



**This electronic thesis or dissertation has been
downloaded from Explore Bristol Research,
<http://research-information.bristol.ac.uk>**

Author:

Abrams, Roman

Title:

Difunctionalisation of Urea-Containing Alkenes by Radical Methods

General rights

Access to the thesis is subject to the Creative Commons Attribution - NonCommercial-No Derivatives 4.0 International Public License. A copy of this may be found at <https://creativecommons.org/licenses/by-nc-nd/4.0/legalcode>. This license sets out your rights and the restrictions that apply to your access to the thesis so it is important you read this before proceeding.

Take down policy

Some pages of this thesis may have been removed for copyright restrictions prior to having it been deposited in Explore Bristol Research. However, if you have discovered material within the thesis that you consider to be unlawful e.g. breaches of copyright (either yours or that of a third party) or any other law, including but not limited to those relating to patent, trademark, confidentiality, data protection, obscenity, defamation, libel, then please contact collections-metadata@bristol.ac.uk and include the following information in your message:

- Your contact details
- Bibliographic details for the item, including a URL
- An outline nature of the complaint

Your claim will be investigated and, where appropriate, the item in question will be removed from public view as soon as possible.

Difunctionalisation of Urea-Containing Alkenes by Radical Methods.

Discovery, development, and mechanistic investigation of
azo-cycloamination and alkyl-arylation alkene difunctionalisations.

Roman Abrams

A dissertation submitted to the University of Bristol in accordance with the
requirements for award of the degree of Doctor of Philosophy in the Faculty of Science

—
School of Chemistry

—
December 2020

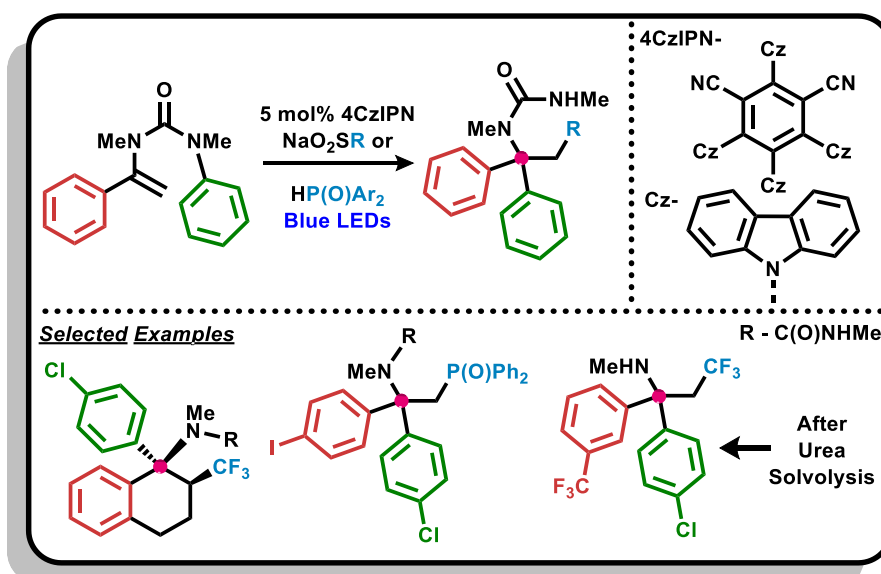
Word count: 73804

Abstract

Chapter 1 - Photocatalytic Difunctionalisation of Vinyl Ureas by Radical-Polar Crossover

The α -tertiary amine is a functional group that is commonly found in natural and synthetic compounds for medicinal and agrochemical applications. For example, α -tertiary amine-based compounds feature as anti-obesity agents, herbicides, fungicides, and anti-depressants. As such, methodologies for the preparation of α -tertiary amines is a topic of continual interest within the synthetic community. In the past, the Clayden group have been able to prepare α -tertiary amines by overcoming the poor reactivity between carbanions and C(sp²) 'electrophiles' by tethering the two coupling components through a urea linkage.

This thesis details the development and scope of conditions for the photoredox catalysed alkyl-arylation and aryl-phosphorylation of vinyl ureas, by use of alkyl sodium sulfinate and diarylphosphine oxide radical precursors. This alkene difunctionalisation process makes use of an organophotocatalyst, allowing the reaction to be driven by visible light. The afforded α -tertiary urea products can be simply converted into their respective α -tertiary amines by solvolysis.

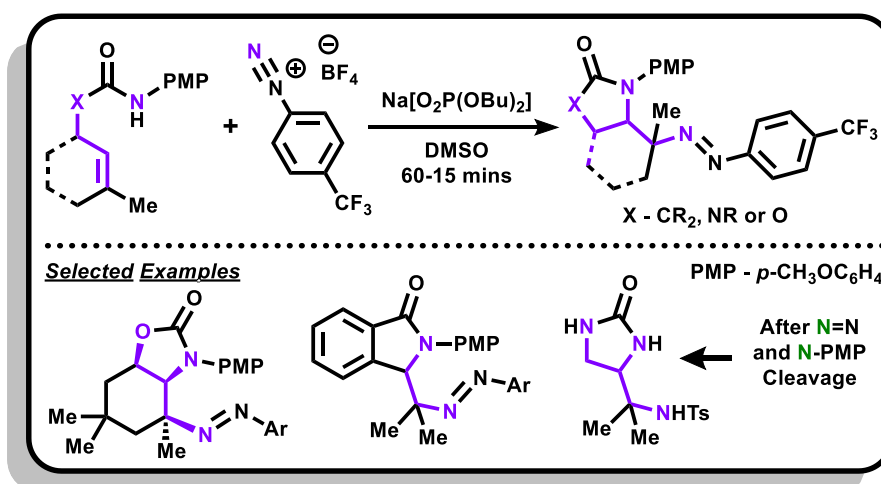


This difunctionalisation process has been probed mechanistically using a suite of methods, which together imply the presence of a reductive quenching photoredox cycle and the formation of α -metallated urea intermediate that undergoes N to C intramolecular arylation across the urea tether.

Chapter 2 - Aryl Diazonium Salt-Promoted Azo-Cycloamination of Allyl Ureas and Carbamates

Vicinal triamines and 1,2,3-diamino alcohols are structural motifs that have captivated the attention of synthetic chemists for the past 50 years, due to their prevalence in natural products, antiviral agents and peptidomimetics. The diamination of allyl amines and allyl alcohols make for attractive routes to vicinal triamines and 1,2,3-diamino alcohols.

This thesis explores an approach based on the aminative cyclisation of allyl ureas and allyl carbamates using photoredox catalysis to generate amidyl radicals by proton-coupled electron-transfer (PCET). However, instead it was discovered that the azo-cycloamination of allyl ureas and carbamates could be conducted in the absence of photocatalyst and light, by simple exposure of certain olefinic starting materials to aryl diazonium salt in the presence of phosphate base. The resulting azo compound products were amenable to deprotection steps, such as hydrogenation of the azo bond to a primary amine.



Preliminary mechanistic investigation of this azo-cycloamination were conducted and comprised of radical trapping experiments and cyclic voltammetry analysis. These experiments imply the presence of a radical-chain process initiated by formation of aryl radical and propagated by PCET N-H homolytic activation.

Acknowledgments

« Living proof that it's better to be lucky than smart. »

Lt. John Bergin – *I, Robot*

Firstly, I thank the EPSRC and the Centre for Doctoral Training in Catalysis for financial support.

So, in no particular order...

Jonathan – Thank you for having me in your group for the last 3.5 years and for guiding me throughout that time. It has been an awesome experience working with you and the people you bring in, you should be so proud of the research institution you have built and I feel blessed to have been a part of it. If I had to go back and redo my PhD, I would still choose the Clayden group again.

Mary – You are one of the most kind-hearted people I have had the pleasure of meeting, and you are going to be a great teacher because of it. Cambridge and Birmingham were a lot of fun and it was a blast working with you on the final project of your PhD.

Frank – My Polish bredren! You have been there from the beginning and my PhD experience has been better for it. You always find the best in people and your political humour has always been a guilty pleasure of mine. I wish you did not have to be shared with the Woolfson group.

MoMoMoMoMoMoMoMoMoMooooo – I have never met anyone like you. You are always so hilarious, happy, and hard-working no matter what comes your way. Portugal was sick, and our friendly poster rivalry was an excellent feature of my PhD.

Rakesh – You are one of the most hard-working individuals I have had the joy of meeting, thank you for your company on all those weekends.

Matthew – Thanks for being a great person to work with and for all the anime recommendations. NAN!!!1

Branca – I have had a great time being a part of BBBB and 24K Magic is definitely the anthem of my PhD. Also, working with someone as curiosity-driven and hard working as yourself has continually been a joy.

Steve – You are one of the most kind and willing to help research fellows I have been lucky to meet, and the group has been a better place to work with you in it.

Ellie – I have had a great time working with you, you were always so chilled, laid-back, and fun. You will always be a great addition to any team you join. Also, thank you for the cyclic voltammetry help.

Mehul – It was awesome working with you in the closing period of my PhD. I am glad the project has been left in such capable hands and I have a good feeling you are going to do great in the group.

Louise – It was so much fun working next to you, never a dull moment and if I could I would happily do it again. Also, thanks for introducing me to SUPing, hoping to do a lot more of it in the future.

Dan – Thanks for your help throughout my PhD, you are probably one of the coolest people I have met.

Makenzie – It was really fun working with you, if something social was planned I could always count on you being there. Also, thanks for the help with the ReactIR.

Dabs – Dude, very soon after I first met you, I felt I had made a genuine friend. Your ability to light up any room you enter was continual a pleasure to see and feel. Thanks for all the help in and out of the lab.

Isabella – It was so jokes sitting next to you for three months, I wish we could have just kept you in the group. #TeamHarvey

Hossay – Thank you so much for your help in and out of the group. You have been patient, always happy to help and a pleasure to work with, but most of all you have been a genuine friend. Also, Italy was amazing and I doubt I would of gone if it was not for you.

Quentin – You were the best in lab mentor anyone could have asked for. Thank you for your patience, your time, and your support. My early experiences with you have shaped me as a scientist throughout my PhD and will continue to do so long afterwards as well.

Romain – Thank you for giving me the best advice of my PhD, you have had more of an influence than you probably know.

Jess – It was a great having you as the first person I worked next to, there was never a dull moment.

Gäel – Thanks for the cyclic voltammetry help, and for saying hi every time you saw me.

Alex – You were sick, supervising you felt like no work at all, instead it felt as if I was working with a friend. Also, you have great taste in music, but you know that already.

Finally, I must give the biggest thank you to my father Robert, my mother Iwona and my partner Emma. Their support goes beyond the mere three years of this PhD. Thank you for standing by me through it all, and accepting my actions and choices in the face of apparent obsession and self-destruction.

Authors Declaration

I declare that the work in this thesis was carried out in accordance with the requirements of the University's Regulations and Code of Practice for Research Degree Programmes and that it has not been submitted for any other academic award. Except where indicated by specific reference in the text, the work is the candidate's own work. Work done in collaboration with, or with the assistance of, others, is indicated as such. Any views expressed in the dissertation are those of the author.

SIGNED: Roman Abrams

DATE: 30/10/20

Contents

Abbreviations	1
Chapter 1	3
1. Importance and Synthesis of α -Tertiary Amines	4
1.1 Cyanate to Isocyanate [3,3]-Sigmatropic Rearrangements	5
1.2 Overman Rearrangement	7
1.3 Curtius Rearrangement	9
1.4 Stevens Rearrangement	11
1.5 Ellman's Auxiliary	14
1.6 Modern Approaches towards α -Tertiary Amines	16
2. Project Background	23
2.1 Photoredox Catalysis	23
2.2 Photoredox-Catalysed Alkene Difunctionalisation by Radical-Polar Crossover	32
2.2.1 Alkene Difunctionalisation by Oxidative-Termination Radical-Polar Crossover ...	34
2.2.2 Alkene Difunctionalisation by Reductive-Termination Radical-Polar Crossover ...	37
2.3 Concerted Nucleophilic Aromatic Substitutions	41
2.4 The Truce-Smiles Rearrangement of α -Metalated Ureas	46
3. Results and Discussion	51
3.1 Project Aims	51
3.2 Reaction Discovery and Optimisation	52
3.3 Scope of Aryl Migrating Groups	62
3.4 Scope of Radical/Anion Stabilising Groups	65
3.5 Radical Precursor Scope	73
3.6 Solvolysis of α -Tertiary Ureas	79
3.7 Mechanistic Investigation	80
3.8 Conclusion	95
Chapter 2	96
4. Vicinal Triamines, 1,2,3-Diamino Alcohols and 1,2,3-Amino Diols	97
4.1 Importance and Synthesis of 1,2,3-Diamino Alcohols and 1,2,3-Amino Diols	97
4.2 Importance and Synthesis of Vicinal Triamines	102
5. Project Background	108
5.1 Photoredox Catalysis and Proton-Coupled Electron Transfer	108
5.2 Aryl Diazonium Salts as Amine Transfer Reagents	115

6. Results and Discussion	120
6.1 Project Aims	120
6.2 Discovery and Optimisation of Azo-Cycloamination Conditions	122
6.3 Scope of Catalyst-Free Azo-Cycloamination Conditions.....	134
6.4 Synthetic Modifications of Azo-Cycloamination Products	143
6.5 Mechanistic Investigation	148
6.6 Conclusion	160
7. Future Work	161
Experimental Section	165
8.1 General Information	166
8.1.1 Solvents, Reagents and Starting Materials	166
8.1.2 Analytical Directions	167
8.1.3 Photochemical Equipment and Setup	169
8.2 Chapter 1 Experimental	170
8.2.1 General Procedures	170
8.2.2 Synthetic Procedures	173
8.2.3 Cyclic Voltammetry Data	235
8.2.4 Stern-Volmer Fluorescence Quenching Studies	237
8.2.4.1 Study at Low Quencher Concentration	237
8.2.4.2 Study at High Quencher Concentration.....	239
8.2.5 Quantum Yield Elucidation	241
8.3 Chapter 2 Experimental	245
8.3.1 General Procedures	245
8.3.2 Synthetic Procedures	247
8.3.3 Cyclic Voltammetry Data	283
8.3.3.1 Initial Investigation	283
8.3.3.2 Follow Up Studies	286
9. References	291

Abbreviations

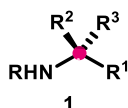
3DPAIPN	2,4,6-tris(diphenylamino)-5-fluoroisophthalonitrile
4CzIPN	1,2,3,5-tetrakis-(carbazol-yl)-4,6-dicyanobenzene
BDE	Bond disassociation energy
CCR1	C-C motif chemokine receptor 1
CFL	Compact fluorescent lamp
cS _N Ar	Concerted nucleophilic aromatic substitution
CT	Charge transfer
CV	Cyclic voltammetry
D-A	Donor-acceptor
DPA	9, 10- Diphenylanthracene
ET	Electron transfer
HAT	Hydrogen atom transfer
IC	Internal conversion
ISC	Inter-system crossing
LED	Light-emitting diode
Mbs	<i>p</i> -Methoxybenzenesulfonyl
OLED	Organic light-emitting diode
PC	Photocatalyst
PCET	Proton-coupled electron-transfer
PMP	<i>p</i> -Methoxyphenyl
PRC	Photoredox catalysis
SCE	Saturated calomel electrode
SES	2-(Trimethylsilyl)ethanesulfonyl
SET	Single electron transfer
TADF	Thermally activated delayed fluorescence
tRNA	Transfer ribonucleic acid
TRPM8	Transient receptor potential cation channel subfamily M member 8

Chapter 1

Photocatalytic Difunctionalisation of Vinyl Ureas by Radical-Polar Crossover

1. Importance and Synthesis of α -Tertiary Amines

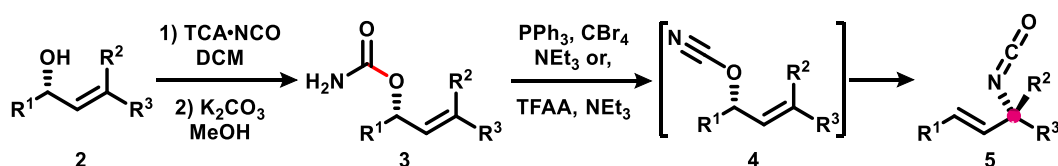
α -Tertiary amines (**1**) are comprised of a carbon atom bonded to three other carbon atoms and one nitrogen atom through single bonds (Scheme 1-1). α -Tertiary amines are commonly found throughout medically relevant molecules. As such, the discovery and development of methods for the synthesis of α -tertiary amines has been and still is an area of interest to synthetic chemists for the past 50 years, resulting in an armamentarium of procedures being developed for their preparation (*vide infra*).



Scheme 1-1. A generic α -tertiary amine, with the tertiary carbon highlighted with a red sphere.

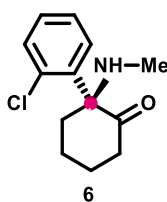
1.1 Cyanate to Isocyanate [3,3]-Sigmatropic Rearrangements

The transposition of allyl cyanates to allyl isocyanates was first reported by Holm and Christophersen in 1970,¹ but due to allyl cyanates being rarely isolable use of this synthetic approach was initially ignored for 20 years.² It was not until methods were established for the conversion of allyl alcohols (**2**) to allyl carbamates (**3**) then in situ formation of allyl cyanates (**4**) by dehydration, that brought this synthetic approach to the mainstream (Scheme 1-2).³ The conversion of allyl cyanates (**4**) to allyl isocyanates (**5**) proceeds by a [3,3]-sigmatropic rearrangement, in which high fidelity of chirality transfer and good *E* stereoselectivity of the new alkene are explained by a chair-like transition state.^{2a,4} Naturally, the transposition of allyl cyanates to allyl isocyanates has been well utilised in the synthesis of allyl amines and α -tertiary amines.⁵



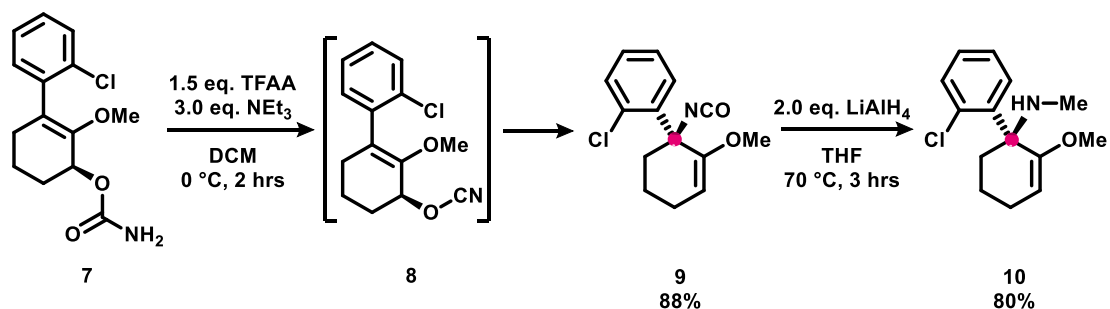
Scheme 1-2. Generalised transformation of allyl alcohol (**2**) to an α -tertiary isocyanate (**5**), by allyl cyanate (**4**) formation.

In 1962, Calvin L. Stevens first synthesised the α -tertiary amine ketamine (**6**, Scheme 1-3), while exploring thermal α -hydroxyimine rearrangements.⁶ Ketamine (**6**) was branded as Ketalar and sold as a human and veterinary anaesthetic.⁷ The anaesthetic potency of the (*S*)-enantiomer of ketamine (**6**) is 3-4 times stronger than the racemic form. Also, for ketamine (**6**) only the (*R*)-enantiomer is responsible for abhorrent side-effects, such as hallucination and agitation.⁸ In addition to its anaesthetic applications, ketamine (**6**) has recently been approved by the US FDA as an antidepressant in the form of a nasal spray.⁹ Due to the medicinal properties ketamine (**6**) exhibits, several of its racemic¹⁰ and asymmetric¹¹ syntheses have been published.



Scheme 1-3. α -Tertiary amine (*S*)-ketamine (**6**).

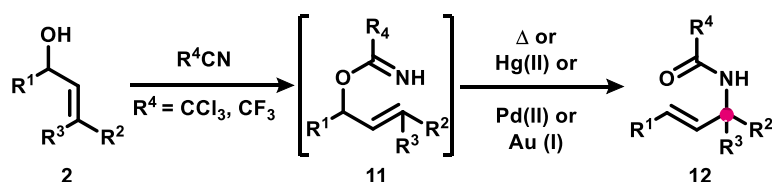
Chen and Li reported a relatively short route to enantiopure (*S*)-ketamine (**6**), by use of the cyanate to isocyanate [3,3]-sigmatropic rearrangement (Scheme 1-4).¹² Firstly, enantiopure allyl carbamate **7** was synthesised by an enantioselective ruthenium-catalysed transfer hydrogenation of the parent enone, followed by carbamate formation. Dehydration of carbamate **7** gives the intermediary cyanate **8**, which spontaneously undergoes [3,3]-sigmatropic rearrangement to give the α -tertiary isocyanate **9** without erosion of enantiopurity. The α -tertiary isocyanate **9** was reduced to the α -tertiary methylamine **10**, which then only requires acid-mediated hydrolysis of the enol ether to form (*S*)-ketamine (**6**).



Scheme 1-4. The [3,3]-sigmatropic rearrangement of carbamate **7** to isocyanate **9** for the synthesis of (*S*)-ketamine (**6**).

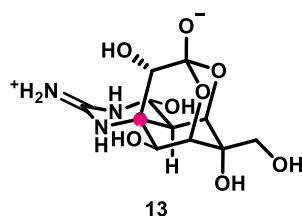
1.2 Overman Rearrangement

The Overman rearrangement, discovered by Larry Overman in 1974,¹³ entails the conversion of allylic alcohols (**2**) to allylic trichloro- or trifluoroacetimidates (**11**), followed by a thermally initiated or transition metal-catalysed [3,3]-sigmatropic rearrangement to yield allylic amides (**12**) (Scheme 1-5).¹⁴ The conversion of an imidate to an amide is exothermic by approximately 15 kcal/mol and so is essentially irreversible.¹⁵ The Overman rearrangement proceeds in a suprafacial concerted manner by a six-membered chair transition state, resulting in excellent *E* selectivity in the newly formed alkene and transfer of chirality from the allylic trichloroacetimidate (**11**) to the allylic amide (**12**).¹⁶ Alternatively, enantio-induction of the Overman rearrangement can be communicated from a separate chiral centre in a diastereoselective fashion.¹⁷ The Overman rearrangement has been used for the formation of carbon-nitrogen bonds in the synthesis of nucleotides, amino acids, *N*-heterocycles, amino sugars, and of course α -tertiary amine-containing molecules.¹⁴



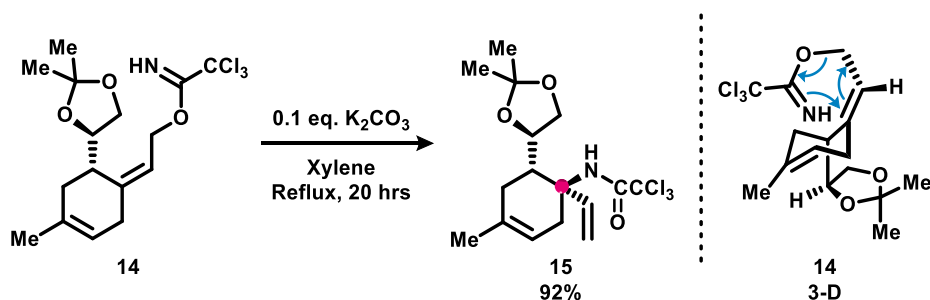
Scheme 1-5. Conversion of allyl alcohols (**2**) to allyl amides (**12**) by the Overman rearrangement.

Tetrodotoxin (**13**, Scheme 1-6) is a key venomous component of puffer-fish poison.¹⁸ Tetrodotoxin (**13**) acts as a potent neurotoxin and performs as a sodium channel blocker to inhibit the stimulation of action potentials within neurons.¹⁹ Due to the pronounced affect tetrodotoxin (**13**) has upon neurological systems it has become a commonly used tool in neurophysiology.²⁰ In addition to possessing potent biological activity, tetrodotoxin (**13**) is also made up of a unique chemical structure, which was elucidated in the 1960s by effort from several academic teams.²¹ Tetrodotoxin (**13**) contains a variety of functionalities, including a cyclic guanidine unit, a polyhydroxylated dioxadamantane containing an ortho ester, and an α -tertiary amine ring junction.



Scheme 1-6. Tetrodotoxin (**13**).

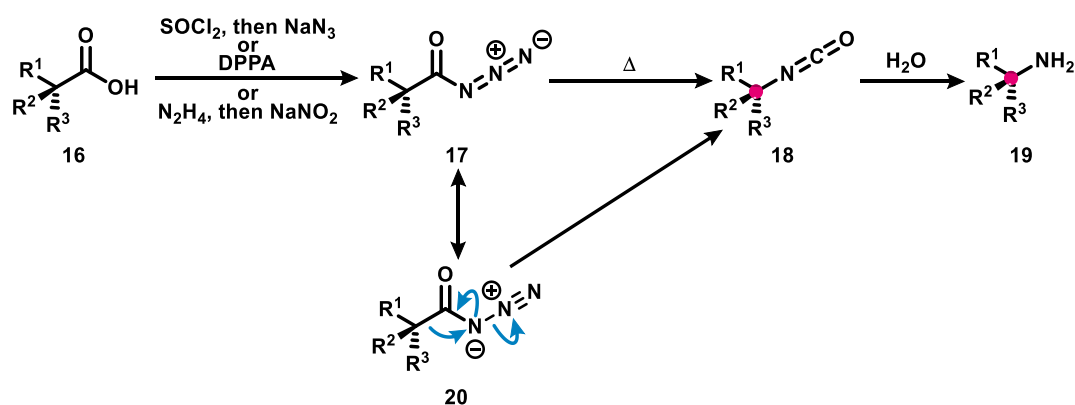
Unsurprisingly, the distinct structure of tetrodotoxin (**13**) has captivated the attention of synthetic chemists with several total syntheses being reported.²² For example, Isobe and co-workers disclosed a concise asymmetric route to tetrodotoxin (**13**) and several of its derivatives.²³ The α -tertiary amine of tetrodotoxin (**13**) was constructed in the opening stages of Isobe's synthesis using levoglucosenone derived allyl trichloroacetimidate **14** (Scheme 1-7). Exposure of allyl trichloroacetimidate **14** to thermal Overman rearrangement conditions gives the α -tertiary amide **15**, with the stereochemistry of the resulting α -tertiary amide being controlled by the adjacent stereocentre.



Scheme 1-7. Thermal Overman rearrangement of allyl imidate **14** to allyl amide **15** for the synthesis of tetrodotoxin (**13**).

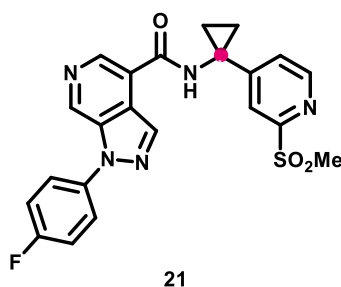
1.3 Curtius Rearrangement

Julius Curtius reported in 1885 that carboxylic acids (**16**) can be converted into acyl azides (**17**), which undergo thermal decomposition to afford isocyanates (**18**) and molecular nitrogen, a process coined the Curtius rearrangement (Scheme 1-8).²⁴ Isocyanates (**18**) are synthetically useful building blocks that can be converted into a variety of functionalities, including amines (**19**) by simple hydrolysis or reduction.^{5,25} The mechanism for the Curtius rearrangement of an acyl azide (**17**) to give isocyanate (**18**) can be thought of as two independent steps that occur in a concerted manner, which include loss of molecular nitrogen to form an acyl nitrene then migration of the adjacent group to the acyl.²⁶ The curly arrow notation of acyl azide **17** to isocyanate **18** can be more clearly seen from the resonance structure **20**. In the Curtius rearrangement the migration of the group adjacent to the acyl occurs with retention of stereochemistry,²⁷ and so has found much application within the context of synthesis.²⁸



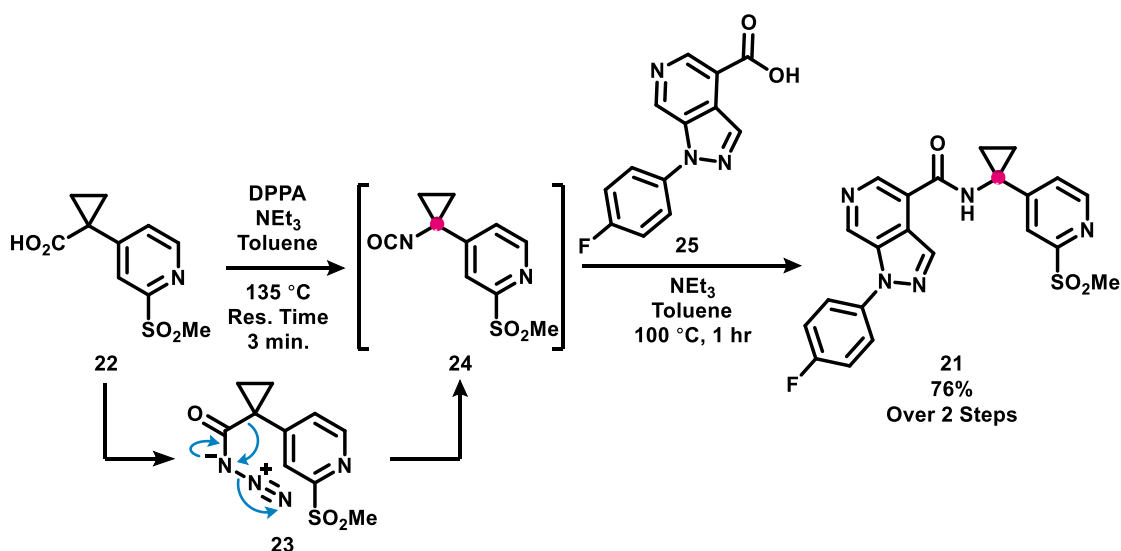
Scheme 1-8. The Curtius rearrangement to convert α -quaternary carboxylic acid **16** to α -tertiary amine **19**, via α -tertiary isocyanate **18**.

Rheumatoid arthritis is a frequently found affliction of the developed world, existing as a chronic inflammatory autoimmune disease resulting in pain, joint destruction, and disability.²⁹ In the search for new treatments of rheumatoid arthritis, CCR1 antagonism has been postulated to reduce inflammation by diminution of macrophage infiltration of synovial tissue.³⁰ As such, CCR1 antagonists have been sought after by several research organisations to combat the symptoms of rheumatoid arthritis. To this end, the α -tertiary amine **21** has been identified as a promising CCR1 antagonist and is being developed as an oral treatment against rheumatoid arthritis (Scheme 1-9).³¹



Scheme 1-9. α -Tertiary amine **21** a CCR1 antagonist.

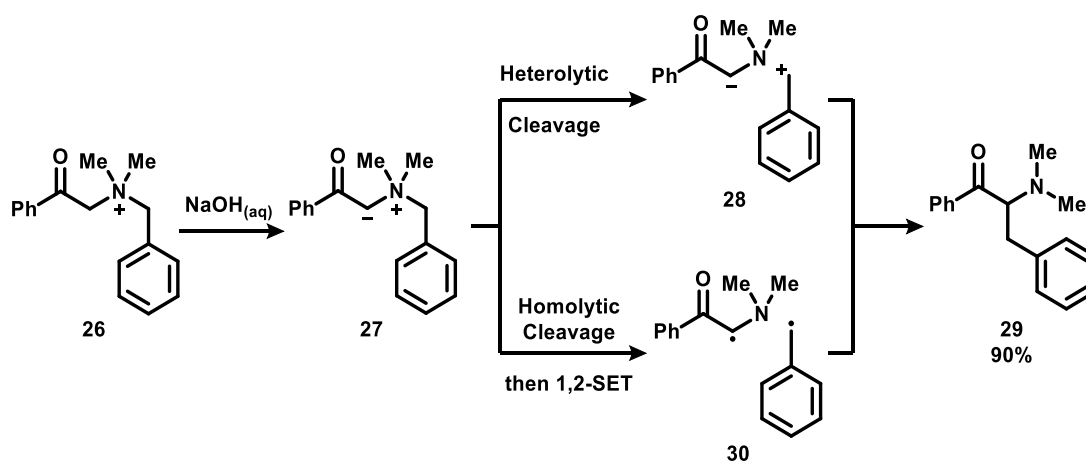
To support the clinical trial investigation of α -tertiary amine **21**, a kilogram scale synthesis with emphasis placed on green chemistry was developed by Marsini and co-workers.³² The key transformation of Marsini's route towards α -tertiary amine **21** is a Curtius rearrangement of carboxylic acid **22**, in which flow protocol was developed for the formation of acyl azide **23**, which under the reaction conditions spontaneously decomposes to α -tertiary isocyanate **24** (Scheme 1-10). α -Tertiary isocyanate **24** is then used in a decarboxylative coupling with fragment **25** to give CCR1 antagonist **21**.



Scheme 1-10. The Curtius rearrangement of carboxylic acid **22** to afford α -tertiary isocyanate **24** for preparation of CCR1 antagonist **21**.

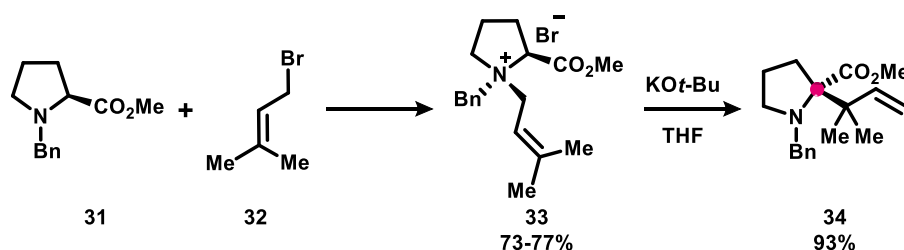
1.4 Stevens Rearrangement

During their investigation of ammonium salts as amine protecting groups, Stevens and co-workers serendipitously found that application of alkali solutions to benzylated ammonium salts (**26**) resulted in a [1,2]-migration of the benzyl group, a reaction later termed the [1,2]-Stevens rearrangement (Scheme 1-11).³³ The mechanism of the [1,2]-Stevens rearrangement has been a controversial subject since its discovery.³⁴ Originally, the [1,2]-Stevens rearrangement was thought to involve the heterolytic dissociation of an ylide (**27**), then reassociation of a close-contact zwitterionic pair (**28**) to afford an α -benzylated amine product (**29**). The zwitterionic mechanism was reasoned as no crossover products were afforded in crossover experiments and that retention of stereochemistry was observed.³⁵ The now more widely accepted mechanism of the [1,2]-Stevens rearrangement is by a homolytic cleavage manifold (**30**), which Stevens and Thomson hypothesised in 1932,^{35b} but was not fully validated until 1970 with work from Lepley³⁶ and Baldwin and co-workers.³⁷



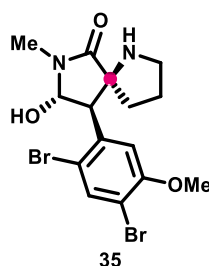
Scheme 1-11. First example of the [1,2]-Stevens rearrangement.

In addition to the migration of benzyl groups, Stevens and co-workers also reported that allylic functionality undergoes migration from an ammonium centre to an adjacent carbon, later known as the [2,3]-Stevens rearrangement.^{35b} Misleadingly, the [1,2]-Stevens rearrangement and the [2,3]-Stevens rearrangement do not share similarities in their mechanisms. The [1,2]-Stevens rearrangement proceeds by a radical manifold (Scheme 1-11), while the [2,3]-Stevens rearrangement is a sigmatropic process.³⁸ A synthetically useful attribute of the [2,3]-Stevens rearrangement is that transfer of chirality is observed. For example, West and co-workers reported the stereoinvertive α -allylation of proline derivatives (**31**), by a diastereoselective *N*-quarternisation with prenyl bromide (**32**) to afford quaternary ammonium salts (**33**) (Scheme 1-12).³⁹ Base-mediated [2,3]-Stevens rearrangement of ammonium **33** yields the α -tertiary amino acid **34**. Over the past 90 years the [1,2]-Stevens rearrangement and [2,3]-Stevens rearrangement have both found significant application in amine synthesis.^{33,35a,40}



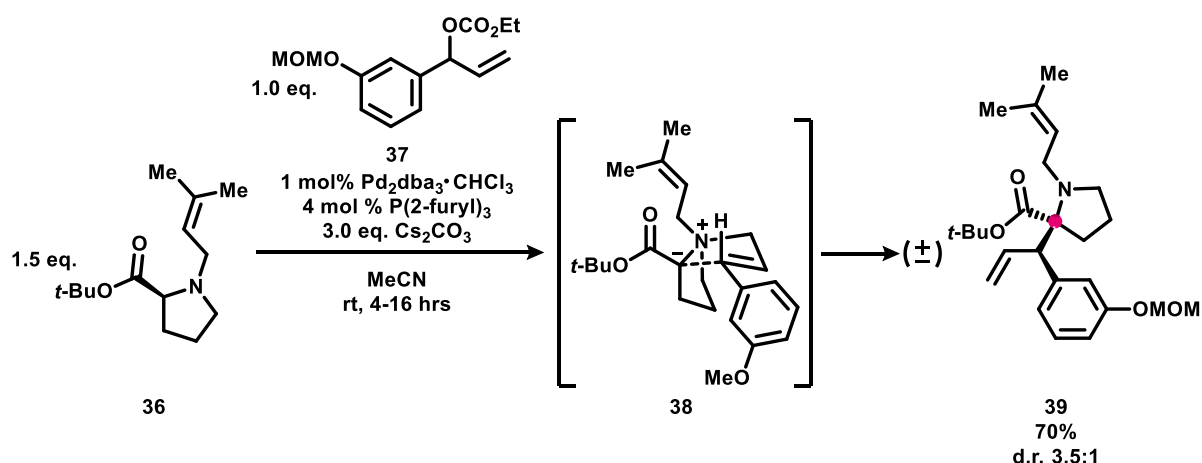
Scheme 1-12. Stereoinvertive [2,3]-Stevens rearrangement of proline derivative **31** to form the α -tertiary amino acid (**34**).

Amathaspiramide F (**35**, Scheme 1-13) is a member of a family of alkaloids isolated from marine bryozoan *Amathia wilsoni* in New Zealand.⁴¹ It has been demonstrated that the amathaspiramide family display a myriad of affects upon biological systems, such as antiviral, cytotoxic, and antimicrobial activities,⁴¹ while also demonstrating promise as β -turn mimics in proteomics.⁴² Members of the amathaspiramide family share a unique aza-spirobicyclic framework, which consists of three contiguous chiral centres, one of which is an α -tertiary amine.



Scheme 1-13. Amathaspiramide F (**35**).

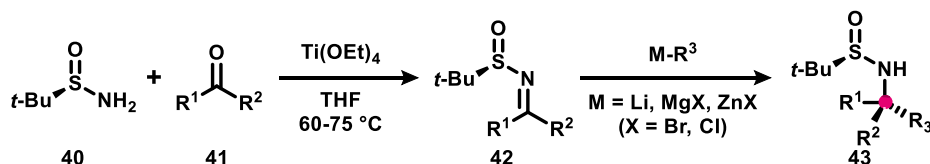
Unsurprisingly, due to the novel structure and medicinal significance of the amathaspiramide family, amathaspiramide F (**35**) has been the subject of total syntheses where the construction of its α -tertiary amine centre is of chief consideration.⁴³ Tambar and Soheili disclosed a route to racemic Amathaspiramide F (**35**), in which a [2,3]-Stevens rearrangement was used to form the α -tertiary amine intermediate **39** (Scheme 1-14).⁴⁴ Firstly, a palladium-catalysed allylic *N*-quaternisation of proline derivative **36** with allylic carbonate **37** was performed to give the ylide **38**, which spontaneously underwent [2,3]-Stevens rearrangement. The afforded α -tertiary amine **39** was obtained with modest diastereocontrol as the *exo* product, which was favoured as to avoid steric clash between the ester and aryl groups.



Scheme 1-14. Palladium-catalysed allylic *N*-quaternisation of allyl amine **36** with allyl carbonate **37**, followed by [2,3]-Stevens rearrangement to give α -tertiary amine **39**.

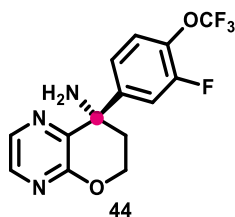
1.5 Ellman's Auxiliary

In 1997, the application of *tert*-butanesulfinamide (**40**, Scheme 1-15) as an auxiliary for the preparation of enantioenriched amines was reported by Ellman and co-workers.⁴⁵ The use of Ellman's auxiliary (**40**) in amine synthesis has impacted multiple chemical fields, including the development of agrochemicals, natural product synthesis, and the preparation of chemical tools for a wide range of biological investigations.⁴⁶ Use of sulfinamide **40** over other sulfinamide auxiliaries⁴⁷ incurs superior stereoselectivity, reduction of nucleophilic additions at sulfur, and ease of synthesis and procurement of both enantiomers.⁴⁸ Furthermore, the condensation of sulfinamide **40** with aldehydes is easily performed at ambient temperature with a catalytic amount of acid.⁴⁹ For the condensation of sulfinamide **40** with ketones (**41**) to form ketimines (**42**) more forcing conditions are employed, with the addition of titanium(IV) ethoxide as a promoter (Scheme 1-15). Ketimine **42** can be used in a variety of synthetic transformations,⁵⁰ the most common being the 1,2-addition of organometallic reagents to form α -tertiary sulfinamides (**43**), which can be converted to α -tertiary amines by acid mediated removal of the auxiliary.⁵¹ The diastereoselectivity observed in the transformation of ketimine **42** to α -tertiary sulfinamide **43** depends on the coordinating strength of the solvent, the cation of the organometallic nucleophile and the chemical functionality present near the ketimine.^{45,49,50e, 52} These parameters will affect whether the addition of an organometallic reagent to ketimine **42** will occur by a closed six-membered transition state or via an open transition state.



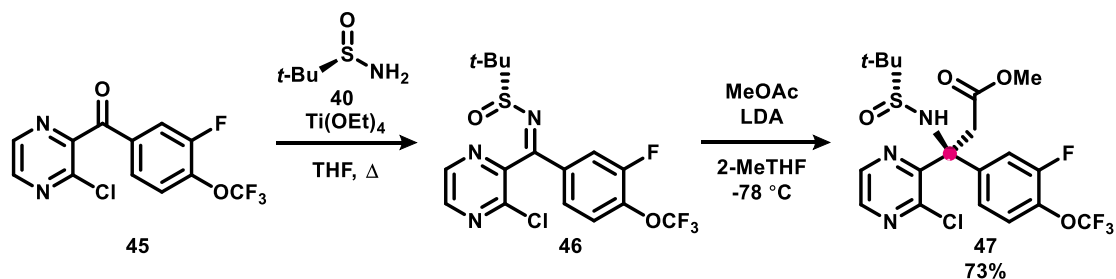
Scheme 1-15. Use of the (*R*) enantiomer of Ellman's auxiliary (**40**) in the synthesis of enantioenriched α -tertiary sulfinamide **43**.

Studies into the neurophysiological basis of cold thermoception and cold nociception using L-menthol-induced cold hypersensitivity relies on direct sensitisation of TRPM8 on A δ and C-fibres.⁵³ Inhibitors of TRPM8 have been touted as potential remedies for migraines and neuropathic pain.⁵⁴ As a result, scientists from Amgen developed a series of chroman derivatives as inhibitors of TRPM8, with the lead candidate identified as α -tertiary amine **44** (Scheme 1-16).⁵⁵



Scheme 1-16. Chroman derived TRPM8 inhibitor **44**.

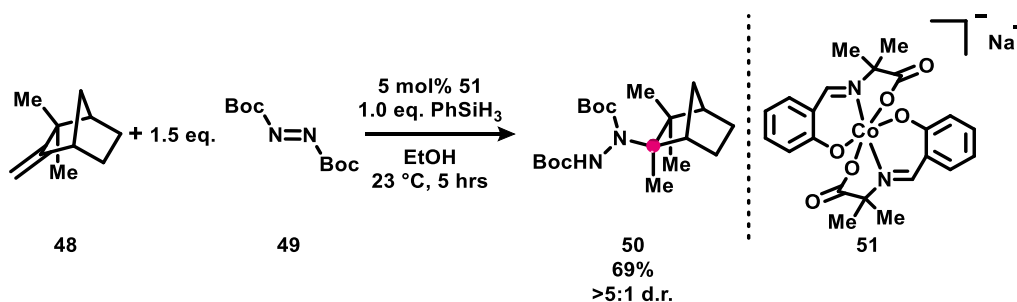
The synthesis of TRPM8 inhibitor **44** begins with the preparation of benzophenone derivative **45**, in which Weinreb ketone synthesis was used (Scheme 1-17).⁵⁵ The titanium(IV) ethoxide promoted condensation of benzophenone derivative **45** with the (*R*) enantiomer of Ellman's auxiliary (**40**) yields the ketimine **46**. Addition of the enolate of methyl acetate to ketimine **46** affords the α -tertiary sulfinamide **47**. Later, the reduction of the ester of **47** to a primary alcohol is carried out and used in the formation of the chroman skeleton of TRPM8 inhibitor **44**, by an intramolecular S_NAr of the chloro-aryl bond.



Scheme 1-17. Enolate addition to ketimine **46** for the preparation of α -tertiary sulfinamide **47**.

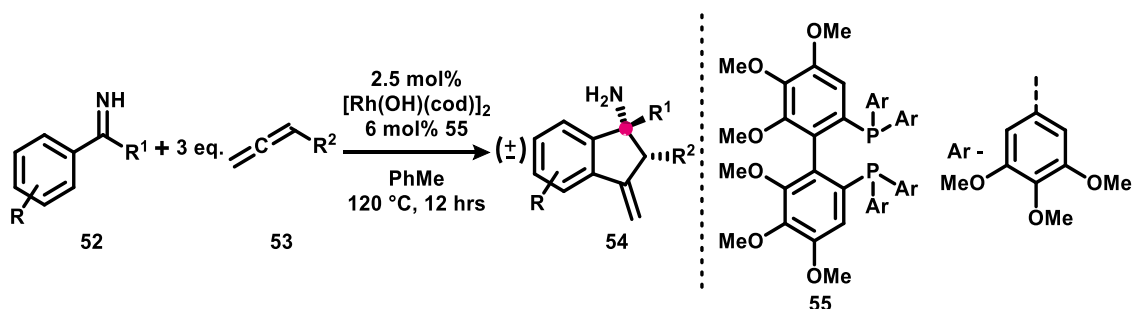
1.6 Modern Approaches towards α -Tertiary Amines

Considering the wide range of appearances α -tertiary amines make throughout biologically potent structures, it is unsurprising that contemporary fields of synthetic chemistry have found application towards their construction. In 2004, Waser and Carreira reported a Markovnikov hydrohydrazination of 1,1-disubstituted alkenes (**48**) with DBAD (**49**) to form α -tertiary hydrazines (**50**) by using cobalt complex **51** (Scheme 1-18).⁵⁶ The mechanism of Scheme 1-18 has been proposed to operate via a cobalt(III)-hydride complex, which performs hydrocobaltation of a double bond, forming a cobalt(III)-alkyl complex. The alkyl portion of the cobalt(III)-alkyl complex disassociates from the cobalt centre as a free radical and adds to DBAD (**49**) to give an amide-coordinated cobalt(III) complex, which undergoes proto-demetalation to yield the desired α -tertiary hydrazine (**48**). Waser and Carreira expanded this protocol to operate under manganese catalysis⁵⁷ and encompass hydroazidations of olefins.⁵⁸ Also Boger and co-workers showed that transformations are applicable under iron catalysis.⁵⁹ α -Tertiary hydrazines⁶⁰ (**50**) and α -tertiary azides⁶¹ can both be converted into their related α -tertiary amines under reductive conditions.



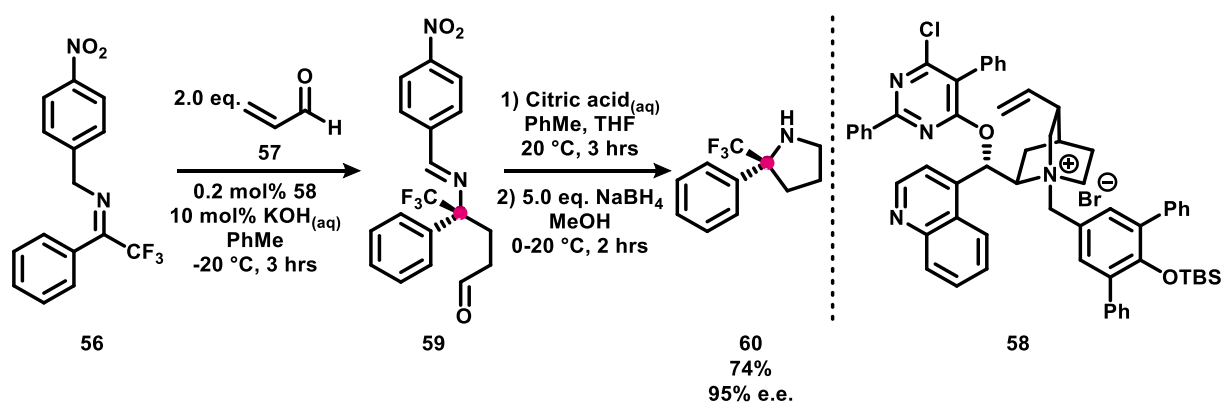
Scheme 1-18. Cobalt-catalysed Markovnikov hydrohydrazination of 1,1-disubstituted olefin **48**.

In 2010, Cramer and co-workers disclosed the rhodium-catalysed [3+2] cycloaddition of acetophenone and benzophenone derived primary ketimines (**52**) with allenes (**53**), to afford α -tertiary amines (**54**) by using ligand **55** (Scheme 1-19).⁶² Scheme 1-19 proceeds by rhodium C-H insertion *ortho* to the imine of **52**, followed by migratory insertion of the aryl into the central carbon of an allene (**53**), forming an allyl rhodium complex that participates in intramolecular nucleophilic allylation of the imine. This rhodium-catalysed [3+2] cycloaddition with primary ketimines has been further developed by Cramer and Zhao independently to also include alkynes as the unsaturated coupling partners⁶³ and enantioselective variants.⁶⁴



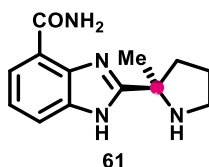
Scheme 1-19. Rhodium-catalysed [3+2] cycloaddition of primary ketimines (**52**) with allenes (**53**) to yield primary α -tertiary amines (**54**).

In 2015, Deng and co-workers reported an enantioselective umpolung approach to the α -functionalisation of trifluoromethylketimines (**56**) with α,β -unsaturated carbonyls (**57**) by phase-transfer catalysis (Scheme 1-20).⁶⁵ Scheme 1-20 operates within an organic-aqueous biphasic reaction medium, where the cinchonine derived phase-transfer catalyst **58** facilitates movement of hydroxide anions from the aqueous into the organic phase. In the organic phase, catalyst **58** associated hydroxide anion deprotonates the benzylic position of trifluoromethylketimines (**56**) forming chiral quaternary ammonium bound 2-azaallyl anions, which couple with acrolein (**57**) through the carbon α to the trifluoromethyl group to form enantio-enriched α -tertiary secondary aldimine (**59**). The absolute stereochemistry of **59** was assigned by its transformation into the pyrrolidine **60**, by acid mediated transimination then reduction of the cyclic secondary aldimine, followed by resolution of the crystal structure of the ammonium chloride salt. This approach was found to be applicable to alkyl trifluoromethylketimines and 1,2-disubstituted acroleins.



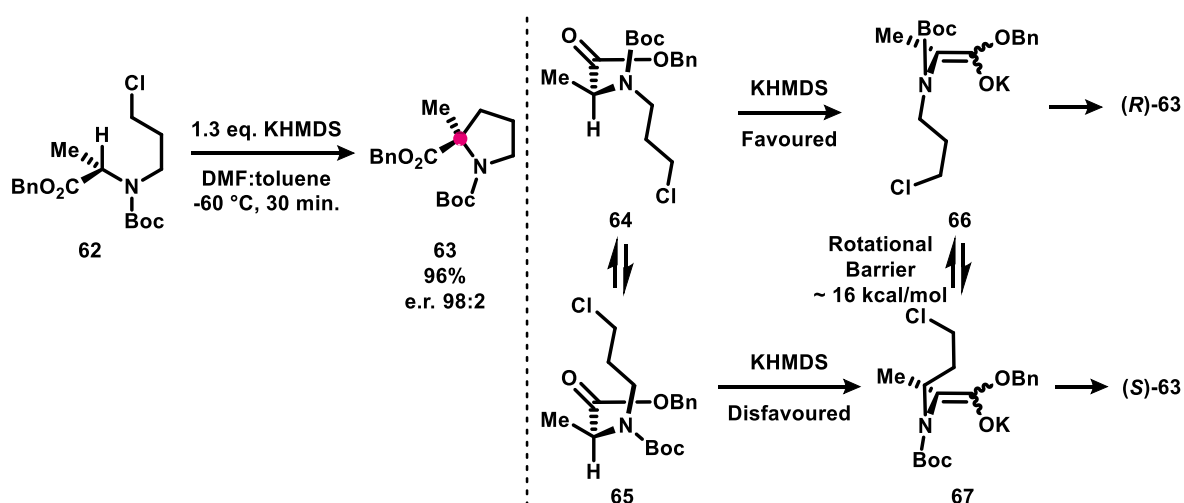
Scheme 1-20. Enantioselective umpolung α -functionalisation of trifluoromethylketimines (**56**) by phase-transfer-catalysis.

Poly(ADP ribose) polymerase is an arbitrator of DNA damage repair within systems susceptible to breast cancer. Preclinical testing has shown that poly(ADP ribose) polymerase inhibitors increase the efficacy of chemotherapeutics and radiation therapy.⁶⁶ Veliparib (**61**, Scheme 1-21) has been touted as a poly(ADP ribose) polymerase inhibitor and is currently under investigation for the treatment of a variety of oncological afflictions.⁶⁷



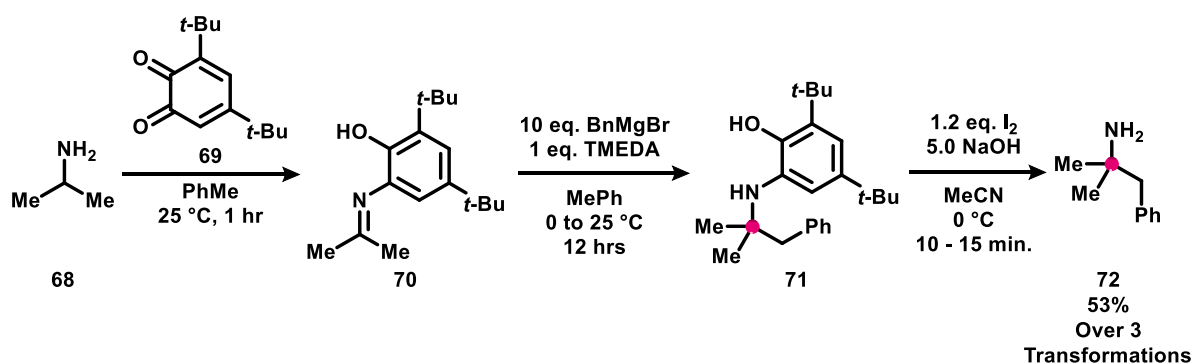
Scheme 1-21. Veliparib (**61**).

The asymmetric synthesis of Veliparib (**61**) was carried out by Kolaczowski and co-workers, where α -tertiary amine **63** is a key intermediate of their route (Scheme 1-22).⁶⁸ The construction of α -tertiary amine **63** was achieved by a cyclization upon alkyl chloride **62**, which proceeds with memory of chirality.⁶⁹ It was proposed that the stereoretentive nature of Scheme 1-22 originates from alkyl chloride **62** predominantly existing in two conformers **64** and **65**, both of which can thermodynamically be deprotonated by KHMDS. However, deprotonation of conformer **65** under the reaction conditions is disfavoured due to an unfavourable steric interaction between the Boc group and the incoming base, an interaction **64** does not incur. Once enolates **66** and **67** are formed they could potentially interconvert with each other by rotation of the nitrogen enolate bond, however **66** and **67** were shown to be atropisomers with a barrier to rotation of 16 kcal/mol.⁷⁰



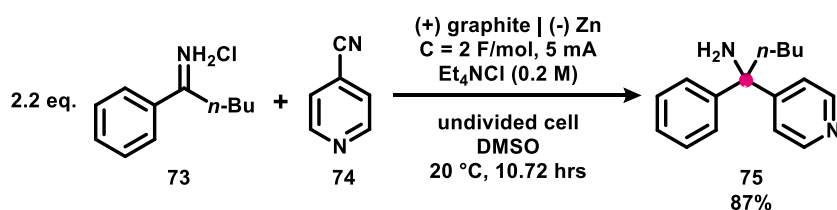
Scheme 1-22. Stereoretentive cyclisation of alkyl chloride **62** to give α -tertiary amine **63** by memory of chirality.

In 2019, Dixon and co-workers looked for inspiration from copper amine oxidases for the development of a novel synthesis of α -tertiary amines. Copper amine oxidases are a class of metalloenzymes that facilitate the oxidation of primary amines into aldehydes, by use of oxygen, a quinone-based co-factor and a copper(II) species.⁷¹ Dixon and co-workers found that the condensation of primary amines (**68**) with quinone **69** formed *N*-aryl ketimines (**70**), by an in situ rearomative [1,5] H-shift of the Schiff base (Scheme 1-23).⁷² It was shown that the newly formed *N*-aryl ketimines (**70**) could be coupled with a variety of organometallic reagents and cyanide, and be a source of α -amino radical by reductive electron transfer for coupling with electron deficient olefins by photoredox catalysis. The utility of this method was underscored by its use in the one-pot preparation of the anorectic drug phentermine (**72**),⁷³ where the primary amine **68** was condensed with quinone **69** to form *N*-aryl ketimine **70**, which was then coupled with benzyl magnesium bromide to give the *N*-aryl α -tertiary amine **71**. *N*-aryl bond cleavage of α -tertiary amine **71** was achieved by hydrolysis under oxidative conditions to give the desired phentermine (**72**).



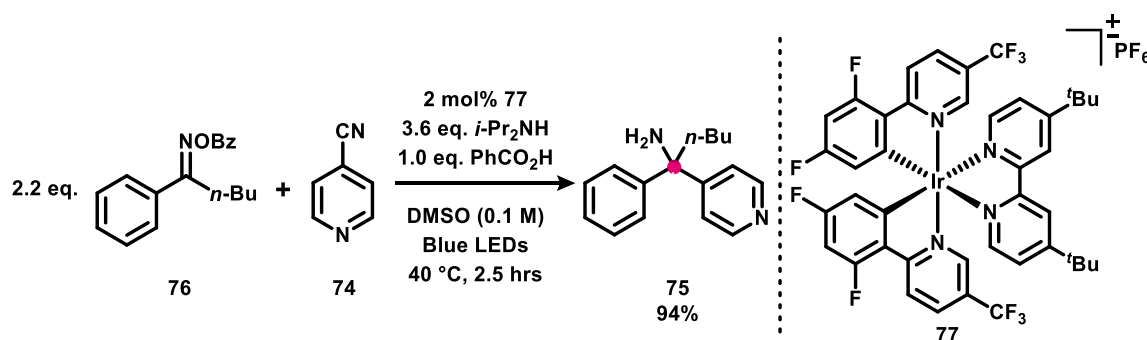
Scheme 1-23. α -C-H functionalisation of α -secondary amines (**68**) by condensation and [1,5] H-shift with quinone **69** then 1,2-addition with Grignard reagent.

In addition to new synthetic disconnections for α -tertiary amine preparation, innovative enabling-technologies are now being used, of which electrochemistry is of particular note for achieving atom-efficient transformations. In 2020, Rovis and co-workers reported the electrochemical reductive coupling of iminium salts (**73**) with cyano functionalised aryl *N*-heterocycles (**74**) to afford α , α -diaryl alkylamines (**75**) (Scheme 1-24).⁷⁴ Multiple mechanistic pathways to exact Scheme 1-24 were probed computationally, leading to the proposition that first cathodic electron transfer to iminium salt (**73**) occurs affording α -amino radical. Simultaneously, aryl *N*-heterocycle (**74**) undergoes reductive proton-coupled electron transfer from the cathode to form a 1,4-dihydropyridine-4-carbonitrile persistent radical, which engages in radical-radical coupling with α -amino radical. Finally, rearomative elimination of hydrogen cyanide furnishes the desired α -tertiary amine (**75**).



Scheme 1-24. Electrochemical coupling of cyano functionalised iminium salts (**73**) with aryl *N*-heterocycles (**74**).

Soon after publishing conditions to exact the electrochemical reductive coupling of iminium salts with cyano functionalised aryl *N*-heterocycles (Scheme 1-24), Rovis and co-workers disclosed the reductive coupling of *O*-benzoyl oximes (**76**) with cyano functionalised aryl *N*-heterocycles (**74**) by photocatalysis (Scheme 1-25).⁷⁵ The mechanism of Scheme 1-25 was probed computationally, leading to the proposition that first photoexcited **77** acts as a triplet sensitizer and engages in Dexter energy-transfer with *O*-benzoyl oxime (**76**), homolysing the N-O bond to form iminyl radical and O-centred benzoyloxyl radical. The iminyl radical hydrogen atom abstracts from the tertiary C-H of DIPA forming imine. Newly formed imine is protonated by benzoic acid, then reduced either by DIPA radical or by photoexcited **77**, forming α -amino radical. Simultaneously, photoexcited **77** is reduced by oxidation of DIPA, then formally reduced **77** engages in reductive proton-coupled electron transfer to cyano functionalised aryl *N*-heterocycle **74**, affording 1,4-dihydropyridine-4-carbonitrile persistent radical. Radical-radical coupling between α -amino radical and 1,4-dihydropyridine-4-carbonitrile radical occurs, followed by rearomative elimination of hydrogen cyanide yielding the desired α -tertiary amine product (**75**). This methodology was also found to be compatible with iminium salts (**73**).



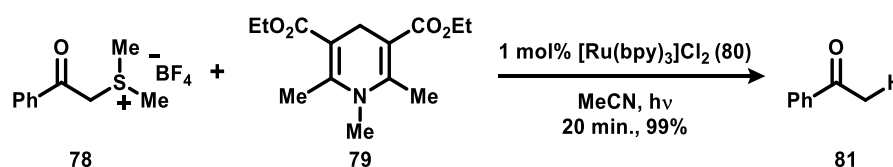
Scheme 1-25. Photochemical α -arylation of *O*-benzoyl oximes (**76**).

2. Project Background

2.1 Photoredox Catalysis

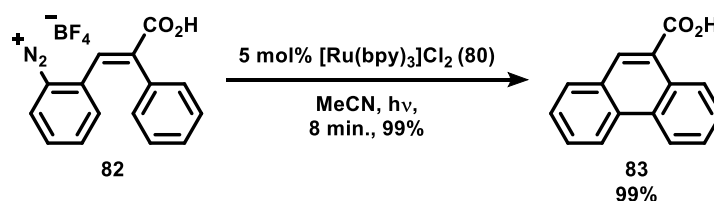
For the last century, the development of photoredox catalysis (PRC) has allowed for the inception of a variety of new chemical technologies. For example, PRC has found application in carbon dioxide reduction,⁷⁶ water splitting⁷⁷ and solar cell materials.⁷⁸ However, use of PRC for organic synthesis has only been truly recognised in the past decade.⁷⁹

The inaugural report of PRC for organic synthesis came from Kellogg in 1978.⁸⁰ Kellogg reported the photoinduced ruthenium complex **80**-catalysed reduction of sulfonium ion **78** to form acetophenone **81** and dimethyl sulfide, using Hantzsch ester derivative **79** as a terminal reductant (Scheme 2-1). Kellogg's reduction protocol was further expanded to other organic functionalities by Pac,⁸¹ Tanaka and Fukuzumi.⁸²



Scheme 2-1. First report of photoredox catalysis for organic synthesis.

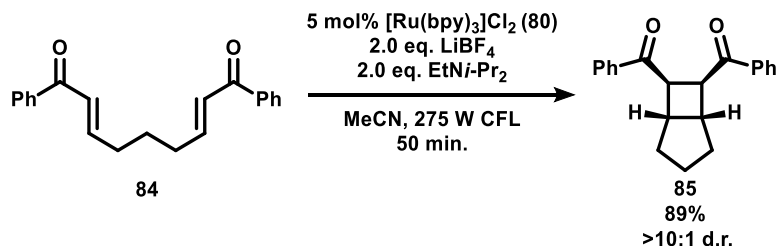
Later, Cano-Yelo and Deronzier disclosed the first redox-neutral photoredox-catalysed transformation in 1984, in the form of a ruthenium complex **80**-catalysed Pschorr reaction to quantitatively convert aryl diazonium salt **82** into phenanthrene derivative **83** (Scheme 2-2).⁸³ In this seminal work it was noted that the reaction occurred with significantly lower quantum efficacy in the absence of photocatalyst **80**.



Scheme 2-2. First example of a redox-neutral photoredox-catalysed process.

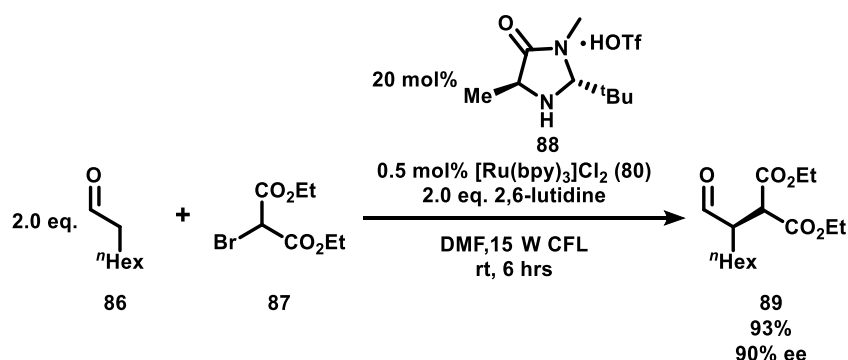
The time between Kellogg's publication and 1991 denotes the first period of sparse academic interest in PRC for application in organic synthesis. During this period, PRC entered a state of dormancy regarding academic attention until the late 2000s. The advent of modern PRC for organic synthesis began in 2008 with two seminal reports.^{84,85}

Firstly, Yoon and co-workers demonstrated the photoredox-catalysed intramolecular [2 + 2] enone cycloaddition of **84** to give the bicyclo[3.2.0]heptane **85**, by use of photocatalyst **80** (Scheme 2-3).⁸⁴ It was found that the addition of LiBF₄ was crucial for Scheme 2-3 to proceed, as it was rationalised that lithium coordination to the carbonyls of **84** activates the enone for reduction by photoexcited **80**.



Scheme 2-3. Ruthenium complex **80**-catalysed [2+2] cycloaddition of enone (**84**).

Soon after Yoon's report, Macmillan and Nicewicz disclosed the enantioselective α -alkylation of aldehydes. This was achieved by use of a dual catalytic system, consisting of chiral organocatalyst **88** and photocatalyst **80** (Scheme 2-4).⁸⁵ This reaction is proposed to initiate by photoexcited **80** oxidising a catalytic quantity of enamine formed by condensation of aldehyde **86** with organocatalyst **88**, yielding formally reduced ruthenium complex **80** and enamine radical cation. Resting state photocatalyst **80** is regenerated from formally reduced ruthenium complex **80** by performing single electron reduction on bromomalonate **87** to generate α -malonyl radical, which adds to enamines (formed in the condensation of aldehyde **86** with organocatalyst **88**) to form α -amino radical. Photoexcited **80** oxidises α -amino radical intermediate, to give an iminium species that is hydrolysed resulting in the desired product **89**, release of the organocatalyst **88** and reforming of formally reduced ruthenium complex **80** to continue the photocatalytic cycle. Since these initial reports from Yoon, and MacMillan and Nicewicz an array of PRC-enabled methodologies have been published.^{79,86}



Scheme 2-4. The enantioselective α -alkylation of aldehydes (**86**) by organo/photoredox dual catalysis.

In addition to the variety of products that are obtainable by PRC, academic attention has also been directed at mechanistic understanding of these processes.⁸⁷ PRC generally begins with excitation of the resting catalyst by absorption of a photon, which promotes an electron from the HOMO to a higher energy orbital by a spin-allowed transition. As the resting catalyst exists in a singlet state, the resulting excited catalyst must occupy a higher energy singlet state in accordance with selection rules of electronic transitions (Figure 2-1). The excited catalyst will then relax to a lower energy singlet state by vibrational quenching, termed internal conversion (IC), where it may then return to its ground state by emission of a lower energy photon than the one it originally absorbed, a process called fluorescence. Alternatively, the lowest energy excited singlet state of the catalyst may undergo the non-radiative transition, intersystem crossing (ISC), and adopt the lowest energy triplet state through IC. Direct relaxation to the ground state from a triplet state requires simultaneous emission of a photon and spin inversion of the excited electron, a forbidden transition termed phosphorescence and so is slow. Therefore, the lowest energy triplet state of the photoredox catalyst is thought to be its long-lived excited state. However, the singlet lifetime of certain photoexcited species can be long enough to facilitate redox processes.^{86d}

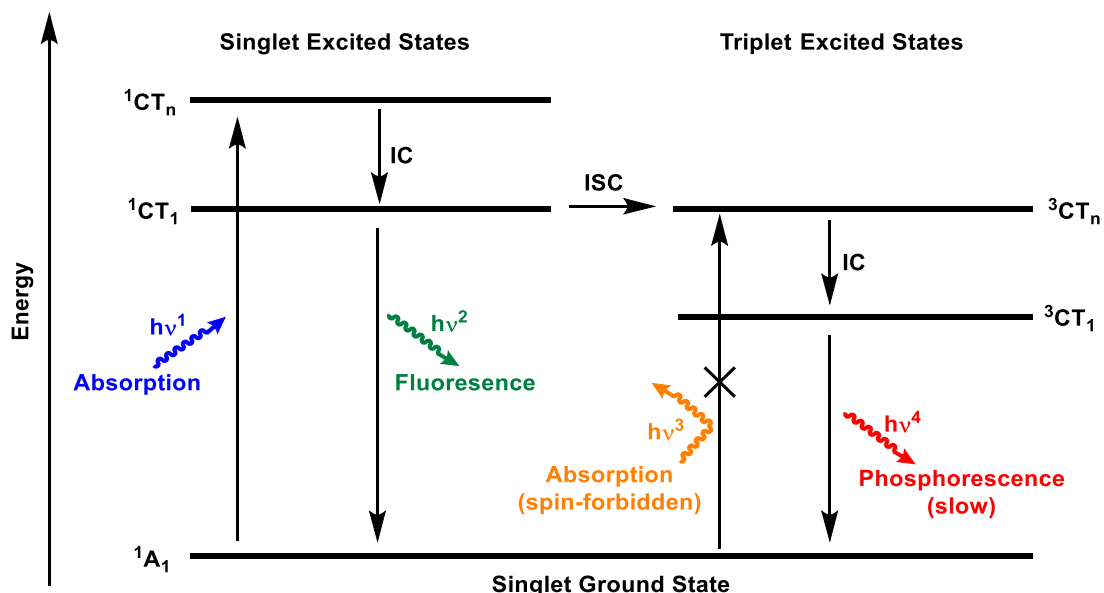


Figure 2-1. Jablonski diagram illustrating the electronic transitions and states a photoredox catalyst will experience during photoexcitation. CT – charge transfer.

If the lifetime of the excited state of the photocatalyst is longer than the timescale of diffusion, it can engage in redox chemistry with a substrate. The electronic structure of an excited photoredox catalyst contains two SOMOs of differing energy (Figure 2-2), so acts as more powerful reducing and oxidising agents compared to their ground state. When an excited photoredox catalyst engages in reduction of a substrate it is formally oxidised. The subsequent oxidation of a substrate by the oxidised photocatalyst to regenerate resting photocatalyst is more exergonic than from its ground or excited state, a process termed oxidative quenching. Conversely, reduction of a substrate by the reduced photocatalyst to regenerate resting photocatalyst is more exergonic than from its ground or excited state, a process termed reductive quenching. Despite the variety of chemical change photoredox catalysis can exact, most processes can be described using these four elementary steps of reduction then oxidation, or oxidation then reduction.^{86b}

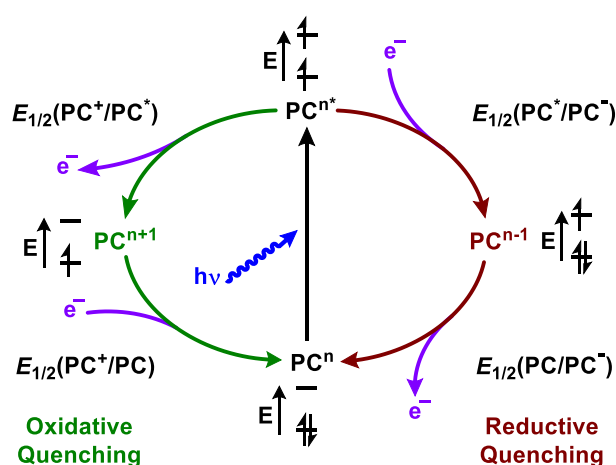
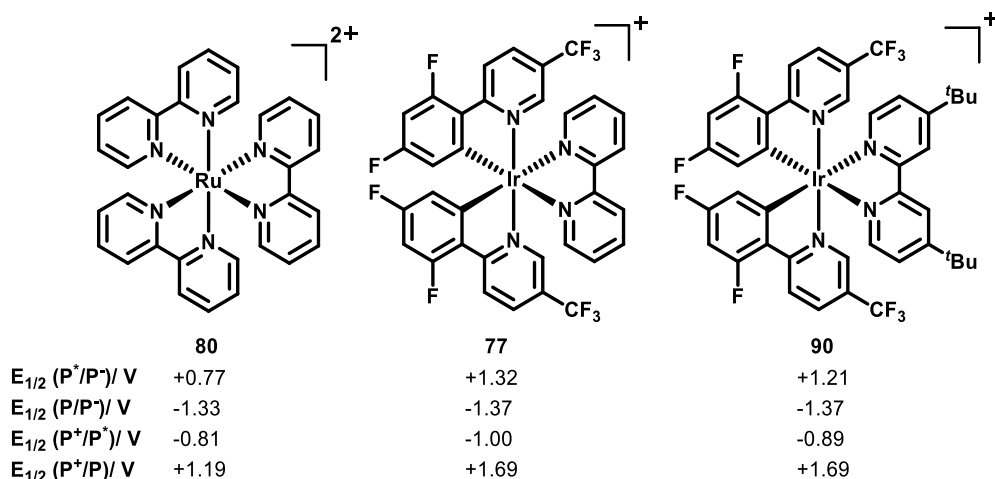


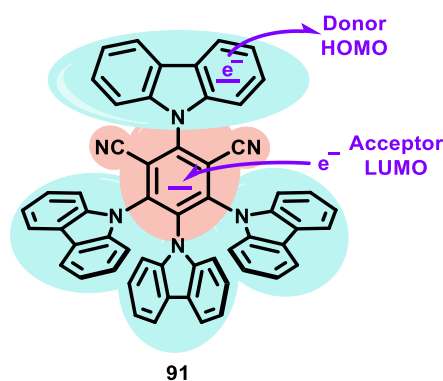
Figure 2-2. Generalised photoredox catalytic cycle, highlighting the two non-radiative regenerative pathways of the ground-state photocatalyst (PC) from its photoexcited state. Asterisks denotes photoexcited state.

In recent years, the most commonly employed families of photoredox catalysts for synthesis have been the polypyridyl complexes of ruthenium and iridium (**77**, **80** and **90**, Scheme 2-5). These complexes absorb visible light, possess long-lived photoexcited states that outcompete unproductive pathways and span a range of redox potentials to exact synthetically useful electron transfers.⁸⁸ However, despite the undeniable influence the polypyridyl complexes of ruthenium and iridium have had in reigniting the field of synthetic photoredox catalysis, they do possess undesirable traits. For one, these complexes are precious metal-centred and so their precursors incur a substantial cost due to their low abundance.⁸⁹ Additionally, multistep syntheses are required for the preparation of iridium and ruthenium photoredox catalysts and their respective bipyridyl ligands, which require the use of palladium precatalysts.⁹⁰ Consequently, academic effort has been directed at the development of new classes of photoredox catalysts that can be attained rapidly from abundant resources, while exhibiting synthetically serviceable redox potentials. For example, endeavours towards the development of earth-abundant metal-centred photoredox catalysts have been undertaken.⁹¹ Furthermore, organic dyes have now recently begun to receive interest as a low cost, high availability, and benign alternatives to precious metal photocatalysts.^{86d}



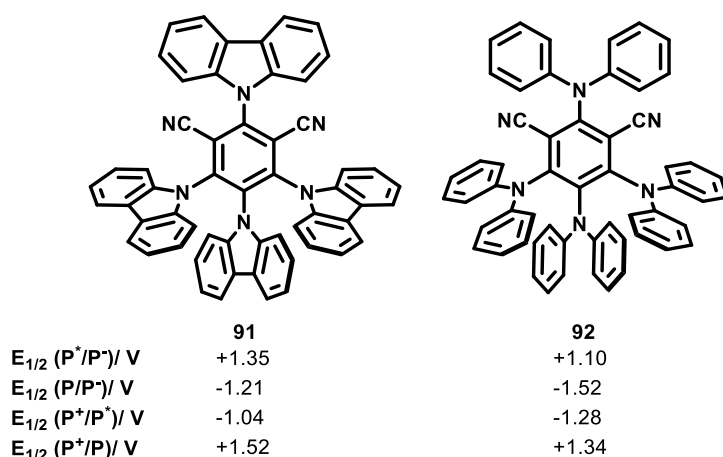
Scheme 2-5. Redox potentials of commonly used precious-metal containing visible light photocatalysts (top).^{86b} Asterisk indicates photoexcited state.

One family of organic photoredox catalysts that have gained particular popularity in recent times as metal-free alternatives to precious metal polypyridyl complexes, are the donor-acceptor dyads of isophthalonitriles.⁹² The first and most widely used of this class is 4CzIPN (**91**), which was originally developed by Adachi and co-workers as a highly efficient, green TADF emitter for use as an OLED (Scheme 2-6).⁹³ 4CzIPN (**91**) possesses a variety of desirable photophysical properties to exact redox processes. Firstly, 4CzIPN (**91**) absorbs light in the visible blue region distinct from most organic substrates, allowing its photoexcitation to be achieved by simple household light sources without perturbation of reactants.⁹⁴ Next, 4CzIPN (**91**) possesses a very small energy gap between its singlet state and triplet state ($\Delta E_{ST} = 0.08$ eV), resulting in a near energetically lossless ISC and therefore maximal conversion of absorbed photonic energy to chemical energy.⁹⁵ Finally, 4CzIPN (**91**) demonstrates photoexcited lifetimes from the triplet state on par with that of commonly used iridium photocatalysts for synthesis.⁹⁶ The donor-acceptor substitution pattern of 4CzIPN (**91**) allows for conceptual visualisation of the spatial separation of the HOMO-LUMO, which are situated on the carbazolyl donors and the cyanoarene acceptor core respectively. Furthermore, the dihedral angle of the carbazolyl donors to the cyanoarene core is typically about 60°, allowing for near independent tuning of the oxidation or reduction power by modifications to the acceptor or donor moieties, respectively.⁹⁷



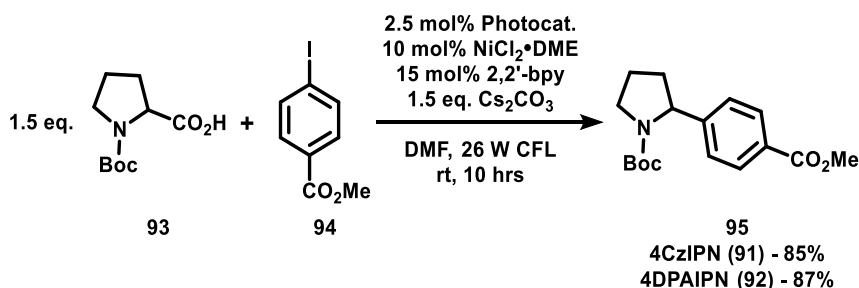
Scheme 2-6. Structure of 4CzIPN (**91**) with its donor (turquoise) and acceptor (beige) moieties highlighted.

The use of 4CzIPN (**91**) in a synthetic context was first investigated by Zhang and Luo, who disclosed the redox potentials of its ground and photoexcited states (Scheme 2-7).⁹⁴ Inspection of the redox potentials of 4CzIPN (**91**) highlights its promise as an inexpensive metal-free iridium photoredox catalyst alternative, especially when compared to iridium complex **77** with respect to the potentials pertaining to a reductive quenching mechanism. Zhang and Luo synthesised a library of 4CzIPN (**91**) derivatives by altering the number of donor moieties and changing the substitution pattern. However, the obtained donor-substituted isophthalalonitriles demonstrated only minor deviations in redox potentials from 4CzIPN (**91**), but significant diminution of stabilities in all cases apart with 4DPAIPN (**92**), a slightly more reducing derivative.



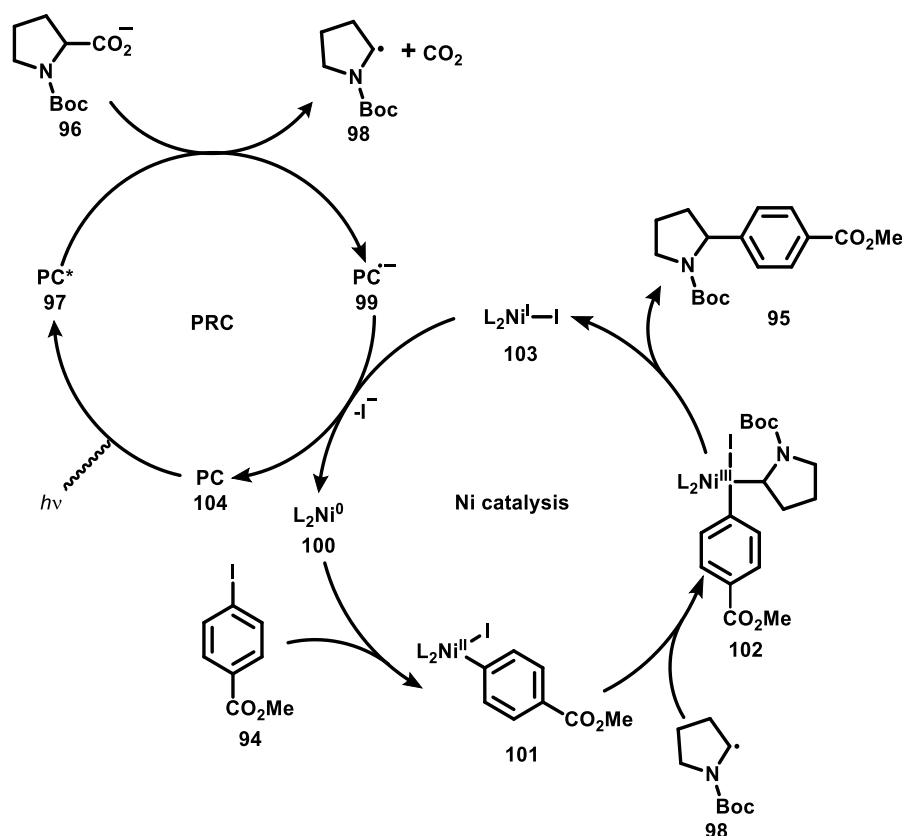
Scheme 2-7. Redox potentials of donor-acceptor fluorophores 4CzIPN (**91**) and 4DPAIPN (**92**) versus SCE. Asterisk indicates photoexcited state.

The method by which Zhang and Luo tested the stability of 4CzIPN (**91**) and 4DPAIPN (**92**) for synthetic purposes was by their application in the decarboxylative cross-coupling of carboxylic acid **93** with aryl iodide **94** to give cross-coupled product **95**, where both catalysts were found to be effective (Scheme 2-8).⁹⁴ Once Scheme 2-8 had reached completion, HPLC analysis of the reaction mixture showed that 58% and 78% of 4CzIPN (**91**) and 4DPAIPN (**92**) remained respectively, indicating these PCs are stable under synthetic reaction conditions and do not simply undergo photodegradation.



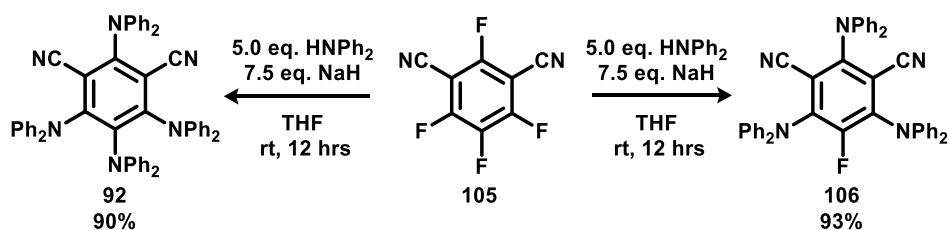
Scheme 2-8. Photoredox/nickel-catalysed decarboxylative cross-coupling facilitated by donor-acceptor dyad photoredox catalysts.

It was proposed that Scheme 2-8 proceeds by initial deprotonation of carboxylic acid **93** to give the carboxylate **96** (Scheme 2-9). Carboxylate **96** has an oxidation potential of +0.95 V versus SCE so is oxidised by excited photocatalyst (**97**), resulting in its decarboxylation to α -amino radical **98** and reduced photocatalyst (**99**).⁹⁸ Simultaneously, the nickel catalytic cycle begins with oxidative addition of nickel(0) complex (**100**) with aryl iodide **94** to give nickel(II) intermediate **101**, which coordinates with free radical **98** to give nickel(III) intermediate **102**. Nickel(III) intermediate **102** performs reductive elimination to yield the desired product **95** and the nickel(I) complex **103**, which is reduced to nickel(0) intermediate **100** by the formally reduced form of the photocatalyst (**99**), regenerating resting photocatalyst (**104**) and closing both catalytic cycles (Scheme 2-9).^{94,99}



Scheme 2-9. Proposed mechanism of Scheme 2-8. Asterisks denotes photoexcited state.

Recently there has been disagreement in the literature over the structure of 4DPAIPN (**92**) (Scheme 2-10). 4DPAIPN (**92**) was originally synthesised by Zhang and Luo, by fourfold-S_NAr of aryl fluoride **105** with diphenylamine.⁹⁴ However, Zeitler and co-workers have reported the attempted reproduction of Zhang's synthesis of 4DPAIPN (**92**) and instead obtained 3DPAFIPN (**106**), the threefold-S_NAr product between aryl fluoride **105** and diphenylamine.^{97a} 4DPAIPN (**92**) and 3DPAFIPN (**106**) were found to possess very similar redox and UV-visible absorption properties, implying that the use of 4DPAIPN (**92**) in Scheme 2-8 may have mistakenly been 3DPAFIPN (**106**).

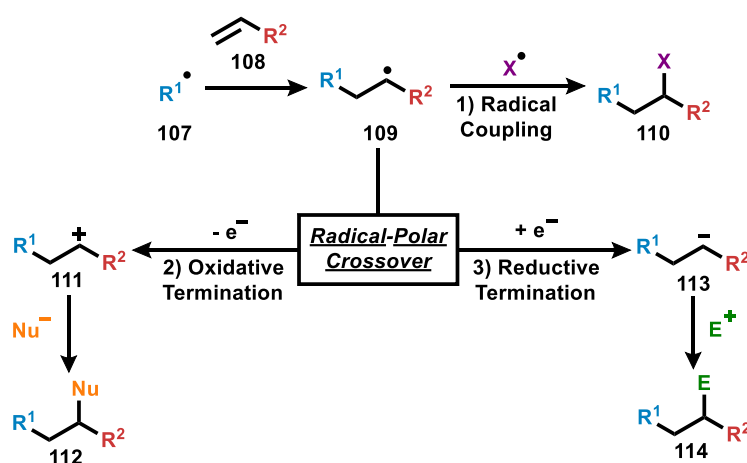


Scheme 2-10. The supposed synthesis of 4DPAIPN (**92**) and 3DPAFIPN (**106**) from aryl fluoride **105**.

2.2 Photoredox-Catalysed Alkene Difunctionalisation by Radical-Polar Crossover

The fundamental power of PRC is that a photoredox cycle consists of two successive opposing single electron redox processes that are mediated by a single entity, the photocatalyst. If a single-electron redox-neutral transformation was attempted on a substrate by two separate electron donor and acceptor entities each facilitating their own separate redox steps, unproductive redox processes between the electron donor and acceptor would be problematic. However, conceptually a photoredox catalyst is an infinite number of single electron donor and acceptor entities in one, by virtue of the photoredox catalytic cycle (Figure 2-2), making PRC effective in performing redox-neutral reactions. The revitalisation of PRC for organic synthesis has led to the discovery of a plethora of new transformations, by allowing for precise small-molecule activation in ways that were not previously possible. For example, PRC has been applied to dual photoredox/transition metal-catalysed cross-coupling reactions, by the generation of mono-valent species to circumvent difficult oxidative addition, transmetalation and reductive elimination steps.¹⁰⁰ Previously benign functional groups have found activation by PRC, such as the α -functionalisation of tertiary aliphatic amines.¹⁰¹ Furthermore, highly impressive late-stage modifications of unactivated C-H bonds have been enabled by PRC, by activation of hydrogen atom transfer catalysts.¹⁰² Lastly, PRC has made a pronounced impression upon the field of alkene difunctionalisations.

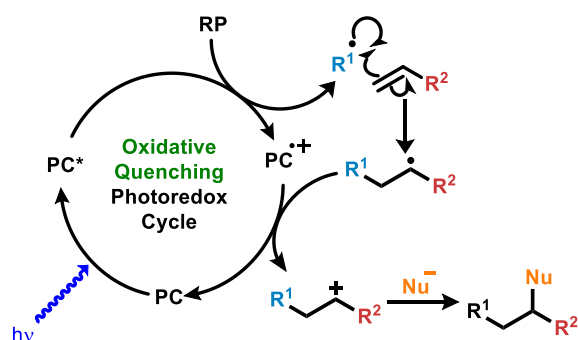
The difunctionalisation of an alkene by PRC will generally initiate by the generation of a radical species (**107**) by reduction or oxidation (Scheme 2-11). Depending on the reaction conditions radical **107** may add to a radical acceptor (**108**) forming new radical species **109**. From here, several mechanistic pathways can occur to determine the fate of radical **109**. 1) A second radical species is generated by the PC through the opposite redox process that formed radical **107**, allowing for transient-radical persistent-radical coupling of radical **109** with another radical to give product **110**.¹⁰³ 2) The PC enables oxidative-termination radical-polar crossover by oxidising radical **109** to carbocation **111**, if radical **107** was formed by reduction. The cationic species **111** can then couple with a nucleophile to give product **112**. 3) Or finally, the PC can mediate a reductive-termination radical-polar crossover and reduce radical **109** to carbanion **113**, if radical **107** was formed by oxidation. The carbanion **113** can then react with an electrophile to give product **114**.



Scheme 2-11. The three mechanistic pathways of PRC enable difunctionalisation of an alkene (**108**), by 1) radical-radical coupling, 2) oxidative-termination radical-polar crossover and 3) reductive-termination radical polar crossover.

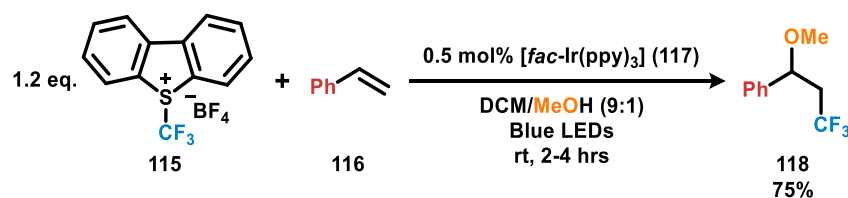
2.2.1 Alkene Difunctionalisation by Oxidative-Termination Radical-Polar Crossover

For the difunctionalisation of an alkene to occur by oxidative-termination radical-polar crossover the PC must engage in an oxidative quenching photoredox cycle, so that a carbocation is formed by oxidation of a radical in the final redox step of the photoredox cycle (Scheme 2-12). The restriction placed upon the PC, that it must first perform a reduction then an oxidation, means that careful consideration of radical precursors and PC selection must be taken. However, despite this mechanistic limitation a variety of PRC-mediated transformations proceed by oxidative-termination radical-polar crossover.¹⁰⁴



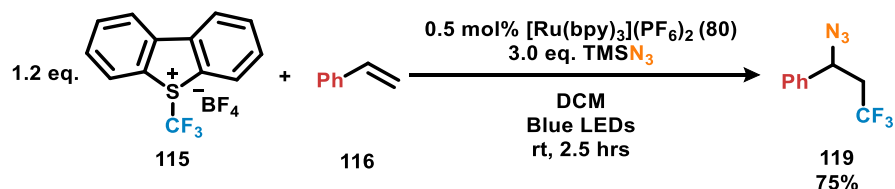
Scheme 2-12. General depiction of an alkene difunctionalisation by oxidative-termination radical-polar crossover. Astrisks denotes photoexcited state.

In 2012, Akita and Koike reported conditions for the three-component oxytrifluoromethylation of alkenes (Scheme 2-13).¹⁰⁵ This transformation was realised by using Umemoto reagent (**115**), a source of trifluoromethyl radical upon reduction by photoexcited **117**. The resultant trifluoromethyl radical adds to an olefin such as styrene (**116**), resulting in a benzylic radical intermediate that is oxidised to a phenyl-stabilised carbocation by formally oxidised **117** (that was generated in trifluoromethyl radical generation). The benzylic carbocationic product of the oxidative quenching photoredox cycle couples with alcoholic solvent to give oxytrifluoromethylation product (**118**).



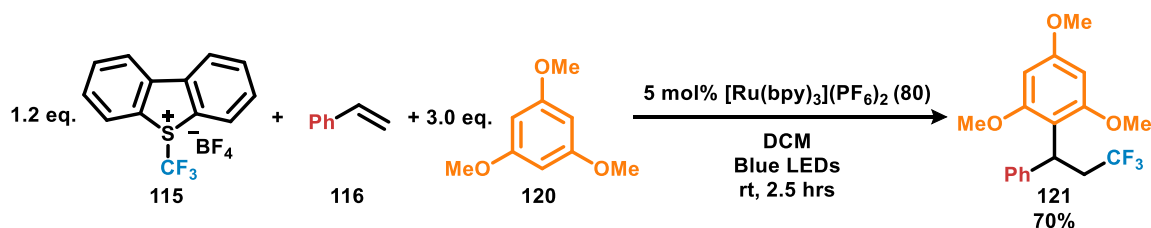
Scheme 2-13. Oxytrifluoromethylation of styrene (**116**) with Umemoto reagent (**115**) in the presence of methanol.

Following on, Magnier and Masson developed a three-component azidotrifluoromethylation of alkenes (Scheme 2-14).¹⁰⁶ Again Umemoto reagent (**115**) is used as a source of trifluoromethyl radical upon reduction (from photoexcited **80**), which adds to styrene (**116**). The resulting benzylic radical is oxidised to a carbenium intermediate by formally oxidised **80**. The benzylic carbocationic intermediate then combines with azidotrimethylsilane to give azidotrifluoromethylation product (**119**).



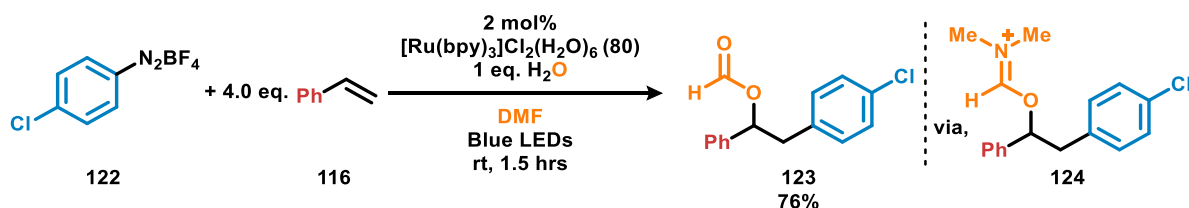
Scheme 2-14. Ruthenium complex **80** catalysed-aminotrifluoromethylation of styrene (**116**).

Later, Masson and co-workers reported the three-component trifluoromethyl-arylation of alkenes (Scheme 2-15).¹⁰⁷ Using similar conditions to Magnier and Masson's aminotrifluoromethylation (Scheme 2-14), the resulting aryl-stabilised carbenium intermediate, formed by trifluoromethyl radical addition to styrene (**116**) followed by oxidation, was used in a Friedel-Crafts-type alkylation with an electron-rich aryl (**120**) to yield the benzhydryl product (**121**). Furthermore, indoles were found to be amenable aryl coupling-partners with the intermediary aryl-stabilised carbenium ions formed.



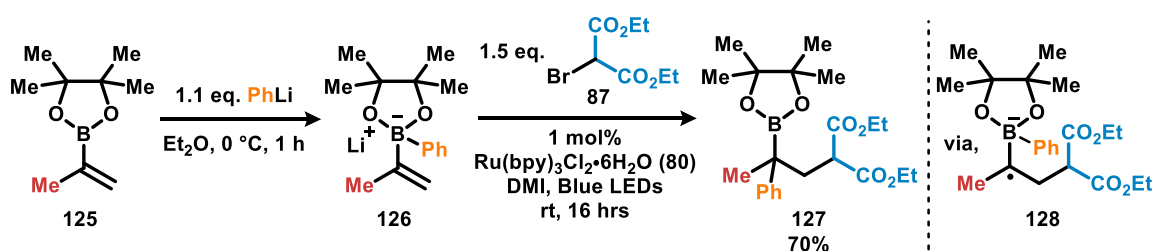
Scheme 2-15. Ruthenium complex **80**-catalysed trifluoromethylation-arylation of styrene (**116**).

In addition to new forms of reactivity being enabled by PRC, the field has also contributed to the improvement of previously well-studied synthetic protocols. In 2015, König and co-workers reported a formyloxylation-arylation of styrenes by a photo-Meerwein arylation (Scheme 2-16).¹⁰⁸ Aryl diazonium salts (**122**) possess very low reduction potentials, as such their reduction by photoexcited **80** is trivial, and yields oxidised **80** and aryl radical.¹⁰⁹ The newly generated aryl radical adds to a styrene (**116**) to give a benzylic radical species that is oxidised to a carbenium ion intermediate by the oxidised form of ruthenium complex **80** (that was formed during aryl radical generation). The aryl-stabilised carbenium ion is quenched by the carbonyl of DMF to generate an iminium intermediate (**124**), which is hydrolysed to give the formyloxylation-arylation product (**123**).



Scheme 2-16. Dormyloxylation-arylation of styrene (**116**) by photo-Meerwein arylation.

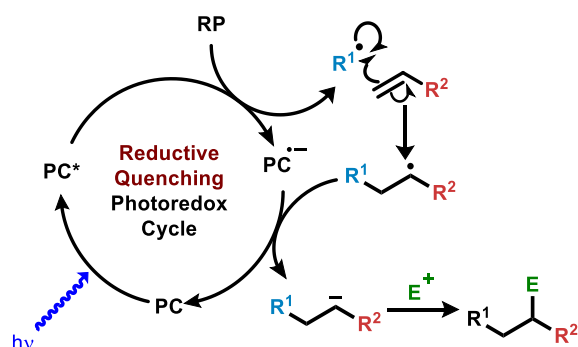
Finally, in 2017 Aggarwal and co-workers developed protocol for a general method of forming two carbon-carbon single bonds across vinyl boronate esters (Scheme 2-17).¹¹⁰ This methodology begins with the union of a lithiated hydrocarbon with a vinyl boronic ester (**125**) to form an intermediary boronate complex (**126**). A solvent switch is performed and boronate **126** is exposed to photocatalyst **80** and an α -bromo ketone (**87**). Scheme 2-17 proceeds by reduction of bromo malonate **87** by photoexcited **80** to yield electrophilic α -malonyl radicals, which add to the electron rich olefin of vinyl borate **126** forming a radical anion species (**128**). The oxidised form of the photocatalyst **80** (generated in α -malonyl radical formation) oxidises radical anion **128** to form an ylide that undergoes 1,2-metalate rearrangement to the desired difunctionalised product (**127**). In some cases, this protocol was found to occur by a radical chain mechanism, that initiates by photolysis of iodoacetophenones and is propagated by electron transfer from intermediary radical anion **128** to iodoacetophenones.¹¹¹



Scheme 2-17. Ruthenium complex **80**-catalysed alkyl-arylation of vinyl boronic ester (**125**) by 1,2-metalate rearrangement.

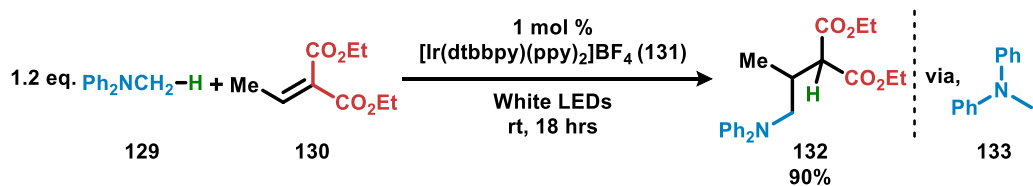
2.2.2 Alkene Difunctionalisation by Reductive-Termination Radical-Polar Crossover

For the functionalisation of an alkene to occur by reductive-termination radical-polar crossover, the PC must partake in a reductive quenching photoredox cycle. In this mechanism a carbanion is formed by reduction of a radical in the final redox process of the photoredox cycle (Scheme 2-18). Contrary to oxidative-termination radical-polar crossover, the requirement placed upon the PC is that it must first perform an oxidation followed by a reduction, hence judicious selection of radical precursors and PC must be undertaken (vide infra).



Scheme 2-18. General mechanistic depiction of an alkene difunctionalisation by reductive-termination radical-polar crossover. Asterisk indicates photoexcited state.

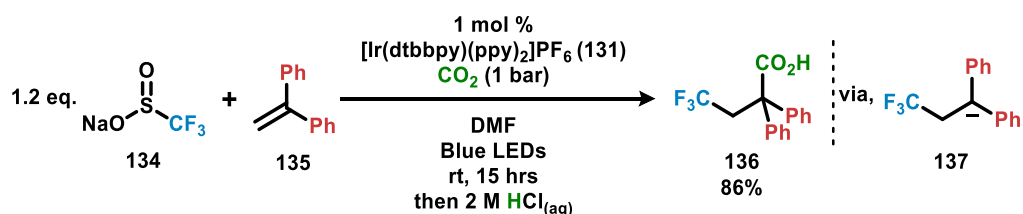
In 2012, Nishibayashi and co-workers reported the α -functionalisation of tertiary amines by PRC (Scheme 2-19).¹¹² This approach proceeds by oxidation of a tertiary amine (**129**) by photoexcited iridium catalyst **131** yielding an N-centred radical cation. The N-centred radical cation greatly destabilises the carbon-hydrogen bond α to it, resulting in its α deprotonation by another separate tertiary amine (**129**) and concurrent 1,2-electron transfer from the α -carbanion to the nitrogen radical cation, yielding an α -aminoalkyl radical (**133**).¹¹³ α -Amino radical **133** is nucleophilic in nature and adds to an electron-deficient radical acceptor, such as methylene malonate **130** to form α -malonyl radical. The intermediary α -malonyl radical is reduced to a carbanion (by formally reduced **131** that was generated in the oxidation of tertiary amine (**129**)), which closes the catalytic cycle. The enolate of **132** is protonated by diphenylmethylammonium formed during α -amino radical **133** generation, yielding the intended product **132**.



Scheme 2-19. Iridium complex **131**-catalysed α -alkylation of tertiary amine **129** with olefin **130**.

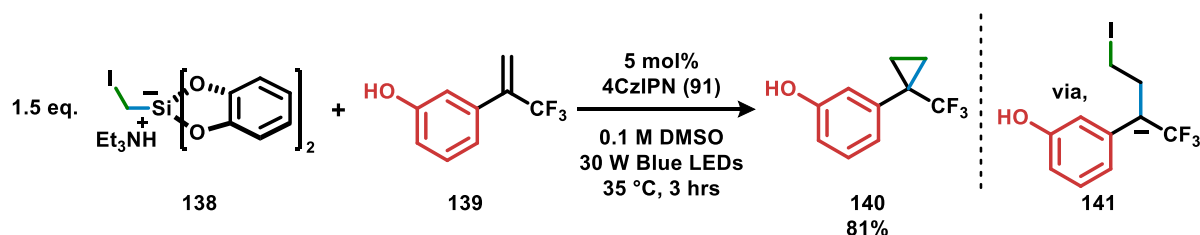
A vast majority of reported accounts of alkene functionalisations by PRC mediated reductive-termination radical-polar crossover start with formation of a nucleophilic radical, by oxidation of a radical precursor. The nucleophilic radical adds to an olefin substituted with an electron-withdrawing group, such as acrylates, vinyl ketones, α,β -unsaturated malonates or acrylonitriles. This yields an intermediary radical adjacent to an electron-withdrawing stabilising group, which is reduced by the formally reduced form of the photocatalyst to a stabilised carbanion. At this point the enolate-type product of PRC is typically protonated, like in Scheme 2-19. Although a variety of fascinating synthetic methodologies have been built around this concept, it does only deliver a monofunctionalisation of an olefin,^{112,114} a fact that is emphasised when compared to the diversity of difunctionalisations of alkenes by oxidative-termination radical-polar crossover. Therefore, recent academic attention has been directed at the difunctionalisation of olefins by reductive-termination radical-polar crossover, in which the carbanion product of PRC is not simply protonated but instead used in another carbon-carbon bond-forming process (*vide infra*).

The first reported difunctionalisation of an alkene by photoredox catalysis mediated reductive-termination radical-polar crossover was by Martin and co-workers in 2017, who disclosed the trifluoromethylation-carboxylation of styrenes (Scheme 2-20).¹¹⁵ Scheme 2-20 proceeds by oxidation of Langlois reagent (**134**) by reduction of photoexcited iridium photocatalyst **131**. Upon oxidation Langlois reagent (**134**) decomposes to sulfur dioxide and trifluoromethyl radical, which adds to alkene **135** yielding benzhydrylic-stabilised C-centred radical. The benzhydrylic-stabilised radical is reduced by reduced **131** (formed in the oxidation of Langlois reagent (**134**)), giving carbanion **137** as the product of the photoredox cycle. Carbanion **137** then attacks carbon dioxide present in solution to give the carboxylate of **136**, which is protonated upon acidic work up.



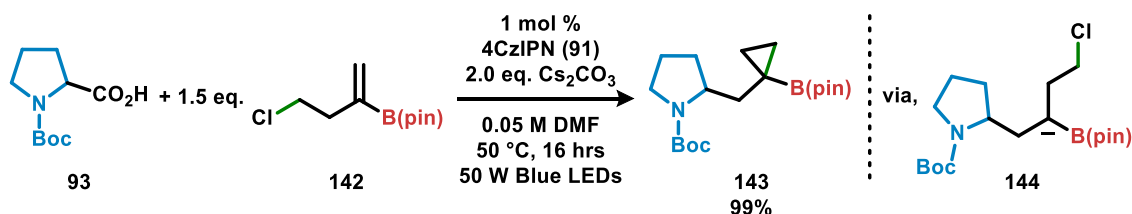
Scheme 2-20. Trifluoromethyl-carboxylation of alkene **135**.

Molander and co-workers and Aggarwal and co-workers independently disclosed methods for the cyclopropanations of olefins by reductive-termination radical-polar crossover. Molander's contribution was the development of a C₁ delivering cyclopropanation reagent (**138**), which contains an alkyl iodide and oxidisable silicate functionality (Scheme 2-21).¹¹⁶ Scheme 2-21 proceeds by oxidation of silicate **138** by photoexcited 4CzIPN (**91**), forming the radical anion of 4CzIPN (**91**) and C-centred iodomethyl radical, which adds to olefin **139** generating a benzyl radical. The intermediary benzyl radical is reduced to carbanion **141** by the radical anion of 4CzIPN (**91**) formed in the oxidation of silicate **138**. Carbanion **141** undergoes intramolecular attack of the pendent alkyl iodide to yield cyclopropane **140**.



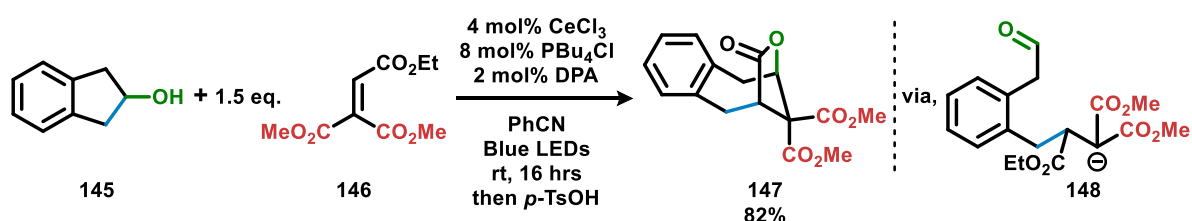
Scheme 2-21. 4CzIPN (**91**)-catalysed formal [2+1]-type cycloaddition of olefin **139** with silicate **138**.

Very soon after Molander's report the Aggarwal group independently published their own PRC-mediated cyclopropanation protocol by reductive-termination radical-polar crossover (Scheme 2-22).¹¹⁷ Aggarwal's protocol again uses 4CzIPN (**91**), but with more emphasis placed upon radical coupling then intramolecular alkylation, rather than [2+1]-type cycloaddition. Scheme 2-22 starts with deprotonation of carboxylic acid **93** by caesium carbonate to give the related caesium carboxylate, which undergoes radical decarboxylation upon oxidation by photoexcited 4CzIPN (**91**) yielding intermediary α -amino radical. The C-centred radical formed is nucleophilic in nature and adds to an electron-deficient olefin (**142**) forming a new C-centred radical species, where the radical is stabilised by an adjacent EWG. This EWG-stabilised C-centred radical is reduced by the radical anion of 4CzIPN (**91**) (formed during the oxidation of deprotonated **93**, generating carbanion **144** that performs intramolecular alkylation to yield the cyclopropane **143**. Later, Aggarwal and co-workers developed protocol for the cyclobutanation of olefins by a similar approach to Scheme 2-22 by homologating the tether between the alkyl chloride and alkene.¹¹⁸



Scheme 2-22. 4CzIPN (**91**)-catalysed decarboxylative radical-addition with subsequent cyclopropanation cascade of vinyl boronic acid **142**.

Lastly, Zuo and co-workers reported a [5+2] cycloaddition by dual catalysis (Scheme 2-23).¹¹⁹ The mechanism of Scheme 2-23 deviates from the one depicted in Scheme 2-18 as an oxidative quenching photoredox cycle occurs. Firstly, photoexcited DPA reduces radical acceptor **146** to form DPA radical cation and the radical anion of **146**. DPA radical cation oxidises cerium(III) chloride to a cerium(IV) species, which complexes to alcohol **145** through its hydroxyl. Cerium(IV) complexed **145** undergoes photolytic Ce-O cleavage forming the O-centred radical of **145** and cerium(III). The O-centred radical of **145** undergoes β -scission to form an aldehyde-containing benzyl radical, which adds to radical acceptor **146** forming α -malonyl radical. The α -malonyl radical is reduced by photoexcited DPA to give enolate **148** and DPA radical cation, which oxidises cerium(III) chloride back to a cerium(IV) species closing both catalytic cycles. Enolate **148** performs an intramolecular aldol reaction forming the related cycloheptanol structure, which is converted to lactone **147** upon addition of acid.

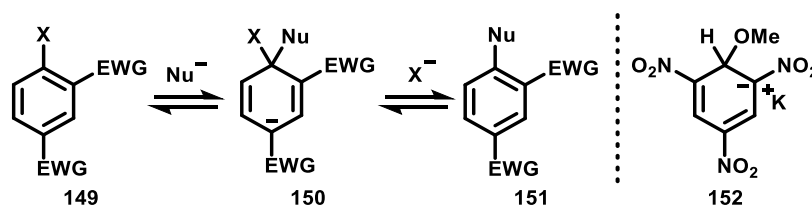


Scheme 2-23. DPA and cerium(III)-catalysed synthesis of lactone **147** by [5+2] cycloaddition.

These seminal reports of photoredox-mediated difunctionalisations of alkenes by reductive-termination radical-polar crossover from Martin, Molander, Aggarwal and Zuo, demonstrate that the carbanion product of the reductive quenching photoredox cycle can couple with carbon dioxide, alkyl halides and aldehydes.

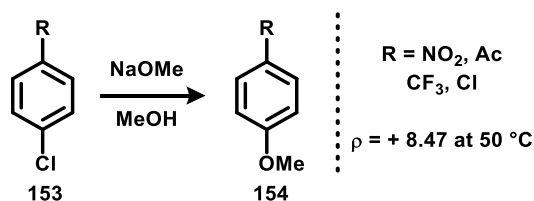
2.3 Concerted Nucleophilic Aromatic Substitutions

The nucleophilic substitution of aromatic rings (S_NAr) represents a long-studied class of reactions, which have been used in a variety of synthetic contexts.¹²⁰ The mechanism of S_NAr has long been accepted to occur in a two-step process (Scheme 2-24).¹²¹ Firstly, a nucleophile adds to an aromatic ring (**149**) substituted with one or more EWGs. The EWGs are positioned *ortho* or *para* to the site of *ipso* substitution to provide resonance stabilisation of the anionic charge introduced by the nucleophile. The anionic dearomatised adduct **150** is commonly termed the Meisenheimer intermediate, as Jakob Meisenheimer in 1901 isolated such species (**152**) when studying the S_NAr of 1,2,3-trinitrobenzenes.¹²² Once the Meisenheimer intermediate (**150**) is formed the second step of the S_NAr mechanism proceeds by ejection of an inductively electron-withdrawing leaving group, with concurrent rearomatisation to give the substituted aromatic ring (**151**). The generation and isolation of a Meisenheimer intermediate will depend on the ability of the aromatic ring's substituents to stabilise anionic charge, the nucleophilicity of the incoming nucleophile, and the nucleofugality of the leaving group.



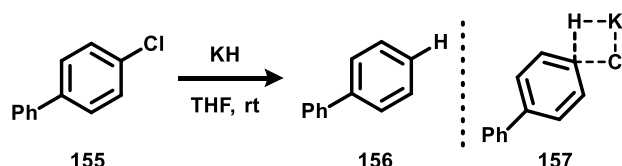
Scheme 2-24. Generalised mechanism of a two-step S_NAr . Common EWGs – $-\text{NO}_2$, $-\text{CN}$, $-\text{C}(\text{O})\text{R}$, $-\text{CF}_3$. Common X – F, Cl, Br, $-\text{OR}$.

The mechanism of two-step S_NAr reactions has been investigated through Hammett analysis by elucidation of the ρ values of such processes. Two-step S_NAr reactions are generally characterised by large and positive ρ values, indicating substantial build-up of negative charge over the rate-determining step and formation of a Meisenheimer intermediate. For example, the ρ value Miller and co-workers obtained in the conversion of *para*-functionalised aryl chlorides (**153**) to *para*-functionalised methoxybenzene by two-step S_NAr was + 8.47 (Scheme 2-25).¹²³



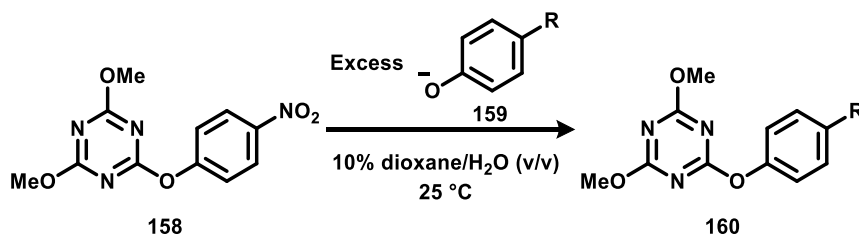
Scheme 2-25. The S_NAr reaction that was the subject of Miller's investigation through Hammett analysis.

Despite the general acceptance of the two-step S_NAr mechanism, anomalous examples appeared to not need the perceived requirements for aryl rings to be substituted with EWGs or halide leaving groups.¹²⁴ A very early example of these supposed abnormal S_NAr processes were from Pierre and co-workers in 1980, who disclosed the dehalogenation of simple electron-neutral aryl halides (**155**) with potassium hydride (Scheme 2-26).¹²⁵ By performing Scheme 2-26 in THF- d_8 and observing no deuterium incorporation into the resulting biphenyl product (**156**) a benzyne intermediate was discounted and instead S_NAr was proposed. Furthermore, the authors found that the reactivity order followed: $ArI > ArBr > ArCl > ArF$, opposite to what is observed in a two-step S_NAr process. To explain a S_NAr mechanism in the absence of substituents that could stabilise a Meisenheimer intermediate, Pierre and co-workers proposed a concerted process by a four-centred transition state (**157**). However, due to lack of computational chemistry the preceding proposition was made without any evidence. Instead Tuttle, Murphy and co-workers later validated Pierre and co-workers' claim that Scheme 2-26 proceeds by a concerted S_NAr (cS_NAr) through DFT computation.¹²⁶



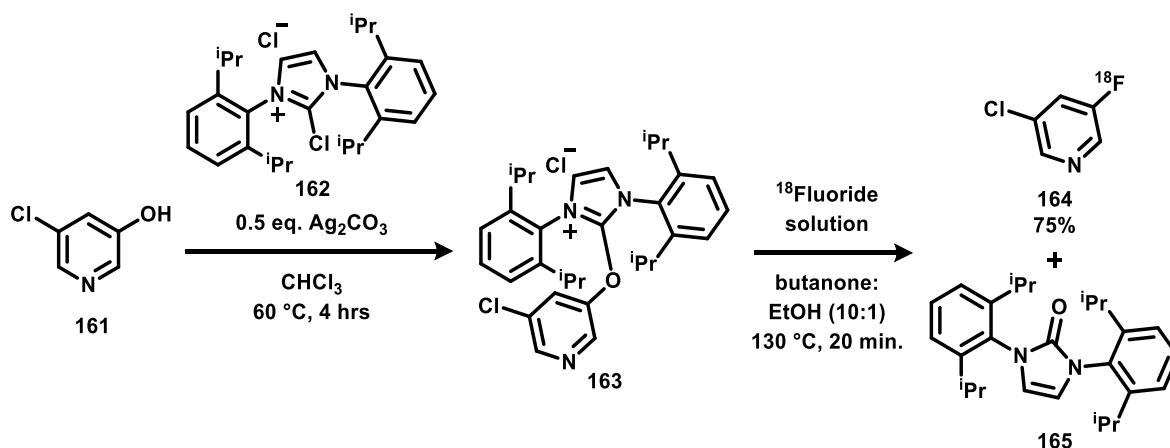
Scheme 2-26. Proto-dehalogenation of aryl chloride **155** by a cS_NAr mechanism.

In 1993 and 1995, Williams and co-workers reported a variety of S_NAr reactions of 1,3,5-triazines (**158**), which involved the exchange of 4-nitrophenol with various phenolate ions (**159**) to form new 1,3,5-triazines (**160**) (Scheme 2-27).¹²⁷ It was found that when the pK_{ArOH} of the substituting phenolate ions (**159**) were incorporated into a Brønsted plot a linear relationship was observed, which suggests no change in mechanism across the phenolate ions used and is consistent with a concerted mechanism. Williams and co-workers also performed Hammett analysis of the S_NAr of 1,3,5-triazine cores substituted with pyridine and aryloxy leaving groups in aminolysis reactions, obtaining ρ values of + 1.65 and + 0.82 when morpholine and *N,N*-dimethylaminopyridine were used respectively as the substituting nucleophiles. These ρ values are considerably less positive than values related to typical two-step S_NAr processes (Scheme 2-25).



Scheme 2-27. Substitution of 1,3,5-triazines (**158**) with phenolate ions (**159**) for Brønsted plot analysis.

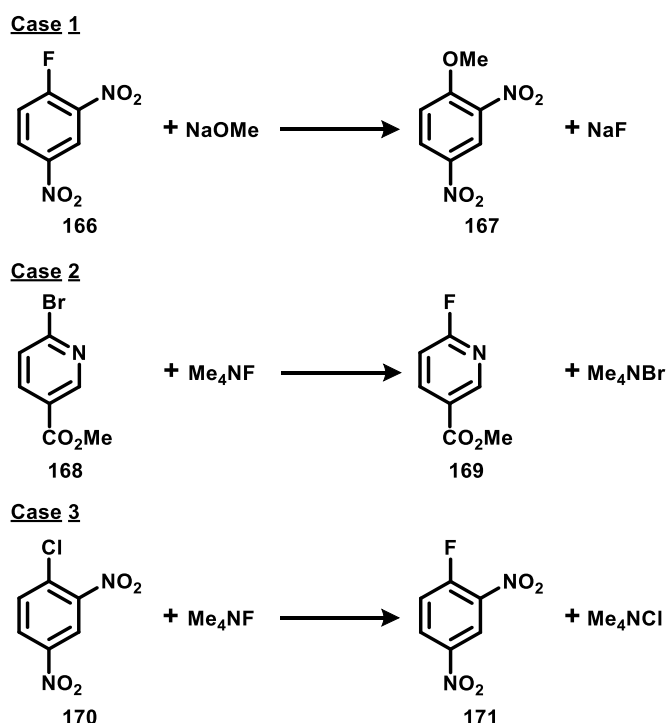
A series of seminal modern acknowledgements and investigations of cS_NAr were carried out by Ritter and co-workers.¹²⁸ Who in 2016 developed a two-step fluorodeoxygenation protocol of phenols by cS_NAr (Scheme 2-28) to chemically install fluorine-18 for application in positron emission tomography.¹²⁹ Scheme 2-28 proceeds by phenol **161** activation from NHC **162** to form the adduct **163**, which is substituted with fluoride to give the aryl fluoride **164** and the urea **165**. Hammett analysis was performed on *para*-substituted phenols for the second step of Scheme 2-28 at 110 °C yielding a ρ value of +1.79, suggesting that a carbanion does not fully develop at the transition state. It was proposed that with Scheme 2-28 proceeding by cS_NAr this would avoid the formation of high energy intermediates on route to a Meisenheimer intermediate, allowing more general reactivity with respect to the electronics of the phenol undergoing substitution compared to if a two-step S_NAr was in operation.



Scheme 2-28. cS_NAr fluorodeoxygenation sequence of phenol **161** by activation from NHC **162**.

Although historically Hammett analysis and ρ value elucidation has been a popular approach to ascertaining whether a S_NAr reaction proceeds in a two-step or concerted fashion, this method can be misleading. Firstly, there are no well-established reference ρ values for cS_NAr reactions. Also, the Hammett slope is temperature-dependent and so comparison of ρ values from different systems conducted at different temperatures is incorrect. Furthermore, during Hammett analysis a transition from a stepwise mechanism to a concerted mechanism may occur over a range of substituents, which have similar ρ values and so hide the transition. These shortcomings were highlighted by Rohrbach, Murphy and Tuttle, who in response developed a computational model to identify changes in mechanism of a S_NAr reaction of aryl fluorides over a range of substituents, by using the electron affinity of the aryl undergoing substitution as an indicator.¹³⁰

The precedent established for the existence of cS_NAr -centred transformations by Pierre,¹²⁵ Williams¹²⁷ and others,¹³¹ followed by Ritter's reintroduction of cS_NAr to the modern synthetic community,^{128,129} led to a seminal investigation by Jacobsen and co-workers.¹³² The aim of the investigation was to uncover the degree of contribution S_NAr reactions operate in a stepwise or concerted manner, by probing three S_NAr reactions (Scheme 2-29). 1) The methoxylation of nitro-substituted aryl fluoride **166** to give aryl methoxy **167**. 2) The fluorination of bromopyridine **168** to give fluoropyridine **169**. 3) The fluorination of nitro-substituted aryl chloride **170** to give aryl fluoride **171**. These three S_NAr examples were selected, as case 1 represents a S_NAr reaction that goes by the classic two-step mechanism. Case 2 exemplifies a S_NAr reaction that proceeds by a concerted process. Finally, case 3 is an example that is in between the classic two-step and concerted mechanisms for S_NAr , as the nitro substituents of **170** provide anion stabilisation, but the chloride leaving group kinetically destabilises formation of a Meisenheimer intermediate.

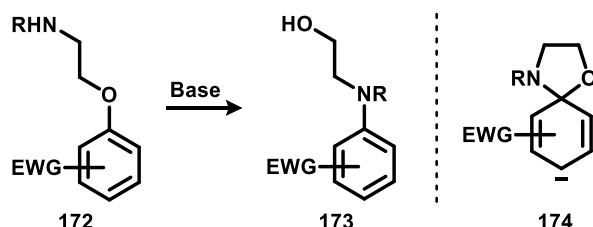


Scheme 2-29. The three S_NAr scenarios studied by Jacobsen and co-workers, representing mechanisms that are a two-step S_NAr , concerted S_NAr and a borderline case.

The experimental method Jacobsen and co-workers used to probe the three scenarios of scheme 2-29 was by indirect measurement of the $^{13}\text{C}/^{12}\text{C}$ kinetic isotope effect (KIE) in the breaking or forming of carbon fluorine bonds, by quantification of the ^{13}C – ^{19}F satellites to the ^{12}C – ^{19}F peak. The maximum KIE observed for any reaction is when the bonds to both the nucleophile and electrophile are weakest in the transition state. Therefore, comparison of experimental KIE measurements against computed maximum KIE values indicates whether a stepwise or concerted $\text{S}_{\text{N}}\text{Ar}$ manifold is present. A two-step mechanism where each bond is altered in succession leads to a small KIE, while a concerted mechanism in which both bonds change simultaneously gives rise to a large KIE. This method demonstrates good agreement with the three cases of Scheme 2-29, with case 1 giving an experimental KIE 47% of the maximum theoretical KIE indicating a two-step mechanism. Case 2 yielded a KIE value that was 87% of the maximum theoretical KIE pointing to a concerted mechanism. Finally, case 3 proceeds by a mechanism in between the extremes of the two-step and concerted mechanisms, with a KIE measurement that is 73% of the maximum theoretical KIE. The most striking finding of Jacobsen and co-workers' investigation was that when their study was extended to 120 other $\text{S}_{\text{N}}\text{Ar}$ reactions, their experimentally determined and computationally obtained KIE values indicated that 99 of the examples proceeded by a concerted mechanism. This seminal result took $\text{cS}_{\text{N}}\text{Ar}$ from being a mechanistic rarity into general acceptance by the synthetic community, allowing the discovery of new methodologies and further understanding of previously developed reactions.^{124,131a,133}

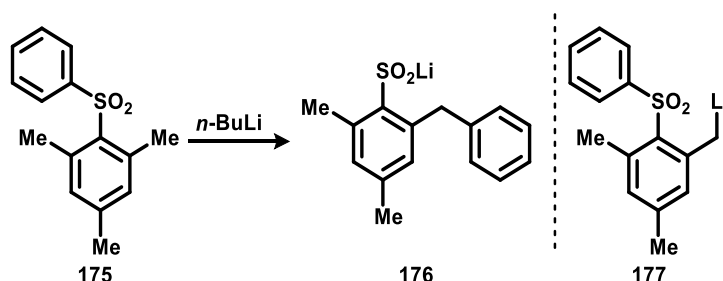
2.4 The Truce-Smiles Rearrangement of α -Metalated Ureas

The first documented report of the Smiles rearrangement was carried out by Henriques in 1894,¹³⁴ with follow up reports by Hinsberg.¹³⁵ However, it was not until the 1930's where the synthetic utility of the Smiles rearrangement was realised by Smiles.¹³⁶ The Smiles rearrangement represents an intramolecular S_NAr between two heteroatoms (alkoxyl aryl **172** to alkyl aniline **173**). Like the classic two-step S_NAr mechanism (Scheme 2-24) the Smiles rearrangement typically requires the migrating aryl group to be furnished with EWGs to lower the activation energy barrier towards accessing the Meisenheimer intermediate (**174**) (Scheme 2-30). In the Smiles rearrangement the collapse of the Meisenheimer intermediate (**174**) is thought to be the rate-determining step of this transformation.¹³⁷ The kinetics of the Smiles rearrangement are dependent on the nucleophilicity of the incoming heteroatom, the nucleofugality of the leaving heteroatom, the degree of activation of the aryl ring undergoing *ipso* substitution, the length of the tether connecting the two hetero-atoms and if substitution on the tether incurs the Thorpe-Ingold effect.¹³⁸



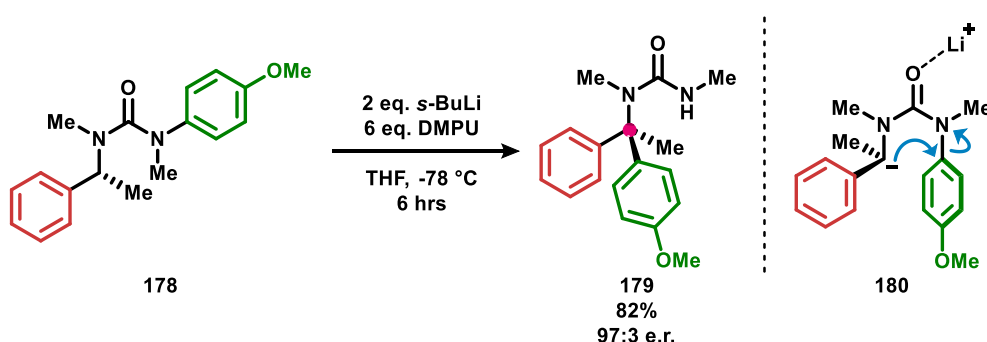
Scheme 2-30. The Smiles rearrangement.

Later, Truce found that carbanions (**177**) were sufficiently nucleophilic to lift the requirement for EWGs on the aryl ring experiencing *ipso* substitution (sulfonyldiaryl **175** to sulfinate **176**) (Scheme 2-31).¹³⁹ The application of a Smiles rearrangement involving the use of a carbanion is termed the Truce-Smiles rearrangement. The Smiles rearrangement and the Truce-Smiles rearrangement have both enjoyed much application over the past 50 years in a variety of synthetic scenarios, in the form of polar,¹⁴⁰ radical¹⁴¹ and transition-metal-catalysed processes.¹⁴²



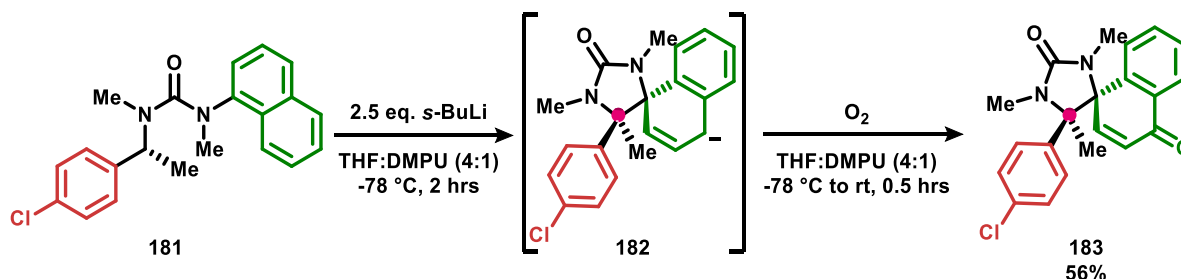
Scheme 2-31. The first reported Truce-Smiles rearrangement.

In 2007, while exploring the lithiation of *N*-aryl ureas, Clayden and co-workers uncovered a unique class of intramolecular aryl migrations.¹⁴³ These processes were originally performed by α C-H bond lithiation of *N*-benzyl ureas (**178**), by exposure to an alkyl lithium base and lithium coordinator DMPU. The α -lithiated *N*-benzyl urea (**180**) undergoes Truce-Smiles aryl migration to give α -tertiary ureas (**179**) (Scheme 2-32). A remarkable trait of this 1,5-aryl shift of α -lithiated *N*-benzyl ureas (**180**) was that even though this transformation proceeds by an S_NAr mechanism, the usual requirement for EWGs to be present on the aryl ring undergoing *ipso* substitution was not necessary, instead EDGs were very well tolerated. Furthermore, enantioenriched α -lithiated *N*-benzyl ureas were configurationally stable on the timescale of the reaction, as such their aryl migration proceeded in a stereoretentive manner, allowing for the synthesis of enantioenriched α -tertiary amines upon solvolysis of the α -tertiary urea products (**179**).¹⁴⁴



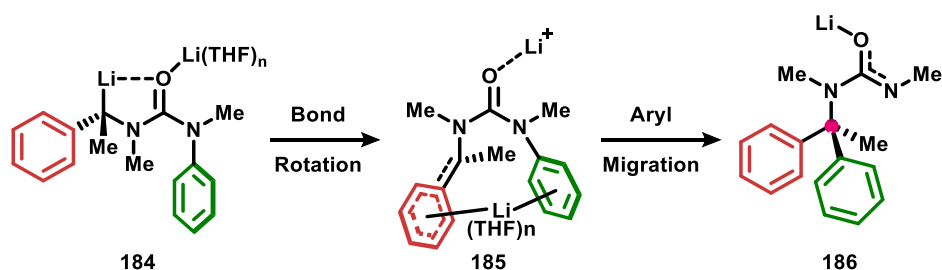
Scheme 2-32. N to C intramolecular electrophilic arylation of α -metalated urea **180**.

In Clayden and co-workers initial report of the Truce-Smiles rearrangement of α -lithiated ureas, it was not completely understood why the excellent variety of electronics for the translocating aryl ring is observed.¹⁴³ The presence of a Meisenheimer intermediate was predicated on the isolation of enone **183**, by performing the Truce-Smiles rearrangement of urea **181** under aerobic conditions. It is presumed that enone **183** is formed by oxidation of the Meisenheimer intermediate **182**. However, as this study was performed a decade earlier than Jacobsen and co-workers' seminal investigation into cS_NAr ,¹³² such a manifold was not suggested for the N to C aryl migration of α -lithiated ureas.



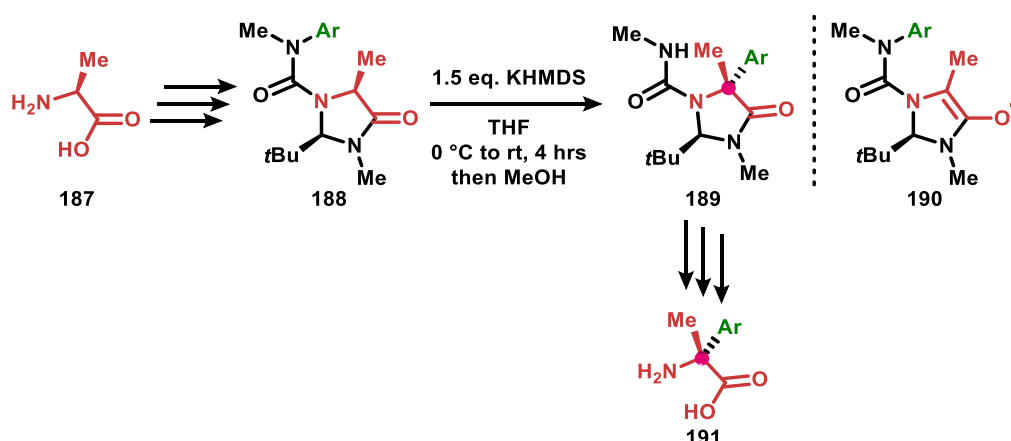
Scheme 2-33. Evidence for a Meisenheimer intermediate during the Truce-Smiles rearrangement of α -metalated urea **182**.

In 2015 a more in-depth mechanistic study of the Truce-Smiles rearrangement of α -lithiated ureas was carried out by Clayden and co-workers using DFT computation.¹⁴⁵ It was found that *N*-aryl ureas exhibit a strong conformational bias for the aryl to be positioned *anti* to the urea carbonyl, to avoid an unfavourable stereo-electronic clash between the aryl π -system and lone pairs of the urea carbonyl, a concept observed in other studies.¹⁴⁶ Next, it was suggested that after α C-H lithiation, the α -lithiated urea adopts the conformation **184**, orienting the benzyllithium *s-cis* to the ureido carbonyl to offer a stabilising interdipolar interaction, which presumably attenuates racemisation of the benzylic position (Scheme 2-34). For aryl translocation to occur the urea carbonyl dipole interaction with the benzyllithium must break, allowing the benzylic group to occupy an *anti*-conformation to the urea carbonyl (**185**). When the α -lithiated urea adopts the conformation **185** both the *N*-aryl and benzyllithium are *anti* to the urea carbonyl, and so are in very close proximity to each other. This is likely the origin of the rate acceleration of the anionic arylation, compared to if such reactions were attempted in an intermolecular fashion. Finally, Truce-Smiles rearrangement of intermediate **185** proceeds to give α -tertiary urea **186**.



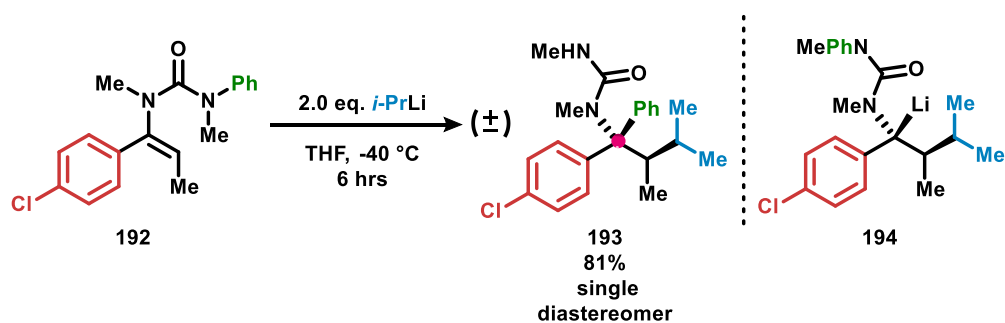
Scheme 2-34. Computed intermediates in the N to C aryl migration of α -lithiated urea **184**.

The degree of stepwise or concerted contribution in the Truce-Smiles rearrangement of α -metalated ureas was first acknowledged and investigated by Clayden and co-workers in 2018,¹⁴⁷ soon after Jacobsen and co-workers study of the cS_NAr mechanism.¹³² In this report Clayden and co-workers disclosed a method for the preparation of enantiopure quaternary amino acids by N to C aryl migration of ureas (Scheme 2-35). This protocol relied on Seebach's concept of Self-Regeneration of Stereocentres,¹⁴⁸ where enantiopure amino acids (**187**) were used to form imidazolidin-4-ones (**188**) that contain a new aminal stereocentre defined by the chirality of the amino acid starting material. Formation of enolate **190** destroys the original source of chirality of the amino acid starting material, however the aminal stereocentre is preserved and controls the stereochemistry of the proceeding Truce-Smiles rearrangement. Like benzylic carbanions, enolates had been previously shown to be viable nucleophiles in the N to C aryl migration of ureas.¹⁴⁹ As such, enolate **190** converts to α -tertiary urea **189** by *anti*-arylation to the aminal stereocentre. Through methylation then hydrolysis of α -tertiary urea **189** the free quaternary amino acid (**191**) is yielded. A ρ value of + 4.5 was obtained at a reaction temperature of $-20\text{ }^{\circ}\text{C}$ by Hammett analysis of the Truce-Smiles rearrangement of enolate **190**, indicating a significant build-up of charge occurring at the transition state, but not full development of a Meisenheimer intermediate.



Scheme 2-35. Preparation of enantiopure quaternary amino acids (**191**) by merging the Truce-Smiles rearrangement of ureas with Seebach's concept of Self-Regeneration of Stereocentres.

In addition to initiating the N to C aryl migration of α -metallated ureas by deprotonation, Clayden and co-workers also reported the carbolithiation of vinyl ureas (**192**) as a second method.¹⁵⁰ Remarkably, it was found that vinyl ureas (**192**) engage in umpolung chemistry, where organolithiums add to the more nucleophilic β -carbon yielding α -lithiated *N*-benzyl ureas (**194**) that undergo 1,5-aryl shift to give β -alkylated- α -arylated α -tertiary ureas (**193**). Due to carbolithiation proceeding *syn*, concurrently yielding configurationally stable α -lithiated *N*-benzyl urea (**194**), the products of this alkyl-arylation difunctionalisation are obtained as a single diastereomer. Later, asymmetric variants of the carbolithiation of vinyl ureas (**192**) were developed by use of (–)-sparteine or (+)-sparteine surrogate to generate enantioenriched α -lithiated *N*-benzyl ureas.¹⁵¹

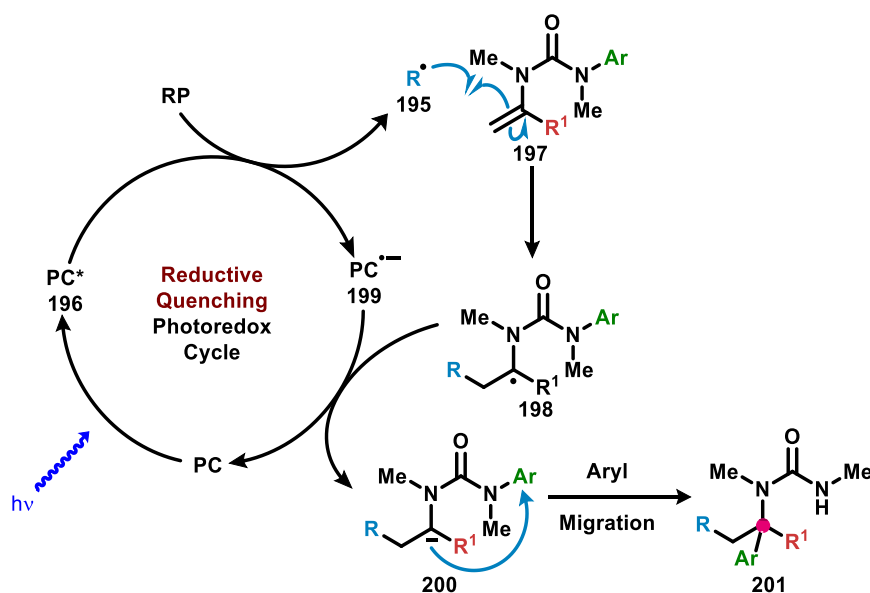


Scheme 2-36. N to C intramolecular electrophilic arylation of metalated urea **194** by carbolithiation of vinyl urea **192**.

3. Results and Discussion

3.1 Project Aims

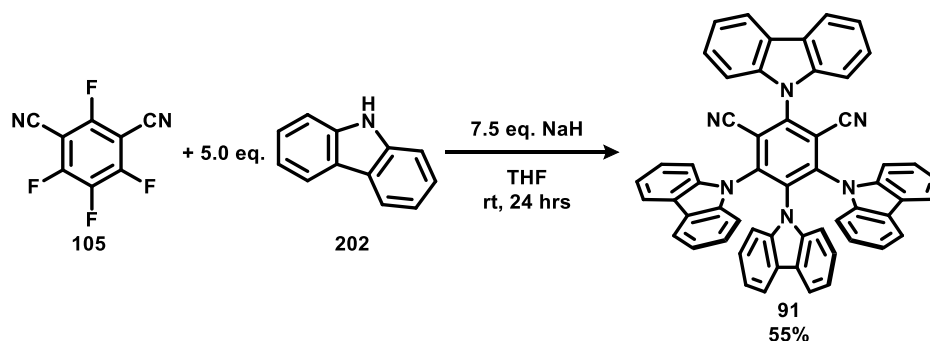
It was intended to develop protocol for the addition of radicals (**195**), generated by reduction of an excited photocatalyst (**196**), to vinyl urea (**197**) (Scheme 3-1). The preceding process would yield intermediary ureido benzyl radical (**198**) that could be reduced by the radical anion of the photocatalyst (**199**), to give α -metalated urea (**200**) that undergoes N to C intramolecular arylation across the urea, yielding α -tertiary urea (**201**). If Scheme 3-1 came to fruition this would represent the first example of a photoredox-catalysed reductive-termination radical polar crossover where the intermediary carbanion product engages in carbon-aryl bond formation. Furthermore, a photoredox mediated intramolecular electrophilic arylation of α -metalated ureas could provide a useful method for the construction of α -tertiary amines. Furthermore, it was intended that to make the transformation of vinyl urea **197** to α -tertiary urea **201** as procedurally simple as possible, cheap and easily accessible photocatalysts 4CzIPN (**91**) and 3DPAFIPN (**106**) would be investigated.



Scheme 3-1. A design plan to perform the intramolecular electrophilic arylation of vinyl urea (**197**), by use of a generic PC and generic radical precursor (RP). Asterisks denotes photoexcited state.

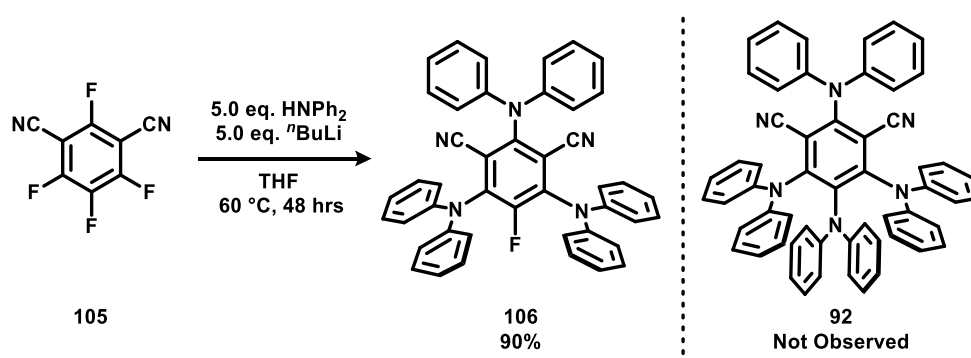
3.2 Reaction Discovery and Optimisation

Firstly, work was undertaken to reproduce the results of Zhang and Luo for the preparation of PCs 4CzIPN (**91**) and 4DPAIPN (**92**). 4CzIPN (**91**) was successfully synthesised by fourfold- S_NAr upon tetrafluoroisophthalonitrile (**105**) with carbazole (**202**) by following literature protocol (Scheme 3-2).⁹⁴ It is noteworthy that the reported cost to synthesise 4CzIPN (**91**) is ~£5/g and no chromatography was required, highlighting its accessibility over the polypyridyl complexes of ruthenium and iridium.⁹⁴



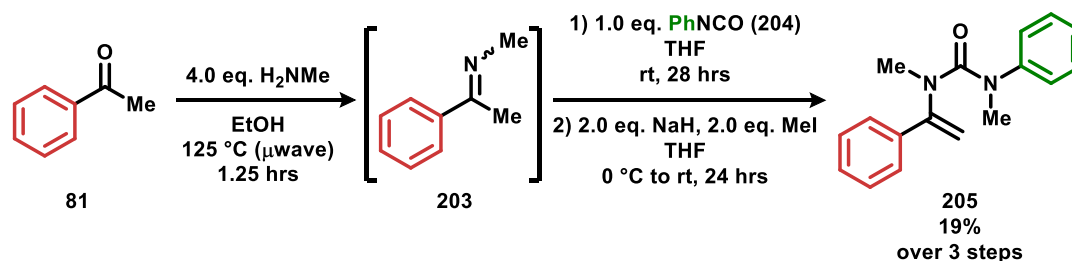
Scheme 3-2. Synthesis of 4CzIPN (**91**).

Attempted synthesis of 4DPAIPN (**92**) by fourfold- S_NAr upon tetrafluoroisophthalonitrile (**105**) with diphenylamine did not give the intended product, but instead photocatalyst 3DPAFIPN (**106**) by threefold- S_NAr (Scheme 3-3). The formation of 3DPAFIPN (**106**) over 4DPAIPN (**92**), even under extended reaction times and elevated temperatures compared to Zhang and Luo's procedure,⁹⁴ gives further support to Zeitler and co-workers claim that 3DPAFIPN (**106**) has been mis-assigned as 4DPAIPN (**92**) (Scheme 2-10).^{97a} However, the use of 3DPAFIPN (**106**) over 4DPAIPN (**91**) is inconsequential to this project, as their redox potentials from the ground state and photoexcited state are similar.



Scheme 3-3. Attempted synthesis of 4DPAIPN (**92**), which yielded 3DPAFIPN (**106**) instead.

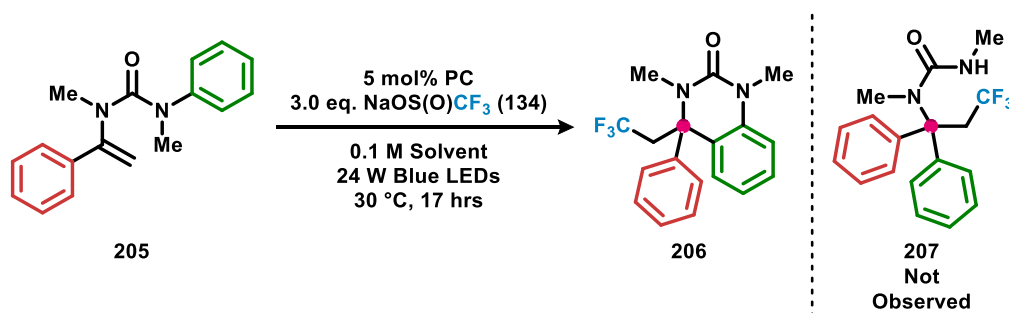
With photocatalysts 4CzIPN (**91**) and 3DPAFIPN (**106**) in hand, work was directed towards the synthesis of vinyl urea **205**, which was selected as a model substrate for initial optimisation studies. Vinyl urea **205** was synthesised by imine condensation between acetophenone (**81**) and methylamine to give imine **203** (Scheme 3-4). Imine **203** was used crude and coupled with phenyl isocyanate (**204**); subsequent one-pot methylation at the carbamoyl nitrogen with methyl iodide gave the desired vinyl urea **205**.¹⁵²



Scheme 3-4. Synthesis of vinyl urea **205**.

Initial forays to achieve a photoredox-mediated intramolecular electrophilic arylation of vinyl urea **205** were performed using photocatalysts 4CzIPN (**91**) and 3DPAFIPN (**106**). Langlois reagent (**134**) was selected as a commercially available radical precursor that upon SET oxidation decomposes to yield sulfur dioxide and trifluoromethyl radical.¹⁵³ Trifluoromethyl radical is well documented in adding to electron-rich olefins such as enamides, giving confidence that it would engage in addition to a vinyl urea.¹⁵⁴ Furthermore, Langlois reagent (**134**) possesses an oxidation potential ($E_{1/2} = 1.05 \text{ V vs SCE}$)¹⁵⁵ of smaller magnitude than that of photoexcited photocatalysts 4CzIPN (**91**) ($E_{1/2} (P^*/P^-) = 1.35 \text{ V vs SCE}$) and 3DPAFIPN (**106**) ($E_{1/2} (P^*/P^-) = 1.09 \text{ V vs SCE}$), giving confidence they will be able to facilitate trifluoromethyl radical generation.⁹⁴

Unexpectedly, initial attempts at the photoredox-mediated intramolecular electrophilic arylation of vinyl urea **205** yielded the 3,4-dihydroquinazolinone **206** and not the intended α -tertiary urea **207** (Table 3-1). Use of 4CzIPN (**91**) (Table 3-1, entries 1-3) over 3DPAFIPN (**106**) (Table 3-1, entries 4 and 5) gave greater productivity for the formation of 3,4-dihydroquinazolinone **206**, which may imply 3DPAFIPN (**106**) is too slow to oxidise Langlois reagent (**134**) under the reaction conditions. With 4CzIPN (**91**) superior yields were observed when DMF was used as solvent over DMSO and THF in the conversion of vinyl urea **205** to 3,4-dihydroquinazolinone **206**.

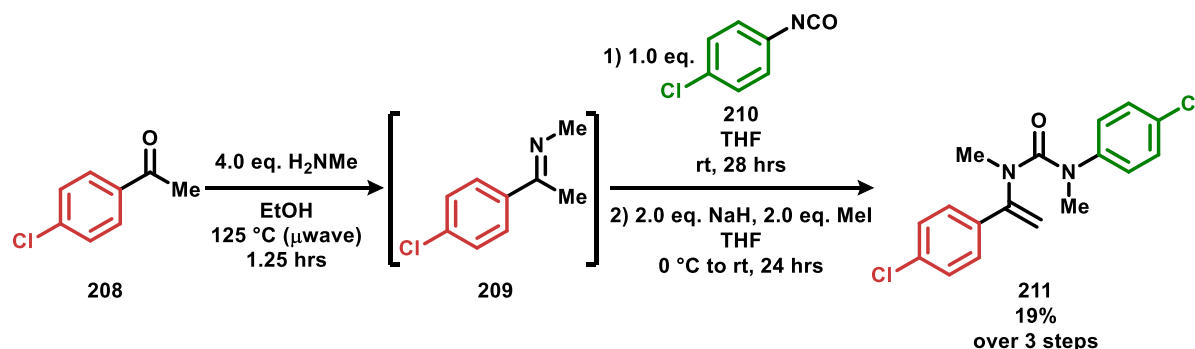


Entry	Photocatalyst	Solvent	206 / % ^[a]
1	4CzIPN (91)	DMF	58 ^[b]
2	4CzIPN (91)	THF	12
3	4CzIPN (91)	DMSO	49
4	3DPAFIPN (106)	DMF	2
5	3DPAFIPN (106)	THF	9

Table 3-1. Initial attempts at the photoredox mediated intramolecular electrophilic arylation of vinyl urea **205**. [a] Yields obtained by ¹⁹F NMR and compared with benzotrifluoride internal standard. [b] Isolated yield.

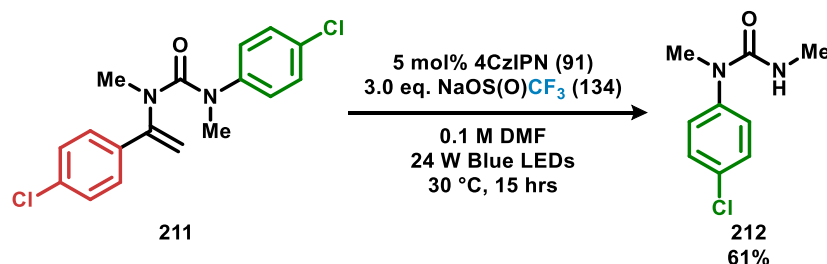
The formation of 3,4-dihydroquinazolinone **206** (Table 3-1), although not the intended product (**207**), does impart some key information. Firstly, under certain conditions 4CzIPN (**91**) can oxidise Langlois reagent (**134**) for trifluoromethyl radical generation. Secondly, the trifluoromethyl radicals formed in situ can add to the olefin of a vinyl urea. It should be highlighted that formation of 3,4-dihydroquinazolinone **206** from vinyl urea **205** is a net-oxidative process, so an unintentional oxidant must be present. As stringent exclusion of oxygen was performed, sulfur dioxide was implicated as a non-innocent by-product of trifluoromethyl radical formation, as it demonstrates a reduction potential ($E_{1/2} = -0.7$ V vs SCE)¹⁵⁶ smaller in magnitude than that of 4CzIPN (**91**) ($E_{1/2} (P/P^-) = -1.21$ V vs SCE).⁹⁴

Condensation of 4'-chloroacetophenone (**208**) with methylamine forms imine **209**, which was subjected to isocyanate **210** and then methylated to give vinyl urea **211** (Scheme 3-5). Vinyl urea **211** was synthesised as the *N*-aryl bears a *para*-chloro substituent. Whether this *para*-chloro relationship is maintained in the 4CzIPN (**91**)-catalysed net-oxidative trifluoromethyl-arylation of vinyl urea **211** would give insight into how this reaction proceeds.



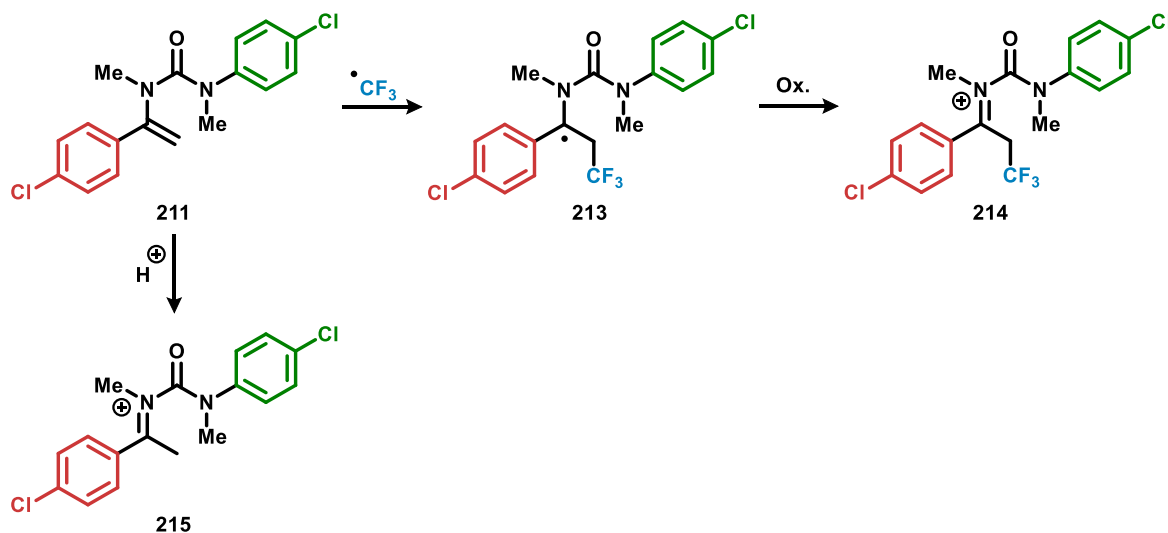
Scheme 3-5. Synthesis of vinyl urea **211**.

Irradiation of 4CzIPN (**91**) in the presence of vinyl urea **211** and Langlois reagent (**134**) in DMF gave predominantly the *N*-aryl urea **212** and a complex mixture of unidentifiable fluorinated products observable by ^{19}F NMR (Scheme 3-6). Attempts at separation of products other than *N*-aryl urea **212** failed, even by preparative TLC.



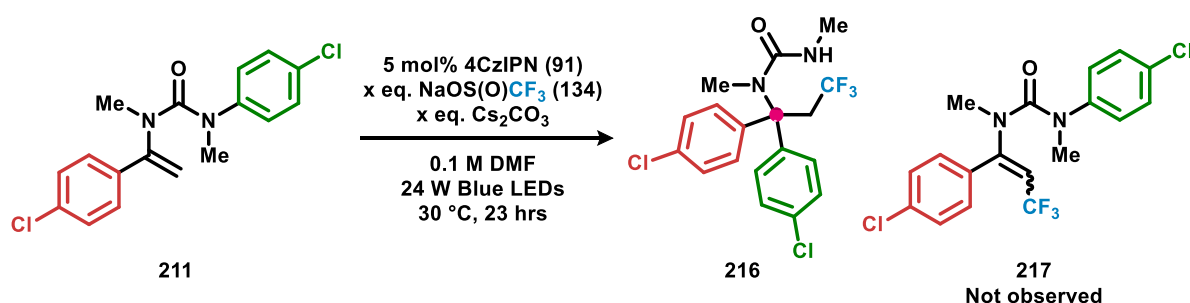
Scheme 3-6. Subjecting of vinyl urea **211** and Langlois reagent (**134**) to 4CzIPN (**91**)-catalysed photoredox conditions.

The significant production of *N*-aryl urea **212** in Scheme 3-6 presumably originates from the hydrolytic cleavage of a uronium species, generated by either PRC-enabled trifluoromethyl radical addition (**213**) then oxidation (**214**), or by acid-catalysed tautomerisation (**215**) (Scheme 3-7).¹⁵² It was hypothesised that the addition of a base to the reaction mixture of Scheme 3-6 would sequester acid by-product generated in net-oxidative processes, potentially limiting the formation of **212** by acid-catalysed tautomerisation of vinyl urea **211**.



Scheme 3-7. Proposed routes to uronium species **214** and **215**.

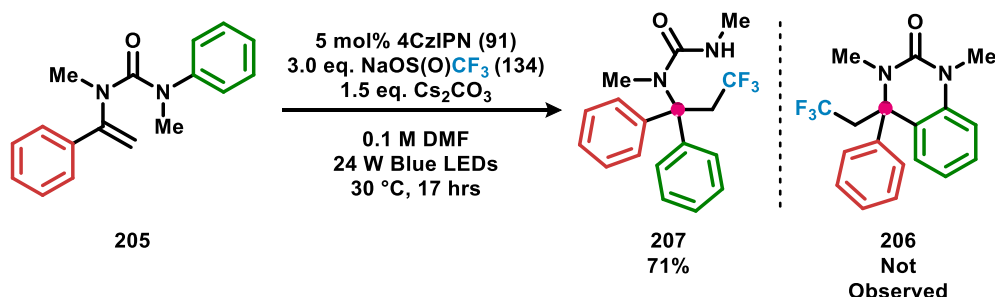
Exposure of vinyl urea **211** and Langlois reagent (**134**) to 4CzIPN (**91**) under blue LED irradiation, with the addition of caesium carbonate as a base was performed (Table 3-2). Remarkably, neither *N*-aryl urea **212** nor vinyl urea **217** were observed as products of Table 3-2, instead the originally sought α -tertiary urea **216** was isolated in moderate yield. The presence of caesium carbonate clearly has a pronounced effect on moving the mechanism of the reaction away from a net-oxidative manifold to a redox-neutral one. Reports exist of caesium carbonate displaying a direct reaction with sulfur dioxide generating caesium sulfite and carbon dioxide, however this appears to only take place at elevated temperatures (>100 °C).¹⁵⁷ Instead, under ambient conditions physisorption of sulfur dioxide onto caesium carbonate is observed. Thus, the effect of caesium carbonate to change the afforded product from *N*-aryl urea **212** to α -tertiary urea **216** may-be by in situ sequestering of sulfur dioxide, which allows 4CzIPN (**91**) radical anion to reduce benzyl radical, formed after trifluoromethyl radical addition to vinyl urea **211**, generating key α -metalated urea intermediate (**200**) for intramolecular electrophilic arylation.



Entry	134 / eq.	Cs ₂ CO ₃ / eq.	216 / % ^[a]
1	3.0	1.5	66 (53) ^[b]
2	2.0	1.5	58
3	1.0	1.0	44

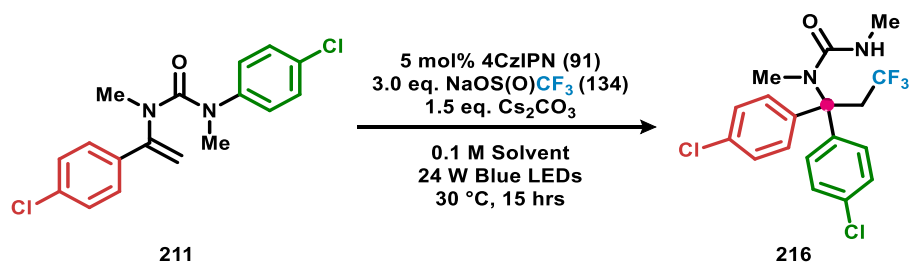
Table 3-2. Discovery of the 4CzIPN (**91**)-catalysed trifluoromethylation followed by intramolecular electrophilic arylation of vinyl urea **211**. [a] Yields obtained by ¹⁹F NMR and compared with benzotrifluoride internal standard. [b] Isolated yield.

With caesium carbonate identified as a key additive to exact the photoredox-mediated intramolecular electrophilic arylation of a vinyl urea, the reliability of this discovery was validated with vinyl urea **205** before optimisation studies were carried out. Gratifyingly, when vinyl urea **205** and Langlois reagent (**134**) were exposed to 4CzIPN (**91**) under blue LED irradiation, with the addition of caesium carbonate, the desired α -tertiary urea **207** was isolated in good yield. Also, no production of the previously afforded 3,4-dihydroquinazolinone **206** was founded (Scheme 3-8).



Scheme 3-8. The 4CzIPN (**91**) mediated trifluoromethyl-arylation of vinyl urea **205**.

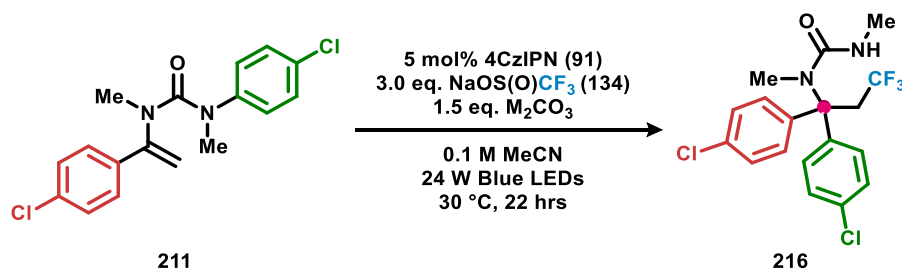
Optimisation studies were performed using vinyl urea **211** as a model substrate. A solvent screen was carried out, where vinyl urea **211** and Langlois reagent (**134**) were exposed to 4CzIPN (**91**) in a reaction mixture containing caesium carbonate (Table 3-3). Use of DMSO as the solvent gave poor productivity for α -tertiary urea **216** (Table 3-3, entry 1), while use of acetone or acetonitrile gave excellent levels of product formation (Table 3-3, entries 2 and 3). Use of benzotrifluoride, dichloromethane or 1,2-dichloroethane as solvent proved detrimental to α -tertiary urea **216** generation (Table 3-3, entries 4-6). Guided by the results of Table 3-3, acetonitrile and acetone were selected as optimum solvents.



Entry	Solvent	216 / % ^[a]
1	DMSO	36
2	MeCN	94
3	Acetone	94
4	PhCF ₃	Trace
5	DCM	Trace
6	DCE	4

Table 3-3. Solvent screen for the 4CzIPN (**91**)-catalysed trifluoromethylation intramolecular electrophilic arylation of vinyl urea **211**. [a] Yields obtained by ¹⁹F NMR and compared with benzotrifluoride internal standard.

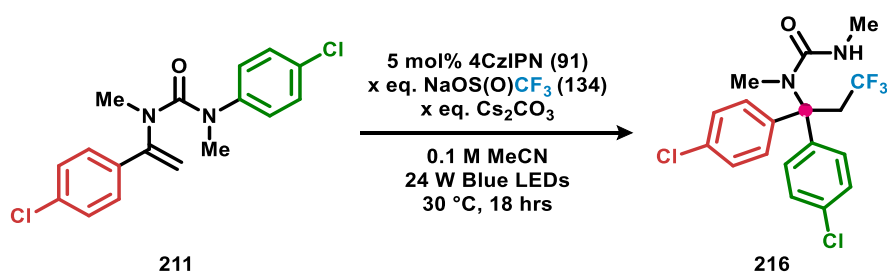
Attention was next directed at whether the cation of the carbonate used in the photoredox mediated formation of α -tertiary urea **216** had any impact upon the reaction (Table 3-4). A trend of increasing yield for α -tertiary urea **216** was observed when going down the rows of group one cationic carbonates.



Entry	M	216 / % ^[a]
1	Cs	93
2	K	79
3	Na	20
4	Li	7

Table 3-4. Carbonate screen for the 4CzIPN (**91**)-catalysed trifluoromethylation then intramolecular electrophilic arylation of vinyl urea **211**. [a] Yields obtained by ¹⁹F NMR and compared with benzotrifluoride internal standard.

Next, an investigation into the optimal stoichiometries of Langlois reagent (**134**) and caesium carbonate were performed. Firstly, productivity for α -tertiary urea **216** decreased upon lowering the stoichiometry of caesium carbonate from 1.5 to 1.0 equivalent (Table 3-5, entries 1, 3 vs 2, 4). Formation of α -tertiary urea **216** was not perturbed by lowering of the stoichiometry of Langlois reagent (**134**) from 3.0 to 1.5 equivalents (Table 3-5, entries 1, 3, 5). As such, 1.5 equivalents of Langlois reagent (**134**) and caesium carbonate were selected as optimum stoichiometries for the transformation of vinyl urea **211** to α -tertiary urea **216**. Finally, an isolated yield for α -tertiary urea **216** was recorded using the optimised conditions outlined in Table 3-5 entry 5, which proved to be in good agreement with the spectroscopic yield obtained.



Entry	134 / eq.	Cs ₂ CO ₃ / eq.	216 / % ^[a]
1	3.0	1.5	79
2	3.0	1.0	40
3	2.0	1.5	83
4	2.0	1.0	58
5	1.5	1.5	89 (87) ^[b]

Table 3-5. Langlois reagent (**134**) and caesium carbonate stoichiometry screen in the conversion of vinyl urea **211** to α -tertiary urea **216**. [a] Yields obtained by ¹⁹F NMR and compared with benzotrifluoride internal standard. [b] Isolated yield.

Optimised conditions for the 4CzIPN (**91**)-catalysed trifluoromethylation with subsequent aryl migration of vinyl urea **211** (Table 3-5, entry 5) were also applicable when acetone was used as solvent (Table 3-6, entry 1). As expected when considering Table 3-1, use of 3DPAFIPN (**106**) resulted in trace α -tertiary urea **216** formation, the same being true when ruthenium photocatalyst **80** was used (Table 3-6, entries 2 and 3). Iridium photocatalyst **90** demonstrates activity in the formation of α -tertiary urea **216** (Table 3-6, entry 4). Iridium photocatalyst **90** displays an oxidation potential from the photoexcited state of ($E_{1/2}$ (P^*/P^-) = 1.21 V vs SCE),^{86b} giving indication that the lack of activity observed with 3DPAFIPN (**106**) ($E_{1/2}$ (P^*/P^-) = 1.09 V vs SCE)^{97a} and ruthenium photocatalyst **80** ($E_{1/2}$ (P^*/P^-) = 0.77 V vs SCE)^{86b} may be due to insufficient oxidation power for trifluoromethyl radical generation from Langlois reagent (**134**) ($E_{1/2}$ = 1.05 V vs SCE).¹⁵⁵

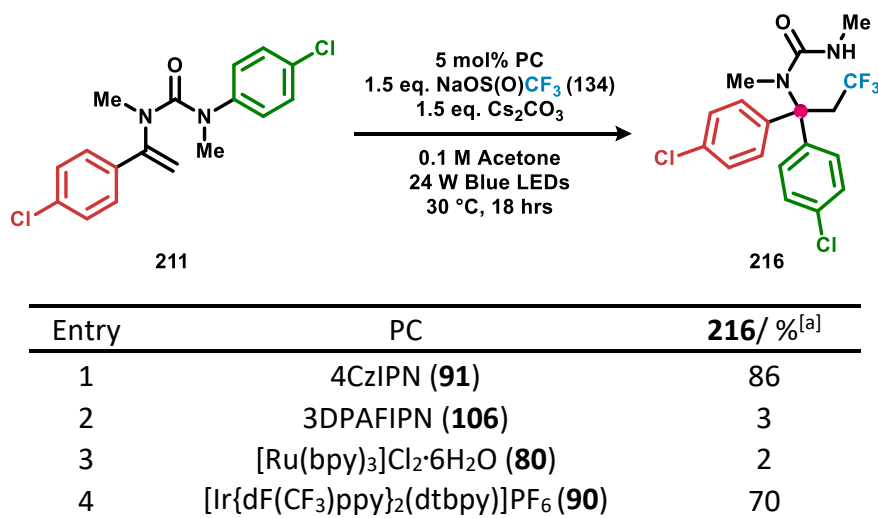
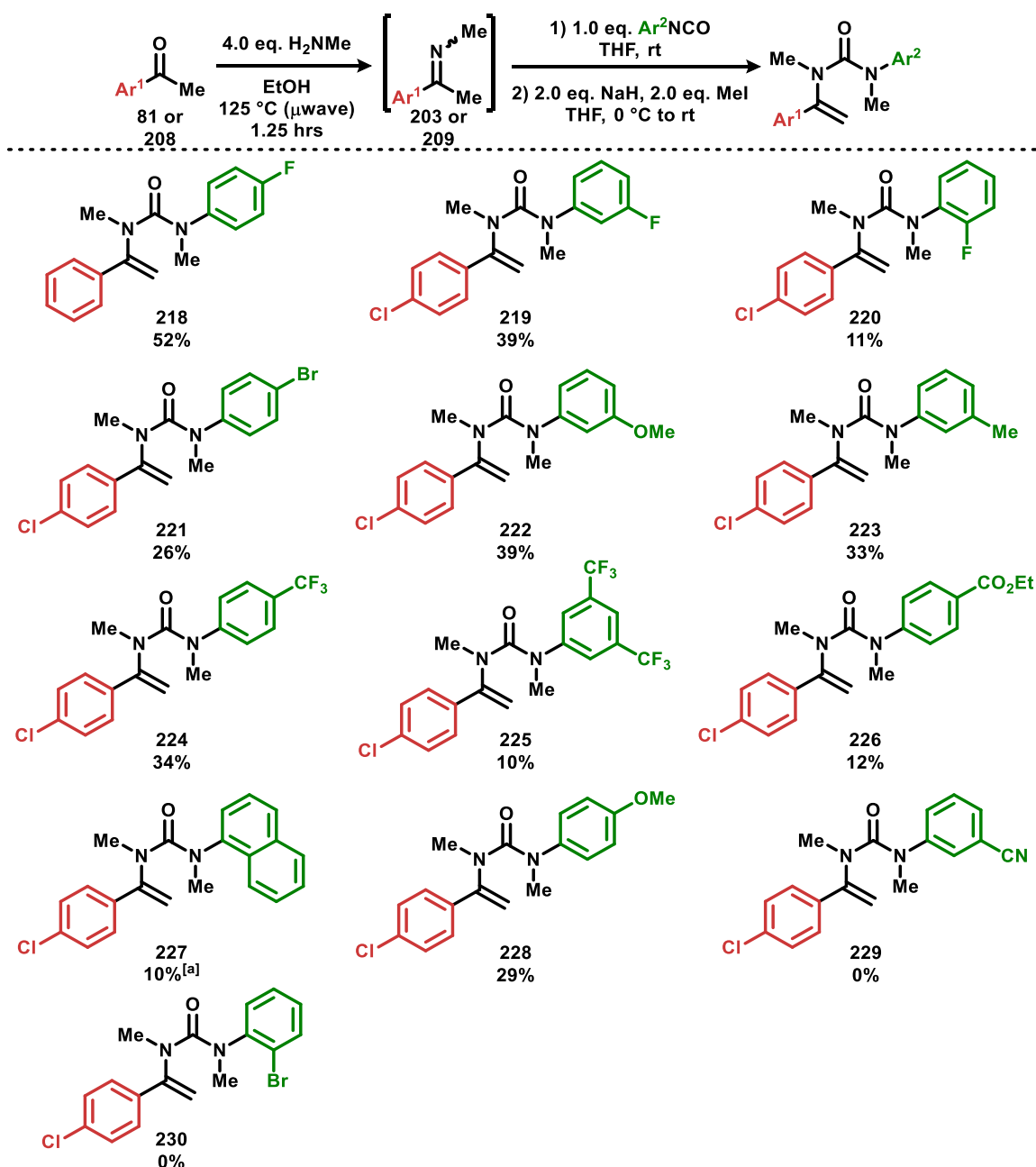


Table 3-6. Photocatalyst screen for the conversion of vinyl urea **211** to α -tertiary urea **216**.
[a] Yields obtained by ¹⁹F NMR and compared with benzotrifluoride internal standard.

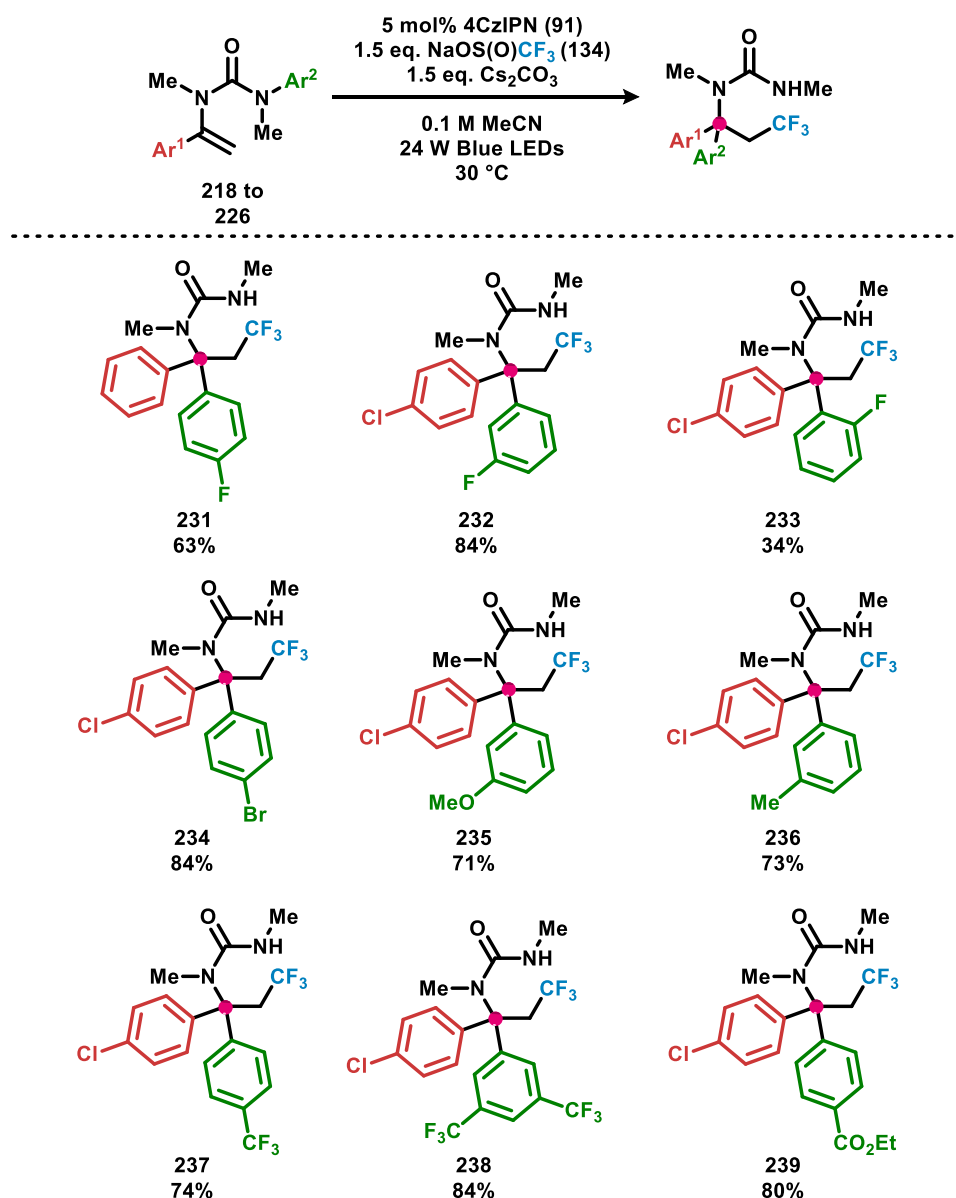
3.3 Scope of Aryl Migrating Groups

With optimised conditions established for the 4CzIPN (**91**)-catalysed transformation of vinyl urea **211** to α -tertiary urea **216**, an investigation into the applicability of these conditions to other vinyl ureas was performed. To this end, acetophenone (**81**) and 4'-chloroacetophenone (**208**) were separately converted into their respective imines (**203** and **209**) by condensation with methylamine (Scheme 3-9). The crude imines obtained were coupled with a variety of different aryl isocyanates then methylated to give an assortment of vinyl ureas (**218** to **228**) all in serviceable yields, apart for vinyl ureas **229** and **230** which failed to give the desired product.



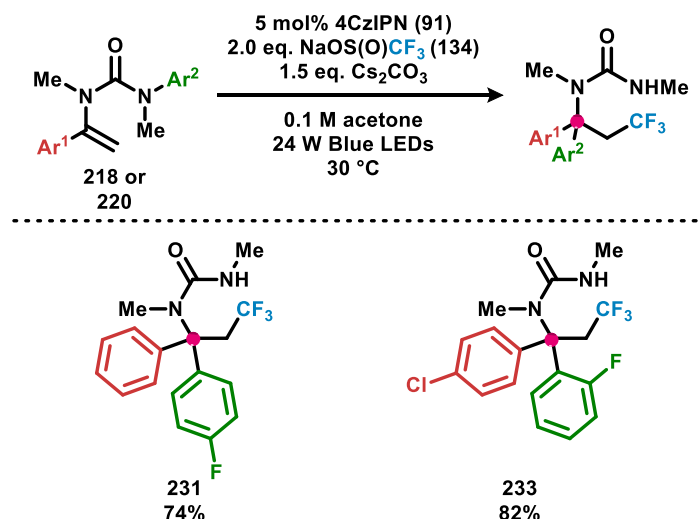
Scheme 3-9. Synthesis of vinyl ureas **218** to **228**. Yields given are over three steps. [a] 2.0 eq. of aryl isocyanate used.

The synthesised library of vinyl ureas (**218** to **228**), possessing a variety of functionality on the *N*-aryl urea, were tested in the 4CzIPN (**91**)-catalysed trifluoromethylation followed by Truce Smiles arylation with Langlois reagent (**134**). Pleasingly, vinyl ureas **218** to **226** gave their respective α -tertiary urea products (**231** to **239**) in mostly good yields (Scheme 3-10). An array of *para*-substituents were found to be compatible under the conditions outlined in Table 3-5 entry 5, including fluoro (**231**), bromo (**234**), trifluoromethyl (**237**) and ethyl ester (**239**). Good representation of successful *meta*-substituted *N*-aryl ureas was obtained, including fluoro (**232**), methoxy (**235**), methyl (**236**) and bis-trifluoromethyl (**238**). Finally, *ortho*-fluorinated *N*-aryl vinyl urea (**233**) was observed to give desired product albeit in poor yield, under the conditions of Scheme 3-10.



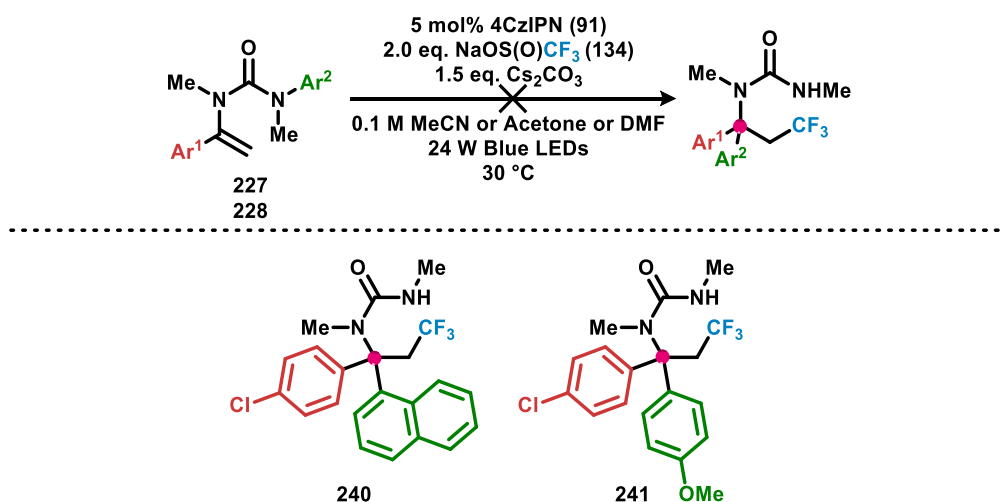
Scheme 3-10. 4CzIPN (**91**)-catalysed trifluoromethylation and subsequent intramolecular electrophilic arylation of vinyl ureas **218** to **226**.

From Scheme 3-10, vinyl ureas **218** and **220** stood out as more difficult substrates and so were selected for re-optimisation. Gratifyingly, the formation of α -tertiary ureas **231** and **233** could be enhanced by simply using acetone in place of acetonitrile and increasing the equivalents of Langlois reagent (**134**) used (Scheme 3-11).



Scheme 3-11. 4CzIPN (**91**)-catalysed trifluoromethylation then subsequent intramolecular electrophilic arylation of vinyl ureas **218** and **220**.

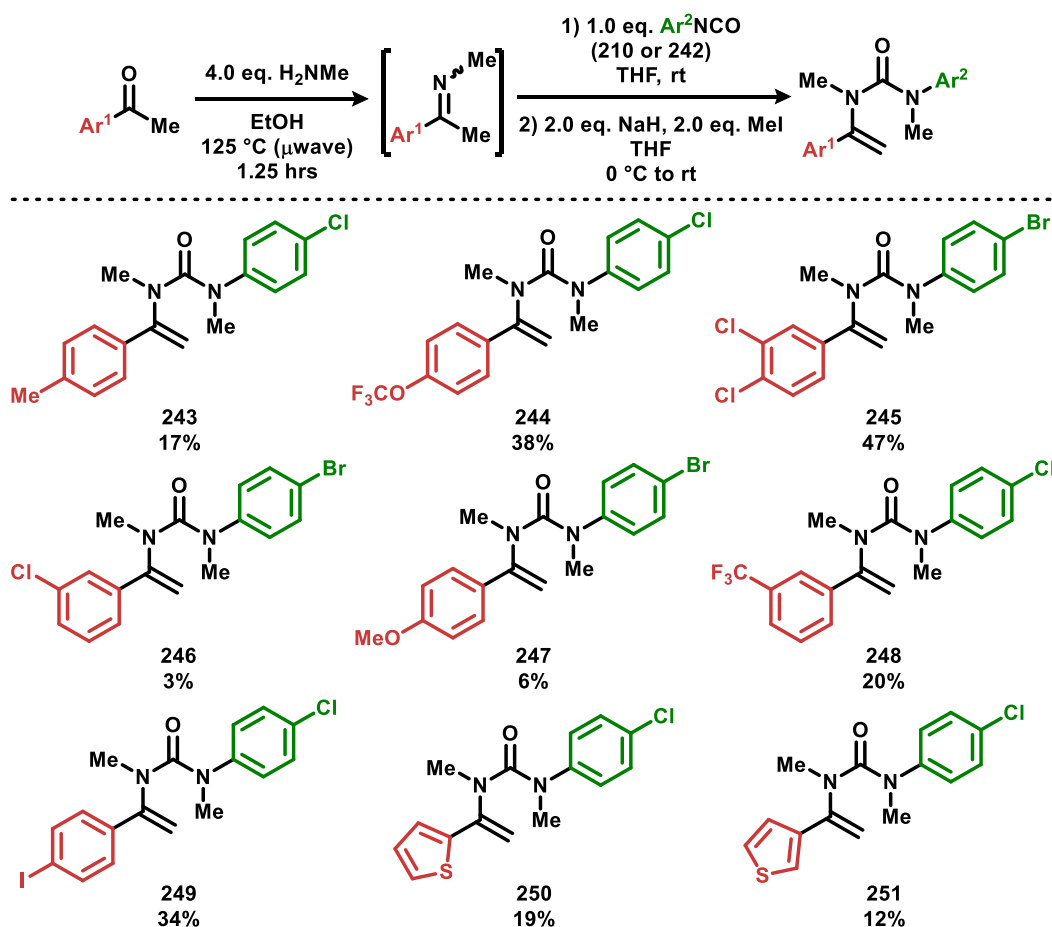
Limitations were identified for the 4CzIPN (**91**)-catalysed trifluoromethyl-arylation of vinyl ureas (Scheme 3-12). Firstly, the attempted conversion of vinyl urea **227** to α -tertiary ureas **240** was unsuccessful, indicating that substitution at the *ortho* position of the migrating aryl ring is problematic. Also, efforts to form α -tertiary urea **241** from vinyl urea **227** resulted only in re-isolation of starting material, suggesting that an electron rich *p*-methoxyphenyl may possess insufficient migratory aptitude for aryl translocation under these conditions. Interestingly, the aryl migration of a 1-naphthyl and *p*-methoxyphenyl have both successfully been achieved previously under base mediated benzylic lithiation conditions, underscoring an advantage of that approach over this newly developed photoredox method.¹⁴³



Scheme 3-12. Attempted 4CzIPN (**91**)-catalysed trifluoromethylation with subsequent intramolecular electrophilic arylation of vinyl ureas **227** and **228**.

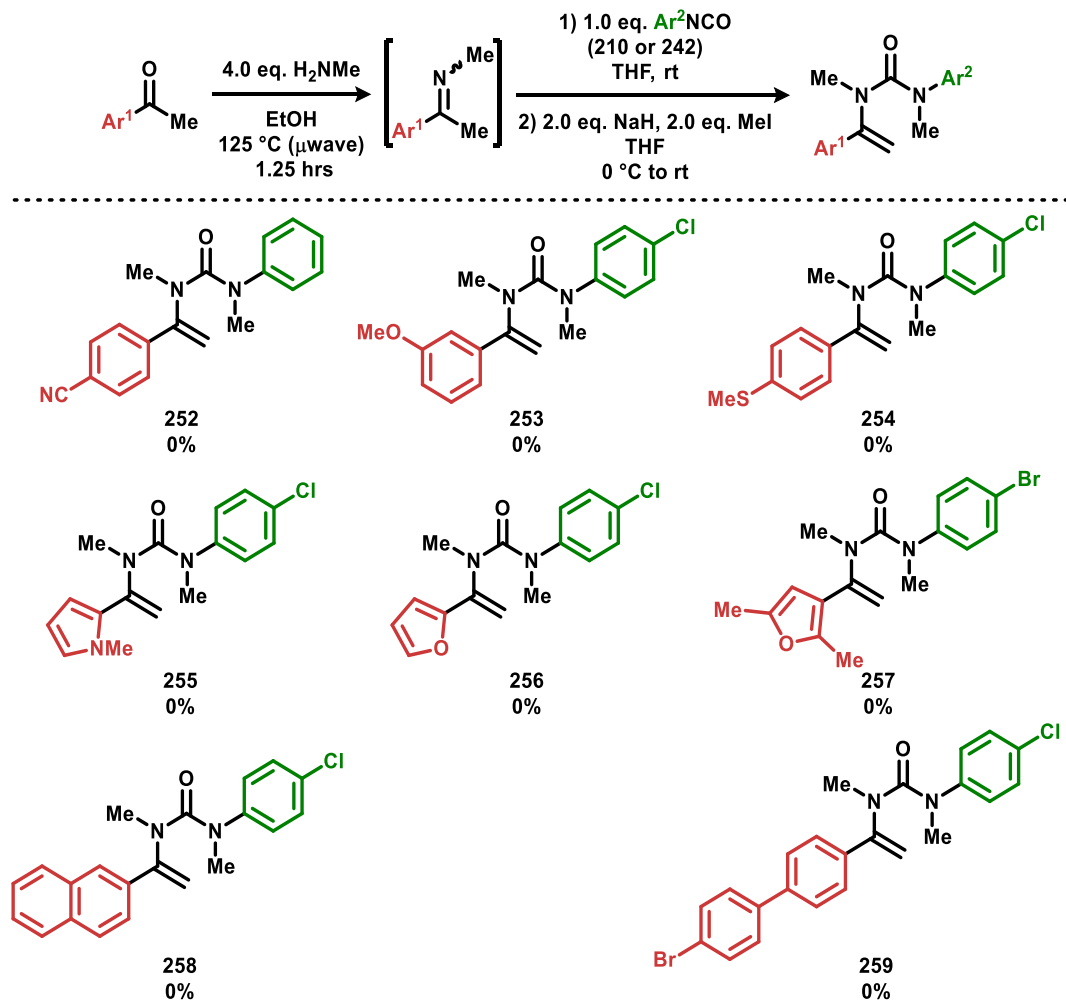
3.4 Scope of Radical/Anion Stabilising Groups

With the 4CzIPN (**91**)-catalysed trifluoromethylation followed by intramolecular electrophilic arylation of vinyl ureas successfully applied to a variety of migrating aromatic rings (Scheme 3-10 and Scheme 3-11), attention was turned to what functionality could be tolerated on the aryl group attached to the vinyl urea. A selection of acetophenone derivatives were transformed into their respective imines by condensation with methylamine (Scheme 3-13). The crude imines obtained were coupled with either 4-chlorophenyl isocyanate (**210**) or 4-bromophenyl isocyanate (**242**), then methylated to give vinyl ureas (**243** to **251**) in moderate to poor yield.



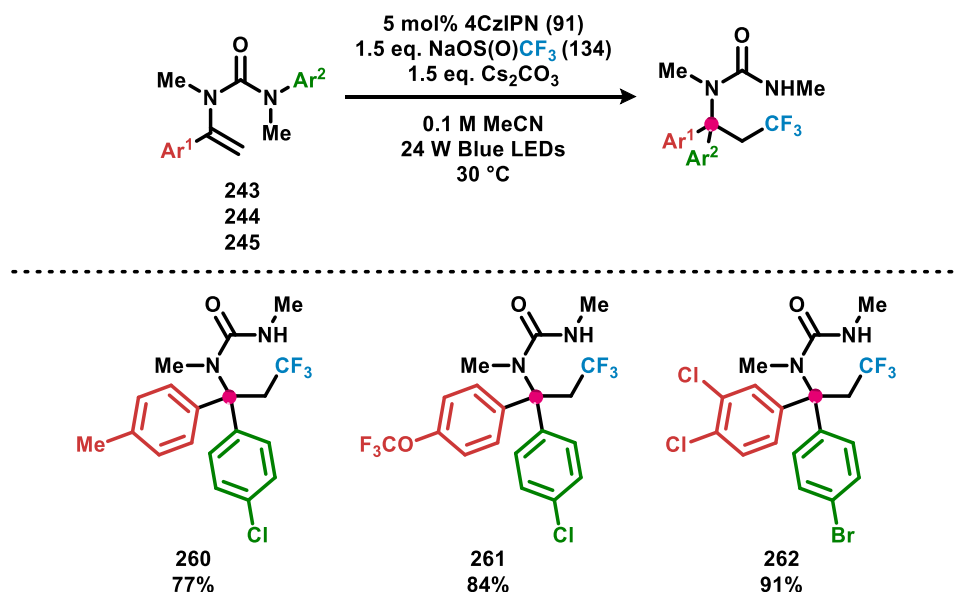
Scheme 3-13. Synthesis of vinyl ureas **243** to **251**. Yields given are over three steps.

It was found that certain vinyl ureas were unobtainable by standard imine-isocyanate coupling conditions (Scheme 3-14). Specifically, the imines required for the preparation of vinyl ureas **252** to **257** were accessible, but their subsequent coupling with aryl isocyanate and methylation proved fruitless. In the attempted synthesis of vinyl ureas **258** and **259**, imine formation resulted in little consumption of starting acetophenone.



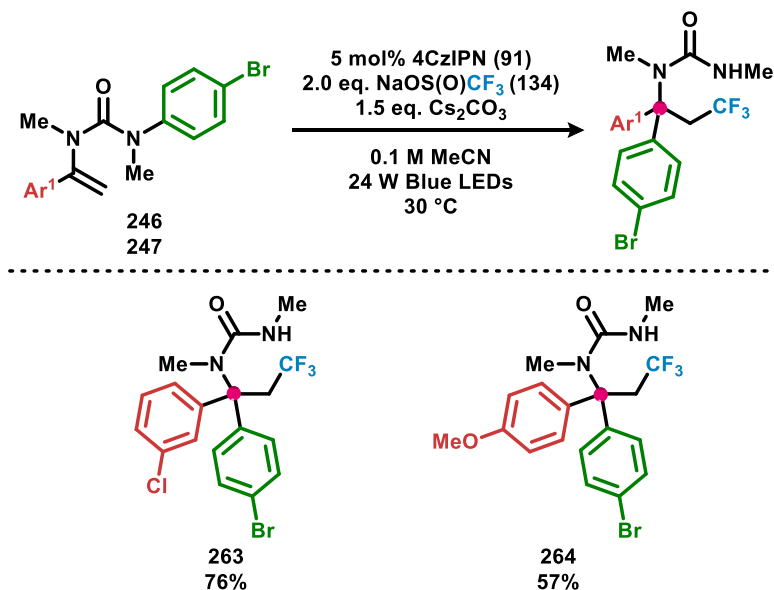
Scheme 3-14. Attempted synthesis of vinyl ureas **252** to **259**.

With an ensemble of vinyl ureas synthesised collectively possessing functional diversity on the aromatic moiety bonded to the olefin (Scheme 3-13), a selection were tested in the 4CzIPN (**91**)-catalysed trifluoromethylation with subsequent Truce-Smiles rearrangement. Vinyl ureas **243**, **244** and **245** were found to be amenable substrates yielding the desired α -tertiary ureas **260**, **261** and **262** in good yields (Scheme 3-15).



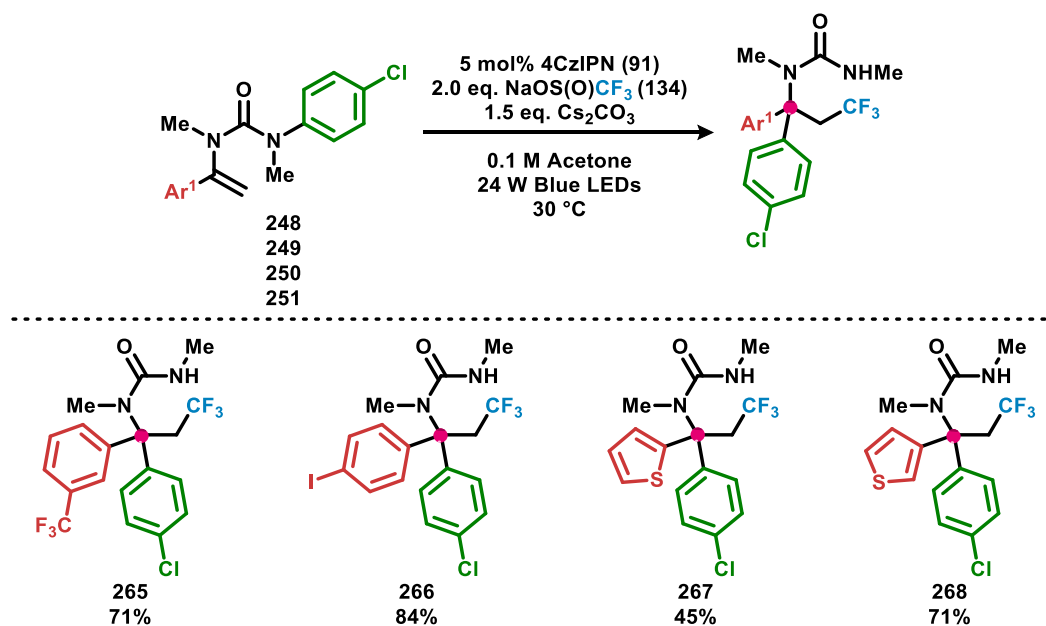
Scheme 3-15. 4CzIPN (**91**)-catalysed trifluoromethylation then subsequent intramolecular electrophilic arylation of vinyl ureas **243**, **244** and **245**.

Vinyl ureas **246** and **247** were found to not achieve full consumption of starting material when optimised conditions were used (Table 3-5, entry 5). To obtain complete conversion of vinyl ureas **246** and **247** the equivalents of Langlois reagent (**134**) used were increased from 1.5 to 2.0, giving the desired α -tertiary ureas **263** and **264** in moderate to good yield (Scheme 3-16).



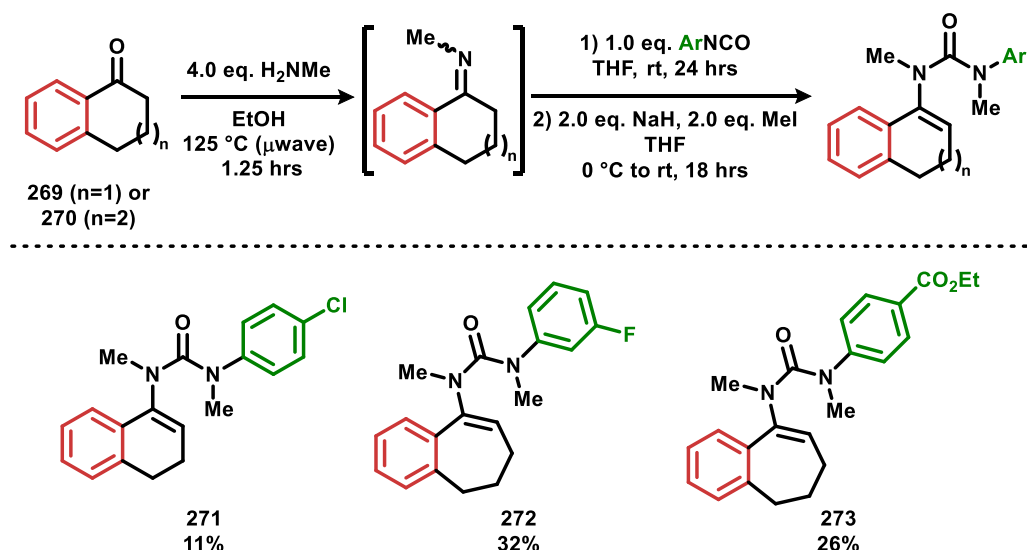
Scheme 3-16. 4CzIPN (**91**)-catalysed trifluoromethylation and subsequent intramolecular electrophilic arylation of vinyl ureas **246** and **247**.

Vinyl ureas **248** to **251** were found to give full conversion when acetone and 2.0 equivalents of Langlois reagent (**134**) were used, to give α -tertiary ureas **265** to **268** (Scheme 3-17). The successful formation of α -tertiary ureas **265** and **266** demonstrates that phenyl rings α to the urea bearing *meta*- trifluoromethyl and *para*- iodo substituents partake in this 4CzIPN (**91**)-catalysed Truce-Smiles rearrangement. Furthermore, the formation of α -tertiary ureas **267** and **268** shows that thiophene heterocycles also stabilise the intermediary ureido benzyl radical and α -metalated urea.



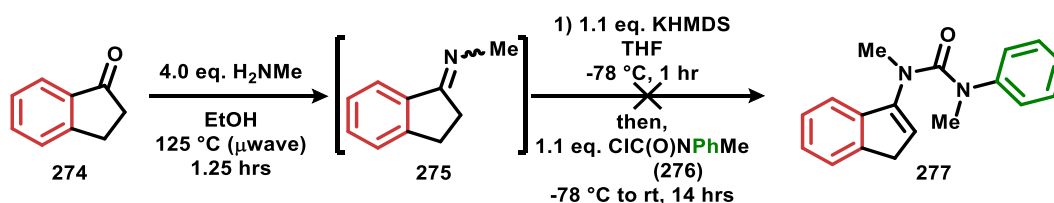
Scheme 3-17. 4CzIPN (**91**)-catalysed trifluoromethylation then subsequent intramolecular electrophilic arylation of vinyl ureas **248** to **251**.

So far only 1,1'-disubstituted vinyl ureas have been used as starting material in this 4CzIPN (**91**)-catalysed trifluoromethyl-arylation of vinyl ureas. More structurally diverse α -tertiary ureas would be accessible if trisubstituted vinyl ureas were also compatible. To this end, α -tetralone (**269**) and 1-benzosuberone (**270**) were used as starting materials in the synthesis of tri-substituted cyclic vinyl ureas **271** to **273** in moderate yield (Scheme 3-18).



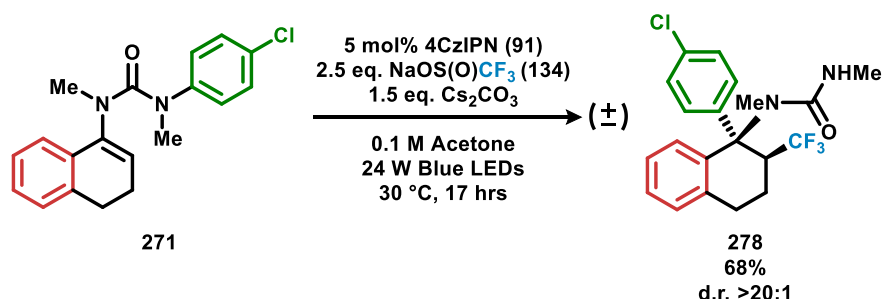
Scheme 3-18. Synthesis of tri-substituted cyclic vinyl ureas **271** to **273**.

For the preparation of the five-membered cyclic vinyl urea **277**, it was postulated that the acidic proton of the indene ring would complicate the methylation step if standard conditions for vinyl urea synthesis were used (Scheme 3-18). An alternative sequence towards vinyl urea **277** was employed, where successful imine condensation of **274** was realised, but subsequent deprotonation of imine **275** with KHMDS and coupling with carbamoyl chloride **276** was unsuccessful (Scheme 3-19).



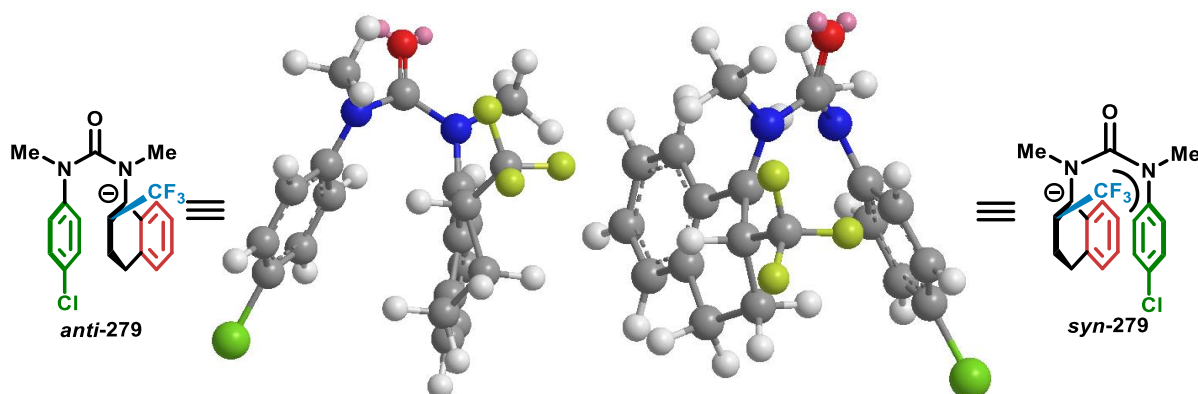
Scheme 3-19. Attempted synthesis of tri-substituted cyclic vinyl urea **277**.

Cyclic vinyl urea **271** was exposed to 4CzIPN (**91**) and Langlois reagent (**134**) under blue LED irradiation with acetone used as solvent, to afford the α -tertiary urea **278** in good yield and excellent diastereoselectivity (Scheme 3-20). NOESY NMR experiments were used to confirm the *anti*-relationship between the trifluoromethyl group and the *para*-chlorophenyl aryl group.



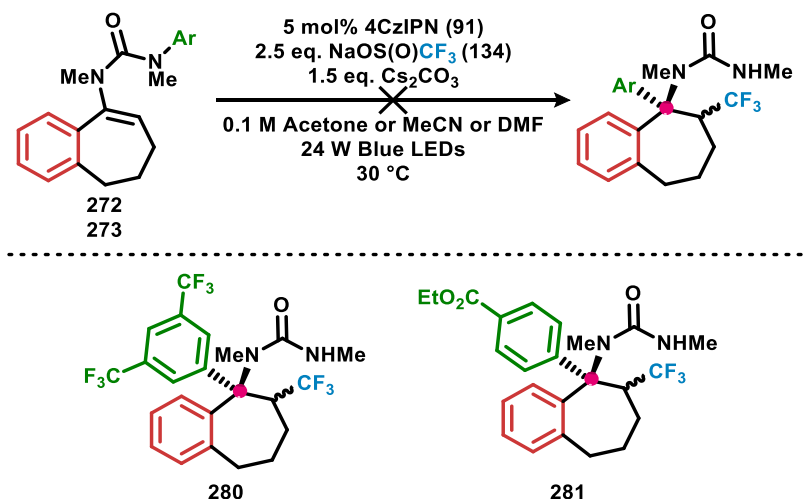
Scheme 3-20. 4CzIPN (**91**)-catalysed trifluoromethyl-arylation of cyclic vinyl urea **271**.

The *anti*-diastereoselectivity observed in Scheme 3-20 presumably is derived from α -metalated urea *anti*-**279** (where the trifluoromethyl group is directed away from the *N*-aryl), being lower in energy than conformation *syn*-**279** (where the trifluoromethyl group is directed towards the *N*-aryl urea) (Scheme 3-21).



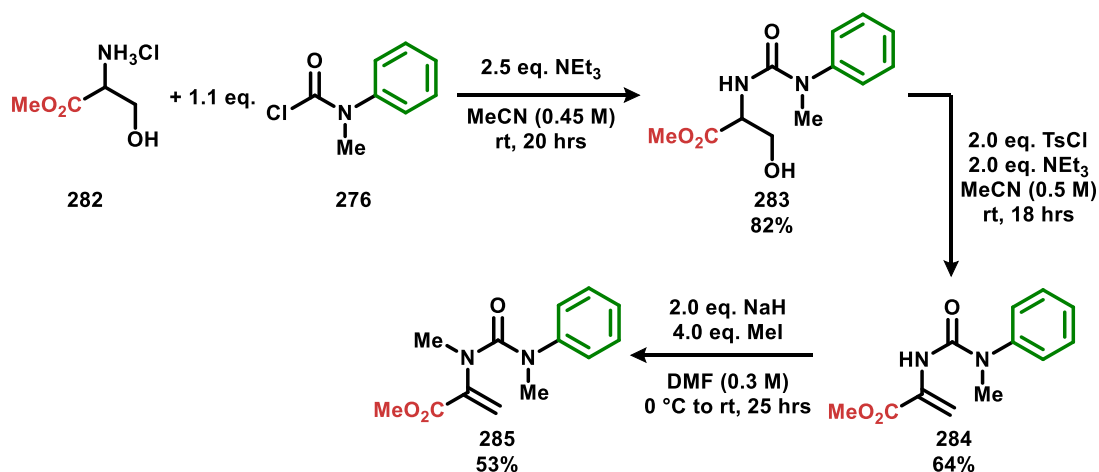
Scheme 3-21. Skeletal and 3-D depiction of the intermediate α -metalated urea in the synthesis of α -tertiary urea **278**, in its two reactive conformations to give *anti* and *syn* diastereoselectivity. Geometries optimised using MM2 energy minimisation in Chem3D.

Unfortunately, when 7-membered cyclic vinyl ureas **272** and **273** were subjected to conditions for 4CzIPN (**91**)-catalysed trifluoromethyl-arylation conditions little consumption of starting material was observed (Scheme 3-22). To the best of this author's knowledge, there are no reported successful attempts at the N to C aryl migration of benzosuberane related α -metalated ureas, potentially indicating that these structures may incur a conformation that is incompatible for Truce-Smiles rearrangement.



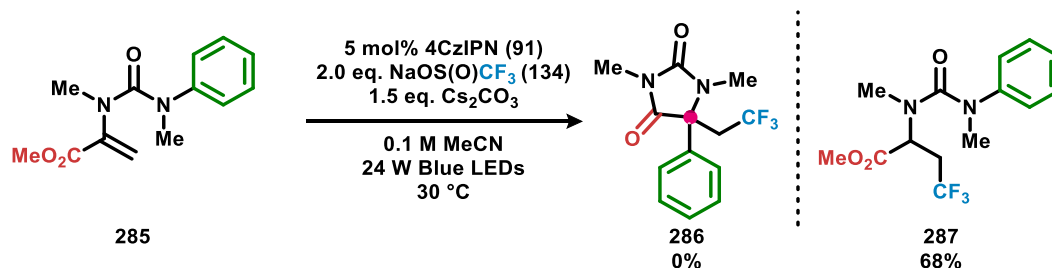
Scheme 3-22. Attempted synthesis of cyclic α -tertiary ureas **280** and **281**.

It was wondered if amino acid derived vinyl ureas would be compatible in this photocatalytic trifluoromethylation followed by Truce-Smiles rearrangement. Towards this end, vinyl urea **285** was selected for synthesis starting from the methyl ester of serine (**282**), which was coupled with carbamoyl chloride **276** to give urea **283** (Scheme 3-23). The hydroxyl of urea **283** underwent 1,2-elimination upon tosylation to give vinyl urea **284**, which was methylated to give the desired vinyl urea **285**.



Scheme 3-23. Synthesis of serine derived vinyl urea **285**.

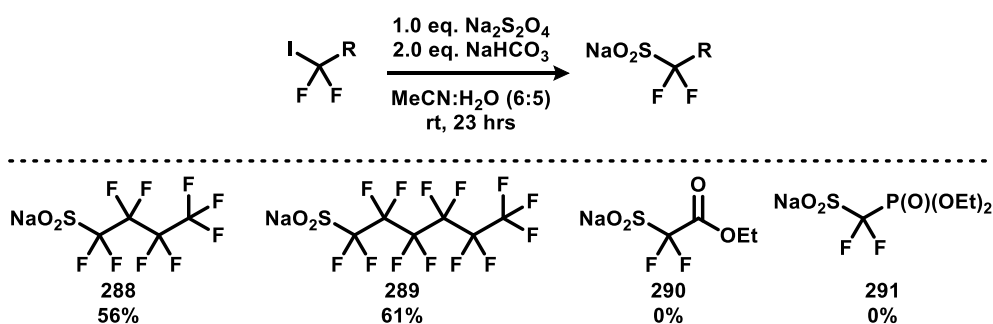
Methyl ester-containing vinyl urea **285** was subjected to conditions for 4CzIPN (**91**)-catalysed trifluoromethylation with ensuing N to C aryl migration, of which the intended product was hydantoin **286**, resulting from urea cyclisation (Scheme 3-24). However, instead only the hydrotrifluoromethylation product **287** was isolated, presumably due to the reduced nucleophilicity of the resulting enolate in comparison to a benzylic anion.



Scheme 3-24. Attempted 4CzIPN (**91**)-catalysed conversion of vinyl urea **288** to hydantoin **290**.

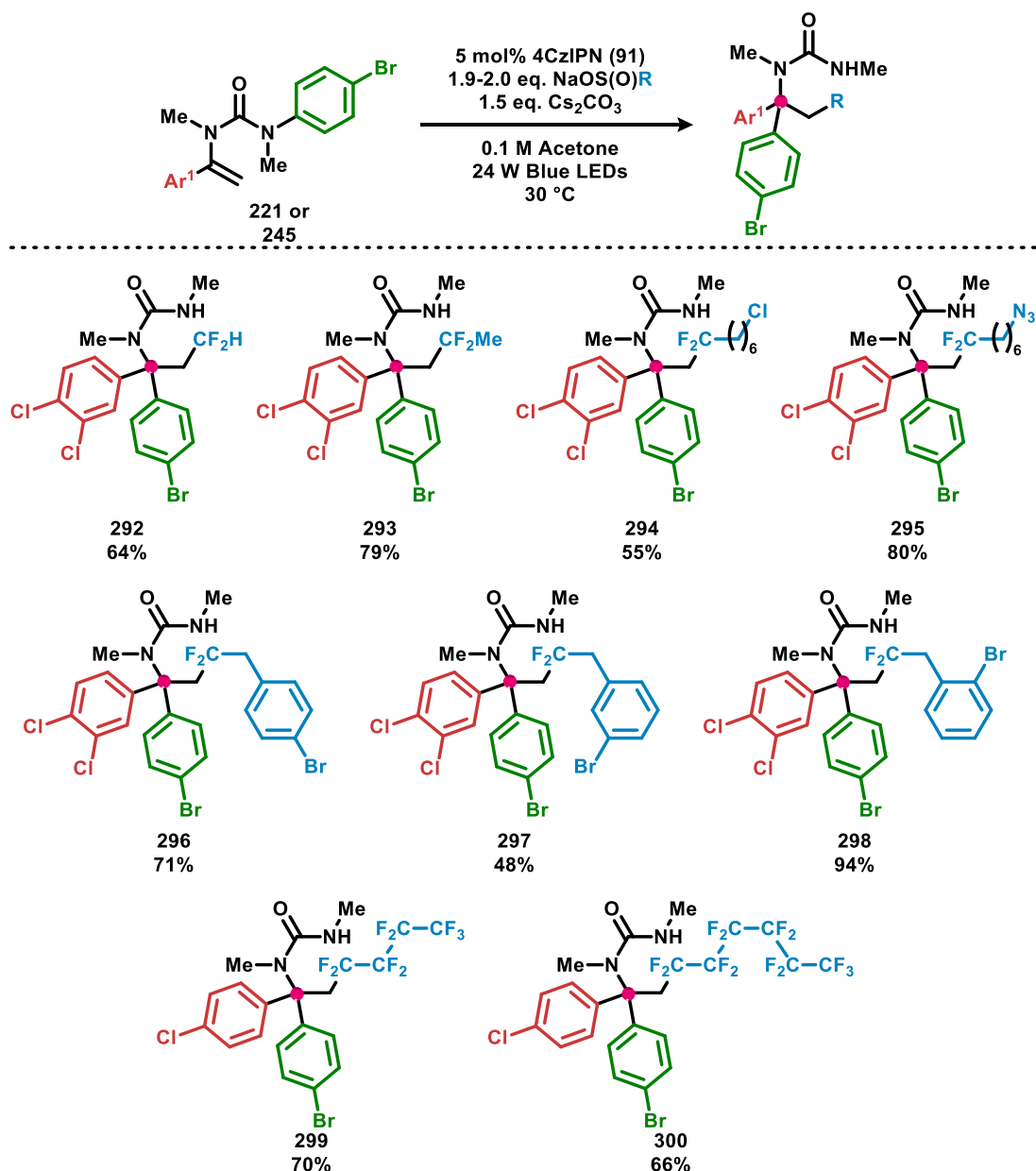
3.5 Radical Precursor Scope

With a variety of aromatic functionality found to be compatible in the 4CzIPN (**91**)-catalysed trifluoromethylation with subsequent intramolecular electrophilic arylation of vinyl ureas, effort was directed to what radical precursors other than Langlois reagent (**91**) could be used. Synthesis of sodium sulfinates from perfluoroalkyl halides were carried out by sulfinate-deiodination of perfluoroalkyl halides (Scheme 3-25). Synthesis of perfluorobutyl- and perfluorohexyl-containing sodium sulfinates **288** and **289** was realised,¹⁵⁸ but preparation of the ethyl ester and ethyl phosphonate containing sodium sulfinates **290** and **291** was unsuccessful.



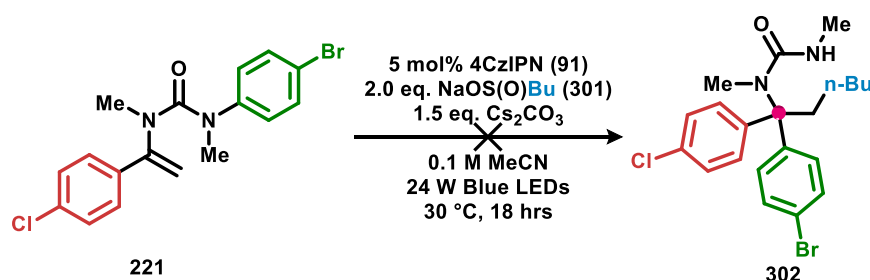
Scheme 3-25. Successful synthesis of perfluoroalkyl sodium sulfinates **288** and **289**, and the attempted synthesis of sodium sulfinates **290** and **291**.

Radical precursors **288** and **289**, along with a variety of other commercially available sodium sulfonates,¹⁵⁹ were successfully used in the alkylation-arylation of vinyl ureas **221** and **245** (Scheme 3-26). Specifically, it was found that difluoromethyl (**292**) and 1,1-difluoroethyl (**293**) could be incorporated into α -tertiary urea products. Formation of α -tertiary urea **293** gave confidence that other 1,1-difluoroalkyl sodium sulfonates would be amenable in this methodology, leading to the successful inclusion of chloride (**294**) and azide (**295**) containing 1,1-difluoroheptyl chains. In addition, (2,2-difluoroethyl)benzenes furnished with a bromide at the *para*- (**296**), *meta*- (**297**) and *ortho*- (**298**) positions were respectively realised. Finally, use of sodium sulfonates **288** and **289** smoothly gave α -tertiary ureas **299** and **300**.



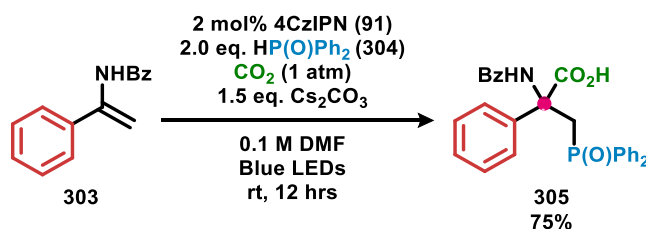
Scheme 3-26. Scope of sodium sulfinate radical precursors.

With a variety of 1,1-difluoroalkyl sodium sulfinate radical precursors found to be effective in achieving the alkyl-arylation of vinyl urea (Scheme 3-26), it was wondered if the geminal difluoro α to the alkyl sodium sulfinate is necessary for reaction. The attempted 4CzIPN (**91**)-catalysed butylation with subsequent intramolecular electrophilic arylation of vinyl urea **221** with sodium butyl sulfinate (**301**) resulted in no formation of α -tertiary urea (**302**) (Scheme 3-27). Scheme 3-27 suggests that the butyl radical, generated upon oxidative decomposition of sodium butyl sulfinate, is maybe too nucleophilic for addition into the electron rich olefin of vinyl urea **221**. The substitution of hydrogen atoms for fluorine increases the electrophilic character of the C-centred radical formed, aiding polarity-matching for the addition to vinyl urea.¹⁶⁰



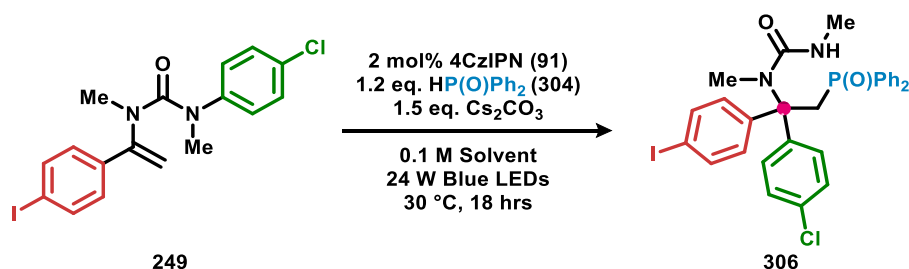
Scheme 3-27. Attempted 4CzIPN (**91**)-catalysed butyl-arylation of vinyl urea **221**.

Effort towards the identification of radical precursors distinct from alkyl sodium sulfinate was undertaken. Yu and co-workers reported the 4CzIPN (**91**)-catalysed phosphonocarboxylation of enamides, with diphenylphosphine oxide and carbon dioxide (Scheme 3-28).¹⁶¹ Scheme 3-28 has been proposed to proceed by oxidation and deprotonation of diphenylphosphine oxide (**304**) by photoexcited 4CzIPN (**91**) and caesium carbonate to yield P-centred radical. Diphenylphosphinoxyl radical adds to enamide (**303**) forming a radical at the benzylic position, which undergoes reductive-termination radical-polar crossover with the radical anion of 4CzIPN (**91**) giving a benzylic anion and closing the photoredox cycle. The generated benzylic anion attacks carbon dioxide forming α -tertiary amide **305** upon acidic work up.



Scheme 3-28. 4CzIPN (**91**)-catalysed phosphonocarboxylation of enamide **303** to give α -tertiary amide **305**.

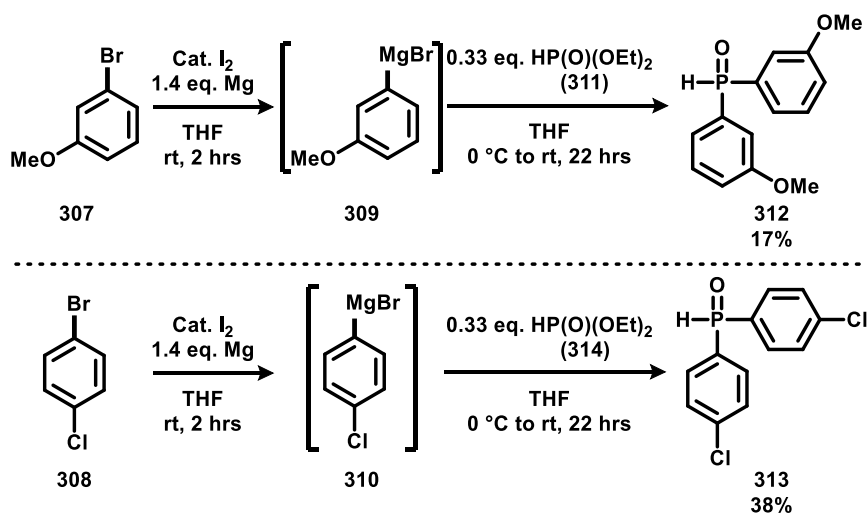
While considering work from Yu and co-workers (Scheme 3-28), it was wondered whether a 4CzIPN (**91**)-mediated diphenylphosphine oxide addition to vinyl urea could be realised to achieve a non-annulative arylphosphonylation of an alkene, a rare class of reaction.¹⁶² To this end, Yu and co-workers' conditions for phosphonocarboxylation of enamides were applied to the attempted arylphosphonylations of vinyl urea **249** (Table 3-7). It was found that the desired diphenylphosphine oxide-containing α -tertiary urea **306** was only observed in trace amounts when DMF and acetone were used as solvent (Table 3-7, entries 1 and 2), but when acetonitrile was used significant levels of product were discerned by ¹H and ³¹P NMR (Table 3-7, entry 3).



Entry	Solvent	306 / % ^[a]
1	DMF	Trace
2	Acetone	Trace
3	MeCN	72

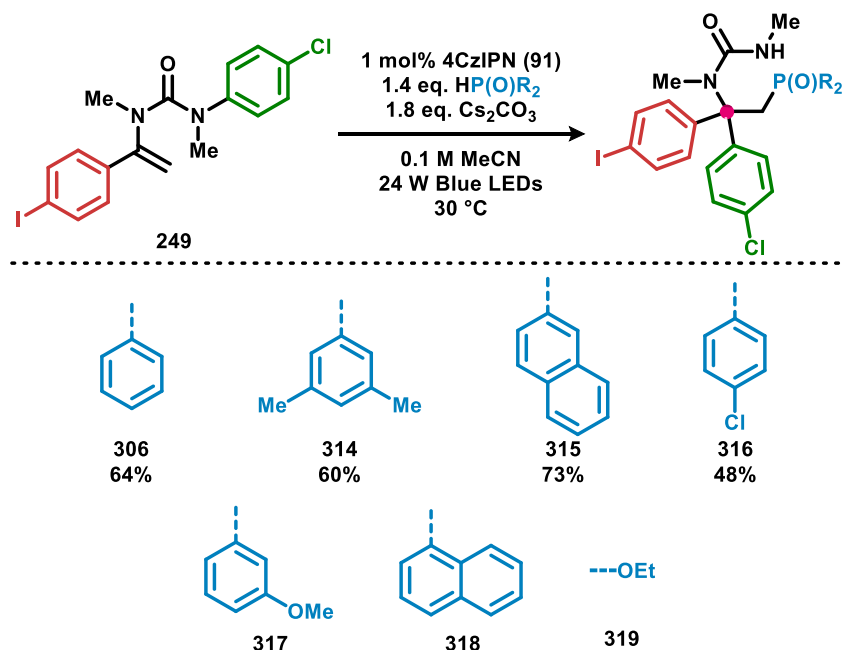
Table 3-7. Solvent screen for the 4CzIPN (**91**)-catalysed phosphonocarboxylation of vinyl urea **249**. [a] Yields obtained by ³¹P NMR and compared with dibutyl phosphate internal standard.

The spectroscopic yield for the 4CzIPN (**91**)-mediated arylphosphonylation of vinyl urea **249** with diphenylphosphine oxide (**304**) gave confidence that other diarylphosphine oxides would perform well in this reaction (Table 3-7, entry 3). Diphenylphosphine oxide derivatives were prepared by conversion of aryl bromides **307** and **308** to aryl magnesium bromides **309** and **310**, which were reacted with diethyl phosphonate (**311**) to afford diarylphosphine oxides **312** and **313** in poor but serviceable yields (Scheme 3-29).



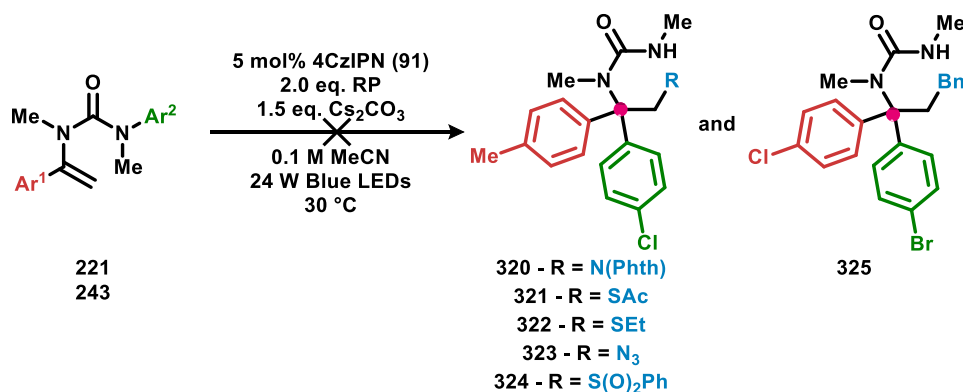
Scheme 3-29. Synthesis of diarylphosphine oxides **312** and **313**.

A scope of diarylphosphine oxides was constructed for the arylphosphonylation of vinyl urea **252**. Diarylphosphine oxide containing α -tertiary ureas **306**, **314**, **315** and **316**, bearing phenyl, *meta*-xylene, 2-naphthyl and *para*-chlorophenyl were successfully yielded (Scheme 3-30). The attempted formation of α -quaternary urea **317** gave low levels of productivity, while α -quaternary urea **318** was found to decompose upon purification attempts. No consumption of starting vinyl urea **252** was observed in the attempted synthesis of **319**.



Scheme 3-30. Scope of diarylphosphine oxides in the arylphosphonylation of vinyl urea **249**.

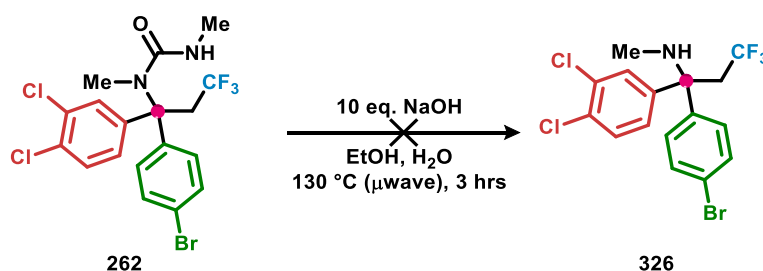
A range of other oxidisable radical precursors were tested in the addition to vinyl ureas **221** and **243** to initiate N to C aryl migration (Scheme 3-31). Unfortunately, attempts at oxidation and addition of potassium phthalimide (**320**), potassium thioacetate (**321**) and sodium ethanethiol (**322**) to vinyl urea **243** proved unsuccessful. Presumably due to their respective radical precursors being insufficiently oxidisable by photoexcited 4CzIPN (**91**), or upon α -metalated urea formation anionic 1,2-elimination of the radical adduct occurs over N to C aryl migration. The attempted arylazidation of vinyl urea **221** with sodium azide to form α -tertiary urea **323** was found to be fruitless. Sodium azide should be oxidisable ($E_{1/2} = 0.9$ V vs SCE)¹⁶³ by photoexcited 4CzIPN (**91**), but the resulting azide radical is most likely nucleophilic in nature. Also, if azide radical addition did occur anionic 1,2-elimination from the α -metalated urea could be envisaged. The photoredox mediated addition of benzyl radical and aryl sulfonyl radical to electron deficient olefins has been documented.¹⁶⁴ However, the attempted phenyl sulfonylation (**324**) and benzylation (**325**) of vinyl ureas **243** and **221** with sodium benzenesulfinate and potassium benzyltrifluoroborate respectively only returned starting material, presumably due to the nucleophilic character of the radicals formed.¹⁶⁰



Scheme 3-31. Scope of unsuccessful radical precursors.

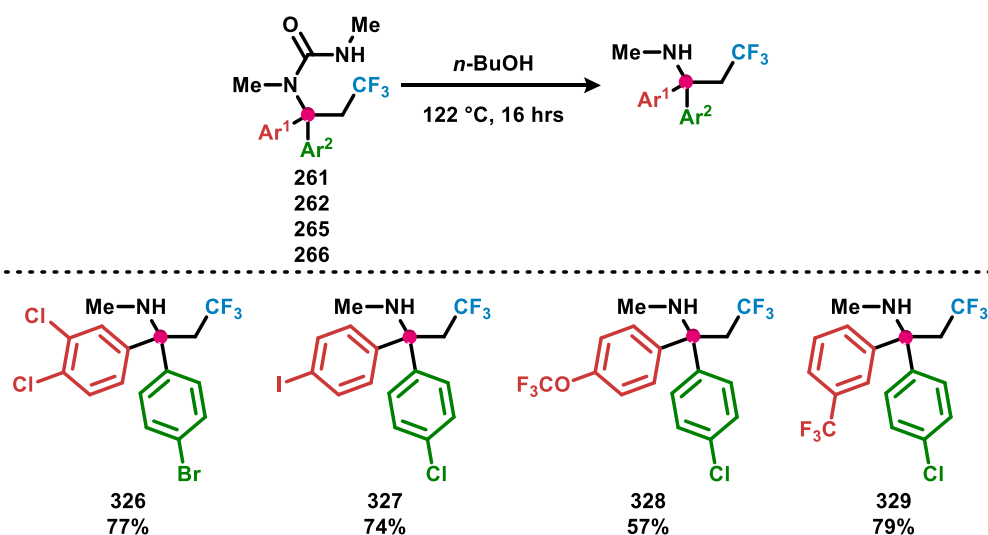
3.6 Solvolysis of α -Tertiary Ureas

With an assortment of α -tertiary ureas synthesised by the 4CzIPN (**91**)-catalysed radical addition with following N to C aryl migration of vinyl ureas, the validity of this methodology for α -tertiary amine synthesis was investigated. Attention was directed towards the removal of the urea of α -tertiary urea **262**. First, hydrolytic conditions were employed in the attempted conversion of α -tertiary urea **262** to α -tertiary amine **329**,¹⁶⁵ however this resulted in starting material decomposition with no discernible indication of α -tertiary amine **329** formation (Scheme 3-32).



Scheme 3-32. Attempted hydrolysis of α -tertiary urea **262**.

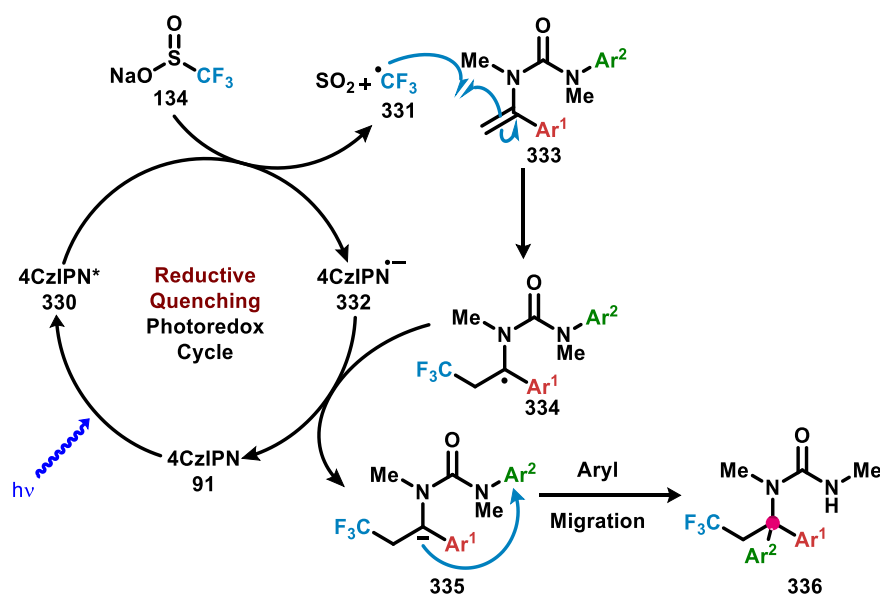
Gratifyingly, the ureas of **261**, **262**, **265** and **266** were removed in refluxing butanol,¹⁴⁴ to yield their corresponding α -tertiary amines **326** to **329**, validating the 4CzIPN (**91**)-catalysed radical addition with subsequent N to C aryl migration as a method for α -tertiary amine synthesis (Scheme 3-33).



Scheme 3-33. Solvolysis of α -tertiary ureas to afford α -tertiary amines **326** to **329**.

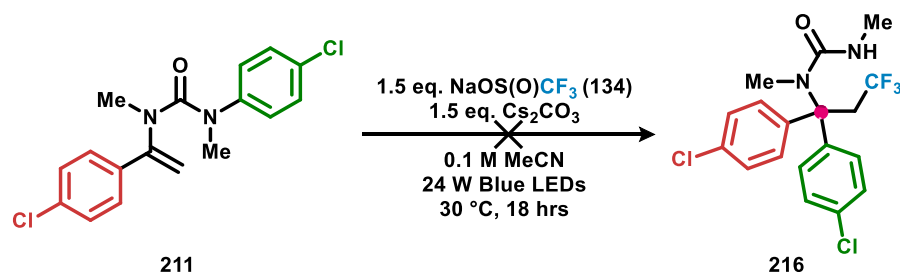
3.7 Mechanistic Investigation

With the synthetic utility for the 4CzIPN (**91**)-catalysed trifluoromethylation followed by Truce-Smith rearrangement of vinyl ureas firmly established, attention was directed at understanding of the mechanism. A proposed mechanism started with resting state 4CzIPN (**91**) reaching its photoexcited state (**330**) by absorption of a photon (Scheme 3-34). Photoexcited 4CzIPN (**330**, $E_{1/2}$ (PC^{*}/PC⁻) = 1.35 V vs SCE)⁹⁴ oxidises Langlois reagent (**134**) ($E_{1/2}$ = 1.05 V vs SCE)¹⁵⁵ resulting in its decomposition to sulfur dioxide and trifluoromethyl radical (**331**), concurrently forming 4CzIPN radical anion (**332**). Trifluoromethyl radical (**331**) adds to a vinyl urea (**333**) forming ureido benzyl radical (**334**) that is reduced by 4CzIPN radical anion (**332**), closing the photoredox cycle and simultaneously generating α -metalated urea (**335**) that undergoes N to C intramolecular arylation, to give an α -tertiary urea (**336**).



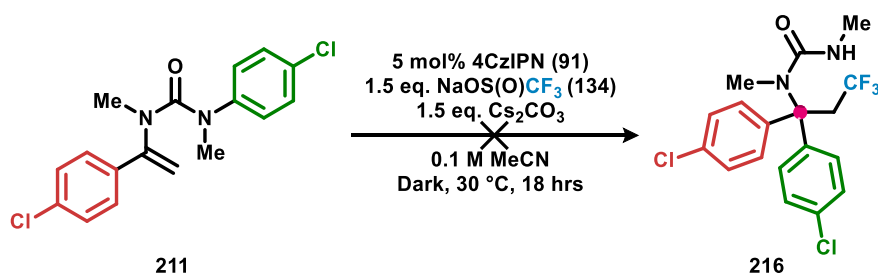
Scheme 3-34. Proposed mechanism for the 4CzIPN (**91**)-catalysed trifluoromethylation followed by intramolecular electrophilic arylation of vinyl ureas. Asterisk denotes photoexcited state.

Work was undertaken to test the validity of the proposed mechanism outlined in Scheme 3-34. Firstly, control experiments were performed, with vinyl urea **211** and Langlois reagent (**134**) being exposed to each other under optimised conditions, but in the absence of photocatalyst 4CzIPN (**91**) (Scheme 3-35). No consumption of the starting vinyl urea **211** was observed, suggesting 4CzIPN (**91**) plays a key role in α -tertiary urea **216** formation.



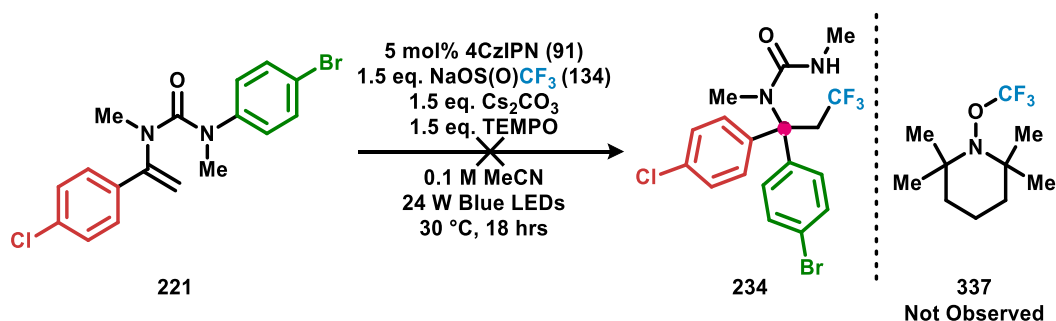
Scheme 3-35. Attempted trifluoromethyl-arylation of vinyl urea **211**, in the absence of photocatalyst 4CzIPN (**91**).

A second control experiment was performed in which vinyl urea **211** was subjected to optimised conditions for trifluoromethylation with subsequent Truce-Smiles rearrangement, but with the omission of any light source (Scheme 3-36). Again, no conversion of vinyl urea **211** was observed, indicating that light is a key component for α -tertiary urea **216** formation.



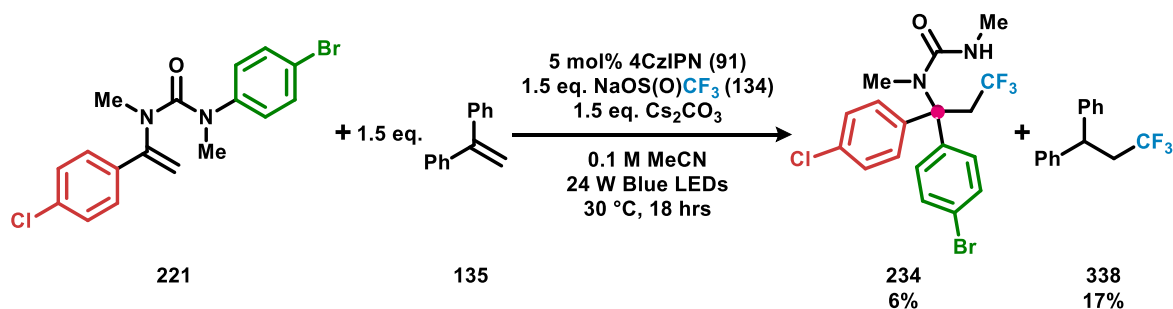
Scheme 3-36. Attempted trifluoromethylation with subsequent intramolecular electrophilic arylation of vinyl urea **211** in the absence of light.

Vinyl urea **221** was subjected to optimised conditions for trifluoromethyl-arylation in the presence of persistent radical TEMPO, which resulted in complete inhibition of α -tertiary urea **234** formation (Scheme 3-37). No obvious TEMPO adducts (**337**) could be discerned from the reaction mixture of Scheme 3-37, implicating the oxidation of TEMPO ($E_{1/2} = 0.62$ V vs SCE)¹⁶⁶ by 4CzIPN (**91**) as its mode of reaction inhibition.



Scheme 3-37. Attempted trifluoromethylation with subsequent intramolecular electrophilic arylation of vinyl urea **221**, in the presence of TEMPO.

A second radical probe experiment was performed, using 1,1-diphenylethylene (**135**)¹⁶⁷ as a radical trap that would not be oxidised or reduced by photoexcited 4CzIPN (**91**). Subjection of vinyl urea **221** to optimised conditions for trifluoromethyl-arylation in the presence of 1,1-diphenylethylene (**135**) drastically attenuated formation of α -tertiary urea **234** (Scheme 3-38). Also, the hydrotrifluoromethylation product **338** was observed confirming the formation of trifluoromethyl radical and highlighting its importance in α -tertiary urea **234** production.



Scheme 3-38. Attenuated trifluoromethylation with subsequent intramolecular electrophilic arylation of vinyl urea **221** in the presence of radical acceptor **135**. Yields obtained by ¹⁹F NMR and compared with benzotrifluoride internal standard.

Scheme 3-38 gives evidence that photoexcited 4CzIPN (**91**) oxidises Langlois reagent (**134**) over other species, however more evidence was sought to substantiate this claim. Stern-Volmer quenching studies can be used to elucidate which substrates a photocatalyst transfers its photonic energy to. A photoexcited species will typically dissipate its absorbed photonic energy by fluorescence (Figure 2-1). However, in the presence of an appropriate substrate a photoexcited species can be quenched by single electron transfer or energy transfer, which reduces the radiative quantum yield of the fluorophore.^{86b,168} This reduction of fluorescence of a photoexcited species can be measured by fluorimetry and compared between quenchers.

Emission quenching of 4CzIPN (**91**) with quenchers Langlois reagent (**134**) and vinyl urea **219** were performed over a quencher concentration range close to the 4CzIPN (**91**):quencher ratio of a typical trifluoromethyl-arylation reaction (Figure 3-1). Figure 3-1 shows that photoexcited 4CzIPN (**91**) is quenched to a greater degree by Langlois reagent (**134**) than vinyl urea **219**, implying a greater rate of photonic energy transfer from 4CzIPN (**91**) to Langlois reagent (**134**) over vinyl urea **219**.

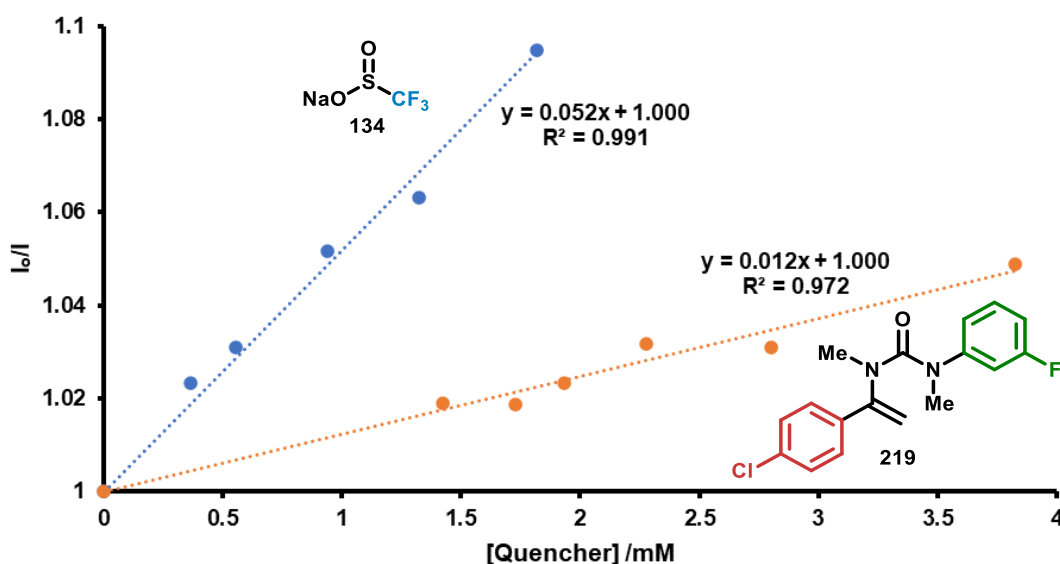


Figure 3-1. Stern-Volmer quenching plot of an 8.0×10^{-6} M solution of 4CzIPN (**91**) in acetonitrile, with quenchers Langlois reagent (**134**) (Blue line) and vinyl urea (**219**) (Orange line).

Stern-Volmer quenching studies of 4CzIPN (**91**) with quenchers Langlois reagent (**134**) and vinyl urea **219** were repeated using a larger quencher concentration range. Like in Figure 3-1, it was observed in Figure 3-2 that photoexcited 4CzIPN (**91**) is quenched to a greater degree by Langlois reagent (**134**) over vinyl urea **219**.

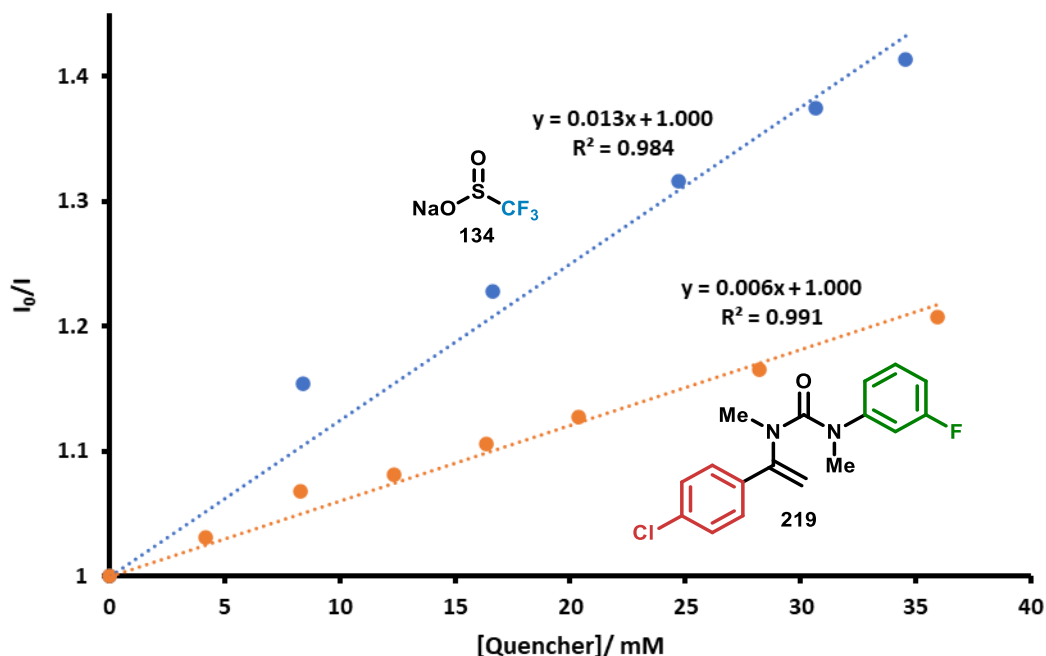


Figure 3-2. Repeated Stern-Volmer quenching plot of a 9.9×10^{-6} M solution of 4CzIPN (**91**) in acetonitrile, over higher concentrations of quenchers Langlois reagent (**134**) (Blue line) and vinyl urea (**219**) (Orange line).

Using the line gradients of Figure 3-2 and the Stern-Volmer equation (1), the quencher rate coefficient (K_q , $M^{-1}.s^{-1}$) can be calculated.¹⁶⁹ In equation (1), I_0 is the emission intensity of the fluorophore in the absence of quencher, I_n is the emission intensity of a fluorophore in the presence of quencher, τ_0 is the fluorescence lifetime of the excited state of a fluorophore (s) (2.37 ns for 4CzIPN (**91**))¹⁷⁰ and $[Q]$ is the quencher concentration (M).

$$\frac{I_0}{I_n} = 1 + K_q \times \tau_0 \times [Q] \quad (1)$$

The quencher rate coefficient between 4CzIPN (**91**) and quenchers Langlois reagent (**134**) and vinyl urea (**219**) were calculated to be $5.31 \times 10^9 M^{-1}.s^{-1}$ and $2.55 \times 10^9 M^{-1}.s^{-1}$ respectively.

Stern-Volmer quenching studies indicate that quenching of photoexcited 4CzIPN (**91**) is observed by vinyl urea **219** (Figure 3-1 and Figure 3-2). To ascertain the cause of this observation, cyclic voltammetry analysis of vinyl urea **219** was performed (Figure 3-3). An irreversible oxidation wave was observed at a potential scan rate of 100 mV.s⁻¹ and 500 mV.s⁻¹. The half wave oxidation potential of vinyl urea **219** was found to be 0.96 V versus the ferrocenium couple and 1.33 V versus the SCE. This gives indication that 4CzIPN (**91**) from its photoexcited state ($E_{1/2}(P^*/P^-) = 1.35$ V vs SCE) may be able to oxidise vinyl urea **219**, possibly indicating how quenching is observed although an energy transfer pathway cannot be discounted.¹⁷¹

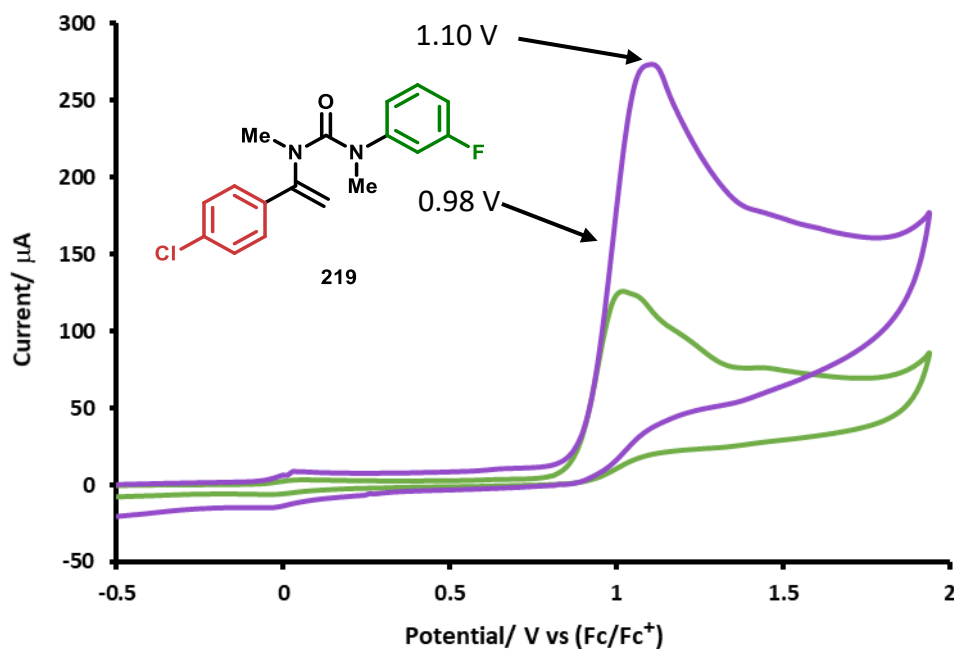
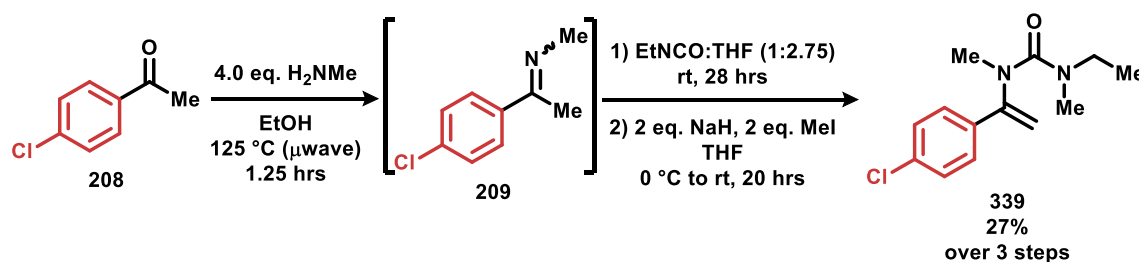


Figure 3-3. Overlaid cyclic voltammogram of vinyl urea **219** at a scan rate of 500 mVs⁻¹ (Purple line) and 100 mVs⁻¹ (Green line).

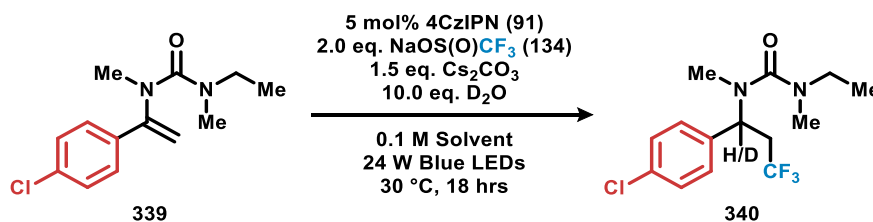
To summarise, Scheme 3-38 gives indication that trifluoromethyl radical is generated in the 4CzIPN (**91**)-catalysed trifluoromethyl-arylation of vinyl urea **221**, as trifluoromethyl radical adduct **338** is observed. Next, Stern-Volmer quenching studies confirm that there is transfer of photonic energy between photoexcited 4CzIPN (**91**) and Langlois reagent (**134**) (Figure 3-1 and Figure 3-2). It is likely the quenching of photoexcited 4CzIPN (**91**) by Langlois reagent (**134**) is derived from electron transfer when considering their respective oxidation potentials (Langlois reagent (**134**): $E_{1/2} = 1.05$ V vs SCE), (4CzIPN (**91**): $E_{1/2} (P^*/P^-) = 1.35$ V vs SCE).^{94,155} Quenching of photoexcited 4CzIPN (**91**) by vinyl urea **219** is observed, the origin of which may be photoexcited 4CzIPN (**91**) oxidising vinyl urea **219** when comparing their oxidation potentials (Figure 3-3), or through energy transfer. However, quenching from vinyl urea **219** occurs to a lesser degree than quenching from Langlois reagent (**134**). Therefore, the results of Scheme 3-38, Figure 3-1, Figure 3-2 and Figure 3-3 together give evidence that photoexcited 4CzIPN (**91**) oxidises Langlois reagent (**134**) for trifluoromethyl radical generation, which then adds to vinyl urea (Scheme 3-34).

Next, effort was made to confirm the reduction of the intermediary ureido benzyl radical (**334**) to an α -metalated urea (**335**) (Scheme 3-34). To this end, vinyl urea **339**, which does not bear a *N*-aryl so cannot undergo N to C aryl migration, was synthesised (Scheme 3-39).



Scheme 3-39. Synthesis of *N*-ethyl vinyl urea **339**.

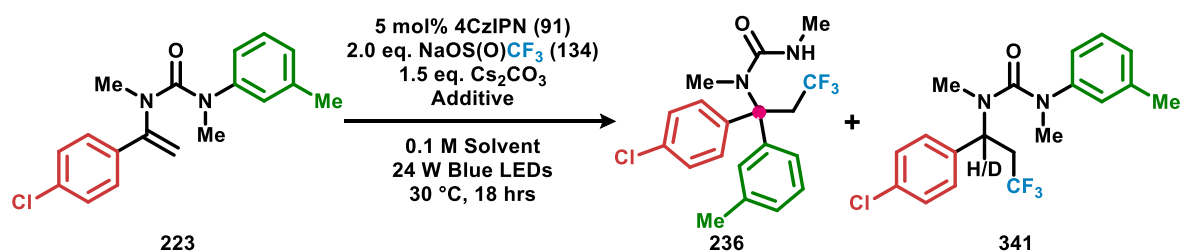
It was thought that the anion of an α -metalated urea (**335**) could be intercepted by an electrophile, such as deuterium from deuterium oxide, which is relatively acidic ($pK_a = 15.9$) but resistant to hydrogen atom transfer ($BDE = 120.9 \text{ kcal.mol}^{-1}$)¹⁷². Vinyl urea **339** was subjected to conditions for trifluoromethyl-arylation, but with deuterium oxide present as an additive (Table 3-8). Conversion of vinyl urea **342** to the hydrotrifluoromethylation product **340** was achieved, furthermore significant deuterium incorporation at the benzylic position was observed. Thus, Table 3-8 gives evidence that under the optimised conditions of this study the formation of α -metalated urea (**335**) is feasible.



Entry	Solvent	340 / %	D-incorporation/ %
1	Acetone	89	76
2	MeCN	77	83
3	DMF	67	82

Table 3-8. The 4CzIPN (**91**)-catalysed hydrotrifluoromethylation of vinyl urea **340**.

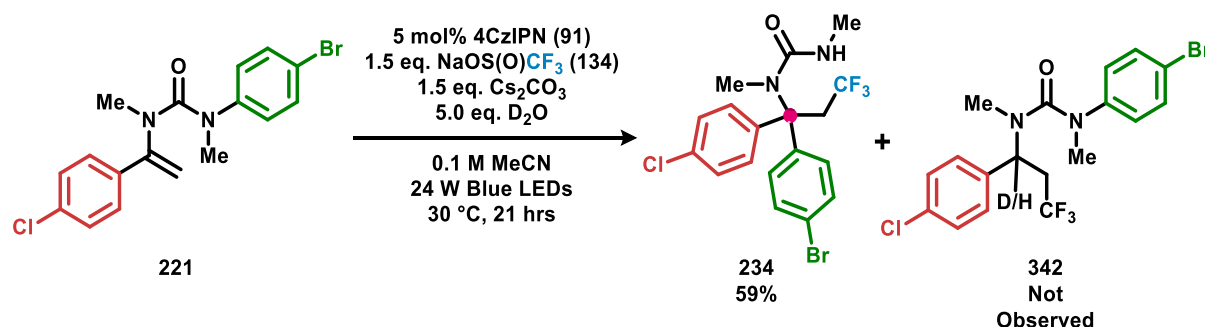
Although the results of Table 3-8 indicate the feasibility of α -metalated urea (**335**) formation under conditions for 4CzIPN (**91**)-catalysed trifluoromethyl-arylation of vinyl urea, it does not distinguish whether the aryl migration occurs by a polar manifold, or by an unprecedented but still conceivable radical process. To answer this, the trifluoromethyl-arylation of vinyl urea **223** was performed in acetone and acetonitrile (Table 3-9, entries 1 and 2), yielding α -tertiary urea **236** and small amounts of the hydrotrifluoromethylation product **341**, presumably due to adventitious traces of water present in Langlois reagent (**134**) and caesium carbonate. Next, the trifluoromethyl-arylation of vinyl urea **223** was repeated, but with the addition of deuterium oxide (Table 3-9, entries 3 and 4) resulting in α -tertiary urea **236** being formed as the minor product and α -secondary urea **341** as the major product. Furthermore, significant levels of deuterium incorporation were observed in α -secondary urea **341**. The results of Table 3-9 indicate that the addition of deuterium oxide interrupts the N to C aryl migration of vinyl urea **223** by protonation of an α -metalated urea (**335**).



Entry	Solvent	Additive	236 /%	341 /%	341 D-incorporation/ %
1	Acetone	None	70	6	-
2	MeCN	None	79	9	-
3	Acetone	D ₂ O (10 eq.)	25	59	69
4	MeCN	D ₂ O (10 eq.)	20	55	82

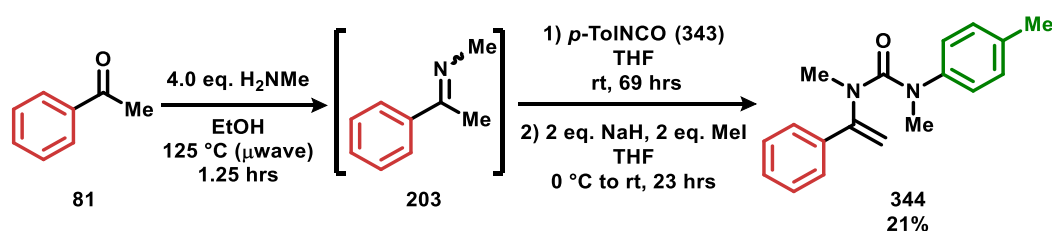
Table 3-9. Isotope labelling studies in the 4CzIPN (**90**)-catalysed hydrotrifluoromethylation of vinyl urea **223**.

In opposition to Table 3-9, the trifluoromethyl-arylation of vinyl urea **221** in the presence of deuterium oxide proceeded to give α -tertiary urea **234**, without the formation of hydrotrifluoromethylation product **342** (Scheme 3-40). An explanation may be that for vinyl urea **221** aryl migration is much faster than protonation of an α -metalated urea, while the converse being true for vinyl urea **223**. Especially when considering an electron deficient migrating aryl is used in Scheme 3-40 and an electron rich migrating aryl is used in Table 3-9.¹⁷³ However, it is still conceivable that the aryl migration for the formation of α -tertiary urea **234** could proceed by a ureido benzyl radical (**334**).



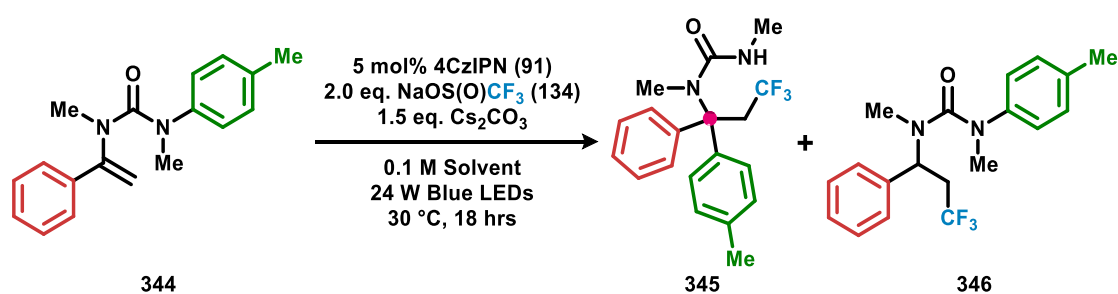
Scheme 3-40. Trifluoromethyl-arylation of vinyl urea **221** in the presence of deuterium oxide.

To ascertain more information of the species undergoing aryl migration under 4CzIPN (**91**)-mediated conditions, vinyl urea **344** was synthesised in moderate yield (Scheme 3-41).



Scheme 3-41. Synthesis of vinyl urea **344**.

The outcome of the 4CzIPN (**91**)-catalysed trifluoromethylation followed by Truce-Smiles rearrangement of vinyl urea **344** was dependent on the solvent used (Table 3-10, entries 1-3). Firstly, the trifluoromethyl-arylation of vinyl urea **344** with DMF used as solvent predominantly yielded α -tertiary urea **345** and a small amount of hydrotrifluoromethylation product **346** (Table 3-10, entry 1). Next, when acetonitrile was used as solvent the α -tertiary urea **345** was formed as the minor product and α -secondary urea **346** was received as the major product (Table 3-10, entry 2). Finally, when acetone was used as solvent the hydrotrifluoromethylation product **346** was exclusively observed (Table 3-10, entry 3). α -Secondary urea **346** is presumably formed by trifluoromethyl radical addition to vinyl urea **344**, resulting in an ureido benzyl radical (**334**) that either undergoes hydrogen atom abstraction with solvent or is reduced by 4CzIPN radical anion (**332**) to an α -metalated urea (**335**) that is protonated.

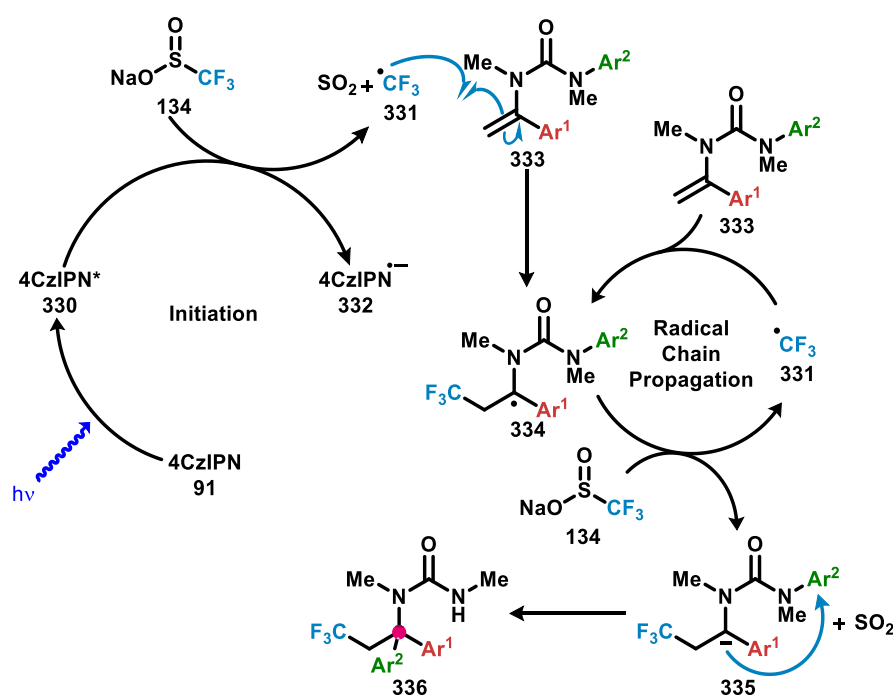


Entry	Solvent	345 / %	346 / %	Solvent pK _a	Solvent BDE/ kcal.mol ⁻¹
1	DMF	66	11	>35 ¹⁷⁴	89.7, ^[a] 89.1 ^{[b]175}
2	MeCN	14	27	31.3 ¹⁷⁶	93.1 ¹⁷⁷
3	Acetone	2	62	26.5 ¹⁷⁸	93.7 ¹⁷⁹

Table 3-10. Solvent dependent 4CzIPN (**91**)-catalysed trifluoromethylation with subsequent intramolecular electrophilic arylation or protonation of vinyl urea **344**. [a] BDE for HC(O)N(CH₃)₂ of DMF. [b] BDE for HC(O)N(CH₃)₂ of DMF.

To rationalise this solvent-dependent outcome of Table 3-10, the propensity for DMF, acetonitrile and acetone to be deprotonated and hydrogen atom abstracted were examined by inspection of their respective pK_a and carbon-hydrogen bond dissociation energies. Acetone was found to have the lowest pK_a followed by acetonitrile then DMF. Conversely, DMF demonstrates the lowest bond dissociation energy for its carbon-hydrogen bonds, followed by acetonitrile then acetone. Therefore, the results of Table 3-10 imply that hydrotrifluoromethylation product **346** is formed by protonation of an α -metalated urea (**335**) and by not hydrogen atom abstraction from a ureido benzyl radical (**334**). As acetone, the solvent most prone to deprotonation with the strongest C-H bonds, leads to significant hydrotrifluoromethylation product **346** formation. While DMF, the solvent least prone to deprotonation with the weakest C-H bonds, does not yield substantial amounts of hydrotrifluoromethylation product **346**. This interpretation of Table 3-10 relies on a thermodynamic explanation; however, a kinetic argument can also be made where the C-H bonds in DMF are viewed as hydric while the C-H bonds of acetone and acetonitrile are seen as electron deficient. So, hydrotrifluoromethylation product **346** may form by preferential HAT from acetone or acetonitrile to nucleophilic ureido benzyl radical (**334**), which occurs to a lesser degree with DMF. Also, the radicals of solvent that have been subjected to HAT can be reduced to their respective anions by the radical anion of 4CzIPN (**332**), a process that is conceivably more exergonic with acetone and acetonitrile over DMF. So, the solvent-dependent outcome of Table 3-10 may be derived from a Curtin–Hammett principle scenario, where the radicals of acetone and acetonitrile formed by HAT to ureido benzyl radical (**334**) are reduced by the radical anion of 4CzIPN (**332**) faster than radicals formed by HAT of DMF.

An alternative mechanism to Scheme 3-34 for the 4CzIPN (**91**)-catalysed trifluoromethyl-arylation of vinyl urea is depicted in Scheme 3-42. Wherein ground state 4CzIPN (**91**) is photoexcited (**330**) by absorption of a photon, then oxidises Langlois reagent (**134**) forming trifluoromethyl radical (**331**), sulfur dioxide and 4CzIPN radical anion (**332**). Trifluoromethyl radical (**331**) adds to vinyl urea (**333**) forming ureido benzyl radical **334**, which is then not reduced by 4CzIPN radical anion (**332**). Instead, the photoredox cycle does not close and ureido benzyl radical **334** is directly reduced by Langlois reagent (**134**), forming α -metalated urea **335**, sulfur dioxide and trifluoromethyl radical (**331**). Newly generated trifluoromethyl radical (**331**) adds to vinyl urea (**333**) propagating the radical chain. α -Metalated urea (**335**) performs N to C intramolecular arylation to give α -tertiary urea (**336**). Thus, the proposed mechanism of Scheme 3-42 renders photocatalyst 4CzIPN (**91**) as an initiator rather than a mediator of a catalytic loop.



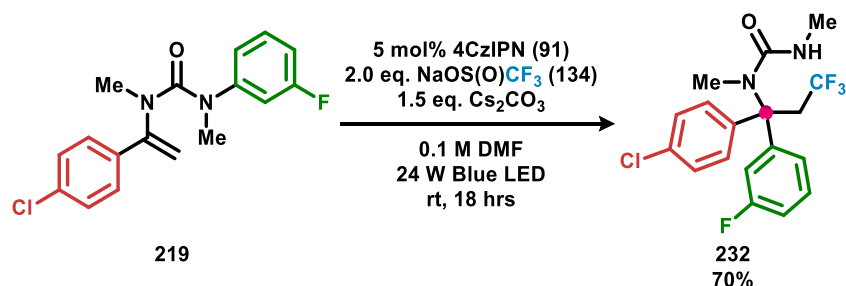
Scheme 3-42. Proposed radical-chain mechanism for the 4CzIPN (**91**) initiated trifluoromethyl-arylation of vinyl ureas. Asterisks denotes photoexcited state.

Quantum yield measurement of photochemical reactions is a useful method of determining the presence of radical chains. A photoredox catalytic cycle can only afford a maximum theoretical quantum yield of one, where every photon absorbed by the photocatalyst results in one molecule of product being produced. Any non-productive photochemical processes such as phosphorescence, internal conversion, or back electron transfer would only decrease the observed quantum yield. With regards to a radical chain mechanism, the quantum yield can be much larger than one, as one initiation from a photon can lead to multiple product formation events.¹⁸⁰

To gain insight into which mechanistic paradigm (Scheme 3-34 vs Scheme 3-42) is present for the trifluoromethyl-arylation of vinyl urea, a quantum yield (Φ) for such a reaction was sought. First the photon flux of a photoreactor set up was determined by ferrioxalate actinometry to be 1.33×10^{-9} Einsteins. s^{-1} (See Experimental for details).^{180,181} The light source of the photoreactor set up was a single 0.1 W blue LED, opposed to an array of 24 W blue LEDs used throughout this study. The change of light source to a weaker LED was to maximise the ratio of propagation events to initiation events in any possible radical chains. With the photon flux of a photoreactor set up determined it can be used calculate the quantum yield of a reaction, using equation (1). Where t is the duration of the reaction in seconds and f is the fraction of absorbed light at $\lambda = 450$ nm for a 5.0×10^{-3} M solution of 4CzIPN (**91**) in DMF measured to be 0.999 (derived from $f = 1 - 10^{-A}$ where A is absorbance at 450 nm measured by UV-Vis spectroscopy).

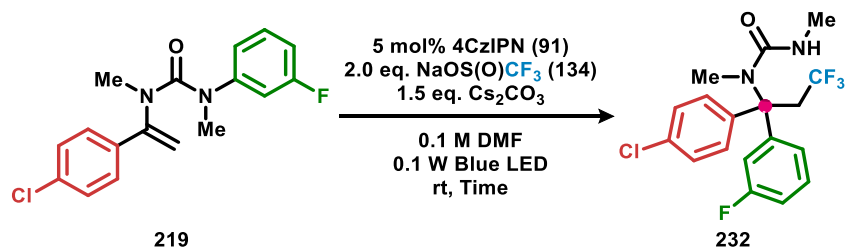
$$\Phi = \frac{\text{mol product}}{\text{photon flux} \times t \times f} \quad (2)$$

A requirement for good quantum yield elucidation is that the reaction mixture is homogeneous to allow for maximum light penetration into solvent and minimal light scattering off particulates. To meet this requirement in the context of the trifluoromethyl-arylation of vinyl urea, which generally gives heterogeneous reaction mixtures in acetone and acetonitrile, DMF was used as solvent to improve reaction homogeneity. The 4CzIPN (**91**)-catalysed trifluoromethylation with subsequent N to C aryl migration of vinyl urea **219** was still found to give good levels of α -tertiary urea **232** productivity, despite the use of DMF as a subpar solvent according to optimisation studies (Scheme 3-43).



Scheme 3-43. 4CzIPN (**91**)-catalysed trifluoromethyl-arylation of vinyl urea **219** with DMF used as solvent.

Finally, the 4CzIPN (**91**)-catalysed trifluoromethyl-arylation of vinyl urea **219** was performed in the photoreactor of known photon flux for 4 hours and 24 hours independently, affording α -tertiary urea **232** in a 1.3% and 13.1% yield respectively (Table 3-11). Using equation (1) the quantum yields of the two runs for the conversion of vinyl urea **219** to α -tertiary urea **232** in DMF were calculated to be 0.13 and 0.23 giving an average value of 0.18. A quantum yield of 0.18 substantiates the claim that 4CzIPN (**91**)-catalysis is in effect (Scheme 3-34), or any present radical chains are very short.

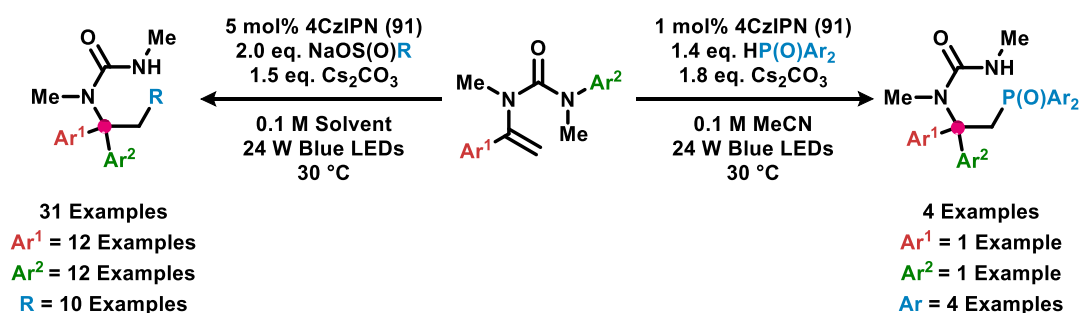


Entry	Time/ hrs	Time/ s	232 / % ^[a]	Moles of 232 / x 10 ⁻⁵	Φ
1	4	14400	1.2	5.0	0.13
2	24	86400	13.1	26.2	0.23

Table 3-11. Quantum yield elucidation for the trifluoromethyl-arylation of vinyl urea **219**.
[a] Yields obtained by ¹⁹F NMR and compared with benzo-trifluoride internal standard.

3.8 Conclusion

A transition metal-free method for the alkyl-arylation of vinyl ureas has been developed, allowing the construction of two carbon-carbon bonds across an olefin in an operationally simple manner (Scheme 3-44). This methodology has been demonstrated through 31 examples to be amenable to a variety of functionality on the migrating aryl group and the aryl group α to the urea tether. Furthermore, studies have shown this method not to be limited to only trifluoromethyl incorporation, but also 1,1-difluoroalkyl groups by use of sodium sulfinate radical precursors other than Langlois reagent. A representative selection of trifluoromethyl-containing α -tertiary urea products have been converted to their respective α -tertiary amines, by solvolysis of the urea. Additionally, preliminary work has been undertaken to demonstrate a photoredox approach for the addition of diarylphosphinoxyl radical to vinyl urea to initiate the N to C aryl migration.



Scheme 3-44. Summarisation of the difunctionalisation protocol developed within this chapter.

This alkyl-arylation approach is built around the use of a photoredox catalyst that is able to generate electrophilic 1,1-difluoroalkyl radical from commercially available sodium sulfonates, which subsequently add to a vinyl urea forming ureido benzyl radical, as shown through radical trapping studies, Stern-Volmer fluorescence quenching and cyclic voltammetry analysis. Direct reduction of the newly generated ureido benzyl radical by sodium sulfinate radical precursor has been shown to be unlikely as an average quantum yield of 0.18 was obtained for a representative example. The ureido benzyl radical is then reduced to α -metalated urea initiating the N to C intramolecular arylation across the urea tether to give an α -tertiary urea, evidence for which is provided through deuterium incorporation studies and a solvent-selectivity study. Thus, this reaction is the first example of a photoredox-catalysed reductive-termination radical-polar crossover where the carbanion product of the photoredox cycle is used in carbon-aryl bond formation.

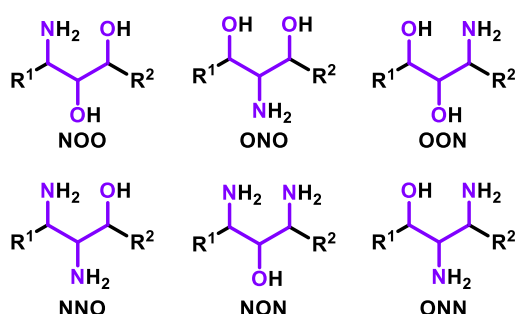
Chapter 2

Aryl Diazonium Salt-Promoted Azo-Cycloamination of Allyl Ureas & Carbamates

4. Vicinal Triamines, 1,2,3-Diamino Alcohols and 1,2,3-Amino Diols

4.1 Importance and Synthesis of 1,2,3-Diamino Alcohols and 1,2,3-Amino Diols

1,2,3-Diamino alcohols and 1,2,3-amino diols (Scheme 4-1) are a commonly found scaffold in medicinally relevant synthetics and natural products, and thus have received the attention of synthetic chemists for the past 50 years.¹⁸² However, the construction of three contiguous carbons each bearing an alcohol or amine functional group is non-trivial. Synthetic challenges related to their construction include avoiding wasteful heteroatom protection and deprotection steps, induction of enantio- and diastereoselectivity, while averting competing substitutions between heteroatoms.



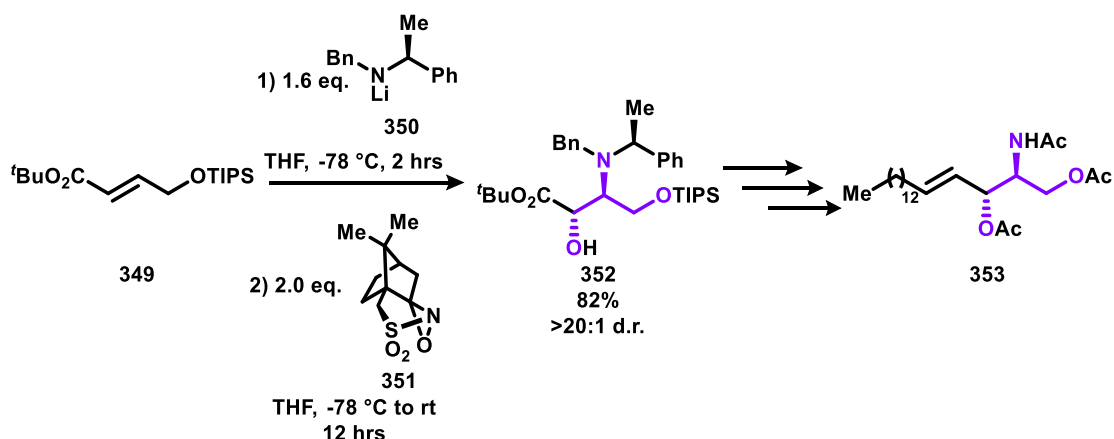
Scheme 4-1. 1,2,3-Amino diols (Top) and 1,2,3-amino diols (Bottom).

1,2,3-Amino diol-containing sphingoid-type bases play significant roles in the plasma membranes of nearly all eukaryotic cells.¹⁸³ Sphingoid-type bases are precursors to sphingolipids, which play significant roles in numerous biological processes¹⁸⁴ and human diseases, including diabetes,¹⁸⁵ cancer¹⁸⁶ and various neurological afflictions.¹⁸⁷ Furthermore, sphingoid-type bases themselves exhibit physiological activity, with both *D*-erythro-sphingosine (**347**) and *D*-erythro-sphinganine (**348**) demonstrating inhibition of protein kinase C (Scheme 4-2).¹⁸⁸



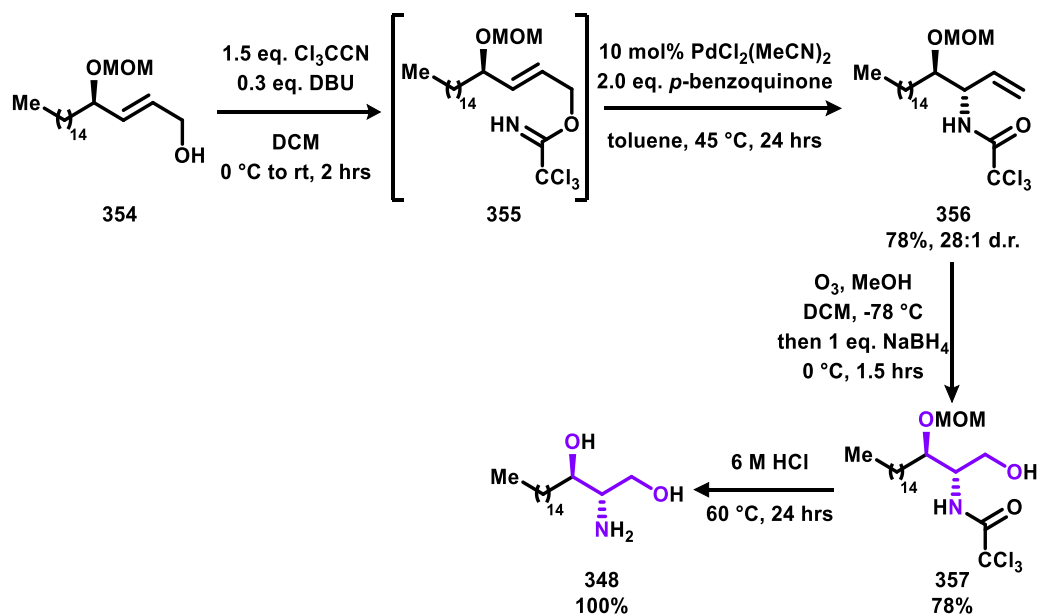
Scheme 4-2. *D*-Erythro-sphingosine (**347**) and *D*-erythro-sphinganine (**348**).

Due to the difficult isolation of sphingolipids from natural sources, various total syntheses of D-*erythro*-sphingosine (**347**) and D-*erythro*-sphinganine (**348**) have been reported.¹⁸⁹ In 2008 Smith and co-workers disclosed a route towards triacylated D-*erythro*-sphingosine (**347**).¹⁹⁰ A diastereoselective *anti*-aminohydroxylation of α,β -unsaturated ester **349** was used for the construction of the 1,2,3-amino diol of **353** (Scheme 4-3). The aminohydroxylation proceeds by conjugate addition with enantiopure secondary lithium amide **350**, followed by one-pot enolate oxidation with (+)-(camphorsulfonyl)oxaziridine (**351**) to give 1,2,3-amino diol **352** as a single diastereomer. 1,2,3-Amino diol **352** was then transformed into the triacylated natural product **353** by using the *tert*-butyl carboxylate as a synthetic handle.



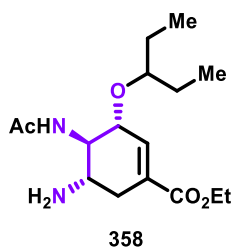
Scheme 4-3. The *anti*-aminohydroxylation of α,β -unsaturated ester **349**.

Synthesis of D-*erythro*-sphinganine (**348**) was completed by Sutherland and co-workers,¹⁹¹ with their 1,2,3-amino diol-forming sequence starting with the acetimidation of allyl alcohol **354** to give trichloroacetimidate **355** (Scheme 4-4). Overman rearrangement of crude trichloroacetimidate **355** gave the 1,2-amino alcohol **356** in a diastereoselective fashion, the selectivity of which was proposed to originate from coordination of palladium(II) with the MOM ether. Next, one-pot ozonolysis and subsequent reduction of 1,2-amino alcohol **356** forms the 1,2,3-amino diol **357**, which upon acid-mediated global deprotection yields the target D-*erythro*-sphinganine (**348**).



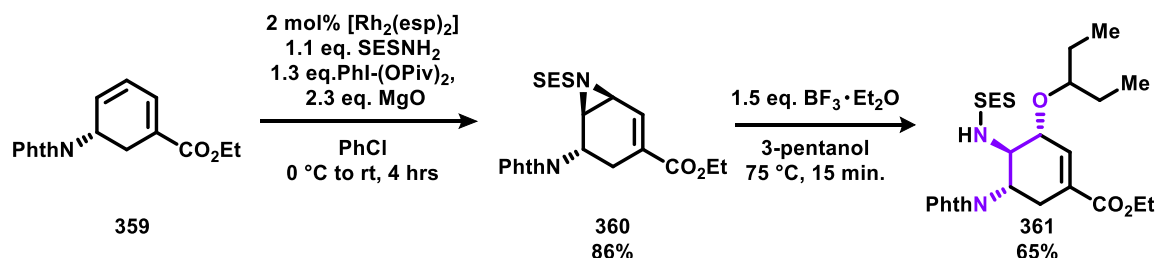
Scheme 4-4. Synthesis of D-*erythro*-sphinganine (**348**) by Overman rearrangement then ozonolysis.

Recently, much academic and media attention has been focused on the very real threat of avian H5N1 influenza virus, which holds a mortality rate of over 50%.¹⁹² (–)-Oseltamivir phosphate (**358**• H_3PO_4 , Scheme 4-5), marketed as Tamiflu is a neuraminidase inhibitor used in the treatment of both type A and type B human influenza,¹⁹³ and represents a promising medicine for combating an H5N1 influenza virus pandemic. However, recent studies have cast a shadow of doubt over the actual effectiveness of (–)-oseltamivir (**358**) in a genuine pandemic, bringing into question the billions of dollars' worth of stockpiling that has been performed by western countries.¹⁹⁴



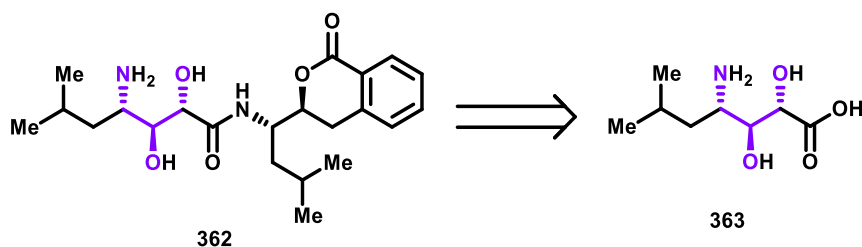
Scheme 4-5. (–)-Oseltamivir (**358**).

Several routes towards (–)-oseltamivir (**358**) have been reported by research groups,¹⁹⁵ with the shortest coming from Trost and co-workers (Scheme 4-6).¹⁹⁶ Their approach to the installation of the 1,2,3-diamino ether of (–)-oseltamivir (**358**) relied on a regio- and diastereoselective rhodium-catalysed aziridination of diene **359** to give aziridine **360**. Lewis acid-mediated opening of aziridine **360** gives the 1,2,3-diamino ether **361**, which is then converted into desired (–)-oseltamivir (**358**) in a few steps.



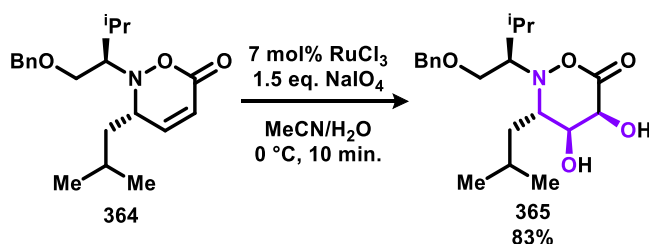
Scheme 4-6. Synthesis of 1,2,3-diamino ether **361** by a rhodium-catalysed aziridination.

In 1997, PM-94128 (**362**) was isolated from the culture broth of *Bacillus* sp. PhM-PHD-090, a bacterium growing in marine sediment. PM-94128 (**362**) demonstrates cytotoxic activity against several tumour cell lines, and is an inhibitor of protein and DNA synthesis.¹⁹⁷ In Vallée and co-workers' synthesis of PM-94128 (**362**), 1,2,3-amino diol fragment (**363**) was identified as a key intermediate for their route (Scheme 4-7).¹⁹⁸



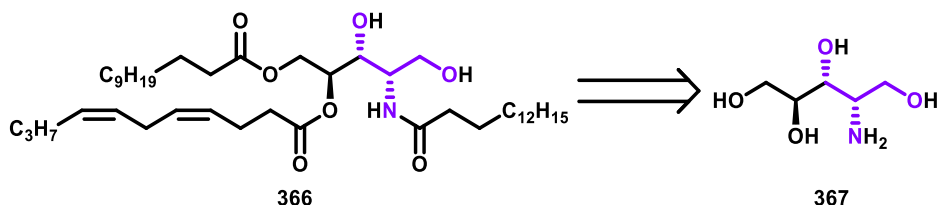
Scheme 4-7. PM-94128 (**362**) and key fragment **363** required for its synthesis.

Vallée and co-workers' approach to the synthesis of 1,2,3-amino diol fragment **363** was by a ruthenium-catalysed dihydroxylation of 1,2-oxazone **364**, which was prepared from (*R*)-valinol (Scheme 4-8).¹⁹⁸ Procedurally, the dihydroxylation of 1,2-oxazone **364** was performed by using Shing's "flash dihydroxylation" conditions to give diol **365** with excellent diastereoselectivity.¹⁹⁹ Subsequent ring-opening of oxazinanone **365** and amide coupling of the resulting carboxylic acid gives access to PM-94128 (**362**).



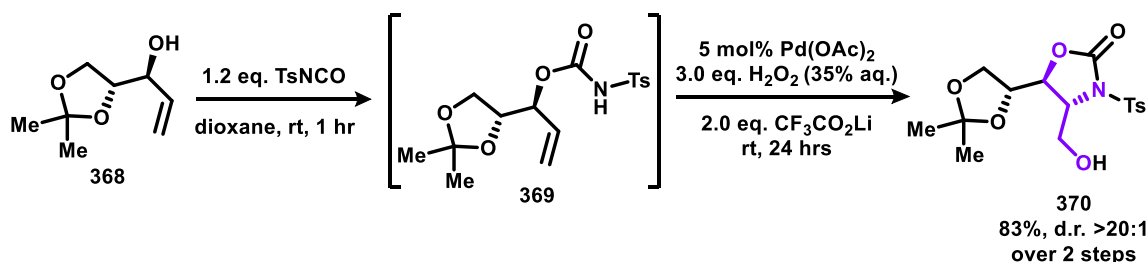
Scheme 4-8. Synthesis of 1,2,3-amino diol **365**, an intermediate for the synthesis of PM-94128 (**362**).

Bathymodiolamide A (**366**), a natural product isolated from the deep-sea hydrothermal vent invertebrate mussel *Bathymodiolus thermophilus*, demonstrates growth inhibition of cervical and breast cancer cell lines.²⁰⁰ Structurally, bathymodiolamide A (**366**) contains an amino alcohol stereo quintad core (**367**), which was of chief consideration to Liu and co-workers in their synthesis (Scheme 4-9).²⁰¹



Scheme 4-9. Bathymodiolamide A (**366**) and its key 1,2,3-amino diol containing core (**367**).

To construct the 1,2,3-amino diol of fragment **367**, Liu and co-workers used a palladium-catalysed aminohydroxylation of allyl alcohol **368**, which was prepared from D-mannitol.²⁰² First, allyl alcohol **368** was converted to carbamate **369** by reaction with tosyl isocyanate. Palladium catalysed aminohydroxylation was then performed in aqueous hydrogen peroxide to access palladium(IV) species and form the 1,2,3-amino diol containing fragment **370** (Scheme 4-10). Completing the amination intramolecularly ensured regioselectivity of the aminohydroxylation across the alkene.



Scheme 4-10. Synthesis of 1,2,3-amino diol containing fragment **370**, by palladium-catalysed aminohydroxylation.

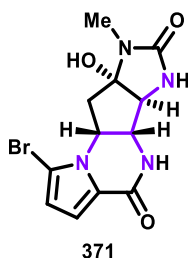
4.2 Importance and Synthesis of Vicinal Triamines

Vicinal triamines, an array of three contiguous carbons each bearing an amine are a feature of numerous bioactive compounds (Scheme 4-11).²⁰³ However, similarly to 1,2,3-amino diols and 1,2,3-diamino alcohols, the construction of vicinal triamines is a challenge that continually requires new approaches to. As such, academic attention has been directed at the development of efficient methodologies for 1,2,3-triamine fragment and natural product preparation.



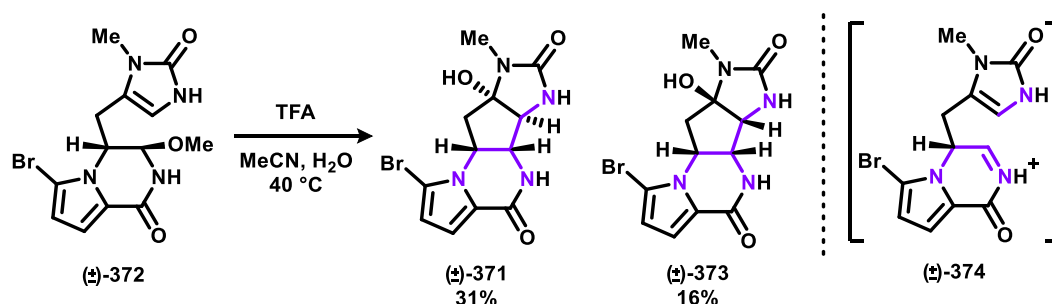
Scheme 4-11. A generic vicinal triamine.

The Agelastatins are a family of cytotoxic pyrrole-imidazole alkaloids, structurally characterised by their unique vicinal triamine containing tetracyclic framework. Agelastatin A (**371**, Scheme 4-12) was isolated in 1993 from the Coral Sea sponge *Agelas dendromorpha* and was found to show antineoplastic activity against multiple tumour cell lines.^{203b,204} Due to the prevalence of agelastatin A (**371**) as a pharmacophore, several syntheses have been explored.²⁰⁵



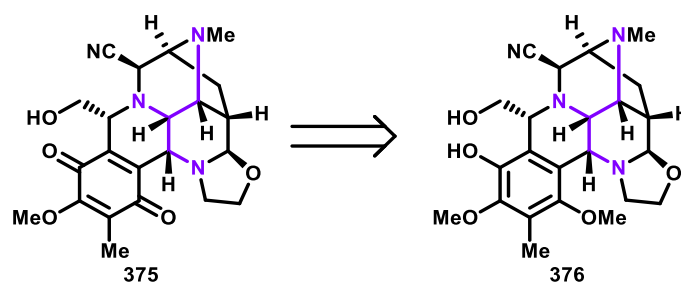
Scheme 4-12. Agelastatin A.

In 2013, Movassaghi and co-workers reported a route towards racemic agelastatin A (**371**) and five other members of the agelastatin family (Scheme 4-13).²⁰⁶ The 1,2,3-triamine of agelastatin A (**371**) was constructed in the final step of the sequence using a bioinspired cyclisation. It was found that late-stage intermediate **372**, derived from aspartic acid,²⁰⁷ undergoes acid-mediated 5-*exo*-trig cyclisation to give agelastatin A (**371**) and its diastereomer **373**. This cyclisation was proposed to initiate by formation of iminium **374** to give the kinetic product **373**, which equilibrates to the thermodynamically favoured agelastatin A (**371**).



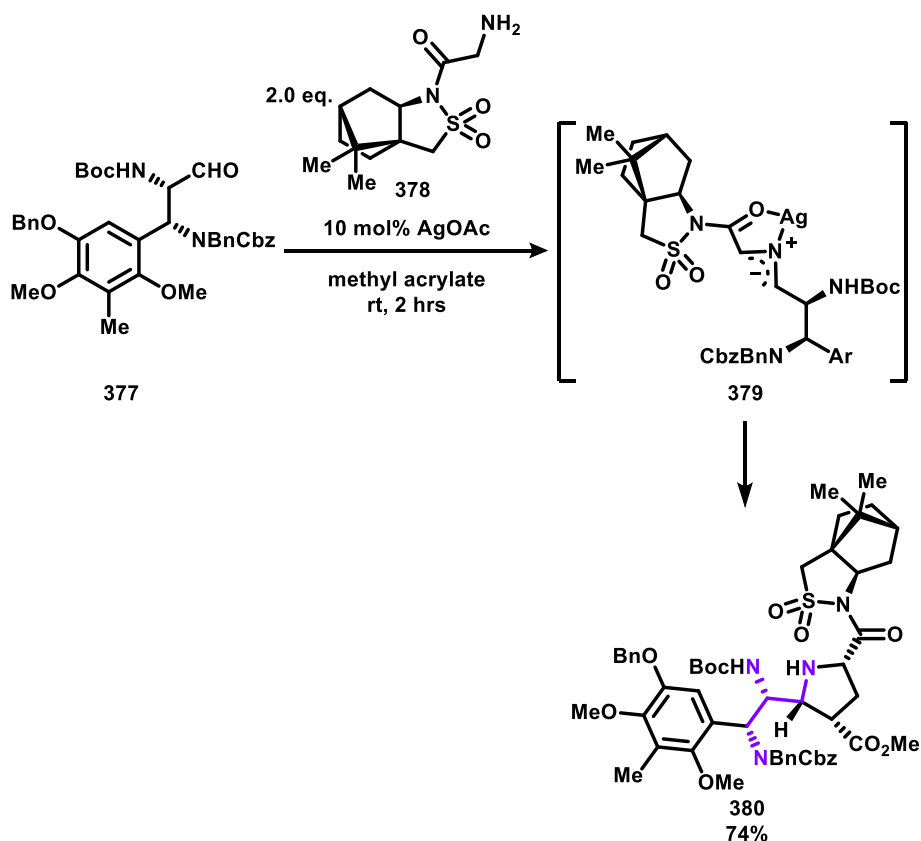
Scheme 4-13. Synthesis of agelastatin A (**371**) and its diastereomer **373** by acid-mediated cyclisation.

Cyanocycline A (**375**, Scheme 4-14) was first isolated in 1982 from the fermentation broth of *Streptomyces flavogriseus* and exhibits a variety of antimicrobial and antitumor activities.^{203c} Cyanocycline A (**375**) contains a vicinal triamine that is a component of five of its six rings. The challenge of reproducing cyanocycline A (**375**) in total synthesis has been completed by several research groups,²⁰⁸ with the shortest route coming Garner and Ümit who completed the synthesis in an impressive 22 steps.²⁰⁹



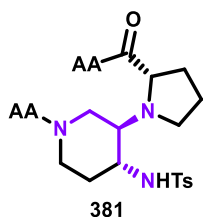
Scheme 4-14. Cyanocycline A (**375**) and a key precursor (**376**) to its synthesis.

Garner and co-worker's synthetic route targeted **376**, a late-stage intermediate of Fukuyama's synthesis of cyanocycline A (**375**) (Scheme 4-14).²⁰⁹ The key transformation of this synthesis was a silver catalysed three-component pyrrolidine formation, by mixing of serine derived aldehyde **377** with L-glycylsultam (**378**) in methyl acrylate to give a single regio- and diastereomer of vicinal triamine **380** (Scheme 4-15). The diastereoselectivity was rationalised to occur by *endo-Si* addition of 2-azaallyl anion **379** to methyl acrylate.



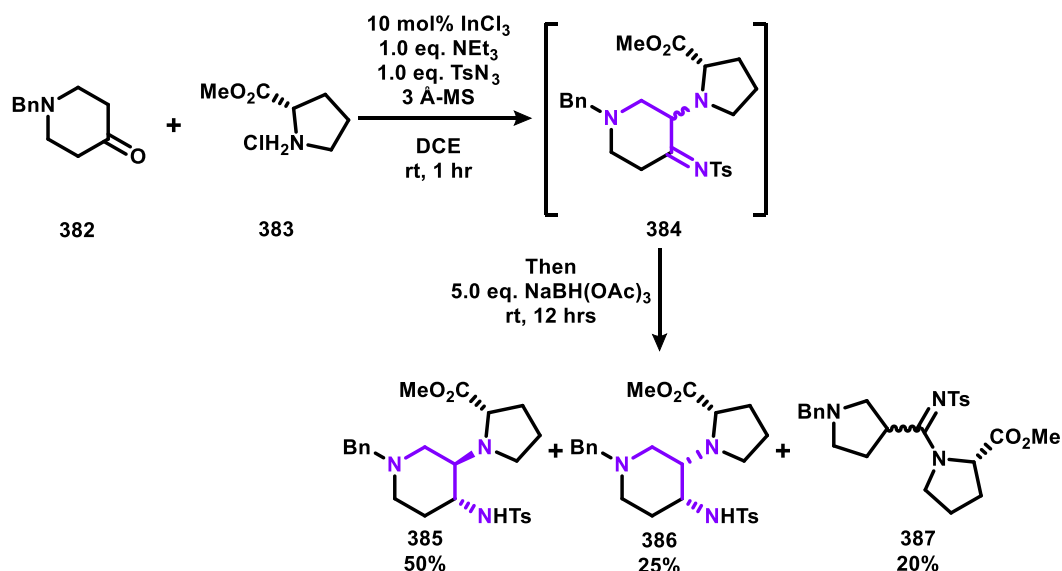
Scheme 4-15. The three-component cyclisation of aldehyde **377** to form key intermediate vicinal triamine **380** for the synthesis of cyanocycline A (**375**).

Peptidomimetics are synthetic molecules able to mimic the folding of peptides and protein fragments, they have widespread application within both chemical biology and medicinal chemistry for the selective perturbation of protein–protein interactions.²¹⁰ The most prevalent nonrepetitive motif of proteins is the four-residue β turn, in which proline and glycine are generally found at the $i+1$ and $i+2$ positions.²¹¹ Numerous synthetic scaffolds that attempt to mimic the β turn of natural peptides have been developed.²¹² In 2014, Pellegrino and co-workers contributed to this field by reporting the vicinal triamine scaffold **381** acts as a β turn nucleator (Scheme 4-16).²¹³



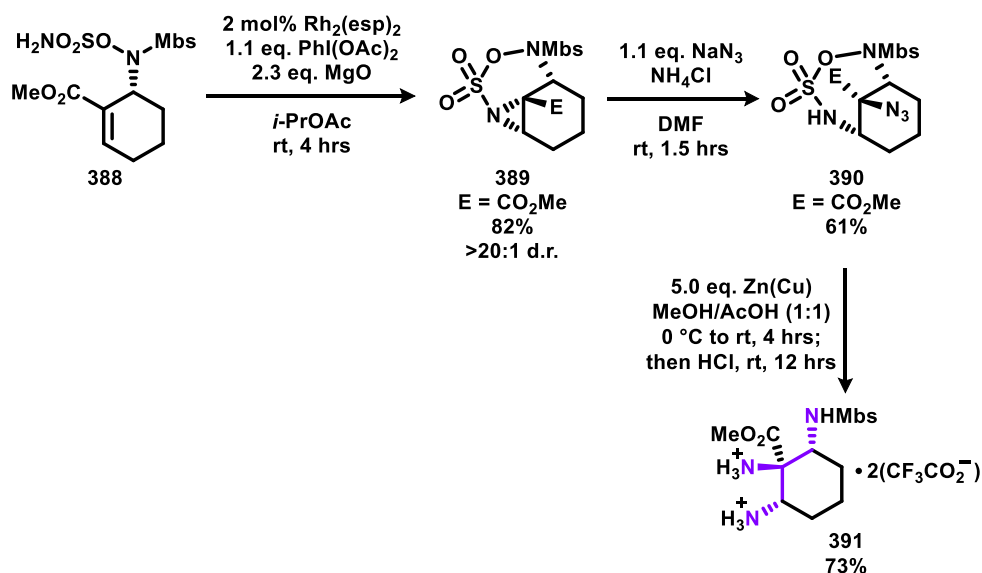
Scheme 4-16. The dipeptide mimic **381** a β turn nucleator. AA - amino acid.

Synthesis of dipeptide mimic **381** is achieved by a three-component coupling between ketone **382**, proline methyl ester (**383**) and tosyl azide (Scheme 4-17).²¹³ The formation of vicinal triamine diastereomers **385** and **386** was proposed to proceed by enamine formation between ketone **382** and proline methyl ester (**383**). The intermediary enamine then engages in [3+2] cycloaddition with tosyl azide, then subsequent concerted proline transposition and expulsion of molecular nitrogen to give imine **384**. Imine **384** is then reduced to vicinal triamine diastereomers **385** and **386**. It was noted that side product **387** is also formed in this reaction, by piperidone contraction instead of proline transposition.



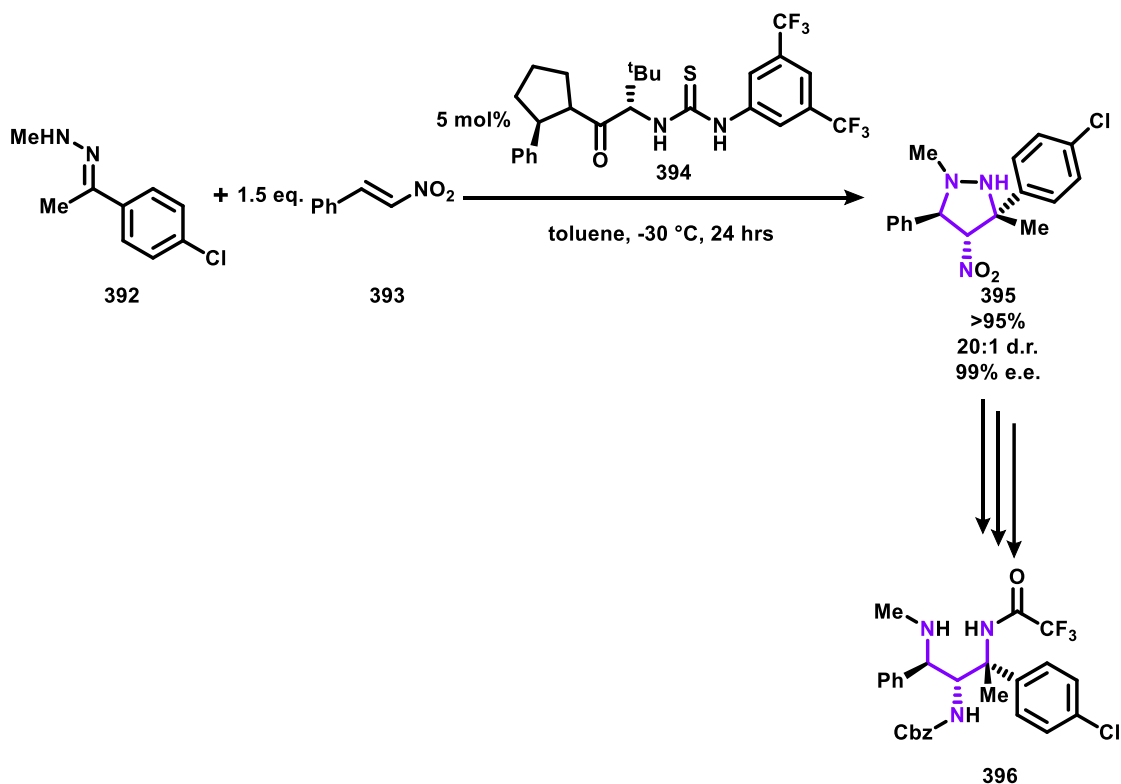
Scheme 4-17. Multicomponent synthesis of vicinal triamine diastereomers **385** and **386**.

Due to the various appearances 1,2,3-triamines make in biologically relevant structures, methodologies have been developed for their specific preparation, away from the context of total synthesis. Trost and co-workers disclosed conditions for the intramolecular aziridination of allylic hydroxylamine-derived sulfamate esters (**388**) to give aziridine (**389**). Aziridine (**389**) was then ring-opened with sodium azide to give the seven-membered heterocycle **390**. Finally, one-pot reduction and deprotection of azide **390** yields the vicinal triamine **391** as an unnatural amino ester.



Scheme 4-18. Synthesis of vicinal triamine **390** by aziridination then aziridine ring-opening.

Finally, Jørgensen and co-workers disclosed conditions for the enantioselective synthesis of 4-nitropyrrolidines as precursors to 1,2,3-triamines (**396**).²¹⁵ This was achieved by a 1,3-dipolar cycloaddition of hydrazones (**392**) with nitro-olefins (**393**), which were activated by hydrogen-bonding thiourea catalyst **394**, allowing control of all three stereocentres of the 4-nitropyrrolidine **395** product. 4-Nitropyrrolidine **395** could then be converted to its corresponding 1,2,3-triamine (**396**) by nitro reduction then N-N reductive cleavage.

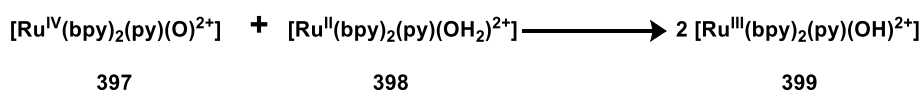


Scheme 4-19. Synthesis of 1,2,3-triamine (**396**) by 1,3-dipolar cycloaddition.

5. Project Background

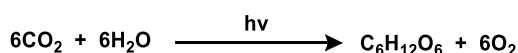
5.1 Photoredox Catalysis and Proton-Coupled Electron Transfer

The term proton-coupled electron transfer (PCET) was first coined in 1981, to describe the elementary step of a simultaneous proton and electron transfer. PCET was originally used to define the comproportionation process between the ruthenium complexes **397** and **398** to give two equivalents of ruthenium complex **399**, in which a proton and electron are synchronously transferred from $\text{Ru}^{\text{II}}\text{-OH}_2^{2+}$ to $\text{Ru}^{\text{IV}}\text{=O}^{2+}$ (Scheme 5-1).²¹⁶ Further distinctions can be made within PCET; if an electron and proton both travel in an elementary step this is said to be a concerted PCET, such as the one depicted in Scheme 5-1. Furthermore, unlike hydrogen atom transfer (HAT), where a proton and electron travel as H^\bullet , in multisite PCET the proton and electron need not originate nor terminate from the same bond or even the same molecule.



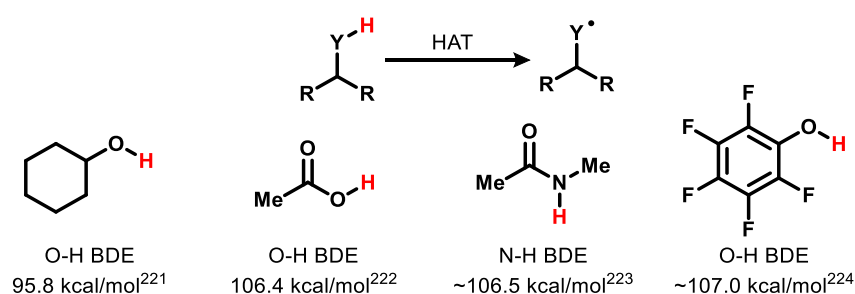
Scheme 5-1. Comproportionation of ruthenium complexes **397** and **398** by PCET.

From its inception, PCET as a terminology has found applicability in various fields of chemistry, such as enzymatic C-H bond oxidation,²¹⁷ biosynthesis of natural products²¹⁸ and several small molecule activation techniques.²¹⁹ Photosynthesis for example is a stunning success of PCET, with 12 electrons and protons being transferred upon photoexcitation from at least 24 photons (Scheme 5-2).²²⁰ However, despite the frequent identification of PCET processes within biological systems, the use of PCET as an enabling mechanism for organic synthesis has only begun to be explored in recent years.



Scheme 5-2. Overall chemical equation of photosynthesis.

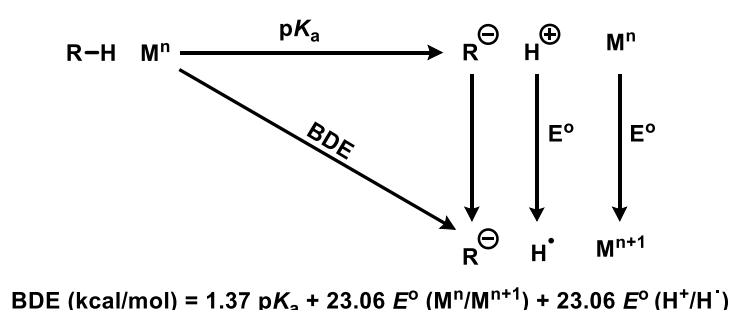
Similarities can be drawn between multisite PCET and HAT, in that both processes involve the transfer of the constitutional parts of H^\bullet to provide a neutral free radical product. The thermodynamic driving force of HAT reactions is correlated to the net increase in bond energy of the bonds being broken and formed. Therefore, the homolytic cleavage of a strong bond between hydrogen and a donor requires the formation of an equally strong or stronger bond between hydrogen and an acceptor. This thermodynamic limitation creates a substantial challenge when developing methodologies by homolytic bond activation, as it typically restricts reactions entirely to exergonic processes (Scheme 5-3).



Scheme 5-3. Examples of organic functionality that possess bonds with high BDEs.

A variety of protic organic functionality display bond-dissociation energies (BDEs) greater than 100 kcal/mol (Scheme 5-3). Consequently, homolytic activation of common O-H and N-H bonds even by the most powerful HAT mediators, such as organometallic tungsten complexes,²²⁵ are usually ineffective. It is also worth noting that typical alkyl C-H bonds possess lower BDEs than O-H and N-H bonds, resulting in unselective homolytic activation across the carbon framework of most saturated organic molecules when strong HAT reagents are used.

The conventional method for defining covalent bond energies, popularised by Bordwell, is through observing the energy required for heterolytic bond cleavage, represented by pK_a , summed together with the energies needed to oxidise the resulting anion and reduce the resulting proton to their respective neutral radicals.²²⁶ In 2010 Mayer brought to attention that the classical method of conceptualising BDEs draws thermodynamic parallels between HAT and multisite PCET, in that a hydrogen atom acceptor may be seen to be equivalent to a Brønsted base and a one-electron oxidant. Despite there being no formal homolytic bond cleavage in an oxidative multisite PCET, the capacity for a base and an oxidant to act as a hydrogen atom acceptor can be assessed by summing of the pK_a and redox potential values to give the 'effective' BDE. This highlights an advantage of multisite PCET over HAT, in that the pK_a and redox potential of the respective base and oxidant (or acid and reductant) can be independently tuned, which are inversely correlated properties and hard to adjust within a sole HAT mediator. This practically manifests as a tool to easily identify acid/reductant combinations and base/oxidant pairings with desirable BDEs (Scheme 5-4).



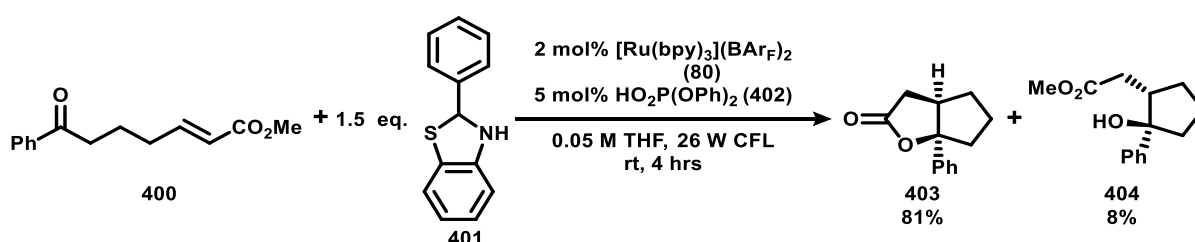
Hydrogen Atom Acceptor Pair

Oxidant	Base	E° (V)	pK_a	'BDE' / kcal.mol ⁻¹
$\text{Fe}^{\text{III}}(\text{bpy})_3$	pyridine	0.70	12.5	87
* $\text{Ru}^{\text{II}}(\text{bpy})_3$	acetate	0.39	23.5	96
* $\text{Ru}^{\text{II}}(\text{bpz})_3$	lutidine	1.07	14.1	100
$\text{Ir}^{\text{III}}(\text{dF}(\text{CF}_3)\text{ppy})_2(\text{bpy})$	DMAP	1.0	18.0	103

Scheme 5-4. Square scheme of a generic multisite PCET manifold to give the 'effective' BDE in acetonitrile. Example bond strengths available by the joint action of a selection of base/oxidant pairs. Asterisks denotes ET from a photoexcited state.²²⁷

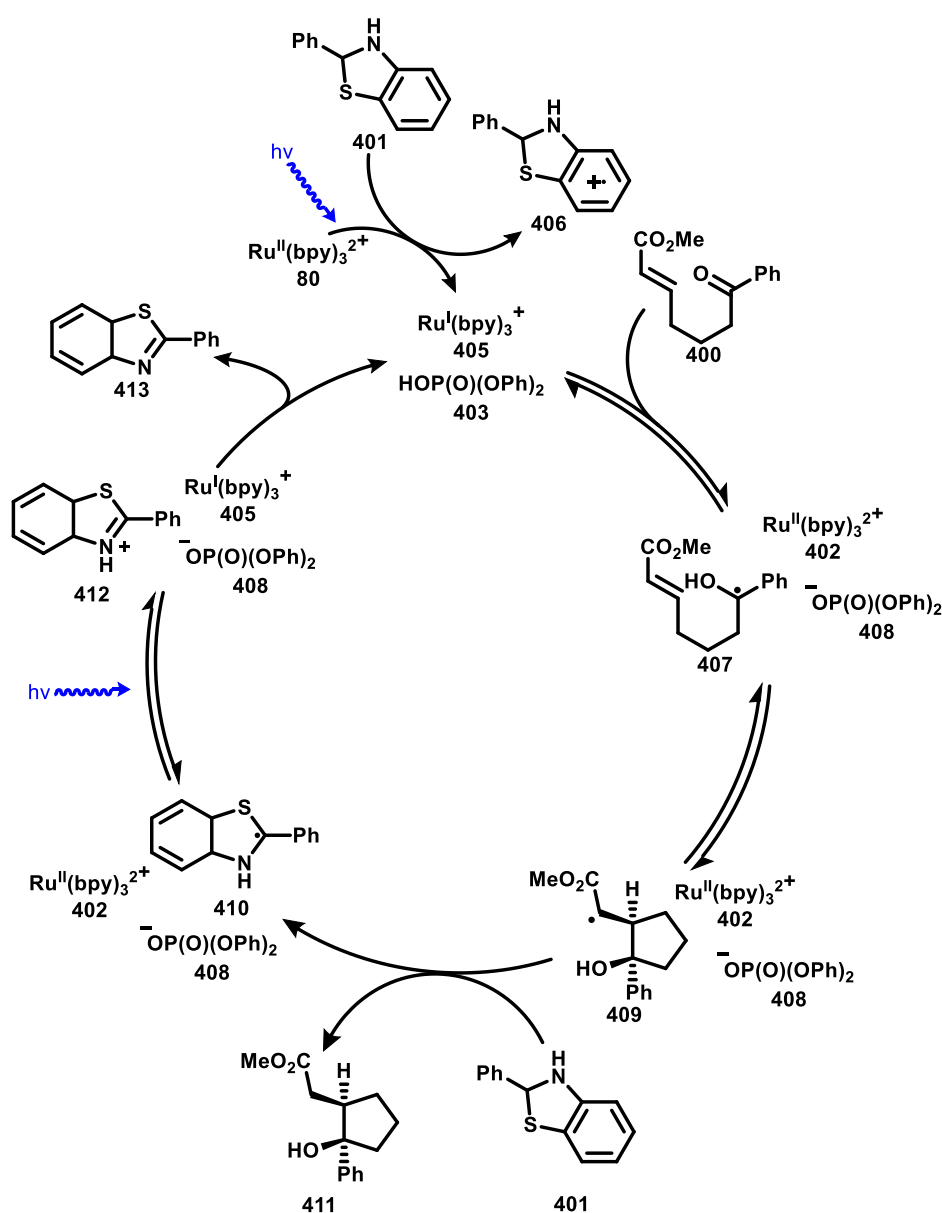
Multisite PCET also allows for the selective homolytic activation of N-H and O-H bonds in the presence of C-H bonds. C-H bonds are typically poor hydrogen bond donors; therefore, a base/oxidant pair can engage in initial pre-association between a polar O-H or N-H bond and a base by hydrogen bonding. Hydrogen bonding of a base with a targeted bond confines the subsequent deprotonation and electron removal to the hydrogen bond donating substrate. Lastly, the formation of a hydrogen bond can be viewed as initial progression through the reaction coordinate of a PCET, allowing for the use of redox mediators that possess insubstantial potentials for electron transfer.²²⁷

Use of PCET for enabling organic synthesis was popularised by Knowles through several seminal reports.^{102c,228} In 2013 Knowles and co-workers disclosed the catalytic generation of ketyl radicals by multisite PCET (Scheme 5-5).²²⁹ The reduction potential of ketones is substantial (acetophenone: $E_{1/2}^{\text{red}} = -2.48 \text{ V vs Fc/Fc}^+$),²³⁰ rendering them an inert functionality to all but the most reducing photocatalysts. In addition, ketones are weakly basic (acetophenone: $\text{p}K_{\text{a}} = -0.1$), so only particularly strong acids are able to generate any practical quantities of the protonated carbonyl.²³¹ However, Knowles and co-workers demonstrated that through reductive multisite PCET, photocatalyst **80** ($\text{Ru}^{\text{I}}/\text{Ru}^{\text{II}} = -1.71 \text{ V vs Fc/Fc}^+$) and diphenyl hydrogen phosphate (**402**) ($\text{p}K_{\text{a}} = 13$) could be used for formal H^{\bullet} donation into ketones for ketyl radical generation, with dihydrobenzothiazole **401** used as a sacrificial electron donor. Ketyl formation from ketone **400** results in a 5-exo-trig radical cyclisation to give bicyclic lactone **403** and ester **404**.



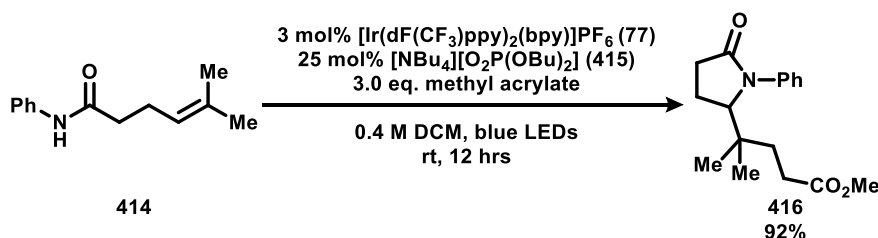
Scheme 5-5. Ketyl-olefin coupling by multisite PCET ketyl radical generation.

The mechanism for Scheme 5-5 was proposed to initiate by photoexcitation of ruthenium complex **80** followed by subsequent reductive quenching with electron donor **401** to give the ruthenium complex **405** and persistent radical cation **406** (Scheme 5-6). Ruthenium complex **405** and diphenyl hydrogen phosphate (**403**) facilitate reductive PCET of ketone **400** to give the ketyl radical **407**, diphenyl phosphate (**408**) and regenerated photocatalyst **80**. The nucleophilic ketyl radical **407** undergoes cyclisation with the pendent electrophilic olefin generating ester-stabilised radical **409**, which abstracts a hydrogen atom from electron donor **401** to yield the phenyl-stabilised radical **410** and the desired product **411**. To complete the catalytic cycle, ruthenium complex **80** undergoes photoexcitation then reductive quenching with phenyl-stabilised radical **410** to give iminium **412** and regenerate ruthenium complex **405**. Diphenyl phosphate (**408**) deprotonates iminium **412** producing thiazole by-product **413** and reforming diphenyl hydrogen phosphate (**403**).²²⁹



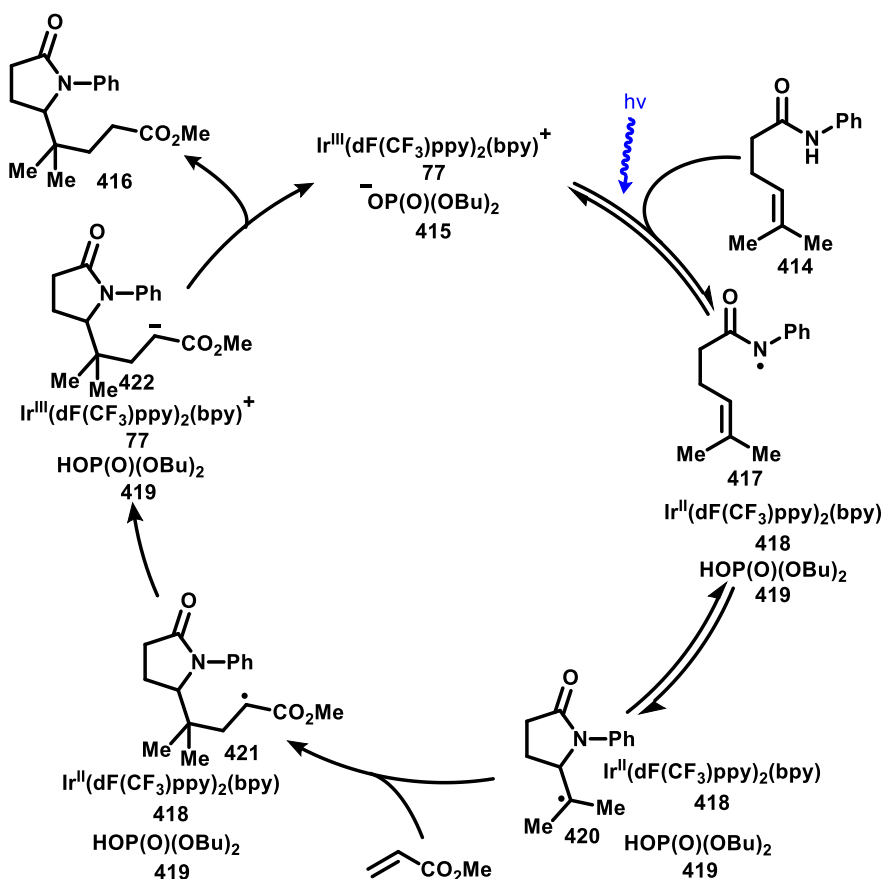
Scheme 5-6. Catalytic cycle for the reductive PCET-mediated ketyl-olefin coupling.

Later, in 2015 Knowles and co-workers reported the carboamination between anilides containing a pendant olefin with electrophilic radical acceptors, by the oxidative PCET of N-H bonds (Scheme 5-7).²³² It was highlighted that the N-H bond of amide **414** possesses large pK_a and oxidation potential values ($pK_a = 32$; $E_{1/2}^{ox} = 1.2$ V vs Fc/Fc⁺). However, it was shown that by using iridium photocatalyst **77** ($E_{1/2}^{ox} = 1.04$ V vs Fc/Fc⁺, from an photoexcited state) and hydrogen-bond acceptor dibutyl phosphate (**415**) ($pK_a = 13$), components that cannot perform an electron or proton transfer individually, amidyl radical formation is achieved. Once amidyl radical formation of amide **414** occurs, cycloamination followed by radical addition to methyl acrylate gives lactam **416**.



Scheme 5-7. Carboamination of olefin-containing amide **414** by oxidative PCET.

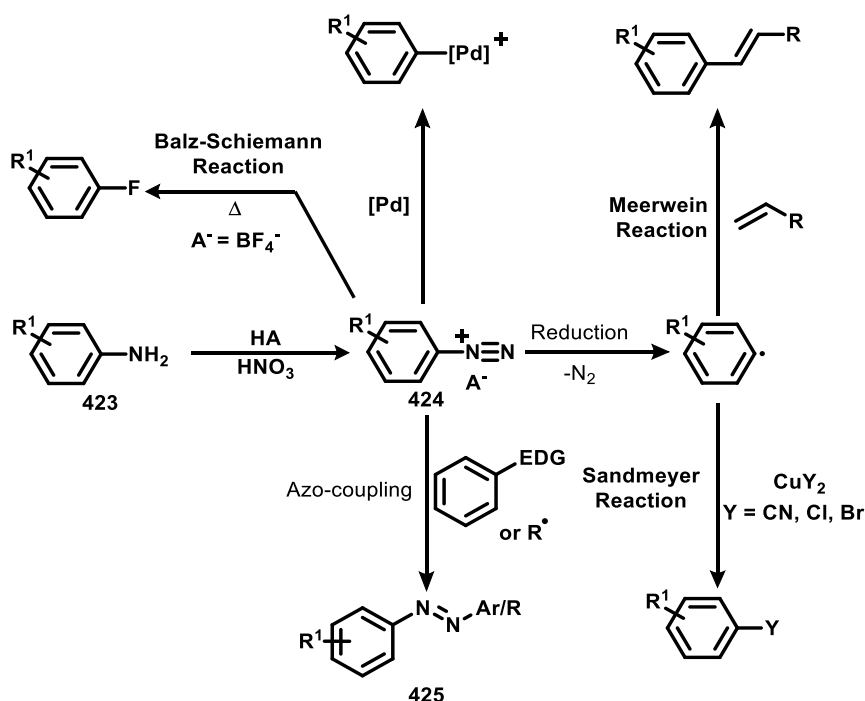
The catalytic cycle of Scheme 5-7 starts with photoexcitation of iridium photocatalyst **77**, which with dibutyl phosphate (**415**) mediates the oxidative PCET of amide **414** to give N-centred radical **417**, iridium complex **418** and dibutyl hydrogen phosphate (**419**). The N-centred radical **417** undergoes cyclisation to give the nucleophilic C-centred radical **420**, which adds to methyl acrylate generating intermediate ester-stabilised radical **421**. Radical **421** is reduced by iridium complex **418** to the carbanion **422**, which is protonated by dibutyl hydrogen phosphate (**419**) and closes the catalytic cycle.



Scheme 5-8. Catalytic cycle for the oxidative PCET-mediated carboamination of anilides containing a distal alkene.

5.2 Aryl Diazonium Salts as Amine Transfer Reagents

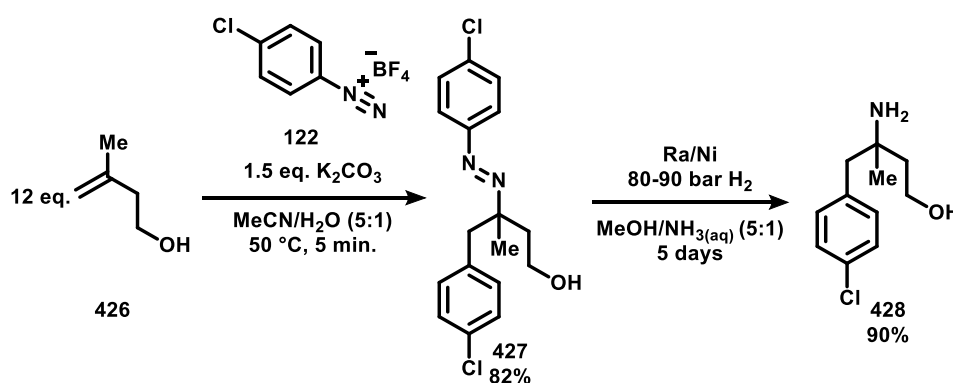
Aryl diazonium salts (**424**) as a class of molecule were first reported in 1858 by Peter Griess, when he disclosed conditions for the diazotization of anilines (**423**) with nitrous acid and picramic acid.²³³ Since the discovery of aryl diazonium salts they have found application in surface chemistry,²³⁴ assembly of soluble carbon nanotubes,²³⁵ molecular optoelectronics²³⁶ and silicon-molecule junctions.²³⁷ However, the field of synthetic chemistry is where aryl diazonium salts have found the most use. Aryl diazonium salts are amenable substrates in a variety of synthetic transformations, such as palladium-catalysed cross-couplings,²³⁸ fluorination by the Balz-Schiemann reaction²³⁹ and aryl radical generation for Meerwein²⁴⁰ or Sandmeyer chemistry (Scheme 5-9).²⁴¹ These transformations are only possible due to the diazonium functional group acting as a very efficient leaving group, by expulsion of molecular nitrogen.



Scheme 5-9. Generalised synthesis of diazonium salts from anilines (**423**) and a selection of their common transformations.

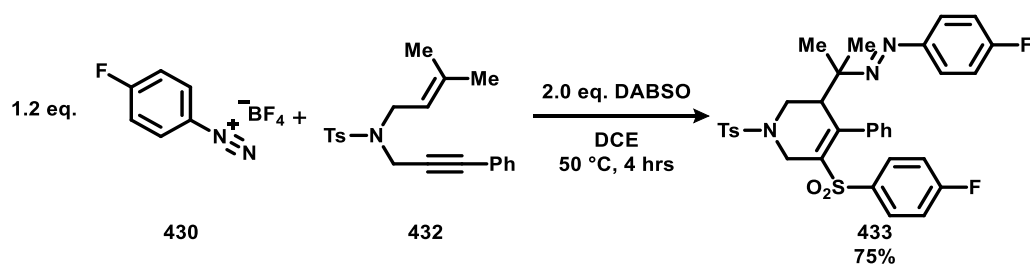
In addition to the reactivity depicted in Scheme 5-9, aryl diazonium salts (**424**) also possess an electrophilic site on the terminal nitrogen, which allows their azo-coupling with electron-rich aryls or radical donors to yield azo compounds (**425**) that find common use as dyes.²⁴² However, azo compounds have recently become of more medicinal and synthetic importance. The azo functional group can be reductively cleaved to give the primary amines of the two constituent parts of the original azo compound. Therefore, the *N*-terminus of an aryl diazonium salt can be viewed as an amine transfer reagent. Furthermore, azo compounds have been investigated as potential prodrugs that adopt an inactive form until they reach the colon, where the therapeutically active amine is revealed upon site-specific reduction catalysed by bacterial extracellular azoreductase.²⁴³ Subsequently, academic attention has been directed at the installation and reductive cleavage of azo functionality (*vide infra*).

In 2015 Heinrich and co-workers reported the Meerwein-type carboamination protocol of 1,1-disubstituted alkenes (**426**) (Scheme 5-10).²⁴⁴ In this reaction aryl diazonium salts (**122**) are used to perform a dual function of being a source of aryl radical donor and electrophilic radical acceptor. The reaction is carried out by slow addition of aryl diazonium salts to a solution of olefin and potassium carbonate. It was proposed that Gomberg–Bachmann-type decomposition of aryl diazonium salt generates aryl radical, which attack 1,1-disubstituted alkene forming nucleophilic tertiary C-centred radical. The newly formed tertiary C-centred radical attacks the *N*-electrophilic site of an aryl diazonium salt, forming a N-centred radical cation that is claimed to be reduced by separate olefin starting material (**426**) to give the final azo product (**427**). One of the azo-compound products (**427**) of this Meerwein-type carboamination was submitted to conditions for reductive cleavage of the azo bond to give the primary amine (**428**).



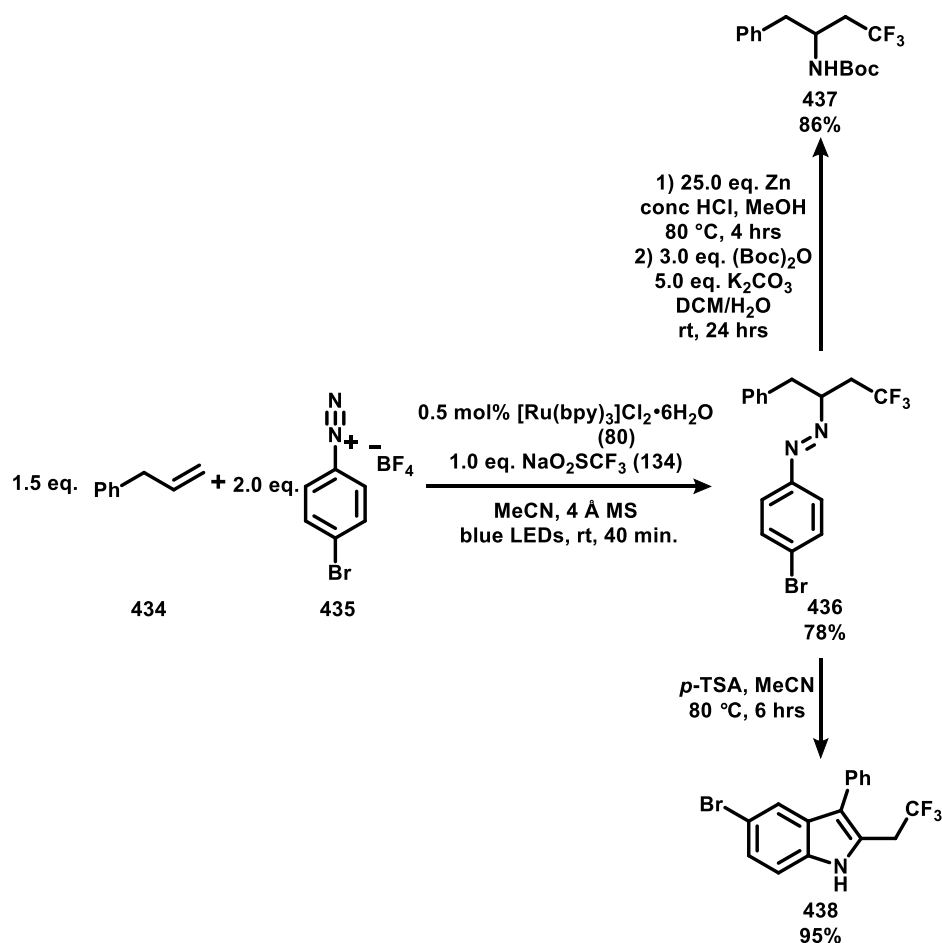
Scheme 5-10. Meerwein-type carboamination of olefin **426**.

Aryl diazonium salts possess very low reduction potentials ($E_{1/2}^{\text{red}} = -0.06$ V vs SCE, for PhN_2BF_4),²⁴⁶ as such they can oxidise other reaction components in addition to reacting in their typical manner. This was used by Wu and co-workers in the in situ oxidation of DABSO by aryl diazonium salts **430** to generate the ammonium cation of $\text{DABCO}\cdot(\text{SO}_2)$, sulfur dioxide and aryl radical (Scheme 5-12).²⁴⁷ The aryl radical is then trapped by sulfur dioxide to give aryl sulfonyl radical, which attacks the alkyne **432** to produce a phenyl-stabilised C-centred radical. The intermediary phenyl-stabilised C-centred radical engages in cyclisation with a distal alkene to yield a nucleophilic tertiary C-centred radical, which attacks diazonium salt **430** forming a N-centred radical cation that oxidises another DABSO to generate the desired product **433**. The newly oxidised DABSO decomposes to ammonium cation of $\text{DABCO}\cdot(\text{SO}_2)$ and sulfur dioxide, which with the previously formed ammonium cation of $\text{DABCO}\cdot(\text{SO}_2)$ eventually forms two equivalents of $\text{DABCO}\cdot(\text{SO}_2)$ and one equivalent sulfonyl fluoride.



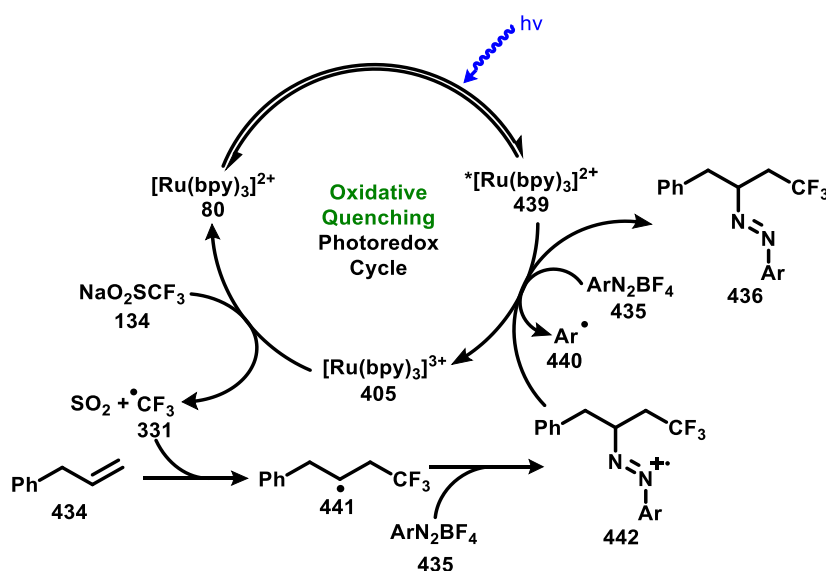
117

Due to the nature of aryl diazonium salts to act as radical acceptors, it is a natural progression for them to be used as substrates in PRC. Xiao and co-workers demonstrated the ruthenium complex **80** catalysed azo-trifluoromethylation of alkenes (**434**) with aryl diazonium salts (**435**) and Langlois reagent (**134**) to give trifluoromethyl-containing azo compounds (**436**) (Scheme 5-13).²⁴⁸ Reductive cleavage of the azo bond of the azo-trifluoromethylation product **436** to the primary amine **437** was demonstrated by use of acid and elemental zinc. Additionally, azo-trifluoromethylation product **436** was shown to participate in an acid facilitated isomerization/cyclization cascade to yield indole **438**.



Scheme 5-13. Azo-trifluoromethylation of alkenes by photoredox catalysis.

The mechanism of Scheme 5-13 was proposed to proceed by photoexcitation of ruthenium complex **80** (**439**) (Scheme 5-14). It was noted that photoexcited ruthenium complex **439** is not a strong enough oxidant ($E_{1/2}(\text{PC}^*/\text{PC}^-) = 0.77 \text{ V vs SCE}$) for the oxidation of Langlois reagent (**134**) ($E_{1/2}^{\text{ox}} = 1.05 \text{ V vs SCE}$).⁸⁶ Instead photoexcited **439** first reduces aryl diazonium salt (**435**) to generate ruthenium complex (**405**), aryl radical (**440**) and molecular nitrogen. Ruthenium complex **405** serves as a powerful oxidant ($E_{1/2}(\text{PC}^+/\text{PC}) = 1.29 \text{ V vs SCE}$), which oxidises Langlois reagent (**134**) and decomposes to trifluoromethyl radical (**331**) and sulfur dioxide. Trifluoromethyl radical attacks the terminal end of olefin **434** to give C-centred radical **441**, which attacks an aryl diazonium salt (**435**) to yield N-centred radical cation **442**. Radical cation **442** is reduced by photoexcited ruthenium complex **80** (**439**) to yield desired product **436** and regenerate ruthenium complex **405**, which continues the catalytic cycle. This work highlights the dual nature of aryl diazonium salts to act as radical acceptors and sacrificial oxidants to promote an oxidative quenching PRC manifold.²⁴⁸

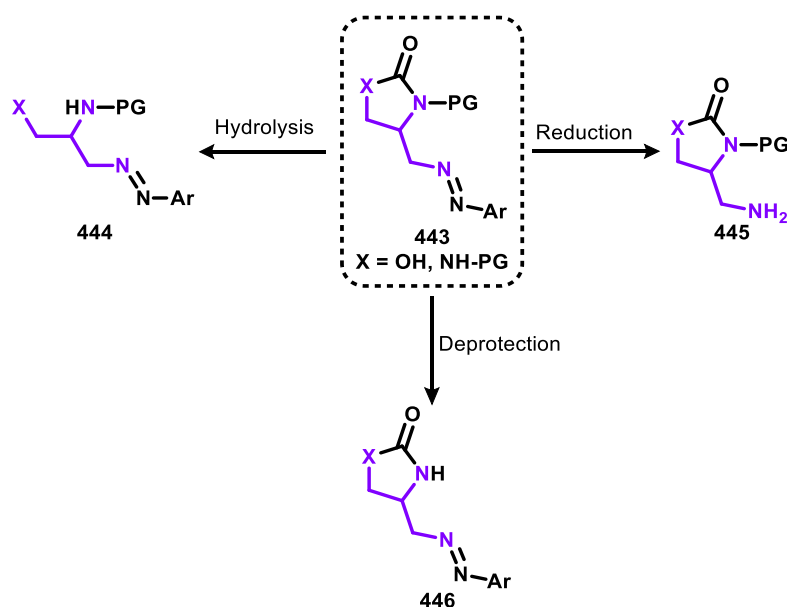


Scheme 5-14. Proposed mechanism for the azo-trifluoromethylation of olefins by photoredox catalysis. Asterisks denotes photoexcited state. Ar - *para*-bromophenyl.

6. Results and Discussion

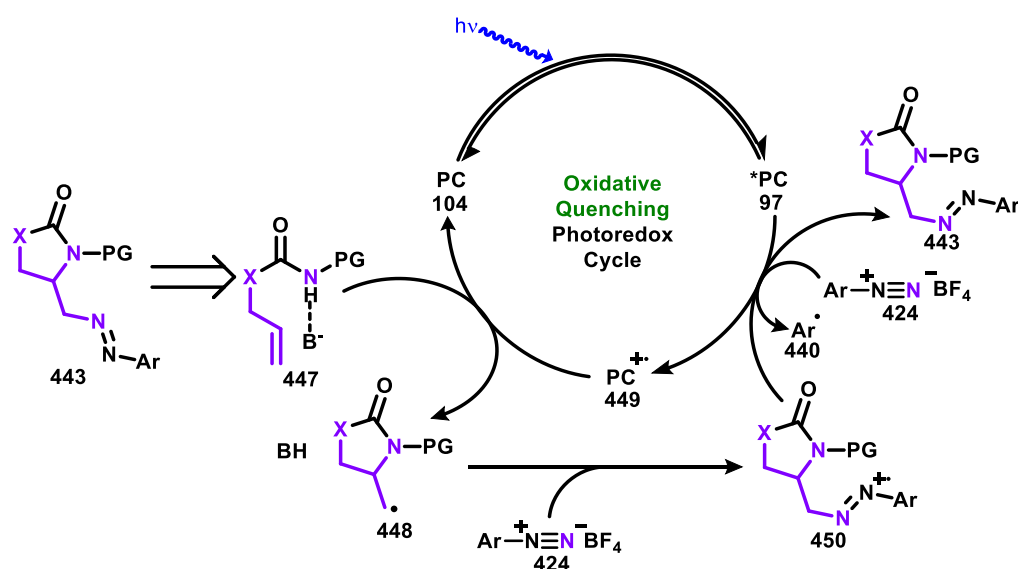
6.1 Project Aims

This project aims to develop methodology for the construction of 1,2,3-triamine and 1,2,3-diamino alcohol fragments, from azo compound derivatives of imidazolidinone and 2-oxazolidone (**443**) (Scheme 6-1). It is reported that imidazolidinones and 2-oxazolidones can be hydrolysed, implying the conversion of common intermediate **443** to azo compound **444** to be possible.²⁴⁹ As previously discussed, azo compounds can be reductively cleaved to primary amines, giving confidence that transformation of common intermediate **443** to primary amine **445** is feasible. Finally, the removal of an appropriate protecting group of the central nitrogen of common intermediate **443** to give azo compound **446** was planned. Therefore, azo compound derivatives of imidazolidinone and 2-oxazolidone (**443**) may practically offer an approach to individually reveal each heteroatom of 1,2,3-triamine and 1,2,3-diamino alcohol fragments for further functionalisation.



Scheme 6-1. Deprotection strategy of each heteroatom of a generalised azo compound derivative of imidazolidinone and 2-oxazolidone (**443**).

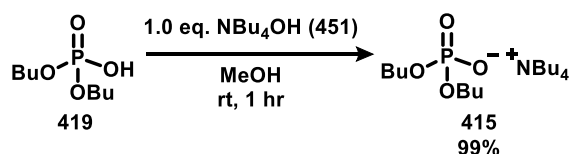
It was envisaged that the generalised azo compound **443** could be formed from a reaction between allyl carbamates or ureas (**447**) and aryl diazonium salts (**424**) (Scheme 6-2). As demonstrated by Knowles and co-workers, oxidative-PCET offers a simple method of forming amidyl radicals of allyl ureas and carbamates, through combinatorial use of reductive-quenching PRC with a hydrogen-bond acceptor.²³¹ Instead, it was hypothesised that the N-centred radical of **447** generated by oxidative-PCET could instead be achieved by an oxidative-quenching photoredox cycle, where a photoexcited PC (**97**) first reduces aryl diazonium salt (**424**) to molecular nitrogen and aryl radical (**440**) forming PC radical cation (**449**), a more potent oxidant than photoexcited PC (**97**). The cooperative action of a hydrogen-bond acceptor and the PC radical cation (**449**) forms N-centred radical by oxidative-PCET, which undergoes 5-membered cycloamination yielding C-centred radical (**448**). As previously discussed, alkyl radicals perform terminal addition into aryl diazonium salts, giving confidence that reaction between C-centred radical **448** and aryl diazonium salts (**424**) to yield radical cation **450** is possible. Lastly, reduction of radical cation **450**, by oxidation of photoexcited PC (**97**), yields the desired azo compound and regenerates PC radical cation (**449**). The joint use of an oxidative quenching redox cycle and oxidative-PCET could mean that only weakly oxidising and reducing PCs (**104**) are required to facilitate this azo-cycloamination.



Scheme 6-2. Hypothesised photoredox cycle to achieve the azo-cycloamination of allyl carbamates or ureas (**443**).

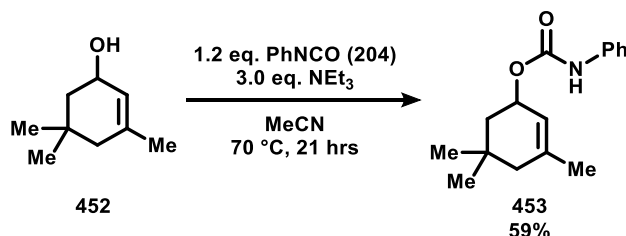
6.2 Discovery and Optimisation of Azo-Cycloamination Conditions

Phosphate **415** is a common hydrogen bond acceptor to facilitate the proton transfer in oxidative PCET activation of ureas and carbamates.²¹⁸ Phosphate **415** was synthesised quantitatively by deprotonation of dibutyl hydrogen phosphate (**419**) with hydroxide **451** (Scheme 6-3).²⁵⁰



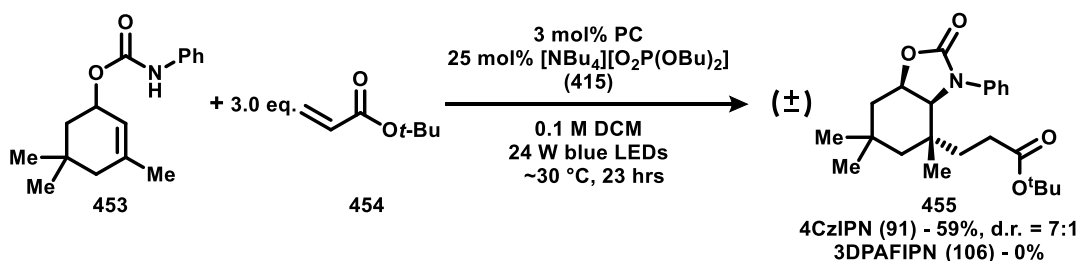
Scheme 6-3. Synthesis of phosphate **415**.

Initial work focused on assessing the ability for PCs 4CzIPN (**91**) and 3DPAFIPN (**106**) to facilitate N-centred radical formation of allyl carbamates by oxidative-PCET. Allyl carbamate **453** was synthesised from allyl alcohol **452** and phenyl isocyanate (**204**) (Scheme 6-4).



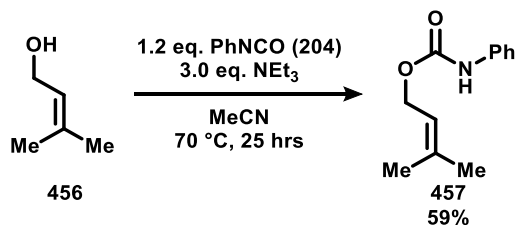
Scheme 6-4. Synthesis of allyl carbamate **453**.

Allyl carbamate **453** was submitted to conditions for 4CzIPN (**91**) and 3DPAFIPN (**106**) catalysed carboamination with *tert*-butyl acrylate (**454**) (Scheme 6-5).²³¹ Gratifyingly, by using 4CzIPN (**91**) allyl carbamate **453** was successfully converted to the carboamination product **455** in reasonable yield and *anti*-diastereoselectivity. Contrarily, use of 3DPAFIPN (**106**) only yielded starting allyl carbamate (**453**), presumably due to being insufficiently oxidising from the photoexcited state to facilitate oxidative-PCET. The observed *anti*-diastereoselectivity is presumably derived from the oxazolidinone ring blocking the required trajectory of the acrylate (**454**) to the C-centred radical post-cycloamination for *syn*-diastereoselectivity.



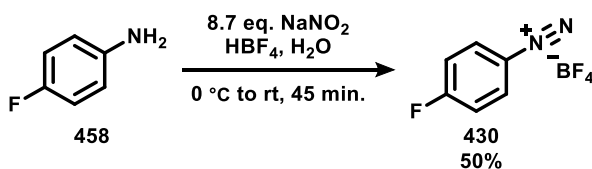
Scheme 6-5. 4CzIPN (**91**) catalysed carboamination of allyl carbamate **453**. Yield is of isolated major diastereomer.

Encouraged by scheme 6-5, focus was directed towards identifying conditions for the azo-cycloamination of allyl carbamates with aryl diazonium salts by PRC. Carbamate **457** was selected as a model substrate to test initial azo-cycloamination activity and was synthesised by coupling prenol (**456**) with phenyl isocyanate (**204**) (Scheme 6-6).



Scheme 6-6. Synthesis of allyl carbamate **457**.

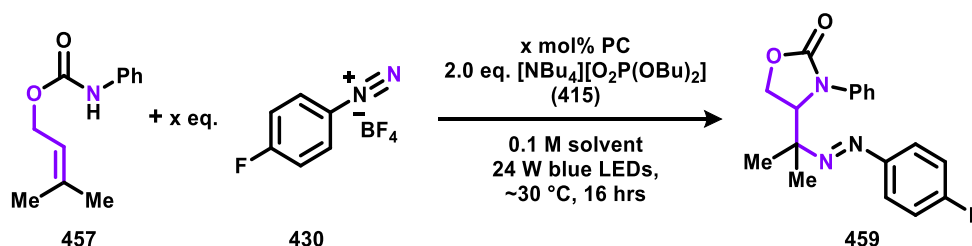
Aryl diazonium salt **430** was synthesised by the diazotisation of aniline **458** in moderate yield (Scheme 6-7).^{241c}



Scheme 6-7. Synthesis of aryl diazonium salt **430**.

The azo-cycloamination of allyl carbamate **457** with aryl diazonium salt **430** to form azo compound **489** was investigated (Table 6-1). Gratifyingly, use of photocatalyst 4CzIPN (**91**) and an excess of hydrogen bond acceptor (**415**) resulted in azo compound (**459**) formation (Table 6-1, Entry 1).²³¹ Switching the reaction solvent to DMSO gave lower azo compound (**459**) generation compared to using DCM (Table 6-1, entry 2). Photocatalyst 3DPAFIPN (**106**) in place of 4CzIPN (**91**) incurred an increase in azo compound (**459**) productivity (Table 6-1, entry 3), despite showing no activity in the carboamination of allyl carbamate **453** (Scheme 6-5). The activity observed in using 3DPAFIPN (**106**) was rationalised to be due to an oxidative quenching photoredox cycle being promoted by reduction of aryl diazonium salt (**430**) (Scheme 6-2). Meaning the oxidative species involved in oxidative-PCET of allyl carbamate **457** could be 3DPAFIPN (**106**) radical cation ($E_{1/2}(P^+/P) = 1.34$ V vs SCE), a similar strength oxidant to photoexcited 4CzIPN (**91**) ($E_{1/2}(P^*/P^-) = 1.35$ V vs SCE).⁹⁴

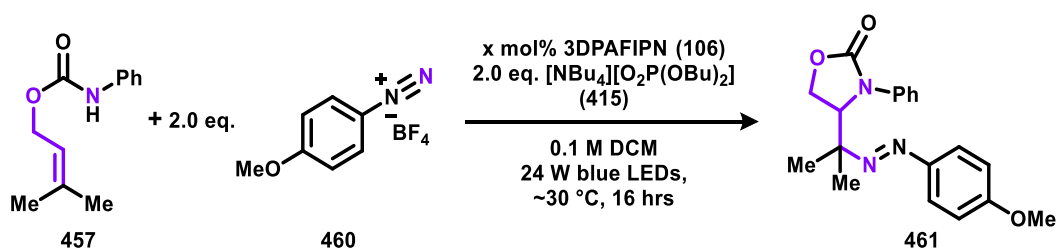
Increasing the 3DPAFIPN (**106**) loading from 3 mol% to 7 mol% gave a small increase in azo compound (**459**) yield (Table 6-1, entry 4), but no more benefit was observed when the loading was increased to 12 mol% (Table 6-1, entry 5). Increasing the stoichiometry of aryl diazonium salt (**430**) was detrimental to azo compound (**459**) productivity (Table 6-1, entry 6), while using 1.5 equivalents gave a small reduction in yield (Table 6-1, entry 7). Remarkably, in the absence of 3DPAFIPN (**106**) and light, significant levels of azo compound (**459**) formation were observed (Table 6-1, entry 8), with blue LED irradiation appearing to have a negligible effect on this catalyst-free reactivity (Table 5-1, entry 9).



Entry	PC (mol%)	430 eq.	Solvent	Yield/ % ^[a]
1	4CzIPN (91) (3)	2.0	DCM	34
2	4CzIPN (91) (3)	2.0	DMSO	8
3	3DPAFIPN (106) (3)	2.0	DCM	42
4	3DPAFIPN (106) (7)	2.0	DCM	54
5	3DPAFIPN (106) (12)	2.0	DCM	52
6	3DPAFIPN (106) (7)	3.0	DCM	8
7	3DPAFIPN (106) (12)	1.5	DCM	43
8 ^[b]	-	2.0	DCM	24
9	-	2.0	DCM	26

Table 6-1. Optimisation of the azo-cycloamination of allyl carbamate **457** with aryl diazonium salt **430**. [a] Yields obtained by ¹⁹F NMR and compared to a benzo-trifluoride internal standard. [b] In the absence of light.

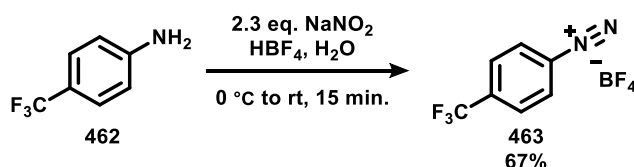
As it is intended to reductively cleave the azo group of azo-cycloamination products, the precise structure of the aryl diazonium salt used is inconsequential, as such an optimal aryl diazonium salt to promote this reaction was sought. Allyl carbamate **457** was exposed to optimised azo-cycloamination conditions for azo compound **459** formation, but instead with aryl diazonium salt **460** (Table 6-2), which pleasingly gave a good yield for azo compound **461** (Table 6-2, entry 1). Interestingly, significant quantities of azo compound **461** were obtained in the absence of 3DPAFIPN (**106**) while still under blue LED irradiation (Table 6-2, entry 2), while near trace amounts of product were returned in the absence of 3DPAFIPN (**106**) and light (Table 2-6, entry 3). These observations imply that a photochemical reaction between allyl carbamate **457** and aryl diazonium salt **460** occurs, which is promoted by 3DPAFIPN (**106**).



Entry	3DPAFIPN (106)/ mol%	Yield / % ^[a]
1	7	74
2	0	47
3	0 ^[b]	<10

Table 6-2. Azo-cycloamination between allyl carbamate **457** and aryl diazonium salt **460**. [a] Isolated yields. [b] In the absence of light.*

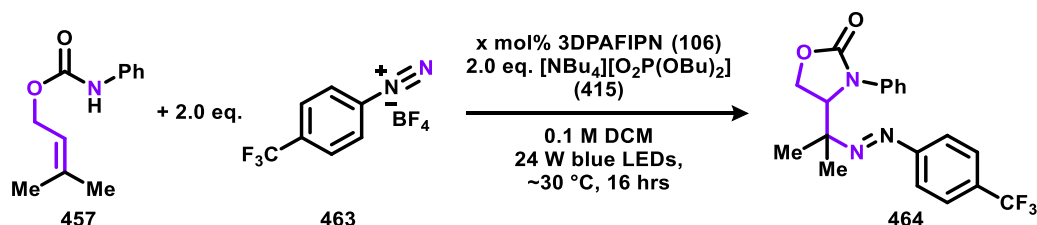
Aryl diazonium salt **463** was synthesised by the diazotisation of aniline **462** in moderate yield (Scheme 6-8).^{241c}



Scheme 6-8. Synthesis of aryl diazonium salt **463**.

* Starting aryl diazonium salt (**460**) synthesised, experiments carried out and products analysed by Dr Quentin Lefebvre.

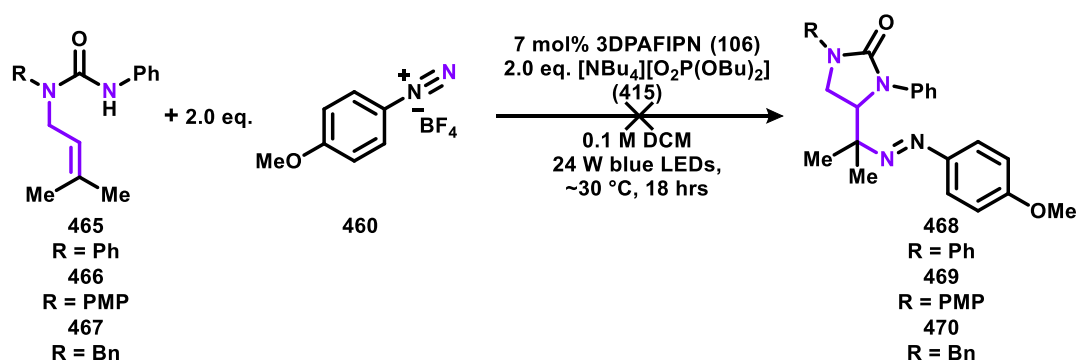
Unlike Table 6-2, when aryl diazonium salt **463** is used in the azo-cycloamination of allyl carbamate **457** to form azo compound **464**, optimal conditions identified were under blue LED irradiation (Table 6-3, entry 2). Addition of 3DPAFIPN (**106**) partially hinders azo compound **464** formation (Table 6-3, entry 1), while in the absence of 3DPAFIPN (**106**) and light product output persists but at an attenuated level (Table 6-3, entry 3).



Entry	3DPAFIPN (106)/ mol%	Yield / % ^[a]
1	7	62
2	0	69
3	0 ^[b]	38

Table 6-3. Azo-cycloamination between allyl carbamate **457** and aryl diazonium salt **463**. [a] Isolated yields. [b] In the absence of light.

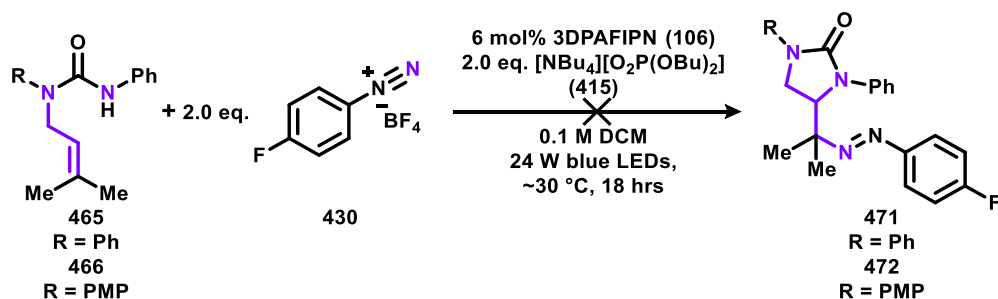
As the 3DPAFIPN (**106**) mediated conversion of allyl carbamate **457** to azo compound **461** (Table 6-2, entry 1) gave the most productive azo-cycloamination, it was hoped that these conditions would also be applicable to allyl ureas, for access to 1,2,3-triamines. In-house prepared allyl ureas **465**, **466** and **467** were submitted to optimised conditions for azo-cycloamination with 3DPAFIPN (**106**) and aryl diazonium salt **460** (Scheme 6-9). Yet disappointingly, no azo-cycloamination product (**468**, **469**, **470**) could be discerned despite full starting material consumption being observed in all cases.



Scheme 6-9. Attempts at the 3DPAFIPN (**106**) mediated azo-cycloamination of allyl ureas with aryl diazonium salt **460**.*

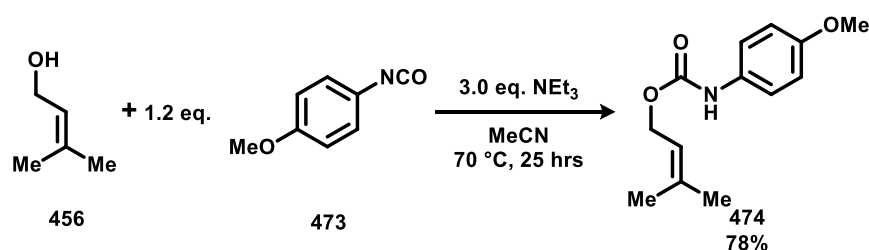
* Starting allyl ureas synthesised and analysed by Dr Quentin Lefebvre.

Undeterred by Scheme 6-9, allyl ureas **465** and **466** were both subjected to optimised 3DPAFIPN (**106**) mediated azo-cycloamination conditions with aryl diazonium salt **430** (Scheme 6-10). Unfortunately, this again resulted in no production of the desired azo compounds **471** and **472** despite achieving reaction completion.



Scheme 6-10. Attempts at the 3DPAFIPN (**106**) mediated azo-cycloamination of allyl ureas with aryl diazonium salt **430**.*

The results of Scheme 6-9 and Scheme 6-10 present a significant flaw in this methodology for achieving the aims of this project (Scheme 6-1), as 1,2,3-triamines would not be accessible by this azo-cycloamination approach. To identify conditions compatible with allyl ureas, an investigation into the electronics of the *N*-aryl of allyl carbamates was performed. Carbamate **474** was synthesised from prenol (**456**) and aryl isocyanate **473** in good yield (Scheme 6-11). It was hypothesised changing the *N*-phenyl of allyl carbamate **457** for a more electron rich aryl may promote oxidative-PCET for *N*-centred radical formation over decomposition pathways, by enhancing the propensity of the *N*-aryl to be oxidised. Adversely, introducing an electron donating-substituent to the *N*-aryl also weakens any hydrogen bond with phosphate base **415** while increasing the N-H bond pK_a , which according to Scheme 5-4 increases the effective BDE of the N-H bond. However, without formal examination of the pK_a and oxidation potential of carbamate **474**, it is not clear to what extent the *para*-methoxy group aids electron transfer and hinders proton transfer for PCET.

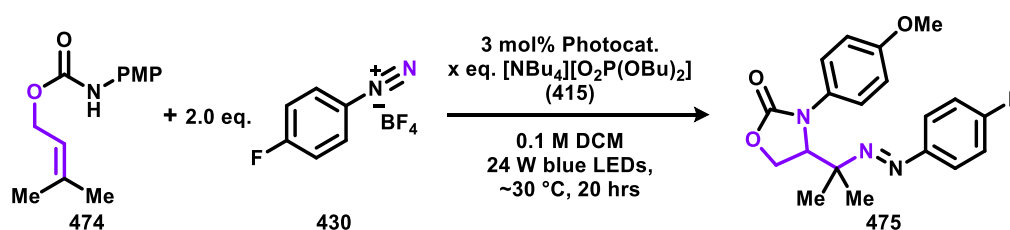


Scheme 6-11. Synthesis of allyl carbamate **474**.

* Starting allyl ureas synthesised and analysed by Dr Quentin Lefebvre.

With allyl carbamate **474** in hand, conditions for PCET of allyl carbamates were used with aryl diazonium salt **430**, which pleasantly gave azo-compound **475** (Table 6-4, entry 1).²³¹ Increasing the equivalents of phosphate base (**415**) from 1.0 to 1.25 to 2.0 each gave a small increase in yield for azo compound **475** (Table 6-4, entries 1-3). Changing the reaction solvent from DCM to DMSO resulted in a significant rise in azo-compound **475** output (Table 6-4, entries 4 and 5), a contradiction to the azo-cycloamination of allyl carbamate **457** (Table 6-1, entries 2 and 3). Finally, using photocatalyst 3DPAFIPN (**106**) in place of 4CzIPN (**91**) gave an increase in yield for azo compound **475** (Table 6-4, entries 6 and 7) and optimised conditions that show good agreement between spectroscopic and isolated yields (Table 6-4, entry 7).

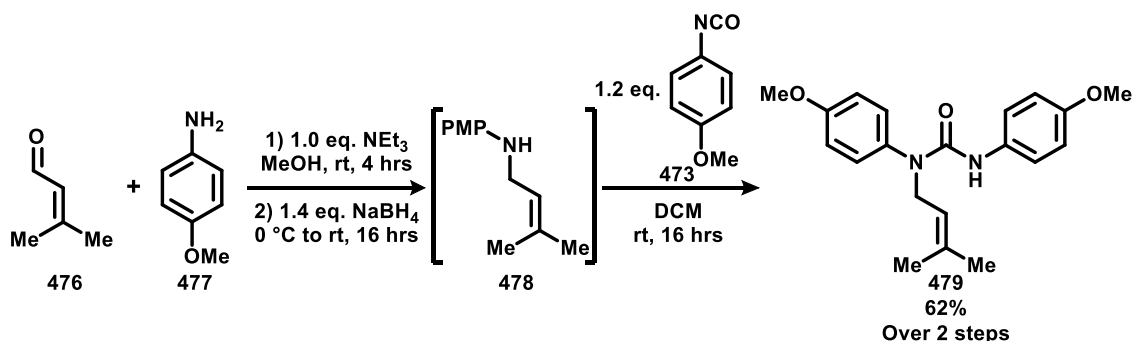
Control experiments implied that photocatalyst 3DPAFIPN (**106**) was necessary for good azo-compound **475** formation when under blue LED irradiation (Table 6-4, entry 8). However surprisingly, in the absence of 3DPAFIPN (**106**) and light the yield for azo compound (**475**) was practically identical to if these components were present (Table 6-4, entry 9). This implies that blue LED irradiation attenuates azo-compound **475** formation, which is overcome by the addition of blue light absorbing 3DPAFIPN (**106**). As such, a serendipitous discovery of conditions for the azo-cycloamination of allyl carbamate **474** with aryl diazonium salt **430** that do not require PRC had occurred, seemingly enabled by the *para*-methoxyphenyl of allyl carbamate **474**.



Entry	PC	415 eq.	Solvent	Yield/ % ^[a]
1	4CzIPN (91)	1.0	DCM	30
2	4CzIPN (91)	1.25	DCM	34
3	4CzIPN (91)	2.0	DCM	47
4	4CzIPN (91)	1.25	DMSO	60
5	4CzIPN (91)	2.0	DMSO	65
6	3DPAFIPN (106)	2.0	DCM	57
7	3DPAFIPN (106)	2.0	DMSO	81 (70) ^[b]
8	-	2.0	DMSO	44
9	- ^[c]	2.0	DMSO	79

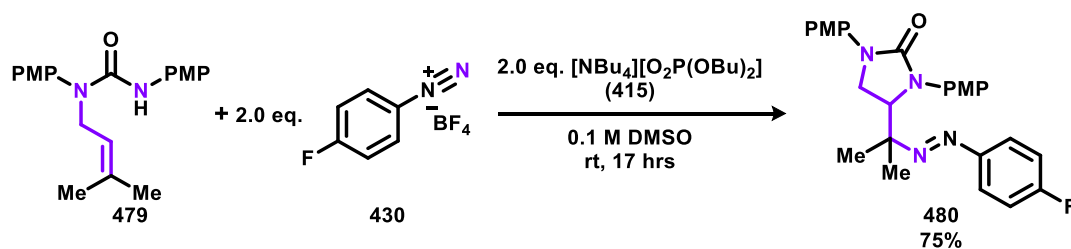
Table 6-4. Optimisation of the azo-cycloamination of allyl carbamate **474** with aryl diazonium salt **430**. [a] Yields obtained by ¹⁹F NMR and compared with benzotrifluoride internal standard. [b] Isolated yield. [c] Performed in the dark at room temperature.

It was questioned whether these new non-catalysed azo-cycloamination conditions would be applicable to allyl ureas. Allyl urea **479** was synthesised by reductive amination of prenal (**476**) with *para*-methoxy aniline (**477**), followed by coupling of the crude allyl amine **478** with *para*-methoxyphenyl isocyanate (**473**) in good yield (Scheme 6-12).



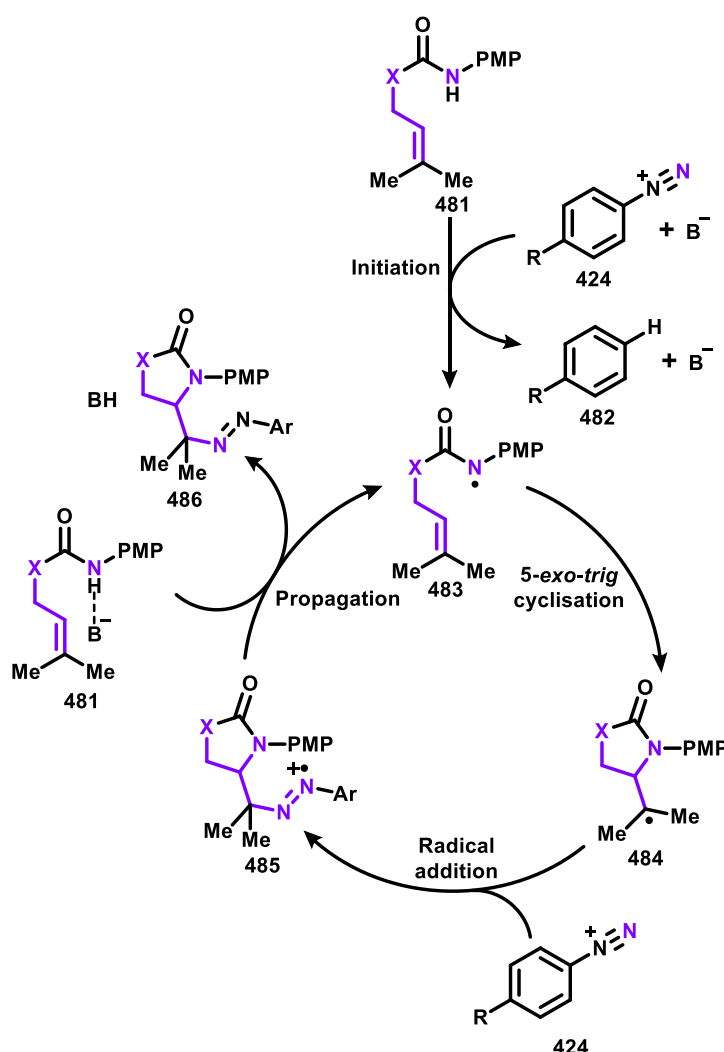
Scheme 6-12. Synthesis of allyl urea **479**.

Allyl urea **479** was subjected to catalyst-free azo-cycloamination conditions with aryl diazonium salt **430** (Scheme 6-13). Remarkably, unlike previous unsuccessful attempts at the 3DPAFIPN (**106**) mediated azo-cycloamination of allyl ureas (Scheme 6-9 and Scheme 6-10), catalyst-free azo-cycloamination conditions gave azo compound **480** in good yield.



Scheme 6-13. Catalyst-free azo-cycloamination of allyl urea **479**.

This new catalyst-free azo-cycloamination method was proposed to proceed by a radical chain mechanism, on the basis that the cycloamination is likely a radical process (Scheme 6-14). As Heinrich and co-workers have previously shown, decomposition of aryl diazonium salt (**424**) to aryl radical (**440**) can occur in the presence of carbonate base, and so the same may be able to occur with phosphate base **415**. The bond dissociation energy of the C-H bonds of aromatics (**482**) (~113 kcal/mol)²⁵¹ is much greater than the N-H bond of *N*-PMP ureas (**481**) (~90.5 kcal/mol),²⁵² suggesting N-H homolytic activation of allyl carbamates and allyl ureas (**481**) can occur by hydrogen atom abstraction from aryl radical **440**. Amidyl radical (**483**) performs cycloamination forming C-centred radical **484**, which attacks aryl diazonium salt (**424**) giving radical cation **485**. It is suspected that radical cation **485** is the key propagating species of the radical chain as observed in other reactions.²⁴⁸ It was postulated that radical cation **485** could oxidise allyl carbamate or allyl urea (**481**) with assistance from a hydrogen-bonding base, resulting in amidyl radical (**483**), azo compound (**486**) and turnover of the radical chain.



Scheme 6-14. Azo-cycloamination of allyl carbamates and allyl ureas by a radical chain mechanism. PMP – *para*-methoxyphenyl.

Aryl diazonium salt optimisation studies for the azo-cycloamination of allyl urea **479** were performed (Table 6-5). Firstly, carrying out the reaction at 30 °C, the temperature of the blue LED photoreactor, incurred a diminishment in azo compound **480** yield compared to using room temperature (Table 6-5, entries 1 and 2). Next, it was found that aryl diazonium salt **460** performed poorly in forming azo compound **487** (Table 6-5, entry 3). While the trifluoromethyl containing aryl diazonium salt **463** gave comparable yields for azo compound **488** to aryl diazonium salt **430** for azo compound **480**, but in a shorter reaction time (Table 6-5, entry 4).

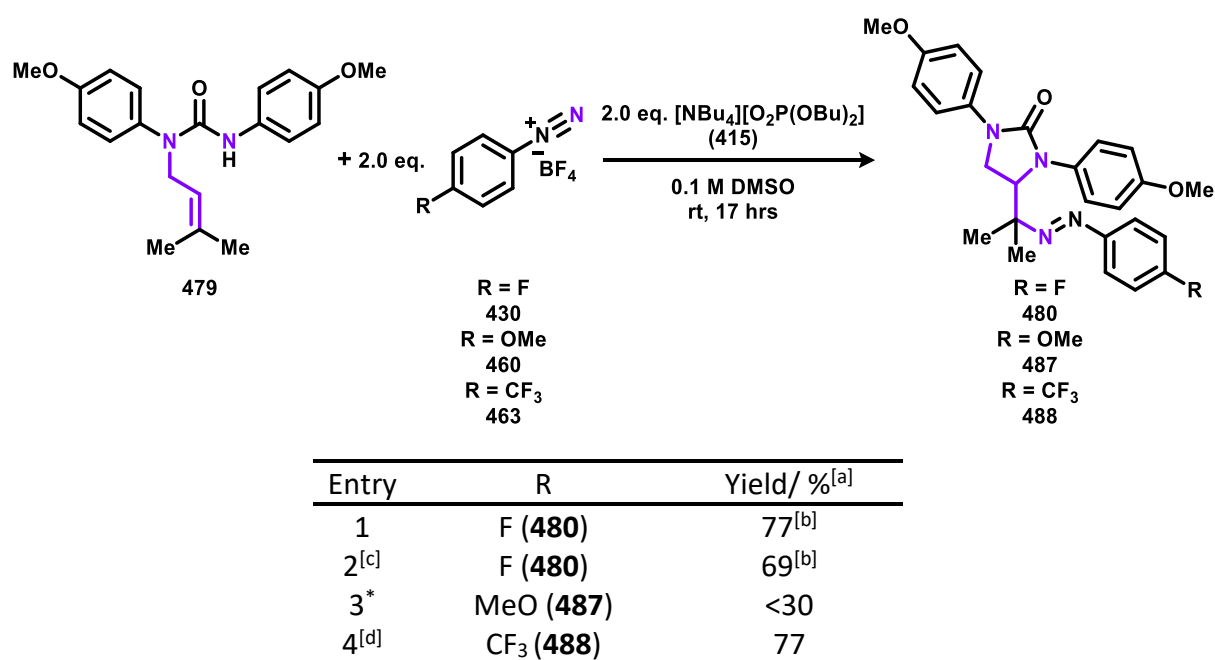
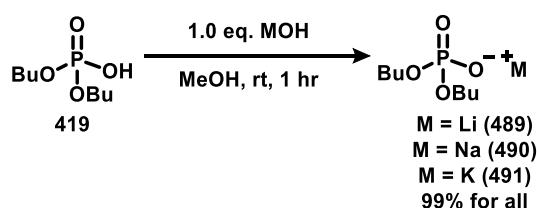


Table 6-5. Aryl diazonium salt optimisation studies for the catalyst-free azo-cycloamination of allyl urea **479**. [a] Isolated yields. [b] Yields obtained by ¹⁹F NMR and compared with benzotrifluoride internal standard. [c] Reaction performed at 30 °C. [d] Reaction performed for 2 hours.

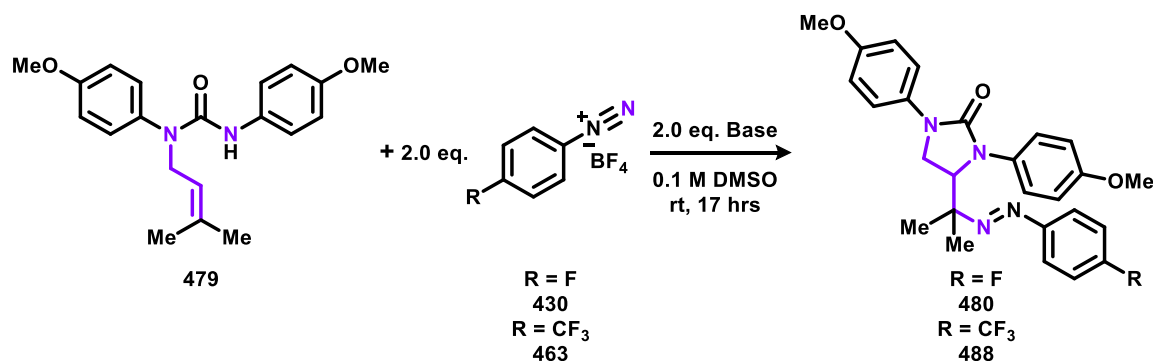
Use of tetrabutylammonium hydroxide (**451**) in the synthesis of phosphate **415** is costly and atom inefficient (Scheme 6-3), furthermore phosphate **415** is hygroscopic making its handling difficult. To address this shortcoming, alkali hydroxide derived phosphate bases **489**, **490** and **491** were all synthesised quantitatively (Scheme 6-15).²⁵⁰



Scheme 6-15. Synthesis of phosphate bases **489**, **490** and **491**.

* Experiment performed and analysed by Dr Quentin Lefebvre.

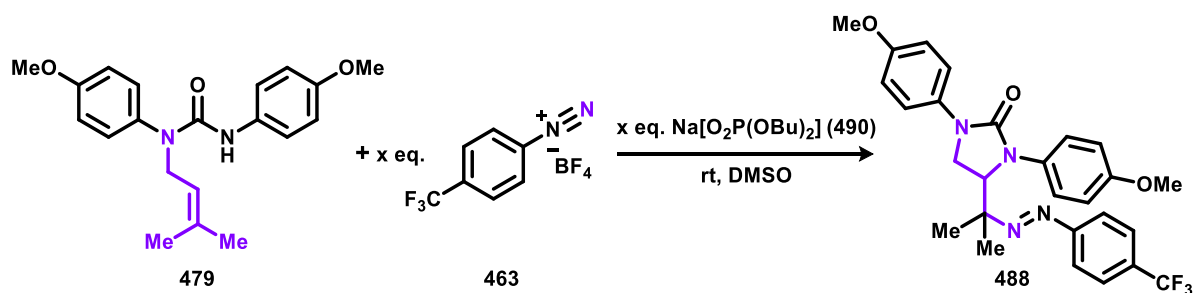
For the azo-cycloamination of allyl urea **479** with aryl diazonium salt **463**, it was found that lithium phosphate **489** and sodium phosphate **490** performed similarly to tetrabutylammonium phosphate **415** (Table 6-5, entry 4 and Table 6-6, entry 1 and 2). A small decrease in azo compound **488** yield occurred when using potassium phosphate **491** (Table 6-6, entry 3). Commercially available bases were also tested, with lithium tribasic phosphate performing similarly to potassium phosphate **491** and sodium tribasic phosphate giving only a moderate yield for azo compound **488** (Table 6-6, entry 4 and 5). Direct use of tetrabutylammonium hydroxide (**451**) yielded only trace amounts of azo compound **480** (Table 6-6, entry 6).



Entry	R	Base	Yield/ % ^[a]
1	CF ₃ (488)	Li[O ₂ P(OBu) ₂] (489)	84
2	CF ₃ (488)	Na[O ₂ P(OBu) ₂] (490)	84
3	CF ₃ (488)	K[O ₂ P(OBu) ₂] (491)	72
4	CF ₃ (488)	Li ₃ PO ₄	72
5	CF ₃ (488)	Na ₃ PO ₄	56
6	F (480)	NBu ₄ OH (451)	2 ^[b]

Table 6-6. Base screen for the azo-cycloamination of allyl urea **479**. [a] Isolated yields. [b] Yields obtained by ¹⁹F NMR and compared with benzotrifluoride internal standard.

Additional optimisation of Table 6-6 entry 2 was performed (Table 6-7). It was found that the azo-cycloamination of allyl urea **479** with aryl diazonium salt **463** reached completion in half an hour (Table 6-7, entry 1). Reducing the equivalents of phosphate base **490** and aryl diazonium salt **463** gave reduced yield for azo compound **488** (Table 6-7, entry 2). Finally, performing the azo-cycloamination of allyl urea **479** at a higher concentration did not alter the yield for azo compound **488**, but did reduce the reaction duration to 15 minutes (Table 6-7, entry 3).

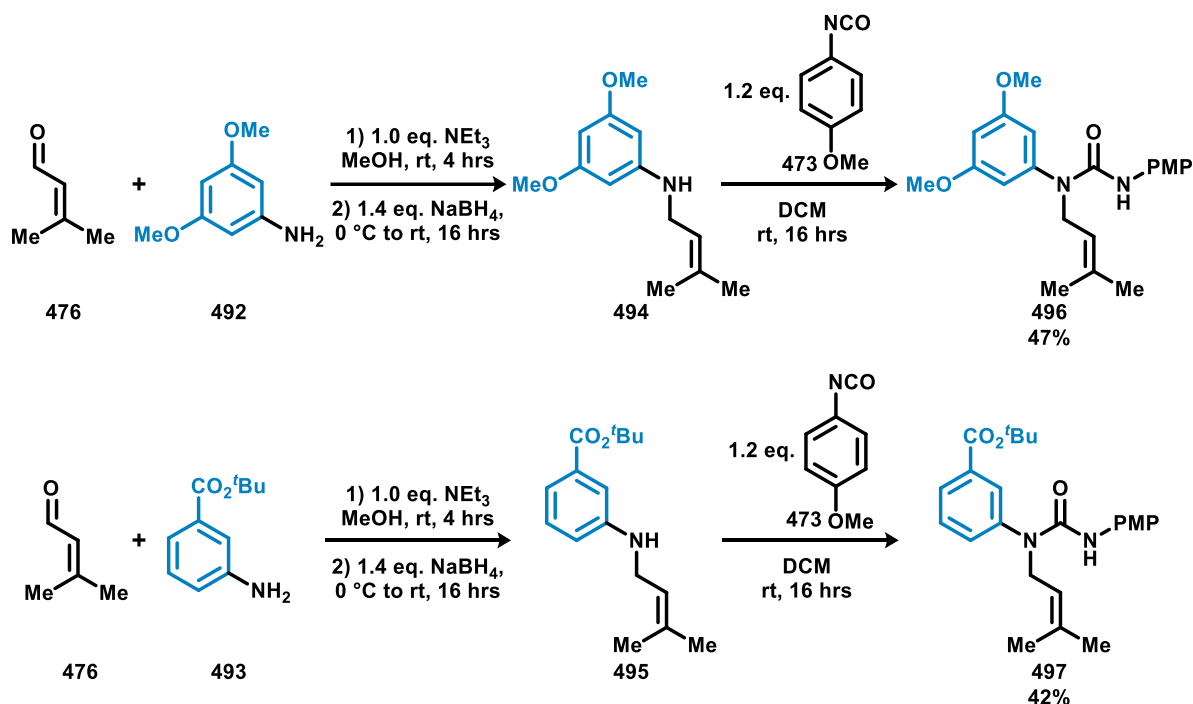


Entry	463/490 eq.	Conc./ M	Time/ min.	Yield/ % ^[a]
1	2.0/2.0	0.1	30	84
2	1.5/1.5	0.1	30	67
3	2.0/2.0	0.2	15	84

Table 6-7. Further optimisation of azo-cycloamination conditions for the synthesis of azo compound **488**. [a] Isolated yields.

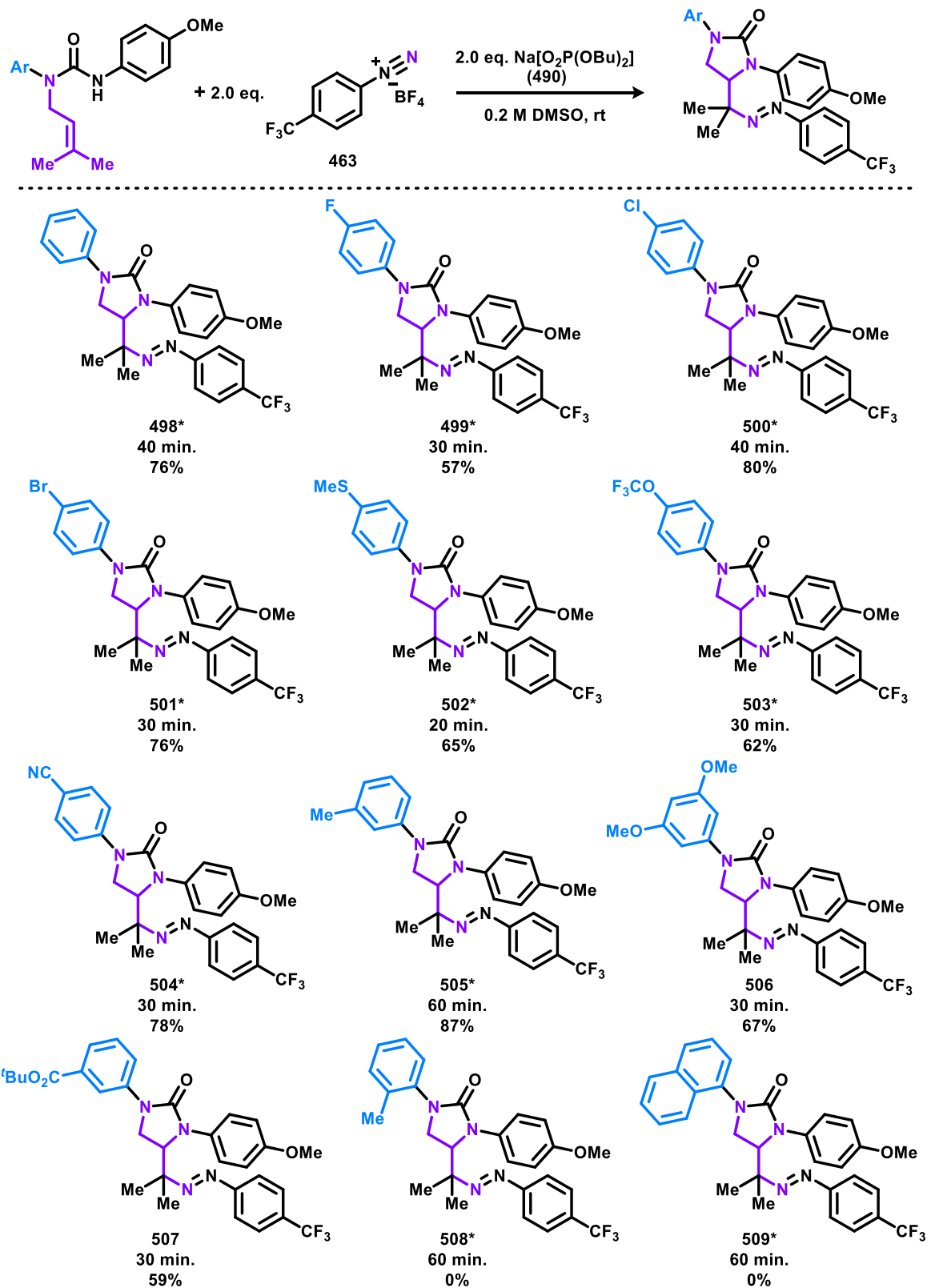
6.3 Scope of Catalyst-Free Azo-Cycloamination Conditions

With optimised conditions identified for the azo-cycloamination of allyl urea **479** by use of aryl diazonium salt **463** and phosphate base **490** (Table 6-7, entry 3), attention was next directed to applying these results to other substrates. Allyl ureas **496** and **497** were synthesised by reductive amination of prenal (**476**) with anilines **492** and **493**, followed by coupling of the crude allyl amines **494** and **495** with *p*-methoxyphenyl isocyanate (**473**) (Scheme 6-16).



Scheme 6-16. Synthesis of allyl ureas **496** and **497**. Yields are over two steps.

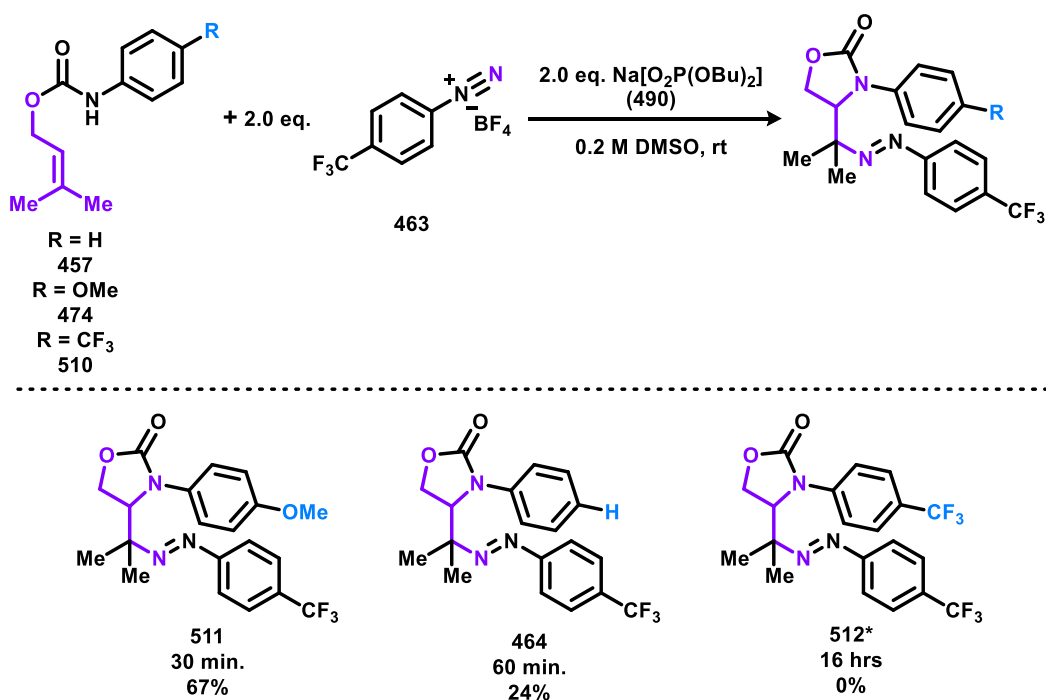
With access to allyl ureas **496** and **497**, and a variety of other in-house prepared prenal (**476**) derived *N'*, *N''* diaryl ureas, an investigation into the functional group tolerance of this new azo-cycloamination method was carried out (Scheme 6-17). Pleasingly, azo compounds **498** to **509** were all successfully synthesised in good to excellent yield. Compatible *para*-aryl substituents included halogens fluoro (**499**), chloro (**500**) and bromo (**501**), thioether (**502**), trifluoromethoxy (**503**) and cyano (**504**). Furthermore, tolerated *meta*-substituents consisted of tolyl (**505**), *tert*-butyl carboxylate (**507**) and di-methoxy (**506**). Unfortunately, *ortho*-functionalised *N*-aryl ureas did not participate in this azo-cycloamination reaction as azo compounds **508** and **509** were not observed, which may be due to promotion of an unfavourable conformation for cycloamination.



Scheme 6-17. Azo-cycloamination of a variety of *N', N''* diaryl ureas.

* Starting allyl urea synthesised and analysed by Dr Quentin Lefebvre.

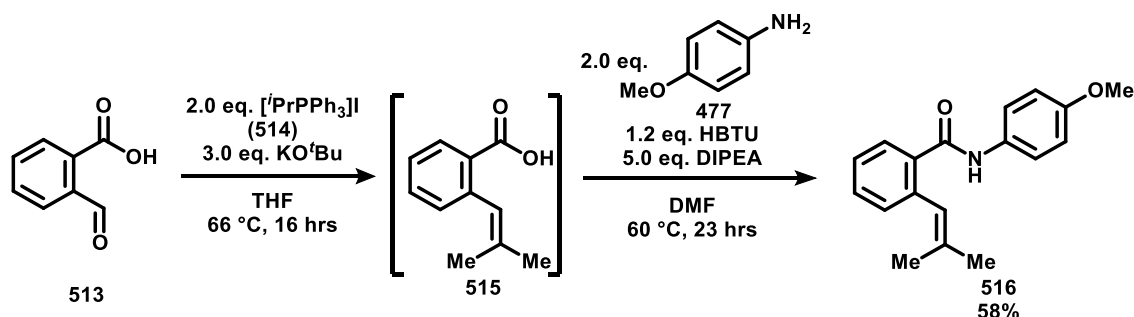
Next, azo-cycloamination conditions were applied to allyl carbamates, using aryl diazonium salt **463** (Scheme 6-18). As previously shown, *N*-PMP allyl carbamate **474** afforded azo compound **511** in good yield. The *N*-phenyl allyl carbamate **457** gave a diminished yield of azo compound **464**. Finally, allyl carbamate **510** containing an electron-deficient *N*-aryl failed to give any azo compound **512**, even with an extended reaction time. Scheme 6-18 implies that the electron density of the *N*-aryl undergoing cycloamination is important for azo compound formation. This may be rationalised in two ways when considering Scheme 6-14: 1) An electron-rich *N*-aryl is more easily oxidised, so may be required to maintain propagation of the radical chain by oxidative-PCET from the radical cation **485**; 2) *para*-trifluoromethylphenyl radical may be weakly electrophilic, so an electron-rich *N*-aryl carbamate may assist N-H hydrogen atom abstraction by the aryl radical through enhanced polarity matching.¹⁶⁰



Scheme 6-18. Azo-cycloamination of allyl carbamates to give azo compounds **511** and **464**.

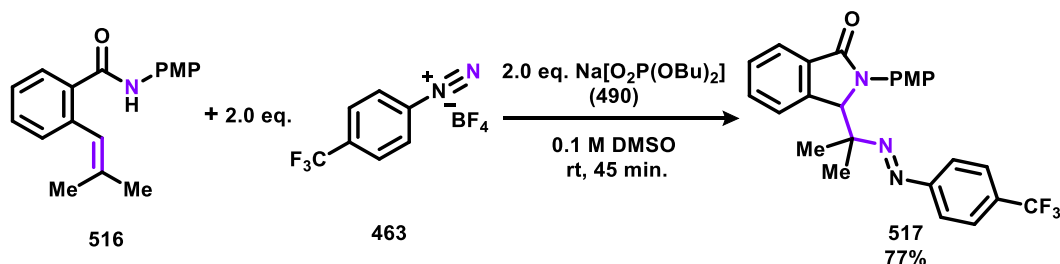
* Starting allyl carbamate synthesised and analysed by Dr Quentin Lefebvre.

As *N*-PMP allyl ureas and allyl carbamates are compatible substrates in azo-cycloamination with aryl diazonium salt **463** (Scheme 6-17 and Scheme 6-18), it was thought *N*-aryl amides would work as well. Amide **516** was synthesised by Wittig olefination of aldehyde **513** with phosphonium **514**; the resulting styrene **515** was then coupled with aniline **477** (Scheme 6-19).



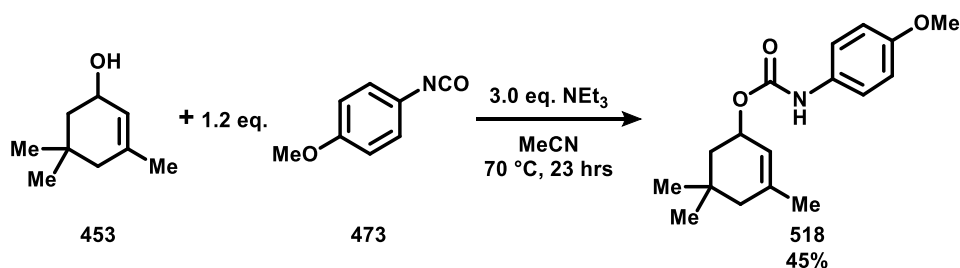
Scheme 6-19. Synthesis of *N*-PMP amide **516**. Yield over two steps.

The azo-cycloamination of amide **516** gave azo compound **517** in good yield, by running the reaction at a concentration of 0.1 M instead of 0.2 M to aid solubility of the starting material (Scheme 6-20).



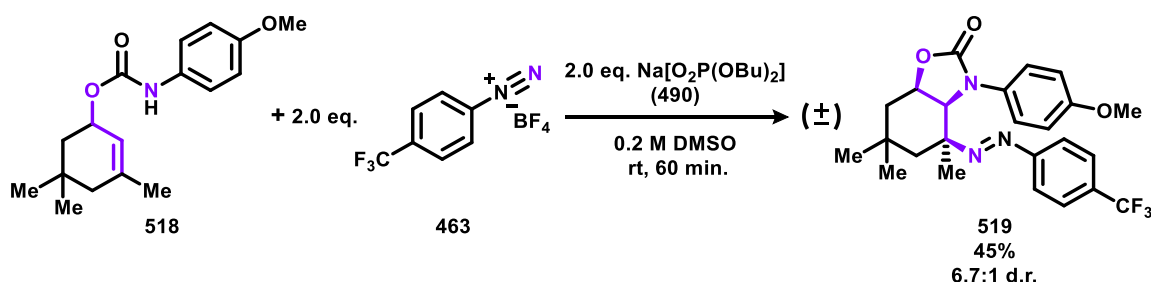
Scheme 6-20. Azo-cycloamination of amide **516**.

So far, this new azo-cycloamination method has only been demonstrated on prenyl derived allyl ureas and allyl carbamates. It was queried whether other allylic carbamates containing more complex carbon skeletons would be applicable substrates in this azo-cycloamination. The cyclic allyl carbamate **518** was synthesised by coupling allylic alcohol **453** with aryl isocyanate **473** (Scheme 6-21).



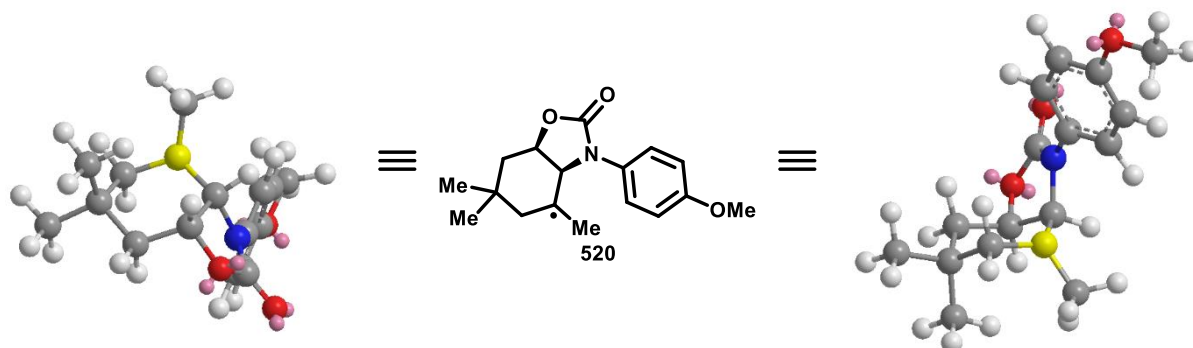
Scheme 6-21. Synthesis of cyclic allyl carbamate **518**.

The azo-cycloamination of cyclic allyl carbamate **518** with aryl diazonium salt **463** pleasingly yielded azo compound **519**, albeit in moderate yield and *syn*-diastereoselectivity (Scheme 6-22).



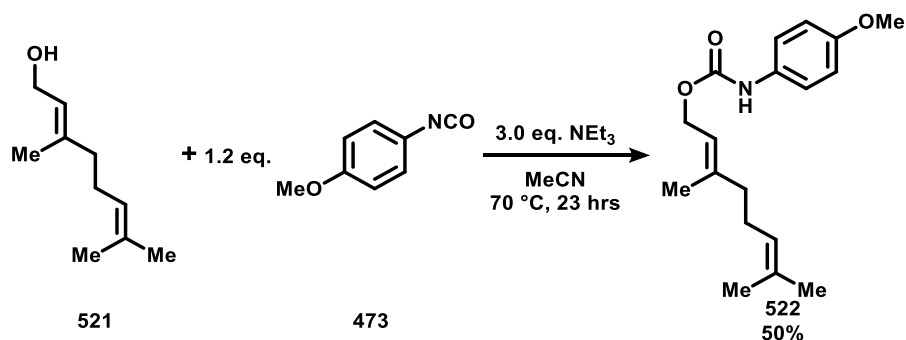
Scheme 6-22. Azo-cycloamination of cyclic allyl carbamate **518**. Yield is of mixture of inseparable diastereomers.

The *syn*-diastereoselectivity observed in the azo-cycloamination of cyclic allyl carbamate **518** can be rationalised by inspecting the computed 3-D structure of the intermediary C-centred radical **520** (Scheme 6-23). The *anti*-diastereoselective outcome requires the trajectory of the aryl diazonium salt **463** to pass through the interior of the cyclohexyl skeleton, near an axial methyl and C-H bond. While for *syn*-diastereoselectivity the aryl diazonium salt **463** must approach from the exterior of the cyclohexyl skeleton near the adjacent oxazolidinone. Scheme 6-5 implies the trajectory for *syn*-diastereoselectivity is likely to be more sterically encumbered than for *anti*-diastereoselectivity, meaning steric shielding does not explain the observed diastereoselective outcome. Instead three propositions may explain the observed selectivity: 1) a π -stacking interaction between the electron-rich *N*-PMP ring and the electron deficient aryl diazonium salt **463** stabilises the approach for *syn*-diastereoselectivity. 2) Radical **520** addition to aryl diazonium salt **463** is reversible and faster than subsequent reduction of radical cation (**485**), so an equilibrium forms favouring the more thermodynamically stable *syn*-epimer of azo compound **519**. 3) Related to proposition 2, a Curtin–Hammett principle scenario could be in play, where a *syn* relationship between the intermediary azo bond radical cation and the *N*-PMP group accelerates the proceeding reduction of radical cation (**485**), potentially by electron transfer between the two aryl rings (See mechanistic investigation).



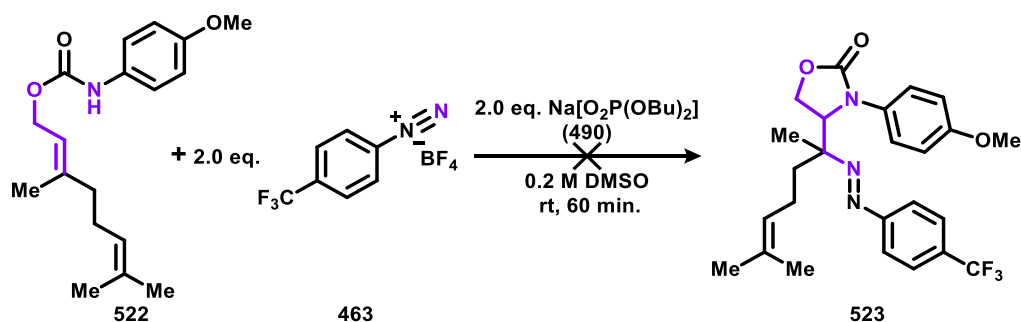
Scheme 6-23. 3-D depictions of the intermediary C-centred radical **520**, with carbon radical highlighted in yellow in 3-D depictions. Geometry optimised using MM2 energy minimalisation in Chem3D.

Encouraged by the results of Scheme 6-24, geraniol (**521**) was coupled with PMP isocyanate **473**, affording allyl carbamate **522** in moderate yield (Scheme 6-24).



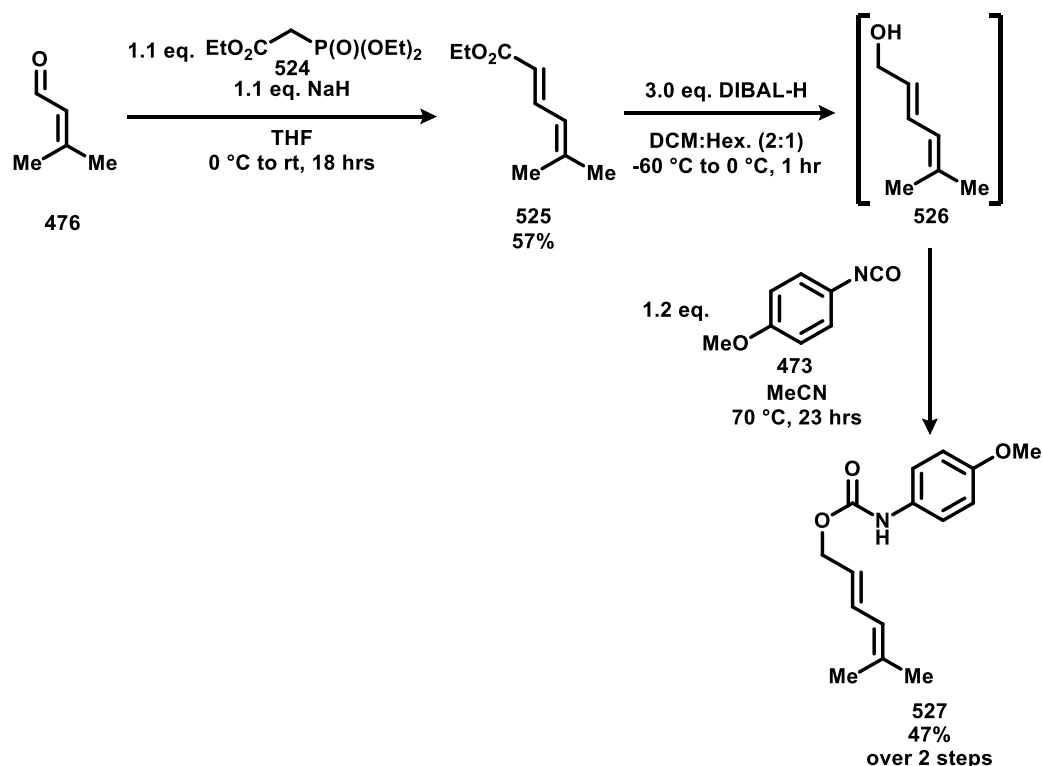
Scheme 6-24. Synthesis of allyl carbamate **522**.

However, when the azo-cycloamination of geraniol derived allyl carbamate **522** with aryl diazonium salt **463** was attempted, only starting material was returned (Scheme 6-25). Scheme 6-25 implies that substrates containing alkenes that are not a part of the allyl carbamate inhibit azo-cycloamination. It may be that the second olefin is subject to addition from aryl radical (**440**) lowering the number of initiation events.^{244,253}



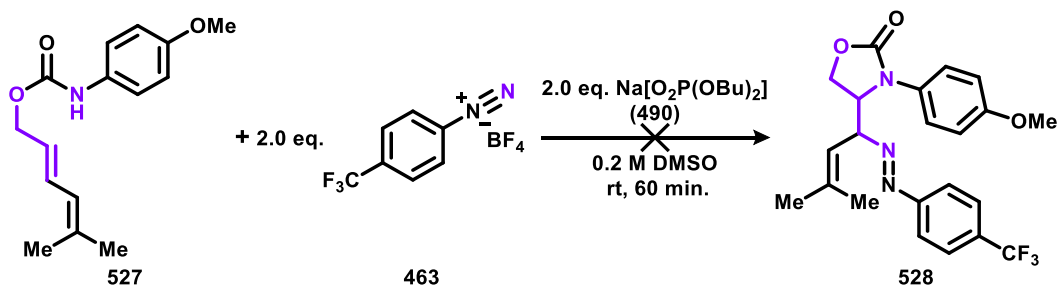
Scheme 6-25. Attempted azo-cycloamination of allyl carbamate **522**.

Next, it was queried whether an allyl carbamate that would form a resonance stabilised C-centred radical (**484**) after cycloamination would partake in subsequent addition to aryl diazonium salt **463**. Dienyl containing allyl carbamate **527** was selected for synthesis in three steps (Scheme 6-26), as radical cycloamination would generate a vinyl-stabilised C-centred radical. First the Horner-Wadsworth-Emmons reaction was applied by coupling prenal (**476**) with phosphonate **524** to form diene **525** in moderate yield. The ester of diene **525** was selectively reduced giving the allyl alcohol **526**, which was coupled with PMP isocyanate **473** giving the desired dienyl carbamate **527**.



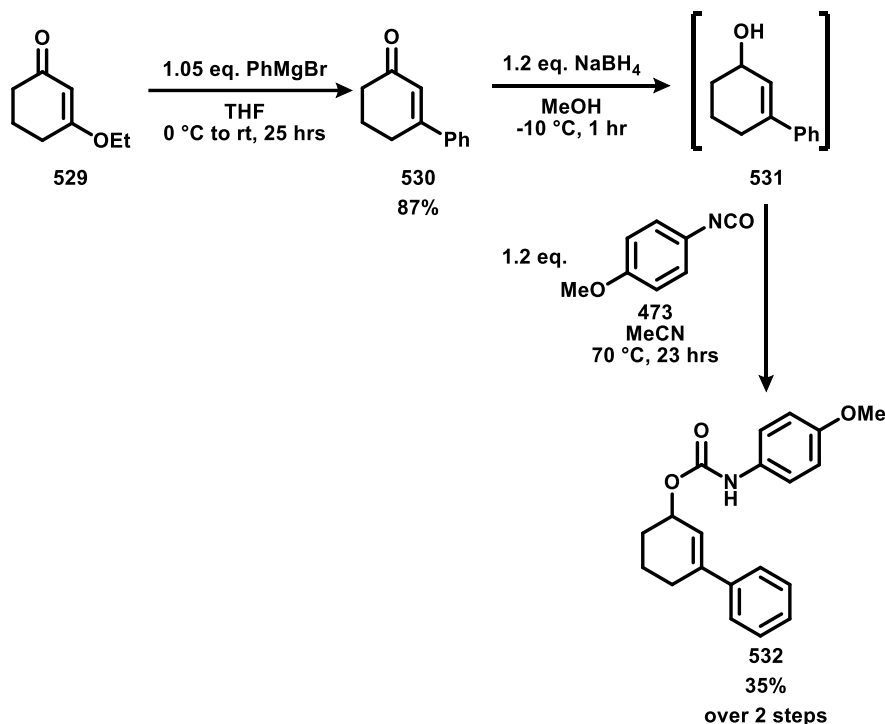
Scheme 6-26. Synthesis of diene containing carbamate **527**.

The attempted azo-cycloamination of dienyl allyl carbamate **527** with aryl diazonium salt **463** only returned starting material and no azo compound **528** (Scheme 6-27).



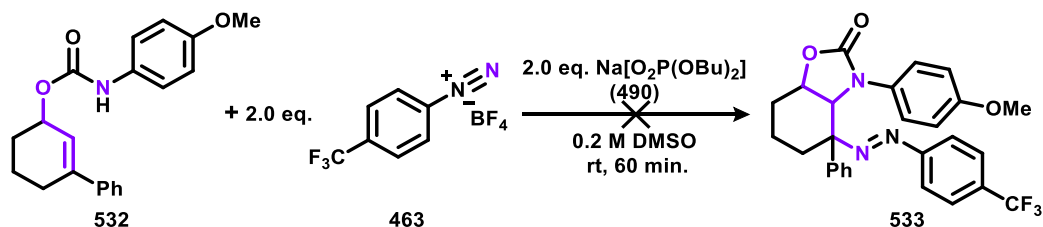
Scheme 6-27. Attempted azo-cycloamination of dienyl carbamate **527**.

Undeterred by Scheme 6-27, styrene containing cyclic allyl carbamate **532** was targeted for synthesis (Scheme 6-28), the C-centred radical of which after radical cycloamination would be phenyl stabilised. First, Michael addition on to enone **529** with phenylmagnesium bromide followed by E1cB elimination of ethoxide formed styrene **530** in good yield. Reduction of enone **530** gives allyl alcohol **531**, which was coupled with aryl isocyanate **473** to give styrene containing allyl carbamate **532**.



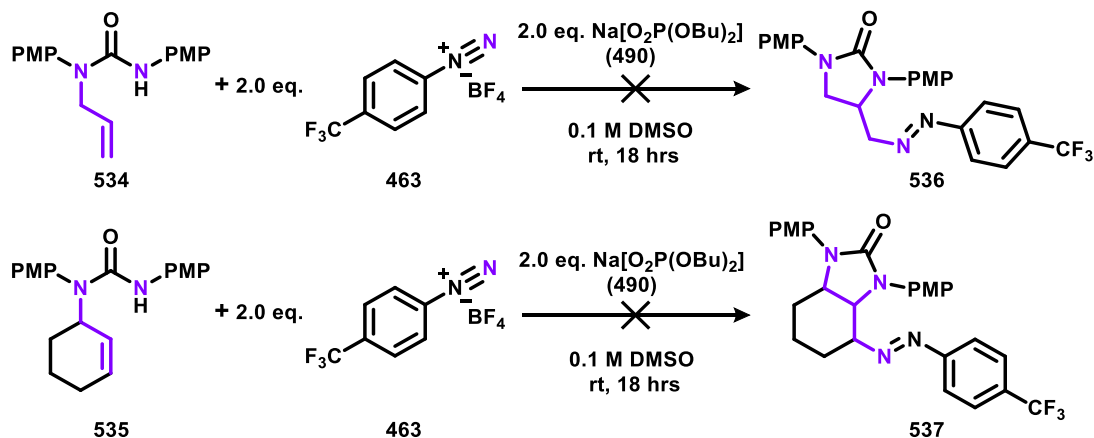
Scheme 6-28. Synthesis of styrene containing allyl carbamate **532**.

Again, like Scheme 6-27 the azo-cycloamination of styrene containing allyl carbamate **532** failed to yield the intended azo compound **533** with only starting material being returned (Scheme 6-29). The negative results of Scheme 6-27 and Scheme 6-29 may indicate that the intermediary C-centred radical (**484**) after cycloamination of carbamates **527** and **532** are too stabilised, potentially resulting in reversible radical addition into aryl diazonium salt **463**.



Scheme 6-29. Attempted azo-cycloamination of styrene containing carbamate **532**.

Finally, it was queried whether allyl ureas that would generate primary or secondary C-centred radicals after cycloamination would engage in azo-cycloamination. Disappointingly, both allyl ureas **534** and **535** failed to give their respective azo compound products (**536** and **537**) and only returned starting material, even with extended reaction times (Scheme 6-30). This outcome is presumably due to the radical cycloaminations being reversible, as the stability of the intermediary primary and secondary C-centred radicals would be lesser than the tertiary C-centred radicals that have proved successful.

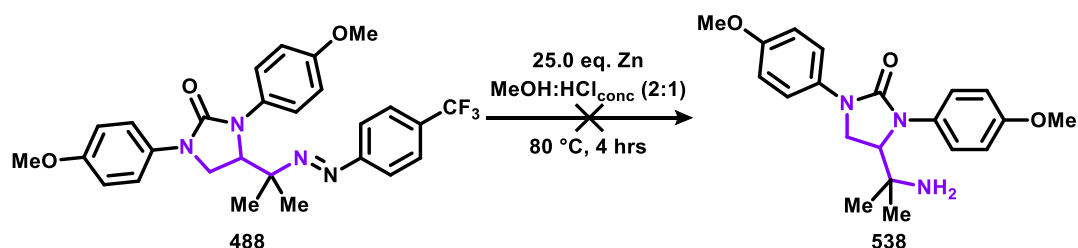


Scheme 6-30. Failed attempts at the azo-cycloamination of allyl ureas **534** and **535**.

* Starting allyl ureas synthesised and analysed by Dr Quentin Lefebvre.

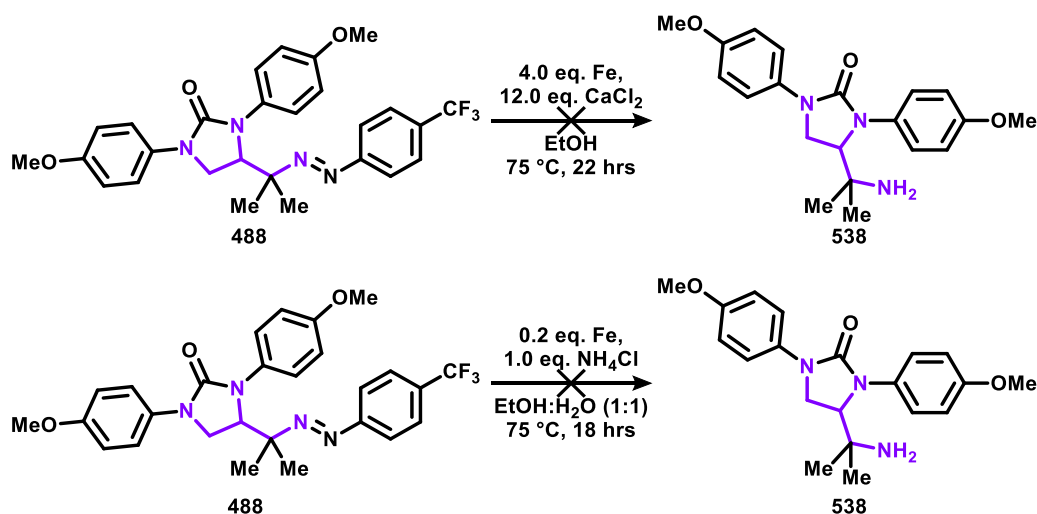
6.4 Synthetic Modifications of Azo-Cycloamination Products

With conditions established for the azo-cycloamination of allyl ureas and allyl carbamates, effort was next directed at the derivatisation of the azo products. First, an investigation was conducted into methods for the reductive cleavage of the azo bond of **488** to access the primary amine **538**. Initial attempts used zinc in an acidic solution (Scheme 6-31), but when azo compound **488** was exposed to acid, its rapid consumption was observed along with no indication of primary amine **538** formation.²⁴⁸



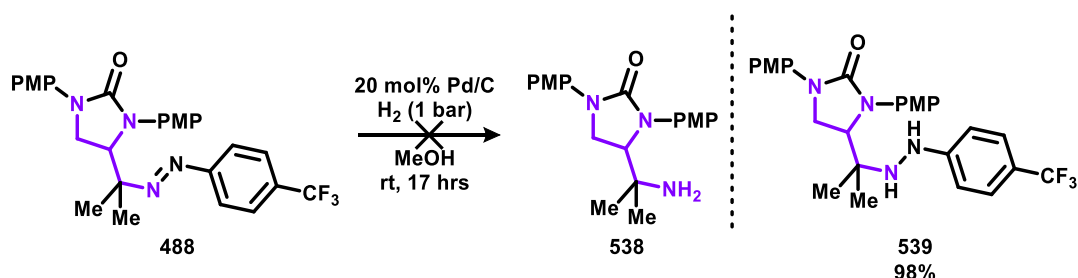
Scheme 6-31. Initial attempt at the reductive cleavage of azo compound **488**.

Now aware azo compound **488** decomposes in acidic media (Scheme 6-31), strong acid-free conditions for its conversion to amine **538** were explored. Disappointingly, when mildly acidic conditions were used only starting material was returned (Scheme 6-32).²⁵⁴



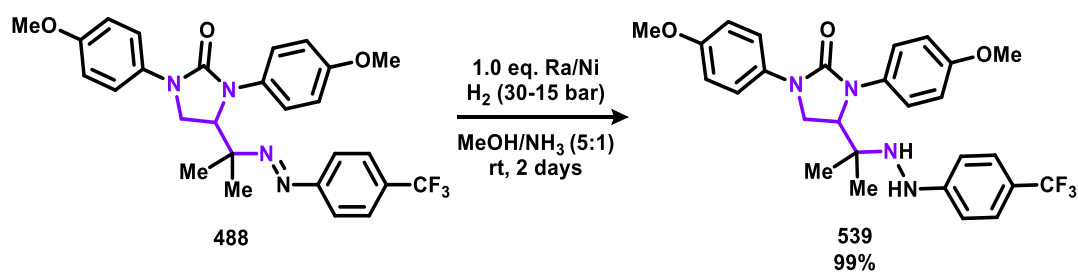
Scheme 6-32. Failed attempts at the reductive cleavage of azo compound **488**.

Literature precedent shows the reductive cleavage of azo bonds can be achieved by transition metal-catalysed hydrogenation (Scheme 6-33).²⁴⁴ A palladium-catalysed hydrogenation of azo compound **488** afforded only the partial reduction product hydrazine **539** (Scheme 6-33).



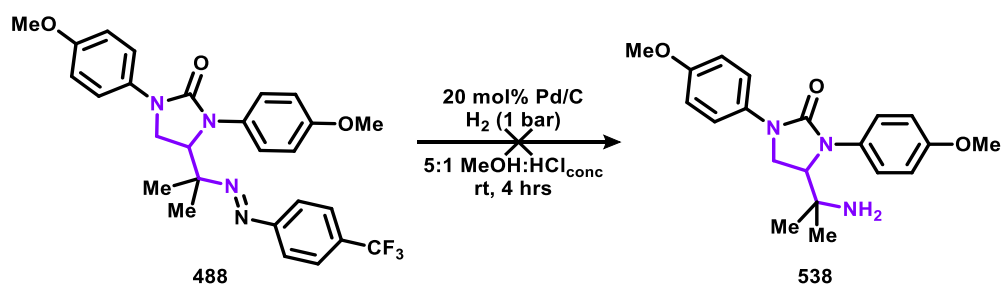
Scheme 6-33. Palladium catalysed hydrogenation of azo compound **488**.

More forcing hydrogenation conditions were tested in the reductive cleavage of azo compound **488**, by using a stoichiometric amount of Raney nickel and a high pressure of hydrogen (Scheme 6-34).²⁴⁴ However, again only the hydrazine product **539** was afforded.



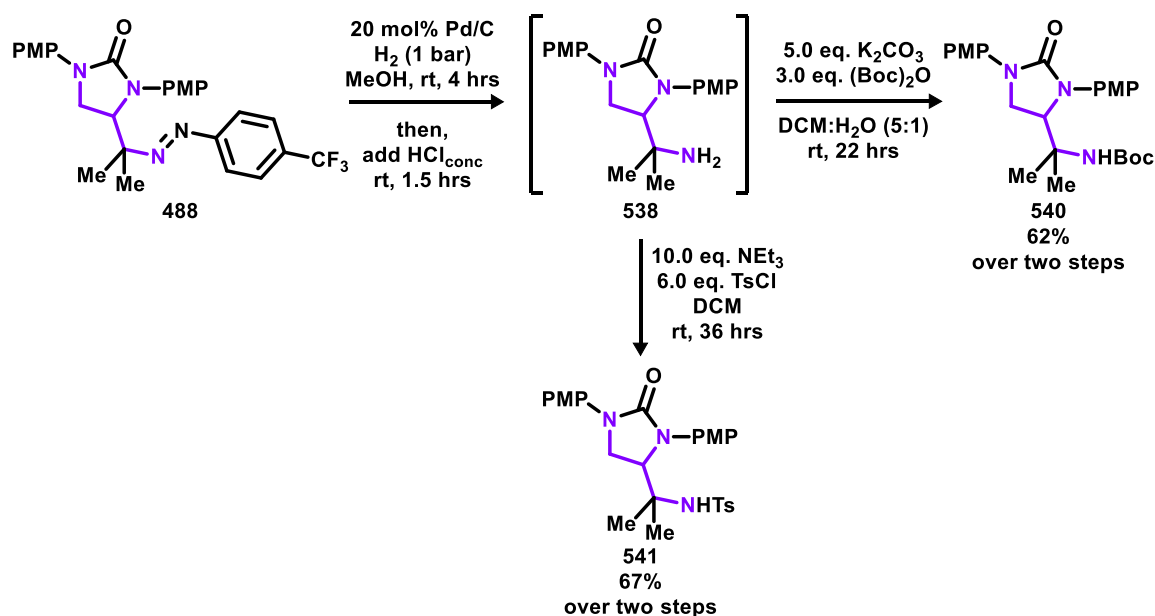
Scheme 6-34. Attempted hydrogenation of azo compound **488** by using Raney nickel.

Reports indicate that palladium-catalysed hydrogenations of azo compounds to amines can be assisted by acid.²⁵⁵ However, when the hydrogenation of azo compound **488** was performed with acid-assistance, complete consumption of starting material was observed without indication of amine **538** formation (Scheme 6-35).



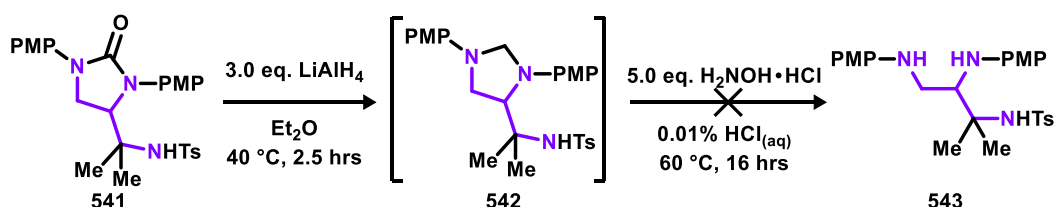
Scheme 6-35. Attempted acid-promoted hydrogenation of azo compound **488**.

As acid mediated approaches to the reductive cleavage of azo compound **488** resulted in decomposition, it was wondered whether hydrazine **539** would demonstrate greater stability. First, azo compound **488** was hydrogenated in the absence of acid quantitatively yielding hydrazine **539**; acid was then added to the reaction mixture and re-exposed to an atmosphere of hydrogen (Scheme 6-36). TLC analysis indicated full consumption of intermediary hydrazine **539**, so in order to aid product isolation the crude mixture was subjected to amine protection separately yielding the *N*-Boc product **540** and *N*-tosyl product **541** in good yields.



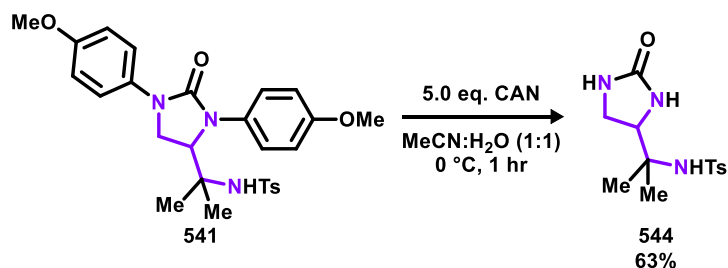
Scheme 6-36. One-pot reductive cleavage of azo compound **488** followed by subsequent *N*-protections.

With a method established for the conversion of azo compound **488** to sulfonamide **571** (Scheme 6-36), next the opening of its imidazolidin-2-one was explored (Scheme 6-37). First, the reduction of sulfonamide **541** to aminal **542** was attempted, with TLC analysis indicating full conversion of starting material (**541**) to a new species, which was presumed to be the desired aminal **542**. Attempts to isolate products from the reduction of sulfonamide **541** curiously only yielded starting material, implying that if aminal **542** had formed it is prone to atmospheric oxidation. Next, the crude product of the reduction of sulfonamide **541** to aminal **542** was immediately exposed to hydrolysis conditions, but instead only sulfonamide **541** was again returned.



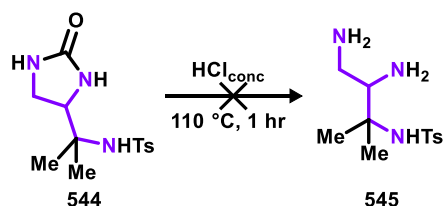
Scheme 6-37. Attempted one-pot conversion of sulfonamide **541** to triamine **543**. PMP – *para*-methoxyphenyl.

With the ring-opening/hydrolysis of sulfonamide **541** proving problematic (Scheme 6-37), attention was turned to the removal of its *para*-methoxyphenyl rings. Ceric ammonium nitrate is commonly used in the oxidative hydrolysis of *N*-electron-rich aryls from amides, carbamates and ureas.²⁵⁶ Exposure of sulfonamide **541** to ceric ammonium nitrate in an aqueous reaction medium yielded imidazolidin-2-one **544** in good yield (Scheme 6-38).



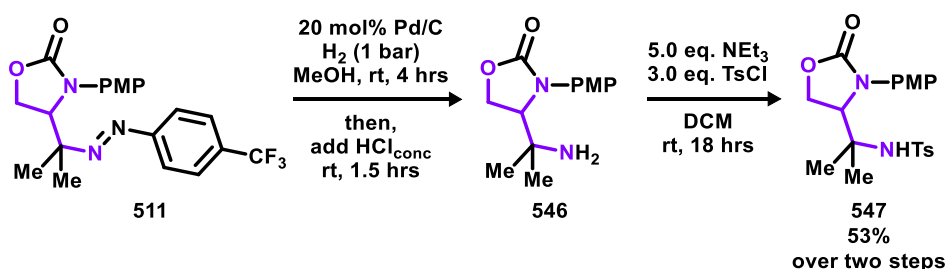
Scheme 6-38. Removal of the *para*-methoxyphenyl rings of sulfonamide **541**.

With access to imidazolidin-2-one **544** its hydrolytic ring opening was attempted; however, the desired triamine (**545**) could not be identified from the reaction crude despite full consumption of starting material (Scheme 6-39). Furthermore, TLC and ¹H NMR analysis indicated that the tosyl protecting group had been removed.



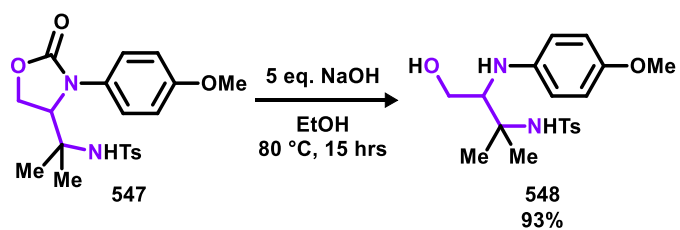
Scheme 6-39. Attempted hydrolysis of imidazolidin-2-one **544**.

Conditions for the reductive cleavage followed by tosyl protection of azo compound **488** were tested on carbamate **511**, yielding the sulfonamide **547** in moderate yield.



Scheme 6-40. Synthesis of sulfonamide **547**.

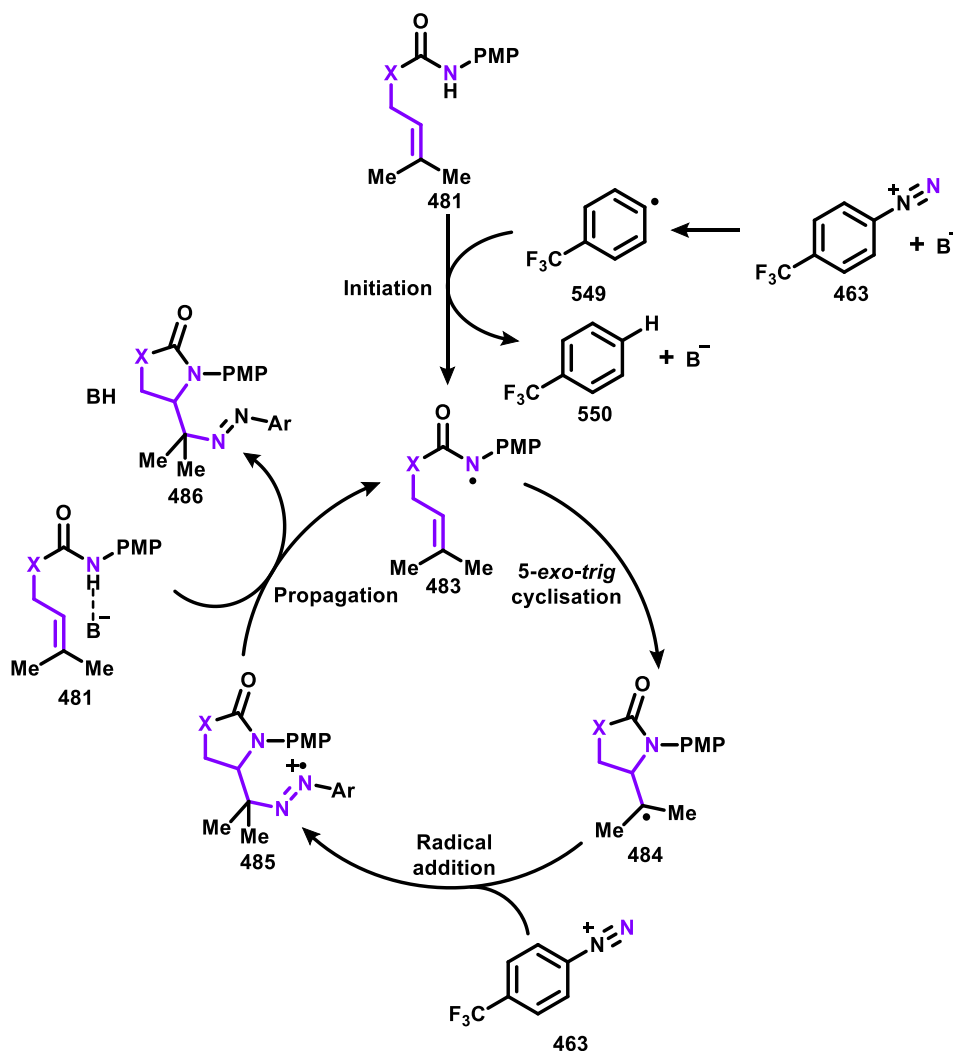
Finally, the oxazolidin-2-one of sulfonamide **547** was opened by basic hydrolysis affording the 1,2,3-diamino alcohol **548** in excellent yield (Scheme 6-41).



Scheme 6-41. Hydrolysis of oxazolidin-2-one **547**.

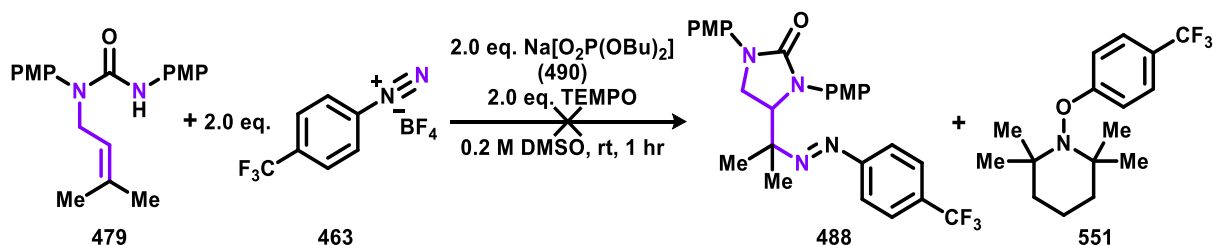
6.5 Mechanistic Investigation

With the synthetic utility established for this newly developed aryl diazonium salt **463** promoted azo-cycloamination of allyl ureas and allyl carbamates, attention was directed towards mechanistic understanding. As previously stated (Scheme 6-14), a preliminary mechanism based on a radical chain process was proposed (Scheme 6-42), which begins with sodium dibutyl phosphate (**490**) facilitated decomposition of aryl diazonium salt **463** forming aryl radical **549**. The aryl radical **549** hydrogen atom-abstracts the N-H of an allyl carbamate or allyl urea (**481**) generating amidyl radical (**483**), which rapidly undergoes cycloamination forming C-centred radical **484** that adds to aryl diazonium salt **463** yielding radical cation **485**. Propagation of the radical-chain by electron transfer from an allyl carbamate or allyl urea (**481**) to radical cation **485** may be feasible by assistance from sodium dibutyl phosphate (**490**) through oxidative-PCET, reforming amidyl radical (**483**) and producing azo compound **486**.



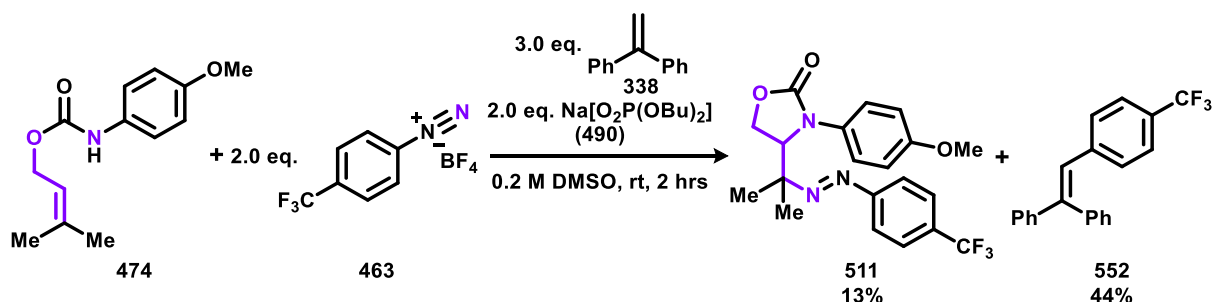
Scheme 6-42. Azo-cycloamination of allyl carbamates and allyl ureas by a radical chain mechanism. B^- - Sodium phosphate **490**.

A TEMPO radical trapping experiment was performed to test for the presence of aryl radical **549** in the azo-cycloamination of allyl urea **479** with aryl diazonium salt **463** (Scheme 6-43). For Scheme 6-43, no azo compound **488**, TEMPO-aryl radical adduct **551**, or any other obvious TEMPO adducts were observed; instead, only the starting allyl urea (**479**), which may imply either an electron transfer mode of TEMPO reaction inhibition or very small quantities of initiator are generated.



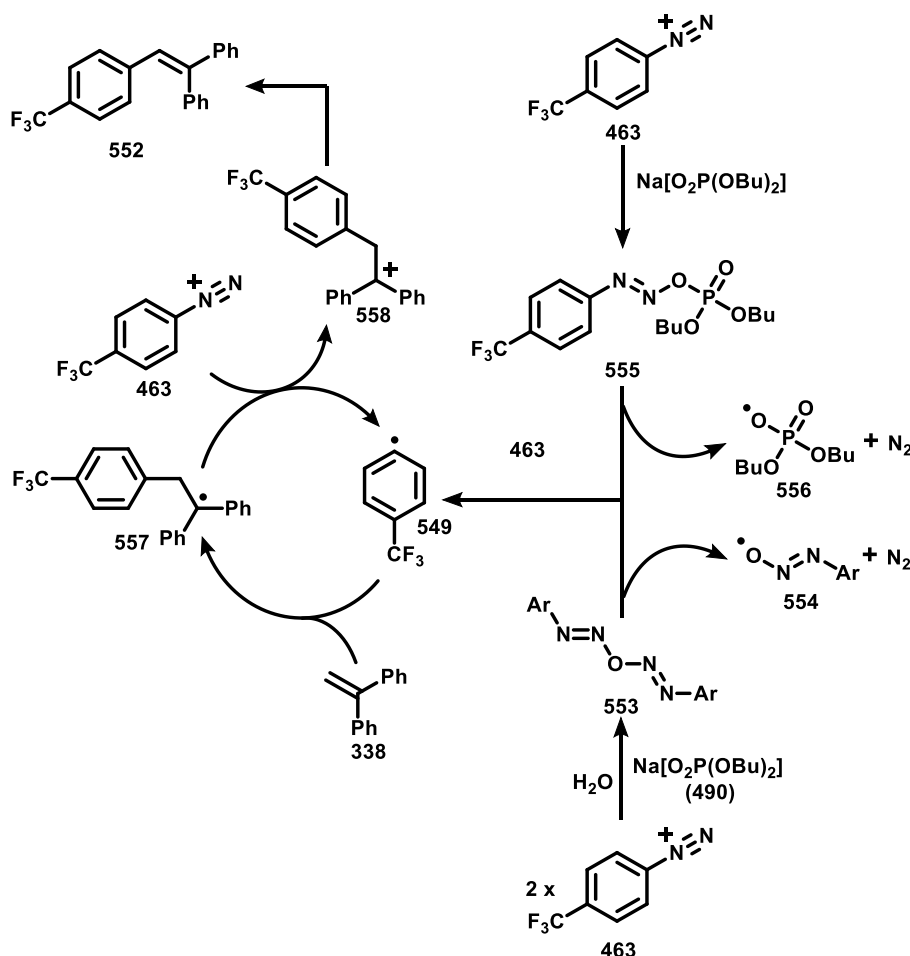
Scheme 6-43. Attempted azo-cycloamination of allyl urea **479** in the presence of TEMPO.

A second radical trapping experiment was performed using 1,1-diphenylethylene (**338**),¹⁶⁷ as it is resistant to electron transfer. The azo-cycloamination of allyl carbamate **474** with aryl diazonium salt **463** in the presence of styrene **338** gave diminished levels of azo compound **511** formation, while forming the triaryl olefin **552** (Scheme 6-44).



Scheme 6-44. Azo-cycloamination of allyl carbamate **474** in the presence of styrene **338**. Yields obtained by ^{19}F NMR and compared with benzotrifluoride internal standard.

The formation of triaryl olefin **552** from styrene **338** under azo-cycloamination conditions is intriguing and presumably proceeds by aryl diazonium salt **463** decomposition to aryl radical **549** (Scheme 6-45). Aryl diazonium salt **463** decomposition could potentially occur in two ways: 1) A Gomberg–Bachmann-type sequence occurs, where adventitious traces of water present in sodium phosphate **490** and aryl diazonium salt **463** lead to the formation of oxybis(diazene) **553**, which decomposes to molecular nitrogen, aryl radical **549** and azoxy radical **554**.^{244,257} 2) Sodium phosphate **490** directly attacks aryl diazonium salt **463** forming compound **555**, which decomposes to molecular nitrogen, aryl radical **549** and O-centred radical **556**. Aryl radical **549** adds to styrene **338** forming benzhydryl radical **557** ($E_{1/2}^{\text{ox}} = 0.27$ V vs SCE, for $\text{Ph}_2\text{C}^+\text{Me}$),²⁵⁸ which may be directly oxidised to carbocation **558** by electron transfer to aryl diazonium salt **463** reforming aryl radical **549** and so propagate a radical chain. Carbocation **558** then undergoes elimination to form triaryl olefin **552**. Alternatively, azoxy radical **554** or O-centred radical **556** could oxidise benzhydryl radical **557** to form carbocation **558**, or hydrogen atom abstract a C-H adjacent to the benzhydryl radical of **557** to directly form triaryl olefin **552**. Regardless of the precise mechanism for triaryl olefin **552** formation in Scheme 6-44, it does confirm that aryl radical **549** is formed under azo-cycloamination conditions and is implicated in azo compound product generation as formation of azo compound **511** was attenuated.



Scheme 6-45. Proposed mechanism for the formation of triaryl olefin **552** in Scheme 6-44.

An investigation into how the reduction of proposed radical cationic intermediate **485** may occur was carried out using cyclic voltammetry. Initial cyclic voltammetry studies used a set-up consisting of a glassy carbon working electrode, a platinum mesh counter electrode, and a silver wire reference electrode. Firstly, the redox window of DMSO was established to be between -1.0 V and 1.0 V versus the ferrocenium couple (Figure 6-1).

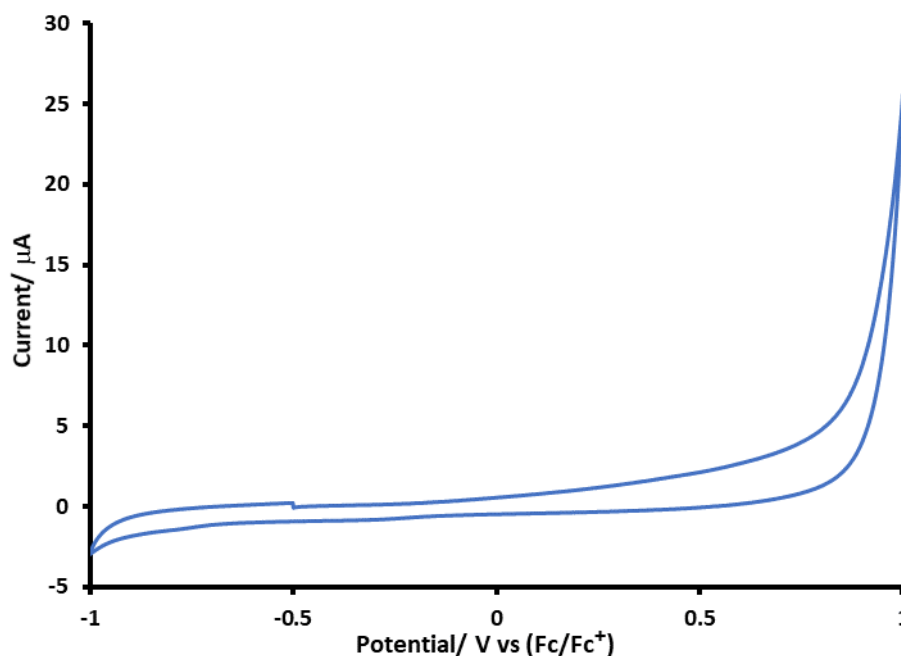


Figure 6-1. Cyclic voltammogram of DMSO.

Next, sodium dibutyl phosphate (**490**) was found to be redox inactive within the redox window of DMSO (Figure 6-2).

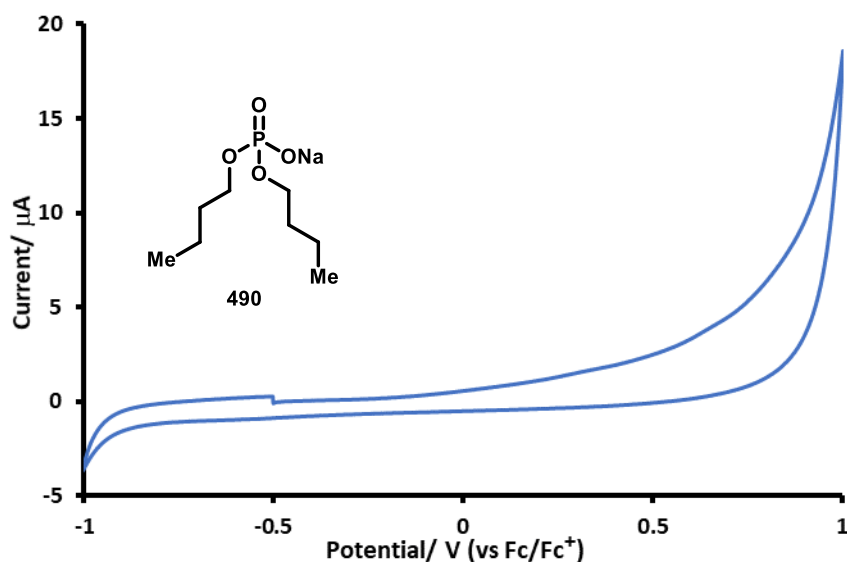


Figure 6-2. Cyclic voltammogram of sodium dibutyl phosphate (**490**).

Aryl diazonium salts exhibit low reduction potentials (PhN_2BF_4 : $E_{1/2}^{\text{red}} = -0.06 \text{ V vs SCE}$),²⁴² this being true as well for aryl diazonium salt **463**, which demonstrates an irreversible half-wave reduction at -0.72 V versus the ferrocenium couple (Figure 6-3). Little change was found upon the addition of sodium dibutyl phosphate (**490**).

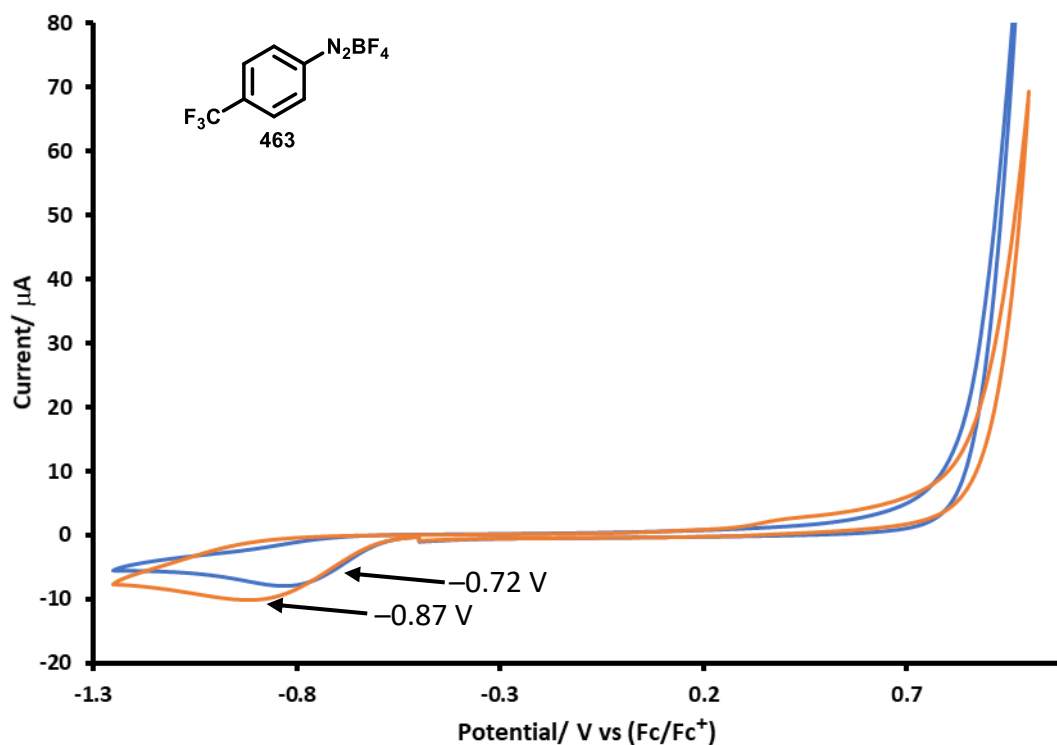


Figure 6-3. Cyclic voltammograms of aryl diazonium salt **463** (Blue) and in the presence of sodium dibutyl phosphate (**490**, 3 eq.) (Orange).

Cyclic voltammetry analysis of allyl urea **479** gives an irreversible half-wave oxidation at 0.57 V vs (Fc/Fc⁺), addition of sodium dibutyl phosphate (**490**) moves the oxidation half-wave to 0.43 V vs (Fc/Fc⁺) (Figure 6-4). This decrease in allyl urea **479** oxidation potential by the introduction of a hydrogen-bonding base (**490**) is indicative of PCET. It is feasible that the oxidation wave of allyl urea **479** originates from the oxidation of the *para*-methoxyphenyl of the tertiary amidyl, however the effect exhibited by the sodium dibutyl phosphate (**490**) implies that it is the *para*-methoxy phenyl of the secondary amidyl that is undergoing oxidation. Also, alkyl olefins demonstrate large oxidation potentials ($E_{1/2}^{ox} = 1.98$ V vs SCE, for amylene),²³⁰ so the prenyl of allyl urea **479** is unlikely to result in this oxidation wave of Figure 6-4. As the oxidation wave of allyl urea **479** and the reduction wave of aryl diazonium salt **463** do not intersect in the absence or presence of sodium dibutyl phosphate (**490**), electron transfer between the two is unlikely (Figure 6-3 and Figure 6-4).

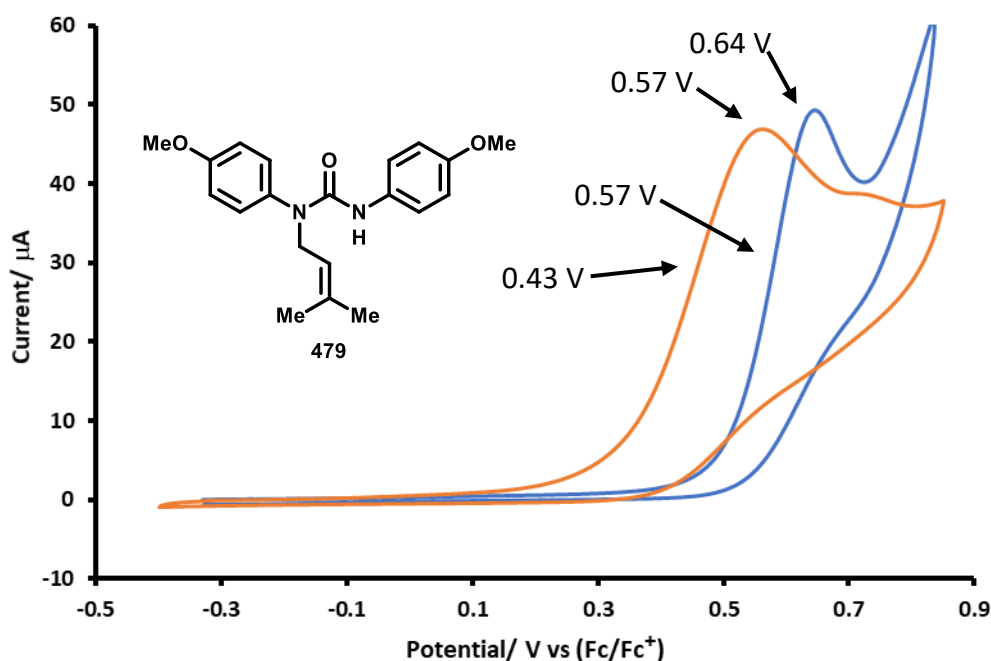


Figure 6-4. Cyclic voltammograms of allyl urea **479** (Blue) and in the presence of sodium dibutyl phosphate (**490**, 4 eq.) (Orange).

Finally for initial cyclic voltammetry studies, analysis of azo compound **488** was performed, giving an irreversible oxidation half-wave at 0.67 V, which decreased by 0.1 V upon addition of sodium dibutyl phosphate (**490**) (Figure 6-5). The observed oxidation wave presumably originates from oxidation of the *para*-methoxyphenyl rings rather than the azo bond. However, all observable oxidation waves of azo compound **488** are at higher potential than the oxidation wave of the secondary amidyl of allyl urea **479** in the presence of sodium dibutyl phosphate (**490**) (Figure 6-4 and Figure 6-5). This may show a thermodynamic driver for the proposed oxidative-PCET of allyl urea (**481**) by radical cation **485**.

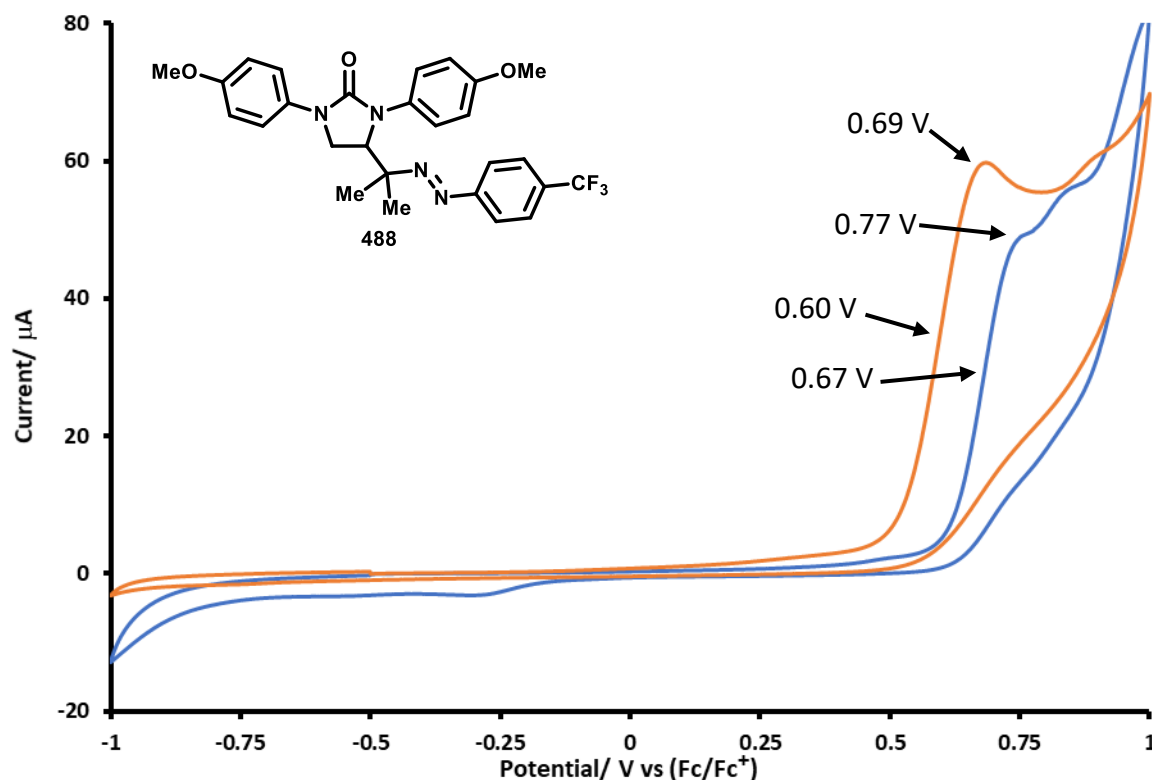


Figure 6-5. Cyclic voltammograms of allyl urea **488** (Blue), and in the presence of sodium dibutyl phosphate (**490**, 6 eq.).

Follow up cyclic voltammetry studies were performed to further clarify the structural motifs of the analytes undergoing electron transfer, by using a glassy carbon working electrode, a platinum wire counter electrode, and a Ag/AgNO₃ reference electrode. Firstly, allyl carbamates **457**, **474** and **510** were analysed by cyclic voltammetry. Allyl carbamate **474** demonstrates an irreversible oxidation half-wave at 0.71 V vs (Fc/Fc⁺), which is shifted to 0.53 V vs (Fc/Fc⁺) upon addition of sodium dibutyl phosphate (**490**) (Figure 6-6).

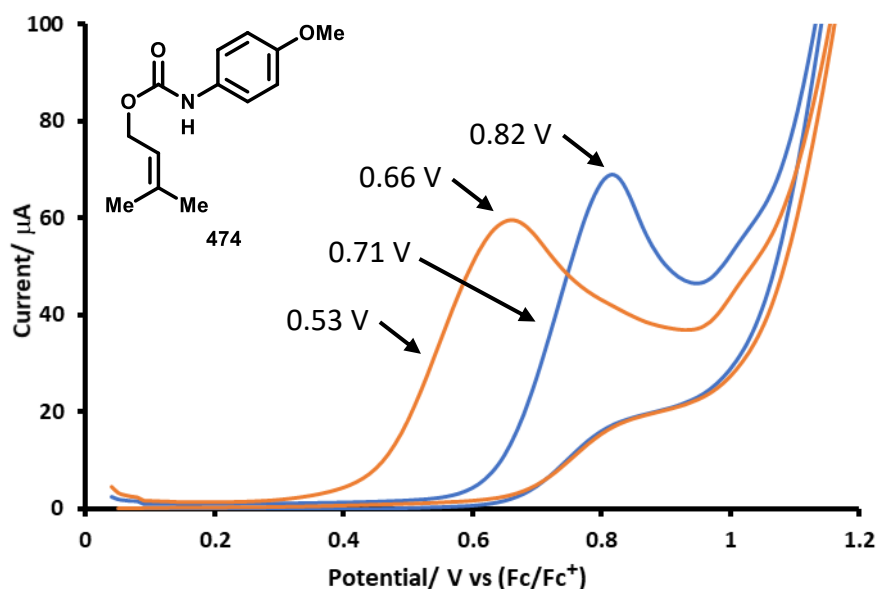


Figure 6-6. Cyclic voltammograms of allyl carbamate **474** (Blue) and in the presence of sodium dibutyl phosphate (**490**, 4 eq.) (Orange).

Next, no oxidation wave was founded within the redox window of DMSO for allyl carbamate **457** (Figure 6-7). However, in the presence of sodium dibutyl phosphate (**490**) an irreversible oxidation half-wave at 0.75 V vs (Fc/Fc⁺) was observed.

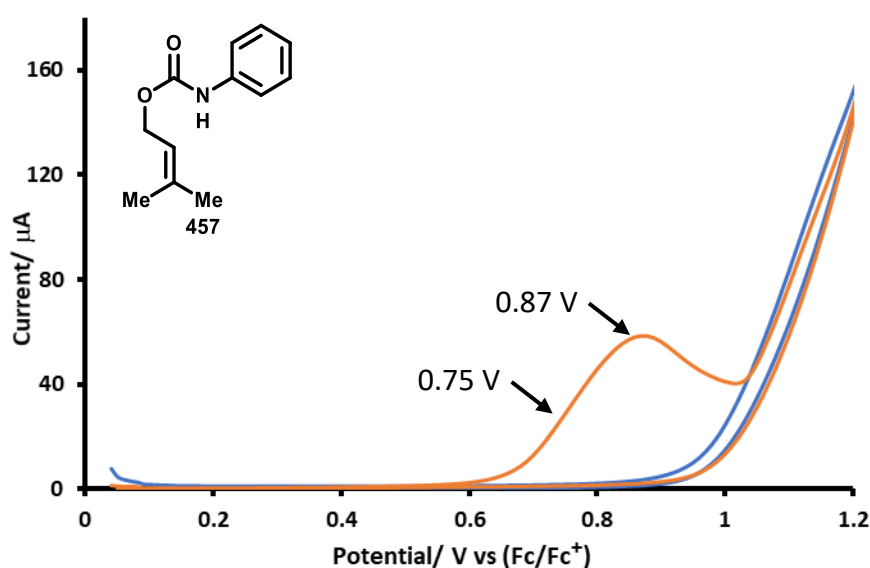


Figure 6-7. Cyclic voltammograms of allyl carbamate **457** (Blue) and in the presence of sodium dibutyl phosphate (**490**, 4 eq.) (Orange).

Lastly, allyl carbamate **510** showed no oxidation wave within the redox window of DMSO, but part of an oxidation half-wave was founded at 0.96 V vs (Fc/Fc⁺) upon addition of sodium dibutyl phosphate (**490**) (Figure 6-8). Figure 6-6, Figure 6-7 and Figure 6-8 indicate an increase in oxidation potential from allyl carbamates **474** to **457** to **510**, confirming the observed oxidation waves stem from oxidation of the *N*-aryl.

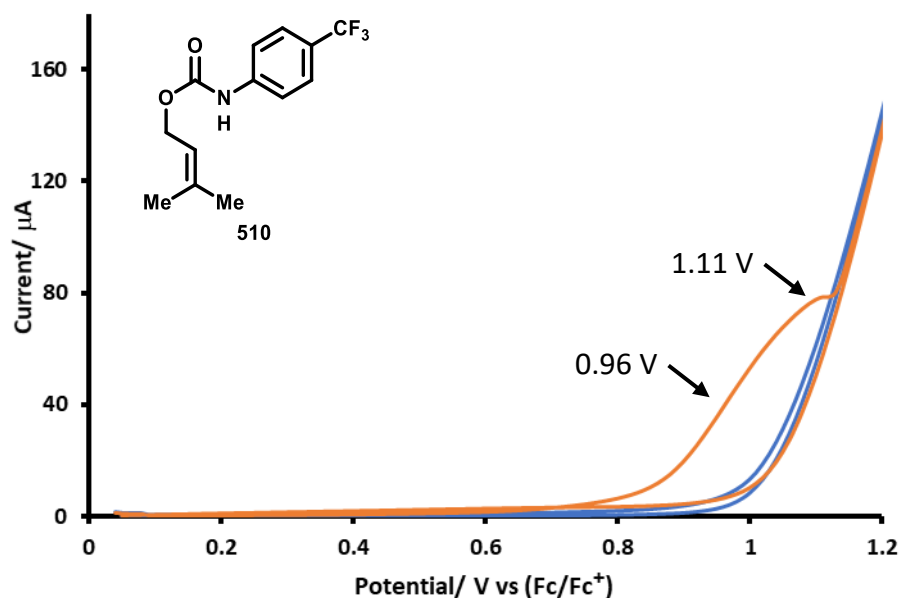


Figure 6-8. Cyclic voltammograms of allyl carbamate **510** (Blue) and in the presence of sodium dibutyl phosphate (**490**, 4 eq.) (Orange).

Following on, azo-cycloamination products **464**, **511** and **513** were analysed by cyclic voltammetry. A partial oxidation wave at 1.04 V vs (Fc/Fc⁺) was observed for azo compound **511**, which did not move upon addition of sodium dibutyl phosphate (Figure 6-9).

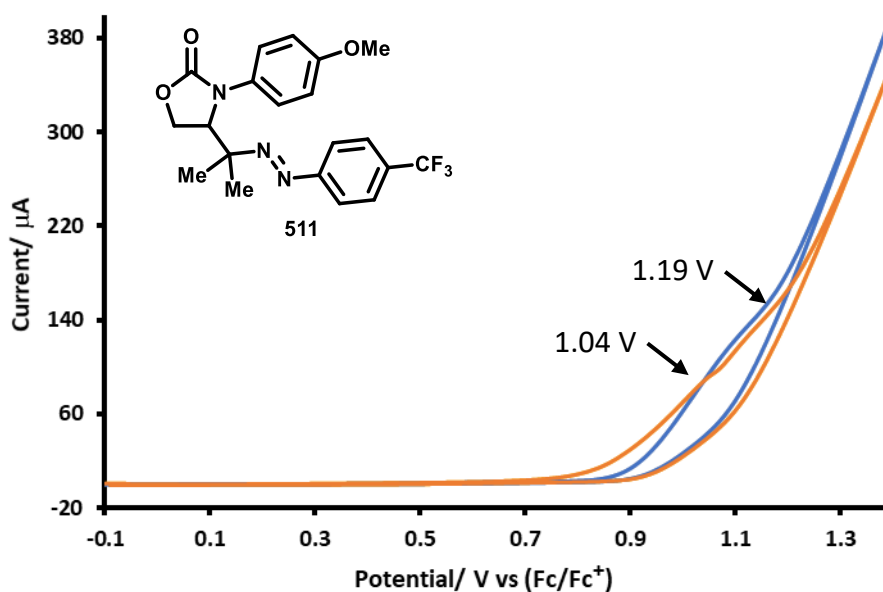


Figure 6-9. Cyclic voltammograms of azo compound **511** (Blue) and in the presence of sodium dibutyl phosphate (**490**, 4 eq.) (Orange).

Next, no oxidation wave was founded within the redox window of DMSO for azo compound **464**, even in the presence of sodium dibutyl phosphate (**490**) (Figure 6-10).

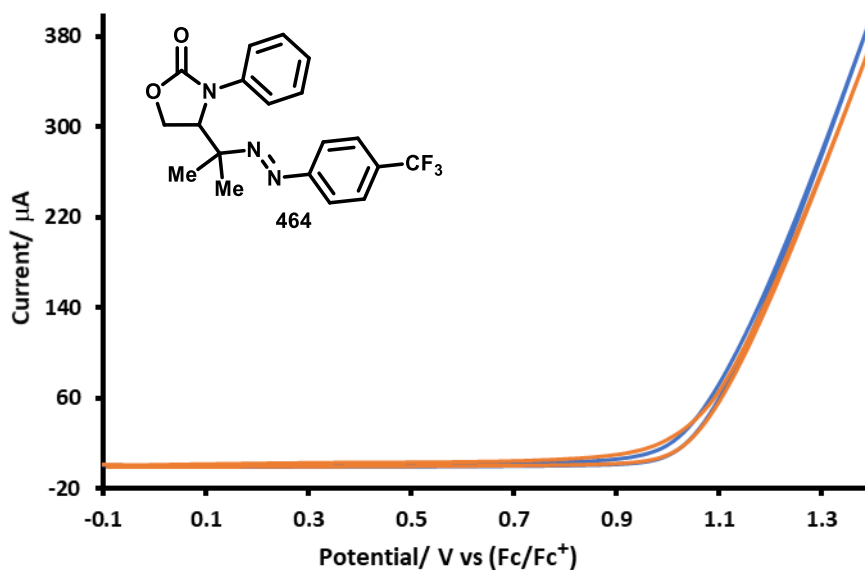


Figure 6-10. Cyclic voltammograms of azo compound **464** (Blue) and in the presence of sodium dibutyl phosphate (**490**, 4 eq.) (Orange).

Finally, like azo compound **464**, azo compound **513** also did not show an oxidation wave within the redox window of DMSO, even upon addition of sodium dibutyl phosphate (**490**) (Figure 6-11).

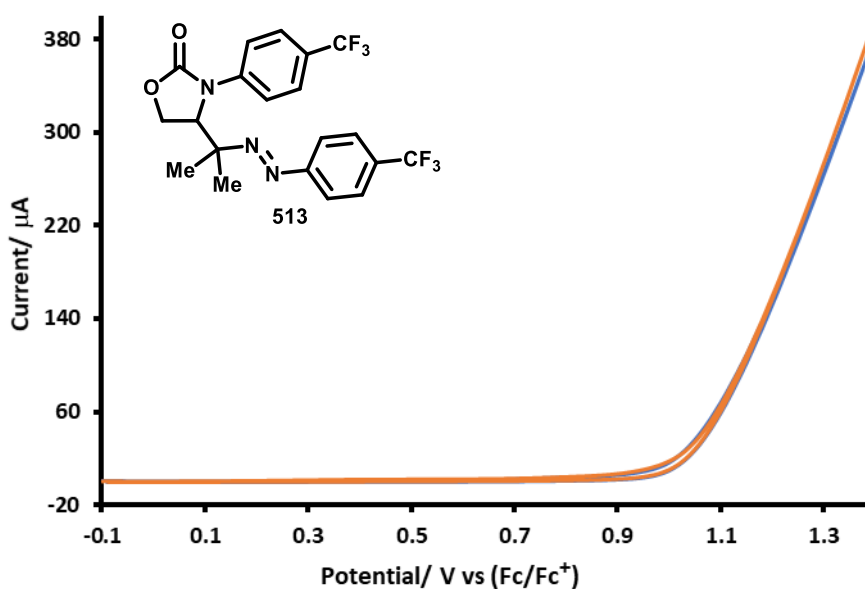
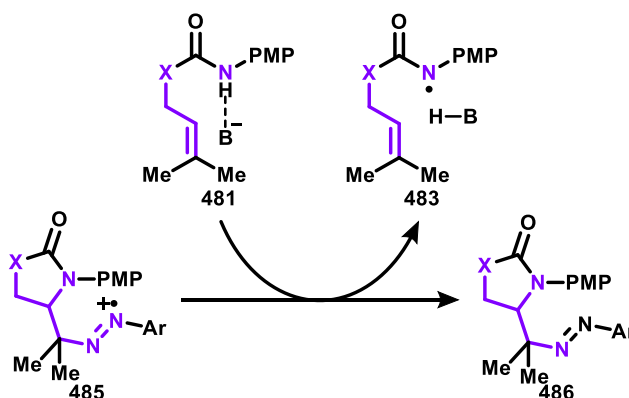


Figure 6-11. Cyclic voltammograms of azo compound **513** (Blue) and in the presence of sodium dibutyl phosphate (**490**, 4 eq.) (Orange).

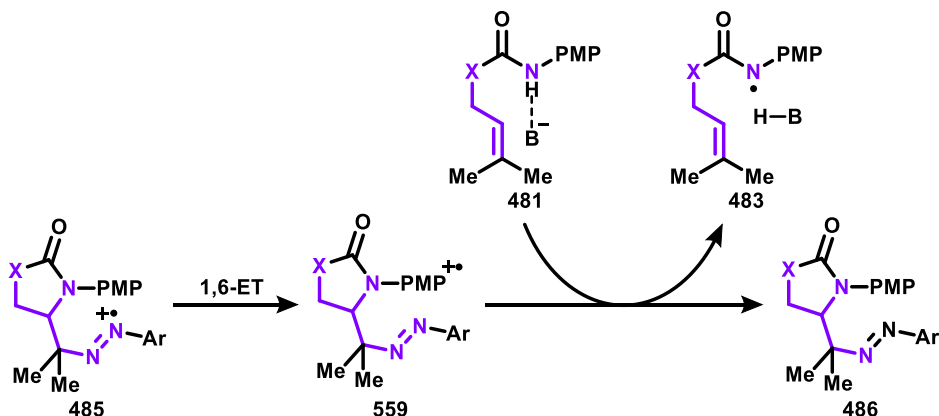
Figure 6-9, Figure 6-10 and Figure 6-11 show that the oxidation waves observed in Figure 6-5 and Figure 6-9 for azo compounds **488** and **511** are derived from oxidation of the *para*-methoxyphenyl rings and not the azo bond. Unfortunately, due to the limited redox window of DMSO, the oxidation potential for the azo bond of the azo-cycloamination products could not be determined, but by consulting literature they are likely to be large (ca. >1.5 V vs SCE).²³⁰ As such, only speculative evidence for the electron transfer of an allyl urea or allyl carbamate (**481**) to radical cation intermediate (**485**) can be given, other than it appears possible that intermediate **485** could perform an intramolecular oxidation of its *para*-methoxyphenyl ring or oxidise the *para*-methoxyphenyl rings of the starting allyl urea or allyl carbamate (**481**). This allows three possible routes for the reduction of radical cation intermediate **485** to azo-cycloamination product (**486**):

1) Scheme 6-42 is correct and direct electron transfer between allyl urea or allyl carbamate (**481**) in a hydrogen bond complex and radical cation **485** occurs (Scheme 6-46). However, this would not explain why allyl carbamates **457** and **510** gave low yields in their respective azo-cycloaminations (Scheme 6-18) when examining Figure 6-7 and Figure 6-8. Unless the *para*-methoxyphenyl ring enhances polarity-matching of the hydrogen-atom abstraction from aryl radical **549**.



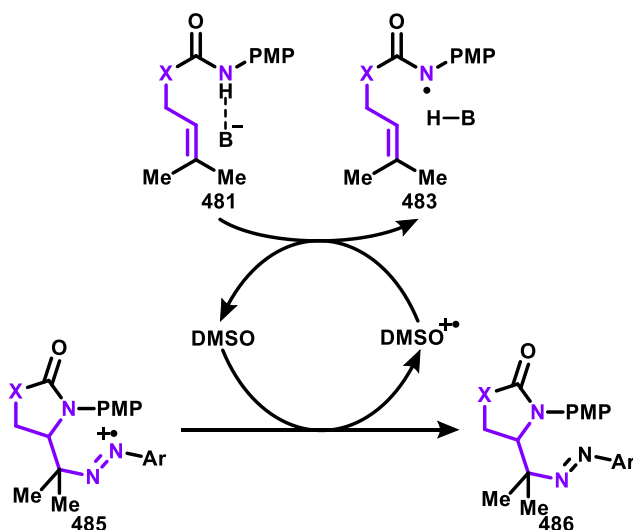
Scheme 6-46. Reduction of radical cation **485** by direct oxidation of allyl urea or allyl carbamate (**481**) in a hydrogen bond complex.

2) Intramolecular electron transfer from the *para*-methoxyphenyl ring to the azo radical cation of intermediate **485** occurs forming the new radical cation **559** (Scheme 6-47), which then through outer-sphere electron transfer oxidises allyl urea or allyl carbamate in a hydrogen bond complex (**481**). This may explain why allyl carbamates **457** and **510** performed poorly in their respective azo-cycloaminations (Scheme 6-18), as it is not clear whether the respective *N*-phenyl or *N-para*-trifluoromethylphenyl rings are oxidisable by radical cation intermediate **485** (Figure 6-10 and Figure 6-11).



Scheme 6-47. Reduction of radical cation **485** by intramolecular electron transfer, then oxidation of hydrogen-bond complex **481**.

3) Lastly, radical cation intermediate **485** could be reduced by DMSO solvent forming DMSO radical cation, which facilitates the oxidation of allyl urea or allyl carbamate in a hydrogen bond complex (**481**) (Scheme 6-48). However like case 1, without invoking enhanced polarity-matching in the initiating N-H hydrogen-atom abstraction from aryl radical **549**, this mechanism does not explain why allyl carbamates **457** and **510** should perform so poorly in their respective azo-cycloaminations (Scheme 6-18).

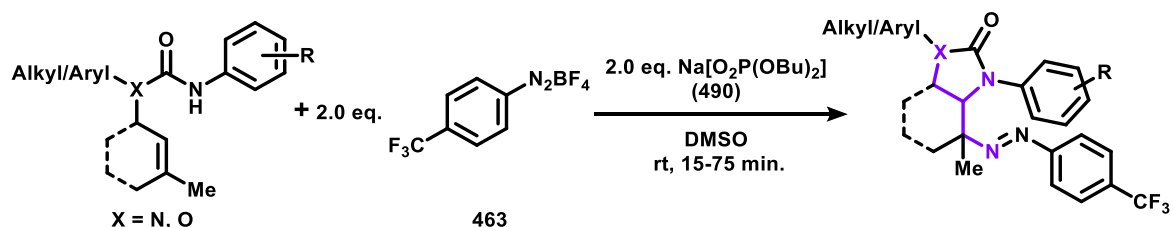


Scheme 6-48. Reduction of radical cation **485** by oxidation of DMSO solvent.

6.6 Conclusion

A new method has been discovered for the synthesis of 2-oxazolidone and imidazolidone containing azo compounds, by azo-cycloamination of allyl ureas and carbamates. This has been achieved by use of the dual reactivity of aryl diazonium salts to act as a source of aryl radicals for oxidative HAT of amidyl N-H and as an electrophilic radical acceptor. It has been found that the electronics of the *N*-aryl undergoing cyclisation and aryl diazonium salt are important in governing whether the reaction is promoted or hindered by light or PRC.

The photocatalyst-free variant of this azo-cycloamination has been applied to a variety of allyl carbamates and allyl ureas (Scheme 6-49). Limitations of this protocol have been identified, in that only tertiary C-centred alkyl radicals have been found to be efficient in aryl diazonium addition.²³¹ A protocol has been developed for the reductive cleavage of the azo-cycloamination products to their protected primary amine analogues plus other deprotections.

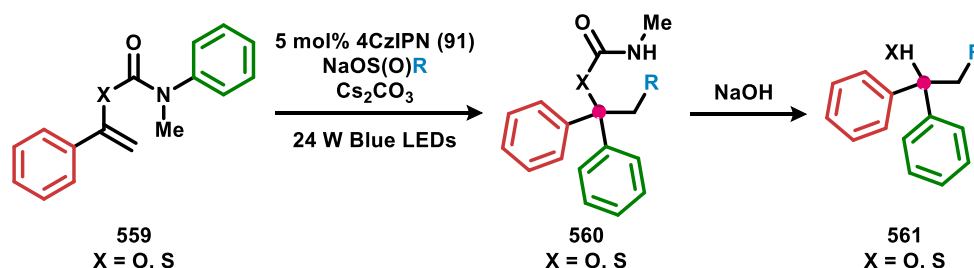


Scheme 6-49. Azo-cycloamination of ureas and carbamates.

Finally, radical trapping experiments were used to give evidence for the existence of a radical chain mechanism that is initiated by the decomposition of the aryl diazonium salt to an aryl radical, that then hydrogen atom abstracts the amidyl N-H to form amidyl radical. Propagation of the radical chain was investigated by CV and is proposed to occur by oxidative PCET from the urea or carbamate starting material, facilitated by the phosphate hydrogen bonding-accepting/base additive and electron transfer to the radical cation of the resulting product.

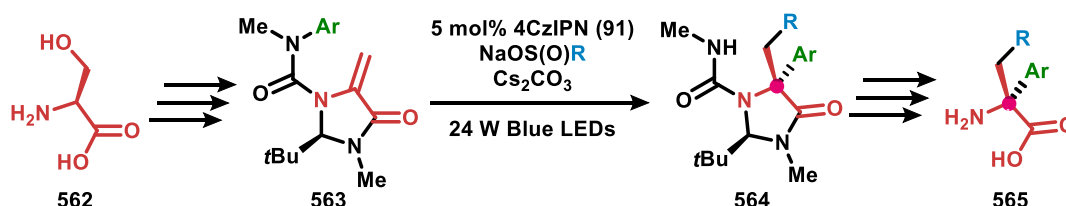
7. Future Work

The contents of this thesis has demonstrated that *N*-aryl vinyl ureas are competent electrophilic radical acceptors that when used in a reductive quenching photoredox cycle result in Truce-Smiles rearrangement, and that aryl diazonium salts initiate and propagate the homolytic activation of amidyl N-H bonds. In principle, this work could be further developed in a variety of manners to establish new synthetic tools. Firstly like the Truce-Smiles rearrangement of α -metalated ureas, Clayden and co-workers have also shown that α -metalated carbamates and thiocarbamates undergo N to C aryl migration in the context of direct C-H lithiation²⁵⁹ and carbolithiation of a vinyl group.²⁶⁰ It is conceivable that conditions for the 4CzIPN (**91**)-catalysed alkyl-arylation of vinyl ureas could be applied to vinyl carbamates and vinyl thiocarbamates (**559**), for the respective preparation of α -tertiary carbamates and α -tertiary thiocarbamates (**560**) (Scheme 7-1). Subsequently allowing access to α -tertiary alcohols and α -tertiary thiols (**561**) by hydrolysis.



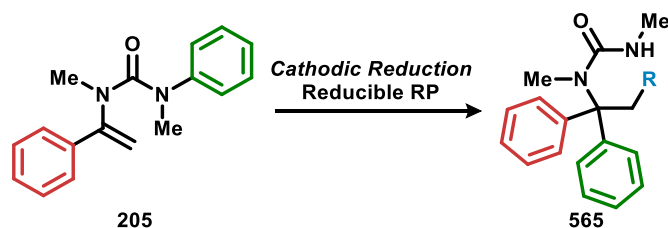
Scheme 7-1. Photoredox-catalysed alkylation-arylation of vinyl carbamates and vinyl thiocarbamates (**559**).

Despite the negative result of Scheme 3-24, implying that 4CzIPN (**91**)-catalysed trifluoromethyl-arylation is incompatible with amino acid-derived vinyl ureas, Scheme 2-35 and other reports by Clayden and co-workers show that such substrates are amenable to Truce-Smiles rearrangement under base-conditions.^{147,149} By applying Seebach's concept of Self-Regeneration of Stereocentres to the preparation of vinyl ureas, imidazolidine-4-one **563** can be formed from serine (**562**) (Scheme 7-2).²⁶¹ Performing the 4CzIPN (**91**)-catalysed radical addition followed by Truce-Smiles rearrangement of vinyl urea **563** to form α -tertiary urea **564** may be possible, as the resulting anion is amide-stabilised and so more nucleophilic than the intermediary ester-stabilised anion formed in Scheme 3-24. α -Tertiary urea **564** could then be converted into enantiopure quaternary amino acids (**565**).



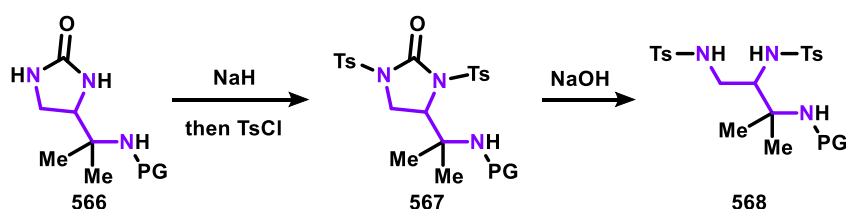
Scheme 7-2. 4CzIPN (**91**)-catalysed radical addition-arylation of vinyl urea **563** for enantiopure quaternary amino acid synthesis.

The concept of photoredox-mediated radical addition to vinyl urea, followed by subsequent reduction of the resulting intermediary ureido benzyl radical (**198**) to an α -metalated urea (**200**) for Truce-Smiles arylation, could be extended to electrochemical-mediation. Use of electrochemistry for radical generation then subsequent α -metalated urea (**200**) formation by cathodic reduction would allow for reducible radical precursors to be used, potentially opening the scope of compatible radicals-partners (Scheme 7-3). This electrochemical approach would require the reduction potential of the radical precursor and the subsequently formed radical to be more negative than the reduction potential of the intermediary ureido benzyl radical (**198**).



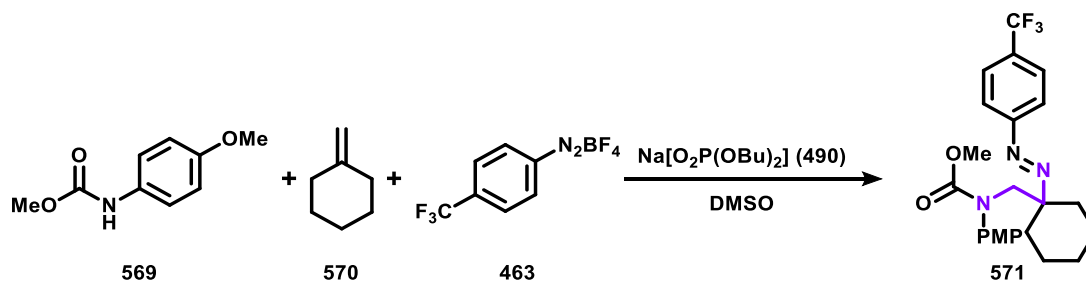
Scheme 7-3. Electrochemically-mediated radical addition followed by Truce-Smiles rearrangement of vinyl urea **205** forming α -tertiary urea (**565**).

For the azo-cycloamination of allyl ureas a method still needs to be identified for the hydrolytic ring-opening of the imidazolidin-2-one of the resulting products after hydrogenation and PMP removal (**566**), to allow this method to access vicinal triamines. So far, attempts at the opening of the imidazolidin-2-one ring have been unsuccessful (Scheme 6-37 and Scheme 6-39). However, another potential method could be tosylation of the imidazolidin-2-one ring of **566** forming **567**, which would be more prone to basic hydrolysis to yield vicinal triamine **568** (Scheme 7-4).



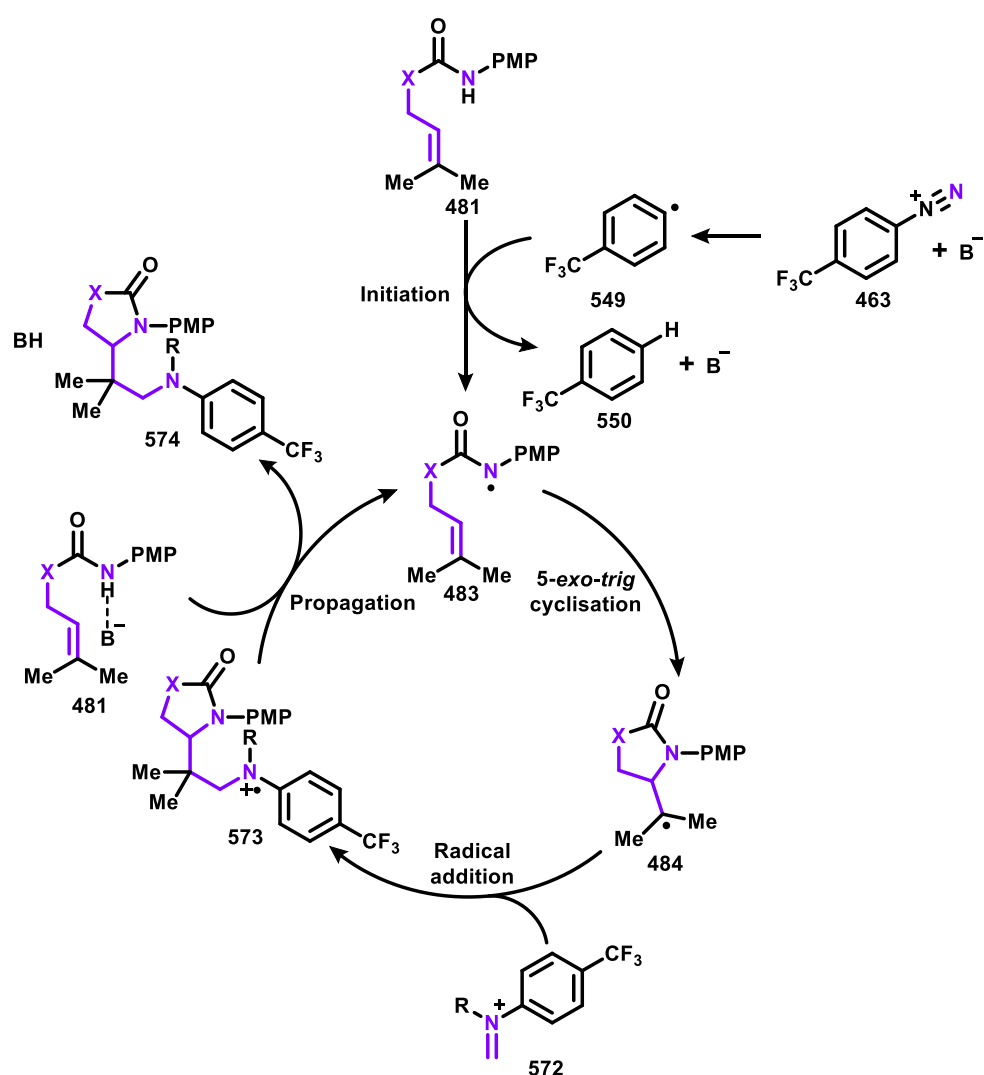
Scheme 7-4. Potential approach to converting the products of azo-cycloamination to vicinal triamines.

It would be noteworthy if this aryl diazonium salt **463** promoted azo-cycloamination of allyl carbamates could be developed into an intermolecular three-component reaction (Scheme 7-5). This approach could be achieved by homolytic activation of N-PMP carbamate (**569**), with the resulting amidyl radical then adding to a 1,1-disubstituted alkene (**570**) forming tertiary C-centered radical that would add to aryl diazonium salt **463**, giving a simple method for the diamination of 1,1-disubstituted alkenes (**571**).



Scheme 7-5. Aryl diazonium salt **463** promoted three-component azo-amination of olefin **570**.

Finally, methods for the homolytic activation of amidyl N-H bonds in the presence of C-H bonds are continually sought. In the proposed radical-chain for the azo-cycloamination of allyl ureas and carbamates, aryl diazonium salt **463** plays a key role in initiation and propagation. It may be possible to decouple the dual function of aryl diazonium salt **463** and render it as only an initiator by introducing a distinct radical acceptor (Scheme 7-6). For example, base-mediated decomposition of aryl diazonium salt **463** yields aryl radical **549**, which hydrogen atom abstracts the N-H of an allyl urea or carbamate (**481**) forming amidyl radical **483**. Cycloamination of amidyl radical **483** forms C-centred radical **484**, which could add to a different radical acceptor to aryl diazonium salt **463**, such as iminium **572** forming radical cation **573**. Radical cation **573** may be able to oxidise an allyl urea or carbamate (**481**) with assistance from a hydrogen-bonding base by PCET, forming 1,2,4-triazine **574** and amidyl radical **483**.



Scheme 7-6. Aryl diazonium salt **463** initiated and iminium **572** propagated alkyl-cycloamination of allyl ureas and carbamates (**481**).

Experimental Section

Preparation and Characterisation of Materials

8.1 General Information

8.1.1 Solvents, Reagents and Starting Materials

Reactions requiring anhydrous conditions (where specified) were performed under dry nitrogen atmosphere in glassware that was dried using a combination of vacuum and heat-gun. Air- and moisture-sensitive liquids and solutions were transferred by syringe or cannula into the reaction vessels through rubber septa. Reactions run in a microwave oven were completed on a Biotage Initiator+. Reaction mixtures were stirred magnetically. Room temperature denotes a temperature range of 19-21 °C.

All reagents were purchased (unless specified) at highest commercial quality and used as received. Non-anhydrous solvents were purchased (unless specified) at the highest commercial quality and used as received. Anhydrous THF, DCM, Et₂O and MeCN were purified by filtration over a column of activated alumina (A-2). Anhydrous DMF was purchased from Sigma-Aldrich and anhydrous acetone was purchased from Acros Organics. DMSO was distilled from CaH₂ and stored under nitrogen in a Young's tube. Langlois reagent (**134**) was purchased from Apollo Scientific and Sigma-Aldrich. Sodium difluoromethanesulfinate was purchased from J&K Scientific. Sodium 1,1-difluoroethane-1-sulfinate, sodium 2-(4-bromophenyl)-1,1-difluoroethane-1-sulfinate, sodium 2-(3-bromophenyl)-1,1-difluoroethane-1-sulfinate, sodium 2-(2-bromophenyl)-1,1-difluoroethane-1-sulfinate, sodium 7-chloro-1,1-difluoroheptane-1-sulfinate, sodium 7-azido-1,1-difluoroheptane-1-sulfinate and sodium 1,1-difluoro-4-(2-methyl-1,3-dioxolan-2-yl)butane-1-sulfinate were all purchased from Sigma-Aldrich as a part of their DiversinatesTM catalogue. Diphenylphosphine oxide, di(naphthalen-2-yl)phosphine oxide and bis(3,5-dimethylphenyl)phosphine oxide were all purchased from FluoroChem. For quantum yield experiments, commercially available potassium ferrioxalate trihydrate (Alfa Aesar) was used for actinometry. Caesium carbonate was purchased from Sigma-Aldrich and Apollo Scientific and stored in an oven at 300 °C.

8.1.2 Analytical Directions

Chromatography: Flash chromatography was performed on an automated Biotage Isolera™ Spektra Four using gradient elution on pre-packed silica gel Biotage® SNAP Ultra or Biotage® Sfär columns. THF used in chromatography was distilled before use to remove BHT inhibitor.

M.p.: Melting points were measured on a Scientific SMP10 melting point apparatus and are uncorrected.

IR: IR spectra were recorded on either neat or films of neat compounds deposited as a solution in DCM, using a Perkin Elmer (Spectrum One) FT-IR spectrometer. Only strong and selected absorbance's (ν_{\max} expressed in cm^{-1}) are reported.

^1H NMR: Spectra were recorded on Bruker Avance (400 MHz or 500 MHz). Chemical shifts (δ_{H}) are quoted in parts per million (ppm) downfield to trimethylsilane and are referenced to the appropriate NMR solvent peak(s). Assignment follow the denotation of ArCH, CH, CH_AH_B (diastereotopic protons), CH_2 , CH_3 , OH and NH. Coupling constants (J) are reported to the nearest 0.1 Hz. The splitting patterns for spectra assignments are abbreviated to singlet (s), doublet (d), triplet (t), quartet (q), quintet (qn), hextet (h), septet (sep.), multiplet (m), broad (br.) and combination of these. 2-D NMR experiments COSY, HSQC and HMBC were used where necessary in assigning NMR spectra.

^{13}C NMR: Spectra were recorded on Bruker Avance (101 MHz or 126 MHz). Chemical shifts (δ_{C}) are quoted in parts per million (ppm) and referenced to the appropriate solvent peak(s) and are assigned C_{quat} , CH, CH_2 , CH_3 , CF_3 , CF_2 and ArCX as determined using 2-D NMR experiments HSQC and HMBC where necessary. Coupling constants (J) are reported to the nearest 0.1 Hz. The splitting patterns for spectra assignments are abbreviated to singlet (s), doublet (d), triplet (t), quartet (q), quintet (qn), hextet (h), septet (sep.), multiplet (m), broad (br.) and combination of these.

^{19}F NMR: Spectra were recorded on Bruker Avance (376 MHz) instruments. Chemical shifts (δ_{F}) are quoted in parts per million (ppm) and referenced to α , α , α -trifluorotoluene internal standard. Coupling constants (J) are reported to the nearest 0.1 Hz. The splitting patterns for spectra assignments are abbreviated to singlet (s), doublet (d), triplet (t), quartet (q), quintet (qn), hextet (h), septet (sep.), multiplet (m), broad (br.) and combination of these.

^{31}P NMR: Spectra were recorded on Bruker Avance (162 MHz) instruments. Chemical shifts (δ_{P}) are quoted in parts per million (ppm).

HRMS: High resolution mass spectra were recorded on a Bruker Daltronics MicroTOF 2 mass spectrometer (ESI).

Cyclic Voltammetry (CV): CV measurements were performed at room temperature using a PalmSens4 or a CH Instruments 600E potentiostat. All working electrodes were polished before each experiment. Before each CV, the solution was stirred for approximately 2 minutes, while being degassed by sparging with nitrogen.

UV/Vis Spectrometry: Absorption spectra were measured using an Agilent Technologies Cary Series UV-Vis Spectrophotometer. Quartz cuvettes of a path length of 1 cm were used.

Fluorescence Spectrometry: Fluorometry was performed on a PerkinElmer LS-45 Fluorescence Spectrometer. Quartz cuvettes of a path length of 1 cm were used.

8.1.3 Photochemical Equipment and Setup

Blue LEDs used were LED Strip Light MINGER 16.4ft(5m) RGB SMD 5050 LED Rope Lighting Colour Changing Full Kit with 44-Keys IR Remote Controller LED Lighting Strips for Kitchen Christmas Decoration (controller was used to set lights to highest blue light intensity). The LEDs required 12 V direct current and were powered by a 2 A power supply resulting in a power output of 24 watts. The LEDs were wrapped around the interior of a glass beaker (diameter: 9 cm, height: 16 cm), with the exterior of the glass beaker wrapped in aluminium foil. During photochemical reactions, the heat generated from the LED strips resulted in a reaction temperature of 30 °C.

Photo reaction set-up:

Photoreaction mixtures were contained in a 10 mL Biotage® Initiator+ microwave vials sealed with a rubber septum that was wrapped with Parafilm, and placed upon the interior wall of the photoreactor (Figure 8-1). The photoreactor could accommodate a maximum of four microwave vials.

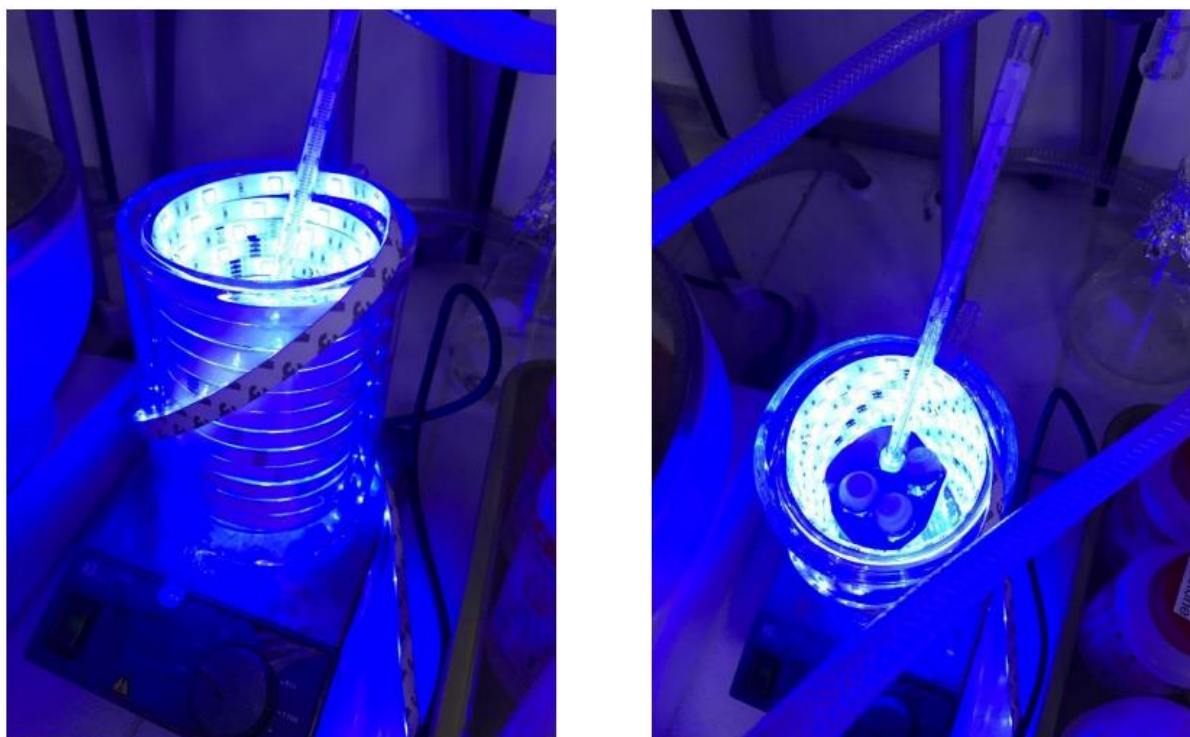
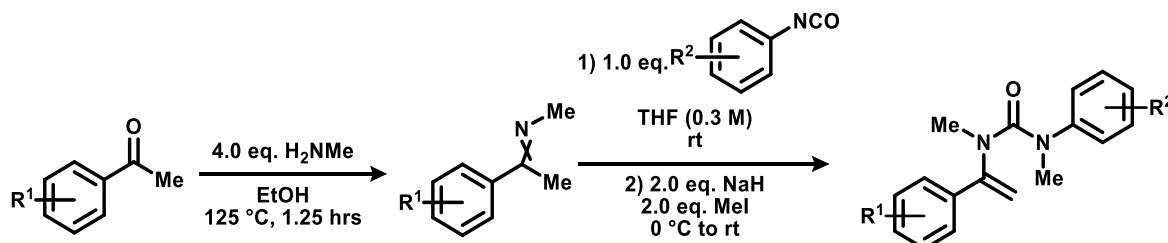


Figure 8-1. Photoredox reaction setup.

8.2 Chapter 1 Experimental

8.2.1 General Procedures

General Procedure 1 (GP1): Synthesis of vinyl ureas by imine formation.

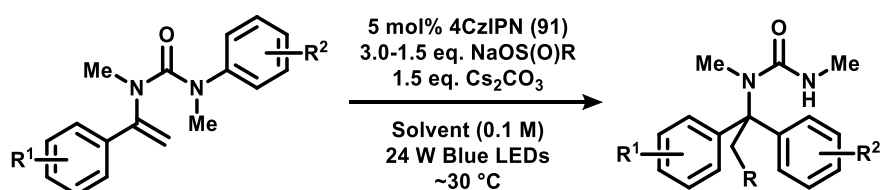


A 20 mL microwave vial was charged with methylamine (5 mL, 40.0 mmol, 8 M in EtOH, 4.0 eq.) and acetophenone derivative (10.0 mmol, 1.0 eq.). The microwave vial was sealed and the contents were heated to 125 °C by microwave irradiation and stirred for 1.25 hours. After which, the reaction mixture was concentrated under reduced pressure to give crude imine that was used without further purification.

A flame-dried Schlenk tube was sequentially charged with nitrogen, crude imine, anhydrous THF (33 mL, 0.3 M) and aryl isocyanate (10.0 mmol, 1 eq.). The resulting reaction mixture was stirred for a defined amount of time at room temperature. After which, the reaction mixture was cooled to 0 °C and 60% sodium hydride dispersed in mineral oil (800 mg, 20.0 mmol, 2.0 eq.) was added portion-wise. The reaction mixture was stirred at 0 °C for 30 minutes, then methyl iodide (1.25 mL, 20.0 mmol, 2.0 eq.) was added. The reaction mixture was warmed to room temperature and allowed to stir for a defined amount of time, after which the reaction was quenched with water (80 mL) and extracted with ethyl acetate (3 x 50 mL). The combined organic extracts were dried (Na_2SO_4), concentrated under reduced pressure and purified by flash column chromatography to give the desired vinyl urea.

Note: Yield of vinyl urea synthesis is sensitive to quality of aryl isocyanate, therefore it is recommended that unopened bottles of aryl isocyanate are used.

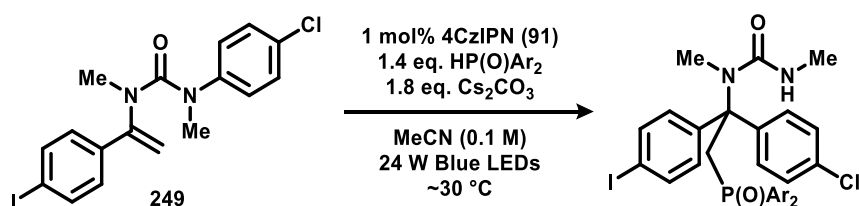
General Procedure 2 (GP2): 4CzIPN catalysed alkylation-arylation of vinyl ureas.



A flame-dried 10 mL microwave vial was charged with starting vinyl urea (0.2 mmol, 1.0 eq.), caesium carbonate (98 mg, 0.3 mmol, 1.5 eq.), 4CzIPN (**91**) (8 mg, 0.01 mmol, 0.05 eq.) and sodium sulfinate radical precursor, then flushed with nitrogen. Anhydrous solvent (0.1 M either DMF, MeCN or acetone) was added, the reaction mixture was stirred and degassed for 10 minutes by sparging with nitrogen. The reaction vessel was exposed to 24 W blue LED irradiation and allowed to stir (600 rpm) for a defined amount of time at 30°C . The reaction was quenched with water (5 mL) and extracted with ethyl acetate (3 x 4 mL). The combined organic extracts were concentrated under reduced pressure, then purified by flash column chromatography (SiO_2 , 0% to 80% Et_2O in *n*-pentane) to obtain the desired product.

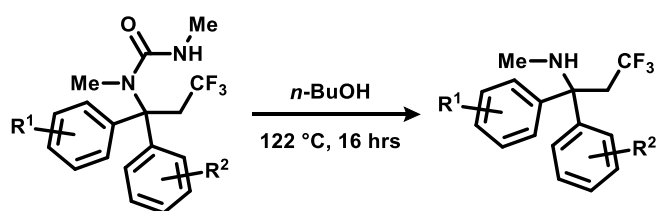
Note: Langlois reagent (**134**) is hygroscopic, if significant amounts of hydrotrifluoromethylation over trifluoromethyl-arylation is observed a new sample of Langlois reagent with a water content below 1% by Karl Fischer titration should be used.

General Procedure 3 (GP3): 4CzIPN mediated arylphosphonylation of vinyl ureas.



A flame-dried 10 mL microwave vial was charged with 1-(4-iodophenyl)-3-(1-(4-chlorophenyl)vinyl)-1,3-dimethylurea (**249**) (43 mg, 0.1 mmol, 1.0 eq.), caesium carbonate (59 mg, 0.18 mmol, 1.8 eq.), 4CzIPN (**91**) (0.8 mg, 1 μmol , 0.01 eq.) and diarylphosphine oxide derivative, then flushed with nitrogen. Anhydrous acetonitrile (1 mL) was added, the reaction mixture was stirred and degassed for 10 minutes by sparging with nitrogen. The reaction vessel was exposed to 24 W blue LED irradiation and allowed to stir (600 rpm) for a defined amount of time at 30°C . The reaction was quenched with water (5 mL) and extracted with ethyl acetate (3 x 4 mL). The combined organic extracts were concentrated under reduced pressure, then purified by flash column chromatography to obtain the desired product.

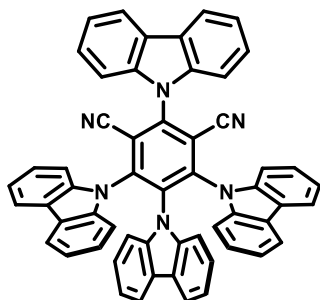
General Procedure 4 (GP4): Solvolysis of α -tertiary ureas.



A flame-dried 10 mL microwave vial was charged with α -tertiary urea starting material and *n*-butanol (1 mL per 10 mg of starting material used). The reaction mixture was briefly exposed to reduced pressure then nitrogen three times. The reaction vessel was sealed and stirred for 16 hours at 122 °C. The reaction mixture was cooled to room temperature and concentrated under reduced pressure to give crude material, which was purified by flash column chromatography (SiO₂, 0% to 30% Et₂O in *n*-pentane) to give the desired product.

8.2.2 Synthetic Procedures

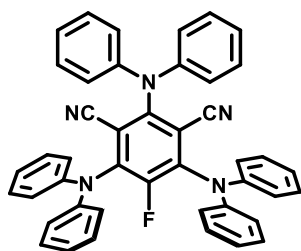
4CzIPN - 2,4,5,6-Tetra(9*H*-carbazol-9-yl)isophthalonitrile (**91**)



To a flame-dried Schlenk tube, carbazole (**202**) (1.67 g, 10.0 mmol) was added under a nitrogen atmosphere followed by anhydrous THF (40 mL), the solution was cooled to 0 °C. 60% Sodium hydride dispersed in mineral oil (600 mg, 15.0 mmol) was added portion-wise to the Schlenk tube. The reaction mixture was warmed to room temperature and allowed to stir for 30 minutes. 2,4,5,6-Tetrafluoroisophthalonitrile (**105**) (400 mg, 2.0 mmol) was added to the Schlenk tube and the contents were stirred for 24 hours at room temperature. The reaction mixture was quenched with water (5 mL) then concentrated under reduced pressure to yield an orange solid as crude product, which was purified by sequentially washing with water (2 x 50 mL), ethanol (2 x 50 mL) and diethyl ether (2 x 50 mL), yielding the title compound (861 mg, 55%) a yellow solid.

¹H NMR (400MHz, DMSO-*d*₆) δ 8.35 (2 H, d, *J* 7.8, 2 x ArCH), 8.19 (2 H, d, *J* 8.3, 2 x ArCH), 7.86 (4 H, d, *J* 7.5, 4 x ArCH), 7.77-7.72 (6 H, m, 6 x ArCH), 7.54 (2 H, d, *J* 8.3, 2 x ArCH), 7.51-7.44 (4 H, m, 4 x ArCH), 7.17-7.07 (8 H, m, 8 x ArCH), 6.81 (2 H, t, *J* 7.7, 2 x ArCH), 6.70 (2 H, t, *J* 7.7, 2 x ArCH). Data in good agreement with literature.⁹⁴

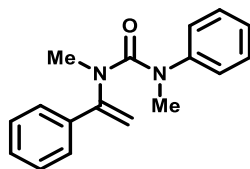
3DPAFIPN - 2,4,6-Tris(diphenylamino)-5-fluoroisophthalonitrile (106)



To a flame-dried Schlenk tube diphenyl amine (1.69 g, 10.0 mmol) was added under a nitrogen atmosphere followed by anhydrous THF (40 mL), the mixture was cooled to 0 °C. A solution of *n*-butyllithium in THF (6.24 mL, 1.6 M, 10.0 mmol) was slowly added to the Schlenk tube. The reaction mixture was warmed to room temperature and allowed to stir for 40 minutes. A solution of 2,4,5,6-tetrafluoroisophthalonitrile (**105**) (400 mg, 2.0 mmol) dissolved in anhydrous THF (8 mL) was added slowly to the Schlenk tube, the contents were heated to 60 °C and stirred for 48 hours. The reaction mixture was quenched with water (5 mL) then concentrated under reduced pressure to yield an orange solid as crude product, which was purified by sequentially washing with water (2 x 50 mL), ethanol (2 x 50 mL) and diethyl ether (2 x 50 mL), yielding the title compound (1.16 g, 90%) a yellow solid.

¹H NMR (400MHz, CDCl₃) δ 7.28-7.22 (12 H, m, 12 x ArCH), 7.08-7.02 (6 H, m, 6 x ArCH), 7.02-6.96 (12 H, m, 12 x ArCH). **¹⁹F NMR (377 MHz, CDCl₃)** δ -121.2 (1 F, s, ArCF). Data in good agreement with literature.^{97a}

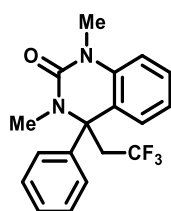
1,3-Dimethyl-3-phenyl-1-(1-phenylvinyl)urea (205)



Formation of the title compound was carried out by following GP1 with acetophenone (**81**) (1.16 mL, 1.20 g, 10.0 mmol) and phenyl isocyanate (**204**) (1.09 mL, 1.19 g, 10.0 mmol) used as starting materials. The imine intermediate was stirred with the requisite aryl isocyanate for 28 hours, subsequent methylation with methyl iodide was stirred for 24 hours. The resulting crude material was purified by flash column chromatography (SiO₂, 0 to 15% THF in 40-60 petroleum ether) yielding the title compound (0.595 g, 22%) as a pale-yellow oil.

IR (film, cm⁻¹) ν_{\max} = 2936, 1655, 1354, 693. **¹H NMR (400 MHz, CDCl₃)** δ 7.27-7.24 (3 H, m, 3 x ArCH), 7.21-7.16 (2 H, m, 2 x ArCH), 7.13-7.08 (2 H, m, 2 x ArCH), 7.07-7.02 (1 H, m, ArCH), 6.82-6.76 (2 H, m, 2 x ArCH), 4.84 (1 H, d, *J* 0.6, CH_aH_b), 4.58 (1 H, d, *J* 0.6, CH_aH_b), 3.23 (3 H, s, CH₃), 2.98 (3 H, s, CH₃). **¹³C NMR (101 MHz, CDCl₃)** δ 160.9 (CO), 150.3 (C_{quat}), 145.0 (C_{quat}), 138.3 (C_{quat}), 128.7 (2 x ArCH), 128.4 (ArCH), 128.1 (2 x ArCH), 125.9 (2 x ArCH), 125.3 (2 x ArCH), 124.8 (ArCH), 107.0 (CH₂), 39.5 (CH₃), 38.6 (CH₃). **HRMS *m/z* (ESI⁺)** *m/z* calcd for C₁₇H₁₉N₂O⁺ [M+H]⁺ 267.1492; found 267.1501.

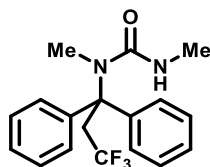
1,3-Dimethyl-4-phenyl-4-(2,2,2-trifluoroethyl)-3,4-dihydroquinazolin-2(1H)-one (206)



Formation of the title compound was carried out by following GP2 with 1,3-dimethyl-3-phenyl-1-(1-phenylvinyl)urea (**205**) (53 mg, 0.2 mmol) and sodium trifluoromethanesulfinate (**134**) (92 mg, 3.0 eq., 0.6 mmol) used as starting materials and DMF used as solvent, but with the omission of caesium carbonate. The reaction mixture was stirred for 17 hours. The resulting crude material was purified by flash column chromatography (SiO₂, 0% to 15% acetone in *n*-pentane) yielding the title compound (39 mg, 58%) as a colourless film.

IR (film, cm⁻¹) ν_{\max} = 2953, 1657, 1379, 1116. **¹H NMR (400 MHz, CDCl₃)** δ 7.42-7.34 (4 H, m, 2 x ArCH + 2 x ArCH), 7.33-7.28 (1 H, m, ArCH), 7.20 (1 H, ddd, *J* 8.3, 7.3, 1.5, ArCH), 6.86 (1 H, dd, *J* 8.3, 1.1, ArCH), 6.80 (1 H, ddd, *J* 7.3, 6.5, 1.1, ArCH), 6.54 (1 H, dd, *J* 7.3, 1.5, ArCH), 3.44 (3 H, s, NCH₃), 3.28-3.16 (1 H, m, CH_aH_b), 3.08-2.96 (1 H, m, CH_aH_b), 2.68 (3 H, s, NCH₃). **¹³C NMR (101 MHz, CDCl₃)** δ 153.2 (CO), 145.6 (C_{quat}), 138.0 (C_{quat}), 129.0 (2 x ArCH), 128.8 (ArCH), 128.3 (ArCH), 128.1 (ArCH), 126.7 (2 x ArCH), 125.9 (CF₃, q, *J*_{CF} 278.9), 124.2 (C_{quat}), 121.7 (ArCH), 112.9 (ArCH), 64.4 (C_{quat}, q, *J*_{CF} 2.0), 40.7 (CH₂, q, *J*_{CF} 25.9), 31.7 (NCH₃), 30.3 (NCH₃). **¹⁹F NMR (377 MHz, CDCl₃)** δ -61.7 (3 F, t, *J* 10.0, CF₃). **HRMS *m/z* (ESI⁺)** *m/z* calcd for C₁₈H₁₈F₃N₂O⁺ [M+H]⁺ 335.1366; found 335.1359.

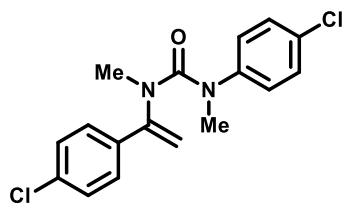
1,3-Dimethyl-1-(3,3,3-trifluoro-1,1-diphenylpropyl)urea (207)



Formation of the title compound was carried out by following GP2 with 1,3-dimethyl-3-phenyl-1-(1-phenylvinyl)urea (**205**) (53 mg, 0.2 mmol) and sodium trifluoromethanesulfinate (**134**) (92 mg, 3.0 eq., 0.6 mmol) used as starting materials and DMF used as solvent. The reaction mixture was stirred for 17 hours to give the title compound (48 mg, 71%) as a white solid.

M.p. 158-161 °C (Et₂O). **IR (film, cm⁻¹)** ν_{\max} 3364, 2945, 1639, 1259, 1117. **¹H NMR (400 MHz, CDCl₃)** δ 7.30 (4 H, dd, *J* 8.1, 1.6, 4 x ArCH), 7.26 (4 H, dd, *J* 8.1, 7.1, 4 x ArCH), 7.14 (2 H, tt, *J* 7.1, 1.6, 2 x ArCH), 4.58 (1 H, br. q, *J* 4.7, NH), 3.96 (2 H, q, *J* 11.0, CH₂), 2.79 (3 H, s, CH₃), 2.77 (3 H, d, *J* 4.7, CH₃). **¹³C NMR (101 MHz, CDCl₃)** δ 159.7 (CO), 144.4 (2 x C_{quat}), 128.3 (4 x ArCH), 126.8 (2 x ArCH), 126.6 (4 x ArCH), 126.5 (CF₃, q, *J*_{CF} 278.0), 68.4 (C_{quat}, q, *J*_{CF} 2.4), 38.8 (CH₂, q, *J*_{CF} 26.9), 36.6 (CH₃), 27.7 (CH₃). **¹⁹F NMR (377 MHz, CDCl₃)** δ -58.3 (3 F, t, *J* 11.0, CF₃). **HRMS *m/z* (ESI⁺)** *m/z* calcd for C₁₈H₂₀N₂OF₃⁺ [M+H]⁺ 337.1522; found 337.1514.

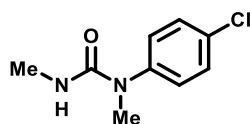
1-(4-Chlorophenyl)-3-(1-(4-chlorophenyl)vinyl)-1,3-dimethylurea (211)



Formation of the title compound was carried out by following GP1 with 1-(4-chlorophenyl)ethan-1-one (**208**) (1.30 mL, 1.54 g, 10.0 mmol) and 1-chloro-4-isocyanatobenzene (**210**) (1.54 g, 10.0 mmol) used as starting materials. The imine intermediate was stirred with the requisite aryl isocyanate for 21 hours, subsequent methylation with methyl iodide was stirred for 18 hours. The resulting crude material was purified by flash column chromatography (SiO₂, 1% to 20% acetone + 3% triethylamine in 40-60 petroleum ether) yielding the title compound (750 mg, 22%) as a white solid.

M.p. 69-72 °C (Et₂O). **IR (film, cm⁻¹)** ν_{\max} = 2939, 1662, 1491, 1351, 1093, 834. **¹H NMR (400 MHz, CDCl₃)** δ 7.24 (2 H, d, *J* 8.7, 2 x ArCH), 7.16 (2 H, d, *J* 8.8, 2 x ArCH), 7.02 (2 H, d, *J* 8.7, 2 x ArCH), 6.70 (2 H, d, *J* 8.8, 2 x ArCH), 4.86 (1 H, d, *J* 0.9, CH_aH_b), 4.61 (1 H, d, *J* 0.9, CH_aH_b), 3.24 (3 H, s, CH₃), 2.95 (3 H, s, CH₃). **¹³C NMR (101 MHz, CDCl₃)** δ 160.3 (CO), 149.2 (C_{quat}), 143.4 (C_{quat}), 136.7 (C_{quat}), 134.4 (ArCCl), 130.3 (ArCCl), 128.9 (2 x ArCH), 128.5 (2 x ArCH), 127.1 (2 x ArCH), 126.4 (2 x ArCH), 107.9 (CH₂), 39.6 (CH₃), 38.6 (CH₃). **HRMS *m/z* (ESI⁺)** *m/z* calcd for C₁₇H₁₇N₂OCl₂⁺ [M+H]⁺ 335.0712; found 335.0727.

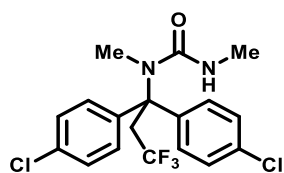
1-(4-Chlorophenyl)-1,3-dimethylurea (212)



Formation of the title compound was carried out by following GP2 with 1-(4-chlorophenyl)-3-(1-(4-chlorophenyl)vinyl)-1,3-dimethylurea (**211**) (65 mg, 0.2 mmol) and sodium trifluoromethanesulfinate (**134**) (92 mg, 3.0 eq., 0.6 mmol) used as starting materials and acetonitrile used as solvent, but with the omission of caesium carbonate. The reaction mixture was stirred for 15 hours to give the title compound (24 mg, 61%) as a white solid.

M.p. 94-97 °C (Et₂O). **IR (film, cm⁻¹)** ν_{\max} = 3355, 2949, 1652, 1525, 1492. **¹H NMR (400 MHz, CDCl₃)** δ 7.38 (2 H, d, *J* 8.7, 2 x ArCH), 7.18 (2 H, d, *J* 8.7, 2 x ArCH), 4.22 (1 H, br. s, NH), 3.24 (3 H, s, NCH₃), 2.74 (3 H, d, *J* 4.7, NCH₃). **¹³C NMR (101 MHz, CDCl₃)** δ 157.8 (CO), 142.2 (C_{quat}), 133.0 (ArCCl), 130.3 (2 x ArCH), 128.9 (2 x ArCH), 37.4 (NCH₃), 27.7 (NCH₃). **HRMS *m/z* (ESI⁺)** *m/z* calcd for C₉H₁₂ClN₂O⁺ [M+H]⁺ 199.0633; found 199.0627.

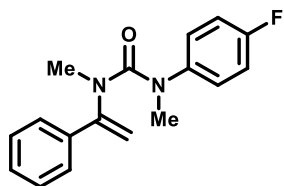
1-(1,1-Bis(4-chlorophenyl)-3,3,3-trifluoropropyl)-1,3-dimethylurea (216)



Formation of the title compound was carried out by following GP2 with 1-(4-chlorophenyl)-3-(1-(4-chlorophenyl)vinyl)-1,3-dimethylurea (**211**) (65 mg, 0.2 mmol) and sodium trifluoromethanesulfinate (**134**) (46 mg, 1.5 eq., 0.3 mmol) used as starting materials and acetonitrile used as solvent. The reaction mixture was stirred for 17 hours to give the title compound (71 mg, 88%) as a pale-yellow solid.

M.p. 176-179 °C (Et₂O). **IR (film, cm⁻¹)** ν_{\max} = 3365, 2958, 1642, 1258, 1105. **¹H NMR (400 MHz, CDCl₃)** δ 7.24 (4 H, d, *J* 8.9, 4 x ArCH), 7.20 (4 H, d, *J* 8.9, 4 x ArCH), 4.63 (1 H, br. q, *J* 4.2, NH), 3.90 (2 H, q, *J* 10.9, CH₂), 2.84-2.70 (6 H, m, 2 x CH₃). **¹³C NMR (101 MHz, CDCl₃)** δ 159.5 (CO), 142.7 (2 x C_{quat}), 132.9 (2 x ArCCl), 128.7 (4 x ArCH), 127.8 (4 x ArCH), 126.2 (CF₃, q, *J*_{CF} 278.1), 67.8 (C_{quat}, q, *J*_{CF} 2.0), 38.4 (CH₂, q, *J*_{CF} 27.4), 36.5 (NCH₃), 27.7 (NCH₃). **¹⁹F NMR (377 MHz, CDCl₃)** δ -58.5 (3 F, t, *J* 10.9, CF₃). **HRMS *m/z* (ESI⁺)** *m/z* calcd for C₁₈H₁₇N₂OCl₂F₃Na⁺ [M+Na]⁺ 427.0562; found 427.0561.

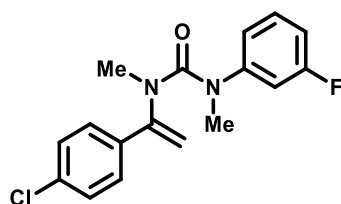
1-(4-Fluorophenyl)-1,3-dimethyl-3-(1-phenylvinyl)urea (218)



Formation of the title compound was carried out by following GP1 with acetophenone (**81**) (1.16 mL, 1.20 g, 10.0 mmol) and 1-fluoro-4-isocyanatobenzene (1.14 mL, 1.37 g, 10.0 mmol) used as starting materials. The imine intermediate was stirred with the requisite aryl isocyanate for 69 hours, subsequent methylation with methyl iodide was stirred for 25 hours. The resulting crude material was purified by flash column chromatography (SiO₂, 1% to 20% acetone + 3% trimethylamine in 40-60 petroleum ether) yielding the title compound (1.49 g, 52%) as a pale-yellow oil.

IR (film, cm⁻¹) ν_{\max} = 3060, 1657, 1508, 1354, 1218, 777. **¹H NMR (400 MHz, CDCl₃)** δ 7.30-7.26 (3 H, m, 3 x ArCH), 7.16-7.10 (2 H, m, 2 x ArCH), 6.89 (2 H, dd, *J* 9.1, 8.3, 2 x ArCH), 6.76 (2 H, dd, *J* 9.1, 4.9, 2 x ArCH), 4.92 (1 H, d, *J* 0.7, CH_aH_b), 4.62 (1 H, d, *J* 0.7, CH_aH_b), 3.23 (3 H, s, CH₃), 2.98 (3 H, s, CH₃). **¹³C NMR (101 MHz, CDCl₃)** δ 160.8 (CO), 160.1 (ArCF, d, *J*_{CF} 244.7), 150.3 (C_{quat}), 141.1 (C_{quat}, d, *J*_{CF} 2.9), 138.0 (C_{quat}), 128.6 (ArCH), 128.2 (2 x ArCH), 127.2 (2 x ArCH, d, *J*_{CF} 8.5), 125.8 (2 x ArCH), 115.5 (2 x ArCH, d, *J*_{CF} 22.7), 107.3 (CH₂), 39.6 (CH₃), 39.0 (CH₃). **¹⁹F NMR (377 MHz, CDCl₃)** δ -117.2—-117.4 (1 F, m, ArCF). **HRMS *m/z* (ESI⁺)** *m/z* calcd for C₁₇H₁₈N₂O⁺ [M+H]⁺ 285.1398; found 285.1408.

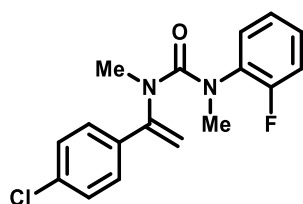
1-(1-(4-Chlorophenyl)vinyl)-3-(3-fluorophenyl)-1,3-dimethylurea (219)



Formation of the title compound was carried out by following GP1 with 1-(4-chlorophenyl)ethan-1-one (**208**) (1.30 mL, 1.54 g, 10.0 mmol) and 1-fluoro-3-isocyanatobenzene (1.14 mL, 1.37 g, 10.0 mmol) used as starting materials. The imine intermediate was stirred with the requisite aryl isocyanate for 18 hours, subsequent methylation with methyl iodide was stirred for 27 hours. The resulting crude material was purified by flash column chromatography (SiO₂, 1% to 20% acetone + 3% trimethylamine in 40-60 petroleum ether) yielding the title compound (1.23 g, 39%) as a pale-yellow oil, which solidified over time to give a white solid.

M.p. 43-45 °C (Et₂O). **IR (film, cm⁻¹)** ν_{max} = 3069, 1662, 1610, 1490, 1354, 1327, 837. **¹H NMR (400 MHz, CDCl₃)** δ 7.23 (2 H, d, *J* 8.9, 2 x ArCH), 7.13 (1 H, dt, *J* 8.2, 6.5, ArCH), 7.03 (2 H, d, *J* 8.9, 2 x ArCH), 6.74 (1 H, tdd, *J* 8.2, 2.3, 0.9, ArCH), 6.56 (1 H, ddd, *J* 8.2, 2.3, 0.9, ArCH), 6.48 (1 H, dt, *J* 10.4, 2.3, ArCH), 4.84 (1 H, d, *J* 1.0, CH_aH_b), 4.63 (1 H, d, *J* 1.0, CH_aH_b), 3.24 (3 H, s, CH₃), 2.95 (3 H, s, CH₃). **¹³C NMR (101 MHz, CDCl₃)** δ 162.8 (ArCF, d, *J*_{CF} 256.6), 160.2 (CO), 149.1 (C_{quat}), 146.3 (C_{quat}, d, *J*_{CF} 10.0), 136.7 (C_{quat}), 134.3 (ArCCl), 129.7 (ArCH, d, *J*_{CF} 9.2), 128.4 (2 x ArCH), 127.0 (2 x ArCH), 120.4 (ArCH, d, *J*_{CF} 2.9), 112.1 (ArCH, d, *J*_{CF} 23.3), 111.5 (ArCH, d, *J*_{CF} 21.1), 107.8 (CH₂), 39.5 (CH₃), 38.3 (CH₃). **¹⁹F NMR (377 MHz, CDCl₃)** δ -112.3—-112.5 (1 F, m, ArCF). **HRMS *m/z* (ESI⁺)** *m/z* calcd for C₁₇H₁₇N₂OFCl⁺ [M+H]⁺ 319.1008; found 319.1020.

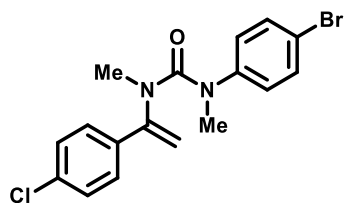
1-(1-(4-Chlorophenyl)vinyl)-3-(2-fluorophenyl)-1,3-dimethylurea (220)



Formation of the title compound was carried out by following GP1 with 1-(4-chlorophenyl)ethan-1-one (**208**) (1.30 mL, 1.54 g, 10.0 mmol) and 1-fluoro-2-isocyanatobenzene (1.12 mL, 1.37 g, 10.0 mmol) used as starting materials. The imine intermediate was stirred with the requisite aryl isocyanate for 20 hours, subsequent methylation with methyl iodide was stirred for 25 hours. The resulting crude material was purified by flash column chromatography (SiO₂, 1% to 20% acetone + 3% trimethylamine in 40-60 petroleum ether), followed by additional purification by flash column chromatography (SiO₂, 0% to 10% Et₂O in DCM), yielding the title compound (339 mg, 11%) as a colourless oil.

IR (film, cm⁻¹) ν_{max} = 1659, 1503, 1353, 1327, 1094, 758. **¹H NMR (400 MHz, CDCl₃)** δ 7.20 (2 H, d, *J* 8.4, 2 x ArCH), 7.09-7.02 (3 H, m, ArCH + 2 x ArCH), 6.98-6.91 (2 H, m, ArCH + ArCH), 6.83 (1 H, t, *J* 7.7, ArCH), 4.94 (1 H, s, CH_aH_b), 4.75 (1 H, s, CH_aH_b), 3.12 (3 H, s, CH₃), 3.06 (3 H, s, CH₃). **¹³C NMR (101 MHz, CDCl₃)** δ 160.8 (CO), 157.7 (ArCF, d, *J*_{CF} 249.9), 148.8 (C_{quat}), 135.5 (C_{quat}), 134.3 (ArCCI), 132.4 (C_{quat}, d, *J*_{CF} 11.6), 129.0 (ArCH, d, *J*_{CF} 1.4), 128.4 (2 x ArCH), 127.6 (ArCH, d, *J*_{CF} 7.9), 127.2 (2 x ArCH), 124.3 (ArCH, d, *J*_{CF} 3.6), 116.4 (ArCH, d, *J*_{CF} 20.3), 107.5 (CH₂), 39.0 (NCH₃), 38.6 (NCH₃). **¹⁹F NMR (377 MHz, CDCl₃)** δ -120.8—-121.0 (1 F, m, ArCF). **HRMS *m/z* (ESI⁺)** *m/z* calcd for C₁₇H₁₇N₂OFCl⁺ [M+H]⁺ 319.1008; found 319.1003.

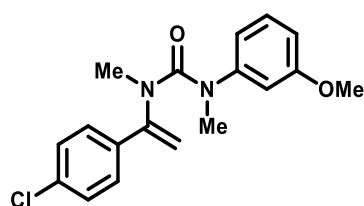
1-(4-Bromophenyl)-3-(1-(4-chlorophenyl)vinyl)-1,3-dimethylurea (221)



Formation of the title compound was carried out by following GP1 with 1-(4-chlorophenyl)ethan-1-one (**208**) (1.30 mL, 1.54 g, 10.0 mmol) and 1-bromo-4-isocyanatobenzene (**245**) (1.98 g, 10.0 mmol) used as starting materials. The imine intermediate was stirred with the requisite aryl isocyanate for 24 hours, subsequent methylation with methyl iodide was stirred for 20 hours. The resulting crude material was purified by flash column chromatography (SiO₂, 5% to 30% Et₂O in 40-60 petroleum ether) yielding the title compound (980 mg, 26%) as a pale-yellow solid.

M.p. 86-89 °C (Et₂O). **IR (film, cm⁻¹)** ν_{max} = 2938, 1659, 1488, 1349, 1327. **¹H NMR (400 MHz, CDCl₃)** δ 7.31 (2 H, d, *J* 8.6, 2 x ArCH), 7.24 (2 H, d, *J* 8.5, 2 x ArCH), 7.02 (2 H, d, *J* 8.5, 2 x ArCH), 6.64 (2 H, d, *J* 8.6, 2 x ArCH), 4.86 (1 H, s, CH_aH_b), 4.61 (1 H, s, CH_aH_b), 3.25 (3 H, s, CH₃), 2.94 (3 H, s, CH₃). **¹³C NMR (101 MHz, CDCl₃)** δ 160.2 (CO), 149.2 (C_{quat}), 143.9 (C_{quat}), 136.8 (C_{quat}), 134.4 (ArCCl), 131.8 (2 x ArCH), 128.5 (2 x ArCH), 127.0 (2 x ArCH), 126.7 (2 x ArCH), 118.0 (ArCBr), 108.0 (CH₂), 39.6 (NCH₃), 38.5 (NCH₃). **HRMS *m/z* (ESI⁺)** *m/z* calcd for C₁₇H₁₇N₂OBrCl⁺ [M+H]⁺ 379.0207; found 379.0215.

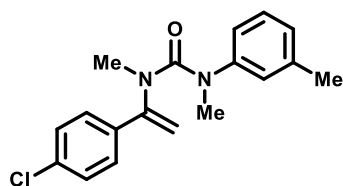
1-(1-(4-Chlorophenyl)vinyl)-3-(3-methoxyphenyl)-1,3-dimethylurea (222)



Formation of the title compound was carried out by following GP1 with 1-(4-chlorophenyl)ethan-1-one (**208**) (1.30 mL, 1.54 g, 10.0 mmol) and 1-isocyanato-3-methoxybenzene (1.31 mL, 1.49 g, 10.0 mmol) used as starting materials. The imine intermediate was stirred with the requisite aryl isocyanate for 17 hours, subsequent methylation with methyl iodide was stirred for 26 hours. The resulting crude material was purified by flash column chromatography (SiO₂, 1% to 20% acetone + 3% trimethylamine in 40-60 petroleum ether) yielding the title compound (1.29 g, 39%) as a yellow oil.

IR (film, cm⁻¹) ν_{max} = 2943, 1659, 1596, 1489, 1353, 836. **¹H NMR (400 MHz, CDCl₃)** δ 7.21 (2 H, d, *J* 8.7, 2 x ArCH), 7.08 (1 H, t, *J* 8.2, ArCH), 7.04 (2 H, d, *J* 8.7, 2 x ArCH), 6.59 (1 H, ddd, *J* 8.2, 2.4, 0.8, ArCH), 6.39 (1 H, ddd, *J* 8.2, 2.4, 0.8, ArCH), 6.30 (1 H, t, *J* 2.4, ArCH), 4.84 (1 H, d, *J* 0.7, CH_aH_b), 4.61 (1 H, d, *J* 0.7, CH_aH_b), 3.72 (3 H, s, OCH₃), 3.20 (3 H, s, CH₃), 2.98 (3 H, s, CH₃). **¹³C NMR (101 MHz, CDCl₃)** δ 160.6 (CO), 159.9 (ArCO), 149.3 (C_{quat}), 146.0 (C_{quat}), 136.8 (C_{quat}), 134.1 (ArCCL), 129.4 (ArCH), 128.3 (2 x ArCH), 127.2 (2 x ArCH), 117.9 (ArCH), 111.6 (ArCH), 110.4 (ArCH), 107.5 (CH₂), 55.4 (OCH₃), 39.4 (CH₃), 38.8 (CH₃). **HRMS *m/z* (ESI⁺)** *m/z* calcd for C₁₈H₂₀N₂O₂Cl⁺ [M+H]⁺ 331.1208; found 331.1223.

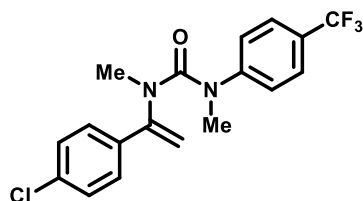
1-(1-(4-Chlorophenyl)vinyl)-1,3-dimethyl-3-(*m*-tolyl)urea (223)



Formation of the title compound was carried out by following GP1 with 1-(4-chlorophenyl)ethan-1-one (**208**) (1.30 mL, 1.54 g, 10.0 mmol) and 1-isocyanato-3-methylbenzene (1.29 mL, 1.33 g, 10.0 mmol) used as starting materials. The imine intermediate was stirred with the requisite aryl isocyanate for 24 hours, subsequent methylation with methyl iodide was stirred for 20 hours. The resulting crude material was purified by flash column chromatography (SiO₂, 5% to 40% Et₂O in 40-60 petroleum ether), followed by additional purification by flash column chromatography (SiO₂, 0% to 10% Et₂O in DCM), yielding the title compound (1.04 g, 33%) as a pale-yellow oil.

IR (film, cm⁻¹) ν_{\max} = 2918, 1657, 1605, 1353, 1327. **¹H NMR (400 MHz, CDCl₃)** δ 7.22 (2 H, d, *J* 8.5, 2 x ArCH), 7.07 (1 H, t, *J* 7.7, ArCH), 7.02 (2 H, d, *J* 8.5, 2 x ArCH), 6.86 (1 H, d, *J* 7.7, ArCH), 6.61 (1 H, d, *J* 7.7, ArCH), 6.56 (1 H, br. s, ArCH), 4.81 (1 H, s, CH_aH_b), 4.59 (1 H, s, CH_aH_b), 3.19 (3 H, s, CH₃), 3.01 (3 H, s, CH₃), 2.25 (3 H, s, ArCCH₃). **¹³C NMR (101 MHz, CDCl₃)** δ 160.7 (CO), 149.3 (C_{quat}), 144.7 (C_{quat}), 138.4 (C_{quat}), 136.8 (C_{quat}), 134.1 (ArCCI), 128.6 (ArCH), 128.2 (2 x ArCH), 127.2 (2 x ArCH), 126.3 (ArCH), 125.8 (ArCH), 122.6 (ArCH), 107.2 (CH₂), 39.3 (NCH₃), 38.9 (NCH₃), 21.4 (ArCCH₃). **HRMS *m/z* (ESI⁺)** *m/z* calcd for C₁₈H₂₀N₂OCl⁺ [M+H]⁺ 315.1259; found 315.1265.

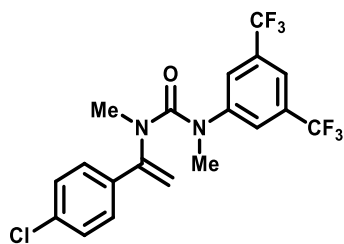
1-(1-(4-Chlorophenyl)vinyl)-1,3-dimethyl-3-(4-(trifluoromethyl)phenyl)urea (224)



Formation of the title compound was carried out by following GP1 with 1-(4-chlorophenyl)ethan-1-one (**208**) (1.30 mL, 1.54 g, 10.0 mmol) and 1-isocyanato-4-(trifluoromethyl)benzene (1.34 mL, 1.87 g, 10.0 mmol) used as starting materials. The imine intermediate was stirred with the requisite aryl isocyanate for 72 hours, subsequent methylation with methyl iodide was stirred for 24 hours. The resulting crude material was purified by flash column chromatography (SiO₂, 1% to 20% acetone + 3% trimethylamine in 40-60 petroleum ether) yielding the title compound (1.24 g, 34%) as a white solid.

M.p. 54-56 °C (Et₂O). **IR (film, cm⁻¹)** ν_{\max} = 1666, 1612, 1321, 1109, 834. **¹H NMR (400 MHz, CDCl₃)** δ 7.44 (2 H, br. d, *J* 8.5, 2 x ArCH), 7.24 (2 H, d, *J* 8.6, 2 x ArCH), 6.99 (2 H, d, *J* 8.6, 2 x ArCH), 6.84 (2 H, br. d, *J* 8.5, 2 x ArCH), 4.85 (1 H, d, *J* 1.0, CH_aH_b), 4.61 (1 H, d, *J* 1.0, CH_aH_b), 3.29 (3 H, s, CH₃), 2.95 (3 H, s, CH₃). **¹³C NMR (101 MHz, CDCl₃)** δ 160.1 (CO), 149.1 (C_{quat}), 147.7 (C_{quat}, q, *J*_{CF} 1.2), 136.8 (C_{quat}), 134.5 (ArCCl), 128.5 (2 x ArCH), 126.9 (2 x ArCH), 126.2 (C_{quat}, q, *J*_{CF} 32.8), 125.9 (2 x ArCH, q, *J*_{CF} 3.8), 124.2 (CF₃, q, *J*_{CF} 271.9), 124.1 (2 x ArCH), 108.2 (CH₂), 39.6 (CH₃), 37.9 (CH₃). **¹⁹F NMR (377 MHz, CDCl₃)** δ -62.0 (3 F, s, CF₃). **HRMS *m/z* (ESI⁺)** *m/z* calcd for C₁₈H₁₇N₂OF₃Cl⁺ [M+H]⁺ 369.0976; found 369.0978.

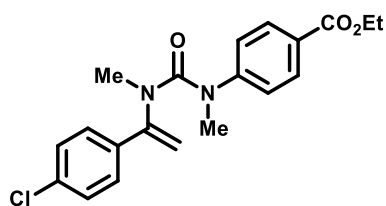
1-(3,5-Bis(trifluoromethyl)phenyl)-3-(1-(4-chlorophenyl)vinyl)-1,3-dimethylurea (225)



Formation of the title compound was carried out by following GP1 with 1-(4-chlorophenyl)ethan-1-one (**208**) (1.30 mL, 1.54 g, 10.0 mmol) and 1-isocyanato-3,5-bis(trifluoromethyl)benzene (1.73 mL, 2.55 g, 10.0 mmol) used as starting materials. The imine intermediate was stirred with the requisite aryl isocyanate for 72 hours, subsequent methylation with methyl iodide was stirred for 24 hours. The resulting crude material was purified by flash column chromatography (SiO₂, 1% to 20% acetone + 3% trimethylamine in 40-60 petroleum ether) yielding the title compound (423 mg, 10%) as a white solid.

M.p. 95-97 °C (Et₂O). **IR (film, cm⁻¹)** ν_{max} = 1669, 1381, 1278, 1126. **¹H NMR (400 MHz, CDCl₃)** δ 7.53 (1 H, br. s, ArCH), 7.24 (2 H, d, *J* 8.7, 2 x ArCH), 7.13 (2 H, br. s, 2 x ArCH), 6.91 (2 H, d, *J* 8.7, 2 x ArCH), 4.85 (1 H, s, CH_aH_b), 4.64 (1 H, s, CH_aH_b), 3.35 (3 H, s, CH₃), 2.99 (3 H, s, CH₃). **¹³C NMR (101 MHz, CDCl₃)** δ 159.3 (CO), 149.1 (C_{quat}), 145.7 (C_{quat}), 136.5 (C_{quat}), 135.0 (ArCCl), 132.1 (2 x C_{quat}, q, *J*_{CF} 33.4), 128.8 (2 x ArCH), 126.7 (2 x ArCH), 124.2 (2 x ArCH, q, *J*_{CF} 3.4), 132.1 (2 x CF₃, q, *J*_{CF} 273.0), 117.4 (ArCH, sep., *J*_{CF} 3.9), 108.4 (CH₂), 40.0 (CH₃), 37.8 (CH₃). **¹⁹F NMR (377 MHz, CDCl₃)** δ -63.1 (6 F, s, 2 x CF₃). **HRMS *m/z* (ESI⁺)** *m/z* calcd for C₁₉H₁₅N₂OClF₆Na⁺ [M+Na]⁺ 459.0669; found 459.0672.

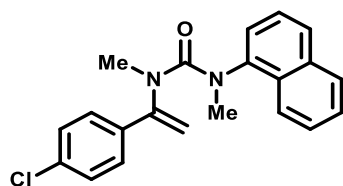
Ethyl 4-(3-(1-(4-chlorophenyl)vinyl)-1,3-dimethylureido)benzoate (226)



Formation of the title compound was carried out by following GP1 with 1-(4-chlorophenyl)ethan-1-one (**208**) (1.30 mL, 1.54 g, 10.0 mmol) and ethyl 4-isocyanatobenzoate (1.91 g, 10.0 mmol) used as starting materials. The imine intermediate was stirred with the requisite aryl isocyanate for 72 hours, subsequent methylation with methyl iodide was stirred for 24 hours. The resulting crude material was purified by flash column chromatography (SiO₂, 0% to 30% THF in 40-60 petroleum ether), yielding the title compound (443 mg, 12%) as a white solid.

M.p. 49-52 °C (Et₂O). **IR (film, cm⁻¹)** ν_{max} = 2981, 1712, 1665, 1604, 1274. **¹H NMR (400 MHz, CDCl₃)** δ 7.88 (2 H, d, *J* 8.7, 2 x ArCH), 7.24 (2 H, d, *J* 8.7, 2 x ArCH), 6.98 (2 H, d, *J* 8.6, 2 x ArCH), 6.76 (2 H, d, *J* 8.7, 2 x ArCH), 4.78 (1 H, d, *J* 0.7, CH_aCH_b), 4.61 (1 H, d, *J* 0.7, CH_aCH_b), 4.36 (2 H, q, *J* 7.1, OCH₂), 3.33 (3 H, s, CH₃), 2.92 (3 H, s, CH₃), 1.40 (3 H, t, *J* 7.1, CH₃). **¹³C NMR (101 MHz, CDCl₃)** δ 166.3 (CO), 160.0 (CO), 149.0 (C_{quat}), 148.6 (C_{quat}), 137.1 (C_{quat}), 134.4 (ArC(Cl)), 130.3 (2 x ArCH), 128.5 (2 x ArCH), 126.9 (2 x ArCH), 125.8 (C_{quat}), 123.2 (2 x ArCH), 108.1 (CH₂), 61.0 (OCH₂), 39.6 (NCH₃), 37.6 (NCH₃), 14.5 (CH₃). **HRMS *m/z* (ESI⁺)** *m/z* calcd for C₂₀H₂₂N₂O₃Cl⁺ [M+H]⁺ 373.1313; found 373.1312.

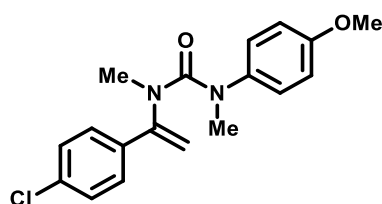
1-(1-(4-Chlorophenyl)vinyl)-1,3-dimethyl-3-(naphthalen-1-yl)urea (227)



Formation of the title compound was carried out by following GP1 with 1-(4-chlorophenyl)ethan-1-one (**208**) (1.30 mL, 1.54 g, 10.0 mmol) and 1-naphthyl isocyanate (1.44 mL, 1.69 g, 10.0 mmol) used as starting materials. The imine intermediate was stirred with the requisite aryl isocyanate for 25 hours, after which additional 1-naphthyl isocyanate (0.72 mL, 0.85 g, 5.0 mmol) was added followed by 21 hours of stirring, then the reaction mixture was concentrated under reduced pressure and the received crude material was purified by flash column chromatography (SiO₂, 0% to 25% MTBE in 40-60 petroleum ether) yielding crude material (505 mg) as a yellow oil. Subsequent methylation with methyl iodide was carried out on a 1.5 mmol scale (by making as if the received crude material was pure) and was stirred for 16 hours. The resulting crude material was purified by flash column chromatography (SiO₂, 0% to 25% MTBE in 40-60 petroleum ether) yielding the title compound (347 mg, 10% over three steps) as an orange oil.

IR (film, cm⁻¹) ν_{\max} = 2971, 1652, 1354, 1093, 775. **¹H NMR (400 MHz, CDCl₃)** δ 7.80-7.76 (1 H, m, ArCH), 7.60-7.56 (2 H, m, 2 x ArCH), 7.49-7.40 (2 H, m, 2 x ArCH), 7.21 (1 H, dd, *J* 7.4, 0.6, ArCH), 7.03 (2 H, d, *J* 8.7, 2 x ArCH), 6.98 (1 H, dd, *J* 7.2, 1.0, ArCH), 6.68 (2 H, d, *J* 8.7, 2 x ArCH), 4.77 (1 H, s, CH_aH_b), 4.47 (1 H, s, CH_aH_b), 3.28 (3 H, s, NCH₃), 3.02 (3 H, s, NCH₃). **¹³C NMR (101 MHz, CDCl₃)** δ 161.9 (CO), 148.8 (C_{quat}), 141.2 (C_{quat}), 135.0 (C_{quat}), 134.5 (C_{quat}), 133.9 (C_{quat}), 130.3 (ArCH), 128.5 (ArCH), 128.2 (2 x ArCH), 127.2 (ArCH), 126.9 (2 x ArCH), 126.5 (ArCH), 126.1 (ArCH), 125.9 (ArCH), 125.5 (ArCH), 122.8 (ArCH), 108.9 (CH₂), 40.1 (NCH₃), 39.3 (NCH₃). **HRMS *m/z* (ESI⁺)** *m/z* calcd for C₂₁H₂₀N₂OCl⁺ [M+H]⁺ 351.1259; found 351.1256.

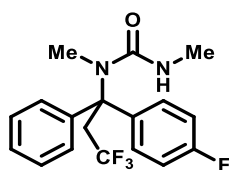
1-(1-(4-Chlorophenyl)vinyl)-3-(4-methoxyphenyl)-1,3-dimethylurea (228)



Formation of the title compound was carried out by following GP1 with 1-(4-chlorophenyl)ethan-1-one (**208**) (1.30 mL, 1.54 g, 10.0 mmol) and 4-methoxyphenyl isocyanate (**473**) (1.29 mL, 1.49 g, 10.0 mmol) used as starting materials. The imine intermediate was stirred with the requisite aryl isocyanate for 21 hours, then concentrated under reduced pressure and the received crude material was purified by flash column chromatography (SiO₂, 0% to 60% Et₂O in 40-60 petroleum ether) yielding crude material (1.24 g) as a yellow oil. Subsequent methylation with methyl iodide was carried out on a 3.9 mmol scale (by making as if the received crude material was pure) and was stirred for 16 hours. The resulting crude material was purified by flash column chromatography (SiO₂, 0% to 30% acetone in 40-60 petroleum ether) yielding the title compound (944 mg, 29% over three steps) as a pale-yellow oil.

IR (film, cm⁻¹) ν_{\max} = 2948, 1655, 1510, 1356, 1246. **¹H NMR (400 MHz, CDCl₃)** δ 7.22 (2 H, d, *J* 8.9, 2 x ArCH), 7.05 (2 H, d, *J* 8.9, 2 x ArCH), 6.75-6.70 (4 H, m, 4 x ArCH), 4.86 (1 H, d, *J* 0.8, CH_aH_b), 4.61 (1 H, d, *J* 0.8, CH_aH_b), 3.76 (3 H, s, OCH₃), 3.17 (3 H, s, NCH₃), 3.00 (3 H, s, NCH₃). **¹³C NMR (101 MHz, CDCl₃)** δ 161.0 (CO), 157.2 (ArCO), 149.4 (C_{quat}), 138.0 (C_{quat}), 136.6 (C_{quat}), 134.1 (ArCCL), 128.3 (2 x ArCH), 127.3 (2 x ArCH), 127.2 (2 x ArCH), 114.0 (2 x ArCH), 107.4 (CH₂), 55.6 (OCH₃), 39.4 (NCH₃), 39.4 (NCH₃). **HRMS *m/z* (ESI⁺)** *m/z* calcd for C₁₈H₁₉N₂O₂ClNa⁺ [M+Na]⁺ 353.1027; found 353.1029.

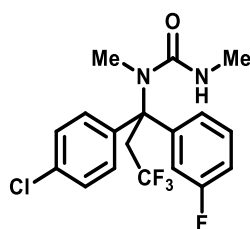
1,3-Dimethyl-1-(3,3,3-trifluoro-1-(4-fluorophenyl)-1-phenylpropyl)urea (**231**)



Formation of the title compound was carried out by following GP2 with 1-(4-fluorophenyl)-1,3-dimethyl-3-(1-phenylvinyl)urea (**218**) (57 mg, 0.2 mmol) and sodium trifluoromethanesulfinate (**134**) (61 mg, 2.0 eq., 0.4 mmol) used as starting materials and acetone used as solvent. The reaction mixture was stirred for 23 hours to give the title compound (53 mg, 74%) as a pale-yellow solid.

M.p. 191-194 °C (Et₂O). **IR (film, cm⁻¹)** ν_{\max} = 3362, 1640, 1509, 1259, 1122. **¹H NMR (400 MHz, CDCl₃)** δ 7.32-7.25 (6 H, m, 6 x ArCH), 7.23-7.15 (1 H, m, ArCH), 6.96 (2 H, t, *J* 8.6, 2 x ArCH), 4.60 (1 H, br. q, *J* 4.1, NH), 3.96 (2 H, q, *J* 10.9, CH₂), 2.86-2.75 (6 H, m, 2 x CH₃). **¹³C NMR (101 MHz, CDCl₃)** δ 161.3 (ArCF, d, *J*_{CF} 246.6), 159.7 (CO), 143.9 (C_{quat}), 140.5 (C_{quat}, d, *J*_{CF} 3.2), 128.4 (2 x ArCH), 128.2 (2 x ArCH, d, *J*_{CF} 7.9), 127.0 (ArCH), 126.8 (2 x ArCH), 126.4 (CF₃, q, *J*_{CF} 279.1), 115.1 (2 x ArCH, d, *J*_{CF} 21.5), 68.1 (C_{quat}, q, *J*_{CF} 2.3), 39.1 (CH₂, q, *J*_{CF} 27.0), 36.5 (CH₃, q, *J*_{CF} 1.8), 27.7 (CH₃). **¹⁹F NMR (377 MHz, CDCl₃)** δ -58.4 (3 F, t, *J* 10.9, CF₃), -116.0—-116.2 (1 F, m, ArCF). **HRMS *m/z* (ESI⁺)** *m/z* calcd for C₁₈H₁₉N₂OF₄⁺ [M+H]⁺ 355.1428; found 355.1425.

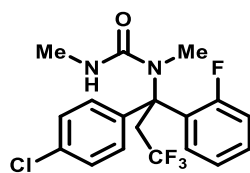
1-(1-(4-Chlorophenyl)-3,3,3-trifluoro-1-(3-fluorophenyl)propyl)-1,3-dimethylurea (**232**)



Formation of the title compound was carried out by following GP2 with 1-(1-(4-chlorophenyl)vinyl)-3-(3-fluorophenyl)-1,3-dimethylurea (**219**) (64 mg, 0.2 mmol) and sodium trifluoromethanesulfinate (**134**) (46 mg, 1.5 eq., 0.3 mmol) used as starting materials and acetonitrile used as solvent. The reaction mixture was stirred for 24 hours to give the title compound (65 mg, 84%) as a pale-yellow solid.

M.p. 145-147 °C (Et₂O). **IR (film, cm⁻¹)** ν_{\max} = 3371, 2926, 1645, 1530, 1488, 1258, 1105. **¹H NMR (400 MHz, CDCl₃)** δ 7.26-7.23 (4 H, m, 2 x ArCH + 2 x ArCH), 7.23-7.19 (1 H, m, ArCH), 7.04 (1 H, d, *J* 8.2, ArCH), 6.98 (1 H, dt, *J* 10.8, 2.0, ArCH), 6.86 (1 H, td, *J* 8.2, 2.0, ArCH), 4.62 (1 H, br. q, *J* 4.2, NH), 3.98-3.83 (2 H, m, CH₂), 2.85-2.75 (6 H, m, 2 x CH₃). **¹³C NMR (101 MHz, CDCl₃)** δ 162.8 (ArCF, d, *J*_{CF} 244.2), 159.5 (CO), 147.1 (C_{quat}), 142.5 (C_{quat}), 132.9 (ArCCl), 130.0 (ArCH, d, *J*_{CF} 8.2), 128.7 (2 x ArCH), 127.9 (2 x ArCH), 126.1 (CF₃, q, *J*_{CF} 276.1), 121.9 (ArCH, d, *J*_{CF} 2.9), 114.1 (ArCH), 113.7 (ArCH, d, *J*_{CF} 24.3), 67.9 (C_{quat}), 38.3 (CH₂, q, *J*_{CF} 27.0), 36.5 (NCH₃, q, *J*_{CF} 2.3), 27.8 (NCH₃). **¹⁹F NMR (377 MHz, CDCl₃)** δ -58.5 (3 F, t, *J* 10.9, CF₃), -111.9—-112.1 (1 F, m, ArCF). **HRMS *m/z* (ESI⁺)** *m/z* calcd for C₁₈H₁₈N₂OClF₄⁺ [M+H]⁺ 389.1038; found 389.1028.

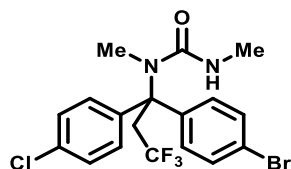
1-(1-(4-Chlorophenyl)-3,3,3-trifluoro-1-(2-fluorophenyl)propyl)-1,3-dimethylurea (233)



Formation of the title compound was carried out by following GP2 with 1-(1-(4-chlorophenyl)vinyl)-3-(2-fluorophenyl)-1,3-dimethylurea (**220**) (64 mg, 0.2 mmol) and sodium trifluoromethanesulfinate (**134**) (62 mg, 2.0 eq., 0.4 mmol) used as starting materials and acetone used as solvent. The reaction mixture was stirred for 18 hours to give the title compound (64 mg, 82%) as a white solid.

M.p. 166-169 °C (Et₂O). **IR (film, cm⁻¹)** ν_{\max} = 3363, 2958, 1642, 1484, 1258, 1105. **¹H NMR (400 MHz, CDCl₃)** δ 7.34-7.20 (6 H, m, 2 x ArCH + 2 x ArCH + ArCH + ArCH), 7.12 (1 H, t, *J* 7.5, ArCH), 6.95 (1 H, dd, *J* 12.7, 7.5, ArCH), 4.63 (1 H, br. s, NH), 4.16-3.96 (2 H, m, CH₂), 2.84 (3 H, s, CH₃), 2.81 (3 H, d, *J* 4.4, CH₃). **¹³C NMR (101 MHz, CDCl₃)** δ 159.7 (ArCF, d, *J*_{CF} 248.3), 159.2 (CO), 140.8 (C_{quat}), 133.0 (ArCCL), 130.9 (C_{quat}, d, *J*_{CF} 10.1), 129.7 (ArCH, d, *J*_{CF} 9.3), 128.7 (2 x ArCH), 128.2 (2 x ArCH), 128.2 (ArCH), 126.2 (CF₃, q, *J*_{CF} 278.4), 124.1 (ArCH, d, *J*_{CF} 3.1), 116.9 (ArCH, d, *J*_{CF} 24.4), 67.1 (C_{quat}, q, *J*_{CF} 2.6), 38.6 (CH₂, q, *J*_{CF} 27.3), 35.4 (NCH₃), 27.7 (NCH₃). **¹⁹F NMR (377 MHz, CDCl₃)** δ -58.5 (3 F, t, *J* 10.8, CF₃), -107.7 (1 F, s, ArCF). **HRMS *m/z* (ESI⁺)** *m/z* calcd for C₁₈H₁₈N₂OClF₄⁺ [M+H]⁺ 389.1038; found 389.1032.

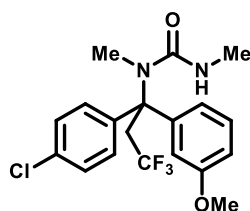
1-(1-(4-Bromophenyl)-1-(4-chlorophenyl)-3,3,3-trifluoropropyl)-1,3-dimethylurea (234)



Formation of the title compound was carried out by following GP2 with 1-(4-bromophenyl)-3-(1-(4-chlorophenyl)vinyl)-1,3-dimethylurea (**221**) (76 mg, 0.2 mmol) and sodium trifluoromethanesulfinate (**134**) (47 mg, 1.5 eq., 0.3 mmol) used as starting materials and acetonitrile used as solvent. The reaction mixture was stirred for 18 hours to give the title compound (76 mg, 84%) as a white solid.

M.p. 184-187 °C (Et₂O). **IR (film, cm⁻¹)** ν_{\max} = 3369, 2971, 1646, 1258, 1105. **¹H NMR (400 MHz, CDCl₃)** δ 7.39 (2 H, d, *J* 8.6, 2 x ArCH), 7.24 (2 H, d, *J* 9.0, 2 x ArCH), 7.20 (2 H, d, *J* 9.0, 2 x ArCH), 7.14 (2 H, d, *J* 8.6, 2 x ArCH), 4.61 (1 H, br. s, NH), 3.90 (2 H, q, *J* 10.8, CH₂), 2.82-2.77 (6 H, m, 2 x CH₃). **¹³C NMR (101 MHz, CDCl₃)** δ 159.5 (CO), 143.4 (C_{quat}), 142.6 (C_{quat}), 132.9 (ArCCL), 131.6 (2 x ArCH), 128.7 (2 x ArCH), 128.1 (2 x ArCH), 127.9 (2 x ArCH), 126.2 (CF₃, q, *J*_{CF} 279.7), 121.0 (ArCBr), 67.8 (C_{quat}, d, *J*_{CF} 2.0), 38.3 (CH₂, q, *J*_{CF} 27.4), 36.4 (NCH₃, q, *J*_{CF} 2.0), 27.7 (NCH₃). **¹⁹F NMR (377 MHz, CDCl₃)** δ -58.5 (3 F, t, *J* 10.8, CF₃). **HRMS *m/z* (ESI⁺)** *m/z* calcd for C₁₈H₁₈N₂OBrClF₃⁺ [M+H]⁺ 449.0238; found 449.0238.

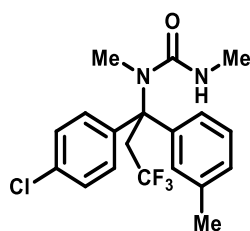
1-(1-(4-Chlorophenyl)-3,3,3-trifluoro-1-(3-methoxyphenyl)propyl)-1,3-dimethylurea (235)



Formation of the title compound was carried out by following GP2 with 1-(1-(4-chlorophenyl)vinyl)-3-(3-methoxyphenyl)-1,3-dimethylurea (**222**) (66 mg, 0.2 mmol) and sodium trifluoromethanesulfinate (**134**) (46 mg, 1.5 eq., 0.3 mmol) used as starting materials and acetonitrile used as solvent. The reaction mixture was stirred for 23 hours to give the title compound (57 mg, 71%) as a pale-yellow solid.

M.p. 70-73 °C (Et₂O). **IR (film, cm⁻¹)** ν_{max} = 3363, 2945, 1642, 1490, 1256, 1105. **¹H NMR (400 MHz, CDCl₃)** δ 7.24-7.20 (4 H, m, 4 x ArCH), 7.18 (1 H, t, *J* 8.1, ArCH), 6.87 (1 H, br. d, *J* 8.1, ArCH), 6.83 (1 H, t, *J* 1.9, ArCH), 6.70 (1 H, dd, *J* 8.1, 1.9, ArCH), 4.59 (1 H, br. q, *J* 4.7, NH), 3.91 (2 H, q, *J* 11.0, CH₂), 3.75 (3 H, s, OCH₃), 2.80 (3 H, s, CH₃), 2.79 (3 H, d, *J* 4.7, CH₃). **¹³C NMR (101 MHz, CDCl₃)** δ 159.6 (CO) 159.5 (ArCO), 145.3 (C_{quat}), 143.7 (C_{quat}), 132.5 (ArCCl), 129.4 (ArCH), 128.5 (2 x ArCH), 127.5 (2 x ArCH), 126.4 (CF₃, q, *J*_{CF} 278.1), 119.2 (ArCH), 114.0 (ArCH), 111.4 (ArCH), 60.0 (C_{quat}), 55.4 (OCH₃), 38.4 (CH₂, q, *J*_{CF} 27.6), 36.5 (CH₃, q, *J*_{CF} 1.9), 27.8 (CH₃). **¹⁹F NMR (377 MHz, CDCl₃)** δ -58.4 (3 F, t, *J* 11.0, CF₃). **HRMS *m/z* (ESI⁺)** *m/z* calcd for C₁₉H₂₀N₂O₂ClF₃Na⁺ [M+Na]⁺ 423.1058; found 423.1055.

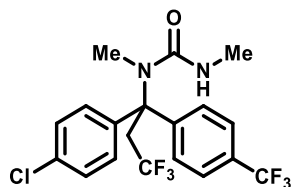
1-(1-(4-Chlorophenyl)-3,3,3-trifluoro-1-(*m*-tolyl)propyl)-1,3-dimethylurea (236)



Formation of the title compound was carried out by following GP2 with 1-(1-(4-chlorophenyl)vinyl)-1,3-dimethyl-3-(*m*-tolyl)urea (**223**) (63 mg, 0.2 mmol) and sodium trifluoromethanesulfinate (**134**) (62 mg, 2.0 eq., 0.4 mmol) used as starting materials and acetonitrile used as solvent. The reaction mixture was stirred for 19 hours to give the title compound (56 mg, 73%) as a white solid.

M.p. 129-131 °C (Et₂O). **IR (film, cm⁻¹)** ν_{\max} = 3360, 2959, 1642, 1258, 1122, 1106. **¹H NMR (400 MHz, CDCl₃)** δ 7.23-7.19 (4 H, m, 4 x ArCH), 7.16 (1 H, t, *J* 7.7, ArCH), 7.09 (1 H, d, *J* 7.7 ArCH), 7.06 (1 H, br. s, ArCH), 6.98 (1 H, d, *J* 7.7 ArCH), 4.58 (1 H, br. s, NH), 3.92 (2 H, dq, *J* 11.0, 3.0, CH₂), 2.83-2.76 (6 H, m, 2 x CH₃), 2.30 (3 H, s, ArCCH₃). **¹³C NMR (101 MHz, CDCl₃)** δ 159.6 (CO), 144.0 (C_{quat}), 143.3 (C_{quat}), 138.0 (C_{quat}), 132.3 (ArCCl), 128.4 (2 x ArCH), 128.3 (ArCH), 127.9 (ArCH), 127.5 (ArCH), 127.5 (2 x ArCH), 126.4 (CF₃, q, *J*_{CF} 279.4), 124.0 (ArCH), 68.1 (C_{quat}, q, *J*_{CF} 2.5), 38.4 (CH₂, q, *J*_{CF} 27.1), 36.5 (NCH₃), 27.7 (NCH₃), 21.9 (CH₃). **¹⁹F NMR (377 MHz, CDCl₃)** δ -58.4 (3 F, t, *J* 11.0, CF₃). **HRMS *m/z* (ESI⁺)** *m/z* calcd for C₁₉H₂₁N₂OCIF₃⁺ [M+H]⁺ 385.1289; found 385.1285.

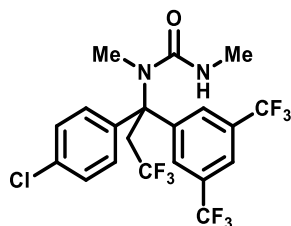
1-(1-(4-Chlorophenyl)-3,3,3-trifluoro-1-(4-(trifluoromethyl)phenyl)propyl)-1,3-dimethylurea (237)



Formation of the title compound was carried out by following GP2 with 1-(1-(4-chlorophenyl)vinyl)-1,3-dimethyl-3-(4-(trifluoromethyl)phenyl)urea (**224**) (74 mg, 0.2 mmol) and sodium trifluoromethanesulfinate (**134**) (46 mg, 1.5 eq., 0.3 mmol) used as starting materials and acetonitrile used as solvent. The reaction mixture was stirred for 19 hours to give the title compound (65 mg, 74%) as a white solid.

M.p. 139-141 °C (Et₂O). **IR (film, cm⁻¹)** ν_{\max} = 3361, 1641, 1530, 1326, 1104. **¹H NMR (400 MHz, CDCl₃)** δ 7.50 (2 H, d, *J* 8.4, 2 x ArCH), 7.36 (2 H, d, *J* 8.4, 2 x ArCH), 7.26-7.21 (4 H, m, 4 x ArCH), 4.64 (1 H, br. q, *J* 4.2, NH), 4.03-3.85 (2 H, m, CH₂), 2.88-2.76 (6 H, m, 2 x CH₃). **¹³C NMR (101 MHz, CDCl₃)** δ 159.5 (CO), 149.0 (C_{quat}), 141.8 (C_{quat}), 132.2 (ArCCl), 128.9 (C_{quat}, q, *J*_{CF} 32.7), 128.8 (2 x ArCH), 128.2 (2 x ArCH), 126.2 (CF₃, q, *J*_{CF} 278.5), 126.2 (2 x ArCH), 125.5 (2 x ArCH, q, *J*_{CF} 3.8), 124.0 (ArCCF₃, q, *J*_{CF} 271.8), 68.0 (C_{quat}, q, *J*_{CF} 2.1), 38.0 (CH₂, q, *J*_{CF} 27.4), 36.4 (NCH₃, q, *J*_{CF} 2.0), 27.7 (NCH₃). **¹⁹F NMR (377 MHz, CDCl₃)** δ -58.6 (3 F, t, *J* 10.7, CF₃), -62.5 (3 F, s, CF₃). **HRMS *m/z* (ESI⁺)** *m/z* calcd for C₁₉H₁₈N₂OCIF₆⁺ [M+H]⁺ 439.1006; found 439.1003.

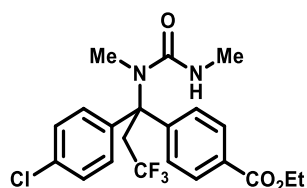
1-(1-(3,5-Bis(trifluoromethyl)phenyl)-1-(4-chlorophenyl)-3,3,3-trifluoropropyl)-1,3-dimethylurea (238)



Formation of the title compound was carried out by following GP2 with 1-(3,5-bis(trifluoromethyl)phenyl)-3-(1-(4-chlorophenyl)vinyl)-1,3-dimethylurea (**225**) (87 mg, 0.2 mmol) and sodium trifluoromethanesulfinate (**134**) (46 mg, 1.5 eq., 0.3 mmol) used as starting materials and acetonitrile used as solvent. The reaction mixture was stirred for 19 hours to give the title compound (85 mg, 84%) as a white solid.

M.p. 140-143 °C (Et₂O). **IR (film, cm⁻¹)** ν_{\max} = 3365, 1642, 1534, 1360, 1278, 1135. **¹H NMR (400 MHz, CDCl₃)** δ 7.66 (1 H, br. s, ArCH), 7.64 (2 H, br. s, 2 x ArCH), 7.30 (2 H, d, *J* 9.0, 2 x ArCH), 7.25 (2 H, d, *J* 9.0, 2 x ArCH), 4.72 (1 H, br. q, *J* 4.7, NH), 4.08-3.94 (1 H, m, CH_aH_b), 3.92-3.79 (1 H, m, CH_aH_b), 2.83 (3 H, s, CH₃), 2.79 (3 H, d, *J* 4.7, CH₃). **¹³C NMR (101 MHz, CDCl₃)** δ 159.3 (CO), 149.0 (C_{quat}), 140.0 (C_{quat}), 133.9 (ArC(Cl)), 131.7 (2 x C_{quat}, q, *J*_{CF} 33.4), 129.2 (2 x ArCH), 128.6 (2 x ArCH), 126.0 (CF₃, q, *J*_{CF} 278.3), 125.3 (2 x ArCH, q, *J*_{CF} 3.1), 123.3 (2 x ArCF₃, q, *J*_{CF} 272.8), 120.6 (ArCH, sep., *J*_{CF} 3.7), 67.7 (C_{quat}), 37.6 (CH₂, q, *J*_{CF} 27.6), 36.3 (NCH₃, q, *J*_{CF} 2.5), 27.7 (NCH₃). **¹⁹F NMR (377 MHz, CDCl₃)** δ -58.4 (3 F, t, *J* 10.5, CF₃), -62.7 (6 F, s, 2 x CF₃). **HRMS *m/z* (ESI⁺)** *m/z* calcd for C₂₀H₁₆N₂OCIF₉Na⁺ [M+Na]⁺ 529.0700; found 529.0697.

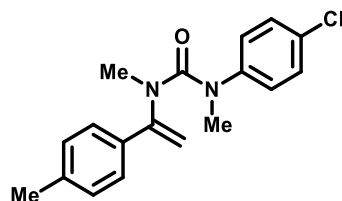
Ethyl 4-(1-(4-chlorophenyl)-1-(1,3-dimethylureido)-3,3,3-trifluoropropyl)benzoate (**239**)



Formation of the title compound was carried out by following GP2 with ethyl 4-(3-(1-(4-chlorophenyl)vinyl)-1,3-dimethylureido)benzoate (**226**) (77 mg, 0.2 mmol) and sodium trifluoromethanesulfinate (**134**) (47 mg, 1.5 eq., 0.3 mmol) used as starting materials and acetonitrile used as solvent. The reaction mixture was stirred for 15 hours to give the title compound (71 mg, 80%) as a white solid.

M.p. 191-194 °C (Et₂O). **IR (film, cm⁻¹)** ν_{\max} = 3369, 2978, 1711, 1643, 1279, 1104. **¹H NMR (400 MHz, CDCl₃)** δ 7.93 (2 H, d, *J* 8.6, 2 x ArCH), 7.34 (2 H, d, *J* 8.6, 2 x ArCH), 7.25-7.21 (4 H, m, 4 x ArCH), 4.64 (1 H, br. q, *J* 4.7, NH), 4.33 (2 H, q, *J* 7.1, OCH₂), 4.05-3.84 (2 H, m, CH₂), 2.82 (3 H, s, NCH₃), 2.80 (3 H, d, *J* 4.7, NHCH₃), 1.35 (3 H, t, *J* 7.1, CH₃). **¹³C NMR (101 MHz, CDCl₃)** δ 166.1 (CO), 159.5 (CO), 149.6 (C_{quat}), 142.1 (C_{quat}), 133.0 (ArCCL), 129.8 (2 x ArCH), 129.0 (C_{quat}), 128.7 (2 x ArCH), 128.1 (2 x ArCH), 125.9 (2 x ArCH), 126.2 (CF₃, q, *J*_{CF} 279.4), 68.1 (C_{quat}, q, *J*_{CF} 2.4), 61.1 (OCH₂), 37.8 (CH₂, q, *J*_{CF} 27.1), 36.5 (NCH₃, q, *J*_{CF} 2.7), 27.7 (NCH₃), 14.4 (CH₃). **¹⁹F NMR (377 MHz, CDCl₃)** δ -58.6 (3 F, t, *J* 10.9, CF₃). **HRMS *m/z* (ESI⁺)** *m/z* calcd for C₂₁H₂₃N₂O₃ClF₃⁺ [M+H]⁺ 443.1344; found 443.1339.

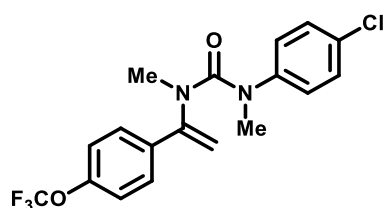
1-(4-Chlorophenyl)-1,3-dimethyl-3-(1-(*p*-tolyl)vinyl)urea (**243**)



Formation of the title compound was carried out by following GP1 with 1-(*p*-tolyl)ethan-1-one (1.33 mL, 1.34 g, 10.0 mmol) and 1-chloro-4-isocyanatobenzene (**210**) (1.54 g, 10.0 mmol) used as starting materials. The imine intermediate was stirred with the requisite aryl isocyanate for 69 hours, subsequent methylation with methyl iodide was stirred for 26 hours. The resulting crude material was purified by flash column chromatography (SiO₂, 1% to 20% acetone + 3% trimethylamine in 40-60 petroleum ether) yielding the title compound (547 mg, 17%) as a pale-yellow oil that solidified over time to give a white solid.

M.p. 46-48 °C (Et₂O). **IR (film, cm⁻¹)** ν_{\max} = 2928, 1660, 1491, 1351, 1324, 824. **¹H NMR (400 MHz, CDCl₃)** δ 7.14 (2 H, d, *J* 8.8, 2 x ArCH), 7.07 (2 H, br. d, *J* 8.2, 2 x ArCH), 7.00 (2 H, d, *J* 8.2, 2 x ArCH), 6.72 (2 H, d, *J* 8.8, 2 x ArCH), 4.86 (1 H, s, CH_aH_b), 4.56 (1 H, s, CH_aH_b), 3.23 (3 H, s, CH₃), 2.94 (3 H, s, CH₃), 2.34 (3 H, s, CH₃). **¹³C NMR (101 MHz, CDCl₃)** δ 160.6 (CO), 150.1 (C_{quat}), 143.6 (C_{quat}), 138.5 (C_{quat}), 135.2 (C_{quat}), 130.0 (ArCCL), 128.9 (2 x ArCH), 128.7 (2 x ArCH), 126.4 (2 x ArCH), 125.7 (2 x ArCH), 106.8 (CH₂), 39.6 (CH₃), 38.5 (CH₃), 21.3 (CH₃). **HRMS *m/z* (ESI⁺)** *m/z* calcd for C₁₈H₂₀N₂OCl⁺ [M+H]⁺ 315.1259; found 315.1272.

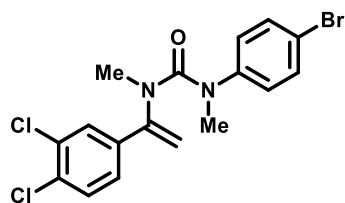
1-(4-Chlorophenyl)-1,3-dimethyl-3-(1-(4-(trifluoromethoxy)phenyl)vinyl)urea (244)



Formation of the title compound was carried out by following GP1 with 1-(4-(trifluoromethoxy)phenyl)ethan-1-one (1.60 mL, 2.04 g, 10.0 mmol) and 1-chloro-4-isocyanatobenzene (**210**) (1.54 g, 10.0 mmol) used as starting materials. The imine intermediate was stirred with the requisite aryl isocyanate for 21 hours, subsequent methylation with methyl iodide was stirred for 24 hours. The resulting crude material was purified by flash column chromatography (SiO₂, 0% to 30% THF in 40-60 petroleum ether), yielding the title compound (1.45 g, 38%) as a pale-yellow oil.

IR (film, cm⁻¹) ν_{\max} = 2943, 1660, 1491, 1252, 1215, 1160. **¹H NMR (400 MHz, CDCl₃)** δ 7.16 (2 H, d, *J* 8.8, 2 x ArCH), 7.13-7.10 (4 H, m, 2 x ArCH + 2 x ArCH), 6.69 (2 H, d, *J* 8.8, 2 x ArCH), 4.89 (1 H, s, CH_aH_b), 4.65 (1 H, s, CH_aH_b), 3.24 (3 H, s, NCH₃), 2.95 (3 H, s, NCH₃). **¹³C NMR (101 MHz, CDCl₃)** δ 160.3 (CO), 149.3 (ArCO, q, *J*_{CF} 2.0), 149.0 (C_{quat}), 143.3 (C_{quat}), 136.8 (C_{quat}), 130.4 (ArCCl), 128.9 (2 x ArCH), 127.2 (2 x ArCH), 126.4 (2 x ArCH), 120.7 (2 x ArCH), 120.6 (CF₃, q, *J*_{CF} 257.2), 108.1 (CH₂), 39.5 (NCH₃), 38.6 (NCH₃). **¹⁹F NMR (377 MHz, CDCl₃)** δ -57.7 (3 F, s, OCF₃). **HRMS *m/z* (ESI⁺)** *m/z* calcd for C₁₈H₁₇N₂O₂F₃Cl⁺ [M+H]⁺ 385.0925 found 385.0918.

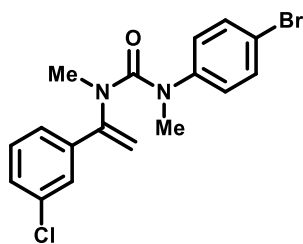
1-(4-Bromophenyl)-3-(1-(3,4-dichlorophenyl)vinyl)-1,3-dimethylurea (245)



Formation of the title compound was carried out by following GP1 with 1-(3,4-dichlorophenyl)ethan-1-one (1.89 g, 10.0 mmol) and 1-bromo-4-isocyanatobenzene (**242**) (1.98 g, 10.0 mmol) used as starting materials. The imine intermediate was stirred with the requisite aryl isocyanate for 71 hours, subsequent methylation with methyl iodide was stirred for 20 hours. The resulting crude material was purified by flash column chromatography (SiO₂, 0% to 30% THF in 40-60 petroleum ether), yielding the title compound (1.94 g, 47%) as pale-yellow solid.

M.p. 139-141 °C (Et₂O). **IR (film, cm⁻¹)** ν_{max} = 2940, 1660, 1488, 1352, 1324. **¹H NMR (400 MHz, CDCl₃)** δ 7.37-7.29 (3 H, m, 2 x ArCH + ArCH), 7.10 (1 H, d, *J* 1.9, ArCH), 6.94 (1 H, dd, *J* 8.3, 1.9, ArCH), 6.67 (2 H, d, *J* 8.7, 2 x ArCH), 4.90 (1 H, s, CH_aH_b), 4.68 (1 H, s, CH_aH_b), 3.20 (3 H, s, NCH₃), 2.98 (3 H, s, NCH₃). **¹³C NMR (101 MHz, CDCl₃)** δ 160.2 (CO), 148.3 (C_{quat}), 143.8 (C_{quat}), 138.2 (C_{quat}), 132.5 (ArCCl), 132.4 (ArCCl), 131.9 (2 x ArCH), 130.2 (ArCH), 127.7 (ArCH), 126.8 (2 x ArCH), 124.9 (ArCH), 118.4 (ArCBr), 108.7 (CH₂), 39.3 (NCH₃), 38.6 (NCH₃). **HRMS *m/z* (ESI⁺)** *m/z* calcd for C₁₇H₁₆N₂OBrCl₂⁺ [M+H]⁺ 412.9818; found 412.9815.

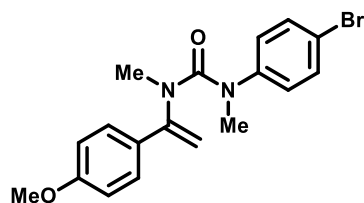
1-(4-Bromophenyl)-3-(1-(3-chlorophenyl)vinyl)-1,3-dimethylurea (246)



Formation of the title compound was carried out by following GP1 with 1-(3-chlorophenyl)ethan-1-one (1.30 mL, 1.55 g, 10.0 mmol) and 1-bromo-4-isocyanatobenzene (**242**) (1.98 g, 10.0 mmol) used as starting materials. The imine intermediate was stirred with the requisite aryl isocyanate for 25 hours, subsequent methylation with methyl iodide was stirred for 18 hours. The resulting crude material was purified by flash column chromatography (SiO₂, 0% to 20% THF in 40-60 petroleum ether), followed by additional purification by flash column chromatography (neutral Al₂O₃, 100% CHCl₃), yielding the title compound (122 mg, 3%) as a colourless oil.

IR (film, cm⁻¹) ν_{max} = 2941, 1659, 1487, 1351, 1324. **¹H NMR (400 MHz, CDCl₃)** δ 7.32 (2 H, d, *J* 8.8, 2 x ArCH), 7.26-7.23 (1 H, m, ArCH), 7.20 (1 H, t, *J* 7.6, ArCH), 7.02 (1 H, t, *J* 1.4, ArCH), 7.00 (1 H, dt, *J* 7.6, 1.4, ArCH), 6.66 (2 H, d, *J* 8.8, 2 x ArCH), 4.91 (1 H, d, *J* 0.7, CH_aH_b), 4.68 (1 H, d, *J* 0.7, CH_aH_b), 3.22 (3 H, s, CH₃), 2.96 (3 H, s, CH₃). **¹³C NMR (101 MHz, CDCl₃)** δ 160.3 (CO), 149.1 (C_{quat}), 143.9 (C_{quat}), 140.0 (C_{quat}), 134.3 (ArCCL), 131.9 (2 x ArCH), 129.5 (ArCH), 128.6 (ArCH), 126.7 (2 x ArCH), 126.1 (ArCH), 123.8 (ArCH), 118.1 (ArCBr), 108.4 (CH₂), 39.4 (NCH₃), 38.5 (NCH₃). **HRMS *m/z* (ESI⁺)** *m/z* calcd for C₁₇H₁₇N₂OBrCl⁺ [M+H]⁺ 379.0207; found 379.0209.

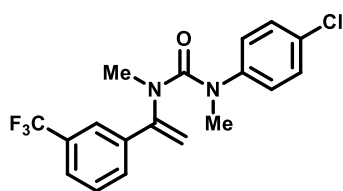
1-(4-Bromophenyl)-3-(1-(4-methoxyphenyl)vinyl)-1,3-dimethylurea (247)



Formation of the title compound was carried out by following GP1 with 1-(4-methoxyphenyl)ethan-1-one (1.50 g, 10.0 mmol) and 1-bromo-4-isocyanatobenzene (**242**) (1.98 g, 10.0 mmol) used as starting materials. The imine intermediate was stirred with the requisite aryl isocyanate for 25 hours, subsequent methylation with methyl iodide was stirred for 17 hours. The resulting crude material was purified by flash column chromatography (SiO₂, 0% to 15% THF in 40-60 petroleum ether), yielding the title compound (213 mg, 6%) as a colourless oil.

IR (film, cm⁻¹) ν_{\max} = 2954, 1659, 1488, 1250. **¹H NMR (400 MHz, CDCl₃)** δ 7.29 (2 H, d, *J* 8.7, 2 x ArCH), 7.03 (2 H, d, *J* 8.9, 2 x ArCH), 6.79 (2 H, d, *J* 8.7, 2 x ArCH), 6.67 (2 H, d, *J* 8.9, 2 x ArCH), 4.80 (1 H, s, CH_aH_b), 4.52 (1 H, s, CH_aH_b), 3.82 (3 H, s, OCH₃), 3.24 (3 H, s, NCH₃), 2.95 (3 H, s, NCH₃). **¹³C NMR (101 MHz, CDCl₃)** δ 160.5 (CO), 160.0 (ArCO), 149.8 (C_{quat}), 144.0 (C_{quat}), 131.7 (2 x ArCH), 130.6 (C_{quat}), 127.1 (2 x ArCH), 126.8 (2 x ArCH), 117.8 (ArCBr), 113.6 (2 x ArCH), 106.1 (CH₂), 55.5 (OCH₃), 39.7 (NCH₃), 38.5 (NCH₃). **HRMS *m/z* (ESI⁺)** *m/z* calcd for C₁₈H₂₀N₂O₂Br⁺ [M+H]⁺ 375.0703; found 375.0697.

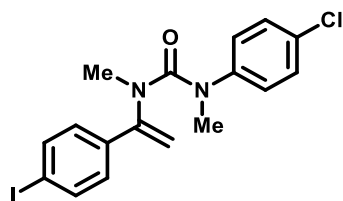
1-(4-Chlorophenyl)-1,3-dimethyl-3-(1-(3-(trifluoromethyl)phenyl)vinyl)urea (248)



Formation of the title compound was carried out by following GP1 with 1-(3-(trifluoromethyl)phenyl)ethan-1-one (1.52 mL, 1.88 g, 10.0 mmol) and 1-chloro-4-isocyanatobenzene (**210**) (1.54 g, 10.0 mmol) used as starting materials. The imine intermediate was stirred with the requisite aryl isocyanate for 22 hours, subsequent methylation with methyl iodide was stirred for 19 hours. The resulting crude material was purified by flash column chromatography (SiO₂, 0% to 30% THF in 40-60 petroleum ether), yielding the title compound (751 mg, 20%) as a white solid.

M.p. 64-67 °C (Et₂O). **IR (film, cm⁻¹)** ν_{max} = 2937, 1663, 1493, 1340, 1307, 1126. **¹H NMR (400 MHz, CDCl₃)** δ 7.54 (1 H, d, *J* 7.9, ArCH), 7.39 (1 H, t, *J* 7.9, ArCH), 7.30 (1 H, d, *J* 7.9, ArCH), 7.26-7.25 (1 H, m, ArCH), 7.16 (2 H, d, *J* 8.9, 2 x ArCH), 6.67 (2 H, d, *J* 8.9, 2 x ArCH), 4.94 (1 H, d, *J* 1.1, CH_aH_b), 4.73 (1 H, d, *J* 1.1, CH_aH_b), 3.24 (3 H, s, NCH₃), 2.94 (3 H, s, NCH₃). **¹³C NMR (101 MHz, CDCl₃)** δ 160.2 (CO), 149.1 (C_{quat}), 143.2 (C_{quat}), 139.0 (C_{quat}), 130.7 (C_{quat}, q, *J*_{CF} 32.4), 130.6 (ArCCl), 129.0 (2 x ArCH), 128.9 (ArCH, q, *J*_{CF} 1.2), 128.7 (ArCH), 126.5 (2 x ArCH), 125.2 (ArCH, q, *J*_{CF} 3.8), 124.1 (CF₃, q, *J*_{CF} 272.4), 122.9 (ArCH, q, *J*_{CF} 3.8), 108.4 (CH₂), 39.4 (NCH₃), 38.6 (NCH₃). **¹⁹F NMR (377 MHz, CDCl₃)** δ -62.7 (3 F, s, CF₃). **HRMS *m/z* (ESI⁺)** *m/z* calcd for C₁₈H₁₇N₂OF₃Cl⁺ [M+H]⁺ 369.0976; found 369.0969.

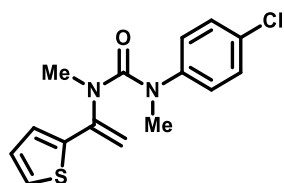
1-(4-Chlorophenyl)-3-(1-(4-iodophenyl)vinyl)-1,3-dimethylurea (249)



Formation of the title compound was carried out by following GP1 with 1-(4-iodophenyl)ethan-1-one (2.46 g, 10.0 mmol) and 1-chloro-4-isocyanatobenzene (**210**) (1.54 g, 10.0 mmol) used as starting materials. The imine intermediate was stirred with the requisite aryl isocyanate for 50 hours, subsequent methylation with methyl iodide was stirred for 24 hours. The resulting crude material was purified by flash column chromatography (SiO₂, 0% to 30% THF in 40-60 petroleum ether), yielding the title compound (1.44 g, 34%) as a yellow solid.

M.p. 82-84 °C (Et₂O). **IR (film, cm⁻¹)** ν_{\max} = 2936, 1653, 1615, 1489, 1350, 1324, 826. **¹H NMR (400 MHz, CDCl₃)** δ 7.58 (2 H, d, *J* 8.6, 2 x ArCH), 7.14 (2 H, d, *J* 8.9, 2 x ArCH), 6.82 (2 H, d, *J* 8.6, 2 x ArCH), 6.68 (2 H, d, *J* 8.9, 2 x ArCH), 4.85 (1 H, s, CH_aH_b), 4.59 (1 H, s, CH_aH_b), 3.22 (3 H, s, NCH₃), 2.93 (3 H, s, NCH₃). **¹³C NMR (101 MHz, CDCl₃)** δ 160.2 (CO), 149.3 (C_{quat}), 143.3 (C_{quat}), 137.8 (C_{quat}), 137.3 (2 x ArCH), 130.3 (ArCCl), 128.8 (2 x ArCH), 127.5 (2 x ArCH), 126.3 (2 x ArCH), 108.0 (CH₂), 94.1 (ArCl), 39.6 (NCH₃), 38.6 (NCH₃). **HRMS *m/z* (ESI⁺)** *m/z* calcd for C₁₇H₁₇N₂OICl⁺ [M+H]⁺ 427.0069; found 427.0062.

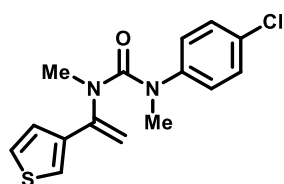
1-(4-Chlorophenyl)-1,3-dimethyl-3-(1-(thiophen-2-yl)vinyl)urea (250)



Formation of the title compound was carried out by following GP1 with 2-acetylthiophene (1.08 mL, 1.26 g, 10.0 mmol) and 1-chloro-4-isocyanatobenzene (**210**) (1.54 g, 10.0 mmol) used as starting materials. The imine intermediate was stirred with the requisite aryl isocyanate for 48 hours, subsequent methylation with methyl iodide was stirred for 22 hours. The resulting crude material was purified by flash column chromatography (SiO₂, 0% to 30% THF in 40-60 petroleum ether), yielding the title compound (581 mg, 19%) as a yellow oil that slowly turned to a brown oil over time.

IR (film, cm⁻¹) ν_{\max} = 2929, 1653, 1491, 1345. **¹H NMR (400 MHz, CDCl₃)** δ 7.18-7.13 (3 H, m, 2 x ArCH + ArCH), 6.91 (1 H, dd, *J* 5.1, 3.7, ArCH), 6.87 (2 H, d, *J* 8.7, 2 x ArCH), 6.85 (1 H, dd, *J* 3.7, 1.2, ArCH), 5.00 (1 H, d, *J* 0.9, CH_aH_b), 4.57 (1 H, d, *J* 0.9, CH_aH_b), 3.16 (3 H, s, NCH₃), 3.10 (3 H, s, NCH₃). **¹³C NMR (101 MHz, CDCl₃)** δ 160.5 (CO), 144.3 (C_{quat}), 143.8 (C_{quat}), 141.7 (C_{quat}), 130.8 (ArCCl), 129.0 (2 x ArCH), 127.2 (2 x ArCH), 127.2 (ArCH), 125.3 (ArCH), 124.9 (ArCH), 108.2 (CH₂), 39.2 (NCH₃), 39.2 (NCH₃). **HRMS *m/z* (ESI⁺)** *m/z* calcd for C₁₅H₁₆N₂OClS⁺ [M+H]⁺ 307.0666; found 307.0658.

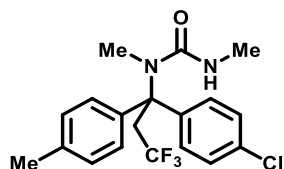
1-(4-Chlorophenyl)-1,3-dimethyl-3-(1-(thiophen-3-yl)vinyl)urea (251)



Formation of the title compound was carried out by following GP1 with 1-(thiophen-3-yl)ethan-1-one (1.26 g, 10.0 mmol) and 1-chloro-4-isocyanatobenzene (**210**) (1.54 g, 10.0 mmol) used as starting materials. The imine intermediate was stirred with the requisite aryl isocyanate for 17 hours, subsequent methylation with methyl iodide was stirred for 24 hours. The resulting crude material was purified by flash column chromatography (SiO₂, 0% to 30% THF in 40-60 petroleum ether), yielding the title compound (359 mg, 12%) as a pale-yellow oil.

IR (film, cm⁻¹) ν_{\max} = 3105, 2937, 1657, 1492, 1350. **¹H NMR** (400 MHz, CDCl₃) δ 7.19 (1 H, dd, *J* 5.1, 3.0, ArCH), 7.13 (2 H, d, *J* 8.9, 2 x ArCH), 7.04-6.99 (1 H, m, ArCH), 6.85 (1 H, d, *J* 5.1, ArCH), 6.76 (2 H, d, *J* 8.9, 2 x ArCH), 4.90 (1 H, s, CH_aH_b), 4.57 (1 H, s, CH_aH_b), 3.19 (3 H, s, NCH₃), 3.04 (3 H, s, NCH₃). **¹³C NMR** (101 MHz, CDCl₃) δ 160.4 (CO), 145.5 (C_{quat}), 143.7 (C_{quat}), 139.8 (C_{quat}), 130.4 (ArCCl), 128.8 (2 x ArCH), 126.9 (2 x ArCH), 125.8 (ArCH), 125.6 (ArCH), 121.8 (ArCH), 107.3 (CH₂), 39.2 (NCH₃), 38.9 (NCH₃). **HRMS *m/z* (ESI⁺)** *m/z* calcd for C₁₅H₁₆N₂O₂SCl⁺ [M+H]⁺ 307.0666; found 307.0662.

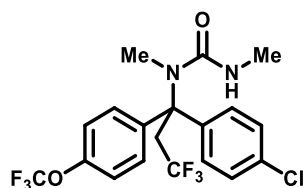
1-(1-(4-Chlorophenyl)-3,3,3-trifluoro-1-(*p*-tolyl)propyl)-1,3-dimethylurea (260)



Formation of the title compound was carried out by following GP2 with 1-(4-chlorophenyl)-1,3-dimethyl-3-(1-(*p*-tolyl)vinyl)urea (**243**) (63 mg, 0.2 mmol) and sodium trifluoromethanesulfinate (**134**) (46 mg, 1.5 eq., 0.3 mmol) used as starting materials and acetonitrile used as solvent. The reaction mixture was stirred for 18 hours to give the title compound (59 mg, 77%) as a pale-yellow solid.

M.p. 148-151 °C (Et₂O). **IR** (film, cm⁻¹) ν_{\max} = 3371, 2962, 1642, 1530, 1258, 1104. **¹H NMR** (400 MHz, CDCl₃) δ 7.23-7.19 (4 H, m, 4 x ArCH), 7.17 (2 H, d, *J* 8.2, 2 x ArCH), 7.07 (2 H, d, *J* 8.2, 2 x ArCH), 4.58 (1 H, br. q, *J* 4.4, NH), 3.99-3.83 (2 H, m, CH₂), 2.81-2.77 (6 H, m, 2 x CH₃), 2.27 (3 H, s, ArCCH₃). **¹³C NMR** (101 MHz, CDCl₃) δ 159.6 (CO), 144.3 (C_{quat}), 140.3 (C_{quat}), 136.9 (C_{quat}), 132.3 (ArCCl), 129.2 (2 x ArCH), 128.5 (2 x ArCH), 127.3 (2 x ArCH), 126.9 (2 x ArCH), 126.4 (CF₃, q, *J*_{CF} 277.7), 67.9 (C_{quat}, q, *J*_{CF} 2.2), 38.5 (CH₂, q, *J*_{CF} 27.1), 36.4 (CH₃, q, *J*_{CF} 2.1), 27.7 (CH₃), 21.0 (CH₃). **¹⁹F NMR** (377 MHz, CDCl₃) δ -58.4 (3 F, t, *J* 10.9, CF₃). **HRMS *m/z* (ESI⁺)** *m/z* calcd for C₁₉H₂₀N₂OClF₃Na⁺ [M+Na]⁺ 407.1108; found 407.1105.

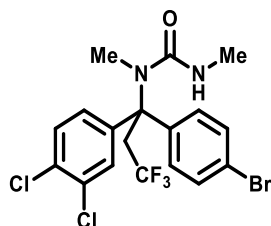
1-(1-(4-Chlorophenyl)-3,3,3-trifluoro-1-(4-(trifluoromethoxy)phenyl)propyl)-1,3-dimethylurea (261)



Formation of the title compound was carried out by following GP2 with 1-(4-chlorophenyl)-1,3-dimethyl-3-(1-(4-(trifluoromethoxy)phenyl)vinyl)urea (**244**) (77 mg, 0.2 mmol) and sodium trifluoromethanesulfinate (**134**) (46 mg, 1.5 eq., 0.3 mmol) used as starting materials and acetonitrile used as solvent. The reaction mixture was stirred for 22 hours to give the title compound (77 mg, 85%) as a white solid.

M.p. 64-67 °C (Et₂O). **IR (film, cm⁻¹)** ν_{max} = 3361, 2930, 1639, 1255, 1220, 1104. **¹H NMR (400 MHz, CDCl₃)** δ 7.29 (2 H, d, *J* 9.0, 2 x ArCH), 7.26-7.21 (4 H, m, 4 x ArCH), 7.10 (2 H, d, *J* 8.4, 2 x ArCH), 4.62 (1 H, br. q, *J* 4.6, NH), 3.92 (2 H, q, *J* 10.8, CH₂), 2.82-2.77 (6 H, m, 2 x NCH₃). **¹³C NMR (126 MHz, CDCl₃)** δ 159.5 (CO), 147.9 (ArCO, q, *J*_{CF} 1.7), 142.6 (C_{quat} + C_{quat}), 132.9 (ArCCl), 128.7 (2 x ArCH), 128.0 (2 x ArCH), 127.9 (2 x ArCH), 126.2 (CF₃, q, *J*_{CF} 278.5), 120.6 (2 x ArCH), 120.5 (OCF₃, q, *J*_{CF} 257.1), 67.8 (C_{quat}, q, *J*_{CF} 2.2), 38.7 (CH₂, q, *J*_{CF} 27.1), 36.5 (NCH₃), 27.7 (NCH₃). **¹⁹F NMR (377 MHz, CDCl₃)** δ -57.6 (3 F, s, OCF₃), -58.5 (3 F, t, *J* 10.8, CF₃). **HRMS *m/z* (ESI⁺)** *m/z* calcd for C₁₉H₁₈N₂O₂ClF₆⁺ [M+H]⁺ 455.0956; found 455.0944.

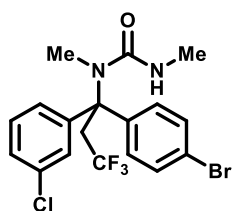
1-(1-(4-Bromophenyl)-1-(3,4-dichlorophenyl)-3,3,3-trifluoropropyl)-1,3-dimethylurea (262)



Formation of the title compound was carried out by following GP2 with 1-(4-bromophenyl)-3-(1-(3,4-dichlorophenyl)vinyl)-1,3-dimethylurea (**245**) (83 mg, 0.2 mmol) and sodium trifluoromethanesulfinate (**134**) (46 mg, 1.5 eq., 0.3 mmol) used as starting materials and acetonitrile used as solvent. The reaction mixture was stirred for 20 hours to give the title compound (88 mg, 91%) as a white solid.

M.p. 92-95 °C (Et₂O). **IR (film, cm⁻¹)** ν_{\max} = 3360, 2967, 1642, 1532, 1255, 1105. **¹H NMR (400 MHz, CDCl₃)** δ 7.41 (2 H, d, *J* 8.7, 2 x ArCH), 7.32 (1 H, d, *J* 8.6, ArCH), 7.31 (1 H, d, *J* 2.4, ArCH), 7.22 (2 H, d, *J* 8.7, 2 x ArCH), 7.11 (1 H, dd, *J* 8.6, 2.4, ArCH), 4.80 (1 H, br. q, *J* 4.6, NH), 4.00-3.75 (2 H, m, CH₂), 2.85-2.74 (6 H, m, CH₃ + CH₃). **¹³C NMR (101 MHz, CDCl₃)** δ 159.4 (CO), 145.4 (C_{quat}), 142.1 (C_{quat}), 132.7 (ArCCl), 131.8 (2 x ArCH), 131.0 (ArCCl), 130.4 (ArCH), 128.5 (2 x ArCH), 127.9 (ArCH), 126.1 (CF₃, q, *J*_{CF} 277.8), 125.3 (ArCH), 121.5 (ArCBr), 67.6 (C_{quat}, q, *J*_{CF} 2.2), 37.9 (CH₂, q, *J*_{CF} 27.2), 36.4 (NCH₃, q, *J*_{CF} 1.9), 27.7 (NCH₃). **¹⁹F NMR (377 MHz, CDCl₃)** δ -58.6 (3 F, t, *J* 10.6, CF₃). **HRMS *m/z* (ESI⁺)** *m/z* calcd for C₁₈H₁₇N₂OBrCl₂F₃⁺ [M+H]⁺ 482.9848; found 482.9841.

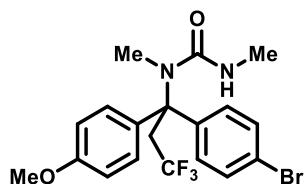
1-(1-(4-Bromophenyl)-1-(3-chlorophenyl)-3,3,3-trifluoropropyl)-1,3-dimethylurea (263)



Formation of the title compound was carried out by following GP2 with 1-(4-bromophenyl)-3-(1-(3-chlorophenyl)vinyl)-1,3-dimethylurea (**246**) (76 mg, 0.2 mmol) and sodium trifluoromethanesulfinate (**134**) (62 mg, 2.0 eq., 0.4 mmol) used as starting materials and acetonitrile used as solvent. The reaction mixture was stirred for 22 hours to give the title compound (68 mg, 76%) as a white solid.

M.p. 81-83 °C (Et₂O). **IR (film, cm⁻¹)** ν_{max} = 3357, 2971, 1642, 1532, 1257, 1129. **¹H NMR (400 MHz, CDCl₃)** δ 7.40 (2 H, d, *J* 8.7, 2 x ArCH), 7.23 (1 H, br. s, ArCH), 7.21-7.12 (5 H, m, 5 x ArCH), 4.63 (1 H, br. s, NH), 3.98-3.82 (2 H, m, CH₂), 2.84-2.77 (6 H, m, 2 x CH₃). **¹³C NMR (126 MHz, CDCl₃)** δ 159.4 (CO), 146.5 (C_{quat}), 143.0 (C_{quat}), 134.5 (ArC(Cl)), 131.7 (2 x ArCH), 129.8 (ArCH), 128.3 (2 x ArCH), 127.2 (ArCH), 126.5 (ArCH), 126.2 (CF₃, q, *J*_{CF} 278.3), 124.4 (ArCH), 121.1 (ArC(Br)), 67.9 (C_{quat}, q, *J*_{CF} 2.2), 38.0 (CH₂, q, *J*_{CF} 27.3), 36.5 (NCH₃, q, *J*_{CF} 1.8), 27.7 (NCH₃). **¹⁹F NMR (377 MHz, CDCl₃)** δ -58.8 (3 F, t, *J* 10.8, CF₃). **HRMS *m/z* (ESI⁺)** *m/z* calcd for C₁₈H₁₈N₂OBrClF₃⁺ [M+H]⁺ 449.0238; found 449.0239.

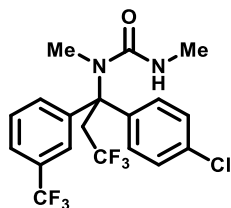
1-(1-(4-Bromophenyl)-3,3,3-trifluoro-1-(4-methoxyphenyl)propyl)-1,3-dimethylurea (264)



Formation of the title compound was carried out by following GP2 with 1-(4-bromophenyl)-3-(1-(4-methoxyphenyl)vinyl)-1,3-dimethylurea (**247**) (75 mg, 0.2 mmol) and sodium trifluoromethanesulfinate (**134**) (62 mg, 2.0 eq., 0.4 mmol) used as starting materials and acetonitrile used as solvent. The reaction mixture was stirred for 17 hours to give the title compound (51 mg, 57%) as a white solid.

M.p. 79-82 °C (Et₂O). **IR (film, cm⁻¹)** ν_{max} = 3369, 2958, 1644, 1513, 1257, 1103. **¹H NMR (400 MHz, CDCl₃)** δ 7.36 (2 H, d, *J* 8.7, 2 x ArCH), 7.19 (2 H, d, *J* 9.0, 2 x ArCH), 7.13 (2 H, d, *J* 8.7, 2 x ArCH), 6.80 (2 H, d, *J* 9.0, 2 x ArCH), 4.58 (1 H, br. s, NH), 3.99-3.79 (2 H, m, CH₂), 3.76 (3 H, s, OCH₃), 2.81-2.76 (6 H, m, 2 x NCH₃). **¹³C NMR (126 MHz, CDCl₃)** δ 159.6 (CO), 158.4 (ArCO), 145.2 (C_{quat}), 134.8 (C_{quat}), 131.4 (2 x ArCH), 128.5 (2 x ArCH), 127.5 (2 x ArCH), 126.4 (CF₃, q, *J*_{CF} 278.4), 120.4 (ArC(Br)), 113.8 (2 x ArCH), 67.7 (C_{quat}, q, *J*_{CF} 2.2), 55.3 (OCH₃), 38.7 (CH₂, q, *J*_{CF} 26.8), 36.3 (NCH₃), 27.7 (NCH₃). **¹⁹F NMR (377 MHz, CDCl₃)** δ -58.4 (3 F, t, *J* 10.8, CF₃). **HRMS *m/z* (ESI⁺)** *m/z* calcd for C₁₉H₂₀N₂O₂BrF₃Na⁺ [M+Na]⁺ 467.0552; found 467.0538.

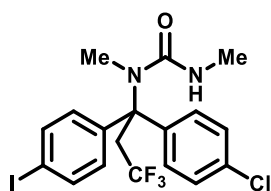
1-(1-(4-Chlorophenyl)-3,3,3-trifluoro-1-(3-(trifluoromethyl)phenyl)propyl)-1,3-dimethylurea (265)



Formation of the title compound was carried out by following GP2 with 1-(4-chlorophenyl)-1,3-dimethyl-3-(1-(3-(trifluoromethyl)phenyl)vinyl)urea (**248**) (74 mg, 0.2 mmol) and sodium trifluoromethanesulfinate (**134**) (62 mg, 2.0 eq., 0.4 mmol) used as starting materials and acetone used as solvent. The reaction mixture was stirred for 17 hours to give the title compound (62 mg, 71%) as a white solid.

M.p. 71-74 °C (Et₂O). **IR (film, cm⁻¹)** ν_{max} = 3360, 2921, 1640, 1327, 1124, 1104. **¹H NMR (400 MHz, CDCl₃)** δ 7.49-7.45 (2 H, m, 2 x ArCH), 7.44-7.37 (2 H, m, 2 x ArCH), 7.28-7.25 (2 H, m, 2 x ArCH), 7.25-7.22 (2 H, m, 2 x ArCH), 4.65 (1 H, br. q, *J* 4.5, NH), 3.95 (1 H, q, *J* 10.8, CH_aH_b), 3.93 (1 H, q, *J* 10.8, CH_aH_b), 2.80 (3 H, s, NCH₃), 2.79 (3 H, d, *J* 4.8 NCH₃). **¹³C NMR (126 MHz, CDCl₃)** δ 159.5 (CO), 145.9 (C_{quat}), 141.9 (C_{quat}), 133.2 (ArCCl), 130.8 (ArCCF₃, q, *J*_{CF} 32.2), 129.3 (ArCH), 129.0 (ArCH), 128.8 (2 x ArCH), 128.1 (2 x ArCH), 126.2 (ArCCF₃, q, *J*_{CF} 278.4), 124.1 (CF₃, q, *J*_{CF} 272.9), 123.8 (ArCH, q, *J*_{CF} 3.7), 122.8 (ArCH, q, *J*_{CF} 3.8), 67.9 (C_{quat}, q, *J*_{CF} 1.9), 38.2 (CH₂, q, *J*_{CF} 27.3), 36.5 (NCH₃, q, *J*_{CF} 2.0), 27.7 (NCH₃). **¹⁹F NMR (377 MHz, CDCl₃)** δ -58.6 (3 F, t, *J* 10.8, CF₃), -62.5 (3 F, s, ArCCF₃). **HRMS *m/z* (ESI⁺)** *m/z* calcd for C₁₉H₁₈N₂OCIF₆⁺ [M+H]⁺ 439.1006; found 439.0993.

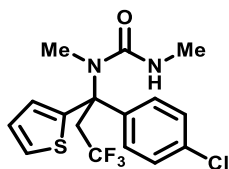
1-(1-(4-Chlorophenyl)-3,3,3-trifluoro-1-(4-iodophenyl)propyl)-1,3-dimethylurea (266)



Formation of the title compound was carried out by following GP2 with 1-(4-chlorophenyl)-3-(1-(4-iodophenyl)vinyl)-1,3-dimethylurea (**249**) (85 mg, 0.2 mmol) and sodium trifluoromethanesulfinate (**134**) (62 mg, 2.0 eq., 0.4 mmol) used as starting materials and acetone used as solvent. The reaction mixture was stirred for 16 hours to give the title compound (83 mg, 84%) as a yellow solid.

M.p. 84-87 °C (Et₂O). **IR (film, cm⁻¹)** ν_{\max} = 3368, 2968, 1641, 1256, 1103, 730. **¹H NMR (400 MHz, CDCl₃)** δ 7.58 (2 H, d, *J* 8.5, 2 x ArCH), 7.26-7.17 (4 H, m, 4 x ArCH), 7.01 (2 H, d, *J* 8.5, 2 x ArCH), 4.63 (1 H, br. s, NH), 3.96-3.82 (2 H, m, CH₂), 2.83-2.76 (6 H, m, 2 x NCH₃). **¹³C NMR (101 MHz, CDCl₃)** δ 159.5 (CO), 144.2 (C_{quat}), 142.6 (C_{quat}), 137.6 (2 x ArCH), 132.9 (ArCCl), 128.7 (2 x ArCH), 128.3 (2 x ArCH), 127.9 (2 x ArCH), 126.2 (CF₃, q, *J*_{CF} 278.6), 92.6 (ArCl), 67.9 (C_{quat}, q, *J*_{CF} 2.2), 38.2 (CH₂, q, *J*_{CF} 27.2), 36.5 (NCH₃, q, *J*_{CF} 2.3), 27.7 (NCH₃). **¹⁹F NMR (377 MHz, CDCl₃)** δ -58.5 (3 F, t, *J* 10.5, CF₃). **HRMS *m/z* (ESI⁺)** *m/z* calcd for C₁₈H₁₈N₂OIF₃Cl⁺ [M+H]⁺ 497.0097; found 497.0091.

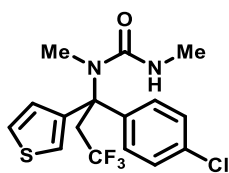
1-(1-(4-Chlorophenyl)-3,3,3-trifluoro-1-(thiophen-2-yl)propyl)-1,3-dimethylurea (267)



Formation of the title compound was carried out by following GP2 with 1-(4-chlorophenyl)-1,3-dimethyl-3-(1-(thiophen-2-yl)vinyl)urea (**250**) (61 mg, 0.2 mmol) and sodium trifluoromethanesulfinate (**134**) (62 mg, 2.0 eq., 0.4 mmol) used as starting materials and acetone used as solvent. The reaction mixture was stirred for 16 hours to give the title compound (34 mg, 45%) as a white solid, which decomposes slowly in solution.

M.p. 132-134 °C (Et₂O). **IR (film, cm⁻¹)** ν_{\max} = 3353, 2957, 1639, 1258, 1117, 1099. **¹H NMR (400 MHz, CDCl₃)** δ 7.26-7.20 (5 H, m, 5 x ArCH), 7.02 (1 H, br. s, ArCH), 6.90-6.84 (1 H, m, ArCH), 4.59 (1 H, br. s, NH), 3.99 (1 H, dq, *J* 15.0, 11.1 CH_aH_b), 3.75 (1 H, dq, *J* 15.0, 11.1 CH_aH_b), 2.81 (3 H, s, NCH₃), 2.75 (3 H, d, *J* 4.4, NCH₃). **¹³C NMR (101 MHz, CDCl₃)** δ 159.2 (CO), 148.4 (C_{quat}), 145.2 (C_{quat}), 132.8 (ArCCl), 128.6 (2 x ArCH), 126.9 (ArCH), 126.6 (2 x ArCH), 126.3 (ArCH, q, *J*_{CF} 2.0), 126.2 (ArCH), 126.1 (CF₃, q, *J*_{CF} 277.8), 65.7 (C_{quat}, q, *J*_{CF} 2.4), 41.6 (CH₂, q, *J*_{CF} 27.4), 35.8 (NCH₃, q, *J*_{CF} 1.7), 27.7 (NCH₃). **¹⁹F NMR (377 MHz, CDCl₃)** δ -58.5 (3 F, t, *J* 11.1, CF₃). **HRMS *m/z* (ESI⁺)** *m/z* calcd for C₁₆H₁₆N₂OSF₃ClNa⁺ [M+Na]⁺ 399.0516; found 399.0506.

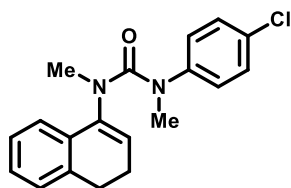
1-(1-(4-Chlorophenyl)-3,3,3-trifluoro-1-(thiophen-3-yl)propyl)-1,3-dimethylurea (268)



Formation of the title compound was carried out by following GP2 with 1-(4-chlorophenyl)-1,3-dimethyl-3-(1-(thiophen-3-yl)vinyl)urea (**251**) (61 mg, 0.2 mmol) and sodium trifluoromethanesulfinate (**134**) (62 mg, 2.0 eq., 0.4 mmol) used as starting materials and acetone used as solvent. The reaction mixture was stirred for 15 hours to give the title compound (54 mg, 71%) as a white solid.

M.p. 143-145 °C (Et₂O). **IR (film, cm⁻¹)** ν_{\max} = 3358, 2963, 1640, 1258, 1108. **¹H NMR (400 MHz, CDCl₃)** δ 7.26-7.17 (5 H, m, 5 x ArCH), 7.14 (1 H, br. s, ArCH), 6.88 (1 H, dd, *J* 5.1, 1.5, ArCH), 4.57 (1 H, br. s, NH), 4.00 (1 H, dq, *J* 15.1, 10.9, CH_aH_b), 3.69 (1 H, dq, *J* 15.1, 10.9, CH_aH_b), 2.80 (3 H, s, NCH₃), 2.78 (3 H, d, *J* 4.7, NCH₃). **¹³C NMR (101 MHz, CDCl₃)** δ 159.2 (CO), 144.8 (C_{quat}), 143.6 (C_{quat}), 132.4 (ArCCl), 128.6 (2 x ArCH), 128.4 (ArCH), 126.5 (2 x ArCH), 126.3 (CF₃, q, *J*_{CF} 278.0), 126.0 (ArCH), 122.4 (ArCH, q, *J*_{CF} 2.1), 65.5 (C_{quat}, q, *J*_{CF} 2.2), 40.0 (CH₂, q, *J*_{CF} 27.4), 35.6 (NCH₃, d, *J*_{CF} 1.7), 27.7 (NCH₃). **¹⁹F NMR (377 MHz, CDCl₃)** δ -58.6 (3 F, t, *J* 10.9, CF₃). **HRMS *m/z* (ESI⁺)** *m/z* calcd for C₁₆H₁₇N₂OSClF₃⁺ [M+H]⁺ 377.0697; found 377.0690.

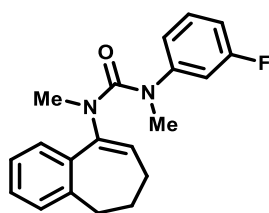
1-(4-Chlorophenyl)-3-(3,4-dihydronaphthalen-1-yl)-1,3-dimethylurea (271)



Formation of the title compound was carried out by following GP1 with α -tetralone (**269**) (1.33 mL, 1.46 g, 10.0 mmol) and 1-chloro-4-isocyanatobenzene (**210**) (1.54 g, 10.0 mmol) used as starting materials. The imine intermediate was stirred with the requisite aryl isocyanate for 24 hours, subsequent methylation with methyl iodide was stirred for 18 hours. The resulting crude material was purified by flash column chromatography (SiO₂, 0% to 30% THF in 40-60 petroleum ether), yielding the title compound (362 mg, 11%) as a colourless oil.

IR (film, cm⁻¹) ν_{\max} = 2937, 1654, 1626, 1491, 1348. **¹H NMR (400 MHz, CDCl₃)** δ 7.15-7.10 (2 H, m, ArCH + ArCH), 7.07 (2 H, d, *J* 8.8, 2 x ArCH), 7.03-6.99 (1 H, m, ArCH), 6.96-6.92 (1 H, m, ArCH), 6.72 (2 H, d, *J* 8.8, 2 x ArCH), 5.46 (1 H, t, *J* 4.7, CH), 3.17 (3 H, s, NCH₃), 3.08 (3 H, s, NCH₃), 2.53-2.23 (2 H, br. m, CH₂), 2.14-1.96 (2 H, br. m, CH₂). **¹³C NMR (101 MHz, CDCl₃)** δ 160.6 (CO), 144.1 (C_{quat}), 141.2 (C_{quat}), 136.6 (C_{quat}), 131.9 (C_{quat}), 130.3 (ArCCl), 128.8 (2 x ArCH), 127.7 (ArCH), 127.6 (ArCH), 127.2 (2 x ArCH), 126.2 (ArCH), 123.5 (CH), 122.2 (ArCH), 39.5 (CH₃), 39.1 (CH₃), 26.8 (CH₂), 22.4 (CH₂). **HRMS *m/z* (ESI⁺)** *m/z* calcd for C₁₉H₂₀N₂OCl⁺ [M+H]⁺ 327.1259; found 327.1249.

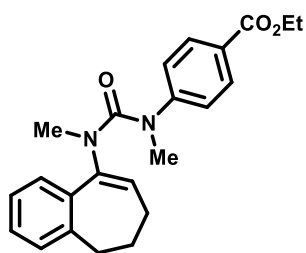
1-(6,7-Dihydro-5H-benzo[7]annulen-9-yl)-3-(3-fluorophenyl)-1,3-dimethylurea (272)



Formation of the title compound was carried out by following GP1 with 1-benzosuberone (**270**) (1.50 mL, 1.60 g, 10.0 mmol) and 1-fluoro-3-isocyanatobenzene (1.14 mL, 1.37 g, 10.0 mmol) used as starting materials. The imine intermediate was stirred with the requisite aryl isocyanate for 72 hours, subsequent methylation with methyl iodide was stirred for 20 hours. The resulting crude material was purified by flash column chromatography (SiO₂, 0% to 30% THF in 40-60 petroleum ether), yielding the title compound (1.02 g, 32%) as a pale-yellow solid.

M.p. 59-61 °C (Et₂O). **IR (film, cm⁻¹)** ν_{max} = 2932, 1656, 1606, 1333, 771. **¹H NMR (400 MHz, CDCl₃)** δ 7.18-7.09 (3 H, m, 3 x ArCH), 7.09 (2 H, m, 2 x ArCH), 6.72-6.63 (2 H, m, 2 x ArCH), 6.57 (1 H, dt, *J* 10.7, 2.2, ArCH), 5.71 (1 H, t, *J* 6.5, CH), 3.12 (3 H, s, NCH₃), 2.96 (3 H, s, NCH₃), 2.12 (2 H, t, *J* 6.5, CH₂), 1.86 (2 H, qn, *J* 6.5, CH₂), 1.78 (2 H, q, *J* 6.5, CH₂). **¹³C NMR (101 MHz, CDCl₃)** δ 162.8 (ArCF, q, *J*_{CF} 245.4), 160.5 (CO), 146.6 (C_{quat}, q, *J*_{CF} 9.6), 142.3 (C_{quat}), 142.3 (C_{quat}), 136.6 (C_{quat}), 129.6 (ArCH, q, *J*_{CF} 9.6), 129.3 (ArCH), 127.6 (ArCH), 125.9 (ArCH), 125.8 (ArCH), 123.6 (CH), 119.4 (ArCH, q, *J*_{CF} 2.9), 111.1 (ArCH, q, *J*_{CF} 23.4), 110.7 (ArCH, q, *J*_{CF} 21.2), 39.3 (NCH₃), 38.2 (NCH₃), 33.6 (CH₂), 32.6 (CH₂), 25.2 (CH₂). **¹⁹F NMR (377 MHz, CDCl₃)** δ -112.5 (1 F, ddd, *J* 10.9, 8.4, 6.6 ArCF). **HRMS *m/z* (ESI⁺)** *m/z* calcd for C₂₀H₂₁N₂OFNa⁺ [M+Na]⁺ 347.1530; found 347.1541.

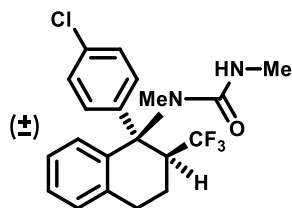
Ethyl 4-(3-(6,7-dihydro-5H-benzo[7]annulen-9-yl)-1,3-dimethylureido)benzoate (273)



Formation of the title compound was carried out by following GP1 with 1-benzosuberone (**270**) (1.50 mL, 1.60 g, 10.0 mmol) and ethyl 4-isocyanatobenzoate (1.91 g, 10.0 mmol) used as starting materials. The imine intermediate was stirred with the requisite aryl isocyanate for 22 hours, subsequent methylation with methyl iodide was stirred for 18 hours. The resulting crude material was purified by flash column chromatography (SiO₂, 0% to 30% THF in 40-60 petroleum ether), yielding the title compound (975 mg, 26%) as a white solid.

M.p. 113-116 °C (Et₂O). **IR (film, cm⁻¹)** ν_{max} = 2932, 1710, 1659, 1603, 1275, 1106. **¹H NMR (400 MHz, CDCl₃)** δ 7.87 (2 H, d, *J* 8.9, 2 x ArCH), 7.17 (1 H, td, *J* 7.3, 1.6, ArCH), 7.12 (1 H, td, *J* 7.3, 1.6, ArCH), 7.09-7.04 (2 H, m, ArCH + ArCH), 6.82 (2 H, d, *J* 8.9, 2 x ArCH), 5.72 (1 H, t, *J* 6.5, CH), 4.32 (2 H, q, *J* 7.1, OCH₂), 3.24 (3 H, s, NCH₃), 2.88 (3 H, s, NCH₃), 1.94 (2 H, t, *J* 6.3, CH₂), 1.85-1.72 (4 H, m, CH₂ + CH₂), 1.35 (3 H, t, *J* 7.1, CH₃). **¹³C NMR (101 MHz, CDCl₃)** δ 166.2 (CO), 160.3 (CO), 148.9 (C_{quat}), 142.3 (C_{quat}), 142.2 (C_{quat}), 137.1 (C_{quat}), 130.3 (2 x ArCH), 129.5 (ArCH), 127.6 (ArCH), 126.0 (ArCH), 125.5 (ArCH), 124.6 (C_{quat}), 123.9 (CH), 121.4 (2 x ArCH), 60.8 (OCH₂), 39.7 (NCH₃), 37.3 (NCH₃), 33.7 (CH₂), 32.4 (CH₂), 25.1 (CH₂), 14.4 (CH₃). **HRMS *m/z* (ESI⁺)** *m/z* calcd for C₂₃H₂₇N₂O₃⁺ [M+H]⁺ 379.2016; found 379.2025.

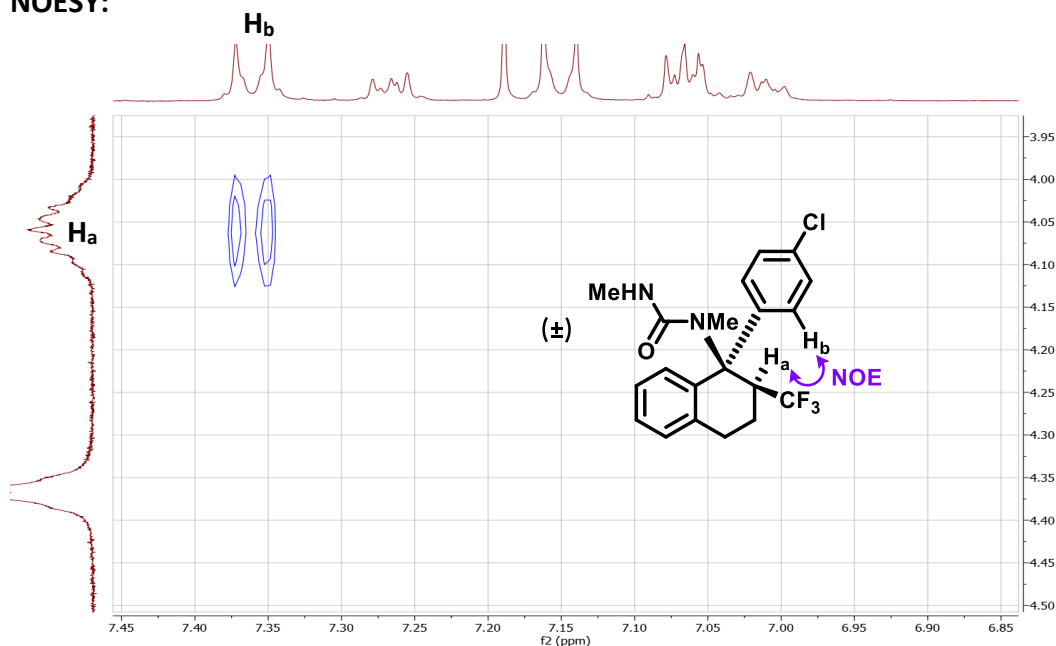
1-(1-(4-Chlorophenyl)-2-(trifluoromethyl)-1,2,3,4-tetrahydronaphthalen-1-yl)-1,3-dimethylurea (278)



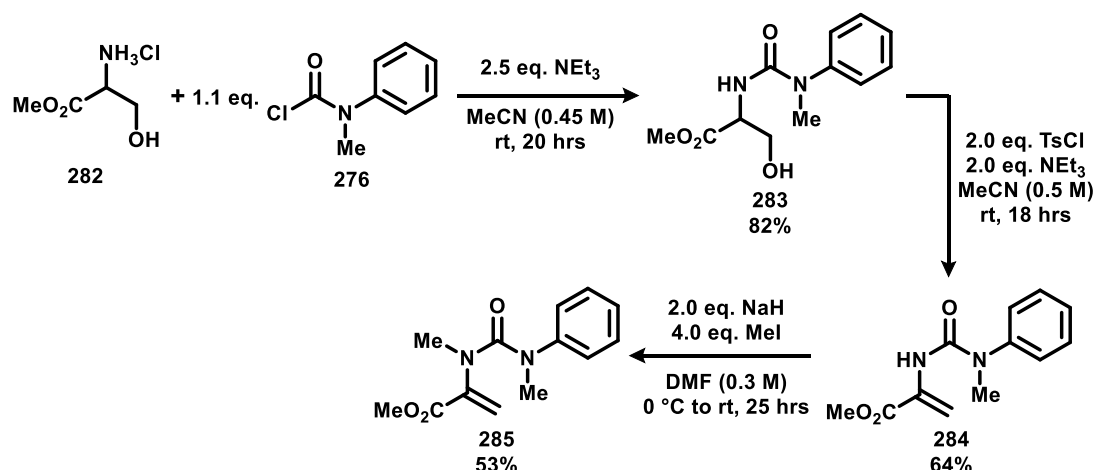
Formation of the title compound was carried out by following GP2 with 1-(4-chlorophenyl)-3-(3,4-dihydronaphthalen-1-yl)-1,3-dimethylurea (**271**) (65 mg, 0.2 mmol) and sodium trifluoromethanesulfinate (**134**) (78 mg, 2.5 eq., 0.5 mmol) used as starting materials and acetone used as solvent. The reaction mixture was stirred for 17 hours to give the title compound (54 mg, 68%, >20:1 d.r.) as a white solid.

M.p. 80-83 °C (Et₂O). **IR (film, cm⁻¹)** ν_{max} = 3352, 2962, 1644, 1530, 1492, 1317, 1123. **¹H NMR (400 MHz, CDCl₃)** δ 7.44 (2 H, d, *J* 8.8, 2 x ArCH), 7.37-7.33 (1 H, m, ArCH), 7.22 (2 H, d, *J* 8.8, 2 x ArCH), 7.16-7.12 (2 H, m, 2 x ArCH), 7.10-7.06 (1 H, m, ArCH), 4.44 (1 H, br. q, *J* 4.6, NH), 4.20-4.07 (1 H, m, CH), 3.01 (1 H, dt, *J* 17.4, 7.5, CH_aH_b), 2.81 (3 H, s, NCH₃), 2.75 (1 H, dt, *J* 17.4, 7.5, CH_aH_b), 2.68 (3 H, d, *J* 4.6, NCH₃), 2.47-2.37 (2 H, m, CH₂). **¹³C NMR (126 MHz, CDCl₃)** δ 159.5 (CO), 145.0 (C_{quat}), 136.9 (C_{quat}), 136.9 (C_{quat}), 132.3 (ArCCl), 130.1 (ArCH), 129.8 (ArCH), 128.2 (2 x ArCH), 128.2 (2 x ArCH), 127.8 (CF₃, q, *J*_{CF} 281.9), 127.4 (ArCH), 126.0 (ArCH), 67.3 (C_{quat}), 45.5 (CH, q, *J*_{CF} 24.3), 37.2 (NCH₃, q, *J*_{CF} 3.2), 27.8 (NCH₃), 27.0 (CH_aH_b), 21.8 (CH₂, q, *J*_{CF} 2.8). **¹⁹F NMR (377 MHz, CDCl₃)** δ -62.4 (3 F, d, *J* 10.4, CF₃). **HRMS *m/z* (ESI⁺)** *m/z* calcd for C₂₀H₂₁N₂OCF₃⁺ [M+H]⁺ 397.1289; found 397.1279.

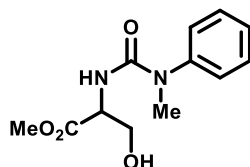
NOESY:



Methyl 2-(1,3-dimethyl-3-phenylureido)acrylate (**285**)

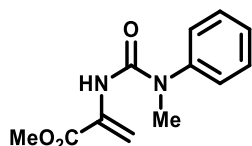


A solution of L-serine methyl ester hydrochloride (**282**) (1.0 g, 6.5 mmol) in anhydrous acetonitrile (14.0 mL) was prepared in a flame-dried RBF under a nitrogen atmosphere. Triethylamine (2.30 mL, 1.65 g, 16.3 mmol) was added to the mixture at room temperature then stirred for 30 minutes. Methyl(phenyl)carbamic chloride (**276**) (1.22 g, 7.2 mmol) was added to the reaction mixture then stirred for 18 hours at room temperature. The reaction was quenched with water (50 mL) and extracted with ethyl acetate (2 x 50 mL). The combined organic extracts were sequentially washed with 1 M $\text{HCl}_{(\text{aq})}$ (50 mL) and saturated $\text{NaHCO}_{3(\text{aq})}$ (50 mL), then dried (Na_2SO_4) and concentrated under reduced pressure yielding methyl (methyl(phenyl)carbamoyl)serinate (**283**) (1.34 g, 82 %) as colourless oil, which was used without further purification.



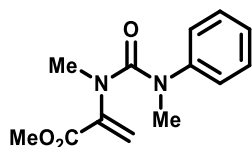
^1H NMR (400 MHz, CDCl_3) δ 7.48-7.43 (2 H, m, 2 x ArCH), 7.36-7.29 (3 H, m, 2 x ArCH + ArCH), 5.31 (1 H, d, J 6.9, NH), 4.56 (1 H, dt, J 6.9, 3.7, CH), 3.94-3.82 (2 H, m, CH_2), 3.74 (3 H, s, OCH_3), 3.29 (3 H, s, NCH_3). OH not observed. Data in good agreement with literature.²⁶²

A solution of methyl (methyl(phenyl)carbamoyl)serinate (**283**) (1.34 g, 5.3 mmol) in anhydrous acetonitrile (10.6 mL) was prepared in a flame-dried RBF under a nitrogen atmosphere. Triethylamine (1.48 mL, 1.07 g, 10.6 mmol) was added to the mixture at room temperature then stirred for 30 minutes at room temperature. *p*-Toluenesulfonyl chloride (2.02 g, 10.6 mmol) was added to the reaction mixture, then stirred for 20 hours at room temperature. The reaction was quenched with water (50 mL) and extracted with ethyl acetate (2 x 50 mL). The combined organic extracts were dried (Na_2SO_4) and concentrated under reduced pressure to yield crude material that was purified by flash column chromatography (SiO_2 , 0% to 60% Et_2O in 40-60 petroleum ether), yielding methyl 2-(3-methyl-3-phenylureido)acrylate (**284**) (795 mg, 64%) as a white solid.



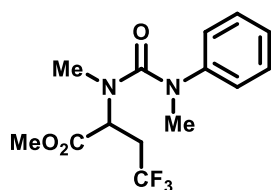
¹H NMR (400 MHz, CDCl₃) δ 7.51-7.45 (2 H, m, 2 x ArCH), 7.37 (1 H, tt, *J* 7.3, 1.2, ArCH), 7.31-7.27 (2 H, m, 2 x ArCH), 7.00 (1 H, br. s, NH), 6.34 (1 H, s, CH_aH_b), 5.66 (1 H, d, *J* 1.26, CH_aH_b), 3.71 (3 H, s, OCH₃), 3.31 (3 H, s, NCH₃). Data in good agreement with literature.²⁶²

A flame-dried Schlenk tube was charged with 2-(3-methyl-3-phenylureido)acrylate (**284**) (795 mg, 3.4 mmol) and anhydrous DMF (11.3 mL) then cooled to 0 °C. 60% Sodium hydride dispersed in mineral oil (271 mg, 6.8 mmol) was added to the Schlenk tube and the contents stirred for 30 minutes at 0 °C. Methyl iodide (0.84 mL, 13.6 mmol) was added to the Schlenk tube at 0 °C, the mixture was warmed to room temperature and stirred for 23 hours. The reaction was quenched with water (80 mL) and extracted with ethyl acetate (3 x 50 mL). The combined organic extracts were dried (Na₂SO₄), concentrated under reduced pressure and purified by flash column chromatography (SiO₂, 0% to 60% Et₂O in 40-60 petroleum ether), yielding the title compound (446 mg, 53%) as a colourless oil.



¹H NMR (400 MHz, CDCl₃) δ 7.31 (2 H, dd, *J* 8.4, 7.3, 2 x ArCH), 7.25-7.21 (2 H, m, 2 x ArCH), 7.13 (1 H, tt, *J* 7.3, 1.2, ArCH), 5.52 (1 H, d, *J* 0.9, CH_aH_b), 4.98 (1 H, d, *J* 0.9, CH_aH_b), 3.77 (3 H, s, OCH₃), 3.25 (3 H, s, NCH₃), 2.85 (3 H, s, NCH₃). Data in good agreement with literature.²⁶²

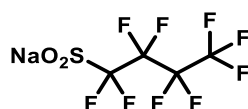
Methyl 2-(1,3-dimethyl-3-phenylureido)-4,4,4-trifluorobutanoate (**287**)



Formation of the title compound was carried out by following GP2 with methyl 2-(1,3-dimethyl-3-phenylureido)acrylate (**285**) (50 mg, 0.2 mmol) and sodium trifluoromethanesulfonate (**134**) (62 mg, 2.0 eq., 0.4 mmol) used as starting materials and acetone used as solvent. The reaction mixture was stirred for 17 hours to give the title compound (43 mg, 68%) as a white solid.

IR (film, cm⁻¹) ν_{max} = 2958, 1746, 1644, 1256, 1104. **¹H NMR (400 MHz, CDCl₃)** δ 7.36-7.30 (2 H, m, 2 x ArCH), 7.17-7.12 (3 H, m, 2 x ArCH + ArCH), 4.39 (1 H, dd, *J* 9.8, 3.4, CH), 3.76 (3 H, s, OCH₃), 3.21 (3 H, s, NCH₃), 2.99-2.85 (1 H, m, CH_aH_b), 2.80-2.65 (1 H, m, CH_aH_b), 2.50 (3 H, s, NCH₃). **¹³C NMR (126 MHz, CDCl₃)** δ 170.5 (CO), 161.1 (CO), 145.9 (C_{quat}), 129.6 (2 x ArCH), 126.2 (CF₃, q, *J*_{CF} 276.8), 125.5 (ArCH), 125.0 (2 x ArCH), 57.0 (CH, q, *J*_{CF} 3.2), 52.9 (OCH₃), 40.4 (NCH₃), 36.9 (NCH₃), 33.6 (CH₂, q, *J*_{CF} 28.9). **¹⁹F NMR (377 MHz, CDCl₃)** δ -64.5 (3 F, t, *J* 10.7, CF₃). **HRMS *m/z* (ESI⁺)** *m/z* calcd for C₁₄H₁₈N₂O₃F₃⁺ [M+H]⁺ 319.1264; found 319.1267.

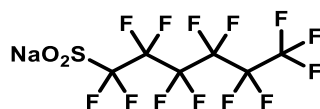
Sodium 1,1,2,2,3,3,4,4,4-nonafluorobutane-1-sulfinate (288)



While open, to air a solution of 1,1,1,2,2,3,3,4,4-nonafluoro-4-iodobutane (1.72 mL, 3.46 g, 10.0 mmol) in acetonitrile (6.0 mL) was prepared and cooled to 0 °C. Sequentially sodium bicarbonate (1.68 g, 20.0 mmol), sodium dithionite (2.05 g, 85 % wt., 10.0 mmol) and water (5.0 mL) were added to the 1,1,1,2,2,3,3,4,4-nonafluoro-4-iodobutane solution. The reaction mixture was warmed to room temperature and stirred for 23 hours. The reaction was quenched by addition of water (5 mL), then extracted with ethyl acetate (3 x 10 mL). The combined organic extracts were dried (Na₂SO₄) and concentrated under reduced pressure yielding white solid as crude product, which was purified by washing with diethyl ether (3 x 10 mL) affording the title compound (1.72 g, 56%) as a white solid.

¹⁹F NMR (377 MHz, DMSO-*d*₆) δ –80.5 (3 F, t, *J* 9.3, CF₃), –122.4 (2 F, br. q, *J* 9.3, CF₂), –126.0 (2 F, t, *J* 11.2, CF₂), –130.5–130.6 (2 F, m, CF₂). Data in good agreement with literature.²⁶³

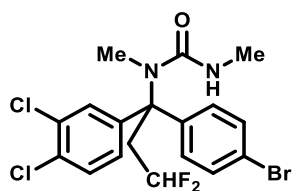
Sodium 1,1,2,2,3,3,4,4,5,5,6,6,6-tridecafluorohexane-1-sulfinate (289)



While open, to air a solution of 1,1,1,2,2,3,3,4,4,5,5,6,6-tridecafluoro-6-iodohexane (2.20 mL, 4.46 g, 10.0 mmol) in acetonitrile (6.0 mL) was prepared and cooled to 0 °C. Sequentially sodium bicarbonate (1.68 g, 20 mmol), sodium dithionite (2.05 g, 85 % wt., 10.0 mmol) and water (5 mL) were added to the 1,1,1,2,2,3,3,4,4,5,5,6,6-tridecafluoro-6-iodohexane solution. The reaction mixture was warmed to room temperature and stirred for 23 hours. The reaction was quenched by addition of water (5 mL), then extracted with ethyl acetate (3 x 10 mL). The combined organic extracts were dried (Na₂SO₄) and concentrated under reduced pressure yielding white solid as crude product, which was purified by washing with diethyl ether (3 x 10 mL) affording the title compound (2.48 g, 61%) as a white solid.

¹⁹F NMR (377 MHz, DMSO-*d*₆) δ –80.5 (3 F, t, *J* 9.6, CF₃), –122.1 (2 F, br. s, CF₂), –122.4 (2 F, br. s, CF₂), –122.9 (2 F, br. s, CF₂), –125.9–126.1 (2 F, m, CF₂), –130.5 (2 F, tt, *J* 12.6, 3.5, CF₂). Data in good agreement with literature.²⁶³

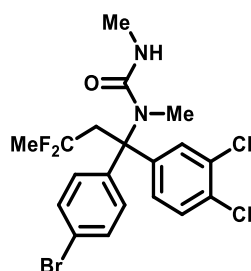
1-(1-(4-Bromophenyl)-1-(3,4-dichlorophenyl)-3,3-difluoropropyl)-1,3-dimethylurea (292)



Formation of the title compound was carried out by following GP2 with 1-(4-bromophenyl)-3-(1-(3,4-dichlorophenyl)vinyl)-1,3-dimethylurea (**245**) (83 mg, 0.2 mmol) and sodium difluoromethanesulfinate (55 mg, 2.0 eq., 0.4 mmol) used as starting materials and acetone used as solvent. The reaction mixture was stirred for 17 hours to give the title compound (60 mg, 64%) as a white solid.

M.p. 72-75 °C (Et₂O). **IR (film, cm⁻¹)** ν_{max} = 3365, 2955, 1640, 1531, 1078. **¹H NMR (400 MHz, CDCl₃)** δ 7.44 (2 H, d, *J* 8.8, 2 x ArCH), 7.35 (1 H, d, *J* 8.6, ArCH), 7.35 (1 H, d, *J* 2.4, ArCH), 7.17 (2 H, d, *J* 8.8, 2 x ArCH), 7.14 (1 H, dd, *J* 8.6, 2.4, ArCH), 5.90 (1 H, tt, *J* 55.9, 4.4, CHF₂), 4.64 (1 H, q, *J* 4.4, NH), 3.34 (2 H, tdd, *J* 15.6, 7.3, 4.4, CH₂), 2.77 (3 H, d, *J* 4.4, NCH₃), 2.70 (3 H, s, NCH₃). **¹³C NMR (126 MHz, CDCl₃)** δ 159.5 (CO), 144.6 (C_{quat}), 142.1 (C_{quat}), 132.7 (ArCCl), 131.9 (2 x ArCH), 131.3 (ArCCl), 130.4 (ArCH), 128.8 (2 x ArCH), 128.6 (ArCH), 126.1 (ArCH), 121.7 (ArCBr), 116.3 (CF₂H, t, *J*_{CF} 239.1), 67.7 (C_{quat}, t, *J*_{CF} 6.1), 42.4 (CH₂, t, *J*_{CF} 22.5), 36.1 (NCH₃), 27.8 (NCH₃). **¹⁹F NMR (377 MHz, CDCl₃)** δ -112.2 (2 F, dt, *J* 55.8, 15.9, CHF₂). **HRMS *m/z* (ESI⁺)** *m/z* calcd for C₁₈H₁₈N₂OF₂Cl₂Br⁺ [M+H]⁺ 464.9942; found 464.9960.

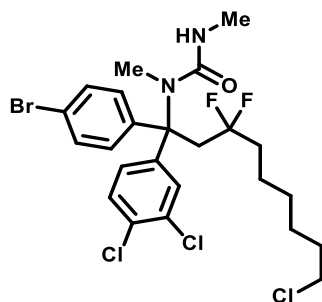
1-(1-(4-Bromophenyl)-1-(3,4-dichlorophenyl)-3,3-difluorobutyl)-1,3-dimethylurea (293)



Formation of the title compound was carried out by following GP2 with 1-(4-bromophenyl)-3-(1-(3,4-dichlorophenyl)vinyl)-1,3-dimethylurea (**245**) (83 mg, 0.2 mmol) and sodium 1,1-difluoroethane-1-sulfinate (61 mg, 2.0 eq., 0.4 mmol) used as starting materials and acetone used as solvent. The reaction mixture was stirred for 17 hours to give the title compound (76 mg, 79%) as a colourless film.

IR (film, cm^{-1}) ν_{max} = 3365, 2960, 1640, 1529, 1479. **^1H NMR (400 MHz, CDCl_3)** 7.37 (2 H, d, J 8.9, 2 x ArCH), 7.31 (1 H, d, J 2.2, ArCH), 7.28 (1 H, d, J 8.6, ArCH), 7.15 (2 H, d, J 8.9, 2 x ArCH), 7.12 (1 H, dd, J 8.6, 2.2, ArCH), 4.64 (1 H, br. s, NH), 3.69-3.45 (2 H, m, CH_2), 2.80 (3 H, s, NCH_3), 2.78 (3 H, d, J 4.8, NCH_3), 1.72 (3 H, t, J 18.6, CH_3). **^{13}C NMR (101 MHz, CDCl_3)** δ 159.6 (CO), 146.8 (C_{quat}), 143.5 (C_{quat}), 132.3 (ArCCl), 131.5 (2 x ArCH), 130.4 (ArCCl), 130.1 (ArCH), 128.7 (2 x ArCH), 128.1 (ArCH), 125.5 (ArCH), 123.8 (CF_2 , t, J_{CF} 241.1), 120.9 (ArCBr), 68.4 (C_{quat}), 40.5 (CH_2 , t, J_{CF} 23.1), 36.6 (NCH_3 , t, J_{CF} 4.0), 27.7 (NCH_3), 26.5 (CH_3 , t, J_{CF} 28.2). **^{19}F NMR (377 MHz, CDCl_3)** δ -87.0--89.7 (2 F, m, CF_2). **HRMS m/z (ESI $^+$)** m/z calcd for $\text{C}_{19}\text{H}_{20}\text{N}_2\text{OCl}_2\text{F}_2\text{Br}^+$ [$\text{M}+\text{H}$] $^+$ 479.0099; found 479.0101.

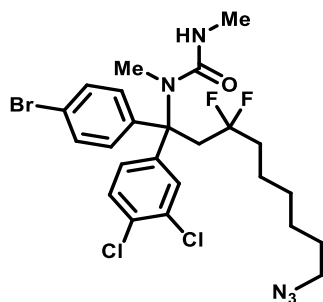
1-(1-(4-Bromophenyl)-9-chloro-1-(3,4-dichlorophenyl)-3,3-difluorononyl)-1,3-dimethylurea (294)



Formation of the title compound was carried out by following GP2 with 1-(4-bromophenyl)-3-(1-(3,4-dichlorophenyl)vinyl)-1,3-dimethylurea (**245**) (83 mg, 0.2 mmol) and sodium 7-chloro-1,1-difluoroheptane-1-sulfinate (103 mg, 2.0 eq., 0.4 mmol) used as starting materials and acetone used as solvent. The reaction mixture was stirred for 18 hours to give the title compound (64 mg, 55%) as a white solid.

M.p. 64-67 °C (Et₂O). **IR (film, cm⁻¹)** ν_{max} = 3368, 2932, 1641, 1527, 1315. **¹H NMR (400 MHz, CDCl₃)** δ 7.37 (2 H, d, *J* 8.6, 2 x ArCH), 7.30 (1 H, d, *J* 2.3, ArCH), 7.28 (1 H, d, *J* 8.9, ArCH), 7.14 (2 H, d, *J* 8.6, 2 x ArCH), 7.11 (1 H, dd, *J* 8.9, 2.3, ArCH), 4.65 (1 H, q, *J* 4.5, NH), 3.63-3.42 (4 H, m, CH₂ + CH₂Cl), 2.80 (3 H, s, NCH₃), 2.78 (3 H, d, *J* 4.5, NCH₃), 1.94 (2 H, dq, *J* 22.5, 8.6, CH₂), 1.78 (2 H, qn, *J* 6.9, CH₂), 1.57 (2 H, qn, *J* 7.8, CH₂), 1.51-1.43 (2 H, m, CH₂), 1.41-1.35 (2 H, m, CH₂). **¹³C NMR (126 MHz, CDCl₃)** δ 159.6 (CO), 146.9 (C_{quat}), 143.6 (C_{quat}), 132.2 (ArCCl), 131.5 (2 x ArCH), 130.3 (ArCCl), 130.1 (ArCH), 128.6 (2 x ArCH), 128.0 (ArCH), 125.5 (ArCH), 124.6 (CF₂, t, *J*_{CF} 244.8), 120.8 (ArCBr), 68.4 (C_{quat}), 45.1 (CH₂Cl), 39.3 (CH₂, t, *J*_{CF} 25.5), 39.0 (CH₂, t, *J*_{CF} 23.0), 36.6 (NCH₃, t, *J*_{CF} 4.0), 32.5 (CH₂), 28.6 (CH₂), 27.7 (NCH₃), 26.7 (CH₂), 22.1 (CH₂, t, *J*_{CF} 4.2). **¹⁹F NMR (377 MHz, CDCl₃)** δ -95.9—-96.1 (2 F, m, CF₂). **HRMS *m/z* (ESI⁺)** *m/z* calcd for C₂₄H₂₉N₂OF₂Cl₃Br⁺ [M+H]⁺ 583.0491; found 583.0503.

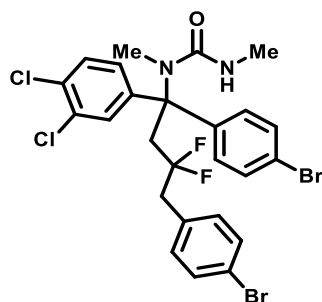
1-(9-Azido-1-(4-bromophenyl)-1-(3,4-dichlorophenyl)-3,3-difluorononyl)-1,3-dimethylurea (295)



Formation of the title compound was carried out by following GP2 with 1-(4-bromophenyl)-3-(1-(3,4-dichlorophenyl)vinyl)-1,3-dimethylurea (**245**) (83 mg, 0.2 mmol) and sodium difluoroheptylazidosulfinate (100 mg, 1.9 eq., 0.38 mmol) used as starting materials and acetone used as solvent. The reaction mixture was stirred for 18 hours to give the title compound (95 mg, 80%) as a white solid.

M.p. 53-57°C (Et₂O). **IR (film, cm⁻¹)** ν_{\max} = 3363, 2934, 2094, 1640, 1313. **¹H NMR (400 MHz, CDCl₃)** δ 7.36 (2 H, d, *J* 8.8, 2 x ArCH), 7.30 (1 H, d, *J* 2.3, ArCH), 7.28 (1 H, d, *J* 8.6, ArCH), 7.14 (2 H, d, *J* 8.8, 2 x ArCH), 7.11 (1 H, dd, *J* 8.6, 2.3, ArCH), 4.67 (1 H, q, *J* 4.6, NH), 3.65-3.41 (2 H, m, CH₂), 3.27 (2 H, t, *J* 6.9, CH₂N₃), 2.79 (3 H, s, NCH₃), 2.77 (3 H, d, *J* 4.6, NCH₃), 2.01-1.85 (2 H, m, CH₂), 1.65-1.52 (4 H, m, CH₂ + CH₂), 1.44-1.33 (4 H, m, CH₂ + CH₂). **¹³C NMR (101 MHz, CDCl₃)** δ 159.6 (CO), 146.9 (C_{quat}), 143.6 (C_{quat}), 132.2 (ArCCl), 131.4 (2 x ArCH), 130.3 (ArCCl), 130.0 (ArCH), 128.6 (2 x ArCH), 128.0 (ArCH), 125.5 (ArCH), 124.6 (CF₂, t, *J*_{CF} 244.2), 120.8 (ArCBr), 68.3 (C_{quat}), 51.5 (CH₂N₃), 39.2 (CH₂, t, *J*_{CF} 25.5), 39.0 (CH₂, t, *J*_{CF} 22.9), 36.6 (NCH₃, t, *J*_{CF} 3.8), 28.9 (CH₂), 28.8 (CH₂), 27.7 (CH₃), 26.6 (CH₂), 22.1 (CH₂, t, *J*_{CF} 4.3). **¹⁹F NMR (377 MHz, CDCl₃)** δ -96.2--96.4 (2 F, m, CF₂). **HRMS *m/z* (ESI⁺)** *m/z* calcd for C₂₄H₂₉N₅OF₂Cl₂Br⁺ [M+H]⁺ 590.0895; found 590.0893.

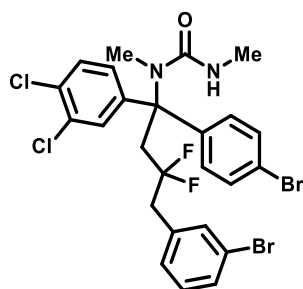
1-(1,4-Bis(4-bromophenyl)-1-(3,4-dichlorophenyl)-3,3-difluorobutyl)-1,3-dimethylurea (296)



Formation of the title compound was carried out by following GP2 with 1-(4-bromophenyl)-3-(1-(3,4-dichlorophenyl)vinyl)-1,3-dimethylurea (**245**) (83 mg, 0.2 mmol) and sodium 2-(4-bromophenyl)-1,1-difluoroethanesulfinate (123 mg, 2.0 eq., 0.4 mmol) used as starting materials and acetone used as solvent. The reaction mixture was stirred for 20 hours to give the title compound (90 mg, 71%) as a white solid.

M.p. 196-200 °C (Et₂O). **IR (film, cm⁻¹)** ν_{\max} = 3367, 2962, 1640, 1489, 1008. **¹H NMR (400 MHz, CDCl₃)** δ 7.53 (2 H, d, *J* 8.2, 2 x ArCH), 7.31 (2 H, d, *J* 8.7, 2 x ArCH), 7.25-7.20 (3 H, m, 2 x ArCH + ArCH), 7.12 (1 H, d, *J* 1.4, ArCH), 6.99-6.93 (3 H, m, 2 x ArCH + ArCH), 4.65 (1 H, q, *J* 4.5, NH), 3.62-3.42 (2 H, m, CH₂), 3.19 (2 H, t, *J* 16.0, CH₂), 2.80-2.76 (6 H, m, 2 x CH₃). **¹³C NMR (126 MHz, CDCl₃)** δ 159.6 (CO), 146.4 (C_{quat}), 143.7 (C_{quat}), 132.5 (2 x ArCH), 132.3 (ArCCl), 132.0 (2 x ArCH), 131.9 (C_{quat}), 131.5 (2 x ArCH), 130.4 (ArCCl), 130.1 (ArCH), 128.3 (2 x ArCH), 127.9 (ArCH), 125.6 (ArCH), 123.3 (CF₂, t, *J*_{CF} 246.5), 122.1 (ArCBr), 120.8 (ArCBr), 68.3 (C_{quat}), 44.7 (CH₂, t, *J*_{CF} 26.5), 38.3 (CH₂, t, *J*_{CF} 22.4), 36.5 (NCH₃, t, *J*_{CF} 3.9), 27.7 (NCH₃). **¹⁹F NMR (377 MHz, CDCl₃)** δ -94.2—-94.4 (2 F, m, CF₂). **HRMS *m/z* (ESI⁺)** *m/z* calcd for C₂₅H₂₃N₂OF₂Cl₂Br₂⁺ [M+H]⁺ 634.9496; found 634.9502.

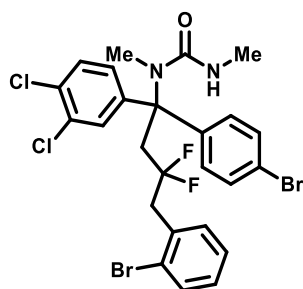
1-(4-(3-Bromophenyl)-1-(4-bromophenyl)-1-(3,4-dichlorophenyl)-3,3-difluorobutyl)-1,3-dimethylurea (297)



Formation of the title compound was carried out by following GP2 with 1-(4-bromophenyl)-3-(1-(3,4-dichlorophenyl)vinyl)-1,3-dimethylurea (**245**) (83 mg, 0.2 mmol) and sodium 2-(3-bromophenyl)-1,1-difluoroethanesulfinate (123 mg, 2.0 eq., 0.4 mmol) used as starting materials and DMF used as solvent. The reaction mixture was stirred for 23 hours to give the title compound (61 mg, 48%) as a pale-yellow solid.

M.p. 179-182 °C (CDCl₃). **IR (film, cm⁻¹)** ν_{max} = 3366, 2929, 1643, 1476. **¹H NMR (400 MHz, CDCl₃)** δ 7.60-7.50 (2 H, m, ArCH + ArCH), 7.35 (2 H, d, *J* 8.5, 2 x ArCH), 7.33-7.26 (3 H, m, ArCH + ArCH + ArCH), 7.18 (1 H, d, *J* 1.2, ArCH), 7.05 (3 H, m, 2 x ArCH + ArCH), 4.68 (1 H, q, *J* 4.5, NH), 3.56-3.44 (2 H, m, CH₂), 3.24 (2 H, t, *J* 16.1, CH₂), 2.90-2.77 (6 H, m, NCH₃ + NCH₃). **¹³C NMR (126 MHz, CDCl₃)** δ 156.9 (CO), 146.5 (C_{quat}), 143.6 (C_{quat}), 135.2 (C_{quat}, *t*, *J*_{CF} 3.9), 133.7 (ArCH), 132.3 (ArCCl), 131.5 (2 x ArCH), 131.1 (ArCH), 130.4 (ArCCl), 130.3 (ArCH), 130.1 (ArCH), 129.4 (ArCH), 128.3 (2 x ArCH), 127.9 (ArCH), 125.5 (ArCH), 123.3 (CF₂, *t*, *J*_{CF} 244.7), 122.8 (ArCBr), 120.8 (ArCBr), 68.3 (C_{quat}), 44.9 (CH₂, *t*, *J*_{CF} 26.2), 38.4 (CH₂, *t*, *J*_{CF} 22.4), 36.5 (NCH₃, *t*, *J*_{CF} 3.9), 27.7 (NCH₃). **¹⁹F NMR (377 MHz, CDCl₃)** δ -94.1—-94.3 (2 F, m, CF₂). **HRMS *m/z* (ESI⁺)** *m/z* calcd for C₂₅H₂₃N₂OF₂Cl₂Br₂⁺ [M+H]⁺ 632.9517; found 632.9513.

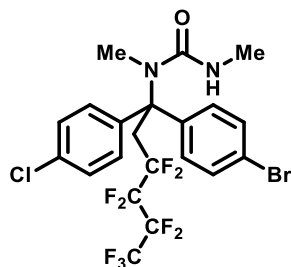
1-(4-(2-Bromophenyl)-1-(4-bromophenyl)-1-(3,4-dichlorophenyl)-3,3-difluorobutyl)-1,3-dimethylurea (298)



Formation of the title compound was carried out by following GP2 with 1-(4-bromophenyl)-3-(1-(3,4-dichlorophenyl)vinyl)-1,3-dimethylurea (**245**) (83 mg, 0.2 mmol) and sodium 2-(2-bromophenyl)-1,1-difluoroethanesulfinate (123 mg, 2.0 eq., 0.4 mmol) used as starting materials and acetone used as solvent. The reaction mixture was stirred for 23 hours to give the title compound (120 mg, 94%) as a beige solid.

M.p. 92-94 °C (CHCl₃). **IR (film, cm⁻¹)** ν_{\max} = 3367, 2936, 1642, 1476. **¹H NMR (400 MHz, CDCl₃)** δ 7.69 (1 H, dd, *J* 7.6, 1.3, ArCH), 7.44 (1 H, d, *J* 7.6, ArCH), 7.36 (1 H, td, *J* 7.6, 1.3, ArCH), 7.27 (2 H, d, *J* 8.8, 2 x ArCH), 7.23 (1 H, td, *J* 7.6, 1.3, ArCH), 7.21 (1 H, d, *J* 8.6, ArCH), 7.16 (1 H, d, *J* 2.3, ArCH), 7.00 (1 H, dd, *J* 8.6, 2.3, ArCH), 6.90 (2 H, d, *J* 8.8, 2 x ArCH), 4.62 (1 H, q, *J* 4.6, NH), 3.67-3.48 (4 H, m, CH₂ + CH₂), 2.80 (3 H, s, NCH₃), 2.79 (3 H, d, *J* 4.6, NCH₃). **¹³C NMR (126 MHz, CDCl₃)** δ 159.5 (CO), 146.8 (C_{quat}), 144.0 (C_{quat}), 135.5 (ArCH), 133.0 (ArCH), 133.0 (C_{quat}), 132.3 (ArCCl), 131.5 (2 x ArCH), 130.2 (ArCCl), 130.1 (ArCH), 129.7 (ArCH), 128.2 (2 x ArCH), 127.8 (ArCH), 127.8 (ArCH), 126.0 (ArCBr), 125.4 (ArCH), 123.8 (CF₂, t, *J*_{CF} 246.8), 120.7 (ArCBr), 68.1 (C_{quat}), 44.4 (CH₂, t, *J*_{CF} 26.6), 38.0 (CH₂, t, *J*_{CF} 22.2), 36.4 (CH₃, t, *J*_{CF} 4.0), 27.7 (CH₃). **¹⁹F NMR (377 MHz, CDCl₃)** δ -93.5--93.7 (2 F, m, CF₂). **HRMS *m/z* (ESI⁺)** *m/z* calcd for C₂₅H₂₃N₂O₂F₂Cl₂Br₂⁺ [M+H]⁺ 632.9517; found 632.9511.

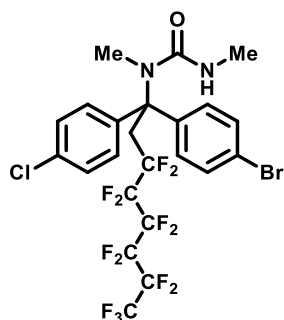
1-(1-(4-Bromophenyl)-1-(4-chlorophenyl)-3,3,4,4,5,5,6,6,6-nonafluorohexyl)-1,3-dimethylurea (299)



Formation of the title compound was carried out by following GP2 with 1-(4-bromophenyl)-3-(1-(4-chlorophenyl)vinyl)-1,3-dimethylurea (**221**) (76 mg, 0.2 mmol) and sodium 1,1,2,2,3,3,4,4,4-nonafluorobutane-1-sulfinate (**288**) (122 mg, 2.0 eq., 0.4 mmol) used as starting materials and acetonitrile used as solvent. The reaction mixture was stirred for 16 hours to give the title compound (84 mg, 70%) as a white solid.

M.p. 172-174 °C (Et₂O). **IR (film, cm⁻¹)** ν_{max} = 3366, 2971, 1639, 1221, 1132. **¹H NMR (400 MHz, CDCl₃)** δ 7.38 (2 H, d, *J* 8.6, 2 x ArCH), 7.23 (2 H, d, *J* 8.7, 2 x ArCH), 7.18 (2 H, d, *J* 8.7, 2 x ArCH), 7.12 (2 H, d, *J* 8.6, 2 x ArCH), 4.64 (1 H, br. q, *J* 4.4, NH), 3.88 (2 H, t, *J* 19.5, CH₂), 2.82 (3 H, s, CH₃), 2.79 (3 H, d, *J* 4.4, CH₃). **¹⁹F decoupled ¹³C NMR (101 MHz, CDCl₃)** δ 159.4 (CO), 143.8 (C_{quat}), 143.1 (C_{quat}), 132.8 (ArCCI), 131.6 (2 x ArCH), 128.7 (2 x ArCH), 127.9 (2 x ArCH), 127.6 (2 x ArCH), 120.9 (ArCBr), 118.7 (CH₂CF₂), 117.5 (CF₃), 110.6 (CF₂), 108.9 (CF₂), 68.2 (C_{quat}), 36.4 (NCH₃), 33.4 (CH₂CF₂), 27.7 (NCH₃). **¹⁹F NMR (377 MHz, CDCl₃)** δ -80.8 (3 F, t, *J* 9.5, CF₃), -110.7 (2 F, br. qn, *J* 15.0, CF₂), -123.8 (2 F, br. s, CF₂), -125.4—125.6 (2 F, m, CF₂). **HRMS *m/z* (ESI⁺)** *m/z* calcd for C₂₁H₁₈N₂OBrClF₉⁺ [M+H]⁺ 599.0142; found 599.0146.

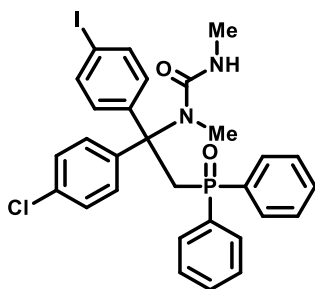
1-(1-(4-Bromophenyl)-1-(4-chlorophenyl)-3,3,4,4,5,5,6,6,7,7,8,8,8-tridecafluorooctyl)-1,3-dimethylurea (300)



Formation of the title compound was carried out by following GP2 with 1-(4-bromophenyl)-3-(1-(4-chlorophenyl)vinyl)-1,3-dimethylurea (**221**) (76 mg, 0.2 mmol) and sodium 1,1,2,2,3,3,4,4,5,5,6,6,6-tridecafluorohexane-1-sulfinate (**289**) (162 mg, 2.0 eq., 0.4 mmol) used as starting materials and acetone used as solvent. The reaction mixture was stirred for 19 hours to give the title compound (93 mg, 66%) as a white solid.

M.p. 87-90 °C (Et₂O). **IR (film, cm⁻¹)** ν_{max} = 3360, 2969, 1642, 1235, 1195, 1143. **¹H NMR (400 MHz, CDCl₃)** δ 7.38 (2 H, d, *J* 8.4, 2 x ArCH), 7.23 (2 H, d, *J* 8.8, 2 x ArCH), 7.18 (2 H, d, *J* 8.8, 2 x ArCH), 7.12 (2 H, d, *J* 8.4, 2 x ArCH), 4.64 (1 H, br. s, NH), 3.88 (2 H, t, *J* 19.2, CH₂), 2.82 (3 H, s, CH₃), 2.79 (3 H, d, *J* 4.1, CH₃). **¹⁹F decoupled ¹³C NMR (101 MHz, CDCl₃)** δ 159.4 (CO), 143.9 (C_{quat}), 143.1 (C_{quat}), 132.8 (ArCCl), 131.6 (2 x ArCH), 128.7 (2 x ArCH), 127.9 (2 x ArCH), 127.6 (2 x ArCH), 120.9 (ArCBr), 118.8 (CH₂CF₂), 117.3 (CF₃), 111.2 (CF₂), 111.1 (CF₂), 110.4 (CF₂), 108.6 (CF₂), 68.2 (C_{quat}), 36.3 (NCH₃), 33.4 (CH₂), 27.7 (NCH₃). **¹⁹F NMR (377 MHz, CDCl₃)** δ -80.6 (3 F, t, *J* 9.4, CF₃), -110.4 (2 F, br. qn, *J* 16.3, CF₂), -121.3 (2 F, br. s, CF₂), -122.6 (2 F, br. s, CF₂), -122.9 (2 F, br. s, CF₂), -126.0 (2 F, br. s, CF₂). **HRMS *m/z* (ESI⁺)** *m/z* calcd for C₂₃H₁₈N₂OBrClF₁₃⁺ [M+H]⁺ 699.0078; found 699.0079.

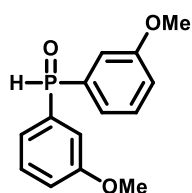
1-(1-(4-Chlorophenyl)-2-(diphenylphosphoryl)-1-(4-iodophenyl)ethyl)-1,3-dimethylurea (306)



Formation of the title compound was carried out by following GP3, with diphenylphosphine oxide (**304**) (28 mg, 1.4 eq., 0.14 mmol) used as starting material. The reaction mixture was stirred for 16 hours, then purified by flash column chromatography (SiO₂, 0% to 55% THF + 3% NEt₃ in *n*-pentane) to give the title compound (40 mg, 64%) as a colourless film.

IR (film, cm⁻¹) ν_{max} = 3343, 2924, 1635, 1534, 1485, 1183. **¹H NMR (500 MHz, CDCl₃)** δ 7.75 (4 H, br. t, *J* 9.0, 4 x ArCH), 7.48 (2 H, d, *J* 8.6, 2 x ArCH), 7.47 (2 H, br. t, *J* 7.3, 2 x ArCH), 7.44-7.38 (4 H, m, 4 x ArCH), 7.29 (2 H, d, *J* 8.6, 2 x ArCH), 7.14 (2 H, d, *J* 8.6, 2 x ArCH), 7.08 (2 H, d, *J* 8.6, 2 x ArCH), 4.37 (1 H, q, *J* 4.5, NH), 4.09 (2 H, d, *J* 11.4, CH₂), 2.63 (3 H, s, CH₃), 2.43 (3 H, d, *J* 4.5, CH₃). **¹³C NMR (126 MHz, CDCl₃)** δ 159.1 (CO), 144.7 (C_{quat}, d, *J*_{CP} 5.7), 143.0 (C_{quat}, d, *J*_{CP} 5.7), 137.1 (2 x ArCH), 134.4 (C_{quat}, d, *J*_{CP} 99.8), 134.2 (C_{quat}, d, *J*_{CP} 99.8), 132.7 (ArCCl), 131.4 (2 x ArCH, t, *J*_{CP} 2.5), 130.8 (4 x ArCH, dd, *J*_{CP} 9.1, 6.4), 129.4 (2 x ArCH), 128.9 (2 x ArCH), 128.5 (4 x ArCH, dd, *J*_{CP} 11.8, 4.6), 128.2 (2 x ArCH), 92.7 (ArCl), 69.6 (C_{quat}, d, *J*_{CP} 5.6), 38.4 (CH₂, d, *J*_{CP} 71.4), 36.9 (CH₃), 27.3 (CH₃). **³¹P NMR (162 MHz, CDCl₃)** δ 24.8 (1 P, br. t, *J* 11.4, PO). **HRMS *m/z* (ESI⁺)** *m/z* calcd for C₂₉H₂₈N₂O₂IClP⁺ [M+H]⁺ 629.0616; found 629.0628.

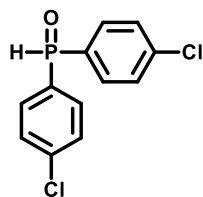
Bis(3-methoxyphenyl)phosphine oxide (**312**)



A solution of 1-bromo-3-methoxybenzene (**307**) (1.89 g, 2.80 g, 15.0 mmol) in anhydrous THF (20.0 mL) was prepared under a nitrogen atmosphere in a flame-dried Schlenk tube. To a separate flame-dried Schlenk tube magnesium turnings (510 mg, 21 mmol) and a single crystal of iodine were added under a nitrogen atmosphere. The solution of 1-bromo-4-chlorobenzene was added to the magnesium turnings at a rate to achieve a gently refluxing solution from the exotherm while stirring. The reaction mixture was stirred for 1.5 hours at room temperature. A solution of diethyl phosphonate (**311**) (0.64 mL, 691 mg, 5 mmol) in anhydrous THF (10 mL) was prepared under a nitrogen atmosphere in a flame-dried Schlenk tube and cooled to 0 °C. The solution of Grignard reagent was added slowly to the solution of diethyl phosphonate. The reaction mixture was warmed to room temperature and stirred 18 hours, then quenched with water (40 mL) and extracted with ethyl acetate (3 x 40 mL). The combined organic extracts were dried (Na_2SO_4) and concentrated under reduced pressure to yield a white solid as crude product. Crude product was purified by flash column chromatography (SiO_2 , 20% to 100% EtOAc in 40-60 petroleum ether) yielding the title compound (229 mg, 17%) as a white solid.

^1H NMR (400 MHz, CDCl_3) δ 8.03 (1 H, d, J 482.0, PH), 7.41 (2 H, td, J 7.9, 3.9, 2 x ArCH), 7.29-7.20 (4 H, m, 4 x ArCH), 3.83 (6 H, s, 2 x OCH_3). Data in good agreement with literature.²⁶⁴

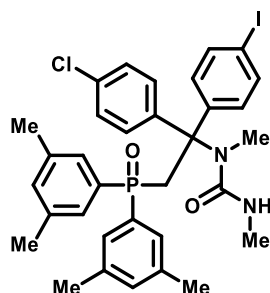
Bis(4-chlorophenyl)phosphine oxide (**313**)



A solution of 1-bromo-4-chlorobenzene (**308**) (2.87 g, 15 mmol) in anhydrous THF (20 mL) was prepared under a nitrogen atmosphere in a flame-dried Schlenk tube. To a separate flame-dried Schlenk tube magnesium turnings (510 mg, 21 mmol) and a single crystal of iodine were added under a nitrogen atmosphere. The solution of 1-bromo-4-chlorobenzene was added to the magnesium turnings at a rate to achieve a gently refluxing solution from the exotherm while stirring. The reaction mixture was stirred for 1.5 hours at room temperature. A solution of diethyl phosphonate (0.64 mL, 691 mg, 5 mmol) (**311**) in anhydrous THF (10 mL) was prepared under a nitrogen atmosphere in a flame-dried Schlenk tube and cooled to 0 °C. The solution of Grignard reagent was added slowly to the solution of diethyl phosphonate. The reaction mixture was warmed to room temperature and stirred 18 hours, then quenched with water (40 mL) and extracted with ethyl acetate (3 x 40 mL). The combined organic extracts were dried (Na₂SO₄) and concentrated under reduced pressure to yield a white solid as crude product. The crude product was purified by flash column chromatography (SiO₂, 20% to 100% Et₂O in 40-60 petroleum ether) yielding the title compound (507 mg, 38%) as a white solid.

¹H NMR (400 MHz, CDCl₃) δ 8.06 (1 H, d, *J* 486.0, *PH*), 7.62 (4 H, dd, *J* 13.2, 8.5, 4 x ArCH), 7.50 (4 H, dq, *J* 8.5, 2.2, 4 x ArCH). Data in good agreement with literature.²⁶⁵

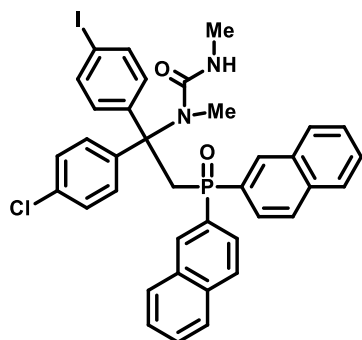
1-(2-(Bis(3,5-dimethylphenyl)phosphoryl)-1-(4-chlorophenyl)-1-(4-iodophenyl)ethyl)-1,3-dimethylurea (314)



Formation of the title compound was carried out by following GP3, with bis(3,5-dimethylphenyl)phosphine oxide (36 mg, 1.4 eq., 0.14 mmol) used as starting material. The reaction mixture was stirred for 20 hours, then purified by flash column chromatography (SiO₂, 0% to 3% MeOH in DCM) then again (SiO₂, 0% to 60% Et₂O in *n*-pentane) to give the title compound (41 mg, 60%) as a colourless film.

IR (film, cm⁻¹) ν_{\max} = 3335, 2924, 1650, 1487, 1179. **¹H NMR (500 MHz, CDCl₃)** δ 7.47 (2 H, d, *J* 8.7, 2 x ArCH), 7.31 (4 H, dd, *J* 9.0, 3.0, 4 x ArCH), 7.3 (2 H, d, *J* 8.7, 2 x ArCH), 7.13 (2 H, d, *J* 8.7, 2 x ArCH), 7.08 (2 H, d, *J* 8.7, 2 x ArCH), 7.06 (2 H, s, 2 x ArCH), 4.48 (1 H, q, *J* 4.7, NH), 3.98 (2 H, d, *J* 11.4, CH₂), 2.64 (3 H, s, CH₃), 2.47 (3 H, d, *J* 4.7, CH₃), 2.31 (12 H, s, 4 x CH₃). **¹³C NMR (126 MHz, CDCl₃)** δ 159.2 (CO), 144.7 (C_{quat}, d, *J*_{CP} 6.1), 143.0 (C_{quat}, d, *J*_{CP} 5.9), 138.1 (4 x C_{quat}, dd, *J*_{CP} 12.3, 6.8), 137.0 (2 x ArCH), 134.3 (C_{quat}, d, *J*_{CP} 99.0), 134.1 (C_{quat}, d, *J*_{CP} 99.0), 133.1 (2 x ArCH, dd, *J*_{CP} 2.9, 1.5), 132.6 (ArCCI), 129.3 (2 x ArCH), 128.9 (2 x ArCH), 128.2 (4 x ArCH, dd, *J*_{CP} 9.0, 6.6), 128.1 (2 x ArCH), 92.7 (ArCI), 69.6 (C_{quat}, d, *J*_{CP} 5.4), 37.9 (CH₂, d, *J*_{CP} 70.6), 36.9 (CH₃), 27.3 (CH₃), 21.5 (4 x CH₃). **³¹P NMR (162 MHz, CDCl₃)** δ 25.2 (1 P, br. t, *J* 11.4, PO). **HRMS *m/z* (ESI⁺)** *m/z* calcd for C₃₃H₃₆ClIN₂O₂P⁺ [M+H]⁺ 685.1242; found 685.1234.

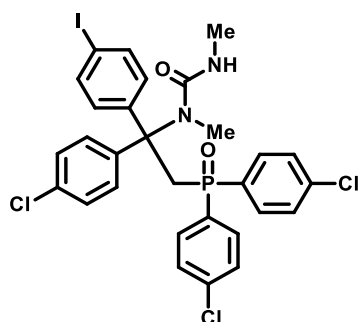
1-(1-(4-Chlorophenyl)-2-(di(naphthalen-2-yl)phosphoryl)-1-(4-iodophenyl)ethyl)-1,3-dimethylurea (315)



Formation of the title compound was carried out by following GP3, with di(naphthalen-2-yl)phosphine oxide (42 mg, 1.4 eq., 0.14 mmol) used as starting material. The reaction mixture was stirred for 18 hours, then purified by flash column chromatography (SiO₂, 0% to 55% THF + 3% NEt₃ in *n*-pentane) then again (SiO₂, 0% to 40% acetone in *n*-pentane) to give the title compound (53 mg, 73%) as a colourless film.

IR (film, cm⁻¹) ν_{\max} = 3349, 2925, 1639, 1485, 1085. **¹H NMR (500 MHz, CDCl₃)** δ 8.41 (2 H, d, *J* 13.3, 2 x ArCH), 7.90 (2 H, d, *J* 8.0, 2 x ArCH), 7.89-7.80 (6 H, m, 6 x ArCH), 7.55 (4 H, pd, *J* 7.2, 2.0, 4 x ArCH), 7.49 (2 H, d, *J* 8.7, 2 x ArCH), 7.33 (2 H, d, *J* 8.8, 2 x ArCH), 7.15 (2 H, d, *J* 8.8, 2 x ArCH), 7.12 (2 H, d, *J* 8.7, 2 x ArCH), 4.31 (2 H, d, *J* 11.1, CH₂), 4.13 (1 H, q, *J* 4.6, NH), 2.65 (3 H, s, CH₃), 2.08 (3 H, d, *J* 4.7, CH₃). **¹³C NMR (126 MHz, CDCl₃)** δ 158.7 (CO), 145.0 (C_{quat}, d, *J*_{CP} 6.0), 143.3 (C_{quat}, d, *J*_{CP} 5.7), 137.0 (2 x ArCH), 134.5 (2 x C_{quat}, d, *J*_{CP} 2.3), 132.7 (ArCCl), 132.5 (2 x ArCH), 132.4 (2 x C_{quat}, d, *J*_{CP} 5.5), 131.4 (C_{quat}, d, *J*_{CP} 100.2), 131.3 (C_{quat}, d, *J*_{CP} 100.2), 129.2 (2 x ArCH), 129.1 (2 x ArCH), 128.8 (2 x ArCH), 128.3 (2 x ArCH, dd, *J*_{CP} 11.5, 7.4), 128.2 (2 x ArCH), 128.2 (2 x ArCH), 127.9 (2 x ArCH), 126.9 (2 x ArCH), 126.0 (2 x ArCH, dd, *J*_{CP} 9.9, 7.0), 92.6 (ArCl), 69.7 (C_{quat}, d, *J*_{CP} 5.5), 37.9 (CH₂, d, *J*_{CP} 71.6), 37.0 (CH₃), 26.8 (CH₃). **³¹P NMR (162 MHz, CDCl₃)** δ 25.0 (1 P, br. t, *J* 11.1, PO). **HRMS *m/z* (ESI⁺)** *m/z* calcd for C₃₇H₃₂ClIN₂O₂P⁺ [M+H]⁺ 729.0929; found 729.0914.

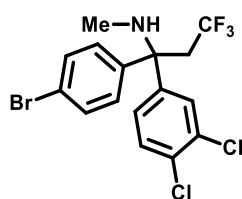
1-(2-(Bis(4-chlorophenyl)phosphoryl)-1-(4-chlorophenyl)-1-(4-iodophenyl)ethyl)-1,3-dimethylurea (316)



Formation of the title compound was carried out by following GP3, with bis(4-chlorophenyl)phosphine oxide (**313**) (38 mg, 1.4 eq., 0.14 mmol) used as starting material. The reaction mixture was stirred for 18 hours, then purified by flash column chromatography (SiO₂, 0% to 50% Et₂O in DCM) to give the title compound (33 mg, 48%) as a colourless film. Note - Product was observed to decompose in CDCl₃ over the course of a night.

IR (film, cm⁻¹) ν_{\max} = 3351, 2919, 1644, 1481, 1088. **¹H NMR (400 MHz, CDCl₃)** δ 7.66 (4 H, dd, *J* 10.9, 8.5, 4 x ArCH), 7.50 (2 H, d, *J* 8.8, 2 x ArCH), 7.39 (4 H, dd, *J* 8.5, 7.4, 4 x ArCH), 7.27 (2 H, d, *J* 8.9, 2 x ArCH), 7.16 (2 H, d, *J* 8.9, 2 x ArCH), 7.06 (2 H, d, *J* 8.8, 2 x ArCH), 4.28 (1 H, q, *J* 4.9, NH), 4.10 (2 H, d, *J* 11.2, CH₂), 2.63 (3 H, s, CH₃), 2.47 (3 H, d, *J* 4.9, CH₂). **¹³C NMR (101 MHz, CDCl₃)** δ 159.0 (CO), 144.4 (C_{quat}, d, *J*_{CP} 6.0), 142.7 (C_{quat}, d, *J*_{CP} 5.8), 138.3 (2 x ArCCl, d, *J*_{CP} 3.1), 137.2 (2 x ArCH), 133.0 (ArCCl), 132.5 (C_{quat}, d, *J*_{CP} 101.2), 132.3 (C_{quat}, d, *J*_{CP} 101.2), 132.2 (4 x ArCH, dd, *J*_{CP} 9.9, 4.7), 129.3 (2 x ArCH), 128.9 (4 x ArCH, dd, *J*_{CP} 12.4, 4.1), 128.9 (2 x ArCH), 128.3 (2 x ArCH), 92.9 (ArCl), 69.6 (C_{quat}, d, *J*_{CP} 5.5), 38.7 (CH₂, d, *J*_{CP} 72.7), 36.9 (CH₃), 27.3 (CH₃). **³¹P NMR (162 MHz, CDCl₃)** δ 25.0 (1 P, br. t, *J* 11.2, PO). **HRMS *m/z* (ESI⁺)** *m/z* calcd for C₂₉H₂₆Cl₃IN₂O₂P⁺ [M+H]⁺ 696.9837; found 696.9803.

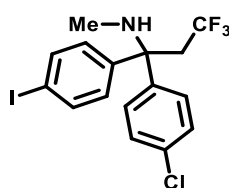
1-(4-Bromophenyl)-1-(3,4-dichlorophenyl)-3,3,3-trifluoro-*N*-methylpropan-1-amine (326)



Formation of the title compound was carried out by following GP4 with 1-(1-(4-bromophenyl)-1-(3,4-dichlorophenyl)-3,3,3-trifluoropropyl)-1,3-dimethylurea (**262**) (75 mg, 0.16 mmol) used as starting material. The reaction gave the title compound (51 mg, 77%) as a colourless oil.

IR (film, cm^{-1}) ν_{max} = 2925, 1257, 1115. **^1H NMR (400 MHz, CDCl_3)** δ 7.46 (1 H, d, J 2.2, ArCH), 7.44 (2 H, d, J 8.6, 2 x ArCH), 7.36 (1 H, d, J 8.5, ArCH), 7.18 (2 H, d, J 8.6, 2 x ArCH), 7.11 (1 H, dd, J 8.5, 2.2, ArCH), 3.14 (2 H, qd, J 10.7, 1.8, CH_2), 2.16 (3 H, s, CH_3), 1.82 (1 H, br. s, NH). **^{13}C NMR (101 MHz, CDCl_3)** δ 145.2 (C_{quat}), 143.2 (C_{quat}), 132.6 (ArCCl), 131.6 (2 x ArCH), 131.3 (ArCCl), 130.3 (ArCH), 128.7 (ArCH), 128.4 (2 x ArCH), 126.3 (ArCH), 125.8 (CF_3 , q, J_{CF} 279.0), 121.4 (ArCBr), 62.3 (C_{quat} , q, J_{CF} 1.8), 38.4 (CH_2 , q, J_{CF} 25.5), 26.3 (NCH_3). **^{19}F NMR (377 MHz, CDCl_3)** δ -59.0 (3 F, t, J 10.7, CF_3). **HRMS m/z (ESI $^+$)** m/z calcd for $\text{C}_{16}\text{H}_{14}\text{NCl}_2\text{BrF}_3^+$ $[\text{M}+\text{H}]^+$ 425.9633; found 425.9626.

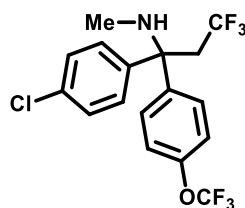
1-(4-Chlorophenyl)-3,3,3-trifluoro-1-(4-iodophenyl)-*N*-methylpropan-1-amine (327)



Formation of the title compound was carried out by following GP4 with 1-(1-(4-chlorophenyl)-3,3,3-trifluoro-1-(4-iodophenyl)propyl)-1,3-dimethylurea (**266**) (49 mg, 0.1 mmol) used as starting material. The reaction gave the title compound (32 mg, 74%) as a colourless oil.

IR (film, cm^{-1}) ν_{max} = 2955, 1259, 1004, 807. **^1H NMR (400 MHz, CDCl_3)** δ 7.62 (2 H, d, J 8.7, 2 x ArCH), 7.27 (2 H, d, J 9.0, 2 x ArCH), 7.23 (2 H, d, J 9.0, 2 x ArCH), 7.05 (2 H, d, J 8.7, 2 x ArCH), 3.15 (2 H, q, J 10.3, CH_2), 2.15 (3 H, s, NCH_3), 1.83 (1 H, br. s, NH). **^{13}C NMR (101 MHz, CDCl_3)** δ 144.8 (C_{quat}), 143.3 (C_{quat}), 137.6 (2 x ArCH), 133.1 (ArCCl), 128.9 (2 x ArCH), 128.6 (2 x ArCH), 128.3 (2 x ArCH), 126.1 (CF_3 , q, J_{CF} 278.6), 92.9 (ArCI), 62.6 (C_{quat} , q, J_{CF} 1.7), 38.7 (CH_2 , q, J_{CF} 25.3), 29.4 (NCH_3). **^{19}F NMR (377 MHz, CDCl_3)** δ -59.0 (3 F, t, J 10.3, CF_3). **HRMS m/z (ESI $^+$)** m/z calcd for $\text{C}_{16}\text{H}_{15}\text{NClIF}_3^+$ $[\text{M}+\text{H}]^+$ 439.9884; found 439.9871.

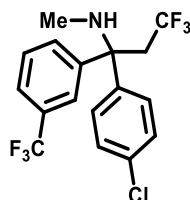
1-(4-Chlorophenyl)-3,3,3-trifluoro-N-methyl-1-(4-(trifluoromethoxy)phenyl)propan-1-amine (328)



Formation of the title compound was carried out by following GP4 with 1-(1-(4-chlorophenyl)-3,3,3-trifluoro-1-(4-(trifluoromethoxy)phenyl)propyl)-1,3-dimethylurea (**261**) (34 mg, 0.08 mmol) used as starting material. The reaction gave the title compound (17 mg, 57%) as a colourless oil.

IR (film, cm⁻¹) ν_{\max} = 3049, 1255, 1211, 1109. **¹H NMR (400 MHz, CDCl₃)** δ 7.33 (2 H, d, *J* 8.9, 2 x ArCH), 7.28 (2 H, d, *J* 9.0, 2 x ArCH), 7.25 (2 H, d, *J* 9.0, 2 x ArCH), 7.14 (2 H, dq, *J* 8.9, 1.0, 2 x ArCH), 3.17 (2 H, q, *J* 10.2, CH₂), 2.16 (3 H, s, NCH₃), 1.88 (1 H, br. s, NH). **¹³C NMR (126 MHz, CDCl₃)** δ 148.2 (C_{quat}), 143.5 (C_{quat}), 143.4 (C_{quat}), 133.2 (ArCCl), 128.7 (2 x ArCH), 128.4 (2 x ArCH), 128.3 (2 x ArCH), 126.0 (CF₃, q, *J*_{CF} 278.3), 120.7 (2 x ArCH), 120.6 (OCF₃, q, *J*_{CF} 257.8), 62.5 (C_{quat}), 38.9 (CH₂, q, *J*_{CF} 25.5), 29.4 (NCH₃). **¹⁹F NMR (377 MHz, CDCl₃)** δ -57.9 (3 F, s, OCF₃), -59.1 (3 F, t, *J* 10.2, CF₃). **HRMS *m/z* (ESI⁺)** *m/z* calcd for C₁₇H₁₅NOCIF₆⁺ [M+H]⁺ 398.0741; found 398.0727; *m/z* calcd for C₁₆H₁₀OCIF₆⁺ [M-NHMe]⁺ 367.0319; found 367.0312. Note - Major mass ion observed is for MeNH loss product.

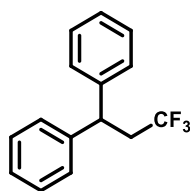
1-(4-Chlorophenyl)-3,3,3-trifluoro-N-methyl-1-(3-(trifluoromethyl)phenyl)propan-1-amine (329)



Formation of the title compound was carried out by following GP4 with 1-(1-(4-chlorophenyl)-3,3,3-trifluoro-1-(3-(trifluoromethyl)phenyl)propyl)-1,3-dimethylurea (**265**) (31 mg, 0.07 mmol) used as starting material. The reaction gave the title compound (21 mg, 79%) as a colourless oil.

IR (film, cm⁻¹) ν_{\max} = 2955, 1328, 1121, 1075. **¹H NMR (400 MHz, CDCl₃)** δ 7.65 (1 H, br. s, ArCH), 7.50 (1 H, br. d, *J* 7.3, ArCH), 7.46 (1 H, td, *J* 8.1, 1.6, ArCH), 7.41 (1 H, dd, *J* 8.1, 7.3, ArCH), 7.29 (2 H, d, *J* 9.0, 2 x ArCH), 7.25 (2 H, d, *J* 9.0, 2 x ArCH), 3.21 (2 H, qd, *J* 10.9, 1.6, CH₂), 2.17 (3 H, s, NCH₃), 1.90 (1 H, br. s, NH). **¹³C NMR (101 MHz, CDCl₃)** δ 146.1 (C_{quat}), 143.0 (C_{quat}), 133.3 (ArCCl), 130.9 (C_{quat}, q, *J*_{CF} 32.3), 130.5 (ArCH), 129.0 (ArCH), 128.8 (2 x ArCH), 128.3 (2 x ArCH), 126.0 (CF₃, q, *J*_{CF} 278.9), 124.2 (ArCCF₃, q, *J*_{CF} 272.2), 124.2 (ArCH, q, *J*_{CF} 3.8), 123.3 (ArCH, q, *J*_{CF} 3.8), 62.8 (C_{quat}, q, *J*_{CF} 1.7), 38.8 (CH₂, q, *J*_{CF} 25.4), 29.4 (NCH₃). **¹⁹F NMR (377 MHz, CDCl₃)** δ -59.1 (3 F, t, *J* 10.9, CF₃), -62.5 (3 F, s, ArCF₃). **HRMS *m/z* (ESI⁺)** *m/z* calcd for C₁₇H₁₅NCIF₆⁺ [M+H]⁺ 382.0792; found 382.0783.

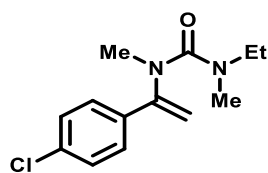
(3,3,3-Trifluoropropane-1,1-diyl)dibenzene (338)



Following GP2 with 1-(4-bromophenyl)-3-(1-(4-chlorophenyl)vinyl)-1,3-dimethylurea (**221**) (76 mg, 0.2 mmol), sodium trifluoromethanesulfinate (**134**) (47 mg, 1.5 eq., 0.3 mmol) and ethene-1,1-diyl dibenzene (**135**) (53 μ L, 1.5 eq., 0.3 mmol) used as starting materials and acetonitrile used as solvent. The reaction mixture was stirred for 15 hours. The obtained crude material was analysed by ^{19}F NMR and yields were calculated by use of α,α,α -trifluorotoluene as an internal standard (0.2 mmol), indicating the presence of 1-(1-(4-bromophenyl)-1-(4-chlorophenyl)-3,3,3-trifluoropropyl)-1,3-dimethylurea (**234**) (6%) and (3,3,3-trifluoropropane-1,1-diyl)dibenzene (**338**) (17%). Isolation of the title compounds was attempted by flash column chromatography (SiO_2 , 0% to 1% Et_2O in *n*-pentane), but could not be separated from ethene-1,1-diyl dibenzene (**135**).

^1H NMR (400 MHz, CDCl_3) δ 7.29-7.19 (10 H, m, 10 x ArCH), 4.32 (1 H, t, J 7.4, CH), 2.89 (2 H, qd, J , 10.4, 7.4, CH_2). ^{19}F NMR (377 MHz, CDCl_3) δ -63.5 (3 F, t, J 10.4, CF_3). Data in good agreement with literature.²⁶⁶

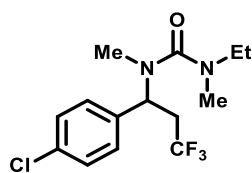
1-(1-(4-Chlorophenyl)vinyl)-3-ethyl-1,3-dimethylurea (339)



Formation of the title compound was carried out by following GP1 with 1-(4-chlorophenyl)ethan-1-one (**208**) (1.30 mL, 1.54 g, 10.0 mmol) and ethyl isocyanate (12.0 mL, 10.7 g, 151 mmol) used as starting materials. The imine intermediate was stirred with the requisite alkyl isocyanate for 28 hours. The excess ethyl isocyanate was removed under reduced pressure and the received crude material was purified by flash column chromatography (SiO₂, 0% to 30% acetone in 40-60 petroleum ether) yielding crude material (1.43 g) as a yellow oil. Subsequent methylation with methyl iodide was carried out on a 6.0 mmol scale (by making as if the received crude material was pure) and was stirred for 20 hours. The resulting crude material was purified by flash column chromatography (SiO₂, 0% to 30% acetone in 40-60 petroleum ether) yielding the title compound (638 mg, 27% over three steps) as a colourless oil.

IR (film, cm⁻¹) ν_{\max} = 2970, 1650, 1487, 1307. **¹H NMR (400 MHz, CDCl₃)** δ 7.43-7.39 (2 H, m, 2 x ArCH), 7.33-7.30 (2 H, m, 2 x ArCH), 5.10 (1 H, d, *J* 0.8, CH_aH_b), 4.79 (1 H, d, *J* 0.8, CH_aH_b), 3.20 (2 H, q, *J* 7.1, CH₂), 2.97 (3 H, s, NCH₃), 2.72 (3 H, s, NCH₃), 0.97 (3 H, t, *J* 7.1, CH₃). **¹³C NMR (101 MHz, CDCl₃)** δ 161.6 (CO), 150.1 (C_{quat}), 136.2 (C_{quat}), 134.5 (ArCCl), 128.8 (2 x ArCH), 127.6 (2 x ArCH), 104.0 (CH₂), 44.3 (NCH₂), 38.0 (NCH₃), 35.0 (NCH₃), 12.3 (CH₃). **HRMS *m/z* (ESI⁺)** *m/z* calcd for C₁₃H₁₈N₂OCl⁺ [M+H]⁺ 253.1102; found 253.1107.

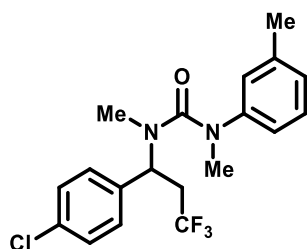
1-(1-(4-Chlorophenyl)-3,3,3-trifluoropropyl)-3-ethyl-1,3-dimethylurea (340)



Formation of the title compound was carried out by following GP2 with 1-(1-(4-chlorophenyl)vinyl)-3-ethyl-1,3-dimethylurea (**339**) (25 mg, 0.1 mmol) and sodium trifluoromethanesulfinate (**134**) (31 mg, 2.0 eq., 0.2 mmol) used as starting materials and acetonitrile used as solvent. The reaction mixture was stirred for 16 hours to give the title compound (25 mg, 76%) as a yellow oil.

IR (film, cm⁻¹) ν_{\max} = 2974, 1634, 1493, 1386, 1122. **¹H NMR (400 MHz, CDCl₃)** δ 7.30-7.36 (2 H, m, 2 x ArCH), 7.34-7.30 (2 H, m, 2 x ArCH), 5.43 (1 H, dd, J 9.9, 5.0, CH), 3.28-3.10 (2 H, m, NCH₂), 2.99-2.83 (1 H, m, CH_aH_b), 2.77 (3 H, s, CH₃), 2.71-2.64 (1 H, m, CH_aH_b), 2.63 (3 H, s, CH₃), 1.14 (3 H, t, J 7.1, CH₃). **¹³C NMR (101 MHz, CDCl₃)** δ 164.7 (CO), 137.2 (C_{quat}), 133.9 (C_{quat}), 129.5 (2 x ArCH), 128.8 (2 x ArCH), 126.3 (CF₃, q, J_{CF} 272.9), 53.7 (CH, q, J_{CF} 3.3), 45.1 (NCH₂), 35.5 (NCH₃), 34.9 (CH₂, q, J_{CF} 27.6), 32.9 (NCH₃), 12.8 (CH₃). **¹⁹F NMR (377 MHz, CDCl₃)** δ -63.9 (3 F, t, J 10.3, CF₃). **HRMS m/z (ESI⁺)** m/z calcd for C₁₄H₁₉N₂OF₃Cl⁺ [M+H]⁺ 323.1133; found 323.1131.

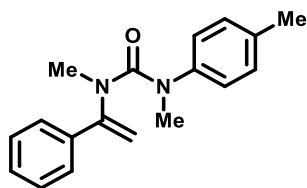
1-(1-(4-Chlorophenyl)-3,3,3-trifluoropropyl)-3-ethyl-1,3-dimethylurea (341)



Formation of the title compound was carried out by following GP2 with 1-(1-(4-chlorophenyl)vinyl)-1,3-dimethyl-3-(*m*-tolyl)urea (**223**) (32 mg, 0.1 mmol), sodium trifluoromethanesulfinate (**134**) (31 mg, 2.0 eq., 0.2 mmol) and water (18 mg, 10 eq., 1.0 mmol) used as starting materials and acetone used as solvent. The reaction mixture was stirred for 16 hours to give the title compound (23 mg, 61%) as a yellow oil.

IR (film, cm⁻¹) ν_{\max} = 2931, 1639, 1493, 1333, 1122. **¹H NMR (400 MHz, CDCl₃)** δ 7.33-7.29 (2 H, m, 2 x ArCH), 7.28-7.24 (2 H, m, 2 x ArCH), 7.18 (1 H, t, J 7.8, ArCH), 6.93 (1 H, br. d, J 7.8, ArCH), 6.84 (1 H, br. d, J 7.8, ArCH), 6.80 (1 H, br. s, ArCH), 5.68 (1 H, dd, J 8.8, 3.3, CH), 3.19 (3 H, s, CH₃), 2.83-2.93 (2 H, m, CH₂), 2.29 (3 H, s, CH₃), 2.26 (3 H, s, ArCCH₃). **¹³C NMR (101 MHz, CDCl₃)** δ 161.8 (CO), 146.3 (C_{quat}), 139.6 (ArCCH₃), 136.8 (C_{quat}), 134.0 (ArCCl), 129.5 (ArCH), 129.3 (2 x ArCH), 128.8 (2 x ArCH), 126.1 (CF₃, q, J_{CF} 278.9), 126.0 (ArCH), 125.6 (ArCH), 122.0 (ArCH), 53.5 (CH, q, J_{CF} 3.9), 40.7 (NCH₃), 34.8 (CH₂, q, J_{CF} 28.2), 32.3 (NCH₃), 21.3 (ArCCH₃). **¹⁹F NMR (377 MHz, CDCl₃)** δ -63.7 (3 F, t, J 10.4, CF₃). **HRMS m/z (ESI⁺)** m/z calcd for C₁₉H₂₁N₂OF₃Cl⁺ [M+H]⁺ 385.1289; found 385.1307.

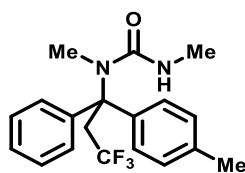
1,3-Dimethyl-1-(1-phenylvinyl)-3-(*p*-tolyl)urea (**344**)



Formation of the title compound was carried out by following GP1 with acetophenone (**81**) (1.16 mL, 1.20 g, 10.0 mmol) and 1-isocyanato-4-methylbenzene (**343**) (1.26 mL, 1.33 g, 10.0 mmol) used as starting materials. The imine intermediate was stirred with the requisite aryl isocyanate for 69 hours, subsequent methylation with methyl iodide was stirred for 23 hours. The resulting crude material was purified by flash column chromatography (SiO₂, 1% to 20% acetone + 3% trimethylamine in 40-60 petroleum ether) yielding the title compound (587 mg, 21%) as a pale-yellow solid.

M.p. 61-63 °C (Et₂O). **IR (film, cm⁻¹)** ν_{max} = 2924, 1656, 1613, 1513, 1353. **¹H NMR (400 MHz, CDCl₃)** δ 7.28-7.23 (3 H, m, ArCH + 2 x ArCH), 7.15-7.10 (2 H, m, 2 x ArCH), 6.99 (2 H, d, *J* 8.7, 2 x ArCH), 6.69 (2 H, d, *J* 8.7, 2 x ArCH), 4.86 (1 H, d, *J* 0.5, CH_aCH_b), 4.60 (1 H, d, *J* 0.5, CH_aCH_b), 3.20 (3 H, s, NCH₃), 2.97 (3 H, s, NCH₃), 2.27 (3 H, s, ArCCH₃). **¹³C NMR (101 MHz, CDCl₃)** δ 161.0 (CO), 150.4 (C_{quat}), 142.5 (C_{quat}), 138.3 (C_{quat}), 134.6 (C_{quat}), 129.3 (2 x ArCH), 128.3 (ArCH), 128.1 (2 x ArCH), 126.0 (2 x ArCH), 125.4 (2 x ArCH), 106.9 (CH₂), 39.4 (NCH₃), 38.8 (NCH₃), 21.0 (ArCCH₃). **HRMS *m/z* (ESI⁺)** *m/z* calcd for C₁₈H₂₁N₂O⁺ [M+H]⁺ 281.1648; found 281.1644.

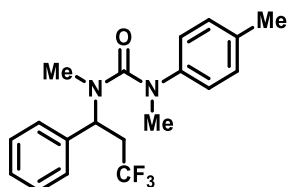
1,3-Dimethyl-1-(3,3,3-trifluoro-1-phenyl-1-(*p*-tolyl)propyl)urea (**345**)



Formation of the title compound was carried out by following GP2 with 1,3-dimethyl-1-(1-phenylvinyl)-3-(*p*-tolyl)urea (**344**) (56 mg, 0.2 mmol) and sodium trifluoromethanesulfinate (**134**) (62 mg, 2.0 eq., 0.4 mmol) used as starting materials and DMF used as solvent. The reaction mixture was stirred for 14 hours and purified by flash column chromatography (SiO₂, 0% to 20% acetone in *n*-pentane) to give the title compound (46 mg, 66%) as a pale-yellow solid.

M.p. 116-120 °C (Et₂O). **IR (film, cm⁻¹)** ν_{\max} = 3369, 2951, 1640, 1529, 1259, 1107. **¹H NMR (400 MHz, CDCl₃)** δ 7.29 (2 H, d, *J* 7.7, 2 x ArCH), 7.26-7.22 (2 H, m, 2 x ArCH), 7.19 (2 H, d, *J* 8.2, 2 x ArCH), 7.14 (1 H, br. t, *J* 7.1, ArCH), 7.06 (2 H, d, *J* 8.2, 2 x ArCH), 4.54 (1 H, br. q, *J* 4.6, NH), 3.94 (1 H, q, *J* 10.9, CH_aH_b), 3.94 (1 H, q, *J* 10.9, CH_aH_b), 2.81 (3 H, s, NCH₃), 2.78 (3 H, d, *J* 4.6, CH₃), 2.26 (3 H, s, ArCCH₃). **¹³C NMR (101 MHz, CDCl₃)** δ 159.7 (CO), 144.8 (C_{quat}), 141.3 (C_{quat}), 136.4 (C_{quat}), 129.0 (2 x ArCH), 128.3 (2 x ArCH), 126.7 (ArCH), 126.7 (2 x ArCH), 126.5 (CF₃, q, *J*_{CF} 279.4), 126.4 (2 x ArCH), 68.2 (C_{quat}, q, *J*_{CF} 1.8), 38.9 (CH₂, q, *J*_{CF} 26.9), 36.5 (NCH₃, q, *J*_{CF} 1.9), 27.7 (NCH₃), 21.0 (ArCCH₃). **¹⁹F NMR (377 MHz, CDCl₃)** δ -58.3 (3 F, t, *J* 10.9, CF₃). **HRMS *m/z* (ESI⁺)** *m/z* calcd for C₁₉H₂₂N₂OF₃⁺ [M+H]⁺ 351.1679; found 351.1675.

1,3-Dimethyl-1-(*p*-tolyl)-3-(3,3,3-trifluoro-1-phenylpropyl)urea (**346**)

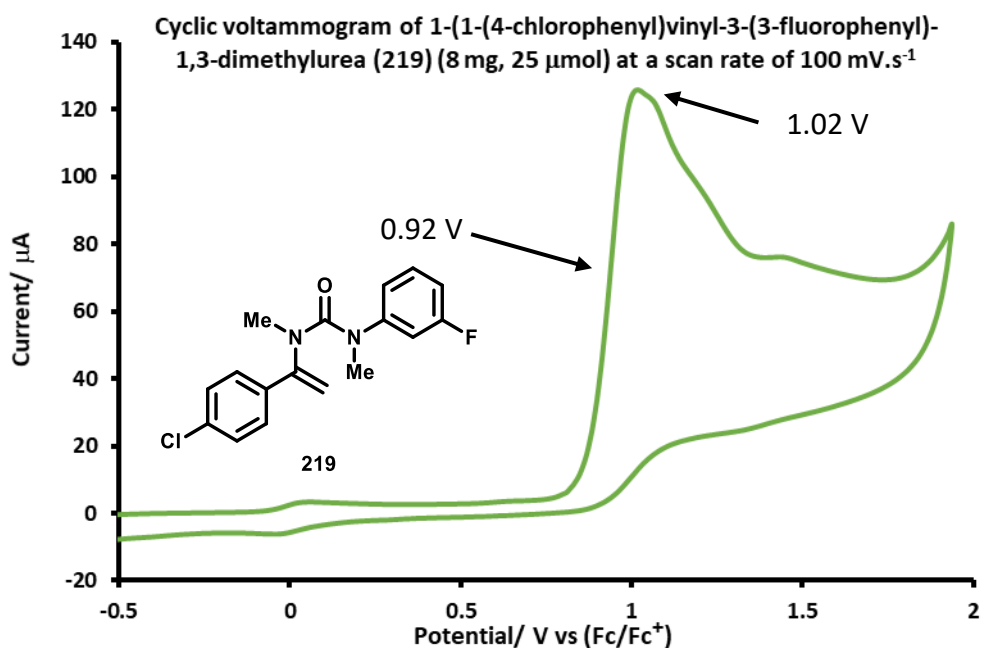
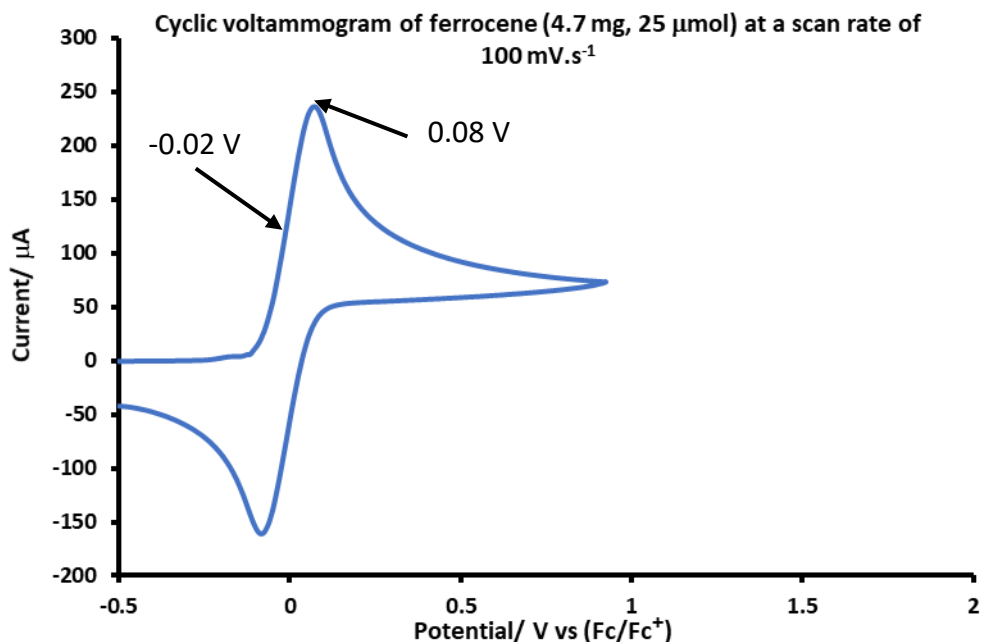


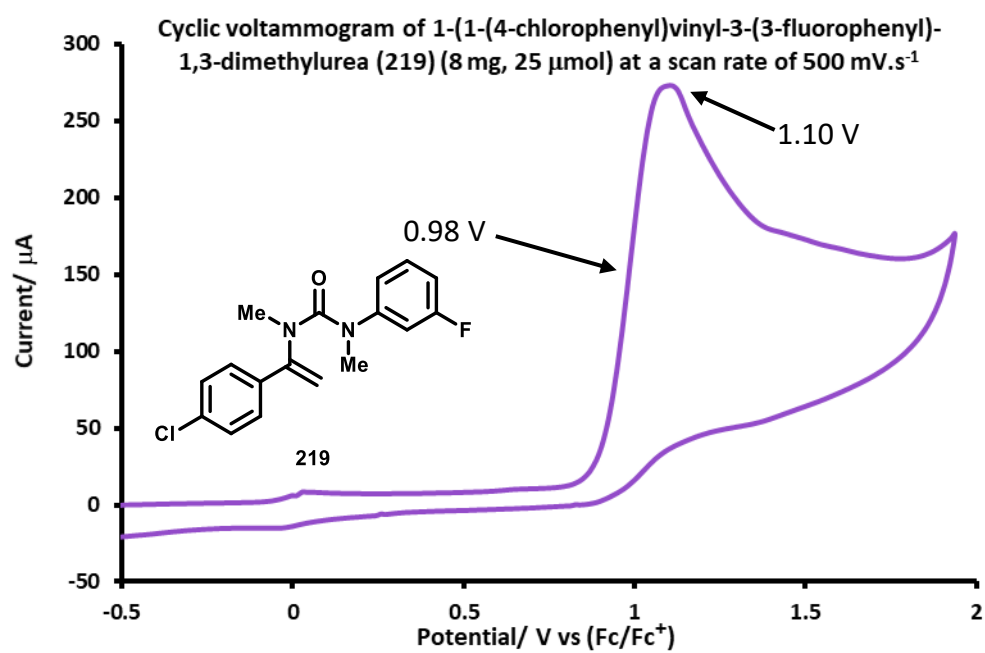
Formation of the title compound was carried out by following GP2 with 1,3-dimethyl-1-(1-phenylvinyl)-3-(*p*-tolyl)urea (**344**) (56 mg, 0.2 mmol) and sodium trifluoromethanesulfinate (**134**) (62 mg, 2.0 eq., 0.4 mmol) used as starting materials and acetone used as solvent. The reaction mixture was stirred for 16 hours to give the title compound (43 mg, 62%) as a yellow oil.

IR (film, cm⁻¹) ν_{\max} = 2925, 1641, 1335, 1123, 1348. **¹H NMR (400 MHz, CDCl₃)** δ 7.36-7.26 (5 H, m, 2 x ArCH + 2 x ArCH + ArCH), 7.08 (2 H, dd, *J* 8.6, 0.7, 2 x ArCH), 6.92 (2 H, d, *J* 8.4, 2 x ArCH), 5.75 (1 H, dd, *J* 8.5, 5.9, CH), 3.19 (3 H, s, NCH₃), 2.85-2.64 (2 H, m, CH₂), 2.30 (3 H, s, ArCCH₃), 2.30 (3 H, s, NCH₃). **¹³C NMR (101 MHz, CDCl₃)** δ 161.9 (CO), 144.0 (C_{quat}), 138.3 (C_{quat}), 135.0 (C_{quat}), 130.2 (2 x ArCH), 128.6 (2 x ArCH), 128.0 (ArCH), 127.8 (2 x ArCH), 126.3 (CF₃, q, *J*_{CF} 277.7), 124.9 (2 x ArCH), 54.0 (CH), 40.8 (NCH₃), 34.7 (CH₂, q, *J*_{CF} 28.0), 32.3 (NCH₃), 21.0 (ArCCH₃). **¹⁹F NMR (377 MHz, CDCl₃)** δ -63.6 (3 F, t, *J* 10.3, CF₃). **HRMS *m/z* (ESI⁺)** *m/z* calcd for C₁₉H₂₂N₂OF₃⁺ [M+H]⁺ 351.1679; found 351.1675.

8.2.3 Cyclic Voltammetry Data

Analyte was added to a 0.1 M solution of tetra-*n*-butylammonium hexafluorophosphate in dry, degassed acetonitrile (5 mL). A glassy carbon working electrode, a silver wire counter electrode and a Ag/AgNO₃ reference electrode were used. A scan rate of 100 or 500 mV.s⁻¹ was applied.



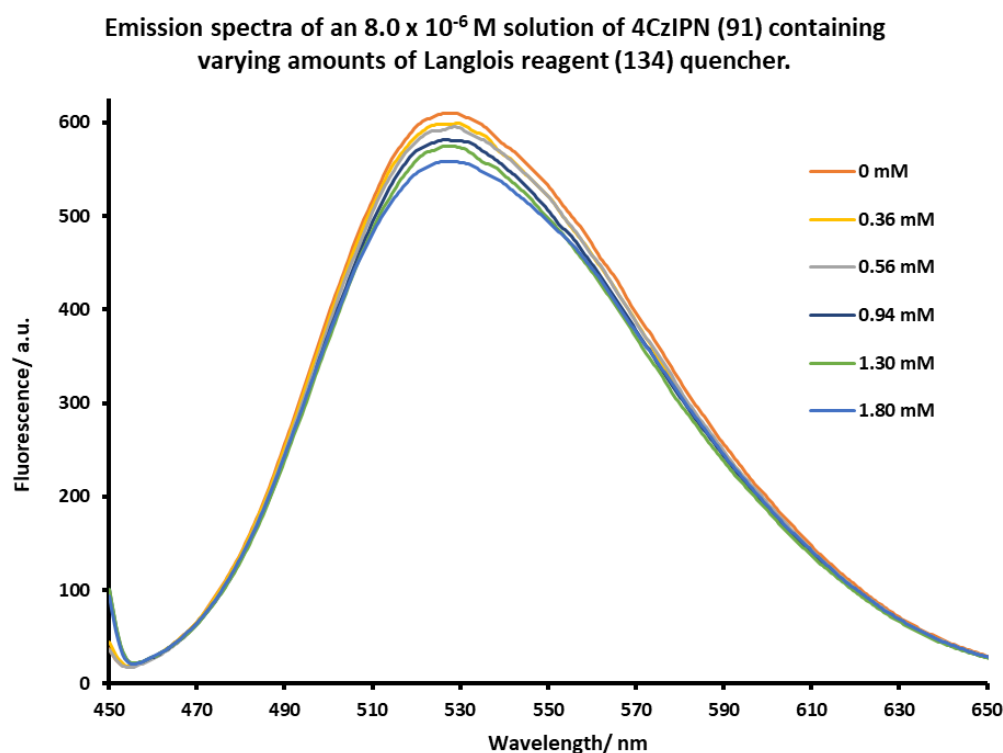


8.2.4 Stern-Volmer Fluorescence Quenching Studies

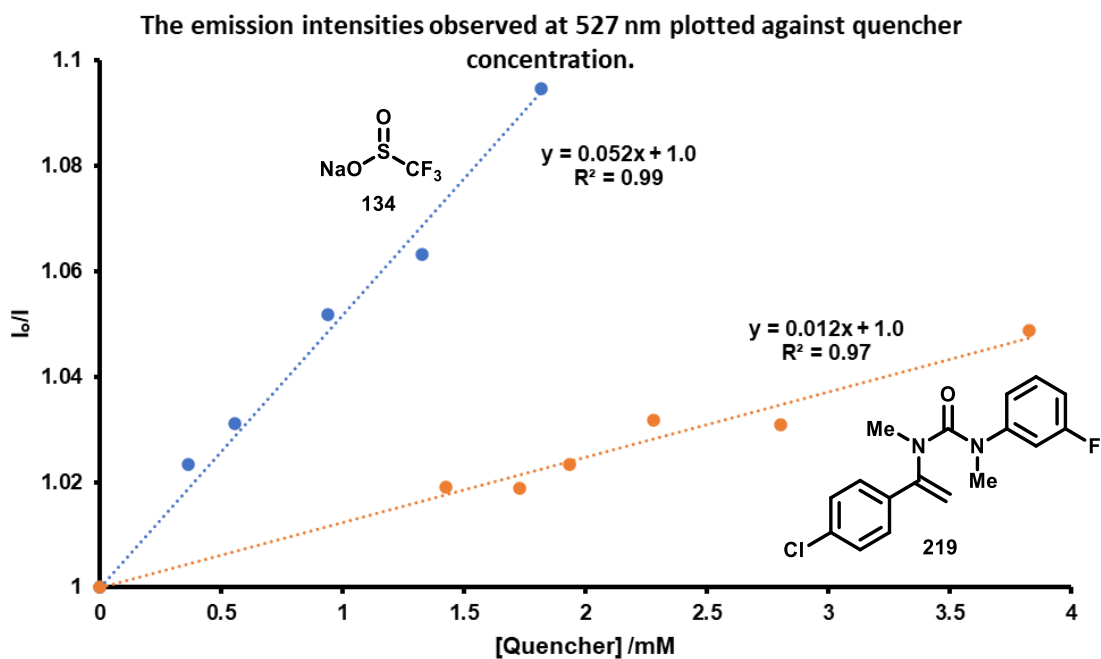
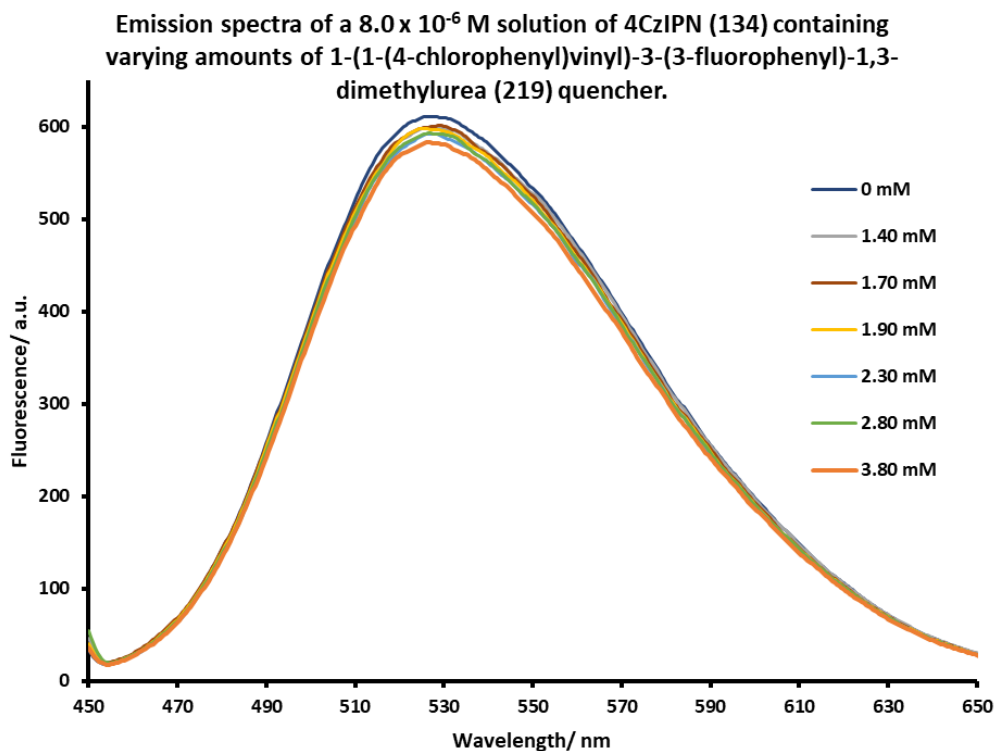
Samples for quenching experiments were prepared in a rubber septum sealed 4 mL quartz cuvette (path length: $l = 1.0$ cm) under an atmosphere of nitrogen. Using fluorometry solutions of 4CzIPN (**91**) in anhydrous and degassed acetonitrile were irradiated at 435 nm and the emission spectrum was recorded. The fluorescence intensities at 527 nm of the collected emission spectra were plotted against quencher concentration.

8.2.4.1 Study at Low Quencher Concentration

An 8.0×10^{-6} M solution of 4CzIPN (**91**) in anhydrous and degassed acetonitrile was prepared. A 4 mL quartz cuvette (path length: $l = 1.0$ cm) was charged with a known amount of Langlois reagent (**134**), sealed with a rubber septum, flushed with nitrogen three times and finally charged with 3.0 mL of the 4CzIPN (**91**) solution, then an emission spectrum was recorded.

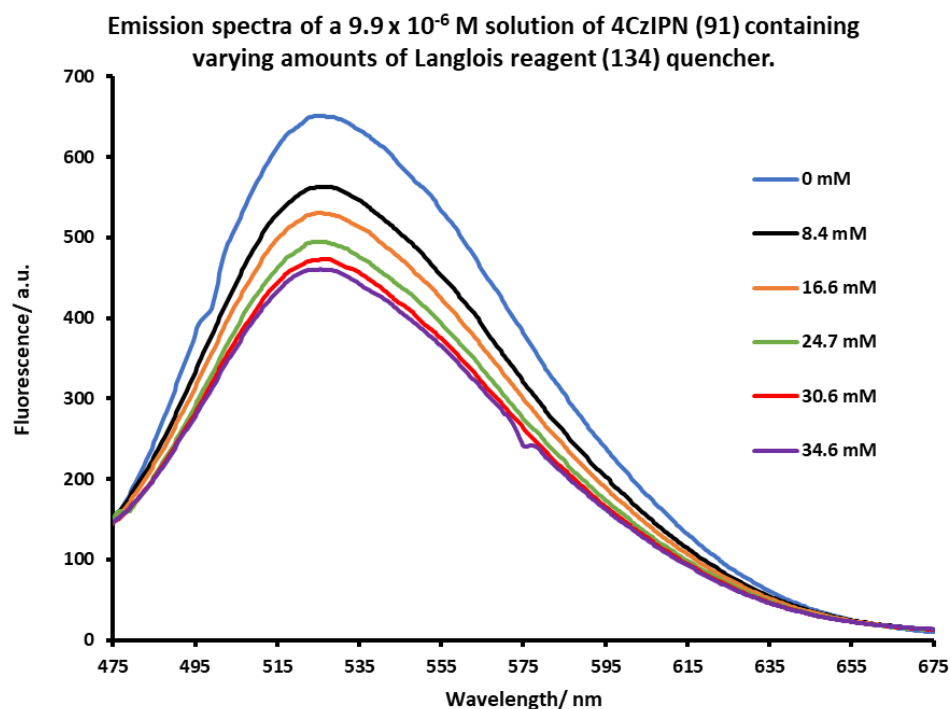


An 8.0×10^{-6} M solution of 4CzIPN (**91**) in anhydrous and degassed acetonitrile was prepared. A 4 mL quartz cuvette (path length: $l = 1.0$ cm) was charged with a known amount of 1-(1-(4-chlorophenyl)vinyl)-3-(3-fluorophenyl)-1,3-dimethylurea (**219**), sealed with a rubber septum, flushed with nitrogen three times and finally charged with 3.0 mL of the 4CzIPN (**91**) solution. An emission spectrum was then recorded.

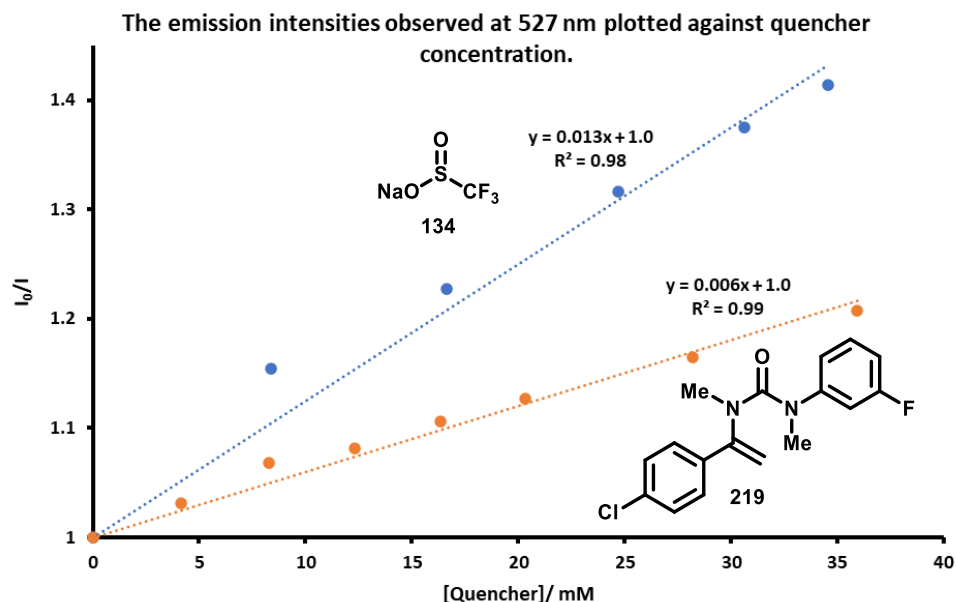
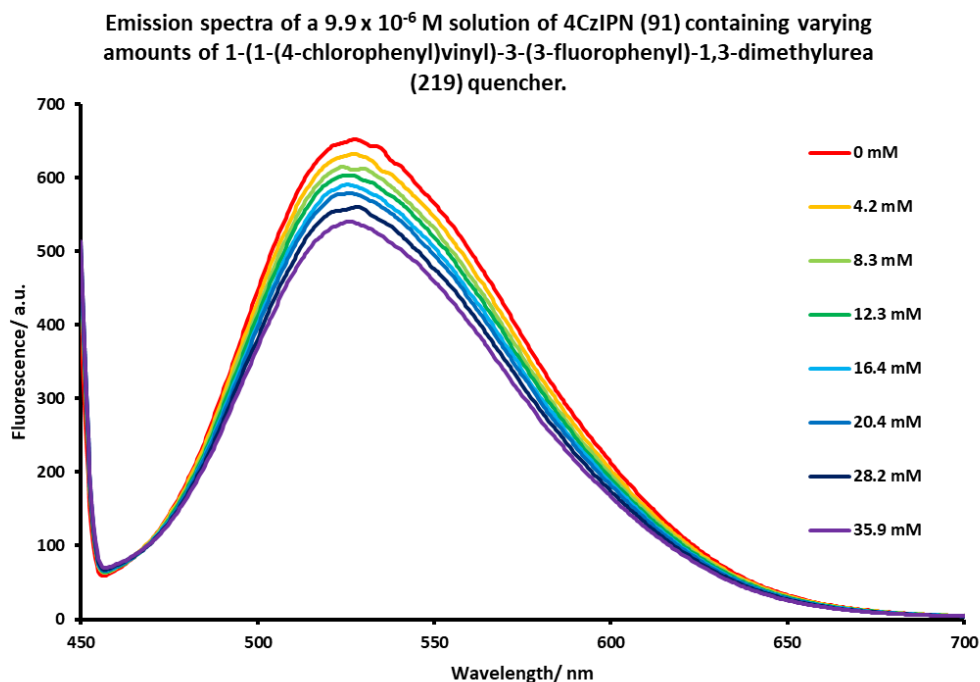


8.2.4.2 Study at High Quencher Concentration

A 9.9×10^{-6} M solution of 4CzIPN (**91**) in anhydrous and degassed acetonitrile was prepared and 2.0 mL were transferred to a 4 mL quartz cuvette (path length: $l = 1.0$ cm) under an atmosphere of nitrogen. A 0.85 M solution of Langlois reagent (**134**) in anhydrous and degassed acetonitrile was prepared under an atmosphere of nitrogen. Aliquots of the Langlois reagent (**134**) solution were added to the solution of 4CzIPN (**91**) contained in the quartz cuvette (path length: $l = 1.0$ cm) under an atmosphere of nitrogen, emission spectra were then recorded.



A 9.9×10^{-6} M solution of 4CzIPN (**91**) in anhydrous and degassed acetonitrile was prepared and 2.0 mL were transferred to a 4 mL quartz cuvette (path length: $l = 1.0$ cm) under an atmosphere of nitrogen. A 0.83 M solution of 1-(1-(4-chlorophenyl)vinyl)-3-(3-fluorophenyl)-1,3-dimethylurea (**219**) in anhydrous and degassed acetonitrile was prepared under an atmosphere of nitrogen. Aliquots of the vinyl urea **219** solution were added to the solution of 4CzIPN (**91**) contained in the quartz cuvette (path length: $l = 1.0$ cm) under an atmosphere of nitrogen, an emission spectrum was then recorded.



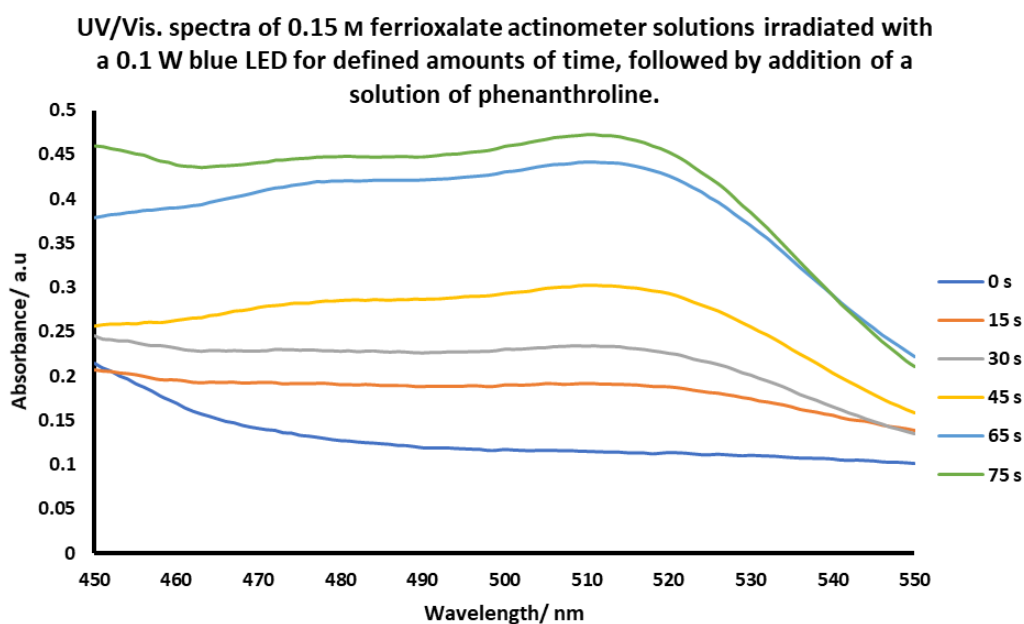
8.2.5 Quantum Yield Elucidation

The quantum yield was measured for the reaction between 1-(1-(4-chlorophenyl)vinyl)-3-(3-fluorophenyl)-1,3-dimethylurea (**219**) (64 mg, 0.2 mmol), sodium trifluoromethanesulfinate (**134**) (46 mg, 1.5 eq., 0.3 mmol), 4CzIPN (**91**) (8 mg, 5 mol%, 10 μ mol) and caesium carbonate (98 mg, 1.5 eq., 0.3 mmol) in DMF. The reaction was performed in a quartz cuvette (path length: $l = 1.0$ cm) positioned 5 cm away from a single 0.1 W blue LED.

Under optimal conditions acetonitrile would be used as solvent, however this provides a heterogeneous reaction mixture reaction soon after irradiation (ca. 30 mins). Heterogeneity will have an impact on light penetration and potentially affect the accuracy of the quantum yield measurements. Therefore, to obtain a more accurate measurement the reaction was performed in DMF, which greatly improved reaction homogeneity and still gave productive formation of α -tertiary urea (**232**) (54 mg, 70%) by following GP2 over 18 hours.

Determination of the Photon Flux:

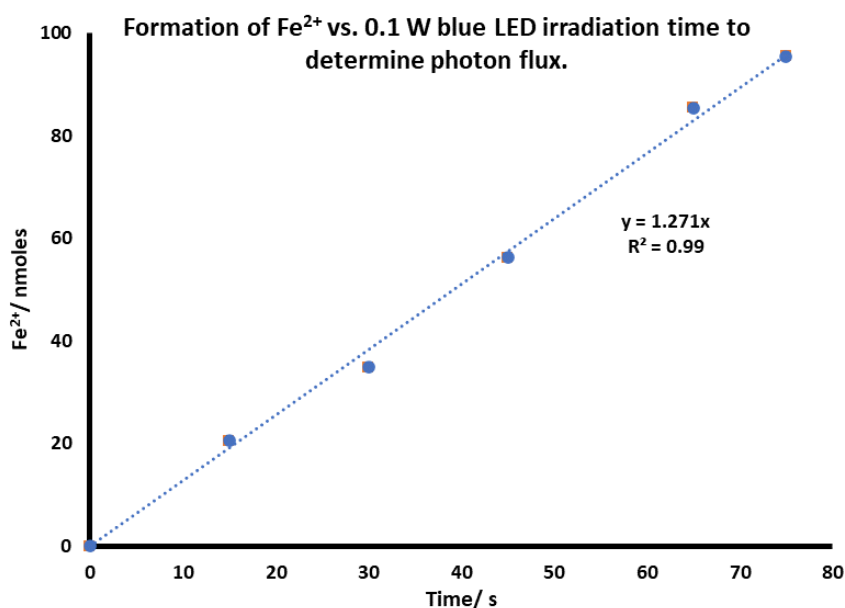
The photon flux of a 0.1 W blue LED setup was determined using standard ferrioxalate actinometry.¹⁸⁰ A 0.15 M ferrioxalate solution was prepared by dissolving 2.21 g of potassium ferrioxalate trihydrate in 30 mL of 0.05 M $\text{H}_2\text{SO}_{4(\text{aq})}$. A buffered 5.5 mM phenanthroline solution was prepared by dissolving 50 mg of 1,10-phenanthroline, 11.25 g of $\text{NaOAc} \cdot 3\text{H}_2\text{O}$ in 50 mL of 0.5 M aq. H_2SO_4 . Both solutions were stored in the dark. Whilst working under low light, 2.0 mL of the 0.15 M ferrioxalate solution was added to a quartz cuvette ($l = 1.0$ cm). The cuvette was placed 5 cm from a single 0.1 W blue LED and irradiated for a specific time (between 15 and 75 seconds). After irradiation, 1.0 mL of the phenanthroline solution was added to the cuvette. The mixture was left to stand for approximately 30 minutes before the absorbance at $\lambda = 510$ nm was measured by UV/Vis. spectroscopy. The absorbance of a non-irradiated sample was also measured. Spectra were zeroed with respect to the 0.15 M ferrioxalate actinometer solution.



The moles of Fe^{2+} formed were calculated using:

$$\text{mol Fe}^{2+} = \frac{V \times \Delta A}{l \times \varepsilon}$$

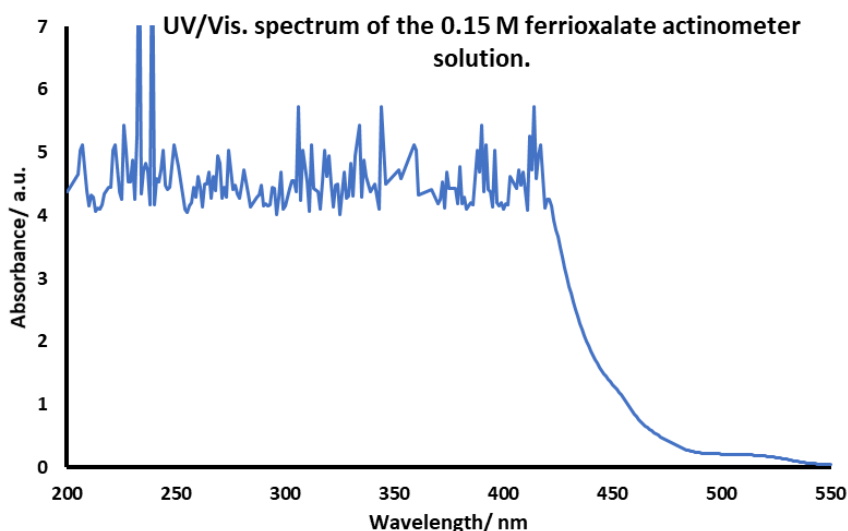
Where V is the total volume of the solution after the addition of 1,10-phenanthroline (0.0030 L), ΔA is the difference in absorbance at $\lambda = 510 \text{ nm}$ between the irradiated and non-irradiated ferrioxalate solutions, l is the optical path length of the irradiation cell (1.0 cm), and ε is the molar absorptivity of the $[\text{Fe}(\text{phen})_3]^{2+}$ complex at $\lambda = 510 \text{ nm}$ ($11,100 \text{ L}\cdot\text{mol}^{-1}\cdot\text{cm}^{-1}$).²⁶⁷



The photon flux was calculated using:

$$\text{Photon Flux} = \frac{\text{mol Fe}^{2+}}{\Phi \times t \times f}$$

Where Φ is the quantum yield of the ferrioxalate actinometer (1.0 at $\lambda = 450 \text{ nm}$),¹⁸¹ t is the irradiation time of the ferrioxalate actinometer solution in seconds and f is the fraction of absorbed light of the 0.15 M ferrioxalate actinometer solution at $\lambda = 450 \text{ nm}$ ($f = 1 - 10^{-A}$ - The absorbance (A) of the ferrioxalate solution at $\lambda = 450 \text{ nm}$ was measured by UV/Vis. spectroscopy (see below) to be 1.131, therefore $f = 0.951$). The terms for mol Fe^{2+} and t were substituted with the gradient of the graph above.



$$\text{Photon Flux} = \frac{1.271 \times 10^{-9}}{1 \times 0.951} = 1.34 \times 10^{-9} \text{ einstein.s}^{-1}$$

Determination of the Quantum Yield:

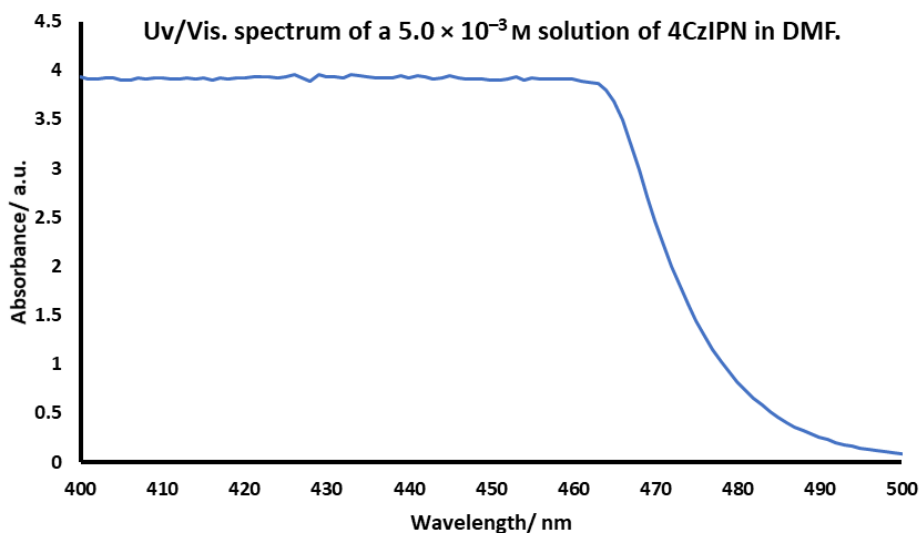
A 4 mL quartz cuvette (path length: $l = 1.0$ cm) was charged with 4CzIPN (**91**) (8 mg, 0.01 mmol), 1-(1-(4-chlorophenyl)vinyl)-3-(3-fluorophenyl)-1,3-dimethylurea (**219**) (64 mg, 0.2 mmol), sodium trifluoromethanesulfinate (**134**) (46 mg, 1.5 eq., 0.3 mmol) and caesium carbonate (98 mg, 1.5 eq., 0.3 mmol). The cuvette was sealed with a rubber septum and the contents were flushed with nitrogen. Under low light, DMF (2 mL) was added and the reaction mixture was degassed by sparging with nitrogen for 10 min. The nitrogen inlet was removed, and the vial further sealed with parafilm. The reaction mixture was positioned 5 cm away from a single 0.1 W blue LED, stirred and irradiated for 4 hours. The reaction was worked up according to GP2 and the yield for α -tertiary urea **232** was determined, by ^{19}F NMR using α,α,α -trifluorotoluene as an internal standard, to be 1.2% (2.4×10^{-6} mol).

The quantum yield (Φ) was calculated using:

$$\Phi = \frac{\text{mol product}}{\text{photon flux} \times t \times f}$$

Where t is the irradiation duration (14400 s) and f is the fraction of light absorbed by 4CzIPN at $\lambda = 450$ nm (for a 5.0×10^{-3} M solution in DMF, this was determined by UV/Vis spectroscopy to be 0.999) (See below).

$$\Phi = \frac{2.40 \times 10^{-6}}{1.34 \times 10^{-9} \times 14400 \times 0.999} = 0.126$$



The reaction with vinyl urea **219** was repeated with an irradiation time of 24 hours (86400 s) to give a 13.1% (2.62×10^{-5} mol) yield of α -tertiary urea **232**.

$$\Phi = \frac{2.62 \times 10^{-5}}{1.34 \times 10^{-9} \times 86400 \times 0.999} = 0.228$$

Average quantum yield (Φ) of the two experiments = 0.177.

8.3 Chapter 2 Experimental

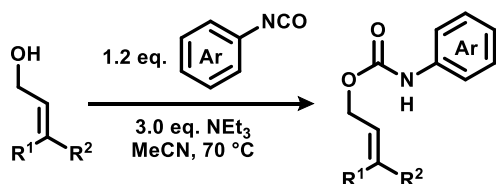
8.3.1 General Procedures

General Procedure 5 (GP5): Synthesis of dibutyl phosphate bases by deprotonation.



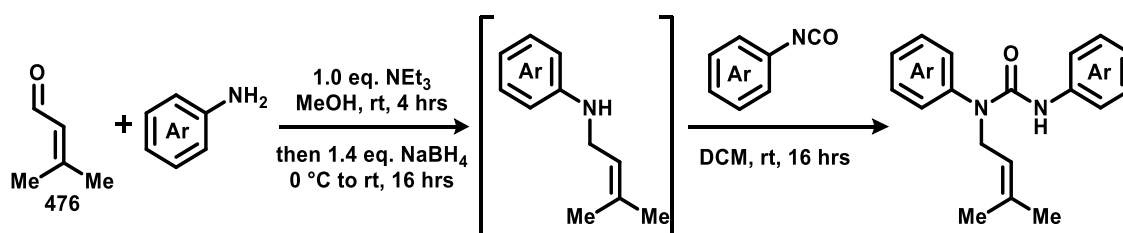
A 50 mL RBF was charged with base (1.0 eq.) and methanol (25 mL), then dibutyl hydrogen phosphate (**419**) (0.94 mL, 1.0 g, 4.8 mmol) was added. The reaction mixture was stirred for 1 hour at room temperature. The reaction mixture was concentrated under reduced pressure and transferred to a Schlenk tube. The contents of the Schlenk tube were placed under vacuum and heated at 80 °C for 4 hours to give the desired product, which was stored under nitrogen.

General Procedure 6 (GP6): Synthesis of allyl carbamates.



A flame-dried RBF was charged with anhydrous acetonitrile (0.25 M), allyl alcohol (5.0 mmol, 1.0 eq.), triethylamine (2.09 mL, 15 mmol, 3.0 eq.) and aryl isocyanate (6.0 mmol, 1.2 eq.) under a nitrogen atmosphere. The reaction mixture was stirred at 70 °C for 23 hours. After which, the reaction mixture was concentrated under reduced pressure and the crude residue was purified by silica column chromatography (2% to 20% EtOAc in 40-60 petroleum ether) to afford the desired product.

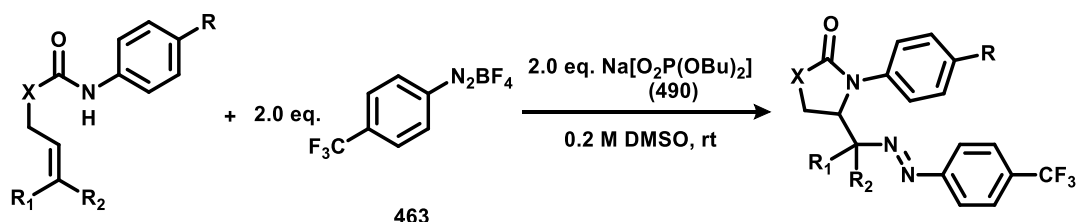
General Procedure 7 (GP7): Synthesis of allyl ureas by reductive amination.



A RBF was charged with aniline derivative (5.0 mmol, 1.0 eq.), methanol (HPLC-grade, 10 mL) and triethylamine (0.70 mL, 5.0 mmol, 1.0 eq.), then 3-methyl-2-butenal (**476**) (0.48 mL, 5.0 mmol, 1.0 eq.). The reaction mixture was stirred at room temperature for 4 hours then cooled to 0 °C and sodium borohydride (270 mg, 7.0 mmol, 1.4 eq.) was added portion wise. The reaction mixture was stirred at room temperature until completion was achieved (followed by TLC, 2-16 hours). Water (1 mL) was added dropwise and half of the solvent was removed under reduced pressure. The mixture was poured onto brine (20 mL) and extracted with ethyl acetate (2 x 20 mL). The combined organic extracts were evaporated under reduced pressure and the resulting residue was purified by flash column chromatography (SiO₂, 5% to 10% EtOAc in *n*-pentane) to give crude intermediary allyl amine.

Crude allyl amine was dissolved in DCM (20 mL) and aryl isocyanate (1.2 eq. based on the mass of the allyl amine) was added dropwise. The reaction mixture was stirred at room temperature until reaction completion (followed by TLC, 2-16 hours). The reaction mixture was evaporated under reduced pressure and the residue was purified by flash column chromatography (SiO₂, 10% to 25% EtOAc in *n*-pentane) to give the desired product.

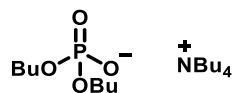
General procedure 8 (GP8): Catalyst-free azo-cycloamination.



A flame-dried 10 mL microwave vial was charged with starting material (0.2 mmol, 1.0 eq.), sodium dibutyl phosphate (**490**) (93 mg, 0.4 mmol, 2.0 eq.) and 4-(trifluoromethyl)benzenediazonium tetrafluoroborate (**463**) (104 mg, 0.4 mmol, 2.0 eq.), then nitrogen. Degassed anhydrous DMSO (1 mL) was added and the reaction was stirred at room temperature for a defined amount of time. The reaction was quenched with water (5 mL) and extracted with ethyl acetate (3 x 3 mL). The combined organic extracts were concentrated under reduced pressure, then purified by silica gel chromatography to afford the desired product.

8.3.2 Synthetic Procedures

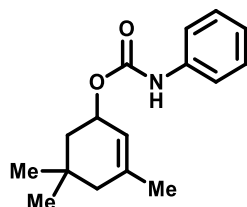
Tetrabutylammonium dibutyl phosphate (415)



Using GP5 and tetrabutylammonium hydroxide 30-hydrate (**451**) (3.84 g, 4.8 mmol), tetrabutylammonium dibutyl phosphate was synthesised (2.15 g, quantitative) as a white solid.

¹H NMR (400 MHz, CDCl₃) 3.85-3.80 (4 H, m, 2 x OCH₂), 3.42-3.35 (8 H, m, 4 x NCH₂), 1.72-1.61 (8 H, m, 4 x CH₂), 1.61-1.53 (4 H, m, 2 x CH₂), 1.50-1.41 (8 H, m, 4 x CH₂), 1.41-1.33 (4 H, m, 2 x CH₂), 0.99 (12 H, t, *J* 7.4, 4 x CH₃), 0.89 (6 H, t, *J* 7.4, 2 x CH₃). Data in good agreement with literature.²⁵⁰

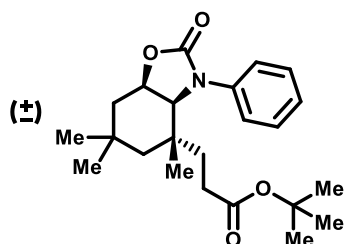
3,5,5-Trimethylcyclohex-2-en-1-yl phenylcarbamate (453)



Using GP6, and starting materials 3,5,5-trimethyl-2-cyclohexen-1-ol (**452**) (0.76 mL, 701 mg, 5.0 mmol) and phenyl isocyanate (**204**) (0.65 mL, 714 mg, 6.0 mmol), the title compound was synthesised (765 mg, 59%) as a white solid.

M.p. 82-84 °C (CDCl₃). **IR (neat, cm⁻¹)** ν_{max} = 3313, 2954, 1692, 1538, 1227, 1051, 691. **¹H NMR (400 MHz, CDCl₃)** δ 7.35 (2 H, d, *J* 8.2, 2 x ArCH), 7.29 (2 H, br. t, *J* 8.2 2 x ArCH), 7.04 (1 H, tt, *J* 8.2, 1.8, ArCH), 6.52 (1 H, s, NH), 5.49-5.45 (1 H, m, CH), 5.37-5.30 (1 H, m, OCH), 1.90 (1 H, d, *J* 16.4, CH_aH_b), 1.82 (1 H, dd, *J* 6.8, 6.4, CH_aH_b), 1.70 (3 H, s, CH₃), 1.68 (1 H, d, *J* 16.4, CH_aH_b), 1.42 (1 H, dd, *J* 8.0, 6.4 CH_aH_b), 1.01 (3 H, s, CH₃), 0.95 (3 H, s, CH₃). **¹³C NMR (101 MHz, CDCl₃)** δ 153.6 (CO) 138.6 (C_{quat}), 138.2 (C_{quat}), 129.1 (2 x ArCH), 123.4 (ArCH), 119.5 (CH), 118.7 (2 x ArCH), 71.2 (OCH), 44.2 (CH₂), 41.1 (CH₂), 30.8 (C_{quat}), 30.6 (CH₃), 27.1 (CH₃), 23.8 (CH₃). **HRMS *m/z* (ESI⁺)** *m/z* calcd for C₁₆H₂₁NO₂Na⁺ [M+Na]⁺ 282.1465; found 282.1469.

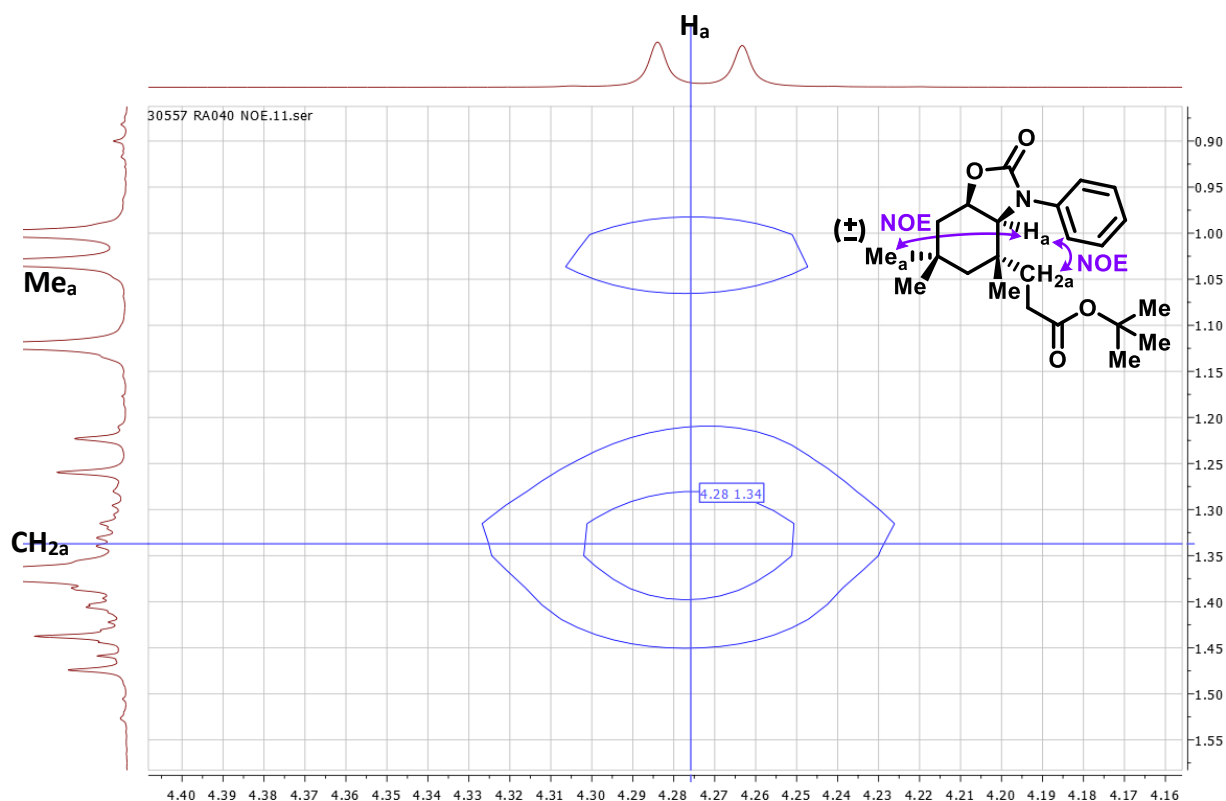
***tert*-Butyl 3-(4,6,6-trimethyl-2-oxo-3-phenyloctahydrobenzo[d]oxazol-4-yl)propanoate (455)**



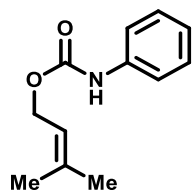
A flame dried 10 mL microwave vial was charged with 3,5,5-trimethylcyclohex-2-en-1-yl phenylcarbamate (**453**) (65 mg, 0.25 mmol), 4CzIPN (**91**) (6 mg, 0.008 mmol) and tetrabutylammonium dibutyl phosphate (**415**) (28 mg, 0.063 mmol). The vial was flushed with nitrogen then anhydrous DCM (2.5 mL) was added. The reaction mixture was degassed by sparging with nitrogen for 5 minutes. *tert*-Butyl acrylate (**454**) (0.11 mL, 96 mg, 0.75 mmol) was added to the reaction mixture then stirred at room temperature for 23 hours under irradiation from 24 W blue LEDs. The reaction was quenched with water (2 mL) and brine (1 mL), then extracted with ethyl acetate (3 x 2 mL). The organic extracts were combined and concentrated under reduced pressure to give crude material, analysis of which by ^1H NMR showed a 10.5:1 diastereomeric mixture of the title compound. The crude material was purified by flash column chromatography (SiO_2 , 10% to 25% EtOAc in *n*-pentane) to give the title compound (57 mg, 59%) as a white solid and single major diastereomer.

M.p. 122-124 °C (CDCl_3). **IR** (neat, cm^{-1}) ν_{max} = 2911, 1730, 1388, 1200, 1143, 763, 693. **^1H NMR (400 MHz, CDCl_3)** δ 7.44 (2 H, d, J 8.3, 2 x ArCH), 7.36 (2 H, t, J 8.3, 2 x ArCH), 7.18 (1 H, tt, J 8.3, 1.4, ArCH), 4.87 (1 H, ddd, J 8.2, 7.1, 6.0, OCH), 4.24 (1 H, d, J 8.2, NCH), 2.03 (2 H, t, J 7.9, (OC)CH₂), 2.01 (1 H, dd, J 14.0, 7.1, CH_aH_b), 1.85 (1 H, dd, J 14.0, 6.0, CH_aH_b), 1.41 (1 H, d, J 12.5, CH_aH_b), 1.41-1.26 (2, m, CH₂), 1.34 (9 H, s, C(CH₃)₃), 1.20 (1 H, d, J 12.5, CH_aH_b), 1.09 (3 H, s, CH₃), 1.00 (3 H, s, CH₃), 0.97 (3 H, s, CH₃). **^{13}C NMR (101 MHz, CDCl_3)** δ 172.7 (CO), 156.5 (CO), 138.9 (C_{quat}), 129.2 (2 x ArCH), 125.9 (ArCH), 124.0 (2 x ArCH), 80.5 (C_{quat}), 74.3 (CH), 62.3 (CH), 45.8 (CH₂), 38.8 (CH₂), 38.7 (C_{quat}), 37.6 (CH₂), 33.0 (CH₃), 32.9 (CH₃), 30.2 (CH₂), 28.5 (C_{quat}), 28.1 (3 x CH₃), 23.4 (CH₃). **HRMS m/z (ESI⁺)** m/z calcd for C₂₃H₃₄NO₄⁺ [M+H]⁺ 388.2482; found 388.2484.

NOSEY:



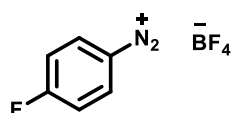
3-Methylbut-2-en-1-yl phenylcarbamate (**457**)



Using GP6 and starting materials 3-methyl-2-buten-1-ol (**456**) (0.51 mL, 431 mg, 5.0 mmol) and phenyl isocyanate (**204**) (0.65 mL, 714 mg, 6.0 mmol), the title compound was synthesised (606 mg, 59%) as a white solid.

1H NMR (301 MHz, $CDCl_3$) δ 7.40-7.34 (2 H, m, 2 x ArCH), 7.33-7.24 (2 H, m, 2 x ArCH), 7.09-7.00 (1 H, m, ArCH), 6.61 (1 H, s, NH), 5.44-5.35 (1 H, m, CH), 4.66 (2 H, d, J 6.8, CH_2), 1.78 (3 H, s, CH_3), 1.75 (3 H, s, CH_3). Data in good agreement with literature.²²⁸

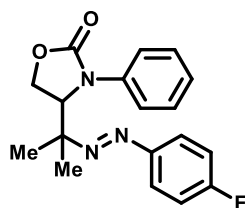
4-Fluorobenzenediazonium tetrafluoroborate (**430**)



4-Fluoroaniline (**458**) (0.95 mL, 1.11 g, 10.0 mmol) was added to a 50% solution of tetrafluoroboric acid in water (3.5 mL) at 0 °C, resulting in a brown suspension that dissolves into solution after warming to room temperature. The reaction mixture was cooled to 5-10 °C and sodium nitrate (0.74 g, 8.7 mmol) dissolved in water (1 mL) was added drop wise over 5 mins. The resulting reaction mixture was stirred for 30 minutes at 5-10 °C, then filtered and the obtained solid was sequentially washed with water (20 mL) and Et₂O (2 x 20 mL), to give the title compound (998 mg, 50%) as a brown solid.

¹H NMR (400 MHz, D₂O) δ 8.73 (2 H, dd, *J* 9.0, 4.2, 2 x ArCH), 7.75 (2 H, t, *J* 9.0, 2 x ArCH). **¹⁹F NMR (377 MHz, D₂O)** δ -83.2 (1 F, s, CF), -150.3 (4 F, s, BF₄). Data in good agreement with literature.²⁶⁸

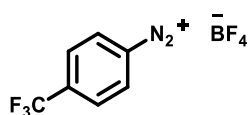
(*E*)-4-(2-((4-Fluorophenyl)diazenyl)propan-2-yl)-3-phenyloxazolidin-2-one (**459**)



A flame-dried 10 mL microwave vial was charged with 3-methylbut-2-en-1-yl (4-methoxyphenyl)carbamate (**457**) (21 mg, 0.1 mmol), 3DPAFIPN (**106**) (4.8 mg, 8 μmol), tetrabutylammonium dibutyl phosphate (**415**) (90 mg, 0.2 mmol) and 4-fluorobenzenediazonium tetrafluoroborate (**430**) (84 mg, 0.4 mmol), then flushed with nitrogen. Anhydrous DCM (1 mL) was added and the reaction mixture was degassed by sparging with nitrogen for two minutes. The reaction mixture was irradiated with 24 W blue LEDs and stirred for 21 hours. The reaction was quenched with water (5 mL) and extracted with ethyl acetate (3 x 3 mL). The combined organic extracts were concentrated under reduced pressure and purified by flash column chromatography (SiO₂, 45% EtOAc in 40-60 petroleum ether) to give the title compound (18 mg, 54%) as a yellow solid.

M.p. 98-102 °C (Et₂O). **IR (neat, cm⁻¹)** ν_{\max} = 2979, 1738, 1412, 1214, 1126, 759, 499. **¹H NMR (400 MHz, CDCl₃)** δ 7.36 (2 H, d, *J* 9.2, 2 x ArCH) 7.34 (2 H, tt, *J* 9.2, 2 x ArCH), 7.26 (2 H, d, *J* 7.5, 2 x ArCH), 7.07 (1 H, tt, *J* 7.5, 1.3 ArCH), 7.02 (2 H, t, *J* 7.5, 2 x ArCH), 5.00 (1 H, dd, *J* 8.9, 3.7, CH), 4.60 (1 H, t, *J* 8.9, CH_aH_b), 4.46 (1 H, dd, *J* 9.4, 3.7, CH_aH_b), 1.21 (3 H, s, CH₃), 1.20 (3 H, s, CH₃). **¹³C NMR (126 MHz, CDCl₃)** δ 164.3 (ArCF, d, *J*_{CF} 251.8), 156.8 (CO), 148.1 (ArCNN, d, *J*_{CF} 3.0), 138.1 (C_{quat}), 129.2 (2 x ArCH), 126.1 (ArCH), 124.8 (2 x ArCH), 124.4 (2 x ArCH, d, *J*_{CF} 9.0), 115.8 (2 x ArCH, d, *J*_{CF} 22.8), 73.8 (C_{quat}), 64.3 (CH₂), 63.7 (CH), 21.3 (CH₃), 20.9 (CH₃). **¹⁹F NMR (377 MHz, CDCl₃)** δ -109.0--109.2 (1 F, m, CF). **HRMS *m/z* (ESI⁺)** *m/z* calcd for C₁₈H₁₈FN₃O₂Na⁺ [M+Na]⁺ 350.1275; found 350.1293.

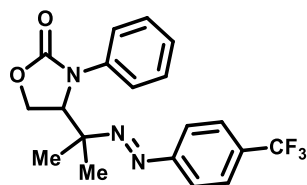
4-(Trifluoromethyl)benzenediazonium tetrafluoroborate (**463**)



4-(Trifluoromethyl)aniline (**462**) (0.63 mL, 806 mg, 5.0 mmol) was added to a 50% solution of tetrafluoroboric acid in water (5 mL) at 0 °C, resulting in a white suspension in solution that dissolves after warming to room temperature. The reaction mixture was cooled to 5-10 °C, then sodium nitrate (0.793 g, 11.5 mmol) dissolved in water (1 mL) was added drop wise over 5 mins. The resulting reaction mixture was stirred for 15 mins at 0 °C, after which the reaction mixture was filtered and the obtained solid was sequentially washed with water (10 mL) and Et₂O (2 x 20 mL) to give the title compound (0.862 g, 67%) as a white solid.

¹H NMR (400 MHz, DMSO-*d*₆) δ 8.90 (2 H, d, *J* 8.6, 2 x ArCH), 8.42 (2 H, d, *J* 8.6, 2 x ArCH). Data in good agreement with literature.²⁶⁸

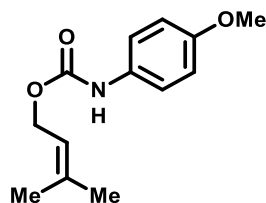
(*E*)-3-Phenyl-4-(2-((4-(trifluoromethyl)phenyl)diazenyl)propan-2-yl)oxazolidin-2-one (**464**)



Following GP8 with 3-methylbut-2-en-1-yl (4-methoxyphenyl)carbamate (**457**) (41 mg, 0.2 mmol) used as starting material. Reaction was stirred for 60 minutes and purified by flash column chromatography (SiO₂, 20% to 50% EtOAc in 40-60 petroleum ether) to give the title compound (18 mg, 24%) as a yellow solid.

M.p. 133-135 °C. IR (film, cm⁻¹) ν_{max} = 2983, 2253, 1753, 1484, 1323, 1065. ¹H NMR (400 MHz, CDCl₃) δ 7.60 (2 H, d, *J* 8.0, 2 x ArCH), 7.38 (2 H, d, *J* 8.0, 2 x ArCH), 7.34 (2 H, d, *J* 8.7, 2 x ArCH), 7.28-7.24 (2 H, m, 2 x ArCH), 7.09-7.05 (1 H, m, ArCH), 5.05 (1 H, dd, *J* 9.1, 3.6, CH), 4.63 (1 H, t, *J* 9.1, CH₂H_b), 4.47 (1 H, dd, *J* 9.1, 3.6, CH_aH_b), 1.26 (3 H, s, CH₃), 1.24 (3 H, s, CH₃). ¹³C NMR (100 MHz, CDCl₃) δ 156.7 (CO), 153.4 (ArCNN), 138.0 (C_{quat}), 132.3 (C_{quat}, *q*, *J*_{CF} 32.4), 129.2 (2 x ArCH), 126.2 (ArCH), 126.1 (2 x ArCH, *q*, *J*_{CF} 3.8), 124.8 (2 x ArCH), 123.9 (CF₃, *q*, *J*_{CF} 272.9), 122.6 (2 x ArCH), 74.8 (C_{quat}), 64.2, (CH₂), 63.6 (CH), 21.4 (CH₃), 20.6 (CH₃). ¹⁹F NMR (377 MHz, CDCl₃) δ -62.6 (3 F, s, CF₃). HRMS *m/z* (ESI⁺) *m/z* calcd for C₁₉H₁₈F₃N₃O₂Na⁺ [M+Na]⁺ 400.1243; found 400.1244.

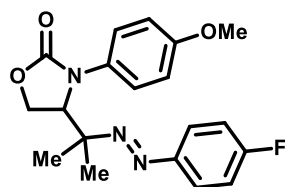
3-Methylbut-2-en-1-yl (4-methoxyphenyl)carbamate (**474**)



Using GP6 and starting materials 3-methyl-2-buten-1-ol (**456**) (0.51 mL, 431 mg, 5.0 mmol) and 4-methoxyphenyl isocyanate (**473**) (0.78 mL, 894 mg, 6.0 mmol), 3-methylbut-2-en-1-yl (4-methoxyphenyl)carbamate was synthesised (0.918 g, 78%) as a white solid.

¹H NMR (400 MHz, CDCl₃) δ 7.26 (2 H, d, *J* 9.1, 2 x ArCH), 6.83 (2 H, d, *J* 9.1, 2 x ArCH), 6.42 (1 H, s, NH), 5.38 (1 H, thep, *J* 7.2, 1.4, CH), 4.63 (2 H, d, *J* 7.2, CH₂), 3.77 (3 H, s, OCH₃), 1.77 (3 H, s, CH₃), 1.73 (3 H, s, CH₃). Data in good agreement with literature.²⁶⁹

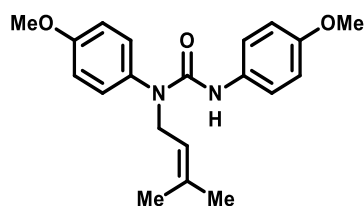
(*E*)-4-(2-((4-Fluorophenyl)oxazolid)propan-2-yl)-3-(4-methoxyphenyl)oxazolidine-2-one (**475**)



A flame-dried 10 mL microwave vial was charged with 3-methylbut-2-en-1-yl (4-methoxyphenyl)carbamate (**474**) (47 mg, 0.2 mmol), 3DPAFIPN (**106**) (4.8 mg, 8 μ mol), tetrabutylammonium dibutyl phosphate (**415**) (180 mg, 0.4 mmol) and 4-fluorobenzenediazonium tetrafluoroborate (**474**) (84 mg, 2.0 eq., 0.4 mmol), then flushed with nitrogen. Anhydrous DMSO (2 mL) was added and the reaction mixture was degassed by sparging with nitrogen for 5 minutes. The reaction mixture was then stirred for 21 hours at room temperature. The reaction was quenched with water (5 mL) and extracted with ethyl acetate (3 x 3 mL). The combined organic extracts were concentrated under reduced pressure and purified by flash column chromatography (SiO₂, 45% EtOAc in 40-60 petroleum ether) to give the title compound (55 mg, 70%) as a yellow solid.

M.p. 120-124 °C (Et₂O). **IR (neat, cm⁻¹)** ν_{max} = 2958, 1731, 1595, 1514, 1479, 1418, 1245, 1224, 1132, 1034, 963, 824. **¹H NMR (400 MHz, CD₂Cl₂)** δ 7.39 (2 H, dd, *J* 9.0, 3.8, 2 x ArCH), 7.18 (2 H, d, *J* 9.1, 2 x ArCH), 7.06 (2 H, t, *J* 9.0, 2 x ArCH), 6.77 (2 H, d, *J* 9.1, 2 x ArCH), 4.93 (1 H, dd, *J* 9.1, 4.3, CH), 4.60 (1 H, t, *J* 9.1, CH_aH_b), 4.44 (1 H, dd, *J* 9.1, 4.3, CH_aH_b), 3.69 (3 H, s, OCH₃), 1.23 (3 H, s, CH₃), 1.19 (3 H, s, CH₃). **¹³C NMR (101 MHz, CD₂Cl₂)** δ 164.7 (CF, d, *J*_{CF} 250.0), 158.3 (ArCO), 157.5 (CO), 148.7 (ArCNN), 131.4 (C_{quat}), 127.2 (2 x ArCH), 124.8 (2 x ArCH, d, *J*_{CF} 9.1), 116.0 (2 x ArCH, d, *J*_{CF} 22.8), 114.7 (2 x ArCH), 74.1 (C_{quat}), 64.7 (CH₂), 64.6 (CH), 55.9 (OCH₃), 21.6 (CH₃), 20.6 (CH₃). **¹⁹F NMR (377 MHz, CDCl₃)** δ -109.0–-109.2 (1 F, m, CF). **HRMS *m/z* (ESI⁺)** *m/z* calcd for C₁₉H₂₀FN₃O₃Na⁺ [M+Na]⁺ 380.1381; found 380.1392.

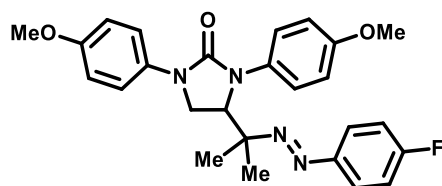
1,3-Bis(*p*-methoxyphenyl)-1-(3-methylbut-2-en-1-yl)urea (479)



Using GP7 and starting materials *p*-anisidine (**477**) (616 mg, 5.0 mmol) and 4-methoxyphenyl isocyanate (**479**) (0.63 mL, 727 mg, 4.9 mmol), the title compound was synthesised (1.20 g, 71%) as a white solid.

M.p. 125-127 °C (CDCl₃). **IR (film, cm⁻¹)** ν_{max} = 3426, 3933, 1661, 1508, 1243, 1225, 728. **¹H NMR (400 MHz, CDCl₃)** δ 7.21-7.16 (4 H, m, 2 \times ArCH + 2 \times ArCH), 6.95 (2 H, d, *J* 8.9, 2 \times ArCH), 6.76 (2 H, d, *J* 9.0, 2 \times ArCH), 5.98 (1 H, br. s, NH), 5.33-5.29 (1 H, m, CH), 4.27 (2 H, d, *J* 7.1, CH₂), 3.84 (3 H, s, OCH₃), 3.74 (3 H, s, OCH₃), 1.67 (3 H, s, CH₃), 1.47 (3 H, s, CH₃). **¹³C NMR (101 MHz, CDCl₃)** δ 159.2 (ArCO), 155.6 (ArCO), 155.0 (CO), 135.6 (C_{quat}), 134.1 (C_{quat}), 132.3 (C_{quat}), 130.2 (2 \times ArCH), 121.5 (2 \times ArCH), 120.6 (CH), 115.3 (2 \times ArCH), 114.1 (2 \times ArCH), 55.6 (2 \times OCH₃), 47.2 (CH₂), 25.8 (CH₃), 17.8 (CH₃). **HRMS *m/z* (ESI⁺)** *m/z* calcd for C₂₀H₂₄N₂O₃Na⁺ [M+Na]⁺ 363.1679; found 363.1679.

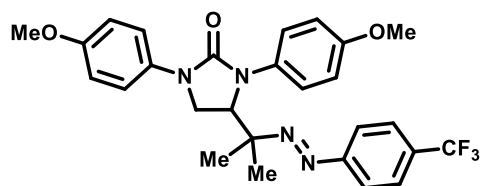
(E)-4-(2-((4-Fluorophenyl)diazenyl)propan-2-yl)-1,3-bis(4-methoxyphenyl)imidazolidin-2-one (480)



A flame-dried 10 mL microwave vial was charged with 1,3-bis(4-methoxyphenyl)-1-(3-methylbut-2-en-1-yl)urea (**479**) (34 mg, 0.1 mmol), tetrabutylammonium dibutyl phosphate (**415**) (90 mg, 0.2 mmol) and 4-(trifluoromethyl)benzenediazonium tetrafluoroborate (**430**) (42 mg, 0.2 mmol) then flushed with nitrogen. Anhydrous DMSO (1 mL) was added and the reaction mixture was degassed by sparging with nitrogen for 5 minutes. The reaction mixture was stirred at room temperature for 17 hours. The reaction was quenched with water (5 mL) and extracted with ethyl acetate (3 x 3 mL). The combined organic extracts were concentrated under reduced pressure and purified by flash column chromatography (SiO₂, 20% to 100% Et₂O in 40-60 petroleum ether) to give the title compound (35 mg, 75%) as a yellow solid.

M.p. 125-128 °C (Et₂O). **IR** (neat, cm⁻¹) ν_{max} = 2933, 1691, 1509, 1241, 1221, 1028, 827. **¹H NMR** (500 MHz, C₆D₆) 7.68 (2 H, d, *J* 8.7, 2 x ArCH), 7.36-7.30 (2 H, m, 2 x ArCH), 7.28 (2 H, d, *J* 8.1, 2 x ArCH), 6.68 (2 H, d, *J* 8.7, 2 x ArCH), 6.71 (2 H, t, *J* 8.1, 2 x ArCH), 6.66 (2 H, d, *J* 8.1, 2 x ArCH), 4.53 (1 H, t, *J* 6.6, CH), 3.54-3.45 (2 H, m, CH₂), 3.35 (3 H, s, OCH₃), 3.23 (3 H, s, OCH₃), 1.12 (3 H, s, CH₃), 1.06 (3 H, s, CH₃). **¹³C NMR** (126 MHz, C₆D₆) δ 164.5 (CF, d, *J*_{CF} 250.4), 157.5 (ArCO), 156.2 (CO), 155.8 (ArCO), 148.6 (ArCNN, d, *J*_{CF} 2.9), 134.4 (C_{quat}), 133.4 (C_{quat}), 127.1 (2 x ArCH), 124.7 (2 x ArCH, d, *J*_{CF} 8.9), 119.5 (2 x ArCH), 115.7 (2 x ArCH, d, *J*_{CF} 22.9), 114.5 (2 x ArCH), 114.3 (2 x ArCH), 74.6 (C_{quat}), 60.6 (CH), 55.1 (OCH₃), 54.9 (OCH₃), 45.1 (CH₂), 21.1 (CH₃), 20.9 (CH₃). **¹⁹F NMR** (377 MHz, C₆D₆) -110.0--110.2 (1 F, m, CF). δ **HRMS *m/z*** (ESI⁺) *m/z* calcd for C₂₆H₂₇FN₄O₃Na⁺ [M+Na]⁺ 485.1959; found 485.1966.

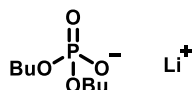
(E)-1,3-Bis(4-methoxyphenyl)-4-(2-((4-(trifluoromethyl)phenyl)diazenyl)propan-2-yl)imidazolidin-2-one (488)



Using GP8 and starting material 1,3-bis(*p*-methoxyphenyl)-1-(3-methylbut-2-en-1-yl)urea (**479**) (68 mg, 0.2 mmol) the title compound was synthesised and purified by flash column chromatography (SiO₂, 20% to 100% Et₂O in 40-60 petroleum ether) to give a yellow solid (85 mg, 83%).

M.p. 183-185 °C (Et₂O). **IR (film, cm⁻¹)** ν_{max} = 3054, 1706, 1512, 1323, 1264, 732. **¹H NMR (500 MHz, CDCl₃)** δ 7.61 (2 H, d, *J* 8.3, 2 × ArCH), 7.50 (2 H, d, *J* 9.1, 2 × ArCH), 7.41 (2 H, d, *J* 8.2, 2 × ArCH), 7.21 (2 H, d, *J* 8.9, 2 × ArCH), 6.90 (2 H, d, *J* 9.1, 2 × ArCH), 6.74 (2 H, d, *J* 8.9, 2 × ArCH), 4.98 (1 H, dd, *J* 9.8, 4.6, CH), 4.18 (1 H, t, *J* 9.7, CH_aH_b), 3.84 (1 H, dd, *J* 9.7, 4.6, CH_aH_b), 3.80 (3 H, s, OCH₃), 3.66 (3 H, s, OCH₃), 1.28 (6 H, s, 2 × CH₃). **¹³C NMR (126 MHz, CDCl₃)** δ 157.4 (ArCO), 156.7 (CO), 155.6 (ArCO), 153.6 (ArCNN), 133.5 (C_{quat}), 132.4 (C_{quat}), 132.2 (C_{quat}, q, *J*_{CF} 32.4), 127.2 (2 × ArCH), 126.0 (2 × ArCH, q, *J*_{CF} 3.7), 124.0 (CF₃, q, *J*_{CF} 272.3), 122.6 (2 × ArCH), 119.7 (2 × ArCH), 114.3 (2 × ArCH), 114.3 (2 × ArCH), 75.4 (C_{quat}), 60.9 (CH), 55.7 (OCH₃), 55.4 (OCH₃), 45.5 (CH₂), 21.5 (CH₃), 20.4 (CH₃). **¹⁹F NMR (470 MHz, CDCl₃)** δ -62.6 (3 F, s, CF₃). **HRMS *m/z* (ESI⁺)** *m/z* calcd for C₂₇H₂₇F₃N₄O₃Na⁺ [M+Na]⁺ 535.1927; found 535.1923.

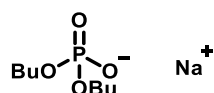
Lithium dibutyl phosphate (489)



Using GP5 and lithium hydroxide (115 mg, 4.8 mmol), lithium dibutyl phosphate was synthesised (1.03 g, quantitative) as a white solid.

¹H NMR (400 MHz, DMSO-*d*₆) 3.63-3.55 (4 H, m, 2 × OCH₂), 1.50-1.38 (4 H, m, 2 × CH₂), 1.36-1.23 (4 H, m, 2 × CH₂), 0.86 (6 H, t, *J* 7.3, 2 × CH₃). **¹³C NMR (101 MHz, DMSO-*d*₆)** δ 63.4 (2 × OCH₂, d, *J*_{CP} 5.7), 33.6 (2 × CH₂, d, *J*_{CP} 7.3), 18.7 (2 × CH₂), 13.7 (2 × CH₃). **³¹P NMR (162 MHz, DMSO-*d*₆)** δ 0.63 (1 P, br. s, P(O)O₃).

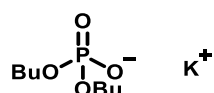
Sodium dibutyl phosphate (490)



Using GP5 and sodium hydroxide (192 mg, 4.8 mmol), sodium dibutyl phosphate was synthesised (1.11 g, quantitative) as a white solid.

¹H NMR (400 MHz, DMSO-*d*₆) δ 3.63-3.56 (4 H, m, 2 x OCH₂), 1.50-1.40 (4 H, m, 2 x CH₂), 1.36-1.24 (4 H, m, 2 x CH₂), 0.86 (6 H, t, *J* 7.3, 2 x CH₃). **¹³C NMR (101 MHz, DMSO-*d*₆)** δ 63.5 (2 x OCH₂, d, *J*_{CP} 5.7), 33.6 (2 x CH₂, d, *J*_{CP} 7.3), 18.7 (2 x CH₂), 13.7 (2 x CH₃). **³¹P NMR (162 MHz, DMSO-*d*₆)** δ 0.56 (1 P, br. s, P(O)₃).

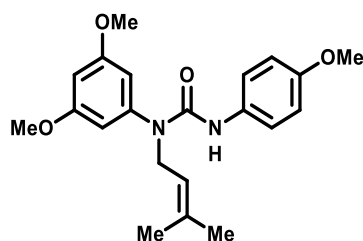
Potassium dibutyl phosphate (491)



Using GP5 and potassium hydroxide (269 mg, 4.8 mmol), potassium dibutyl phosphate was synthesised (1.18 g, quantitative) as a white solid.

¹H NMR (400 MHz, DMSO-*d*₆) δ 3.62-3.55 (4 H, m, 2 x OCH₂), 1.50-1.39 (4 H, m, 2 x CH₂), 1.36-1.23 (4 H, m, 2 x CH₂), 0.86 (6 H, t, *J* 7.3, 2 x CH₃). **¹³C NMR (101 MHz, DMSO-*d*₆)** δ 63.4 (2 x OCH₂, d, *J*_{CP} 5.7), 33.6 (2 x CH₂, d, *J*_{CP} 7.3), 18.7 (2 x CH₂), 13.7 (2 x CH₃). **³¹P NMR (162 MHz, DMSO-*d*₆)** δ 0.19 (1 P, br. s, P(O)O₃).

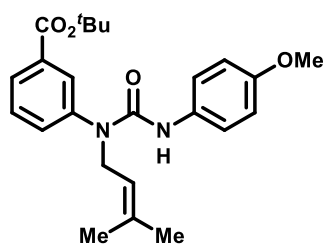
3-(*p*-Methoxyphenyl)-1-(*o,o'*-dimethoxyphenyl)-1-(3-methylbut-2-en-1-yl)-urea (496)



Using GP7 and starting materials 3,5-dimethoxyaniline (**492**) (0.766 g, 5.0 mmol) and 4-methoxyphenyl isocyanate (**473**) (0.49 mL, 564 mg, 3.8 mmol), the title compound was synthesised (0.870 g, 47%) as a white solid.

M.p. 125-127 °C (CDCl₃). **IR (neat, cm⁻¹)** *v*_{max} = 3382, 2972, 2932, 1708, 1664, 1509, 1294, 1220, 1154, 1035, 747. **¹H NMR (400 MHz, CDCl₃)** 7.20 (2 H, d, *J* 9.0, 2 x ArCH), 6.78 (2 H, d, *J* 9.0, 2 x ArCH), 6.44 (3 H, s, 2 x ArCH + ArCH), 6.20 (1 H, s, NH), 5.37-5.30 (1 H, m, CH), 4.29 (2 H, d, *J* 7.0, CH₂), 3.79 (6 H, s, 2 x OCH₃), 3.75 (3 H, s, OCH₃), 1.69 (3 H, s, CH₃), 1.54 (3 H, s, CH₃). **¹³C NMR (101 MHz, CDCl₃)** δ 161.8 (2 x ArCO), 155.7 (ArCO), 154.4 (CO), 143.6 (C_{quat}), 135.4 (C_{quat}), 132.2 (C_{quat}), 121.6 (2 x ArCH), 120.8 (CH), 114.1 (2 x ArCH), 106.7 (2 x ArCH), 100.0 (ArCH), 55.7 (2 x OCH₃), 55.6 (OCH₃), 47.3 (CH₂), 25.8 (CH₃), 17.9 (CH₃). **HRMS *m/z* (ESI⁺)** *m/z* calcd for C₂₁H₂₆N₂O₄Na⁺ [M+Na]⁺ 393.1785; found 393.1781.

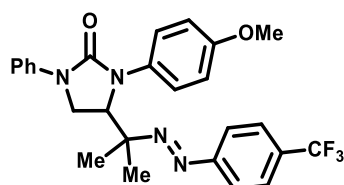
***tert*-Butyl 3-(3-(4-methoxyphenyl)-1-(3-methylbut-2-en-1-yl)ureido)benzoate (497)**



Using GP7 and starting materials *tert*-butyl 3-aminobenzoate (**493**) (0.966 g, 5.0 mmol) and 4-methoxyphenyl isocyanate (**473**) (0.36 mL, 418 mg, 2.8 mmol), the title compound was synthesised (0.869 g, 42%) as a yellow solid.

M.p. 79-81 °C (CDCl₃). **IR** (neat, cm⁻¹) ν_{\max} = 3382, 2972, 2932, 1708, 1664, 1509, 1294, 1220, 1154, 1035, 747. **¹H NMR** (400 MHz, CDCl₃) δ 7.97 (1 H, dt, *J* 7.4, 1.3, ArCH), 7.90 (1 H, t, *J* 1.3, ArCH), 7.49 (1 H, t, *J* 7.4, ArCH), 7.45 (1 H, dt, *J* 7.4, 1.3, ArCH), 7.17 (2 H, d, *J* 8.9, 2 x ArCH), 6.78 (2 H, d, *J* 8.9, 2 x ArCH), 5.94 (1 H, s, NH), 5.33 (1 H, t, *J* 6.9, CH), 4.32 (2 H, d, *J* 6.9, CH₂), 3.74 (3 H, s, OCH₃), 1.68 (3 H, s, CH₃), 1.60 (9 H, s, C(CH₃)₃), 1.48 (3 H, s, CH₃). **¹³C NMR** (101 MHz, CDCl₃) δ 164.8 (CO), 155.9 (C_{quat}), 154.5 (CO), 142.0 (C_{quat}), 136.0 (C_{quat}), 134.2 (C_{quat}), 132.8 (ArCH), 131.9 (C_{quat}), 130.0 (ArCH), 129.5 (ArCH), 128.8 (ArCH), 121.8 (2 x ArCH), 120.4 (CH), 114.1 (2 x ArCH), 81.9 (C(CH₃)₃), 55.6 (OCH₃), 47.4 (CH₂), 28.3 (C(CH₃)₃), 25.8 (CH₃), 17.8 (CH₃). **HRMS *m/z* (ESI⁺)** *m/z* calcd for C₂₄H₃₁N₂O₄⁺ [M+H]⁺ 411.2278; found 411.2279.

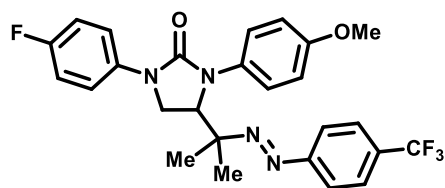
(*E*)-3-(4-Methoxyphenyl)-1-phenyl-4-(2-((4-(trifluoromethyl)phenyl)diazenyl)propan-2-yl)imidazolidin-2-one (498)



Following GP8 with 3-(*p*-methoxyphenyl)-1-(3-methylbut-2-en-1-yl)-1-(phenyl)urea (62 mg, 0.2 mmol) used as starting material. Reaction was stirred for 40 minutes and purified by flash column chromatography (SiO₂, 0% to 10 % MeOH in DCM) to give the title compound (73 mg, 76%) as a yellow solid.

M.p. 154-155 °C (Et₂O). **IR** (neat, cm⁻¹) ν_{\max} = 2934, 1696, 1599, 1502, 1412, 1321, 1243, 1163, 1120, 1100, 1062, 835, 751, 689. **¹H NMR** (400 MHz, CDCl₃) δ 7.63-7.58 (4 H, m, 2 x ArCH + 2 x ArCH), 7.42 (2 H, d, *J* 8.3, 2 x ArCH), 7.35 (2 H, t, *J* 7.4, 2 x ArCH), 7.21 (2 H, d, *J* 8.9, 2 x ArCH), 7.07 (1 H, t, *J* 7.4, ArCH), 6.75 (2 H, d, *J* 8.9, 2 x ArCH), 4.99 (1 H, dd, *J* 9.9, 4.6, CH), 4.21 (1 H, t, *J* 9.9, CH₂H_b), 3.88 (1 H, dd, *J* 9.9, 4.6, CH_aH_b), 3.66 (3 H, s, OCH₃), 1.28 (6 H, s, 2 x CH₃). **¹³C NMR** (126 MHz, CDCl₃) δ 157.5 (ArCO), 156.4 (CO), 153.5 (ArCNN), 140.1 (C_{quat}), 132.1 (C_{quat}), 132.1 (C_{quat}, q, *J*_{CF} 32.4), 129.0 (2 x ArCH), 127.2 (2 x ArCH), 125.9 (2 x ArCH, q, *J*_{CF} 3.6), 123.9 (CF₃, q, *J*_{CF} 272.3), 122.8 (ArCH), 122.6 (2 x ArCH), 117.7 (2 x ArCH), 114.3 (2 x ArCH), 75.3 (C_{quat}), 60.8 (CH), 55.4 (OCH₃), 45.0 (CH₂), 21.5 (CH₃), 20.2 (CH₃). **¹⁹F NMR** (377 MHz, CDCl₃) δ -62.6 (3 F, s, CF₃). **HRMS *m/z* (ESI⁺)** *m/z* calcd for C₂₆H₂₆F₃N₄O₂⁺ [M+H]⁺ 483.2002; found 483.1997.

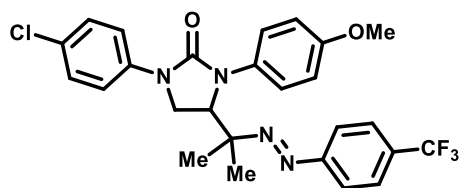
(E)-1-(4-Fluorophenyl)-3-(4-methoxyphenyl)-4-(2-((4-(trifluoromethyl)phenyl)diazenyl)propan-2-yl)imidazolidin-2-one (499)



Following GP8 with 1-(*p*-fluorophenyl)-3-(*p*-methoxyphenyl)-1-(3-methylbut-2-en-1-yl)-urea (66 mg, 0.2 mmol) used as starting material. Reaction was stirred for 30 minutes and purified by flash column chromatography (SiO₂, DCM) to give the title compound (57 mg, 57%) as a yellow solid.

M.p. 184–186 °C (Et₂O). **IR** (neat, cm⁻¹) ν_{max} = 2927, 1697, 1509, 1411, 1324, 1250, 1222, 1128, 1065, 833, 530. **¹H NMR** (400 MHz, CDCl₃) δ 7.61 (2 H, d, *J* 8.3, 2 × ArCH), 7.55 (2 H, dd, *J* 8.7, 4.6, 2 × ArCH), 7.42 (2 H, d, *J* 8.3, 2 × ArCH), 7.20 (2 H, d, *J* 9.0, 2 × ArCH), 7.04 (2 H, t, *J* 8.7, 2 × ArCH), 6.75 (2 H, d, *J* 9.0, 2 × ArCH), 4.98 (1 H, dd, *J* 9.8, 4.6, CH), 4.18 (1 H, t, *J* 9.8, CH_aH_b), 3.85 (1 H, dd, *J* 9.8, 4.6, CH_aH_b), 3.66 (3 H, s, OCH₃), 1.28 (6 H, s, 2 × CH₃). **¹³C NMR** (126 MHz, CDCl₃) δ 158.7 (ArCF, d, *J*_{CF} 242.4), 157.6 (ArCO), 156.5 (CO), 153.5 (ArC_{NN}), 136.2 (C_{quat}, d, *J*_{CF} 2.6), 132.2 (C_{quat}, q, *J*_{CF} 32.6), 132.1 (C_{quat}), 127.2 (2 × ArCH), 126.0 (2 × ArCH, q, *J*_{CF} 3.7), 123.9 (CF₃, q, *J*_{CF} 272.3), 122.6 (2 × ArCH), 119.3 (2 × ArCH, d, *J*_{CF} 7.6), 115.6 (2 × ArCH, d, *J*_{CF} 22.4), 114.3 (2 × ArCH), 75.3 (C_{quat}), 60.8 (CH), 55.4 (OCH₃), 45.3 (CH₂), 21.5 (CH₃), 20.3 (CH₃). **¹⁹F NMR** (377 MHz, CDCl₃) δ -62.6 (3 F, s, CF₃), -120.3–-120.5 (1 F, m, ArCF). **HRMS** *m/z* (ESI⁺) *m/z* calcd for C₂₆H₂₅F₄N₄O₂⁺ [M+H]⁺ 501.1908; found 501.1909.

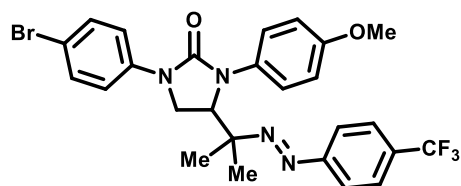
(E)-1-(4-Chlorophenyl)-3-(4-methoxyphenyl)-4-(2-((4-(trifluoromethyl)phenyl)diazenyl)propan-2-yl)imidazolidin-2-one (500)



Following GP8 with 1-(*p*-chlorophenyl)-3-(*p*-methoxyphenyl)-1-(3-methylbut-2-en-1-yl)urea (69 mg, 0.2 mmol) used as starting material. Reaction was stirred for 40 minutes and purified by flash column chromatography (SiO₂, DCM) to give the title compound (82 mg, 80%) as a yellow solid.

M.p. 179-181 °C (Et₂O). **IR** (neat, cm⁻¹) ν_{max} = 2986, 1694, 1496, 1419, 1321, 1244, 1160, 1125, 828. **¹H NMR** (400 MHz, CDCl₃) δ 7.61 (2 H, d, *J* 8.3, 2 × ArCH), 7.56 (2 H, d, *J* 9.0, 2 × ArCH), 7.42 (2 H, d, *J* 8.3, 2 × ArCH), 7.30 (2 H, d, *J* 9.0, 2 × ArCH), 7.20 (2 H, d, *J* 9.0, 2 × ArCH), 6.75 (2 H, d, *J* 9.0, 2 × ArCH), 4.99 (1 H, dd, *J* 9.8, 4.6, CH), 4.17 (1 H, t, *J* 9.8, CH_aH_b), 3.84 (1 H, dd, *J* 9.8, 4.6, CH_aH_b), 3.66 (3 H, s, OCH₃), 1.27 (6 H, s, 2 × CH₃). **¹³C NMR** (126 MHz, CDCl₃) δ 157.6 (ArCO), 156.2 (CO), 153.5 (ArCNN), 138.7 (C_{quat}), 132.2 (C_{quat}, q, *J*_{CF} 32.7), 131.9 (ArCCl), 128.9 (2 × ArCH), 127.8 (C_{quat}), 127.2 (2 × ArCH), 125.9 (2 × ArCH, q, *J*_{CF} 3.1), 123.9 (CF₃, q, *J*_{CF} 272.8), 122.6 (2 × ArCH), 118.8 (2 × ArCH), 114.3 (2 × ArCH), 75.2 (C_{quat}), 60.8 (CH), 55.4 (OCH₃), 45.0 (CH₂), 21.5 (CH₃), 20.3 (CH₃). **¹⁹F NMR** (377 MHz, CDCl₃) δ -62.6 (3 F, s, CF₃). **HRMS *m/z*** (ESI⁺) *m/z* calcd for C₂₆H₂₄ClF₃N₄O₂Na⁺ [M+Na]⁺ 539.1432; found 539.1433.

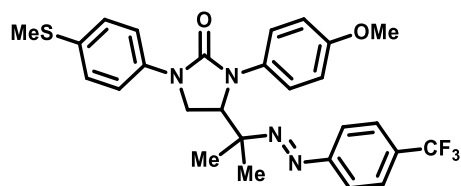
(E)-1-(4-Bromophenyl)-3-(4-methoxyphenyl)-4-(2-((4-(trifluoromethyl)phenyl)diazenyl)propan-2-yl)imidazolidin-2-one (501)



Following GP8 with 1-(*p*-bromophenyl)-3-(*p*-methoxyphenyl)-1-(3-methylbut-2-en-1-yl)urea (78 mg, 0.2 mmol) used as starting material. Reaction was stirred for 30 minutes and purified by flash column chromatography (SiO₂, 0% to 10% Et₂O in DCM) to give the title compound (87 mg, 76%) as a yellow solid.

M.p. 192-194 °C (Et₂O). **IR** (neat, cm⁻¹) ν_{max} = 2983, 1692, 1492, 1417, 1321, 1286, 1243, 1160, 1124, 1064, 827. **¹H NMR** (400 MHz, CDCl₃) δ 7.61 (2 H, d, *J* 8.4, 2 × ArCH), 7.51 (2 H, d, *J* 9.2, 2 × ArCH), 7.44 (2 H, d, *J* 9.2, 2 × ArCH), 7.42 (2 H, d, *J* 8.4, 2 × ArCH), 7.20 (2 H, d, *J* 9.0, 2 × ArCH), 6.75 (2 H, d, *J* 9.0, 2 × ArCH), 4.98 (1 H, dd, *J* 9.8, 4.6, CH), 4.16 (1 H, t, *J* 9.8, CH_aH_b), 3.83 (1 H, dd, *J* 9.8, 4.7, CH_aH_b), 3.66 (3 H, s, OCH₃), 1.27 (6 H, s, 2 × CH₃). **¹³C NMR** (126 MHz, CDCl₃) δ 157.6 (ArCO), 156.2 (CO), 153.5 (ArCNN), 139.2 (C_{quat}), 132.2 (C_{quat}, q, *J*_{CF} 32.5), 131.8 (2 × ArCH), 131.8 (C_{quat}), 127.2 (2 × ArCH), 125.9 (2 × ArCH, q, *J*_{CF} 3.8), 123.9 (CF₃, q, *J*_{CF} 272.6), 122.6 (2 × ArCH), 119.1 (2 × ArCH), 115.4 (ArCBr), 114.3 (2 × ArCH), 75.2 (C_{quat}), 60.7 (CH), 55.4 (OCH₃), 44.9 (CH₂), 21.5 (CH₃), 20.3 (CH₃). **¹⁹F NMR** (377 MHz, CDCl₃) δ -62.6 (3 F, s, CF₃). **HRMS *m/z* (ESI⁺)** *m/z* calcd for C₂₆H₂₄BrF₃N₄O₂Na⁺ [M+Na]⁺ 583.0927 found 583.0928.

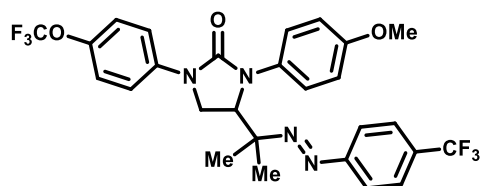
(E)-3-(4-Methoxyphenyl)-1-(4-(methylthio)phenyl)-4-(2-((4-(trifluoromethyl)phenyl)diazenyl)propan-2-yl)imidazolidin-2-one (502)



Following GP8 with 3-(*p*-methoxyphenyl)-1-(3-methylbut-2-en-1-yl)-1-(*p*-methylthiophenyl)urea (71 mg, 0.2 mmol) used as starting material. Reaction was stirred for 20 minutes and purified by flash column chromatography (SiO₂, 0% to 10% EtO₂ in DCM) to give the title compound (69 mg, 65%) as a yellow solid.

M.p. 150-152 °C (Et₂O). **IR** (neat, cm⁻¹) ν_{\max} = 2983, 1692, 1498, 1417, 1320, 1243, 1159, 1122, 1063, 829. **¹H NMR** (400 MHz, CDCl₃) δ 7.61 (2 H, d, *J* 8.3, 2 × ArCH), 7.55 (2 H, d, *J* 8.9, 2 × ArCH), 7.42 (2 H, d, *J* 8.3, 2 × ArCH), 7.28 (2 H, d, *J* 8.9, 2 × ArCH), 7.20 (2 H, d, *J* 8.9, 2 × ArCH), 6.74 (2 H, d, *J* 8.9, 2 × ArCH), 4.98 (1 H, dd, *J* 9.8, 4.6, CH), 4.18 (1 H, t, *J* 9.8, CH_aH_b), 3.84 (1 H, dd, *J* 9.8, 4.6, CH_aH_b), 3.65 (3 H, s, OCH₃), 2.47 (3 H, s, SCH₃) 1.27 (6 H, s, 2 × CH₃). **¹³C NMR** (126 MHz, CDCl₃) δ 157.5 (ArCO), 156.3 (CO), 153.5 (ArCNN), 138.0 (C_{quat}), 132.1 (C_{quat}, q, *J*_{CF} 32.3), 132.1 (C_{quat}), 131.7 (C_{quat}), 128.5 (2 × ArCH), 127.2 (2 × ArCH), 125.9 (2 × ArCH, q, *J*_{CF} 3.7), 124.0 (CF₃, q, *J*_{CF} 272.3), 122.6 (2 × ArCH), 118.3 (2 × ArCH), 114.3 (2 × ArCH), 75.3 (C_{quat}), 60.8 (CH), 55.4 (OCH₃), 45.0 (CH₂), 21.5 (CH₃), 20.3 (CH₃), 17.2 (SCH₃). **¹⁹F NMR** (377 MHz, CDCl₃) δ -62.6 (3 F, s, CF₃). **HRMS *m/z* (ESI⁺)** *m/z* calcd for C₂₇H₂₇F₃N₄O₂SN⁺ [M+Na]⁺ 551.1699; found 551.1678.

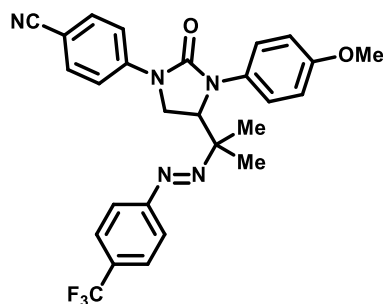
(E)-3-(4-Methoxyphenyl)-1-(4-(trifluoromethoxy)phenyl)-4-(2-((4-(trifluoromethyl)phenyl)diazenyl)propan-2-yl)imidazolidin-2-one (503)



Following GP8 with 3-(*p*-methoxyphenyl)-1-(3-methylbut-2-en-1-yl)-1-(*p*-trifluoromethoxyphenyl)urea (79 mg, 0.2 mmol) used as starting material. Reaction was stirred for 30 minutes and purified by flash column chromatography (SiO₂, 0% to 10% EtO₂ in DCM) to give the title compound (70 mg, 62%) as a yellow solid.

M.p. 172-174 °C (Et₂O). **IR** (neat, cm⁻¹) ν_{max} = 2985, 1694, 1509, 1413, 1245, 1223, 1160, 1124, 1064, 831. **¹H NMR** (400 MHz, CDCl₃) δ 7.63 (2 H, d, *J* 9.1, 2 x ArCH), 7.61 (2 H, d, *J* 8.1, 2 x ArCH), 7.42 (2 H, d, *J* 8.1, 2 x ArCH), 7.24-7.17 (4 H, m, 4 x ArCH), 6.76 (2 H, d, *J* 8.9, 2 x ArCH), 4.99 (1 H, dd, *J* 9.9, 4.6, CH), 4.19 (1 H, t, *J* 9.9, CH_aH_b), 3.86 (1 H, dd, *J* 9.9, 4.6, CH_aH_b), 3.66 (3 H, s, OCH₃), 1.27 (6 H, s, 2 x CH₃). **¹³C NMR** (126 MHz, CDCl₃) δ 157.7 (ArCO), 156.3 (CO), 153.5 (ArC_{NN}, *q*, *J* 1.2), 144.3 (ArCO, *q*, *J* 1.8), 138.8 (C_{quat}), 132.2 (C_{quat}, *q*, *J*_{CF} 32.2), 131.9 (C_{quat}), 127.3 (2 x ArCH), 126.0 (2 x ArCH, *q*, *J*_{CF} 3.8), 123.9 (CF₃, *q*, *J*_{CF} 272.3), 122.6 (2 x ArCH), 121.8 (2 x ArCH), 120.7 (CF₃, *q*, *J*_{CF} 256.5), 118.5 (2 x ArCH), 114.4 (2 x ArCH), 75.2 (C_{quat}), 60.8 (CH), 55.4 (OCH₃), 45.1 (CH₂), 21.5 (CH₃), 20.3 (CH₃). **¹⁹F NMR** (377 MHz, CDCl₃) δ -58.2 (3 F, s, OCF₃), -62.6 (3 F, s, CF₃). **HRMS *m/z* (ESI⁺)** *m/z* calcd for C₂₇H₂₅F₆N₄O₃⁺ [M+H]⁺ 567.1825; found 567.1805.

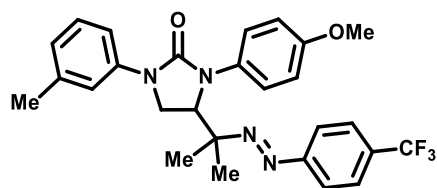
(E)-4-(3-(4-Methoxyphenyl)-2-oxo-4-(2-((4-(trifluoromethyl)phenyl)diazenyl)propan-2-yl)imidazolidin-1-yl)benzonitrile (504)



Following GP8 with 1-(4-cyanophenyl)-3-(4-methoxyphenyl)-1-(3-methylbut-2-en-1-yl)urea (67 mg, 0.2 mmol) used as starting material. Reaction was stirred for 30 minutes and purified by flash column chromatography (SiO₂, 0% to 10% EtO₂ in DCM) to give the title compound (79 mg, 78%) as a yellow solid.

M.p. 234-237 °C (Et₂O). **IR** (neat, cm⁻¹) ν_{max} = 2970, 2936, 2843, 2220, 1700, 1606, 1510, 1410, 1321, 1250, 1162, 1128, 835. **¹H NMR** (400 MHz, CDCl₃) δ 7.73 (2 H, d, *J* 8.9, 2 x ArCH), 7.65-7.59 (4 H, m, 2 x ArCH + 2 x ArCH), 7.43 (2 H, d, *J* 8.2, 2 x ArCH), 7.20 (2 H, d, *J* 8.9, 2 x ArCH), 6.76 (2 H, d, *J* 8.9, 2 x ArCH), 5.01 (1 H, dd, *J* 9.9, 4.4, CH), 4.21 (1 H, t, *J* 9.9, CH_aH_b), 3.88 (1 H, dd, *J* 9.9, 4.4, CH_aH_b), 3.66 (3 H, s, OCH₃), 1.28 (3 H, s, CH₃), 1.26 (3 H, s, CH₃). **¹³C NMR** (126 MHz, CDCl₃) δ 157.9 (ArCO), 155.8 (CO), 153.4 (ArCNN), 143.9 (C_{quat}), 133.2 (2 x ArCH), 132.4 (C_{quat}, q, *J*_{CF} 32.2), 131.4 (C_{quat}), 127.3 (2 x ArCH), 126.0 (2 x ArCH, q, *J*_{CF} 3.6), 123.9 (CF₃, q, *J*_{CF} 272.3), 122.6 (2 x ArCH), 119.3 (ArCCN), 117.2 (2 x ArCH), 114.5 (2 x ArCH), 105.4 (ArCCN), 75.1 (C_{quat}), 60.8 (CH), 55.4 (OCH₃), 44.7 (CH₂), 21.5 (CH₃), 20.4 (CH₃). **¹⁹F NMR** (377 MHz, CDCl₃) δ -62.6 (3 F, s, CF₃). **HRMS *m/z* (ESI⁺)** *m/z* calcd for C₂₇H₂₄F₃N₅O₂Na⁺ [M+Na]⁺ 530.1774; found 530.1757.

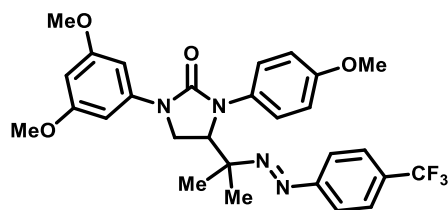
(E)-3-(4-Methoxyphenyl)-1-(*m*-tolyl)-4-(2-((4-(trifluoromethyl)phenyl)diazenyl)propan-2-yl)imidazolidin-2-one (505)



Following GP8 with 3-(*p*-methoxyphenyl)-1-(3-methylbut-2-en-1-yl)-1-(*m*-tolyl)urea (65 mg, 0.2 mmol) used as starting material. Reaction was stirred for 1 hour and purified by flash column chromatography (SiO₂, 0% to 15% DCM in Et₂O) to give the title compound (86 mg, 87%) as a yellow solid.

M.p. 147-149 °C (Et₂O). **IR** (neat, cm⁻¹) ν_{max} = 2952, 1696, 1586, 1514, 1412, 1323, 1244, 1160, 1121, 1063, 835. **¹H NMR** (400 MHz, CDCl₃) δ 7.61 (2 H, d, *J* 8.2, 2 × ArCH), 7.51 (1 H, s, ArCH), 7.42 (2 H, d, *J* 8.2, 2 × ArCH), 7.35 (1 H, d, *J* 7.9, ArCH), 7.24 (1 H, t, *J* 7.9, ArCH), 7.21 (2 H, d, *J* 8.9, 2 × ArCH), 6.89 (1 H, d, *J* 7.9, ArCH), 6.74 (2 H, d, *J* 8.9, 2 × ArCH), 4.98 (1 H, dd, *J* 9.8, 4.6, CH), 4.20 (1 H, t, *J* 9.8, CH_aH_b), 3.87 (1 H, dd, *J* 9.8, 4.6, CH_aH_b), 3.66 (3 H, s, OCH₃), 2.36 (3 H, s, CH₃), 1.28 (6 H, s, 2 × CH₃). **¹³C NMR** (126 MHz, CDCl₃) δ 157.4 (ArCO), 156.4 (CO), 153.5 (ArC_{NN}), 140.0 (C_{quat}), 138.8 (C_{quat}), 132.2 (C_{quat}), 132.1 (C_{quat}, q, *J*_{CF} 32.2), 128.8 (ArCH), 127.2 (2 × ArCH), 125.9 (2 × ArCH, q, *J*_{CF} 3.6), 124.0 (CF₃, q, *J*_{CF} 272.2), 123.7 (ArCH), 122.6 (2 × ArCH), 118.6 (ArCH), 114.8 (ArCH), 114.2 (2 × ArCH), 75.4 (C_{quat}), 60.8 (CH), 55.3 (OCH₃), 45.1 (CH₂), 21.8 (CH₃), 21.5 (CH₃), 20.2 (CH₃). **¹⁹F NMR** (377 MHz, CDCl₃) δ -62.6 (3 F, s, CF₃). **HRMS *m/z* (ESI⁺)** *m/z* calcd for C₂₇H₂₈F₃N₄O₂⁺ [M+H]⁺ 497.2159; found 497.2160.

(E)-1-(3,5-Dimethoxyphenyl)-3-(4-methoxyphenyl)-4-(2-((4-(trifluoromethyl)phenyl)diazenyl)propan-2-yl)imidazolidin-2-one (506)

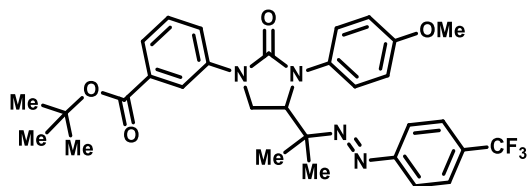


Following GP8 with 3-(*p*-methoxyphenyl)-1-(*o,o'*-dimethoxyphenyl)-1-(3-methylbut-2-en-1-yl)-urea (**496**) (74 mg, 0.2 mmol) used as starting material. Reaction was stirred for 30 minutes and purified using deactivated silica gel chromatography (Et₂O) to give the title compound (61 mg, 67%) as an yellow solid.

M.p. 142-144 °C (Et₂O). **IR** (neat, cm⁻¹) ν_{\max} = 2937, 1697, 1584, 1513, 1411, 1322, 1245, 1154, 1062, 833, 813. **¹H NMR** (400 MHz, CDCl₃) δ 7.61 (2 H, d, *J* 8.3, 2 × ArCH), 7.41 (2 H, d, *J* 8.3, 2 × ArCH), 7.19 (2 H, d, *J* 9.0, 2 × ArCH), 6.90 (2 H, d, *J* 2.1, 2 × ArCH), 6.75 (2 H, d, *J* 9.0, 2 × ArCH), 6.20 (1 H, t, *J* 2.1, ArCH), 4.97 (1 H, dd, *J* 10.0, 4.9, CH), 4.14 (1 H, t, *J* 10.0, CH_aH_b), 3.86 (1 H, dd, *J* 10.0, 4.9, CH_aH_b), 3.79 (6 H, s, 2 × OCH₃), 3.65 (3 H, s, OCH₃), 1.27 (6 H, s, 2 × CH₃). **¹³C NMR** (126 MHz, C₆D₆) δ 161.9 (2 × ArCO), 157.5 (ArCO), 155.8 (CO), 153.7 (ArCNN), 142.9, (C_{quat}), 132.8 (C_{quat}), 132.0 (C_{quat}, q, *J*_{CF} 32.1), 127.2 (2 × ArCH), 126.0 (2 × ArCH, q, *J*_{CF} 3.6), 124.6 (CF₃, q, *J*_{CF} 272.1), 122.9 (2 × ArCH), 114.2 (2 × ArCH), 96.7 (2 × ArCH), 95.1 (ArCH), 75.6 (C_{quat}), 60.4 (CH), 55.0 (2 × OCH₃), 54.8 (OCH₃), 44.9 (CH₂), 21.5 (CH₃), 19.8 (CH₃). **¹⁹F NMR** (377 MHz, CDCl₃) δ -62.6 (3 F, s, CF₃). **HRMS *m/z* (ESI⁺)** *m/z* calcd for C₂₈H₂₉F₃N₄O₄Na⁺ [M+Na]⁺ 565.2033; found 565.2033.

***tert*-Butyl**

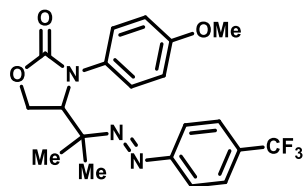
(*E*)-3-(3-(4-methoxyphenyl)-2-oxo-4-(2-((4-(trifluoromethyl)phenyl)diazenyl)propan-2-yl)imidazolidin-1-yl)benzoate (507)



Following GP8 with *tert*-butyl 3-(3-(4-methoxyphenyl)-1-(3-methylbut-2-en-1-yl)ureido)benzoate (**497**) (82 mg, 0.2 mmol) used as starting material. Reaction was stirred for 30 minutes and purified by flash column chromatography (SiO₂, 0% to 10% EtO₂ in DCM) to give the title compound (69 mg, 59%) as a yellow solid.

M.p. 176-178 °C (Et₂O). **IR** (neat, cm⁻¹) ν_{max} = 2979, 2935, 1712, 1691, 1514, 1416, 1322, 1248, 1160, 1124, 1065, 848, 833, 759. **¹H NMR** (400 MHz, CDCl₃) δ 8.19 (1 H, ddd, *J* 8.2, 2.5, 1.1, ArCH), 7.87 (1 H, dd, *J* 2.5, 1.6, ArCH), 7.67 (1 H, ddd, *J* 7.6, 1.6, 1.1, ArCH), 7.61 (2 H, d, *J* 8.2, 2 × ArCH), 7.42 (2 H, d, *J* 8.8, 2 × ArCH), 7.37 (1 H, t, *J* 8.2, ArCH), 7.21 (2 H, d, *J* 9.0, 2 × ArCH), 6.75 (2 H, d, *J* 9.0, 2 × ArCH), 5.01 (1 H, dd, *J* 9.8, 4.6, CH), 4.24 (1 H, t, *J* 9.8, CH_aH_b), 3.94 (1 H, dd, *J* 9.8, 4.6, CH_aH_b), 3.65 (3 H, s, OCH₃), 1.60 (9 H, s, 3 × C(CH₃)₃), 1.28 (6 H, s, 2 × CH₃). **¹³C NMR** (126 MHz, CDCl₃) δ 165.9 (CO), 157.6 (ArCO), 156.4 (CO), 153.5 (ArCNN), 140.2 (C_{quat}), 132.6 (C_{quat}), 132.2 (C_{quat}, q, *J*_{CF} 32.5), 132.0 (C_{quat}), 129.0 (ArCH), 127.3 (2 × ArCH), 125.9 (2 × ArCH, q, *J*_{CF} 3.5), 124.0 (CF₃, q, *J*_{CF} 272.3), 122.6 (ArCH), 122.4 (2 × ArCH), 122.5 (ArCH), 117.3 (ArCH), 114.3 (2 × ArCH), 81.4 (C(CH₃)₃), 75.3 (C_{quat}), 60.9 (CH), 55.4 (OCH₃), 45.0 (CH₂), 28.3 (C(CH₃)₃), 21.5 (CH₃), 20.2 (CH₃). **¹⁹F NMR** (377 MHz, CDCl₃) δ -62.6 (3 F, s, CF₃). **HRMS** *m/z* (ESI⁺) *m/z* calcd for C₃₁H₃₃F₃N₄O₄Na⁺ [M+Na]⁺ 605.2346; found 605.2344.

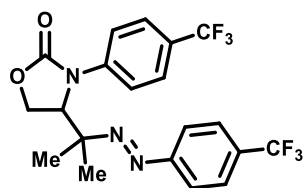
(E)-3-(4-Methoxyphenyl)-4-(2-((4-(trifluoromethyl)phenyl)diazenyl)propan-2-yl)oxazolidin-2-one (511)



Following GP8 with 3-methylbut-2-en-1-yl (4-methoxyphenyl)carbamate (**474**) (47 mg, 0.2 mmol) used as starting material. Reaction was stirred for 30 minutes and purified by flash column chromatography (SiO₂, 20% to 100% Et₂O in 40-60 petroleum ether) to give the title compound (54 mg, 67%) as a yellow solid.

M.p. 142-144 °C (Et₂O). **IR** (neat, cm⁻¹) ν_{max} = 2986, 1733, 1513, 1324, 1243, 1166, 1128, 1062, 823. **¹H NMR** (400 MHz, CDCl₃) δ 7.62 (2 H, d, *J* 8.2, 2 × ArCH), 7.42 (2 H, d, *J* 8.2, 2 × ArCH), 7.18 (2 H, d, *J* 8.8, 2 × ArCH), 6.74 (2 H, d, *J* 8.8, 2 × ArCH), 4.98 (1 H, dd, *J* 9.2, 4.0, CH), 4.63 (1 H, t, *J* 9.2, CH_aH_b), 4.45 (1 H, dd, *J* 9.2, 4.0, CH_aH_b), 3.65 (3 H, s, OCH₃), 1.28 (3 H, s, CH₃), 1.23 (3 H, s, CH₃). **¹³C NMR** (126 MHz, CDCl₃) δ 157.9 (ArCO), 157.1 (CO), 153.4 (ArCNN), 132.3 (C_{quat}, q, *J*_{CF} 32.7), 130.6 (C_{quat}), 126.6 (2 × ArCH), 126.0 (2 × ArCH, q, *J*_{CF} 3.8), 123.9 (CF₃, q, *J*_{CF} 272.9), 122.6 (2 × ArCH), 114.5 (2 × ArCH), 74.7 (C_{quat}), 64.1 (CH₂), 64.1 (CH), 55.4 (OCH₃), 21.4 (CH₃), 20.1 (CH₃). **¹⁹F NMR** (377 MHz, CDCl₃) δ -62.6 (3 F, s, CF₃). **HRMS *m/z*** (ESI⁺) *m/z* calcd for C₂₀H₂₀F₃N₃O₃Na⁺ [M+Na]⁺ 430.1349; found 430.1340.

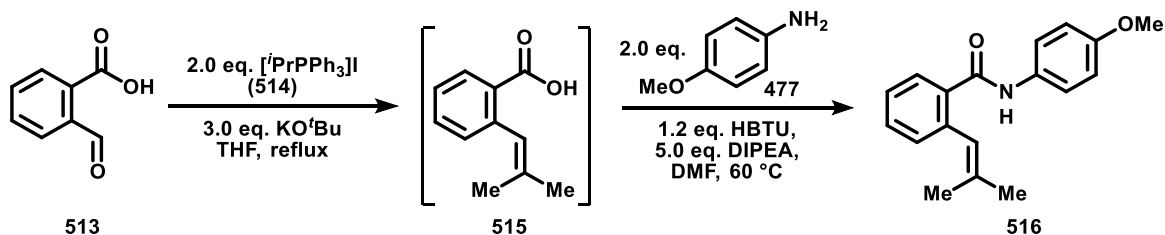
(E)-3-(4-(Trifluoromethyl)phenyl)-4-(2-((4-(trifluoromethyl)phenyl)diazenyl)propan-2-yl)oxazolidin-2-one (512)



A flame-dried 10 mL microwave vial was charged with 3-methylbut-2-en-1-yl (4-(trifluoromethyl)phenyl)carbamate (**510**) (55 mg, 0.2 mmol), sodium dibutyl phosphate (**490**) (93 mg, 0.2 mmol) and 4-(trifluoromethyl)benzenediazonium tetrafluoroborate (**463**) (104 mg, 0.4 mmol), then flushed with nitrogen and anhydrous DCM (2 mL) was added. The reaction mixture was stirred at room temperature for 18 hours under irradiation from 24 W blue LEDs. The reaction was quenched with water (5 mL) and extracted with ethyl acetate (3 x 3 mL). The combined organic extracts were concentrated under reduced pressure and purified by flash column chromatography (SiO₂, 20% to 100% Et₂O in 40-60 petroleum ether) to give the title compound (30 mg, 34%) as a yellow solid.

M.p. 184-187 °C (CDCl₃). **IR (film, cm⁻¹)** ν_{max} = 2982, 1732, 1330, 1120, 1069. **¹H NMR (400 MHz, CDCl₃)** δ 7.60 (2 H, d, *J* 8.4, 2 x ArCH), 7.47-7.44 (4 H, m, 4 x ArCH), 7.35 (2 H, d, *J* 8.4, 2 x ArCH), 5.13 (1 H, dd, *J* 8.9, 3.2, CH), 4.69 (1 H, t, *J* 8.9, CH_aH_b), 4.54 (1 H, dd, *J* 8.9, 3.2, CH_aH_b), 1.31 (3 H, s, CH₃), 1.27 (3 H, s, CH₃). **¹³C NMR (126 MHz, CDCl₃)** δ 156.0 (CO), 153.0 (ArCNN), 141.1 (C_{quat}), 132.8 (C_{quat}, q, *J*_{CF} 32.5), 127.6 (C_{quat}, q, *J*_{CF} 33.0), 126.2 (2 x ArCH, q, *J*_{CF} 3.7), 126.2 (2 x ArCH, q, *J*_{CF} 3.9), 124.2 (2 x ArCH), 123.8 (CF₃, q, *J*_{CF} 272.2), 123.7 (CF₃, q, *J*_{CF} 271.9), 122.4 (2 x ArCH), 75.2 (C_{quat}), 64.2 (CH₂), 63.0 (CH), 21.8 (CH₃), 19.5 (CH₃). **¹⁹F NMR (377 MHz, CDCl₃)** δ -62.5 (3 F, s, CF₃), -62.7 (3 F, s, CF₃). **HRMS m/z (ESI⁺)** m/z calcd for C₂₀H₁₇F₆N₃O₂Na⁺ [M+Na]⁺ 468.1117; found 468.1122.

N-(4-Methoxyphenyl)-2-(2-methylprop-1-en-1-yl)benzamide (516)

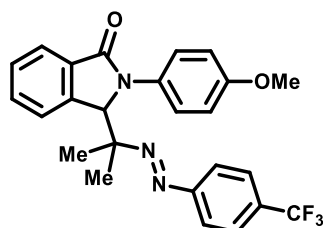


A solution of isopropyltriphenylphosphonium iodide (**514**) (4.31 g, 10.0 mmol) and potassium *tert*-butoxide (1.69 g, 15.0 mmol) in THF (20 mL) was stirred at room temperature for 1.5 hours. 2-Carboxybenzaldehyde (**513**) (0.75 g, 5.0 mmol) was added and the solution was refluxed for 18 hours. The reaction was cooled to room temperature and quenched with a saturated NH₄Cl_(aq) (30 mL). The solution was diluted with ethyl acetate (20 mL) and the organic layer extracted with 2 M NaOH_(aq) (6 x 25 mL). The combined aqueous layers were acidified with concentrated HCl and extracted with EtOAc (35 mL x 6). The combined organic layers were dried (Na₂SO₄) and concentrated under reduced pressure to yield crude material (460 mg) as a white solid that was used without further purification.

The crude material (460 mg) was dissolved in DMF (5.2 mL); HBTU (1.20 g, 3.1 mmol) and DIPEA (2.3 mL, 5.0 eq., 13 mmol) were sequentially added to the reaction mixture, which was stirred at room temperature for 10 minutes at room temperature. 4-Methoxyaniline (**477**) (0.640 g, 2 eq., 5.2 mmol) was added to the reaction mixture, which was stirred for 23 hours at 60 °C. The reaction was quenched with water (50 mL) and extracted with ethyl acetate (2 x 50 mL). The combined organic extracts were sequentially washed with NaHCO_{3(aq)} (50 mL) and brine (50 mL), then dried (Na₂SO₄). The organic extracts were concentrated under reduced pressure to afford crude residue, which was purified by flash column chromatography (SiO₂, 10% to 40% ethyl acetate in 40-60 petroleum ether) to give the title compound (425 mg, 30% over two steps) as a white solid.

M.p. 99-101 °C (CDCl₃). **IR** (neat, cm⁻¹) ν_{max} = 3336, 2956, 1692, 1527, 1415, 1246, 1230, 1175, 1059, 1027, 825. **¹H NMR** (400 MHz, CDCl₃) δ 8.01 (1 H, s, NH), 7.84 (1 H, d, *J* 7.5, ArCH), 7.49 (2 H, d, *J* 8.9, 2 x ArCH), 7.41 (1 H, t, *J* 7.5, ArCH), 7.31 (1 H, t, *J* 7.5, ArCH), 7.22 (1 H, d, *J* 7.5, ArCH), 6.88 (2 H, d, *J* 8.9, 2 x ArCH), 6.50 (1 H, s, CH), 3.79 (3 H, s, OCH₃), 1.97 (3 H, s, CH₃), 1.78 (3 H, s, CH₃). **¹³C NMR** (101 MHz, CDCl₃) δ 166.6 (CO), 156.5 (ArCO), 138.7 (C_{quat}), 136.0 (C_{quat}), 134.8 (C_{quat}), 131.4 (C_{quat}), 130.6 (ArCH), 130.4 (ArCH), 129.1 (ArCH), 127.0 (ArCH), 123.7 (CH), 121.5 (2 x ArCH), 114.3 (2 x ArCH), 55.6 (OCH₃), 26.3 (CH₃), 19.5 (CH₃). **HRMS *m/z*** (ESI⁺) *m/z* calcd for C₁₈H₁₉NO₂Na⁺ [M+Na]⁺ 304.1308; found 304.1320.

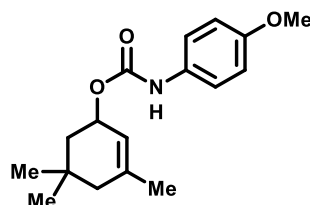
(E)-2-(4-Methoxyphenyl)-3-(2-((4-(trifluoromethyl)phenyl)diazenyl)propan-2-yl)isoindolin-1-one (517)



Following GP8 at a reaction concentration of 0.1 M, with *N*-(4-methoxyphenyl)-2-(2-methylprop-1-en-1-yl)benzamide (**516**) (56 mg, 0.2 mmol) used as starting material. Reaction was stirred for 45 minutes and purified by flash column chromatography (SiO₂, 0% to 10% Et₂O in DCM) to give the title compound (70 mg, 77%) as a yellow solid.

M.p. 184-187 °C (Et₂O). **IR** (neat, cm⁻¹) ν_{\max} = 2991, 2936, 1675, 1515, 1327, 1248, 1120, 1065, 831, 739. **¹H NMR** (400 MHz, CDCl₃) δ 7.99-7.94 (1 H, m, ArCH), 7.61 (2 H, d, *J* 8.4, 2 × ArCH), 7.57-7.50 (3 H, m, ArCH + ArCH + ArCH), 7.46 (2 H, d, *J* 8.4, 2 × ArCH), 7.22 (2 H, d, *J* 8.9, 2 × ArCH), 6.74 (2 H, d, *J* 8.9, 2 × ArCH), 5.93 (1 H, s, CH), 3.62 (3 H, s, OCH₃), 1.32 (3 H, s, CH₃), 1.01 (3 H, s, CH₃). **¹³C NMR** (126 MHz, CDCl₃) δ 168.2 (CO), 157.7 (ArCO), 153.3 (ArCNN), 142.7 (C_{quat}), 133.3 (C_{quat}), 132.2 (C_{quat}, q, *J*_{CF} 32.2), 131.5 (ArCH), 131.3 (C_{quat}), 129.0 (ArCH), 127.5 (2 × ArCH), 125.9 (2 × ArCH, q, *J*_{CF} 3.8), 124.5 (ArCH), 124.2 (ArCH), 124.0 (CF₃, q, *J*_{CF} 272.3), 122.7 (2 × ArCH), 114.3 (2 × ArCH), 75.8 (C_{quat}), 68.9 (CH), 55.3 (OCH₃), 22.7 (CH₃), 20.3 (CH₃). **¹⁹F NMR** (377 MHz, CDCl₃) δ -62.6 (3 F, s, CF₃). **HRMS *m/z* (ESI⁺)** *m/z* calcd for C₂₅H₂₂F₃N₃O₂Na⁺ [M+Na]⁺ 476.1556; found 476.1559.

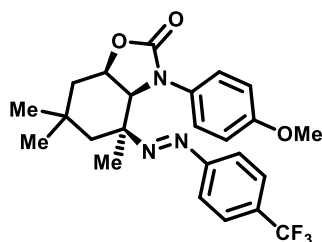
3,5,5-Trimethylcyclohex-2-en-1-yl (4-methoxyphenyl)carbamate (518)



Using GP6 and starting materials 3,5,5-trimethyl-2-cyclohexen-1-ol (**453**) (0.76 mL, 701 mg, 5.0 mmol) and 4-methoxyphenyl isocyanate (**473**) (0.78 mL, 895 mg, 6.0 mmol), the title compound was synthesised (0.654 g, 45%) as a white solid.

M.p. 99-101 °C (CDCl₃). **IR** (neat, cm⁻¹) ν_{\max} = 3336, 2956, 1692, 1527, 1415, 1246, 1230, 1175, 1059, 1027, 825. **¹H NMR** (400 MHz, CDCl₃) δ 7.28 (2 H, br. d, *J* 9.0, 2 × ArCH), 6.82 (2 H, d, *J* 9.0, 2 × ArCH), 6.68 (1 H, s, NH), 5.47 (1 H, s, CH), 5.33 (1 H, br. s, OCH), 3.76 (3 H, s, OCH₃), 1.86 (1 H, d, *J* 18.3, CH_aH_b), 1.81 (1 H, dd, *J* 13.1, 6.0, CH_aH_b), 1.69 (3 H, s, CH₃), 1.67 (1 H, d, *J* 18.3, CH_aH_b), 1.43 (1 H, dd, *J* 13.1, 8.1, CH_aH_b), 1.00 (3 H, s, CH₃), 0.94 (3 H, s, CH₃). **¹³C NMR** (101 MHz, CDCl₃) δ 155.9 (ArCO), 154.0 (CO), 138.2 (C_{quat}), 131.3 (C_{quat}), 120.6 (2 × ArCH), 119.7 (CH), 114.2 (2 × ArCH), 70.9 (CH), 55.5 (OCH₃), 44.1 (CH₂), 41.0 (CH₂), 30.7 (C_{quat}), 30.5 (CH₃), 27.0 (CH₃), 23.7 (CH₃). **HRMS *m/z* (ESI⁺)** *m/z* calcd for C₁₇H₂₃NO₃Na⁺ [M+Na]⁺ 312.1570; found 312.1573.

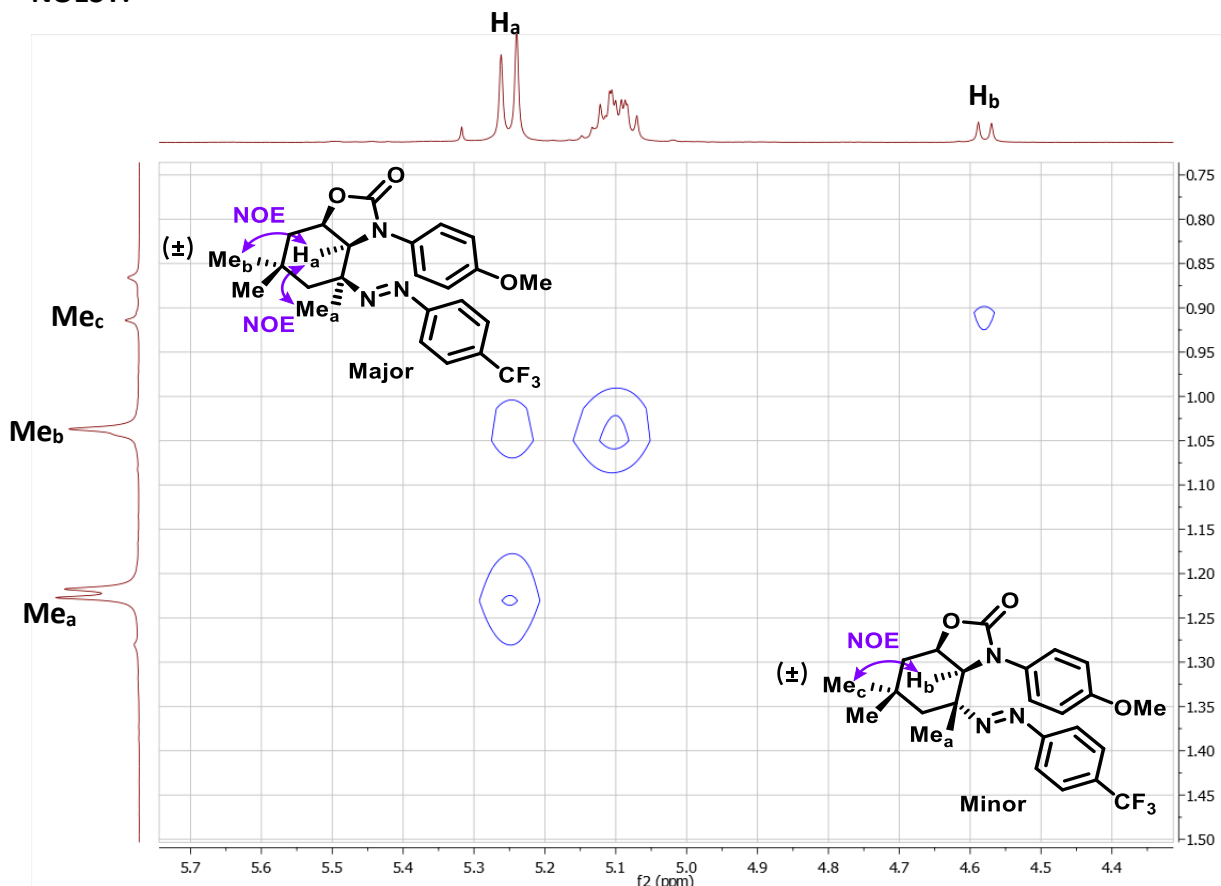
(E)-3-(4-Methoxyphenyl)-4-(1-((4-(trifluoromethyl)phenyl)diazenyl)cyclohexyl)oxazolidin-2-one (519)



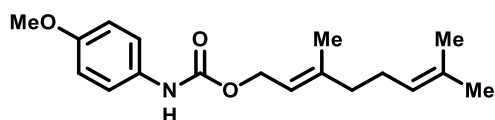
Following GP8 with 3,5,5-trimethylcyclohex-2-en-1-yl (4-methoxyphenyl)carbamate (**518**) (58 mg, 0.2 mmol) used as starting material. Reaction was stirred for 60 minutes and purified by flash column chromatography (SiO₂, 10% to 50% EtOAc in 40-60 petroleum ether) to give the title compound (41 mg, 45%) as an orange solid in a 6.7:1 ratio of inseparable diastereomers.

M.p. 159-161 °C (Et₂O). **IR** (neat, cm⁻¹) ν_{max} = 2952, 1737, 1512, 1407, 1320, 1244, 1169, 1118, 1061, 1038, 824. **¹H NMR** (400 MHz, CDCl₃) δ 7.82 (0.3 H, d, *J* 8.5, 2 × min. ArCH), 7.76 (0.3 H, d, *J* 8.5, 2 × min. ArCH), 7.68 (2 H, d, *J* 8.5, 2 × maj. ArCH), 7.55 (2 H, d, *J* 8.5, 2 × maj. ArCH), 7.29 (2 H, d, *J* 9.0, 2 × maj. ArCH), 7.17 (0.3 H, d, *J* 9.0, 2 × min. ArCH), 6.80-6.78 (0.3 H, m, 2 × min. ArCH), 6.76 (2 H, d, *J* 9.0, 2 × maj. ArCH), 5.23 (1 H, d, *J* 9.0, maj. NCH), 5.12-5.03 (1.3 H, m, maj. OCH + min. OCH), 4.55 (0.15 H, d, *J* 7.4, min. NCH), 3.73 (0.45 H, s, min. OCH₃), 3.69 (3 H, s, maj. OCH₃), 2.11-2.07 (0.15 H, m, min. CH_aH_b), 2.04 (1 H, dd, *J* 14.7, 6.7, maj. CH_aH_b), 1.93-1.87 (0.15 H, m, min. C'H_aH_b), 1.90 (1 H, d, *J* 14.7, maj. C'H_aH_b), 1.85-1.82 (0.15 H, m, min. CH_aH_b), 1.75 (1 H, dd, *J* 14.7, 5.3, maj. CH_aH_b), 1.62 (1 H, d, *J* 14.7, maj. C'H_aH_b), 1.51 (0.15 H, d, *J* 14.7, min. C'H_aH_b), 1.20 (3 H, s, maj. CH₃), 1.19 (3 H, s, maj. CH₃), 1.01 (3.45 H, s, maj. CH₃ + min. CH₃), 0.89 (0.45 H, s, min. CH₃), 0.84 (0.45 H, s, min. CH₃). **¹³C NMR** (101 MHz, CDCl₃) δ 157.7 (min. ArCO), 157.4 (maj. ArCO), 157.2 (min. CO), 156.7 (maj. CO), 153.4 (min. ArCNN), 153.4 (maj. ArCNN), 132.6 (min. C_{quat}, q, *J*_{CF} 32.2), 132.4 (maj. C_{quat}, q, *J*_{CF} 32.2), 131.3 (min. C_{quat}), 131.0 (maj. C_{quat}), 126.7 (min. 2 × ArCH, q, *J*_{CF} 3.8), 126.7 (maj. 2 × ArCH, q, *J*_{CF} 3.8), 126.3 (min. 2 × ArCH), 125.3 (maj. 2 × ArCH), 123.9 (maj. CF₃, q, *J*_{CF} 272.3), 122.9 (min. 2 × ArCH), 122.5 (maj. 2 × ArCH), 114.4 (min. 2 × ArCH), 114.2 (maj. 2 × ArCH), 75.2 (maj. C_{quat}), 74.4 (min. OCH), 73.6 (maj. OCH), 72.3 (min. C_{quat}), 65.1 (min. NCH), 61.0 (maj. NCH), 55.5 (maj. OCH₃), 55.5 (min. OCH₃), 49.7 (min. CH₂), 44.7 (maj. CH₂), 39.3 (min. CH₂), 38.3 (maj. CH₂), 33.0 (maj. CH₃), 33.0 (maj. CH₃), 32.7 (min. CH₃), 31.5 (min. CH₃), 28.9 (min. C_{quat}), 28.7 (maj. C_{quat}), 26.7 (min. CH₃), 22.4 (maj. CH₃). Minor CF₃ signal not observed. **¹⁹F NMR** (377 MHz, CDCl₃) δ -62.6 (3 F, s, maj. CF₃ + min. CF₃). **HRMS** *m/z* (ESI⁺) *m/z* calcd for C₂₄H₂₆F₃N₃O₃Na⁺ [M+Na]⁺ 484.1818; found 484.1807.

NOESY:



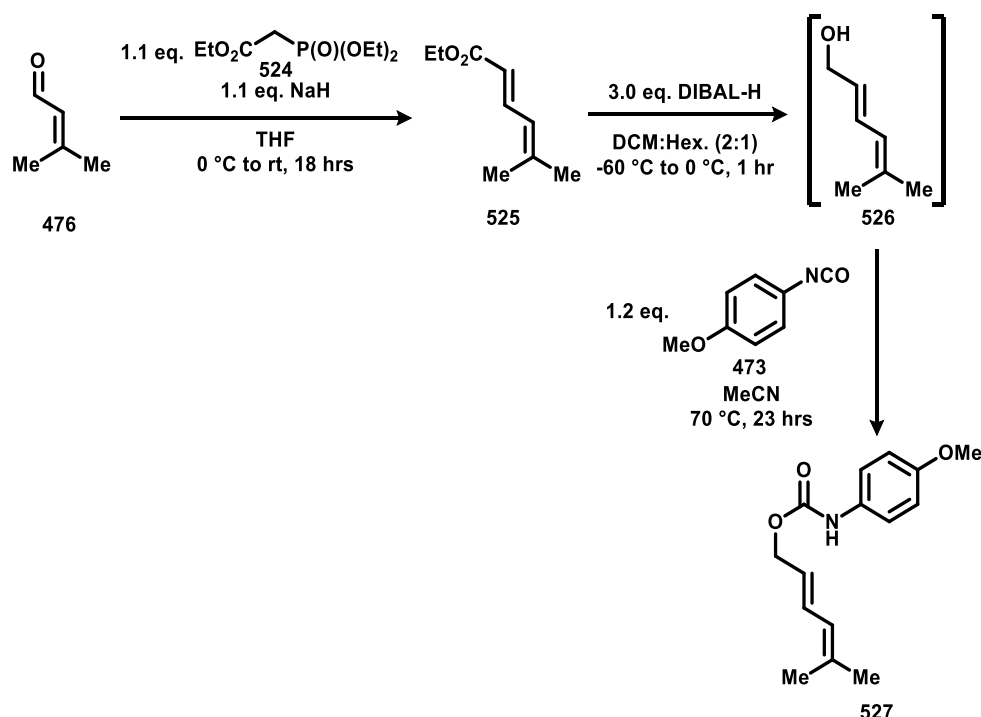
(E)-3,7-Dimethylocta-2,6-dien-1-yl (4-methoxyphenyl)carbamate (522)



Using GP6 and starting materials geraniol (**521**) (0.88 mL, 771 mg, 5.0 mmol) and 4-methoxyphenyl isocyanate (**473**) (0.78 mL, 894 mg, 6.0 mmol), the title compound was synthesised (0.766 g, 50%) as an orange oil.

IR (film, cm^{-1}) ν_{max} = 3323, 2913, 1698, 1512, 1030. **^1H NMR (400 MHz, CDCl_3)** δ 7.28 (2 H, br. d, J 8.9, 2 x ArCH), 6.85 (2 H, d, J 8.9, 2 x ArCH), 6.46 (1 H, br. s, NH), 5.39 (1 H, tq, J 7.2, 1.2, CH), 5.12-5.06 (1 H, m, CH), 4.67 (2 H, d, J 7.1, CH_2), 3.78 (3 H, s, OCH_3), 2.15-2.02 (4 H, m, $\text{CH}_2 + \text{CH}_2$), 1.73 (3 H, s, CH_3), 1.68 (3 H, s, CH_3), 1.61 (3 H, s, CH_3). **^{13}C NMR (126 MHz, CDCl_3)** δ 156.1 (ArCO), 154.1 (CO), 142.6 (C_{quat}), 132.0 (C_{quat}), 131.2 (C_{quat}), 123.9 (CH), 120.7 (2 x ArCH), 118.6 (CH), 114.4 (2 x ArCH), 62.1 (CH_3), 55.7 (OCH_3), 39.7 (CH_2), 26.5 (CH_2), 25.8 (CH_3), 17.8 (CH_3), 16.7 (CH_3). **HRMS m/z (ESI $^+$)** m/z calcd for $\text{C}_{18}\text{H}_{25}\text{NO}_3\text{Na}^+$ $[\text{M}+\text{Na}]^+$ 326.1727; found 326.1736.

(E)-5-Methylhexa-2,4-dien-1-yl (4-methoxyphenyl)carbamate (527)



A solution of 60% sodium hydride in mineral oil (448 mg, 11.2 mmol) in anhydrous THF (15 mL) was prepared in a flame-dried Schlenk tube. The sodium hydride solution was cooled to 0 °C and charged with triethyl phosphonoacetate (**524**) (2.22 mL, 2.51 g, 11.2 mmol) in a dropwise fashion. The mixture was stirred at 0 °C for 20 minutes, then 3-methyl-2-butenal (**476**) (1.18 mL, 858 mg, 10.2 mmol) was added dropwise. The reaction mixture was warmed to room temperature and stirred for 18 hours. The reaction was quenched with saturated $\text{NH}_4\text{Cl}_{(\text{aq})}$ (20 mL) and extracted with ethyl acetate (3 x 10 mL). The combined organic extracts were dried (MgSO_4), concentrated under reduced pressure and purified by flash column chromatography (SiO_2 , 0% to 10% Et_2O in 40-60 petroleum ether) yielding ethyl (E)-5-methylhexa-2,4-dienoate (**525**) (902 mg, 57%) as a yellow oil.

^1H NMR (400 MHz, CDCl_3) δ 7.55 (1 H, dd, J 15.1, 11.6, CH), 5.98 (1 H, d, J 11.6, CH), 5.75 (1 H, d, J 15.1, CH), 4.16 (2 H, q, J 7.1, OCH_2), 1.89 (3 H, s, CH_3), 1.87 (3 H, s, CH_3), 1.29 (3 H, t, J 7.1, CH_3). Data in good agreement with literature.²⁷⁰

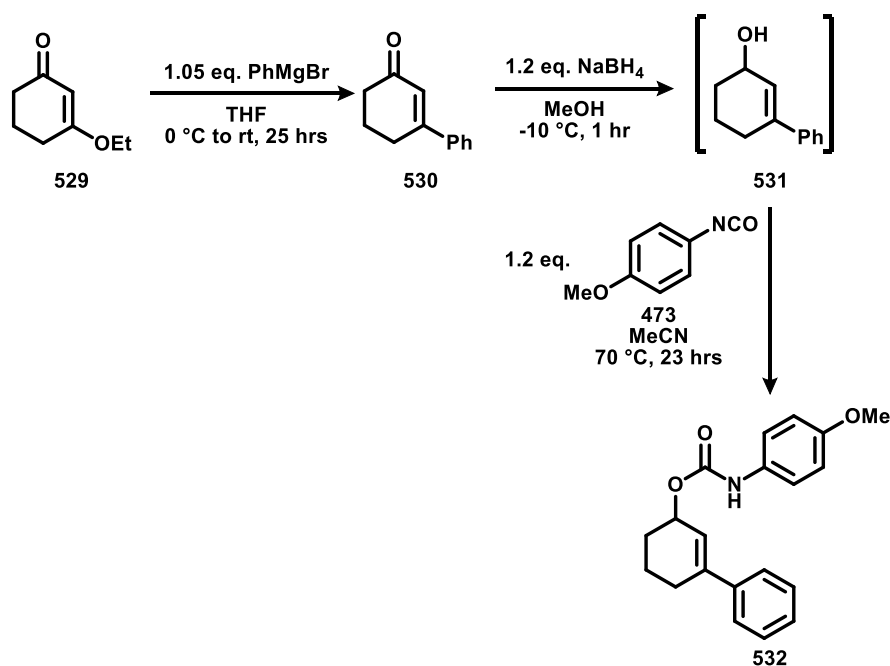
Under a nitrogen atmosphere a flame dried RBF was charged with ethyl (E)-5-methylhexa-2,4-dienoate (**525**) (902 mg, 5.8 mmol) and anhydrous DCM (32 mL), then cooled to -60 °C. 1 M Diisobutylaluminum hydride in hexanes (17.4 mL, 17.4 mmol) was added to the reaction mixture slowly at -60 °C. The reaction mixture was warmed to 0 °C and allowed to stir for one hour. The reaction mixture was quenched with water (5 mL), followed by 15% $\text{NaOH}_{(\text{aq})}$ (5 mL) forming a white precipitate. The mixture was vigorously stirred at room temperature for one hour. Magnesium sulfate was added, the mixture was filtered over a pad of celite and washed with DCM (20 mL). The organic filtrate was concentrated under reduced pressure yielding crude (E)-5-methylhexa-2,4-dien-1-ol (**526**) as a yellow oil, which was used without further purification.

¹H NMR (400 MHz, CDCl₃) δ 6.45 (1 H, dd, *J* 15.1, 10.9, CH), 5.84 (1 H, d, *J* 10.9, CH), 5.71 (1 H, dt, *J* 15.1, 6.1, CH), 4.18 (2 H, d, *J* 6.1, CH₂), 1.78 (3 H, s, CH₃), 1.76 (3 H, s, CH₃). OH not observed. Data in good agreement with literature.²⁷¹

Using GP6 on a 5.8 mmol scale and starting materials crude (*E*)-5-methylhexa-2,4-dien-1-ol (**526**) and 4-methoxyphenyl isocyanate (**473**) (0.90 mL, 1.04 g, 7.0 mmol), the title compound was synthesised (709 mg, 47% over two steps) as a white solid.

M.p. 97-99 °C (Et₂O). **IR (film, cm⁻¹)** ν_{max} = 3312, 2909, 1697, 1511, 1032, 827. **¹H NMR (400 MHz, CDCl₃)** δ 7.28 (2 H, br. d, *J* 8.9, 2 x ArCH), 6.84 (2 H, d, *J* 8.9, 2 x ArCH), 6.62 (1 H, br. s, NH), 6.53 (1 H, dd, *J* 15.2, 11.1, CH), 5.84 (1 H, d, *J* 11.1, CH), 5.66 (1 H, dt, *J* 15.2, 6.7, CH), 4.68 (2 H, d, *J* 6.7, CH₂), 3.77 (3 H, s, OCH₃), 1.79 (3 H, s, CH₃), 1.77 (3 H, s, CH₃). **¹³C NMR (126 MHz, CDCl₃)** δ 156.1 (ArCO), 153.9 (CO), 137.6 (C_{quat}), 131.5 (CH), 131.1 (C_{quat}), 124.1 (CH), 123.8 (CH), 120.8 (2 x ArCH), 114.3 (2 x ArCH), 66.1 (CH₂), 55.6 (OCH₃), 26.2 (CH₃), 18.5 (CH₃). **HRMS *m/z* (ESI⁺)** *m/z* calcd for C₁₅H₁₉NO₃Na⁺ [M+Na]⁺ 284.1257; found 284.1257.

3,4,5,6-Tetrahydro-[1,1'-biphenyl]-3-yl (4-methoxyphenyl)carbamate (x-x-x)



Under a nitrogen atmosphere a flame-dried Schlenk tube was charged with 3 M phenyl magnesium bromide (5 mL, 15.0 mmol) in diethyl ether and anhydrous THF (10 mL). The Schlenk tube was cooled to 0 °C and a solution of 3-ethoxycyclohex-2-enone (**529**) (1.92 mL, 2.0 g, 14.3 mmol) in anhydrous THF (2 mL) was added slowly while stirring. The reaction mixture was warmed to room temperature and allowed to stir for 25 hours. The reaction was quenched with 1 M HCl (50 mL) and extracted with DCM (3 x 50 mL). The combined organic extracts were dried (MgSO₄), concentrated under reduced pressure and purified by flash column chromatography (SiO₂, 0% to 50% Et₂O in 40-60 petroleum ether) to yield 5,6-dihydro-[1,1'-biphenyl]-3(4H)-one (**530**) (2.15 g, 87%) as a white solid.

¹H NMR (400 MHz, CDCl₃) δ 7.56-7.51 (2 H, m, 2 x ArCH), 7.44-7.39 (3 H, m, 3 x ArCH), 6.42 (1 H, t, *J* 1.4, CH), 2.78 (2 H, td, *J* 6.2, 1.4, CH₂), 2.49 (2 H, t, *J* 6.2, CH₂), 2.16 (2 H, qn, *J* 6.2, CH₂). Data in good agreement with literature.²⁷²

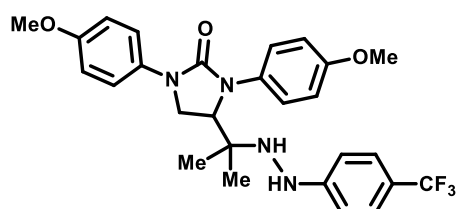
A flame-dried 250 mL RBF was charged with 5,6-dihydro-[1,1'-biphenyl]-3(4H)-one (**530**) (2.15 g, 12.5 mmol), flushed with nitrogen and charged with methanol (70 mL). The reaction mixture was cooled to -10 °C, then under stirring sodium borohydride (568 mg, 15.0 mmol) was added in portions. The reaction mixture was stirred for 1 hour at -10 °C, then quenched with saturated NH₄Cl_(aq) (100 mL) and extracted with diethyl ether (2 x 100 mL). The combined organic extracts were washed with brine (2 x 50 mL), dried (MgSO₄) and concentrated under reduced pressure to yield crude 3,4,5,6-tetrahydro-[1,1'-biphenyl]-3-ol (**531**) as a brown solid, which was used without further purification.

¹H NMR (400 MHz, CDCl₃) δ 7.43-7.39 (2 H, m, 2 x ArCH), 7.36-7.30 (2 H, m, 2 x ArCH), 7.26 (1 H, tt, *J* 7.2, 1.4, ArCH), 6.13 (1 H, dt, *J* 3.6, 1.8, CH), 4.43-4.37 (1 H, m, CH), 2.52-2.43 (1 H, m, CH_aH_b), 2.41-2.32 (1 H, m, CH_aH_b), 2.00-1.85 (2 H, m, CH₂), 1.80-1.63 (2 H, m, CH₂). OH not observed. Data in good agreement with literature.²⁷³

Using GP6 on a 12.5 mmol scale and starting materials crude 3,4,5,6-tetrahydro-[1,1'-biphenyl]-3-ol (**531**) and 4-methoxyphenyl isocyanate (**473**) (1.95 mL, 2.24 g, 15.0 mmol), the title compound was synthesised (1.42 g, 35% over two steps) as a brown solid.

M.p. 108-110 °C (Et₂O). **IR** (film, cm⁻¹) ν_{max} = 3316, 2936, 1693, 1512, 1215, 1030. **¹H NMR** (400 MHz, CDCl₃) δ 7.39-7.37 (2 H, m, 2 x ArCH), 7.33-7.22 (5 H, m, ArCH + 2 x ArCH + 2 x ArCH), 6.81 (2 H, d, *J* 9.0, 2 x ArCH), 6.74 (1 H, br. s, NH), 6.15 (1 H, dt, *J* 3.9, 1.6, CH), 5.46 (1 H, *J*, br. q, 4.0, CH), 3.74 (3 H, s, OCH₃), 2.54-2.44 (1 H, m, CH_aH_b), 2.39-2.29 (1 H, m, CH_aH_b), 1.99-1.74 (4 H, m, CH₂ + CH₂). **¹³C NMR** (126 MHz, CDCl₃) δ 155.9 (ArCO), 153.9 (CO), 142.1 (C_{quat}), 141.0 (C_{quat}), 131.2 (C_{quat}), 128.4 (2 x ArCH), 127.7 (ArCH), 125.5 (2 x ArCH), 122.6 (CH), 120.7 (2 x ArCH), 114.2 (2 x ArCH), 69.6 (CH), 55.5 (OCH₃), 28.3 (CH₂), 27.4 (CH₂), 19.4 (CH₂). **HRMS *m/z* (ESI⁺)** *m/z* calcd for C₂₀H₂₁NO₃Na⁺ [M+Na]⁺ 346.1414; found 346.1415.

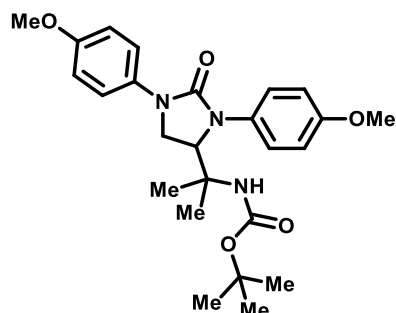
1,3-Bis(4-methoxyphenyl)-4-(2-(2-(4-(trifluoromethyl)phenyl)hydrazineyl)propan-2-yl)imidazolidin-2-one (539**)**



A 10 mL RBF was charged with (*E*)-1,3-bis(4-methoxyphenyl)-4-(2-((4-(trifluoromethyl)phenyl)diazene)propan-2-yl)imidazolidin-2-one (**488**) (102 mg, 0.2 mmol), methanol (5 mL) and 10 wt% palladium on carbon (42 mg, 0.4 mmol). The reaction mixture was exposed to an atmosphere of hydrogen and stirred at room temperature for 16 hours. The reaction mixture was filtered through celite, concentrated under reduced pressure and purified by flash column chromatography (0% to 100% Et₂O in 40-60 petroleum ether) to give title compound (101 mg, 98%.) as a white solid.

M.p. 157-159 °C (Et₂O). **IR** (film, cm⁻¹) ν_{max} = 3302, 2974, 1693, 1617, 1321, 1245, 1105. **¹H NMR** (400 MHz, CDCl₃) δ 7.50 (2 H, d, *J* 9.2, 2 x ArCH), 7.39-7.35 (4 H, m, 4 x ArCH), 6.95 (2 H, d, *J* 9.0, 2 x ArCH), 6.91 (2 H, d, *J* 9.2, 2 x ArCH), 6.79 (2 H, d, *J* 8.6, 2 x ArCH), 5.00 (1 H, br. s, NH), 4.40 (1 H, dd, *J* 9.5, 4.6, CH), 4.03 (1 H, t, *J* 9.5, CH_aH_b), 3.86 (1 H, dd, *J* 9.5, 4.6, CH_aH_b), 3.80 (6 H, s, OCH₃ + OCH₃), 3.26 (1 H, br. s, NH), 1.09 (3 H, s, CH₃), 1.07 (3 H, s, CH₃). **¹³C NMR** (126 MHz, CDCl₃) δ 158.0 (ArCO), 156.9 (CO), 155.7 (ArCO), 152.9 (ArCNN, *q*, *J*_{CF} 1.1), 133.4 (C_{quat}), 133.0 (C_{quat}), 126.9 (2 x ArCH), 126.5 (2 x ArCH, *q*, *J*_{CF} 3.8), 124.9 (CF₃, *q*, *J*_{CF} 271.1), 120.7 (C_{quat}, *q*, *J*_{CF} 32.6), 119.7 (2 x ArCH), 114.9 (2 x ArCH), 114.3 (2 x ArCH), 121.1 (2 x ArCH), 60.3 (C_{quat}), 58.9 (CH), 55.7 (OCH₃), 55.6 (OCH₃), 45.9 (CH₂), 21.7 (CH₃), 21.6 (CH₃). **¹⁹F NMR** (377 MHz, CDCl₃) δ -61.1 (3 F, s, CF₃). **HRMS *m/z* (ESI⁺)** *m/z* calcd for C₂₇H₃₀F₃N₄O₃⁺ [M+H]⁺ 515.2265; found 515.2256.

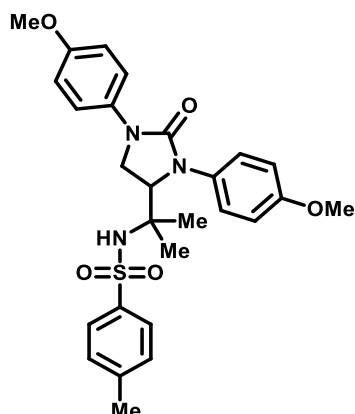
***tert*-Butyl (2-(1,3-bis(4-methoxyphenyl)-2-oxoimidazolidin-4-yl)propan-2-yl)carbamate (540)**



A 10 mL RBF was charged with (*E*)-1,3-bis(4-methoxyphenyl)-4-(2-((4-(trifluoromethyl)phenyl)diazenyl)propan-2-yl)imidazolidin-2-one (**488**) (102 mg, 0.2 mmol), methanol (5 mL) and 10 wt% palladium on carbon (42 mg, 0.4 mmol). The reaction mixture was exposed to an atmosphere of hydrogen and stirred at room temperature for 4 hours. Concentrated HCl_(aq) (1 mL) was added to the reaction mixture then re-exposed to an atmosphere of hydrogen for 1.5 hours at room temperature with stirring. The reaction mixture was filtered through celite and concentrated under reduced pressure to give a colourless residue, which was dissolved in DCM (4 mL) and water (0.5 mL). Potassium carbonate (138 mg, 1.0 mmol) and di-*tert*-butyl decarbonate (131 mg, 0.6 mmol) were added to the reaction mixture, which was stirred for 21 hours at room temperature. The reaction was quenched with water (20 mL) and extracted with DCM (3 x 20 mL). The combined organic extracts were dried (Na₂SO₄) and concentrated under reduced pressure to give a yellow residue, which was purified by flash column chromatography (0% to 50% EtOAc in 40-60 petroleum ether) to give the title compound (56 mg, 62%) as a white solid.

M.p. 151-154 °C (CDCl₃). **IR** (neat, cm⁻¹) ν_{max} = 3292, 2977, 1699, 1678, 1508, 1410, 1243, 1157, 1075, 829. **¹H NMR** (400 MHz, CDCl₃) δ 7.49 (2 H, d, *J* 9.1, 2 x ArCH), 7.31 (2 H, d, *J* 8.8, 2 x ArCH), 6.95-6.84 (4 H, m, 4 x ArCH), 5.06 (1 H, br. s, CH), 4.35 (1 H, s, NH), 4.01 (1 H, t, *J* 9.8, CH_aH_b), 3.80 (3 H, s, OCH₃), 3.79 (3 H, s, OCH₃), 3.68 (1 H, dd, *J* 9.8, 4.5, CH_aH_b), 1.35 (9 H, s, C(CH₃)₃), 1.27 (3 H, s, CH₃), 1.16 (3 H, s, CH₃). **¹³C NMR** (101 MHz, CDCl₃) δ 157.4 (ArCO), 156.8 (CO), 155.4 (ArCO), 154.2 (CO), 133.4 (C_{quat}), 132.9 (C_{quat}), 126.5 (2 x ArCH), 119.5 (2 x ArCH), 114.4 (2 x ArCH), 114.1 (2 x ArCH), 79.3 (C_{quat}), 57.6 (CH), 56.1 (C_{quat}), 55.5 (OCH₃), 55.4 (OCH₃), 45.4 (CH₂), 28.4 (C(CH₃)₃), 24.0 (CH₃), 23.1 (CH₃). **HRMS *m/z* (ESI⁺)** *m/z* calcd for C₂₅H₃₃N₃O₅Na⁺ [M+Na]⁺ 478.2312; found 478.2312.

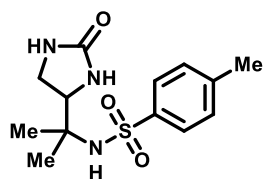
***N*-(2-(1,3-Bis(4-methoxyphenyl)-2-oxoimidazolidin-4-yl)propan-2-yl)-4-methylbenzenesulfonamide (541)**



A 10 mL RBF was charged with (*E*)-1,3-bis(4-methoxyphenyl)-4-(2-((4-(trifluoromethyl)phenyl)diazanyl)propan-2-yl)imidazolidin-2-one (**488**) (102 mg, 0.2 mmol), methanol (5 mL) and 10 wt% palladium on carbon (42 mg, 0.04 mmol). The reaction mixture was exposed to an atmosphere of hydrogen and stirred at room temperature for 4 hours. Concentrated aqueous HCl (1 mL) was added to the reaction mixture, then re-exposed to an atmosphere of hydrogen for 1.5 hours at room temperature with stirring. The reaction mixture was filtered through Celite and concentrated under reduced pressure to give a colourless residue. The hydrogenated residue was dissolved in DCM (5 mL), then charged with triethylamine (0.14 mL, 1.0 mmol,) and *p*-toluenesulfonyl chloride (114 mg, 0.6 mmol). The reaction mixture was stirred for 18 hours at room temperature. The reaction mixture was charged with additional triethylamine (1.0 mmol, 5.0 eq., 0.14 mL) and *p*-toluenesulfonyl chloride (114 mg, 0.6 mmol), then stirred at room temperature for an additional 18 hours. The reaction was quenched with water (10 mL) and extracted with ethyl acetate (3 x 20 mL). The combined organic extracts were dried (Na₂SO₄) and concentrated under reduced pressure to give a yellow residue, which was purified by flash column chromatography (0% to 50% EtOAc in 40-60 petroleum ether) to give the title compound (68 mg, 67%) as a white solid.

M.p. 170-173 °C (CDCl₃). **IR (film, cm⁻¹)** ν_{max} = 3281, 2921, 1687, 1510, 1433, 1246, 1161, 830. **¹H NMR (400 MHz, CDCl₃)** δ 7.67 (2 H, d, *J* 8.3, 2 x ArCH), 7.44 (2 H, d, *J* 9.0, 2 x ArCH), 7.28 (2 H, d, *J* 9.0, 2 x ArCH), 7.22 (2 H, d, *J* 8.3, 2 x ArCH), 6.93-6.84 (4 H, m, 4 x ArCH), 5.03 (1 H, s, NH), 4.53 (1 H, dd, *J* 9.5, 4.5, CH), 3.95 (1 H, t, *J* 9.5, CH_aH_b), 3.82-3.76 (7 H, m, 2 x OCH₃ + CH_aH_b), 2.39 (3 H, s, CH₃), 1.08 (3 H, s, CH₃), 0.99 (3 H, s, CH₃). **¹³C NMR (101 MHz, CDCl₃)** δ 157.8 (ArCO), 156.8 (CO), 155.7 (ArCO), 143.4 (C_{quat}), 140.2 (C_{quat}), 133.1 (C_{quat}), 132.8 (C_{quat}), 129.8 (2 x ArCH), 127.0 (2 x ArCH), 126.7 (2 x ArCH), 199.9 (2 x ArCH), 114.6 (2 x ArCH), 114.3 (2 x ArCH), 61.2 (CH), 59.9 (C_{quat}), 55.7 (OCH₃), 55.6 (OCH₃), 45.5 (CH₂), 25.0 (CH₃), 23.7 (CH₃), 21.6 (CH₃). **HRMS m/z (ESI⁺)** m/z calcd for C₂₇H₃₂N₃O₅S⁺ [M+H]⁺ 510.2057; found 510.2056.

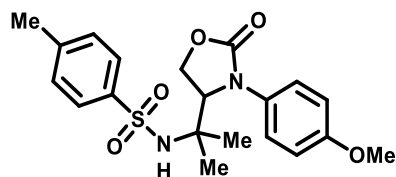
4-Methyl-*N*-(2-(2-oxoimidazolidin-4-yl)propan-2-yl)benzenesulfonamide (**544**)



A 10 mL RBF was charged with *N*-(2-(1,3-bis(4-methoxyphenyl)-2-oxoimidazolidin-4-yl)propan-2-yl)-4-methylbenzenesulfonamide (**541**) (68 mg, 0.13 mmol) and acetonitrile (3 mL). The mixture was cooled to 0 °C and a solution of ceric ammonium nitrate (367 mg, 0.67 mmol) dissolved in water (3 mL) was added drop wise over 3 minutes. The reaction mixture was stirred at 0 °C for 1 hour, then quenched with water (10 mL) and extracted with ethyl acetate (3 x 10 mL). The combined organic extracts were dried (Na₂SO₄) and concentrated under reduced pressure to give an orange residue, which was purified by flash column chromatography (0% to 10% MeOH in DCM) to give the title compound (25 mg, 63%) as a colourless film.

IR (film, cm⁻¹) ν_{\max} = 3266, 2923, 1689, 1318, 1147, 1093, 663, 556. **¹H NMR (400 MHz, CDCl₃)** δ 7.84 (2 H, d, *J* 8.3, 2 x ArCH), 7.26 (2 H, d, *J* 8.3, 2 x ArCH), 7.12 (1 H, br. s, NH), 6.74 (1 H, br. s, NH), 6.01 (1 H, br. s, NH), 3.65-3.57 (1 H, m, CH), 3.50-3.38 (2 H, m, CH₂), 2.41 (3 H, s, CH₃), 1.16 (3 H, s, CH₃), 1.13 (3 H, s, CH₃). **¹³C NMR (101 MHz, CDCl₃)** δ 165.0 (CO), 142.9 (C_{quat}), 140.8 (C_{quat}), 129.6 (2 x ArCH), 127.1 (2 x ArCH), 62.7 (CH), 57.6 (C_{quat}), 42.2 (CH₂), 26.5 (CH₃), 21.7 (CH₃), 21.6 (CH₃). **HRMS *m/z* (ESI⁺)** *m/z* calcd for C₁₃H₁₉N₃O₃SN⁺ [M+Na]⁺ 320.1040; found 320.1039.

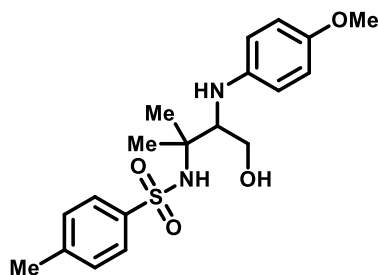
***N*-(2-(3-(4-Methoxyphenyl)-2-oxooxazolidin-4-yl)propan-2-yl)-4-methylbenzenesulfonamide (547)**



A 10 mL RBF was charged (*E*)-3-(4-methoxyphenyl)-4-(2-((4-(trifluoromethyl)phenyl)diazenyl)propan-2-yl)oxazolidin-2-one (**511**) (82 mg, 0.2 mmol), methanol (5 mL) and 10 wt% palladium on carbon (42 mg, 0.04 mmol). The reaction mixture was exposed to an atmosphere of hydrogen and stirred at room temperature for 4 hours. Concentrated aqueous HCl (1 mL) was added to the reaction mixture then exposed again to an atmosphere of hydrogen for 1.5 hours at room temperature with stirring. The reaction mixture was filtered through Celite and concentrated under reduced pressure to give a colourless residue, which was dissolved in DCM (5 mL). Triethylamine (0.14 mL, 1.0 mmol) and *p*-toluenesulfonyl chloride (114 mg, 0.6 mmol) were added to the reaction mixture, which was stirred for 18 hours at room temperature. The reaction was quenched with water (10 mL) and extracted with ethyl acetate (3 x 10 mL). The combined organic extracts were dried (Na₂SO₄) and concentrated under reduced pressure to give a colourless residue, which was purified by flash column chromatography (0% to 100% EtOAc in 40-60 petroleum ether) to give the title compound (43 mg, 53%) as a white solid.

M.p. 111-113 °C (CDCl₃). **IR (film, cm⁻¹)** ν_{\max} = 3256, 2983, 1732, 1513, 1248, 1131, 727. **¹H NMR (400 MHz, CDCl₃)** δ 7.65 (2 H, d, *J* 8.2, 2 x ArCH), 7.28-7.19 (4 H, m, 4 x ArCH), 6.85 (2 H, d, *J* 8.8, 2 x ArCH), 5.32 (1 H, s, NH), 4.66 (1 H, t, *J* 6.2, CH), 4.39 (2 H, d, *J* 6.3, CH₂), 3.75 (3 H, s, OCH₃), 2.37 (3 H, s, CH₃), 1.07 (3 H, s, CH₃), 0.85 (3 H, s, CH₃). **¹³C NMR (101 MHz, CDCl₃)** δ 158.0 (ArCO), 157.4 (CO), 143.6 (C_{quat}), 140.0 (C_{quat}), 130.8 (C_{quat}), 129.8 (2 x ArCH), 126.9 (2 x ArCH), 126.0 (2 x ArCH), 114.7 (2 x ArCH), 64.5 (CH₂), 63.8 (CH), 59.4 (C_{quat}), 55.6 (OCH₃), 25.4 (CH₃), 22.4 (CH₃), 21.6 (CH₃). **HRMS *m/z* (ESI⁺)** *m/z* calcd for C₂₀H₂₅N₂O₅S⁺ [M+H]⁺ 405.1479; found 405.1474.

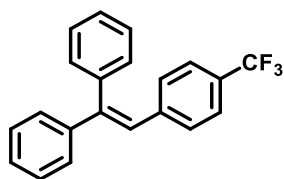
***N*-(4-Hydroxy-3-((4-methoxyphenyl)amino)-2-methylbutan-2-yl)-4-methylbenzenesulfonamide (548)**



A 5 mL RBF was charged with *N*-(2-(3-(4-methoxyphenyl)-2-oxooxazolidin-4-yl)propan-2-yl)-4-methylbenzenesulfonamide (**547**) (40 mg, 0.1 mmol), ethanol (1 mL) and sodium hydroxide (40 mg 1.0 mmol). The reaction mixture was heated to 80 °C for 15 hours. The reaction mixture was concentrated under reduced pressure and the crude residue was dissolved in water (10 mL). The pH of the aqueous solution was adjusted to 7 by addition of aqueous hydrochloric acid (1 M), then extracted with ethyl acetate (3 x 10 mL). The combined organic extracts were dried (Na₂SO₄) and concentrated under reduced pressure to give the title compound (33 mg, 93%) as a red film.

IR (film, cm⁻¹) ν_{max} = 3271, 2929, 1510, 1234, 1145, 1092, 815, 659, 548. **¹H NMR (400 MHz, CDCl₃)** δ 7.78 (2 H, d, *J* 7.8, 2 x ArCH), 7.28 (2 H, d, *J* 7.8, 2 x ArCH), 6.74 (2 H, d, *J* 8.2, 2 x ArCH), 6.59 (2 H, d, *J* 8.2, 2 x ArCH), 5.86 (1 H, s, NH), 3.85-3.79 (2 H, m, CH₂), 3.73 (3 H, s, OCH₃), 3.37-2.92 (3 H, m, CH + OH + NH), 2.41 (3 H, s, CH₃), 1.25 (3 H, s, CH₃), 1.24 (3 H, s, CH₃). **¹³C NMR (101 MHz, CDCl₃)** δ 152.7 (ArCO), 143.1 (C_{quat}), 142.2 (C_{quat}), 140.4 (C_{quat}), 129.8 (2 x ArCH), 127.1 (2 x ArCH), 115.4 (2 x ArCH), 115.1 (2 x ArCH), 64.0 (CH), 61.4 (CH₂), 60.2 (C_{quat}), 55.9 (OCH₃), 26.4 (CH₃), 25.0 (CH₃), 21.6 (CH₃). **HRMS *m/z* (ESI⁺)** *m/z* calcd for C₁₉H₂₆N₂O₄Na⁺ [M+Na]⁺ 401.1500; found 401.1505.

(2-(4-(Trifluoromethyl)phenyl)ethene-1,1-diyl)dibenzene (552)



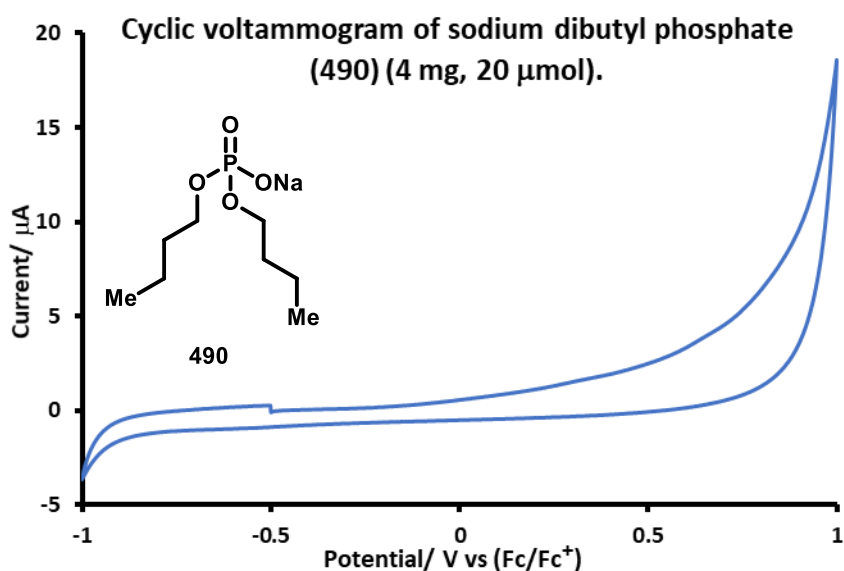
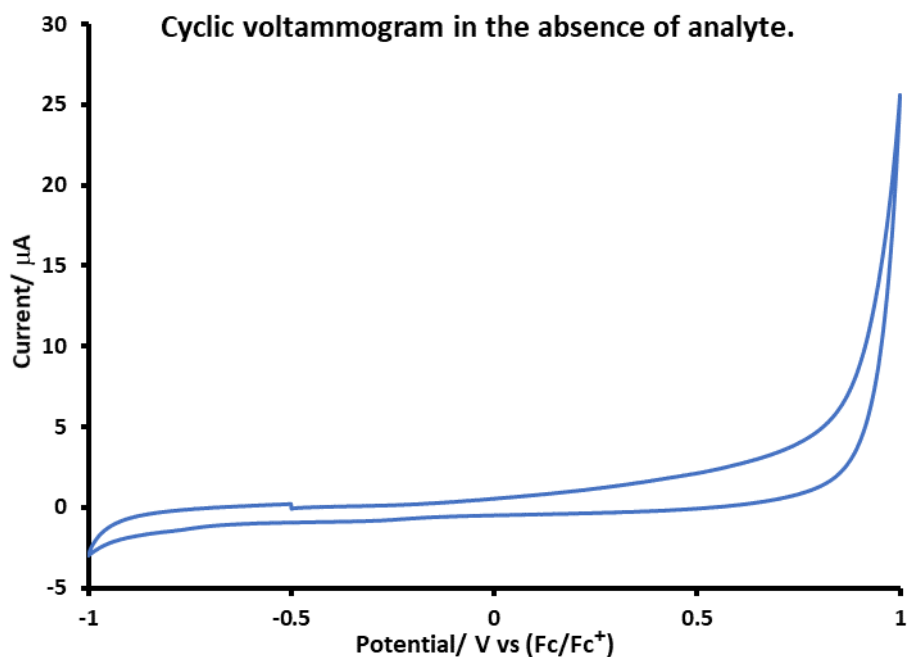
A flame-dried 10 mL microwave vial was charged with 3-methylbut-2-en-1-yl (4-methoxyphenyl)carbamate (**474**) (47 mg, 0.2 mmol), sodium dibutyl phosphate (**490**) (93 mg, 0.2 mmol) and 4-(trifluoromethyl)benzenediazonium tetrafluoroborate (**463**) (104 mg, 0.4 mmol), then flushed with nitrogen and charged with a solution of ethene-1,1-diyl dibenzene (**338**) (0.11 mL, 0.6 mmol) in anhydrous DMSO (1 mL). The reaction mixture was stirred at room temperature for 2 hours. The reaction was quenched with water (5 mL) and extracted with ethyl acetate (3 x 3 mL). The combined organic extracts were concentrated under reduced pressure. The obtained crude material was analysed by ^{19}F NMR and yields were calculated by use of α,α,α -trifluorotoluene as an internal standard (0.2 mmol), indicating the presence of (*E*)-3-(4-methoxyphenyl)-4-(2-((4-(trifluoromethyl)phenyl)diaz-enyl)propan-2-yl)oxazolidin-2-one (**511**) (13%) and (2-(4-(trifluoromethyl)phenyl)ethene-1,1-diyl)dibenzene (**552**) (44%). Isolation of the title compounds was attempted by flash column chromatography (SiO_2 , 0% to 1% Et_2O in *n*-pentane), but could not be separated from ethene-1,1-diyl dibenzene (**338**) starting material.

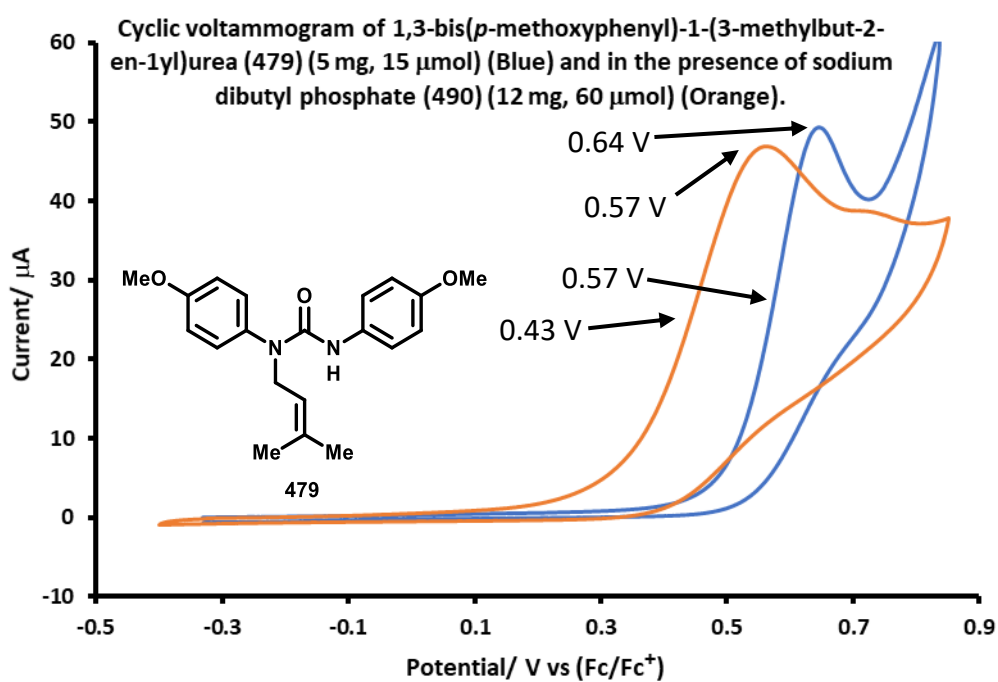
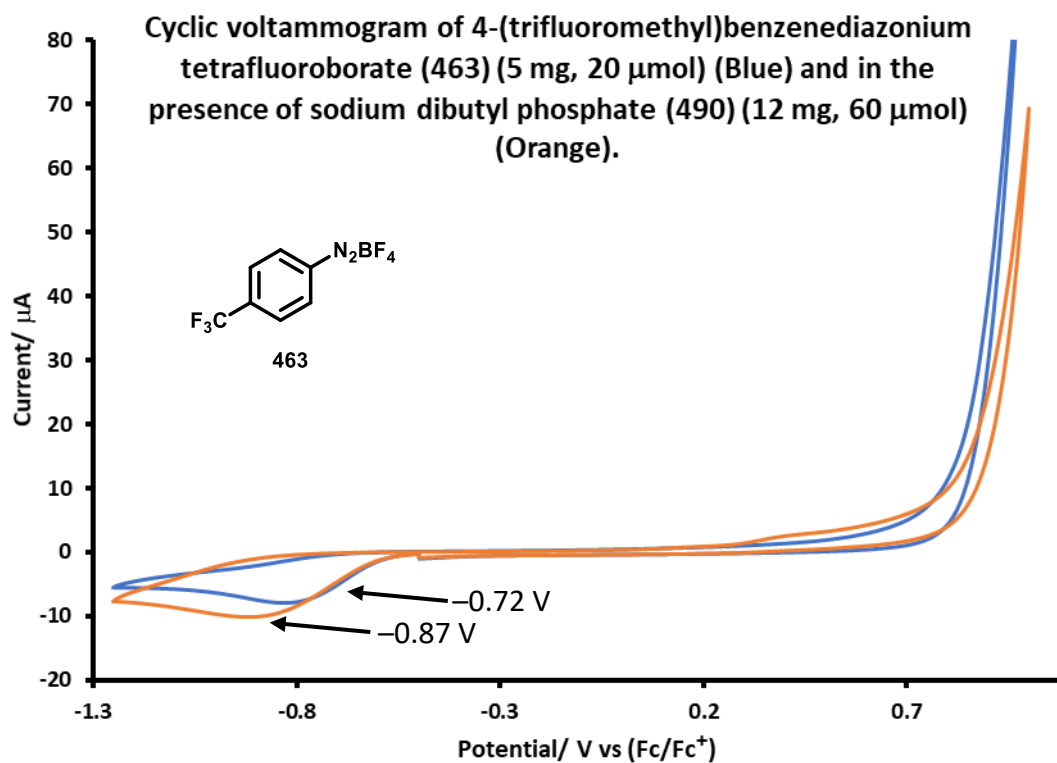
^1H NMR (400 MHz, CDCl_3) δ 7.38-7.30 (10 H, m, 10 x ArCH), 7.21-7.17 (2 H, m, 2 x ArCH), 7.11 (2 H, d, *J* 8.3, 2 x ArCH), 6.98 (1 H, s, CH). ^{19}F NMR (377 MHz, CDCl_3) δ -62.5 (3 F, s, CF_3). LRMS m/z (EI^+) m/z calcd for $\text{C}_{21}\text{H}_{15}\text{F}_3^+$ [$\text{M}+\text{Na}$] $^+$ 324.11; found 324.11. Data in good agreement with literature.²⁷⁴

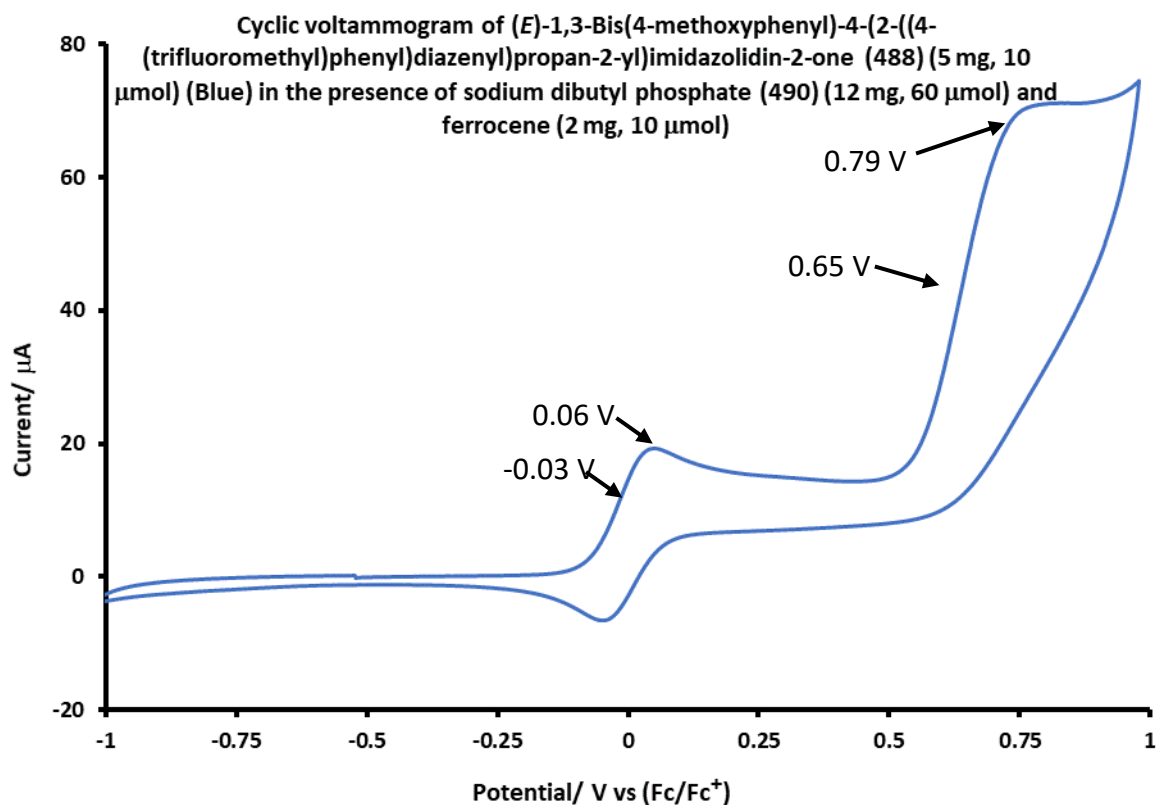
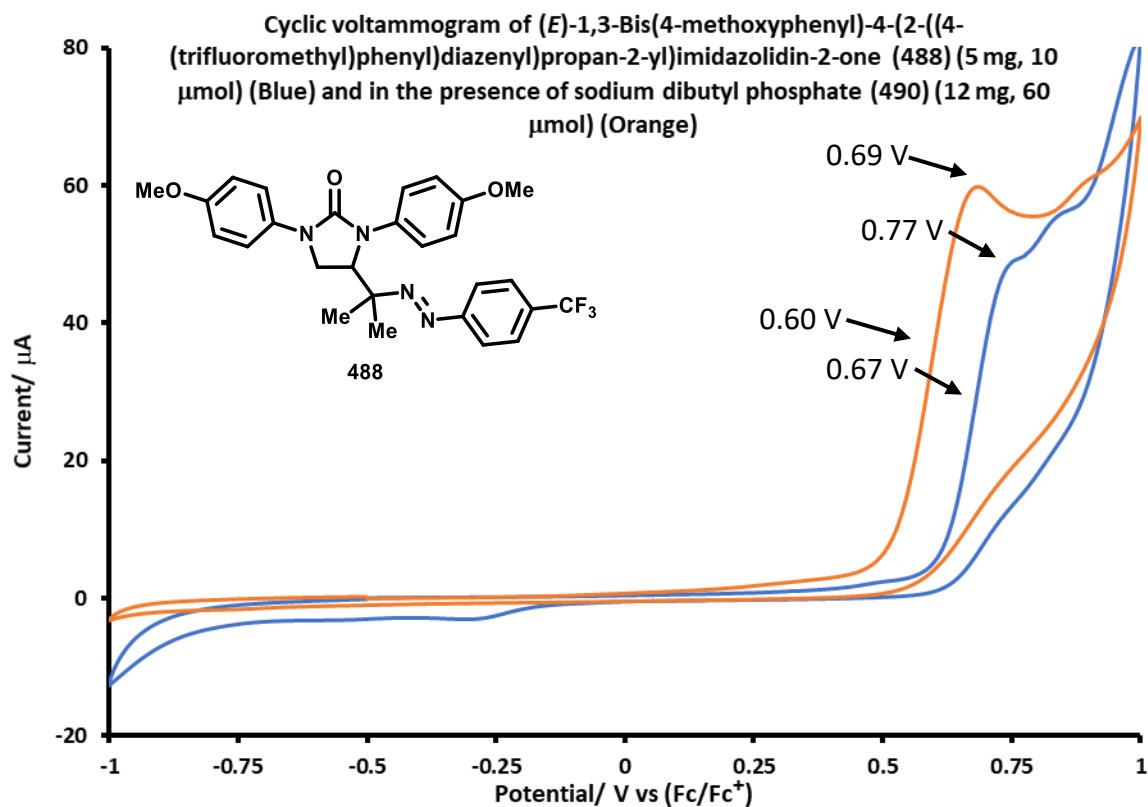
8.3.3 Cyclic Voltammetry Data

8.3.3.1 Initial Investigation

Analyte was added to a 0.1 M solution of tetra-*n*-butylammonium hexafluorophosphate in dry, degassed DMSO (5 mL). Experiments were run using a glassy carbon working electrode, a platinum mesh counter electrode and a silver wire reference electrode, at scan rate of 100 mV/s.

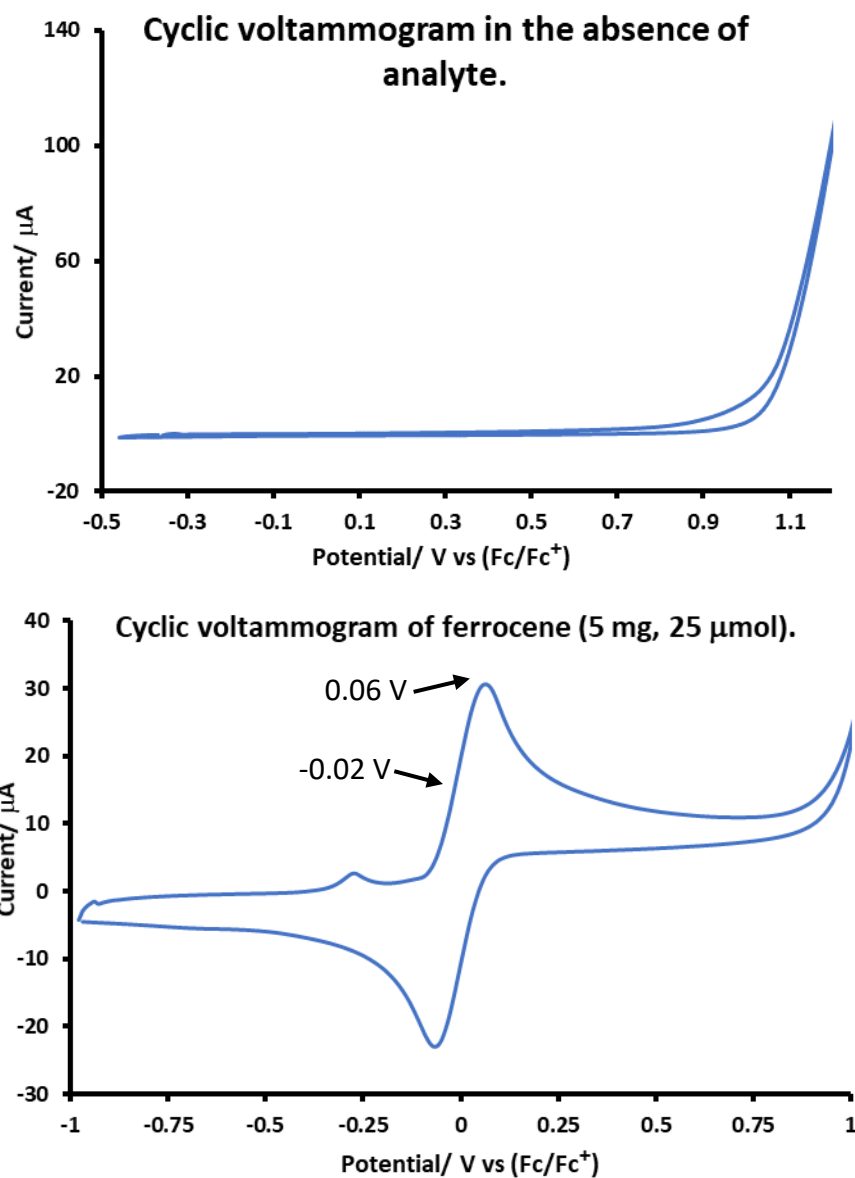


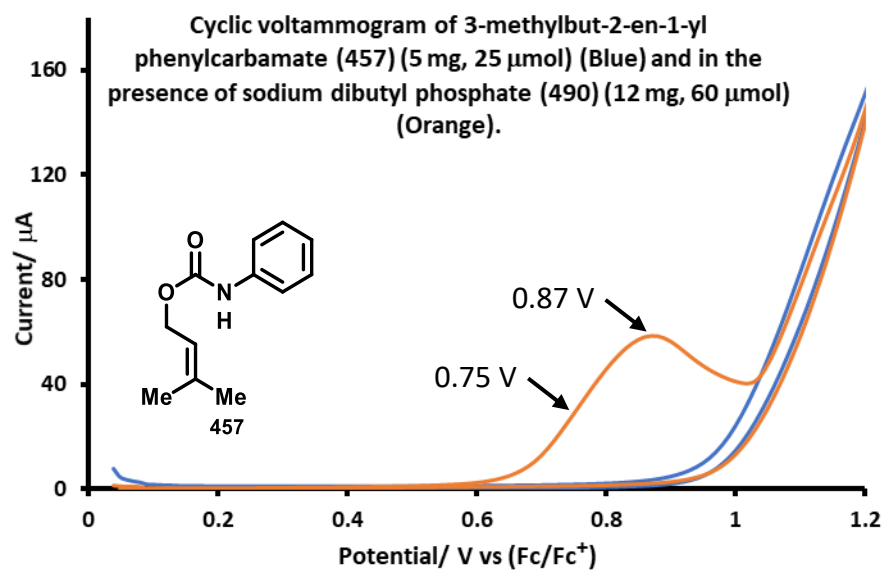
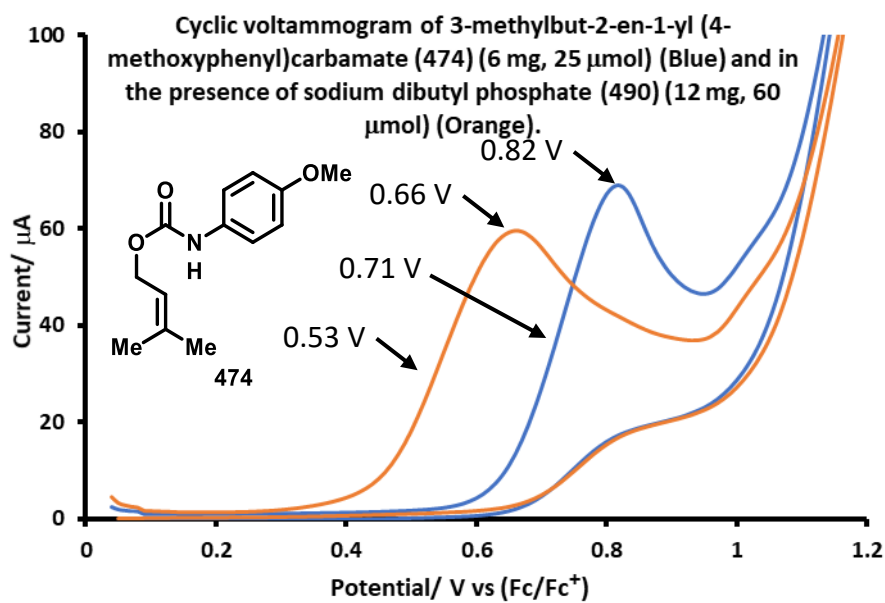


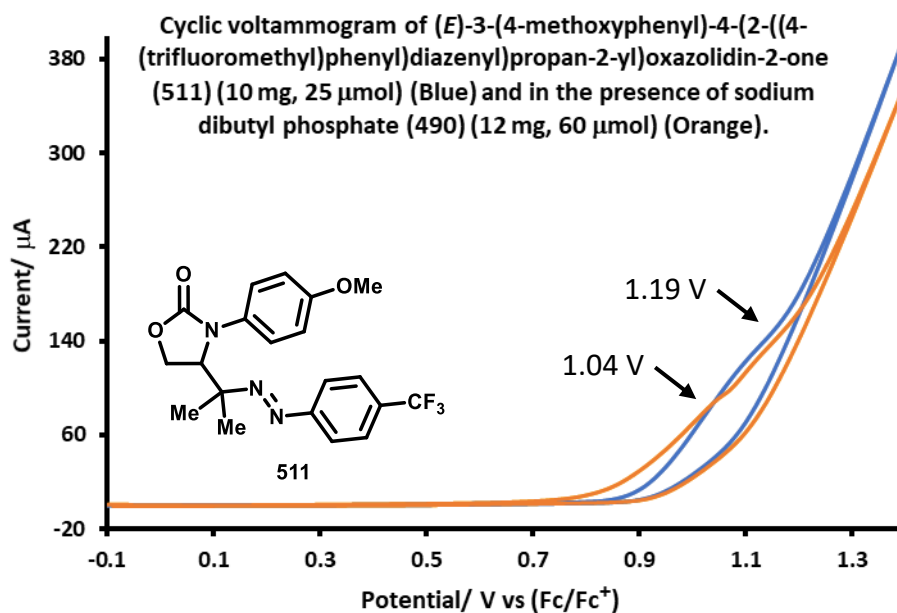
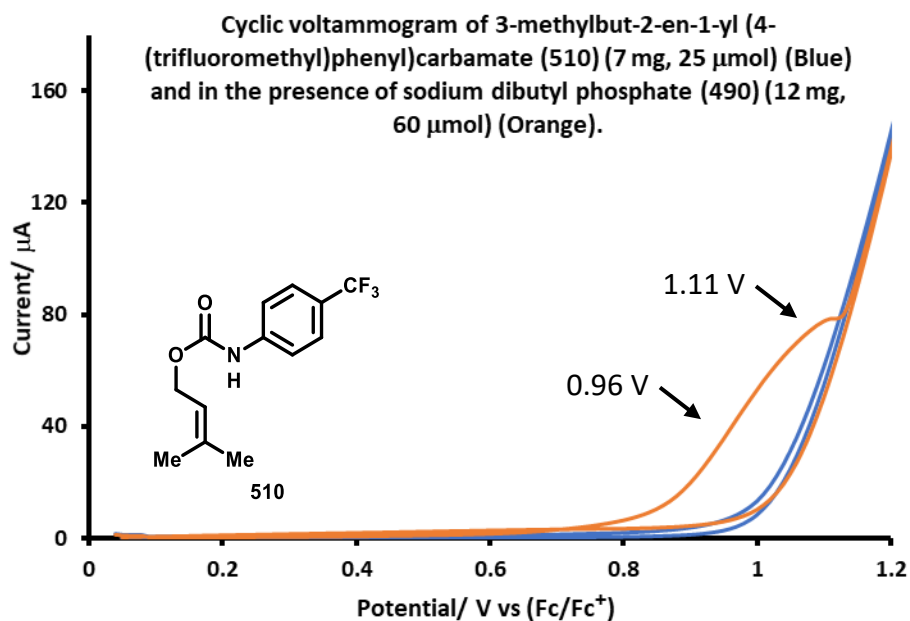


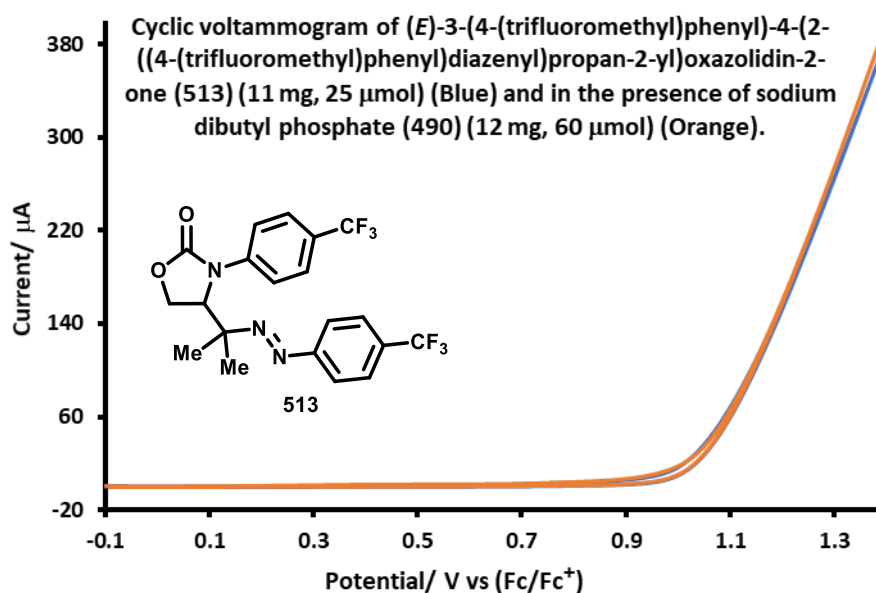
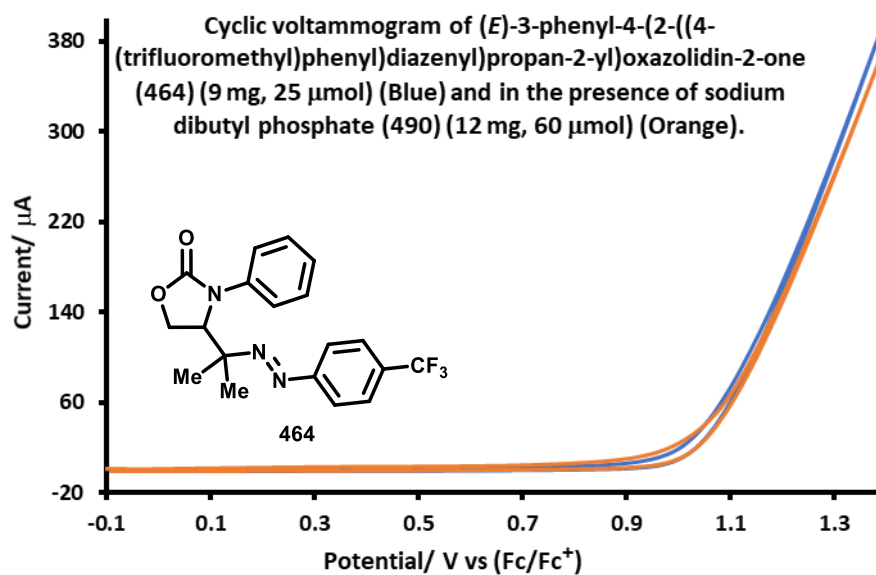
8.3.3.2 Follow Up Studies

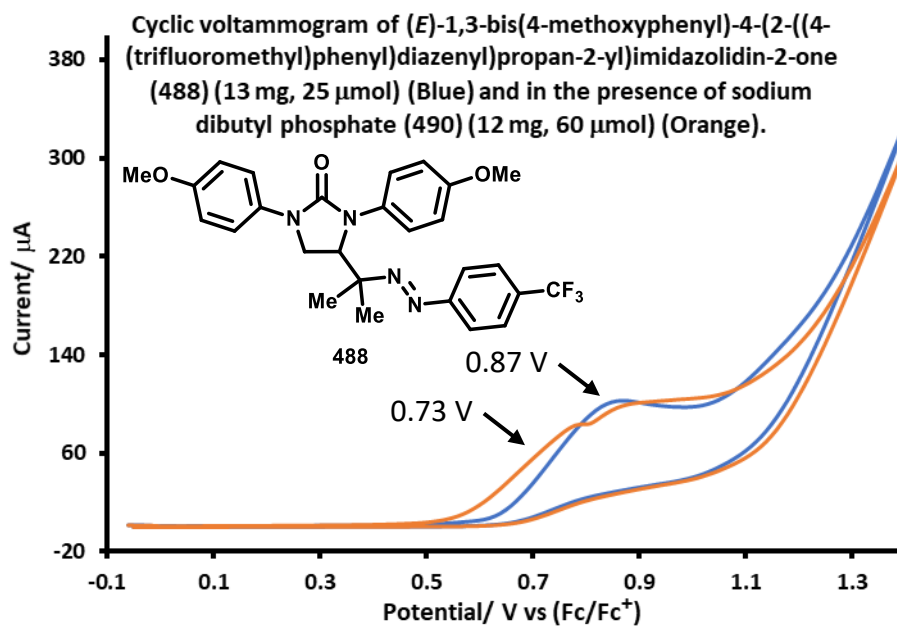
Analyte was added to a 0.1 M solution of tetra-*n*-butylammonium hexafluorophosphate in dry, degassed DMSO (5 mL). Experiments were run using a glassy carbon working electrode, a platinum wire counter electrode, and a Ag/AgNO₃ reference electrode. A scan rate of 100 mV/s was applied.











9. References

- ¹ C. Christophersen, A. Holm, *Acta Chem. Scand.*, 1970, **24**, 1512-1526.
- ² [a] K. Banert, A. Melzer, *Tetrahedron Lett.*, 2001, **42**, 6133-6135; [b] R. Koch, J. J. Finnerty, S. Murali, C. Wentrup, *J. Org. Chem.*, 2012, **77**, 1749-1759.
- ³ Y. Ichikawa, *Synlett*, 2007, 2927-2936.
- ⁴ [a] P. Kapferer, F. Sarabia, A. Vasella, *Helv. Chim. Acta*, 1999, **82**, 645-656; [b] Y. Ichikawa, E. Yamauchi, M. Isobe, *Biosci. Biotechnol. Biochem.*, 2005, **69**, 939-943; [c] S. Roy, C. Spino, *Org. Lett.*, 2006, **8**, 939-942.
- ⁵ P.-A. Nocquet, S. Henrion, A. Macé, B. Carboni, J. M. Villagordo, F. Carreaux, *Eur. J. Org. Chem.*, 2017, 1295-1307.
- ⁶ C. L. Stevens, R. D. Elliott, B. L. Winch, *J. Am. Chem. Soc.*, 1963, **85**, 1464-1470.
- ⁷ [a] W. E. Childers, R. B. Baudy, *J. Med. Chem.*, 2007, **50**, 2557-2562; [b] B. A. Chizh, P. M. Headley, *Curr. Pharm. Des.*, 2005, **11**, 2977-2994; [c] A. Leung, M. S. Wallance, B. Ridgeway, T. Yaksh, *Pain*, 2001, **91**, 177-187.
- ⁸ [a] L. A. Nguyen, H. He, C. Pham-Huy, *Int. J. Biomed. Sci.*, 2006, **2**, 85-100; [b] J. Liu, X.-Q. Ji, X.-Z. Zhu, *Life Sci.*, 2006, **78**, 1839-1844; [c] L. E. Mather, *Minerva Anesthesiol.*, 2005, **71**, 507-516; [d] C. Nau, G. R. Strichartz, *Anesthesiology*, 2002, **97**, 497-502.
- ⁹ P. Molero, J. A. Ramos-Quiroga, E. Calvo-Sánchez, J. A. Ramos-Quiroga, E. Calvo-Sánchez, R. Martin-Santos, L. Gutiérrez-Rojas, J. J. Meana, *CNS Drugs*, 2018, **32**, 411-420.
- ¹⁰ [a] C. L. Stevens, A. Thuillier, F. A. Daniher, *J. Org. Chem.*, 1965, **30**, 2962-2966; [b] C. L. Stevens, I. L. Klundt, M. E. Munk, M. D. Pillai, *J. Org. Chem.*, 1965, **30**, 2967-2972; [c] C. L. Stevens, H. T. Hanson, K. G. Taylor, *J. Am. Chem. Soc.*, 1966, **88**, 2769-2774; [d] C. L. Stevens, A. B. Ash, A. Thuillier, J. H. Amin, A. Balys, W. E. Dennis, J. P. Dickerson, R. P. Glinski, H. T. Hanson, M. D. Pillai, J. W. Stoddard, *J. Org. Chem.*, 1966, **31**, 2593-2601; [e] C. L. Stevens, A. Thuillier, K. G. Taylor, F. A. Daniher, J. P. Dickerson, H. T. Hanson, N. A. Nielsen, N. A. Tikotkar, R. M. Weier, *J. Org. Chem.*, 1966, **31**, 2601-2607; [f] C. L. Stevens, F. E. Glenn, P. M. Pillai, *J. Am. Chem. Soc.*, 1973, **95**, 6301-6308.
- ¹¹ [a] K. Steiner, S. Gangkofner, J. M. Grunenwald, Int. Appl. WO 9743244 A1, Nov 20, 1997; [b] C. Chen, O. Floegel, M. Justus, A. Maurer, K. Reuter, T. Strittmatter, T. Wedel, PCT Int. Appl. WO 2016180984 A1, Nov 17, 2016; [c] I. Dimitrov, J. Jose, W. A. Denny, *Synthesis*, 2018, **50**, 4201-4215; [d] R. Yokoyama, S. Matsumoto, S. Nomura, T. Higaki, T. Yokoyama, S. Kiyooka, *Tetrahedron*, 2009, **65**, 5181-5191; [e] T. Yokoyama, R. Yokoyama, S. Nomura, S. Matsumoto, R. Fujiyama, S. Kiyooka, *Bull. Chem. Soc. Jpn.*, 2009, **82**, 1528-1532.
- ¹² C. Chen, X. Li, *Org. Lett.* 2019, **21**, 6575-6578.
- ¹³ L. E. Overman, *J. Am. Chem. Soc.*, 1974, **96**, 597-599.
- ¹⁴ [a] *The Claisen Rearrangement* (Eds.: M. Hiersemann, U. Nubbemeyer), Wiley-VCH, Weinheim, Germany, 2007; [b] K. C. Majumdar, T. Bhattacharyya, B. Chattopadhyay, B. Sinha, *Synthesis*, 2009, 2117-2142; [c] H. Nomura, C. J. Richards, *Chem. Asian J.*, 2010, **5**, 1726-1740; [d] J. S. Arnold, Q. Zhang, H. M. Nguyen, *Eur. J. Org. Chem.*, 2014, 4925-4948; [e] J. S. Cannon, L. E. Overman, *Acc. Chem. Res.*, 2016, **49**, 2220-2231; [f] R. A. Fernandes, P. Kattanguru, S. P. Gholap, D. A. Chaudhari, *Org. Biomol. Chem.*, 2017, **15**, 2672-2710.
- ¹⁵ [a] P. Beak, J. Bonham, J. T. Lee, *J. Am. Chem. Soc.*, 1968, **90**, 1569-1582; [b] P. Beak, D. S. Mueller, J. Lee, *J. Am. Chem. Soc.*, 1974, **96**, 3867-3874.
- ¹⁶ Y. Yamamoto, H. Shimoda, J. Oda, Y. Inouye, *Bull. Chem. Soc. Jpn.*, 1976, **49**, 3247-3249.
- ¹⁷ H. Yamanaka, K. Sato, H. Sato, M. Iida, T. Oishi, N. Chida, *Tetrahedron*, 2009, **65**, 9188-9201.
- ¹⁸ "Tetrodotoxin, Saxitoxin, and the Molecular Biology of the Sodium Channel" (Eds.: C. Y. Kao, S. Lovinson), *Ann. N. Y. Acad. Sci.*, 1986, **479**, 1-445.
- ¹⁹ V. Bane, M. Lehane, M. Dikshit, A. O'Riordan, A. Furey, *Toxins*, 2014, **6**, 693-755.
- ²⁰ [a] T. Narahashi, J. W. Moore, W. R. Scott, *J. Gen. Physiol.*, 1964, **47**, 965-974; [b] F. Hucho, *Angew. Chem. Int. Ed.*, 1995, **34**, 39-50.

- ²¹ [a] T. Goto, Y. Kishi, S. Takahashi, Y. Hirata, *Tetrahedron*, 1965, **21**, 2059-2088; [b] K. Tsuda, S. Ikuma, M. Kawamura, R. Tachikawa, K. Sakai, C. Tamura, O. Amakasu, *Chem. Pharm. Bull.*, 1964, **12**, 1357-1374; [c] R. B. Woodward, *Pure. Appl. Chem.*, 1964, **9**, 49-74.
- ²² [a] Y. Kishi, M. Aratani, T. Fukuyama, F. Nakatsubo, T. Goto, S. Inoue, H. Tanino, S. Sugiura, H. Kakoi, *J. Am. Chem. Soc.*, 1972, **94**, 9217-9219; [b] Y. Kishi, T. Fukuyama, M. Aratani, F. Nakatsubo, T. Goto, S. Inoue, H. Tanino, S. Sugiura, H. Kakoi, *J. Am. Chem. Soc.*, 1972, **94**, 9219-9221; [c] A. Hinman, J. Du Bois, *J. Am. Chem. Soc.*, 2003, **125**, 11510-11511.
- ²³ [a] T. Nishikawa, D. Urabe, M. Isobe, *Angew. Chem. Int. Ed.*, 2004, **43**, 4782-4785; [b] T. Nishikawa, M. Asai, N. Ohyabu, N. Yamamoto, Y. Fukuda, M. Isobe, *Tetrahedron*, 2001, **57**, 3875-3883.
- ²⁴ [a] T. Curtius, *Ber. Dtsch. Chem. Ges.*, 1890, **23**, 3023-3033; [b] T. Curtius, *J. Prakt. Chem.*, 1894, **50**, 275-294; [c] *Organic Reactions*, vol. III (Eds.: W. Bachmann, L. F. Fieser, J. R. Johnson, H. R. Snyder), John Wiley & Sons, London, 1946.
- ²⁵ [a] R. M. Stollé, N. J. Merkle, *Prakt. Chem.*, 1928, **119**, 275-278; [b] R. G. Arnold, J. A. Nelson, J. J. Verbanc, *Chem. Rev.*, 1957, **57**, 47-76; [c] A. L. Wilds, N. F. Woolsey, J. V. D. Berghé, C. H. Winestock, *Tetrahedron Lett.*, 1965, 4841-4846; [d] H. Saikachi, T. Kitagawa, *Chem. Pharm. Bull.*, 1978, **26**, 1054-1060; [e] A. K. Ghosh, A. Sarkar, M. Brindisi, *Org. Biomol. Chem.*, 2018, **16**, 2006-2027.
- ²⁶ [a] J. Stieglitz, *Am. Chem. J.*, 1896, **18**, 756; [b] S. Linke, G. T. Tisue, W. Lwowski, *J. Am. Chem. Soc.*, 1967, **89**, 6308-6310; [c] W. Lwowski, G. T. Tisue, *J. Am. Chem. Soc.*, 1965, **87**, 4022-4023; [d] R. A. Abramovitch, B. A. Davis, *Chem. Rev.*, 1964, **64**, 149-185; [e] C. Wentrup, H. Bornemann, *Eur. J. Org. Chem.*, 2005, 4521-4524; [f] S. Vyas, J. Kubicki, H. L. Luk, Y. L. Zhang, N. P. Gritsan, C. M. Hadad, M. S. Platz, *J. Phys. Org. Chem.*, 2012, **25**, 693-703; [g] K. Banert, C. Berndt, M. Hagedorn, H. Liu, T. Anacker, J. Friedrich, G. Rauhut, *Angew. Chem. Int. Ed.*, 2012, **51**, 4718-4721.
- ²⁷ A. Campell, J. Kenyon, *J. Chem. Soc.*, 1946, 25-27.
- ²⁸ [a] R. Imof, D. W. Ladner, J. M. Muchowski, *J. Org. Chem.*, 1977, **41**, 3709-3713; [b] S. Sasmal, A. Geyer, M. E. Maier, *J. Org. Chem.*, 2002, **67**, 6260-6263; [c] B. S. Patil, G. R. Vasanthakumar, V. V. S. Babu, *J. Org. Chem.*, 2003, **68**, 7274-7280; [d] F. Zhang, J. M. Fox, *Org. Lett.*, 2006, **8**, 2965-2968; [e] M. Lasa, P. López, C. Cativiela, *Tetrahedron: Asymmetry*, 2005, **16**, 4022-4033; [f] M. Chaumontet, R. Piccardi, O. Baudoin, *Angew. Chem. Int. Ed.*, 2009, **48**, 179-182.
- ²⁹ [a] D. L. Scott, F. Wolfe, T. W. J. Huzinga, *Lancet*, 2010, **376**, 1094-1108; [b] M. Ally, B. Hodgkinson, *S. Afr. Fam. Pract.*, 2014, **56**, 166-171; [c] T. Bongartz, A. J. Sutton, M. J. Sweeting, I. Buchan, E. L. Mateson, V. Montori, *J. Am. Med. Assoc.*, 2006, **295**, 2275-2285; [d] V. Majithia, S. A. Geraci, *Am. J. Med.*, 2007, **120**, 936-939; [e] B. Bresnihan, *J. Rheumatol.*, 1999, **26**, 717-719.
- ³⁰ [a] S. L. Kunkel, N. Lukacs, T. Kasama, R. M. Strieter, *J. Leukocyte Biol.*, 1996, **59**, 6-12; [b] X. Yu, Y. Huang, P. Collin-Osdoby, P. J. Osdoby, *Bone Miner. Res.*, 2004, **19**, 2065-2077; [c] J. M. Lean, C. Murphy, K. Fuller, T. J. Chambers, *J. Cell. Biochem.*, 2002, **87**, 386-393.
- ³¹ [a] R. Betageri, B. N. Cook, D. Disalvo, C. Harcken, D. Kuzmich, P. Liu, J. Lord, C. Mao, H. Razavi, *PCT Int. Appl*, WO2012087782A120120628, 2012; [b] B. N. Cook, D. Disalvo, D. R. Fandrick, C. Harcken, D. Kuzmich, T. W.-H. Lee, P. Liu, J. Lord, C. Mao, J. Neu, B. C. Raudenbush, H. Razavi, J. T. Reeves, J. J. Song, A. D. Swinamer, Z. Tan, *PCT Int. Appl*, WO2010036632A120100401, 2010.
- ³² M. A. Marsini, F. G. Buono, J. C. Lorenz, B.-S. Yang, J. T. Reeves, K. Sidhu, M. Sarvestani, Z. Tan, Y. Zhang, N. Li, H. Lee, J. Brazzillo, L. J. Nummy, J. C. Chung, I. K. Luvaga, B. A. Narayanan, X. Wei, J. J. Song, F. Roschangar, N. K. Yee, C. H. Senanayake, *Green Chem.*, 2017, **19**, 1454-1461.
- ³³ T. S. Stevens, E. M. Creighton, A. B. Gordon, M. MacNicol, *J. Chem. Soc.*, 1928, 3193-3197.
- ³⁴ [a] S. Bhakat, *J. Chem. Pharm. Res.*, 2011, **3**, 115-121; [b] D. Baidilov, *Synthesis*, 2020, **52**, 21-26.
- ³⁵ [a] T. S. Stevens, *J. Chem. Soc.*, 1930, 2107-2119; [b] T. Thomson, T. S. Stevens, *J. Chem. Soc.*, 1932, 1932-1940; [c] A. Campbell, A. H. J. Houston, J. Kenyon, *J. Chem. Soc.* 1947, 93-95.
- ³⁶ A. R. Lepley, *J. Am. Chem. Soc.*, 1969, **91**, 1237-1239.
- ³⁷ J. E. Baldwin, W. F. Erickson, R. E. Hackler, R. M. Scott, *J. Chem. Soc. D.*, 1970, 576b-578.
- ³⁸ G. Ghigo, S. Cagnina, A. Maranzana, G. Tonachini, *J. Org. Chem.*, 2010, **75**, 3608-3617.

- ³⁹ K. W. Glaeske, F. G. West, *Org. Lett.*, 1999, **1**, 31-33.
- ⁴⁰ [a] T. S. Stevens, W. W. Snedden, E. T. Stiller, T. Thomson, *J. Chem. Soc.*, 1930, 2119-2125; [b] T. Thomson, T. S. Stevens, *J. Chem. Soc.*, 1932, 55-69; [c] T. Thomson, T. S. Stevens, *J. Chem. Soc.*, 1932, 69-73; [d] J. L. Dunn, T. S. Stevens, *J. Chem. Soc.*, 1932, 1926-1931; [e] J. L. Dunn, T. S. Stevens, *J. Chem. Soc.*, 1934, 279-282; [f] W. R. Bamford, T. S. Stevens, J. W. Wright, *J. Chem. Soc.*, 1952, 4334-4338; [g] R. A. W. Johnstone, T. S. Stevens, *J. Chem. Soc.*, 1955, 4487-4488; [h] W. R. Bamford, T. S. Stevens, *J. Chem. Soc.*, 1952, 4675-4678; [i] K. W. Glaeske, F. G. West, *Org. Lett.*, 1999, **1**, 31-34; [j] A. P. A. Arboré, D. J. Cane-Honeysett, I. Coldham, M. L. Middleton, *Synlett*, 2000, 236-238; [k] J. S. Clark, M. D. Middleton, *Org. Lett.*, 2002, **4**, 765-768.
- ⁴¹ B. D. Morris, M. R. Prinsep, *J. Nat. Prod.*, 1999, **62**, 688-693.
- ⁴² M. F. Braña, M. Garranzo, B. de Pascual-Teresa, J. Pérez-Castells, M. R. Torres, *Tetrahedron*, 2002, **58**, 4825-4836.
- ⁴³ [a] C. C. Hughes, D. Trauner, *Angew. Chem. Int. Ed.*, 2002, **41**, 4556-4559; [b] K. Sakaguchi, M. Ayabe, Y. Watanabe, T. Okada, K. Kawamura, T. Shiada, Y. Ohfune, *Org. Lett.*, 2008, **10**, 5449-5452; [c] K. Sakaguchi, M. Ayabe, Y. Watanabe, T. Okada, K. Kawamura, T. Shinada, Y. Ohfune, *Tetrahedron*, 2009, **65**, 10355-10364; [d] K. Chiyoda, J. Shimokawa, T. Fukuyama, *Angew. Chem. Int. Ed.*, 2012, **51**, 2505-2508.
- ⁴⁴ A. Soheili, U. K. Tambar, *Org. Lett.*, 2013, **15**, 5138-5141.
- ⁴⁵ G. Liu, D. A. Cogan, J. A. Ellman, *J. Am. Chem. Soc.*, 1997, **119**, 9913-9914.
- ⁴⁶ [a] P. Zhou, B.-C. Chen, F. A. Davis, *Tetrahedron*, 2004, **60**, 8003-8030; [b] C. H. Senanayake, D. Krishnamurthy, Z.-H. Lu, Z. Han, I. Gallou, *Aldrichim. Acta*, 2005, **38**, 93-103; [c] C. H. Senanayake, Z. Han, D. Krishnamurthy, *Organosulfur Chemistry in Asymmetric Synthesis*; (Eds.: T. Toru, C. Bolm), Wiley, Weinheim, Germany, 2008; [d] J. A. Ellman, T. D. Owens, T. P. Tang, *Acc. Chem. Res.*, 2002, **35**, 984-995; [e] F. Ferreira, C. Botuha, F. Chemla, A. Perez-Luna, *Chem. Soc. Rev.*, 2009, **38**, 1162-1186.
- ⁴⁷ F. A. Davis, A. J. Friedman, E. W. Kluger, *J. Am. Chem. Soc.*, 1974, **96**, 5000.
- ⁴⁸ M. Robak, M. Herbage, J. A. Ellman, *Chem. Rev.*, 2010, **110**, 3600-3740.
- ⁴⁹ G. Liu, D. A. Cogan, T. D. Owens, T. P. Tang, J. A. Ellman, *J. Org. Chem.*, 1999, **64**, 1278-1284.
- ⁵⁰ [a] D. Morton, D. Pearson, R. A. Field, R. A. Stockman, *Synlett*, 2003, **13**, 1985-1988; [b] F. Chemia, F. Ferreira, *J. Org. Chem.*, 2004, **69**, 8244-8250; [c] H. A. Dondas, N. De Kimpe, *Tetrahedron Lett.*, 2005, **46**, 4179-4182; [d] L. B. Schenkel, J. A. Ellman, *Org. Lett.*, 2004, **6**, 3621-3624; [e] K. M. Brinner, J. A. Ellman, *Org. Biomol. Chem.*, 2005, **3**, 2109-2113.
- ⁵¹ V. K. Aggarwal, N. Barbero, E. M. McGarrigle, G. Mickle, R. Navas, J. R. Suárez, M. G. Unthank, M. Yar, *Tetrahedron Lett.*, 2009, **50**, 3482-3484.
- ⁵² [a] S. D. Kuduk, R. M. DiPardo, R. K. Chang, C. Ng, M. G. Bock, *Tetrahedron Lett.*, 2004, **45**, 6641-6643; [b] Z. Han, D. Krishnamurthy, D. Pflum, P. Grover, S. A. Wald, C. H. Senanayake, *Org. Lett.*, 2002, **4**, 4025-4028.
- ⁵³ [a] G. Wasner, J. Schattschneider, A. Binder, R. Baron, *Brain*, 2004, **127**, 1159-1171; [b] F. Seifert, C. Maihöfner, *Neuroimage*, 2007, **35**, 1168-1180; [c] K. Tajino, K. Matsumura, K. Kosada, T. Shibakusa, K. Inoue, T. Fushiki, H. Hosokawa, S. Kobayashi, *Am. J. Physiol. Regul. Integr. Comp. Physiol.*, 2007, **293**, R2128-R2135; [d] U. Baumgärtner, W. Greffrath, R.-D. Treede, *Neurophysiol. Clin.*, 2012, **42**, 267-280.
- ⁵⁴ Y. Hu, D. Cai, J. Zhu, P. Dong, M. Li, K. L. Greenman, J. Dong, T.-L. Wang, Patent WO 2018130227 A1, July, 2018.
- ⁵⁵ K. Biswas, J. Brown, J. J. Chen, V. K. Gore, S. Harried, D. B. Horne, M. R. Kaller, V. V. Ma, T. T. Nguyen, K. Sham, W. Zhong, Patent WO 2014025651 A1, February, 2014.
- ⁵⁶ J. Waser, E. M. Carreira, *J. Am. Chem. Soc.*, 2004, **126**, 5676-5677.
- ⁵⁷ J. Waser, E. M. Carreira, *Angew. Chem. Int. Ed.*, 2004, **43**, 4099-4102.
- ⁵⁸ [a] J. Waser, H. Nambu, E. M. Carreira, *J. Am. Chem. Soc.*, 2005, **127**, 8294-8295; [b] J. Waser, B. Gaspar, H. Nambu, E. M. Carreira, *J. Am. Chem. Soc.*, 2006, **128**, 11693-11712.
- ⁵⁹ E. K. Leggans, T. J. Barker, K. K. Duncan, D. L. Boger, *Org. Lett.*, 2012, **14**, 1428-1431.

- ⁶⁰ [a] Y. Zhang, Q. Tang, M. Luo, *Org. Biomol. Chem.*, 2011, **9**, 4977-4982; [b] H. Vogt, S. Vanderheiden, S. Bräse, *Chem. Commun.*, 2003, **19**, 2448-2449; [c] R. Chênevert, F. Jacques, *Tetrahedron Asymmetry*, 2006, **17**, 1017-1021; [d] G. Guanti, L. Banfi, E. Narisano, *Tetrahedron*, 1988, **44**, 5553-5562; [e] R. Fernández, A. Ferrete, J. M. Lassaletta, J. M. Llera, E. Martín-Zamora, *Angew. Chem. Int. Ed.*, 2002, **41**, 831-833; [f] R. K. Saunthwal, M. T. Cornall, R. Abrams, J. W. Ward, J. Clayden, *Chem. Sci.*, 2019, **10**, 3408-3412.
- ⁶¹ [a] S. Chandrasekhar, S. Y. Prakash, C. L. Rao, *J. Org. Chem.*, 2006, **71**, 2196-2199; [b] L. Benati, G. Bencivenni, R. Leardini, D. Nanni, M. Minozzi, P. Spagnolo, R. Scialpi, G. Zanardi, *Org. Lett.*, 2006, **8**, 2499-2502; [c] A. Kamal, N. Shankaraiah, N. Markandeya, Ch. S. Reddy, *Synlett*, 2008, 1297-1300; [d] S. Ahammed, A. Saha, B. C. Ranu, *J. Org. Chem.*, 2011, **76**, 7235-7239; [e] H. Sajiki, *Tetrahedron Lett.*, 1995, **36**, 3465-3468; [f] E. J. Corey, J. O. Link, *J. Am. Chem. Soc.*, 1992, **114**, 1906-1908; [g] A. Postigo, S. Kopsov, C. Ferreri, C. Chatgililoglu, *Org. Lett.*, 2007, **9**, 5159-5162.
- ⁶² D. N. Tran, N. Cramer, *Angew. Chem. Int. Ed.*, 2010, **49**, 8181-8184.
- ⁶³ J. Zhang, A. Ugrinov, P. Zhao, *Angew. Chem. Int. Ed.*, 2013, **52**, 6681-6684.
- ⁶⁴ [a] D. N. Tran, N. Cramer, *Angew. Chem. Int. Ed.*, 2011, **50**, 11098-11102; [b] D. N. Tran, N. Cramer, *Angew. Chem. Int. Ed.*, 2013, **52**, 10630-10634.
- ⁶⁵ Y. Wu, L. Hu, Z. Li, L. Deng, *Nature*, 2015, **523**, 445-450.
- ⁶⁶ C. K. Donawho, Y. Luo, Y. Luo, T. D. Penning, J. L. Bauch, J. J. Bouska, V. D. Bontcheva-Diaz, B. F. Cox, T. L. DeWeese, L. E. Dillehay, D. C. Ferguson, N. S. Ghoreishi-Haack, D. R. Grimm, R. Guan, E. K. Han, R. R. Holley-Shanks, B. Hristov, K. B. Idler, K. Jarvis, E. F. Johnson, L. R. Kleinberg, V. Klinghofer, L. M. Lasko, X. Liu, K. C. Marsh, T. P. McGonigal, J. A. Meulbroek, A. M. Olson, J. P. Palma, L. E. Rodriguez, Y. Shi, J. A. Stavropoulos, A. C. Tsurutani, G.-D. Zhu, S. H. Rosenberg, V. L. Giranda, D. Frost, *Clin. Cancer Res.*, 2007, **13**, 2728-2737.
- ⁶⁷ [a] J. P. Palma, Y.-C. Wang, L. E. Rodriguez, D. Montgomery, P. A. Ellis, G. Bukofzer, A. Niquette, X. Liu, Y. Shi, L. Lasko, G.-D. Zhu, T. D. Penning, V. L. Giranda, S. H. Rosenberg, D. J. Frost, C. K. Donawho, *Clin. Cancer Res.*, 2009, **15**, 7277-7290; [b] H. S. Han, V. Dieras, M. Robson, M. Palacova, P. K. Marcom, A. Jager, I. Bondarenko, D. Citrin, M. Campone, M. L. Telli, S. M. Domchek, M. Friedlander, B. Kaufman, J. E. Garber, Y. Shparyk, E. Chmielowska, E. H. Jakobsen, V. Kaklamani, W. Gradishar, C. K. Ratajczak, C. Nickner, Q. Qin, J. Qian, S. P. Shepherd, S. J. Isakoff, S. Puhalla, *Ann. Oncol.*, 2018, **29**, 154-161; [c] S. S. Ramalingam, N. Blais, J. Mazieres, M. Reck, C. M. Jones, E. Juhasz, L. Urgan, S. Orlov, F. Barlesi, E. Kio, U. Keiholz, Q. Qin, J. Qian, C. Nickner, J. Dziubinski, H. Xiong, P. Ansell, M. McKee, V. Giranda, V. Gorbunova, *Clin. Cancer Res.*, 2017, **23**, 1937-1944.
- ⁶⁸ L. Kolaczowski, J. Barkalow, D. M. Barnes, A. Haight, W. Pritts, A. Schellinger, *J. Org. Chem.*, 2019, **84**, 4837-4845.
- ⁶⁹ T. Kawabata, S. Kawakami, S. Majumdar, *J. Am. Chem. Soc.*, 2003, **125**, 13012-13013.
- ⁷⁰ T. Kawabata, H. Suzuki, Y. Nagae, K. Fujii, *Angew. Chem. Int. Ed.*, 2000, **39**, 2155-2157.
- ⁷¹ *Copper Amine Oxidases: Structures, Catalytic Mechanisms, and Role in Pathophysiology*, (Ed.: G. Floris, B. Mondovi), CRC Press, Taylor and Francis Group Publishing, New York, 2009.
- ⁷² D. Vasu, A. L. Fuentes de Arriba, J. A. Leitch, A. de Gombert, D. J. Dixon, *Chem. Sci.*, 2019, **10**, 3401-3407.
- ⁷³ [a] B. V. Shetty, *J. Org. Chem.*, 1961, **26**, 3002-3004; [b] P. G. Gildner, A. A. S. Gietter, D. Cui, D. A. Watson, *J. Am. Chem. Soc.*, 2012, **134**, 9942-9945.
- ⁷⁴ D. Lehnher, Y. Lam, M. C. Nicastrì, J. Liu, J. A. Newman, E. L. Regalado, D. A. DiRocco, T. Rovis, *J. Am. Chem. Soc.*, 2020, **142**, 468-478.
- ⁷⁵ M. C. Nicastrì, D. Lehnher, Y. Lam, D. A. DiRocco, T. Rovis, *J. Am. Chem. Soc.*, 2020, **142**, 987-998.
- ⁷⁶ H. Takeda, O. Ishitani, *Coord. Chem. Rev.*, 2010, **254**, 346-354.
- ⁷⁷ [a] M. Grätzel, *Acc. Chem. Res.*, 1981, **14**, 376-384; [b] T. Meyer, *J. Acc. Chem. Res.*, 1989, **22**, 163-170.
- ⁷⁸ K. Kalyanasundaram, M. Grätzel, *Coord. Chem. Rev.*, 1998, **177**, 347-414.
- ⁷⁹ M. H. Shaw, J. Twilton, D. W. C. MacMillan, *J. Org. Chem.*, 2016, **81**, 6898-6926.
- ⁸⁰ [a] D. M. Hedstrand, W. M. Kruizinga, R. M. Kellogg, *Tetrahedron Lett.*, 1978, **19**, 1255-1258; [b] T. J. van Bergen, D. M. Hedstrand, W. H. Kruizinga, R. M. Kellogg, *J. Org. Chem.*, 1979, **44**, 4953-4962.

- ⁸¹ [a] C. Pac, M. Ihama, M. Yasuda, Y. Miyauchi, H. Sakurai, *J. Am. Chem. Soc.*, 1981, **103**, 6495-6497; [b] C. Pac, Y. Miyauchi, O. Ishitani, M. Ihama, M. Yasuda, H. Sakurai, *J. Org. Chem.*, 1984, **49**, 26-34; [c] O. Ishitani, M. Ihama, Y. Miyauchi, C. Pac, *J. Chem. Soc. Perkin Trans. 1*, 1985, 1527-1531; [d] O. Ishitani, C. Pac, H. Sakurai, *J. Org. Chem.*, 1983, **48**, 2941-2942; [e] O. Ishitani, S. Yanagida, S. Takamuku, C. Pac, *J. Org. Chem.*, 1987, **52**, 2790-2796.
- ⁸² [a] K. Hironaka, S. Fukuzumi, T. Tanaka, *J. Chem. Soc. Perkin Trans. 2*, 1984, 1705-1709; [b] S. Fukuzumi, S. Koumitsu, K. Hironaka, T. Tanaka, *J. Am. Chem. Soc.*, 1987, **109**, 305-316; [c] S. Fukuzumi, S. Mochizuki, T. Tanaka, *J. Phys. Chem.*, 1990, **94**, 722-726.
- ⁸³ [a] H. Cano-Yelo, A. Deronzier, *J. Chem. Soc. Perkin Trans. 2*, 1984, 1093-1098; [b] H. Cano-Yelo, A. Deronzier, *J. Photochem.*, 1987, **37**, 315-321.
- ⁸⁴ M. A. Ischay, M. E. Anzovino, J. Du, T. P. Yoon, *J. Am. Chem. Soc.*, 2008, **130**, 12886-12887.
- ⁸⁵ D. A. Nicewicz, D. W. C. MacMillan, *Science*, 2008, **322**, 77-80.
- ⁸⁶ [a] J. M. R. Narayanam, C. R. J. Stephenson, *Chem. Soc. Rev.*, 2011, **40**, 102-113; [b] C. K. Prier, D. A. Rankic, D. W. C. MacMillan, *Chem. Rev.*, 2013, **113**, 5322-5363; [c] X. Lang, J. Zhaob, X. Chen, *Chem. Soc. Rev.*, 2016, **45**, 3026-3038; [d] N. A. Romero, D. A. Nicewicz, *Chem. Rev.*, 2016, **116**, 10075-10166; [e] C.-S. Wang, P. H. Dixneuf, J.-F. Soulé, *Chem. Rev.*, 2018, **118**, 7532-7585; [f] R. C. McAtee, E. J. McClain, C. R. J. Stephenson, *Trends Chem.*, 2019, **1**, 111-125.
- ⁸⁷ J. W. Tucker, C. R. J. Stephenson, *J. Org. Chem.*, 2012, **77**, 1617-1622.
- ⁸⁸ A. Juris, V. Balzani, P. Belser, A. von Zelewsky, *Helv. Chim. Acta*, 1981, **64**, 2175-2182.
- ⁸⁹ D. L. Anderson, *"Chemical Composition of the Mantle" Theory of the Earth*, Blackwell, Boston, 1989.
- ⁹⁰ C. B. Kelly, N. R. Patel, D. N. Primer, M. Jouffroy, J. C. Tellis, G. A. Molander, *Nat. Protoc.*, 2017, **12**, 472-492.
- ⁹¹ For Cu photoredox catalysis see- [a] S. Paria, O. Reiser, *ChemCatChem*, 2014, **6**, 2477-2483; [b] D. B. Bagal, G. Kachkovskiy, M. Knorn, T. Rawnner, B. M Bhanage, O. Reiser, *Angew. Chem. Int. Ed.*, 2015, **54**, 6999-7002. For Cr photoredox catalysis see- S. M. Stevenson, M. P. Shores, E. M. Ferreira, *Angew. Chem. Int. Ed.*, 2015, **54**, 6506-6510. For Fe photoredox catalysis see- A. Gualandi, M. Marchini, L. Mengozzi, M. Natali, M. Lucarini, P. Ceroni, P. G. Cozzi, *ACS Catal.*, 2015, **5**, 5927-5931.
- ⁹² T.-Y. Shang, L.-H. Lu, Z. Cao, Y. Liu, W.-M. He, B. Yu, *Chem. Commun.*, 2019, **55**, 5408-5419.
- ⁹³ H. Uoyama, K. Goushi, K. Shizu, H. Nomura, C. Adachi, *Nature*, 2012, **492**, 234-238.
- ⁹⁴ J. Luo, J. Zhang, *ACS Catal.*, 2016, **6**, 873-877.
- ⁹⁵ N. Yanai, M. Kozue, S. Amemori, R. Kabe, C. Adachic, N. Kimizuka, *J. Mater. Chem. C*, 2016, **4**, 6447-6451.
- ⁹⁶ H. Nakanotani, K. Masui, J. Nishide, T. Shibata, C. Adachi, *Sci. Rep.*, 2013, **3**, 2127.
- ⁹⁷ [a] E. Speckmeier, T. G. Fischer, K. Zeitler, *J. Am. Chem. Soc.*, 2018, **140**, 15353-15365; [b] F. Le Vaillant, M. Garreau, S. Nicolai, G. Gryn'ova, C. Corminboeuf, J. Waser, *Chem. Sci.*, 2018, **9**, 5883-5889.
- ⁹⁸ Z. Zuo, D. W. MacMillan, *J. Am. Chem. Soc.*, 2014, **136**, 5257-5260.
- ⁹⁹ Z. Zuo, D. T. Ahneman, L. Chu, J. A. Terrett, A. G. Doyle, D. W. C. MacMillan, *Science*, 2014, **345**, 437-440.
- ¹⁰⁰ [a] S. E. Creutz, K. J. Lotito, G. C. Fu, J. C. Peters, *Science*, 2012, **338**, 647-651; [b] J. C. Tellis, D. N. Primer, G. A. Molander, *Science*, 2014, **345**, 433-436; [c] O. Gutierrez, J. C. Tellis, D. N. Primer, G. A. Molander, M. C. Kozłowski, *J. Am. Chem. Soc.*, 2015, **137**, 4896-4899; [d] J. C. Tellis, C. B. Kelly, D. N. Primer, M. Jouffroy, N. R. Patel, G. A. Molander, *Acc. Chem. Res.*, 2016, **49**, 1429-1439; [e] M. Jouffroy, D. N. Primer, G. A. Molander, *J. Am. Chem. Soc.*, 2016, **138**, 475-478; [f] E. R. Welin, C. Le, D. M. Arias-Rotondo, J. K. McCusker, D. W. C. MacMillan, *Science*, 2017, **355**, 380-385.
- ¹⁰¹ [a] J. W. Beatty, C. R. J. Stephenson, *J. Am. Chem. Soc.*, 2014, **136**, 10270-10273; [b] D. Staveness, T. M. Sodano, K. Li, E. A. Burnham, K. D. Jackson, C. R. J. Stephenson, *Chem.*, 2019, **5**, 215-226.
- ¹⁰² [a] H. Tanaka, K. Sakai, A. Kawamura, K. Oisaki, M. Kanai, *Chem. Commun.*, 2018, **54**, 3215-3218; [b] D.-F. Chen, J. C. K. Chu, T. Rovis, *J. Am. Chem. Soc.*, 2017, **139**, 14897-14900; [c] J. C. K. Chu, T. Rovis, *Nature*, 2016, **539**, 272-275; [c] G. J. Choi, Q. Zhu, D. C. Miller, C. J. Gu, R. R. Knowles, *Nature*, 2016, **539**, 268-271.
- ¹⁰³ [a] A. Studer, D. P. Curran, *Angew. Chem. Int. Ed.*, 2016, **55**, 58-102; [b] D. Leifert, A. Studer, *Angew. Chem. Int. Ed.*, 2019, **59**, 74-108.

- ¹⁰⁴ [a] T. Koike, M. Akita, *Acc. Chem. Res.*, 2016, **49**, 1937-1945; [b] T. Courant, G. Masson, *J. Org. Chem.*, 2016, **81**, 6945-6952; [c] B. Sahoo, J. L. Li, F. Glorius, *Angew. Chem. Int. Ed.*, 2015, **54**, 11577-11580; [d] R. Honeker, R. A. Garza-Sanchez, M. N. Hopkinson, F. Glorius, *Chem. - Eur. J.*, 2016, **22**, 4395-4399; [e] G. Bergonzini, C. Cassani, H. Lorimer-Olsson, J. Hörberg, C. Wallentin, *Chem. - Eur. J.*, 2016, **22**, 3292-3295; [f] H.-L. Huang, H. Yan, C. Yang, W. Xia, *Chem. Commun.*, 2015, **51**, 4910-4913; [g] Y. Li, B. Liu, X.-H. Ouyang, R.-J. Song, J.-H. Li, *Org. Chem. Front.*, 2015, **2**, 1457-1467.
- ¹⁰⁵ Y. Yasu, T. Koike, M. Akita, *Angew. Chem. Int. Ed.*, 2012, **51**, 9567-9571.
- ¹⁰⁶ G. Dagousset, A. Carboni, E. Magnier, G. Masson, *Org. Lett.*, 2014, **16**, 4340-4343.
- ¹⁰⁷ A. Carboni, G. Dagousset, E. Magnier, G. Masson, *Chem. Commun.*, 2014, **50**, 14197-14200.
- ¹⁰⁸ C.-J. Yao, Q. Sun, N. Rastogi, B. König, *ACS Catal.*, 2015, **5**, 2935-2938.
- ¹⁰⁹ R. Abrams, Q. Lefebvre, J. Clayden, *Angew. Chem. Int. Ed.*, 2018, **57**, 13587-13591.
- ¹¹⁰ M. Silvi, C. Sandford, V. K. Aggarwal, *J. Am. Chem. Soc.*, 2017, **139**, 5736-5739.
- ¹¹¹ L. Pitzer, F. Sandfort, F. Strieth-Kalthoff, F. Glorius, *J. Am. Chem. Soc.*, 2017, **139**, 13652-13655.
- ¹¹² Y. Miyake, K. Nakajima, Y. Nishibayashi, *J. Am. Chem. Soc.*, 2012, **134**, 3338-3341.
- ¹¹³ J. W. Beatty, C. R. J. Stephenson, *Acc. Chem. Res.*, 2015, **48**, 1474-1484.
- ¹¹⁴ [a] K. Okada, K. Okamoto, N. Morita, K. Okubo, M. Oda, *J. Am. Chem. Soc.*, 1991, **113**, 9401-9402; [b] P. Kohls, D. Jadhav, G. Pandey, O. Reiser, *Org. Lett.*, 2012, **14**, 672-675; [c] Y. Yasu, T. Koike, M. Akita, *Adv. Synth. Catal.*, 2012, **354**, 3414-3420; [d] L. Chu, C. Ohta, Z. Zuo, D. W. C. MacMillan, *J. Am. Chem. Soc.*, 2014, **136**, 10886-10889.
- ¹¹⁵ V. R. Yatham, Y. Shen, R. Martin, *Angew. Chem.* 2017, **129**, 11055-11059.
- ¹¹⁶ J. P. Phelan, S. B. Lang, J. S. Compton, C. B. Kelly, R. Dykstra, O. Gutierrez, G. A. Molander, *J. Am. Chem. Soc.*, 2018, **140**, 8037-8047.
- ¹¹⁷ C. Shu, R. S. Mega, B. J. Andreassen, A. Noble, V. K. Aggarwal, *Angew. Chem. Int. Ed.*, 2018, **57**, 15430-15434.
- ¹¹⁸ C. Shu, A. Noble, V. K. Aggarwal, *Angew. Chem. Int. Ed.*, 2019, **58**, 3870-3874.
- ¹¹⁹ A. Hu, Y. Chen, J.-J. Guo, N. Yu, Q. An, Z. Zuo, *J. Am. Chem. Soc.*, 2018, **140**, 13580-13585.
- ¹²⁰ F. Terrier, *Modern Nucleophilic Aromatic Substitution*, Wiley-VCH, Weinheim, 2013.
- ¹²¹ A. Williams, *Concerted Organic and Bio-Organic Mechanisms*, CRC, Boca Raton, FL, 1999.
- ¹²² J. Meisenheimer, *Liebigs Ann. Chem.*, 1902, **323**, 205-246.
- ¹²³ [a] J. Miller, *Aust. J. Chem.*, 1956, **9**, 61-73; [b] J. Miller, K.-Y. Wan, *J. Chem. Soc.*, 1963, 3492-3495.
- ¹²⁴ S. Rohrbach, A. J. Smith, J. H. Pang, D. L. Poole, T. Tuttle, S. Chiba, J. A. Murphy, *Angew. Chem. Int. Ed.*, 2019, **58**, 16368-16388.
- ¹²⁵ H. Handel, M. A. Pasquini, J. L. Pierre, *Tetrahedron*, 1980, **36**, 3205-3208.
- ¹²⁶ J. P. Barham, S. E. Dalton, M. Allison, G. Nocera, A. Young, M. P. John, T. McGuire, S. Campos, T. Tuttle, J. A. Murphy, *J. Am. Chem. Soc.*, 2018, **140**, 11510-11518.
- ¹²⁷ [a] A. Hunter, M. Renfrew, J. A. Taylor, J. M. J. Whitmore, A. Williams, *J. Chem. Soc. Perkin Trans. 2*, 1993, 1703-1704; [b] A. Hunter, M. Renfrew, D. Rettura, J. A. Taylor, J. M. J. Whitmore, A. Williams, *J. Am. Chem. Soc.*, 1995, **117**, 5484-5491.
- ¹²⁸ [a] P. Tang, W. Wang, T. Ritter, *J. Am. Chem. Soc.*, 2011, **133**, 11482-11484; [b] T. Fujimoto, F. Becker, T. Ritter, *Org. Process Res. Dev.*, 2014, **18**, 1041-1044; [c] C. N. Neumann, T. Ritter, *Acc. Chem. Res.*, 2017, **50**, 2822-2833.
- ¹²⁹ C. N. Neumann, J. M. Hooker, T. Ritter, *Nature*, 2016, **534**, 369-373.
- ¹³⁰ S. Rohrbach, J. A. Murphy, T. Tuttle, *J. Am. Chem. Soc.*, 2020, **142**, 14871-14876.

- ¹³¹ [a] K. Kikushima, M. Grellier, M. Ohashi, S. Ogoshi, *Angew. Chem. Int. Ed.*, 2017, **56**, 16191-16196; [b] D. Y. Ong, C. Tejo, K. Xu, H. Hirao, S. Chiba, *Angew. Chem. Int. Ed.*, 2017, **56**, 1840-1844; [c] H. Sun, S. DiMagno, *Angew. Chem. Int. Ed.*, 2006, **45**, 2720-2725; [d] Y.-J. Zheng, T. C. Bruice, *J. Am. Chem. Soc.*, 1997, **119**, 3868-3877; [e] J. Baker, M. Muir, *Can. J. Chem.*, 2010, **88**, 588-597; [f] M. N. Glukhovtsev, R. D. Bach, S. Laiter, *J. Org. Chem.*, 1997, **62**, 4036-4046; [g] T. Giroldo, L. A. Xavier, J. M. Riveros, *Angew. Chem. Int. Ed.*, 2004, **43**, 3588-3590; [h] I. Fernández, G. Frenking, E. Uggerud, *J. Org. Chem.*, 2010, **75**, 2971-2980; [i] M. Liljenberg, T. Brinck, T. Rein, M. Svensson, *Beil. J. Org. Chem.*, 2013, **9**, 791-799.
- ¹³² E. E. Kwan, Y. Zeng, H. A. Besser, E. N. Jacobsen, *Nat. Chem.*, 2018, **10**, 917-923.
- ¹³³ [a] J. M. Quibell, G. J. P. Perry, D. M. Cannas, I. Larrosa, *Chem. Sci.*, 2018, **9**, 3860-3865; [b] S. D. Schimler, M. A. Cismesia, P. S. Hanley, R. D. J. Froese, M. J. Jansma, D. C. Bland, M. S. Sanford, *J. Am. Chem. Soc.*, 2017, **139**, 1452-1455; [c] A. Kaga, H. Hayashi, H. Hakamata, M. Oi, M. Uchiyama, R. Takita, S. Chiba, *Angew. Chem. Int. Ed.*, 2017, **56**, 11807-11811.
- ¹³⁴ R. Henriques, *Ber. Dtsch. Chem.*, 1894, **27**, 2993-3005.
- ¹³⁵ [a] O. Hinsberg, *J. Prakt. Chem.*, 1914, **90**, 345-353; [b] O. Hinsberg, *J. Prakt. Chem.*, 1916, **93**, 277-301.
- ¹³⁶ [a] L. A. Warren, S. Smiles, *J. Chem. Soc.*, 1930, 1327-1331; [b] A. Levi, L. A. Warren, S. Smiles, *J. Chem. Soc.*, 1933, 1490-1493; [c] L. A. Warren, S. Smiles, *J. Chem. Soc.*, 1930, 956-963; [d] L. A. Warren, S. Smiles, *J. Chem. Soc.*, 1932, 2774-2778; [e] W. J. Evans, S. Smiles, *J. Chem. Soc.*, 1935, 181-188; [f] F. Galbraith, S. L. Smiles, *J. Chem. Soc.*, 1935, 1234-1238; [g] C. S. McClement, S. Smiles, *J. Chem. Soc.*, 1937, 1016-1021.
- ¹³⁷ A. C. Knipe, N. Sridhar, *J. Chem. Soc., Chem. Commun.*, 1979, 791-792.
- ¹³⁸ C. M. Holden, M. F. Greaney, *Chem. Eur. J.*, 2017, **23**, 8992-9008.
- ¹³⁹ [a] W. E. Truce, W. J. Ray, O. L. Norman, D. B. Eickemeyer, *J. Am. Chem. Soc.*, 1958, **80**, 3625-3629; [b] W. E. Truce, W. J. Ray, *J. Am. Chem. Soc.* 1959, **81**, 481-484.
- ¹⁴⁰ [a] L. El Kaïm, L. Grimaud, J. Oble, *Angew. Chem. Int. Ed.*, 2005, **44**, 7961-7964; [b] L. El Kaïm, L. Grimaud, *Eur. J. Org. Chem.*, 2014, 7749-7762; [c] B. Preger, G. E. Hofmeister, C. B. Jacobsen, D. G. Alberg, M. Nielsen, K. A. Jorgensen, *Chem. Eur. J.*, 2010, **16**, 3783-3790; [d] W. R. Erickson, M. J. McKennon, *Tetrahedron Lett.*, 2000, **41**, 4541-4544; [e] L. H. Mitchell, N. C. Barvian, *Tetrahedron Lett.*, 2004, **45**, 5669-5671; [f] O. K. Rasheed, I. R. Hardcastle, J. Raftery, P. Quayle, *Org. Biomol. Chem.*, 2015, **13**, 8048-8052; [g] M. W. Wilson, S. E. Ault-Justus, J. C. Hodges, J. R. Rubin, *Tetrahedron*, 1999, **55**, 1647-1656; [h] V. Lupi, M. Penso, F. Foschi, F. Gassa, V. Mihali, A. Tagliabue, *Chem. Commun.*, 2009, 5012-5014; [i] C. Dey, D. Katayev, K. E. O. Ylijoki, E. P. Kendig, *Chem. Commun.*, 2012, **48**, 10957-10959.
- ¹⁴¹ [a] M. Pudlo, I. Allart-Simon, B. Tinant, S. Gerard, J. Sapi, *Chem. Commun.*, 2012, **48**, 2442-2444; [b] W. Kong, M. Casimiro, N. Fuentes, E. Merino, C. Nevado, *Angew. Chem. Int. Ed.*, 2013, **52**, 13086-13090; [c] N. Fuentes, W. Kong, L. Fernandez-Sanchez, E. Merino, C. Nevado, *J. Am. Chem. Soc.*, 2015, **137**, 964-973; [d] S. W. Crossley, R. M. Martinez, S. Guevara-Zuluaga, R. A. Shenvi, *Org. Lett.*, 2016, **18**, 2620-2623; [e] H. Huang, Y. Li, *J. Org. Chem.*, 2017, **82**, 4449-4457; [f] J. Yu, D. Wang, Y. Xu, Z. Wu, C. Zhu, *Adv. Synth. Catal.*, 2018, **360**, 744-750; [g] T. M. Monos, R. C. McAtee, C. R. J. Stephenson, *Science*, 2018, **361**, 1369-1373; [h] M.-W. Zheng, X. Yuan, Y.-S. Cui, J.-K. Qiu, G. Li, K. Guo, *Org. Lett.*, 2018, **20**, 7784-7789; [i] D. M. Whalley, H. A. Duong, M. F. Greaney, *Chem. Eur. J.*, 2019, **25**, 1927-1930.
- ¹⁴² [a] M. O. Kitching, T. E. Hurst, V. Snieckus, *Angew. Chem. Int. Ed.*, 2012, **51**, 2925-2929; [b] T. E. Hurst, M. O. Kitching, L. C. R. M. da Frota, K. G. Guimaraes, M. E. Dalziel, V. Snieckus, *Synlett*, 2015, 1455-1460; [c] N. C. Ganguly, P. Mondal, S. Roy, P. Mitra, *RSC Adv.*, 2014, **4**, 55640-55648; [d] Y. Zhou, J. Zhu, B. Li, Y. Zhang, J. Feng, A. Hall, J. Shi, W. Zhu, *Org. Lett.*, 2016, **18**, 380-383; [e] P. Sang, M. Yu, H. Tu, J. Zou, Y. Zhang, *Chem. Commun.*, 2013, **49**, 701-703.
- ¹⁴³ J. Clayden, J. Dufour, D. M. Grainger, M. Helliwell, *J. Am. Chem. Soc.*, 2007, **129**, 7488-7489.
- ¹⁴⁴ [a] J. Clayden, U. Hennecke, *Org. Lett.*, 2008, **10**, 3567-3570; [b] R. Bach, J. Clayden, U. Hennecke, *Synlett*, 2009, 421-424; [c] D. J. Tetlow, U. Hennecke, J. Raftery, M. J. Waring, D. S. Clarke, J. Clayden, *Org. Lett.*, 2010, **12**, 5442-5445; [d] W. Zawodny, S. L. Montgomery, J. R. Marshall, J. D. Finnigan, N. J. Turner, J. Clayden, *J. Am. Chem. Soc.*, 2018, **140**, 17872-17877.
- ¹⁴⁵ M. A. Vincent, J. Maury, I. H. Hillier, J. Clayden, *Eur. J. Org. Chem.*, 2015, 953-959.

- ¹⁴⁶ [a] J. Clayden, U. Hennecke, M. A. Vincent, I. H. Hillier, M. Helliwell, *Phys. Chem. Chem. Phys.*, 2010, **12**, 15056-15064; [b] J. Clayden, L. Lemiègre, M. Pickworth, L. Jones, *Org. Biomol. Chem.*, 2008, **6**, 2908-2913; [c] J. Clayden, H. Turner, M. Helliwell, E. Moir, *J. Org. Chem.*, 2008, **73**, 4415-4423.
- ¹⁴⁷ D. J. Leonard, J. W. Ward, J. Clayden, *Nature*, 2018, **562**, 105-109.
- ¹⁴⁸ D. Seebach, A. R. Sting, M. Hoffmann, *Angew. Chem. Int. Ed.*, 1996, **35**, 2708-2748.
- ¹⁴⁹ [a] R. C. Atkinson, D. J. Leonard, J. Maury, D. Castagnolo, N. Volz, J. Clayden, *Chem. Commun.*, 2013, **49**, 9734-9736; [b] R. C. Atkinson, F. Fernández-Nieto, J. M. Roselló, J. Clayden, *Angew. Chemie. Int. Ed.*, 2015, **54**, 8961-8965.
- ¹⁵⁰ J. Clayden, M. Donnard, J. Lefranc, A. Minassi, D. J. Tetlow, *J. Am. Chem. Soc.*, 2010, **132**, 6624-6625.
- ¹⁵¹ [a] D. Castagnolo, L. Degennaro, R. Luisi, J. Clayden, *Org. Biomol. Chem.*, 2015, **13**, 2330-2340; [b] M. Tait, M. Donnard, A. Minassi, J. Lefranc, B. Bechi, G. Carbone, P. O'Brien, J. Clayden, *Org. Lett.*, 2013, **15**, 34-37.
- ¹⁵² J. Lefranc, D. J. Tetlow, M. Donnard, E. Gálvez, J. Clayden, *Org. Lett.*, 2011, **13**, 296-299.
- ¹⁵³ C. Zhang, *Adv. Synth. Catal.*, 2014, **356**, 2895-2906.
- ¹⁵⁴ [a] V. Krishnamutri, S. B. Munoz, X. Ispizua-Rodriguez, J. Vickerman, T. Mathew, G. K. Surya Prakash, *Chem. Comm.*, 2018, **54**, 10574-10577; [b] H. Wang, Y. Cheng, S. Yu, *Sci. China Chem.*, 2016, **59**, 195-198; [c] H.-B. Yang, N. Selander, *Org. Biomol. Chem.*, 2017, **15**, 1771-1775.
- ¹⁵⁵ P. Allongue, M. Delamar, B. Desbat, O. Fagebaume, R. Hitmi, J. Pinson, J.-M. Savéant, *J. Am. Chem. Soc.*, 1997, **119**, 201-207.
- ¹⁵⁶ L. Cui, Y. Matusaki, N. Tada, T. Mirura, B. Uno, A. Itoh, *Adv. Synth. Catal.*, 2013, **355**, 2203-2207.
- ¹⁵⁷ [a] T. C. Keener, W. T. Davis, *JAPCA*, 1984, **34**, 651-654; [b] S. Kimura, J. M. Smith, *AIChE J.*, 1987, **33**, 1522-1532; [c] H. T. Dang, V. D. Nguyen, H. H. Pham, H. D. Arman, O. V. Larionov, *Tetrahedron*, 2019, **75**, 3258-3264.
- ¹⁵⁸ C. Hu, F. Qing, W. Huang, *J. Org. Chem.*, 1991, **56**, 2801-2804.
- ¹⁵⁹ [a] Y. Fujiwara, J. A. Dixon, F. O'Hara, E. D. Funder, D. D. Dixon, R. A. Rodriguez, R. D. Baxter, B. Herlé, N. Sach, M. R. Collins, Y. Ishihara, P. S. Baran, *Nature*, 2012, **492**, 95-99; [b] R. Gianatassio, S. Kawamura, C. L. Eprile, K. Foo, J. Ge, A. C. Burns, M. R. Collins, P. S. Baran, *Angew. Chem. Int. Ed.*, 2014, **53**, 9851-9855; [c] Q. Zhou, J. Gui, C.-M. Pan, E. Albone, X. Cheng, E. M. Suh, L. Grasso, Y. Ishihara, P. S. Baran, *J. Am. Chem. Soc.*, 2013, **135**, 12994-12997.
- ¹⁶⁰ F. De, Vleeschouwer, V. Van Speybroeck, M. Waroquier, P. Geerlings, F. De Proft, *Org. Lett.*, 2007, **9**, 14, 2721-2724.
- ¹⁶¹ Q. Fu, Z. Bo, J. Ye, T. Ju, H. Huang, L.-L. Liao, D.-G. Yu, *Nat. Commun.*, 2019, **10**, 3592.
- ¹⁶² [a] X.-Q. Chu, Y. Zi, H. Meng, X.-P. Xu, S.-J. Ji, *Chem. Commun.*, 2014, **50**, 7642-7645; [b] L. Li, Q.-S. Gu, N. Wang, P. Song, Z.-L. Li, X.-H. Li, F.-L. Wang, X.-Y. Liu, *Chem. Commun.*, 2017, **53**, 4038-4041; [c] W. Kong, E. Merino, C. Nevado, *Angew. Chem. Int. Ed.*, 2014, **53**, 5078-5082; [d] D. Chen, Z. Wu, Y. Yao, C. Zhu, *Org. Chem. Front.*, 2018, **5**, 2370-2374.
- ¹⁶³ A. S. H. Ryder, W. B. Cunningham, G. Ballantyne, T. Mules, A. G. Kinsella, J. Turner-Dore, C. M. Alder, L. J. Edwards, B. S. J. McKay, M. N. Grayson, A. J. Cresswell, *Angew. Chem. Int. Ed.*, 2020, **59**, 14986-14991.
- ¹⁶⁴ [a] D. R. Heitz, K. Rizwan, G. A. Molander, *J. Org. Chem.*, 2016, **81**, 7308-7313; [b] S. M. Hell, C. F. Meyer, A. Misale, J. B. I. Sap, K. E. Christensen, M. C. Willis, A. A. Trabanco, V. Gouverneur, *Angew. Chem. Int. Ed.*, 2020, **59**, 11620-11626.
- ¹⁶⁵ J. Maury, W. Zawodny, J. Clayden, *Org. Lett.*, 2017, **19**, 472-475.
- ¹⁶⁶ X.-Y. Qian, S.-Q. Li, J. Song, H.-C. Xu, *ACS Catal.*, 2017, **7**, 2730-2734.
- ¹⁶⁷ [a] J. J. Lubinkowski, J. W. Knapczyk, J. L. Calderon, L. R. Petit, W. E. McEwen, *J. Org. Chem.*, 1975, **40**, 3010-3015; [b] H. Seo, M. H. Katcher, T. F. Jamison, *Nat. Chem.*, 2017, **9**, 453-456.
- ¹⁶⁸ K. P. L. Kuijpers, C. Bottecchia, D. Cambié, K. Drummen, N. J. König, T. Noël, *Angew. Chem. Int. Ed.* 2018, **57**, 11278-11282.
- ¹⁶⁹ O. Stern, M. Volmer, *Phys. Z.*, 1919, **20**, 183-188.
- ¹⁷⁰ H. Takeda, M. Takeda, H. Yoshioka, H. Minamide, Y. Oki, C. Adachi, *Opt. Mater. Express*, 2019, **9**, 1150-1160.

-
- ¹⁷¹ D. M. Arias-Rotondo, J. K. McCusker, *Chem. Soc. Rev.*, 2016, **45**, 5803-5820.
- ¹⁷² X.-M. Qian, Y. Song, K.-C. Lau, C. Y. Ng, J. Liu, W. Chen, G. Z. He, *Chem. Phys. Lett.*, 2002, **353**, 19-26.
- ¹⁷³ C. Hansch, A. Leo, R. W. Taft, *Chem. Rev.*, 1991, **91**, 165-195.
- ¹⁷⁴ D. Heseck, M. Lee, B. C. Noll, J. F. Fisher, S. Mobashery, *J. Org. Chem.*, 2009, **74**, 2567-2570.
- ¹⁷⁵ J. H. Markgraf, R. Chang, J. R. Cort, J. L. Durant, M. Finkelstein, A. W. Gross, M. H. Lavyne, W. M. Moore, R. C. Petersen, S. D. Ross, *Tetrahedron*, 1997, **53**, 10009-10018.
- ¹⁷⁶ W. S. Matthews, J. E. Bares, J. E. Bartmess, F. G. Bordwell, F. J. Cornforth, G. E. Drucker, Z. Margolin, R. J. McCallum, G. J. McCollum, N. R. Vanier, *J. Am. Chem. Soc.*, 1975, **97**, 7006-7014.
- ¹⁷⁷ F. G. Bordwell, X. Zhang, *J. Org. Chem.*, 1990, **55**, 6078-6079.
- ¹⁷⁸ F. G. Bordwell, *Acc. Chem. Res.*, 1988, **21**, 456-463.
- ¹⁷⁹ M. S. Alnajjar, X.-M. Zhang, G. J. Gleicher, S. V. Truksa, J. A. Franz, *J. Org. Chem.*, 2002, **67**, 9016-9022.
- ¹⁸⁰ M. A. Cismesia, T. P. Yoon, *Chem. Sci.*, 2015, **6**, 5426-5434.
- ¹⁸¹ M. Montalti, A. Credi, L. Prodi, M. T. Gandolfi, *Handbook of Photochemistry*, 3rd ed.; CRC/Taylor & Francis: Boca Raton, USA, 2006.
- ¹⁸² [a] H. H. Baer, F. Rajabalee, *Carbohydr. Res.*, 1970, **12**, 241-251; [b] V. Bailliez, A. Olesker, J. Cleophax, *Tetrahedron*, 2004, **60**, 1079-1085; [c] W. Meyer zu Reckendorf, N. Wassiliadou-Micheli, *Chem. Ber.*, 1974, **107**, 1188-1194; [d] W. Meyer zu Reckendorf, *Chem. Ber.*, 1971, **104**, 1976-1980.
- ¹⁸³ B. Cinque, L. Di Marzio, C. Centi, C. Di Rocco, C. Riccardi, M. G. Cifone, *Pharmacol. Res.*, 2003, **47**, 421-437.
- ¹⁸⁴ C. F. Snook, J. A. Jones, Y. A. Hannun, *Biochim. Biophys. Acta*, 2006, **1761**, 927-946.
- ¹⁸⁵ S. A. Summers, D. H. Nelson, *Diabetes*, 2005, **54**, 591-602.
- ¹⁸⁶ D. E. Modrak, D. V. Gold, D. M. Goldenberg, *Mol. Cancer Ther.*, 2006, **5**, 200-208.
- ¹⁸⁷ T. Kolter, K. Sandhoff, *Biochim. Biophys. Acta*, 2006, **1758**, 2057-2079.
- ¹⁸⁸ C. Rodriguez-Lafrasse, R. Rousson, S. Valla, P. Antignac, P. Louisot, M. T. Vanier, *Biochem. J.*, 1997, **325**, 787-791.
- ¹⁸⁹ [a] P. M. Koskinen, A. M. P. Koskinen, *Synthesis*, 1998, 1075-1091; [b] A. R. Howell, R. C. So, S. K. Richardson, *Tetrahedron*, 2004, **60**, 11327-11347; [c] J. A. Morales-Serna, J. Llaveria, Y. Díaz, M. I. Matheu, S. Castillon, *Curr. Org. Chem.*, 2010, **14**, 2483-2521.
- ¹⁹⁰ E. Abraham, S. G. Davies, N. L. Millican, R. L. Nicholson, P. M. Roberts, A. D. Smith, *Org. Biomol. Chem.*, 2008, **6**, 1655-1664.
- ¹⁹¹ E. D. D. Calder, A. M. Zaed, A. Sutherland, *J. Org. Chem.*, 2013, **78**, 7223-7233.
- ¹⁹² V. Farina, J. D. Brown, *Angew. Chem. Int. Ed.*, 2006, **45**, 7330-7334.
- ¹⁹³ C. U. Kim, W. Lew, M. A. Williams, H. Liu, L. Zhang, S. Swaminathan, N. Bishofberger, M. S. Chen, D. B. Mendel, C. Y. Tai, W. G. Laver, R. C. Stevens, *J. Am. Chem. Soc.*, 1997, **119**, 681-690.
- ¹⁹⁴ [a] T. Jefferson, M. Jones, P. Doshi, E. A. Spencer, I. Onakpoya, C. Heneghan, *Br. Med. J.*, 2014, **348**, g2545; [b] C. Heneghan, I. Onakpoya, M. Thompson, E. A. Spencer, M. Jones, T. Jefferson, *Br. Med. J.*, 2014, **348**, g2547.
- ¹⁹⁵ [a] J. C. Rohloff, K. M. Kent, M. J. Postich, M. W. Becker, H. H. Chapman, D. E. Kelly, W. Lew, M. S. Louie, L. R. McGee, *J. Org. Chem.*, 1998, **63**, 4545-4550; [b] M. Karpf, R. Trussardi, *J. Org. Chem.*, 2001, **66**, 2044-2051; [c] Y.-Y. Yeung, S. Hong, E. J. Corey, *J. Am. Chem. Soc.*, 2006, **128**, 6310-6311; [d] N. Satoh, T. Akiba, S. Yokoshima, T. Fukuyama, *Angew. Chem. Int. Ed.*, 2007, **46**, 5734-5736; [e] H. Ishikawa, T. Suzuki, Y. Hayashi, *Angew. Chem. Int. Ed.*, 2009, **48**, 1304-1307.
- ¹⁹⁶ B. M. Trost, T. Zhang, *Angew. Chem. Int. Ed.*, 2008, **47**, 3759-3761.
- ¹⁹⁷ L. M. Cañedo, J. L. Fernández Puentes, J. Pérez Baz, C. Acebal, F. de la Calle, D. Garcia Grávalos, T. Garcia de Quesada, *Antibiot.*, 1997, **50**, 175-176.
- ¹⁹⁸ S. K. Patel, K. Murat, S. Py, Y. Vallée, *Org. Lett.*, 2003, **5**, 4081-4084.

- ¹⁹⁹ [a] T. K. M. Shing, V. W. F. Tai, E. K. W. Tam, *Angew. Chem. Int. Ed.*, 1994, **33**, 2312-2313; [b] T. K. M. Shing, E. W. Tam, *Tetrahedron Lett.*, 1999, **40**, 2179-2180.
- ²⁰⁰ E. H. Andrianasolo, L. Haramaty, K. L. McPhail, E. White, C. Vetriani, P. Falkoski, R. J. Lutz, *Nat. Prod.*, 2011, **74**, 842-846.
- ²⁰¹ H. Zhu, P. Chen, G. Liu, *J. Am. Chem. Soc.*, 2014, **136**, 1766-1769.
- ²⁰² [a] Y. Le Merrer, A. Duréault, C. Greck, D. Micas-Languin, C. Gravier, J.-C. Depezay, *Heterocycles*, 1987, **25**, 541-548; [b] M. Chandrasekhar, K. L. Chandra, V. K. Singh, *J. Org. Chem.*, 2003, **68**, 4039-4045; [c] J. S. Reddy, A. R. Kumar, B. V. Rao, *Tetrahedron, Asymm.*, 2005, **16**, 3154-3159; [d] W. Lu, G. Zheng, J. C. Cai, *Tetrahedron*, 1999, **55**, 7157-7168.
- ²⁰³ [a] Daiichi Sankyo Company, US Pat. 8088796 B2, 2012; [b] G. R. Pettit, S. Ducki, D. L. Herald, D. L. Doubek, J. M. Schmidt, J.-C. Chapuis, *Oncol. Res.*, 2005, **15**, 11-20; [c] T. Hayashi, T. Noto, Y. Nawata, H. Okazaki, M. Sawada, K. J. Ando, *Antibiot.*, 1982, **35**, 771-777; [d] G. Dinos, D. N. Wilson, Y. Teraoka, W. Szaflarski, P. Fucini, D. Kalpaxis, K. H. Nierhaus, *Mol. Cell*, 2004, **13**, 113-124.
- ²⁰⁴ [a] M. D'Ambrosio, A. Guerriero, C. Debitus, O. Ribes, J. Pusset, S. Leroy, F. Pietra, *J. Chem. Soc., Chem. Commun.*, 1993, 1305-1306; [b] M. D'Ambrosio, A. Guerriero, G. Chiasera, F. Pietra, *Helv. Chim. Acta*, 1994, **7**, 1895-1902; [c] M. D'Ambrosio, A. Guerriero, M. Ripamonti, C. Debitus, J. Waikedre, F. Pietra, *Helv. Chim. Acta*, 1996, **79**, 727-735; [d] S. Tilvi, C. Morioux, M. Martin, J. Gallard, J. Sorres, K. Patel, S. Petek, C. Debitus, L. Ermolenko, A. Al-Mourabit, *J. Nat. Prod.*, 2010, **73**, 720-723.
- ²⁰⁵ G. Dong, *Pure Appl. Chem.*, 2010, **82**, 2231-2246.
- ²⁰⁶ S. Han, D. S. Siegel, K. C. Morrison, P. J. Hergenrother, M. Movassaghi, *J. Org. Chem.*, 2013, **78**, 11970-11984.
- ²⁰⁷ T. Negoro, M. Murata, S. Ueda, B. Fujitani, Y. Ono, A. Kuromiya, M. Komiya, K. Suzuki, J. Matsumoto, *J. Med. Chem.*, 1998, **41**, 4118-4129.
- ²⁰⁸ [a] A. Evans, C. A. Illig, J. C. Saddler, *J. Am. Chem. Soc.*, 1986, **108**, 2476-2478; [b] T. Fukuyama, L. Li, A. A. Laird, R. K. Frank, *J. Am. Chem. Soc.*, 1987, **109**, 1587-1589.
- ²⁰⁹ H. Ümit, P. Garner, *J. Am. Chem. Soc.*, 2007, **129**, 15460-15461.
- ²¹⁰ [a] S. R. Harvey, M. Porri, C. Stachl, D. MacMillan, G. Zinzalla, P. E. Barran, *J. Am. Chem. Soc.*, 2012, **134**, 19384-19392; [b] L. R. Whitby, D. L. Boger, *Acc. Chem. Res.*, 2012, **45**, 1698-1709; [c] M. Vidal, M. E. Cusick, A.-L. Barabasi, *Cell*, 2011, **144**, 986-998.
- ²¹¹ E. G. Hutchinson, J. M. Thornton, *Protein Sci.*, 1994, **3**, 2207-2216.
- ²¹² [a] R. V. Nair, A. S. Kotmale, S. A. Dhokale, R. L. Gawade, V. G. Puranik, P. R. Rajamohan, G. Sanjayan, *J. Org. Biomol. Chem.*, 2014, **12**, 774-782; [b] V. H. Thorat, T. S. Ingole, K. N. Vijayadas, R. V. Nair, S. S. Kale, V. V. E. Ramesh, H. C. Davis, P. Prabhakaran, R. G. Gonnade, R. L. Gawade, V. G. Puranik, P. R. Rajamohan, G. Sanjayan, *J. Eur. J. Org. Chem.*, 2013, 3529-3542; [c] G. Lesma, R. Cecchi, A. Cagnotto, M. Gobbi, F. Meneghetti, M. Musolino, A. Sacchetti, A. Silvani, *J. Org. Chem.*, 2013, **78**, 2600-2610; [d] P. A. Ottersbach, J. Schmitz, G. Schnakenburg, M. Gütschow, *Org. Lett.*, 2013, **15**, 448-451; [e] C.-F. Wu, X. Zhao, W.-X. Lan, C. Cao, J.-T. Liu, X.-K. Jiang, Z.-T. Li, *J. Org. Chem.*, 2012, **77**, 4261-4270.
- ²¹³ S. Pellegrino, A. Contini, M. L. Gelmi, L. L. Presti, R. Soave, E. Erba, *J. Org. Chem.*, 2014, **79**, 3094-3102.
- ²¹⁴ B. M. Trost, S. Malhotra, D. E. Olson, A. Maruniak, J. Du Bois, *J. Am. Chem. Soc.*, 2009, **131**, 4190-4191.
- ²¹⁵ L. Lykke, B. D. Carlsen, R. S. Rambo, K. A. Jørgensen, *J. Am. Chem. Soc.*, 2014, **136**, 11296-11299.
- ²¹⁶ [a] N. Iordanova, S. Hammes-Schiffer, *J. Am. Chem. Soc.*, 2002, **124**, 4848-4856; [b] R. A. Binstead, T. J. Meyer, *J. Am. Chem. Soc.*, 1987, **109**, 3287-3297; [c] B. T. Farrer, H. H. Thorp, *Inorg. Chem.*, 1999, **38**, 2497-2502; [d] B. A. Moyer, T. J. Meyer, *J. Am. Chem. Soc.*, 1978, **100**, 3601-3603; [e] R. A. Binstead, B. A. Moyer, G. J. Samuels, T. J. Meyer, *J. Am. Chem. Soc.*, 1981, **103**, 2897-2899; [f] T. J. Meyer, M. H. V Huynh, *Inorg. Chem.*, 2003, **42**, 8140-8160.
- ²¹⁷ [a] N. Lehnert, E. I. Solomon, *J. Biol. Inorg. Chem.*, 2003, **8**, 294-305; [b] E. Hatcher, A. Soudackov, S. Hammes-Schiffer, *J. Am. Chem. Soc.*, 2004, **126**, 5763-5775.
- ²¹⁸ Y. Wang, H. Chen, M. Makino, Y. Shiro, S. Nagano, S. Asamizu, H. Onaka, S. Shaik, *J. Am. Chem. Soc.*, 2009, **131**, 6748-6762.

- ²¹⁹ [a] C. Constantin, S. Drouet, M. Robert, J. M. Saveant, *Science*, 2012, **338**, 90-94; [b] M. D. Symes, Y. Surendranath, D. A. Lutterman, D. G. Nocera, *J. Am. Chem. Soc.*, 2011, **133**, 5174-5177.
- ²²⁰ T. J. Meyer, M. H. V. Huynh, H. H. Thorp, *Angew. Chem. Int. Ed.*, 2007, **46**, 5284-5304.
- ²²¹ J. B. Pedley, R. D. Naylor, S. P. Kirby, *Thermodynamic Data of Organic Compounds*, 2nd ed., Chapman and Hall, New York, 1986.
- ²²² L. Eberson, *Acta Chem. Scand.*, 1963, **17**, 2004-2018.
- ²²³ F. G. Borwell, S. Zhang, X. M. Zhang, W. Z. Liu, *J. Am. Chem. Soc.*, 1995, **117**, 7092-7096.
- ²²⁴ K. Y. Choo, D. M. Golden, S. W. Brenson, *Int. J. Chem. Kinet.*, 1975, **7**, 713.
- ²²⁵ J. G. West, D. Huang, E. J. Sorensen, *Nat. Commun.*, 2015, **6**, 10093-10100.
- ²²⁶ F. G. Bordwell, J. P. Cheng, J. A. Harrelson, *J. Am. Chem. Soc.*, 1988, **110**, 1229-1231.
- ²²⁷ D. C. Miller, K. T. Tarantino, R. R. Knowles, *Top. Curr. Chem.*, 2016, 374.
- ²²⁸ [a] L. J. Rono, H. G. Yayla, D. Y. Wang, M. F. Armstrong, R. R. Knowles, *J. Am. Chem. Soc.*, 2013, **135**, 17735-17738; [b] D. C. Miller, G. J. Choi, H. S. Orbe, R. R. Knowles, *J. Am. Chem. Soc.*, 2015, **137**, 13492-13495; [c] H. G. Yayla, H. Wang, K. T. Tarantino, H. S. Orbe, R. R. Knowles, *J. Am. Chem. Soc.*, 2016, **138**, 10794-10797.
- ²²⁹ K. T. Tarantino, P. Liu, R. R. Knowles, *J. Am. Chem. Soc.*, 2013, **135**, 10022-10025.
- ²³⁰ H. G. Roth, N. A. Romero, D. A. Nicewicz, *Synlett*, 2016, **27**, 714-723.
- ²³¹ I. M. Kolthoff, M. K. Chantooni, *J. Am. Chem. Soc.*, 1973, **95**, 8539-8546.
- ²³² G. J. Choi, R. R. Knowles, *J. Am. Chem. Soc.*, 2015, **137**, 9226-9229.
- ²³³ P. Griess, *Liebigs, Ann.*, 1858, **106**, 123-125.
- ²³⁴ [a] O. Ghodbane, G. Chamoulaud, D. Bélanger, *Electrochem. Commun.*, 2004, **6**, 254-258; [b] S. Betelu, C. Vautrin-UI, A. Chaussé, *Electrochem. Commun.*, 2009, **11**, 383-386.
- ²³⁵ J. L. Bahr, J. Yang, D. V. Kosynkin, M. J. Bronikowski, R. E. Smalley, J. M. Tour, *J. Am. Chem. Soc.*, 2001, **123**, 6536-6542.
- ²³⁶ Y. Pan, B. Tong, J. Shi, W. Zhao, J. Shen, J. Zhi, Y. Dong, *J. Phy. Chem. C*, 2010, **114**, 8040-8047.
- ²³⁷ D. K. Aswall, S. P. Koiry, B. Jousselmé, S. K. Gupta, S. Palacin, J. V. Yakhmi, *Phys. E.*, 2009, **41**, 325-344.
- ²³⁸ A. Roglans, A. Pla-Quintana, M. Moreno-Mañas, *Chem. Rev.*, 2006, **106**, 4622-4643.
- ²³⁹ [a] G. Balz, G. Schiemann, *Chem. Ber.*, 1927, **60**, 1186-1190; [b] A. Roe, *Org. React.*, 1949, **5**, 193-228.
- ²⁴⁰ [a] C. S. Rondestvedt, *Org. React.*, 1960, **11**, 189-260; [b] C. S. Rondestvedt, *Org. React.*, 1976, **24**, 225-259.
- ²⁴¹ [a] C. Galli, *Chem. Rev.*, 1988, **88**, 765-792; [b] P. Hanson, S. C. Rowell, A. B. Taylor, P. H. Walton, A. W. Timms, *J. Chem. Soc. Perkin Trans. 2*, 2002, 1126-1134; [c] P. Hanson, J. R. Jones, A. B. Taylor, P. H. Walton, A. W. Timms, *J. Chem. Soc. Perkin Trans. 2*, 2002, 1135-1150.
- ²⁴² M. Solís, A. Solís, H. I. Pérez, N. Manjarrez, M. Flores, *Process Biochem.*, 2012, **47**, 1723-1748.
- ²⁴³ [a] M. Roldo, E. Barbu, J. F. Brown, D. W. Laight, J. D. Smart, J. Tsibouklis, *Expert Opin. Drug Deliv.*, 2007, **4**, 547-560; [b] A. Jain, Y. Gupta, S. K. Jain, *Crit. Rev. Ther. Drug Carrier Syst.*, 2006, **23**, 349-400.
- ²⁴⁴ S. Kindt, K. Wicht, M. R. Heinrich, *Org. Lett.*, 2015, **17**, 6122-6125.
- ²⁴⁵ H. Jiang, Y. Chen, B. Chen, H. Xu, W. Wan, H. Deng, K. Ma, S. Wu, J. Hao, *Org. Lett.*, 2017, **16**, 2406-2409.
- ²⁴⁶ C. P. Andrieux, J. Pinson, *J. Am. Chem. Soc.*, 2003, **125**, 14801-14806.
- ²⁴⁷ Y. An, J. Wu, *Org. Lett.*, 2017, **19**, 6028-6031.
- ²⁴⁸ X.-L. Yu, J.-R. Chen, D.-Z. Chen, W.-J. Xiao, *Chem. Commun.*, 2016, **52**, 8275-8278.
- ²⁴⁹ [a] M. W. Kirkwood, G. F. Wright, *J. Org. Chem.*, 1953, **18**, 629-642; [b] O. Meth-Cohn, Z. Yan, *J. Chem. Soc., Perkin Trans. 1*, 1998, 423-436.
- ²⁵⁰ Q. Zhu, D. E. Graff, R. R. Knowles, *J. Am. Chem. Soc.*, 2018, **140**, 741-747.
- ²⁵¹ D. R. Reed, M. C. Hare, A. Fattahi, G. Chung, M. S. Gordon, S. R. Kass, *J. Am. Chem. Soc.*, 2003, **125**, 4643-4651.
- ²⁵² J.-P. Cheng, M. Xian, K. Wang, X. Zhu, Z. Yin, P. G. Wang, *J. Am. Chem. Soc.*, 1998, **120**, 10266-10267.
- ²⁵³ [a] M. Hartmann, Y. Li, A. Studer, *J. Am. Chem. Soc.*, 2012, **134**, 16516-16519; [b] H. Jasch, Y. Landais, M. R. Heinrich, *Chem. Eur. J.*, 2013, **19**, 8411-8416; [c] O. Blank, A. Wetzel, D. Ullrich, M. R. Heinrich, *Eur. J. Org. Chem.*, 2008, 3179-3189.
- ²⁵⁴ [a] S. Chandrappa, K. Vinaya, T. Ramakrishnappa, K. S. Rangappa, *Synlett.*, 2010, **20**, 3019-3022; [b] A. Mobinikhaledi, N. Foroughifar, H. F. Jirandehi, *Monatsh. Chem.*, 2007, **138**, 755-757.

-
- ²⁵⁵ J. E. Baldwin, R. M. Adlington, I. M. Newington, *J. Am. Chem. Soc.*, 1986, **2**, 176-178.
- ²⁵⁶ [a] A. Jarrahpour, M. Zarei, *Molecules*, 2006, **11**, 49-58; [b] G. Cainelli, P. Galletti, D. Giacomini, *Tetrahedron Lett.*, 1998, **39**, 7779-7782; [c] A. Macías, A. M. Ramallal, E. Alonso, C. del Pozo, J. González, *J. Org. Chem.*, 2006, **71**, 7721-7730; [d] K. C. Nicolaou, P. S. Baran, Y.-L. Zhong, J. A. Vega, *Angew. Chem. Int. Ed.*, 2000, **39**, 2525-2529.
- ²⁵⁷ [a] M. Gomberg, W. E. Bachmann, *J. Am. Chem. Soc.*, **42**, 2339-2343; [b] G. Pratsch, T. Wallaschkowski, M. R. Heinrich, *Chem. Eur. J.*, 2012, **18**, 11555-11559.
- ²⁵⁸ D. D. M. Wayner, D. J. McPhee, D. Griller, *J. Am. Chem. Soc.*, 1988, **110**, 132-137.
- ²⁵⁹ [a] J. Clayden, W. Farnaby, D. M. Grainger, U. Hennecke, M. Mancinelli, D. J. Tetlow, I. H. Hillier, M. A. Vincent, *J. Am. Chem. Soc.*, 2009, **131**, 3410-3411; [b] P. MacLellan, J. Clayden, *Chem. Commun.*, 2011, 3395-3397; [c] G. Mingat, P. MacLellan, M. Laars, J. Clayden, *Org. Lett.*, 2014, **16**, 1252-1255;
- ²⁶⁰ [a] A. M. Fournier, J. Clayden, *Org. Lett.*, 2012, **14**, 142-145; [b] D. Castagnolo, D. J. Foley, H. Berber, R. Luisi, J. Clayden, *Org. Lett.*, 2013, **15**, 2116-2119; [c] D. Castagnolo, L. Degennaro, R. Luisi, J. Clayden, *Org. Biomol. Chem.*, 2015, **13**, 2330-2340.
- ²⁶¹ M. A. Okoh, PhD thesis, University of Bristol, 2020.
- ²⁶² E. Wadsworth, Master's Dissertation, University of Bristol, 2019.
- ²⁶³ J. Dai, Z. Li, T. Wang, W. Bai, R. Bai, *Org. Lett.*, 2017, **19**, 1418-1421.
- ²⁶⁴ Y. Sato, S. Kawaguchia, A. Ogawa, *Chem. Commun.*, 2015, **51**, 10385-10388.
- ²⁶⁵ L. Deng, Y. Wang, H. Mei, Y. Pan, J. Han, *J. Org. Chem.*, 2019, **84**, 949-956.
- ²⁶⁶ M. Ali, L.-P. Liu, G. B. Hammond, B. Xu, *Tetrahedron Lett.*, 2009, **50**, 4078-4080.
- ²⁶⁷ C. G. Hatchard, C. A. Parker, *Proc. Roy. Soc.*, 1956, **A235**, 518-536.
- ²⁶⁸ Z. Gonda, F. Béke, O. Tischler, M. Petró, Z. Novák, B. L. Tóth, *Eur. J. Org. Chem.*, 2017, 2112-2117.
- ²⁶⁹ L. Zhu, P. Xiong, Z.-Y. Mao, Y.-H. Wang, X. Yan, X. Lu, H.-C. Xu, *Angew. Chem.*, 2016, **55**, 2226-2229.
- ²⁷⁰ C. Curti, A. Sartori, L. Battistini, N. Brindani, G. Rassu, G. Pelosi, A. Lodola, M. Mor, G. Casiraghi, F. Zanardi, *Chem. Eur. J.*, 2015, **21**, 6433-6442.
- ²⁷¹ B. DeBoef, R. W. Counts, S. R. Gilbertson, *J. Org. Chem.*, 2007, **72**, 3, 799-804.
- ²⁷² X. Chen, H. Zhou, K. Zhang, J. Li, H. Huang, *Org. Lett.*, 2014, **16**, 3912-3915.
- ²⁷³ J. Li, C. Tan, J. Gong, Z. Yang, *Org. Lett.*, 2014, **16**, 20, 5370-5373.
- ²⁷⁴ Y.-F. Liang, R. Steinbock, L. Yang, L. Ackermann, *Angew. Chem. Int. Ed.*, 2018, **57**, 10625-10629.